HETEROGENEOUS SHALLOW-SHELF CARBONATE BUILDUPS IN THE PARADOX BASIN, UTAH AND COLORADO: TARGETS FOR INCREASED OIL PRODUCTION AND RESERVES USING HORIZONTAL DRILLING TECHNIQUES

FINAL REPORT

Thomas C. Chidsey, Jr., Compiler and Editor
Utah Geological Survey
Salt Lake City, Utah

March 2007

Performed Under Contract No. DE-FC26-00BC15128

Virginia Weyland, Contract Manager
U.S. Department of Energy
National Petroleum Technology Laboratory
1 West 3rd Street
Tulsa, OK 74103-3532

DISCLAIMER

FINAL

HETEROGENEOUS SHALLOW-SHELF CARBONATE BUILDUPS IN THE PARADOX BASIN, UTAH AND COLORADO: TARGETS FOR INCREASED OIL PRODUCTION AND RESERVES USING HORIZONTAL DRILLING TECHNIQUES

FINAL REPORT

Thomas C. Chidsey, Jr., Compiler and Editor

Date of Report: March 2007

Work Performed Under Contract No. DE-FC26-00BC15128

Prepared for
U.S. Department of Energy
Assistant Secretary for Fossil Energy

Virginia Weyland, Project/Contract Manager
National Petroleum Technology Laboratory
1 West 3rd Street
Tulsa, OK 74103-3532

Submitting Organization: **Utah Geological Survey**
1594 West North Temple, Suite 3110
P.O. Box 146100
Salt Lake City, Utah 84114-6100
(801) 537-3300

ABSTRACT

The Paradox Basin of Utah, Colorado, Arizona, and New Mexico contains nearly 100 small oil fields producing from carbonate buildups within the Pennsylvanian (Desmoinesian) Paradox Formation. These fields typically have one to 10 wells with primary production ranging from 700,000 to 2,000,000 barrels (111,300-318,000 m^3) of oil per field and a 15 to 20 percent recovery rate of the original oil in place. At least 200 million barrels (31.8 million m^3) of oil will not be recovered from these small fields because of inefficient recovery practices and undrained heterogeneous reservoirs. With the exception of the giant Greater Aneth field, the value of horizontal drilling has not been demonstrated in any of the small shallow-shelf carbonate reservoirs in the Paradox Basin. These reservoirs are heterogeneous due to lithofacies changes and extensive diagenesis, leaving untapped compartments.

The two main producing zones of the Paradox Formation are informally named the Ismay and the Desert Creek. The Ismay zone is dominantly limestone comprising small, equant buildups of phylloid-algal material; locally variable, inner-shelf, skeletal calcarenites; rare, open-marine, bryozoan mounds; and anhydrite caps. The Ismay produces oil from fields in the southern Blanding sub-basin. The Desert Creek zone is dominantly dolomite comprising regional, nearshore, shoreline trends with highly aligned, linear lithofacies tracts. The Desert Creek produces oil in fields in the central Blanding sub-basin. Both the Ismay and Desert Creek buildups generally trend northwest-southeast.

Four case-study fields were evaluated as candidates for horizontal drilling and enhanced oil recovery based upon geological characterization and reservoir modeling studies during Budget Period I of the project: Bug field, San Juan County, Utah, in the Desert Creek trend; and Cherokee field, San Juan County, Utah, and Little Ute and Sleeping Ute fields, Montezuma County, Colorado, in the Ismay trend. Geological characterization on a local scale focused on reservoir heterogeneity, quality, and lateral continuity, as well as possible reservoir compartmentalization to grade each field's potential for drilling horizontal laterals from existing development wells. The work consisted of (1) description and analysis of cores, (2) correlation of geophysical well logs, (3) reservoir mapping and lithofacies determination, (4) petrographic description of thin sections (including scanning electron microscopy, epifluorescence, and cathodoluminescence analyses), (5) cross plotting of permeability and porosity data, (6) capillary pressure/mercury injection analysis, (7) production analysis, (8) three-dimensional reservoir modeling, (9) reservoir calculations, and (10) development of horizontal drilling strategies. From these evaluations, specific untested or under-produced compartments were identified as targets for horizontal drilling.

The project's primary objective was to enhance domestic petroleum production by demonstration and transfer of horizontal drilling technology in the Paradox Basin. If this project demonstrated technical and economic feasibility, then the technique could be applied to approximately 100 additional small fields in the Paradox Basin alone, and result in increased recovery of an additional 25 to 50 million barrels (4-8 million m^3) of oil. Based on our evaluations, we chose Cherokee and Bug fields as the best candidates for pilot demonstration projects to drill horizontal wells, monitor well performance, and report associated validation activities. Our work showed that horizontal laterals drilled from existing vertical wells in each field would likely encounter unproduced oil reserves, and could be done economically. Both field operators elected not to participate in the demonstration project (Budget Period II) citing limited drilling budgets and commitments elsewhere as the primary reasons for their decisions.

The UGS conducted an aggressive promotion plan to offer the opportunity for other operators to participate in the project. Although the UGS received inquires from numerous operators about the offer, none followed up with a proposal. Finally, the UGS and DOE elected to terminate the project without the field horizontal drilling demonstration. However, the results of the various project studies can be applied in the future to similar fields elsewhere in the Paradox Basin and the Rocky Mountain region, the Michigan and Illinois Basins, and the Midcontinent region.

The core-derived vertical sequence of lithofacies from the case-study fields was tied to its corresponding log response to identify reservoir and non-reservoir rock and determine potential units suitable for horizontal drilling projects. Reservoir maps showed buildup trends, defined limits of field potential, and also indicated possible horizontal drilling targets. The diagenetic fabrics and porosity types found at the fields are indicators of reservoir flow capacity, storage capacity, and potential for horizontal drilling. The reservoir quality has been affected by multiple generations of dissolution, anhydrite plugging, and various types of cementation which act as barriers or baffles to fluid flow. The most significant and unique diagenetic characteristics were intense, late-stage microporosity and early-stage micro-boxwork porosity.

Examination of regional upper Ismay cores identified seven depositional lithofacies: open marine, middle shelf, inner shelf/tidal flat, bryozoan mound, phylloid-algal mound, quartz sand dune, and anhydritic salina. Lower Desert Creek lithofacies include open marine, middle shelf, proto-mound/collapse breccia, and phylloid-algal mound. Mapping the upper Ismay zone lithofacies delineates very prospective reservoir trends that contain porous, productive buildups around the anhydrite-filled intra-shelf basins. Lithofacies and reservoir controls imposed by the anhydritic intra-shelf basins should be considered when selecting the optimal location and orientation of any horizontal drilling from known phylloid-algal reservoirs to undrained reserves, as well as identifying new exploration trends. Although intra-shelf basins are not present in the lower Desert Creek zone of the Blanding sub-basin, drilling horizontally along linear shoreline trends could also encounter previously undrilled porous intervals and buildups.

Production "sweet spots" and potential horizontal drilling candidates were identified for Cherokee and Bug fields. For Cherokee field, the total volume of the reservoir porosity units is 17,522 acre-feet, and may contain over 350,000 barrels of oil (55,000 m^3) and 6.6 billion cubic feet of gas (BCFG) (0.19 BCMG) primary recovery. Based on these calculations, the remaining recoverable oil and gas reserves are nearly 168,000 barrels of oil (26,700 m^3) and 3 BCFG (0.08 BCMG), suggesting the presence of additional undrained zones. For Bug field, the volume calculated for porosity greater than 10 percent is 99,057 acre-feet. This also suggests the presence of additional undrained zones. The lower Desert Creek may contain recoverable oil and gas reserves of nearly 2,440,000 barrels of oil (388,000 m^3) and 5.7 BCFG (0.16 BCMG).

Strategies for horizontal drilling were developed for case-study and similar fields in the Paradox Basin. All strategies involve drilling stacked, parallel, horizontal laterals. Depositional lithofacies are targeted in both the Ismay and Desert Creek zones where, for example, multiple buildups can be penetrated with two opposed sets of stacked, parallel, horizontal laterals. Similarly, a second strategy involves penetrating multiple zones of diagenetically enhanced reservoir intervals in these mound buildups. Microporosity, micro-boxwork porosity, and meteoric overprint represent important sites for untapped hydrocarbons.

CONTENTS

FIGURES

TABLES

ACKNOWLEDGEMENTS

Project Financial Support

This research was performed under the Class II Oil Revisit Program of the U.S. Department of Energy (DOE), National Petroleum Technology Laboratory, Tulsa, Oklahoma, contract number DE-FC26-00BC15128. The Contracting Officer's Representatives were Gary D. Walker (retired), Dan Furguson, and Virginia Weyland. Additional funding and support was also provided by the Utah Geological Survey and Colorado Geological Surveys; Eby Petrography & Consulting, Inc., Littleton, Colorado; and Seeley Oil Company, Salt Lake City, Utah.

Project Contributors

Principal Investigator/Program Manager

Thomas C. Chidsey, Jr., Utah Geological Survey, Salt Lake City, Utah

Financial Officers

John Kingsley, Dan Kelly (now with the U.S. Department of Defense), Kathi Galusha, Utah Geological Survey, Salt Lake City, Utah

Task Contributing Scientists and Organizations

Roger L. Bon, Thomas C. Chidsey, Jr., Kevin McClure (now with Castle Inspection Services), Craig D. Morgan, and Sharon Wakefield, Utah Geological Survey, Salt Lake City, Utah

David E. Eby, Eby Petrography & Consulting, Inc., Littleton, Colorado

Laura L. Wray, Colorado Geological Survey (now with Williams Production Co.), Denver, Colorado

Stephen T. Nelson, Brigham Young University, Provo, Utah

Core and petrophysical data were provided by Anadarko Petroleum Co., Burlington Resources, Marathon Oil Co., PetroCorp, Inc., Samedan Oil Corp., Seeley Oil Co., and Wexpro Co. Pore casting and SEM analyses were produced and interpreted by Louis H. Taylor, Standard Geological Services, Inc., Littleton, Colorado. Capillary pressure/mercury injection analysis was conducted by TerraTek, Inc., Salt Lake City, Utah. Isotopic analysis was conducted by Melissa Schlegel, Brigham Young University Department of Geology Stable Isotope Laboratory, Provo, Utah. The Nuclide ELM 2-R Luminoscope used for this study is part of the instrumentation in the Department of Geological Engineering, Colorado School of Mines. John Humphrey assisted with the setup and instruction on this instrument. Core descriptions also incorporated interpretations by Carl R. Cannizzaro, Rensselaer Polytechnic Institute, Troy, New York; M. Randal Skinner, Brigham Young University, Provo, Utah; and Michael H. Roylance, University of Kansas, Lawrence, Kansas. Technical oversight and support was provided by the Ute Mountain Ute Indian Tribe.

Utah Geological Survey *Petroleum News* was edited by Roger Bon. The project Web page was managed by Christine Wilkerson. Vicky Clarke, Tom Dempster, Cheryl Gustin, Sharon Hamre, Kevin McClure, Carolyn Olsen, and Jim Parker, (Utah Geological Survey), and Nicole Koenig (Colorado Geological Survey) drafted figures, designed displays, photographed core, and assembled reports. Desktop publishing was by Cheryl Gustin, Utah Geological Survey.

This report, or portions of it, were reviewed by David Tabet, Mike Hylland, Robert Ressetar, Bryce Tripp, and Kimm Harty, Utah Geological Survey; Gary D. Walker, Daniel Ferguson, Viola Rawn-Schatzinger, and Virginia Weyland, National Petroleum Technology Laboratory, U.S. Department of Energy, Tulsa, Oklahoma.

EXECUTIVE SUMMARY

The Paradox Basin of Utah, Colorado, Arizona, and New Mexico contains nearly 100 small oil fields producing from carbonate buildups within the Pennsylvanian (Desmoinesian) Paradox Formation. These fields typically have one to 10 wells with primary production ranging from 700,000 to 2,000,000 barrels (111,300-318,000 m^3) of oil per field and a 15 to 20 percent recovery rate of the original oil in place. At least 200 million barrels (31.8 million m^3) of oil will not be recovered from these small fields because of inefficient recovery practices and undrained heterogeneous reservoirs.

The two main producing zones of the Paradox Formation are informally named the Ismay and the Desert Creek. The Ismay zone is dominantly limestone comprising small, equant buildups of phylloid-algal material; locally variable, inner-shelf, skeletal calcarenites; rare, open-marine, bryozoan mounds; and anhydrite caps. The Ismay produces oil from fields in the southern Blanding sub-basin. The Desert Creek zone is dominantly dolomite comprising regional, nearshore, shoreline trends with highly aligned, linear lithofacies tracts. The Desert Creek produces oil in fields in the central Blanding sub-basin. Both the Ismay and Desert Creek buildups generally trend northwest-southeast. Various lithofacies changes and extensive diagenesis have created complex reservoir heterogeneity within these two diverse zones.

Four case-study fields were selected for local-scale reservoir characterization and evaluation during Budget Period I of the project: Bug field, San Juan County, Utah, in the Desert Creek trend; and Cherokee field, San Juan County, Utah, and Little Ute and Sleeping Ute fields, Montezuma County, Colorado, in the Ismay trend. Geological characterization on a local scale focused on reservoir heterogeneity, quality, and lateral continuity, as well as possible reservoir compartmentalization, within these fields. This study utilized representative cores, geophysical logs, and thin sections to characterize and grade each field’s potential for drilling horizontal laterals from existing development wells.

The project’s primary objective was to enhance domestic petroleum production by demonstration and transfer of horizontal drilling technology in the Paradox Basin. If this project demonstrated technical and economic feasibility, then the technique could be applied to approximately 100 additional small fields in the Paradox Basin alone, and result in increased recovery of an additional 25 to 50 million barrels (4-8 million m^3) of oil. Based on our evaluations, we chose the best candidate fields for pilot demonstration projects to drill horizontally from existing vertical wells, monitor well performance, and report associated validation activities. The two case-study fields were Cherokee field, operated by our industry partner Seeley Oil Company, and Bug field, operated by Wexpro Company. Our work showed that horizontal wells drilled from existing vertical wells in each field would likely encounter unproduced oil reserves, and could be done so economically. Both operators elected not to participate in the demonstration project (Budget Period II) citing limited drilling budgets and commitments elsewhere as the primary reasons for their decisions.

The UGS conducted an aggressive promotion plan to offer the opportunity for other operators to participate in the project demonstration to drill a lateral(s) from an existing vertical well(s) or new horizontal well(s) in the Ismay and Desert Creek zones of Paradox Basin fields in Utah or Colorado. Although the UGS received inquires from numerous operators about the offer, none followed up with a proposal. Finally, the UGS and DOE elected to terminate the project without the field horizontal drilling demonstration. However, the results of the various project studies can be applied in the future to similar fields elsewhere in the Paradox Basin and the Rocky Mountain region, the Michigan and Illinois Basins, and the Midcontinent region.

Lithofacies

The depositional environments of the Ismay and Desert Creek zones, based on the core descriptions, show that the controlling factors on lithofacies deposition were water depth, salinity, prevailing wave energy, and in the case of phylloid-algal growth, paleostructural position. Lithofacies from the middle shelf, principally the phylloid-algal mounds, form the dominant producing reservoirs in the Ismay and Desert Creek zones. Examination of upper Ismay cores identified seven depositional lithofacies: open marine, middle shelf, inner shelf/ tidal flat, bryozoan mound, phylloid-algal mound, quartz sand dune, and anhydritic salina. Lower Desert Creek lithofacies include open marine, middle shelf, proto-mound/collapse breccia, and phylloid-algal mound.

A grid of regional log cross sections within the Utah portion of the Blanding sub-basin shows the development of “clean carbonate” packages which contain all of the productive reservoir lithofacies. These clean carbonates abruptly change laterally into thick anhydrite packages. Isochore maps of the upper Ismay clean carbonates and the locally thick anhydrites are consistent with a broad carbonate shelf containing several small intra-shelf basins. The intra-shelf basin centers filled with anhydrite following carbonate sedimentation on the remainder of the carbonate shelf. Mapping the upper Ismay zone lithofacies into two intervals (upper and lower parts) delineated very prospective reservoir trends that contain porous, productive buildups. The mapped lithofacies trends clearly define anhydrite-filled intra-shelf basins. Intra-shelf basins are not present in the lower Desert Creek zone of the Blanding sub-basin.

Case-Study Field Evaluation

The log-based correlation scheme developed for the project ties the typical, vertical, core-derived sequence or cycle of depositional lithofacies from Cherokee and Bug case-study fields to their corresponding gamma-ray and neutron-density curves from geophysical well logs. The correlation scheme identifies major zone contacts, seals or barriers, baffles, producing or potential reservoirs, and depositional lithofacies. Seals or barriers include anhydrite layers and shales. Baffles are those rock units that restrict fluid flow in some parts of the field, but may develop enough porosity and permeability in other parts through diagenetic processes or lithofacies changes to provide a conduit for fluid flow or even oil storage. In Cherokee field for example, six porosity units were identified in the upper Ismay zone. In Bug field, the porosity unit is the entire Desert Creek mound. However, geophysical logs often exhibit a "false porosity" for some units which led to wasteful completion attempts. The cores reveal these zones to actually represent barriers or baffles to fluid flow. Log-defined units with real porosity represent potential targets for horizontal drilling.

The typical vertical sequence or lithofacies from the case-study fields, as determined from conventional core and tied to its corresponding log response, helped identify reservoir and non-reservoir rock (such as false porosity zones on geophysical well logs) and determine potential units suitable for horizontal drilling projects. Structure contour maps on the top of the Ismay and Desert Creek zones and seals such as the Chimney Rock shale, and isochore maps of various units of the Ismay and lower Desert Creek for case-study fields show carbonate buildup trends, lithofacies distribution, defined limits of field potential, and also indicated possible horizontal drilling targets.

The diagenetic fabrics and porosity types found in the various hydrocarbon-bearing rocks of the case-study fields are indicators of reservoir flow capacity, storage capacity, and potential for horizontal drilling. The reservoir quality of these fields has been affected by multiple generations of dissolution, anhydrite plugging, and various types of cementation which act as barriers or baffles to fluid flow. The most significant and unique diagenetic characteristic observed in thin sections from Cherokee field was intense, late-stage microporosity development along hydrothermal solution fronts. This late-stage diagenetic overprint is not present in the Little Ute and Sleeping Ute fields of Colorado. The thin sections from Bug field show extensive, early-stage, micro-boxwork porosity due to dissolution related to subaerial exposure of the carbonate buildup. Based on cross plots of permeability and porosity data, the reservoir quality of the rocks in the case-study fields is most dependent on pore types and diagenesis, and in the Colorado fields, lithofacies as well.

Scanning Electron Microscope and Pore Casting

Scanning electron microscope and/or pore casting analyses helped disclose the diagenetic fabrics and porosity types found in the various hydrocarbon-bearing rocks of Cherokee and Bug fields. All samples exhibit microporosity in the form of intercrystalline (primarily in Cherokee field) or micro-boxwork porosity (primarily in Bug field). Dissolution has contributed to porosity in most samples by creating moldic, vuggy, and channel porosity. Anhydrite, calcite, smectite clays, and pyrobitumen are present in some samples. The dominant cement occluding porosity and permeability in the Cherokee wells is anhydrite. The general diagenetic sequence for samples studied by SEM and pore casting analyses was: (1) deposition of calcite cement, (2) dissolution, (3) dolomitization, (4) dissolution, (5) fracturing, (6) calcite cementation, (7) quartz cementation, (8) clay deposition, (9) anhydrite cementation, and (10) pyrobitumen emplacement.

Epifluorescence Petrography

Epifluorescence petrography makes it possible to clearly identify grain types and shapes within both limestone and dolomite reservoir intervals in upper Ismay zone thin sections from the Cherokee field cores examined in this study. In particular, peloids, skeletal grain types, and coated grains are easy to see in rocks where these grains have been poorly preserved, partially leached, or completely dolomitized. Epifluorescence petrography clearly and rapidly images pore spaces that cannot otherwise be seen in standard viewing under transmitted polarized lighting. In many of the microporous limestones and finely crystalline dolomites, the differences between muddy and calcarenitic fabrics can only be clearly appreciated with fluorescence lighting.

Much of the upper Ismay zone porosity is very heterogeneous and poorly connected as viewed under epifluorescence. The epifluorescence examination helps in seeing the dissolution origin of most types of the microporosity. Transmitted polarized lighting does not image microporosity in carbonate samples very well, even though blue-dyed epoxy can impregnate very small pores. This porosity does not show up very well because the pores are much smaller than the thickness of the thin section, and hence carbonate crystallites on either side of micropores are seen rather than the pores. In addition, opaque bitumen linings prevent light from passing through some of the pores to the observer. Without the aid of the epifluorescence view, the amount of visible open pore space would be underestimated in the plane-light image.

Where dolomitization has occurred, epifluorescence petrography often shows the crystal size, shape, and zonation far better than transmitted plane or polarized lighting. This information is often very useful when considering the origin and timing of dolomitization as well as evaluating the quality of the pore system within the dolomite. Low-permeability carbonates from this study area show bright yellow fluorescence due to trapped live oil that is retained within tighter parts of the reservoir system. Rocks with greater permeability show red fluorescence due to the epoxy fluorescence where oil has almost completely drained from the better quality portions of the reservoir. Epifluorescence frequently reveals small compartments of good porosity separated from much tighter rocks by subhorizontal stylolitic seams. Hence, some of the stylolites and wispy seams with concentrations of insoluble residues act as barriers to vertical fluid flow between the porous compartments.

Cathodoluminescence Petrography

Cathodoluminescence is the emission of light resulting from the bombardment of materials using a cathode ray. This petrographic technique can be an invaluable tool in petrographic studies of carbonate rocks. It provides important information about the complex modification of rock fabrics and porosity within the lower Desert Creek and upper Ismay zones of the Blanding sub-basin. Examination of upper Ismay limestones and lower Desert Creek dolomites under cathodoluminescence makes it possible to more clearly identify grain types and shapes, early cements (such as botryoidal, fibrous marine, bladed calcite cements), and brecciated phylloid-algal mound fabrics. In addition, identification of pelleted fabrics in muds, as well as various types of skeletal grains, is improved by cathodoluminescence examination in rocks where these grains have been poorly preserved, partially leached or completely dolomitized. In many ways, cathodoluminescence imaging of samples nicely complements the types of information derived from epifluorescence of carbonate thin sections.

Cathodoluminescence imaging clearly and rapidly images pore spaces that cannot be easily seen in standard viewing under transmitted, plane-polarized light. In addition, the cross sectional size, shape, and boundaries of pores are easy to determine. This information is often very useful when considering the origin and timing of dolomitization as well as evaluating the quality of the pore system within the dolomite. Imaging of microfractures as well as dissolution along microstylolites is greatly facilitated under cathodoluminescence. Many open microfractures cannot be easily seen in a normal 3-μm–thick petrographic thin section, especially within dense, lower Desert Creek dolomites. Routine cathodoluminescence examination of the same thin section often reveals the presence of individual microfractures or microfracture swarms. Examination of saddle dolomites, when present within the clean carbonate intervals of the upper Ismay or lower Desert Creek interval, can provide more information about these late, elevated temperate (often hydrothermal) mineral phases. For instance, saddle dolomites from the Cherokee Federal No. 22-14 well showed nice growth banding. They also exhibited the difference between replacement and cement types of saddle dolomites under cathodoluminescence.

Isotope Geochemistry

Diagenesis is the main control on the quality of Ismay and Desert Creek reservoirs.

Most of the carbonates present within the lower Desert Creek and Ismay have retained a marine-influenced carbon isotope geochemistry throughout marine cementation, as well as through post-burial recycling of marine carbonate components during dolomitization, stylolitization, dissolution, and late cementation. Meteoric waters do not appear to have had any effect on the composition of these lower Desert Creek dolomites. Based on Bug field dolomite samples, the lower Desert Creek zone shows carbon isotope compositions that are very close in value to modern marine carbonates and Holocene botryoidal, marine, aragonite cements. As with the Bug field dolomite samples, the Cherokee field carbonates fall within the same range of carbon isotope compositions as modern marine sediments, skeletons, and marine cements.

Light oxygen values obtained from reservoir samples for wells located along the margins or flanks of Bug field may be indicative of exposure to higher temperatures, to fluids depleted in ^{18}O relative to sea water, or to hypersaline waters during burial diagenesis. The samples from Bug field with the lightest oxygen isotope compositions are from wells that have produced significantly higher amounts of hydrocarbons. There is no significant difference between the oxygen isotope compositions from lower Desert Creek dolomite samples in Bug field and the upper Ismay limestones and dolomites from Cherokee field.

Carbon isotopic compositions for samples of an upper Ismay cemented limestone buildup in Patterson Canyon field of Utah can be divided into two populations with regard to carbon isotopic composition: isotopically heavier mound cement and isotopically lighter oolite and banded cement. Mound cements were confined to a “closed hydrologic system” that allowed a fluid with heavier carbon to evolve. The oolite and banded cement therein may have formed in a more open system, allowing exchange with isotopically lighter waters which were involved in the lithification and diagenesis of the capping oolite.

Capillary Pressure/Mercury Injection Analysis

Capillary pressure/mercury injection analysis for Cherokee field indicates a relatively high injection pressure is required for mercury to occupy more than the last 70 percent of the pores. A steep saturation profile indicates greater microporosity that corresponds to the lower initial flowing potential and productivity, but high potential for untapped reserves. Half of the pore-size distribution for the Cherokee reservoir falls in the microporosity realm. The pore-throat radii for the Bug reservoir show that some zones also have significant microporosity (micro-boxwork porosity) while other zones are dominated by moldic porosity. As in Cherokee field, relatively high injection pressures in Bug field are required for mercury to occupy more than the last 70 percent of the pores. The steeper saturation profiles indicate the presence of micro-boxwork porosity and thus, excellent horizontal drilling targets.

Production Analysis

Production “sweet spots” and potential horizontal drilling candidates were identified for Cherokee and Bug fields. In Cherokee field, the most productive wells are located on the crest of the structural nose where the upper-Ismay-zone buildup developed and in the thickest part of the mound facies. These wells likely penetrated a thick section of microporosity - pore type with the greatest hydrocarbon storage capacity and potential horizontal drilling target in the field. In Bug field, the most productive wells are located structurally downdip from the updip porosity pinch-out that forms the trap, and in the main part of the lower-Desert-Creek-zone carbonate buildup. These wells likely penetrated significant micro-boxwork porosity – the diagenetic pore type with the greatest hydrocarbon storage and flow capacity in this dolomitized reservoir.

Three-Dimensional Modeling and Reserve Calculations

Cherokee field 3-D diagrams with structural contours on top of the upper and lower Ismay zone and Gothic shale show the same general southwest-dipping structural nose upon which the carbonate-buildup reservoir developed. There is an abrupt end of the structure suggesting the possible presence of a normal fault where late-stage microporosity may have developed. Cherokee wells that contain phylloid-algal buildups and lie along the edge of thick anhydrite follow the regional, upper-Ismay-facies pattern where intrashelf basins contain thick anhydrite accumulations. Phylloid-algal buildups developed on innershelf and tidal flats within curvilinear bands that rim the intrashelf basins. Three-dimensional models of the thickness of the entire Ismay zone, upper Ismay, lower Ismay, and upper Ismay clean carbonate, display a general west-northwest to east-southeast trend, punctuated by elongate to slightly equant thicks. Five reservoir porosity units with porosity greater than 6 percent are present in the upper Ismay mound and separated from each other by low-porosity/permeability barriers. These porosity units represent the phylloid-algal buildups and, typical of the upper-Ismay trend in the Blanding sub-basin, are viewed in 3-D as small equant-shaped pods. Porosity unit 5 is the largest and most likely the major production contributor, as well as holding the bulk of the remaining reserves. The 3-D thickness diagrams suggest all five porosity units have an untested northeastern area.

Bug field 3-D diagrams with structural contours on top of the lower Desert Creek zone and Chimney Rock shale show a southwest regional dip and a subtle, elongate, northwest-southeast-trending anticline. A 3-D model of the entire thickness of the Desert Creek zone likewise displays the same general northwest-southeast trend as do the structural diagrams, with elongate thins and thicks. The 3-D models of the thickness of lower Desert Creek intervals display an elongate, northwest-southeast-trending carbonate buildup depicting the typical, nearshore, shoreline-linear facies tracts of the Desert Creek zone in the northern Blanding sub-basin. The 3-D diagrams of the net feet of log-derived porosity greater than 10 and 12 percent in the lower Desert Creek show an elongate reservoir buildup with two subsidiary thicks separated by a slightly thinner saddle that may represent an intermound trough. Both porosity diagrams show a decrease along the northeast flank of the buildup, which when combined with a coincident high in the top of the lower Desert Creek create a combination stratigraphic/ structural trap.

Reservoir volumes (in acre-feet) were calculated for Cherokee and Bug fields. Recovery factors of 20 barrels of oil (3 m^3) and 380 thousand cubic feet of gas (MCFG) (11 MCMG) per acre-foot, respectively, were used for Cherokee field to determine the upper Ismay primary oil and gas recovery. The total volume of Cherokee field porosity units 1 through 5 is 17,522 acre-feet, and may contain over 350,000 barrels of oil (55,000 m^3) and 6.6 BCFG (billion cubic feet of gas) (0.19 BCMG) primary recovery. Based on these calculations, the remaining recoverable oil and gas reserves at Cherokee field are nearly 168,000 barrels of oil (26,700 m^3) and 3 BCFG (0.08 BCMG), suggesting the presence of additional undrained zones (microporosity). Using a price of $30/barrel and $4/MCFG, the unrisked value of the remaining recoverable reserves is over $5 million and $11 million for oil and gas, respectively.

Recovery factors of 41 barrels of oil (6.5 m^3) and 103 MCFG (3 MCMG) per acre-foot were used for Bug field to determine the lower Desert Creek clean carbonate primary oil and gas recovery. The volume calculated for net feet porosity greater than 10 percent by log analysis is 99,057 acre-feet. This suggests the presence of additional undrained zones (micro-boxwork porosity). The lower Desert Creek clean carbonate may contain recoverable oil and gas reserves of nearly 2,440,000 barrels of oil (388,000 m^3) and 5.7 BCFG (0.16 BCMG). Again, using prices of $30/barrel and $4/MCFG, the unrisked value of the remaining reserves is over $73 million and $22 million for oil and gas, respectively.

Horizontal Drilling Opportunities

With the exception of the giant Greater Aneth field, the value of horizontal drilling has not been demonstrated in any of the small shallow-shelf carbonate reservoirs in the Paradox Basin. These reservoirs are heterogeneous due to lithofacies changes and extensive diagenesis within the Ismay and Desert Creek zones, leaving untapped compartments. Production and injection laterals should be drilled into the porosity zones to sweep oil that vertical wells could not reach.

Lithofacies and reservoir controls imposed by the anhydritic intra-shelf basins should be considered when selecting the optimal location and orientation of any horizontal drilling for undrained reserves, as well as identifying new exploration trends. In the Ismay zone, projections of the inner shelf/tidal flat and mound trends around the intra-shelf basins identify potential exploration targets that could be developed using horizontal drilling techniques. Drilling horizontally from known phylloid-algal reservoirs along the inner shelf/tidal flat trend could encounter previously undrilled porous buildups. In the Desert Creek zone, drilling horizontally from productive mound lithofacies along linear shoreline trends could also encounter previously undrilled porous intervals and buildups.

Strategies for horizontal drilling were developed for case-study and similar fields in the Paradox Basin. All strategies involve drilling stacked, parallel, horizontal laterals. Depositional lithofacies are targeted in both the Ismay and Desert Creek zones where, for example, multiple buildups can be penetrated with two opposed sets of stacked, parallel, horizontal laterals. Much of the elongate, brecciated, beach-mound depositional lithofacies in the Desert Creek zone of Bug field could be penetrated by opposed sets of stacked, parallel, horizontal laterals. Similarly, a second strategy involves penetrating multiple zones of diagenetically enhanced reservoir intervals in these mound buildups. The microporosity in Cherokee, the micro-boxwork porosity in Bug, and the meteoric overprint at Little Ute/Sleeping Ute fields represent important sites for untapped hydrocarbons and possible targets for horizontal drilling. The hydrothermally induced microporosity in the Ismay zone of Cherokee field does not appear to be lithofacies dependent and therefore could be drained with radially stacked, horizontal laterals and splays.

The UGS made five alternative horizontal drilling recommendations to the operator of Cherokee field based on the conclusion that multiple potential Ismay intervals have not been drained due to reservoir heterogeneity, particularly to the northeast of the main field area. All alternatives would use existing vertical development wells, rather than drilling new wells to minimize costs and surface disturbances in the environmentally sensitive areas of southeastern

Utah. For Bug field, the UGS proposed drilling opposing, dual, long-radius, horizontal laterals from the center of the field. These laterals would target the thickest and highest porosity and permeability in lower Desert Creek clean carbonate and would extend along the length of the field, following the nearshore, shoreline trend or phylloid-algal mound lithofacies.

CHAPTER I
INTRODUCTION

Thomas C. Chidsey, Jr.,
Utah Geological Survey

Project Overview

Over 450 million barrels (bbls) of oil (72 million m^3) have been produced from the shallow-shelf carbonate reservoirs in the Pennsylvanian (Desmoinesian) Paradox Formation in the Paradox Basin, southeastern Utah and southwestern Colorado (figure 1-1) (Colorado Oil and Gas Conservation Commission, 2006; Utah Division of Oil, Gas and Mining, 2007). The two main producing zones of the Paradox Formation are informally named the Ismay and the Desert Creek (figure 1-2). The Ismay zone is dominantly limestone comprising small, equant buildups of phylloid-algal material; locally variable, inner-shelf, skeletal calcarenites; rare, open-marine, bryozoan mounds; and anhydrite caps. The Ismay produces oil from fields in the southern Blanding sub-basin (figure 1-3). The Desert Creek zone is dominantly dolomite comprising regional, nearshore, shoreline trends with highly aligned, linear lithofacies tracts. The Desert Creek produces oil in fields in the central Blanding sub-basin (figure 1-3). Both the Ismay and Desert Creek buildups generally trend northwest-southeast. Various lithofacies changes and extensive diagenesis have created complex reservoir heterogeneity within these two diverse zones.

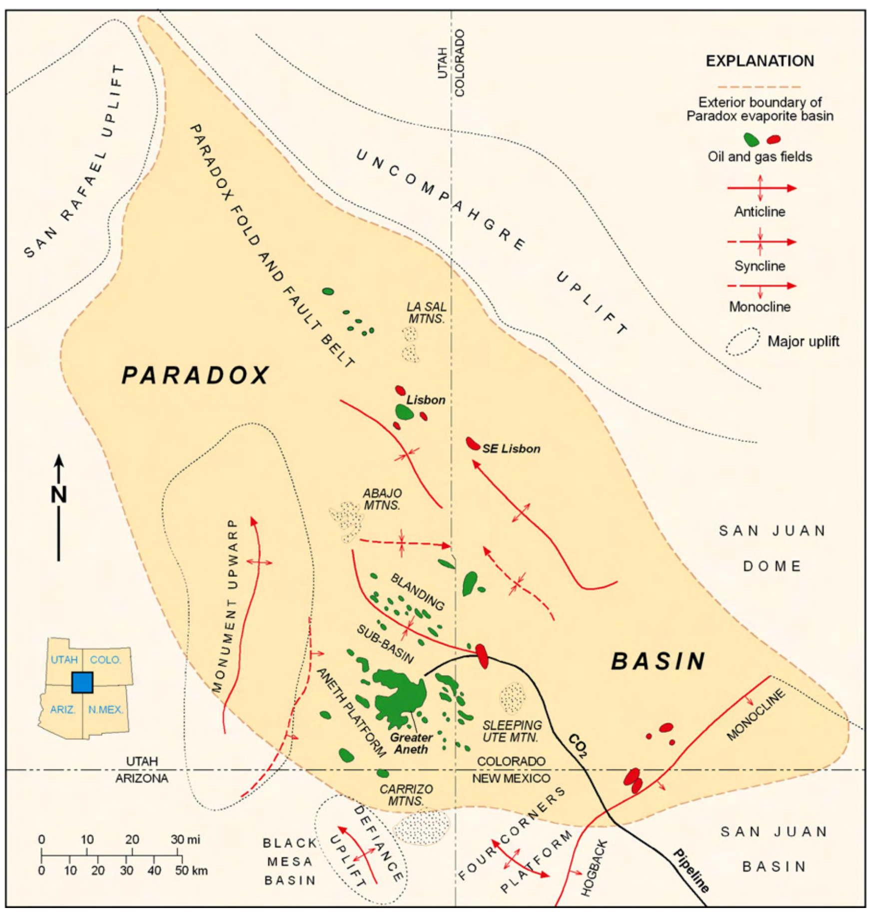

Figure 1-1. Location map of the Paradox Basin, Utah, Colorado, Arizona, and New Mexico showing producing oil and gas fields, the Paradox fold and fault belt, and Blanding sub-basin as well as surrounding Laramide basins and uplifts (modified from Harr, 1996).

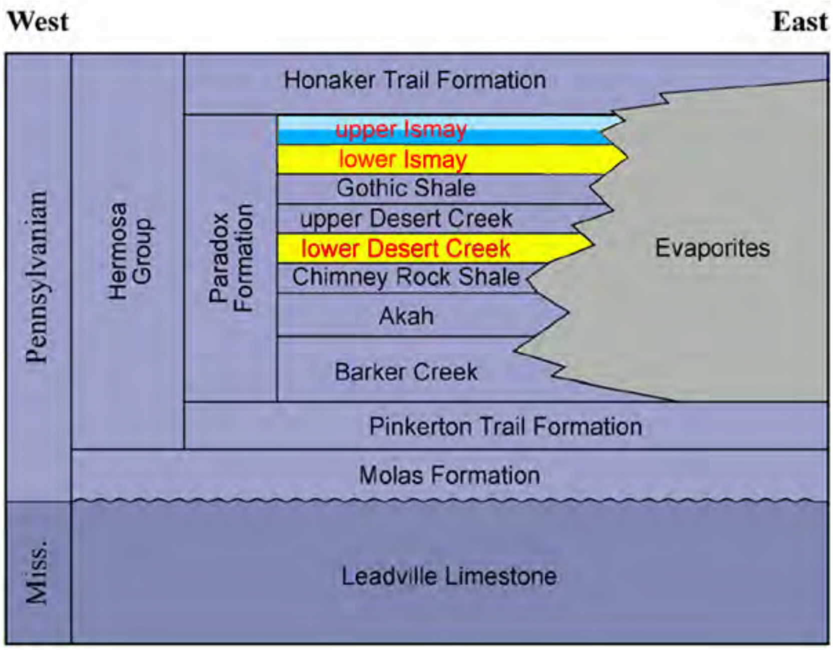

Figure 1-2. Pennsylvanian stratigraphy of the southern Paradox Basin including informal zones of the Paradox Formation; the Ismay and Desert Creek zones productive in the case-study fields described in this report are highlighted. For the regional lithofacies evaluation the upper Ismay zone has been further divided into two units – the "upper part" and the "lower part."

With the exception of the giant Greater Aneth field, the other 100-plus oil fields in the basin typically contain 2 to 10 million bbls (0.3-1.6 million m^3) of original oil in place. Most of these fields are characterized by high initial production rates followed by a very short productive life (primary), and hence premature abandonment. Only 15 to 25 percent of the original oil in place is recoverable during primary production from conventional vertical wells.

An extensive and successful horizontal drilling program has been conducted in the giant Greater Aneth field. However, to date, only two horizontal wells have been drilled in small Ismay and Desert Creek fields. The results from these wells were disappointing due to the previously poor understanding of the carbonate lithofacies and diagenetic fabrics that create reservoir heterogeneity. These small fields, and similar fields in the basin, are at high risk of premature abandonment. At least 200 million bbls (31.8 million m^3) of oil will be left behind in these small fields because current development practices leave compartments of the heterogeneous reservoirs undrained. Through proper geological evaluation of the reservoirs, production may be increased by 20 to 50 percent through the drilling of low-cost, single, or multilateral horizontal legs from existing vertical development wells (figure 1-4). In addition, horizontal drilling from existing wells minimizes surface disturbances and costs for field development, particularly in the environmentally sensitive areas of southeastern Utah and southwestern Colorado.

The Utah Geological Survey (UGS), Colorado Geological Survey (CGS), Eby Petrography & Consulting, Inc., and Seeley Oil Company entered into a cooperative agreement with the U.S. Department of Energy (DOE) as part of its Class II Oil Revisit Program. A three-phase, multidisciplinary approach was planned to increase production and reserves from the shallow-shelf carbonate reservoirs in the Ismay and Desert Creek zones of the Paradox Basin.

<u>Phase 1</u> was a geological and reservoir characterization of selected, diversified, small fields, including Cherokee and Bug fields in San Juan County, Utah, and Little Ute and Sleeping Ute fields in Montezuma County, Colorado (figure 1), to identify those field(s) having the greatest potential as targets for increased well productivity and ultimate recovery in a pilot demonstration project. This phase included: (a) determination of regional geological setting;

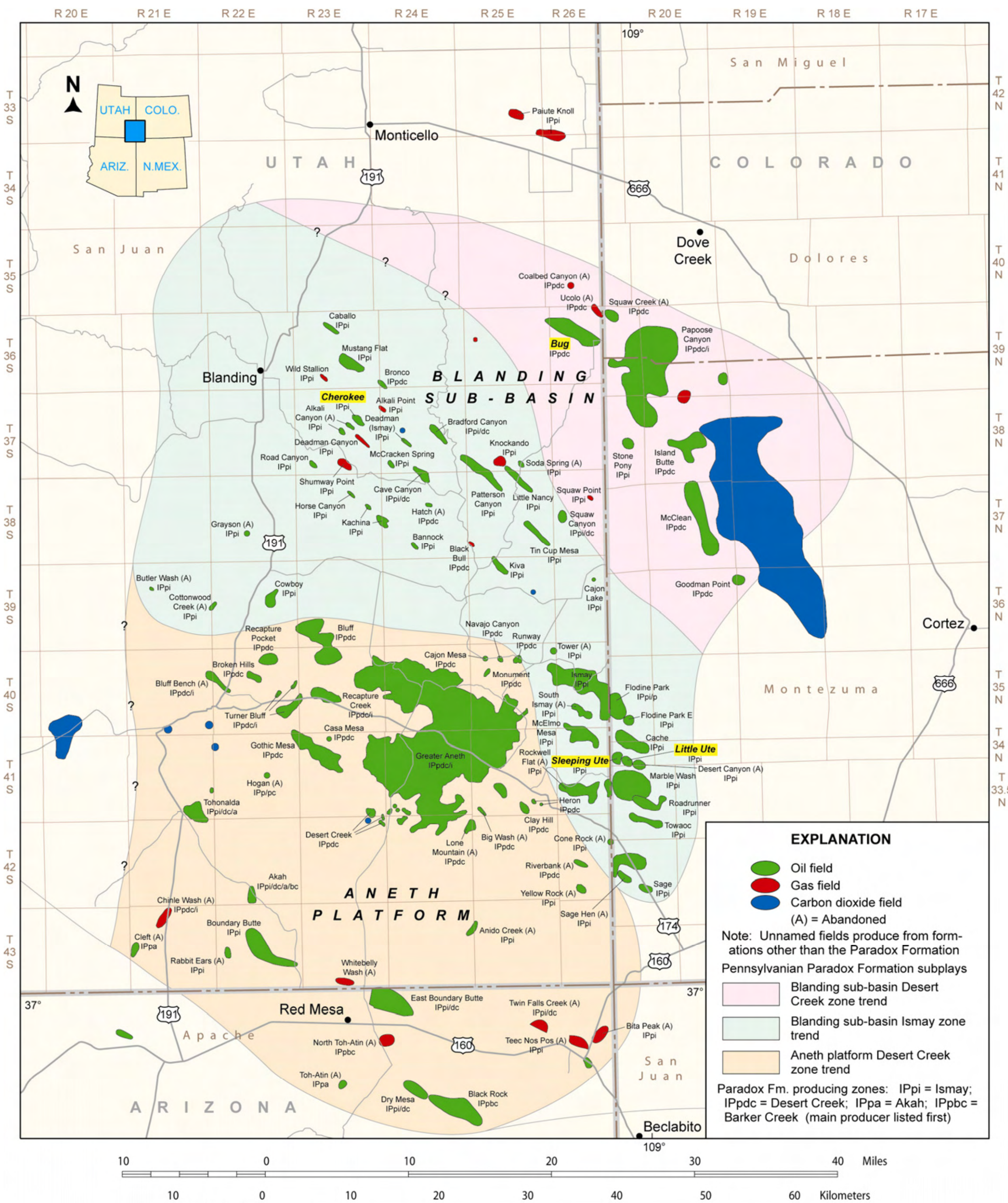

Figure 1-3. Map showing the project study area and fields (case-study fields in black) within the Ismay and Desert Creek producing trends in the Blanding sub-basin, Utah and Colorado. Fields shown in the Aneth platform area of the map, including the giant Greater Aneth field, produce primarily from the Desert Creek zone on the shelf margin of the Paradox Basin. Modified from Wray and others (2002); Chidsey and others (2004).

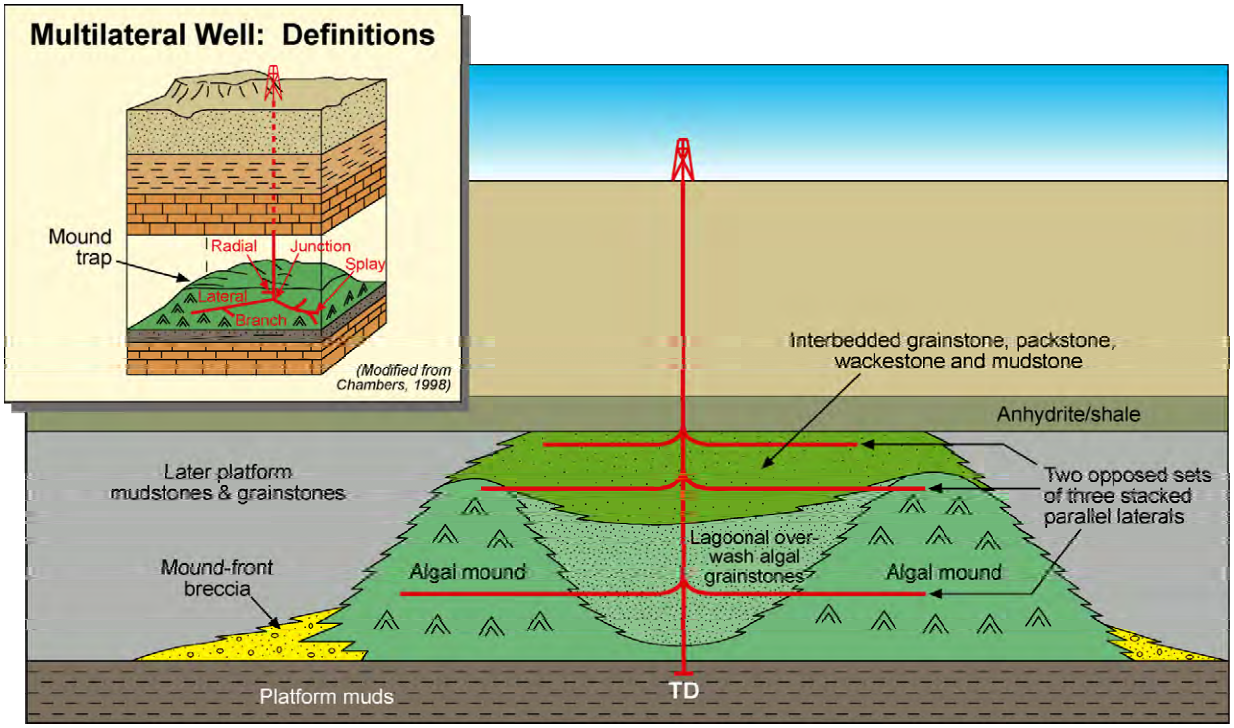

Figure 1-4. Schematic diagram of Ismay zone drilling targets by multilateral (horizontal) legs from an existing field well.

(b) analysis of the reservoir heterogeneity, quality, lateral continuity, and compartmentalization within the fields; (c) construction of lithologic, microfacies, porosity, permeability, and net pay maps of the fields; (d) determination of field reserves and recovery; and (e) integration of geological data to design single or multiple horizontal laterals from existing vertical wells.

Phase 2 was to be a field demonstration project of the horizontal drilling techniques identified as having the greatest potential for increased field productivity and ultimate recovery. The demonstration project was to include drilling one or more horizontal laterals from the existing, vertical, field well(s) to maximize production from the zones of greatest potential.

Phase 3 was to include: (a) reservoir management and production monitoring, (b) economic evaluation of the results, and (c) determination of the ability to transfer project technologies to other similar fields in the Paradox Basin and throughout the U.S.

The UGS selected two fields, Cherokee field, operated by our industry partner Seeley Oil Company, and Bug field, operated by Wexpro Company, for detailed case studies (figure 1-3). These two fields are representative of the two main producing trends in the Paradox Basin of Utah and Colorado – the Ismay and Desert Creek zones of the Pennsylvanian Paradox Formation. Our work showed that horizontal wells drilled from existing vertical wells in each field would likely encounter unproduced oil reserves, and could be done so economically. Both operators elected not to participate in the demonstration project (Budget Period II). They cited limited drilling budgets and commitments elsewhere, particularly Wexpro which is involved in major gas plays in Wyoming, as the primary reasons for their decisions.

The UGS conducted an aggressive promotion program encourage other operators, including the operator of Little Ute and Sleeping Ute fields, to participate in the project demonstration whereby they would receive 35 percent (up to $200,000), for the cost to drill a lateral(s) from an existing vertical well(s) or new horizontal well(s) in the Ismay and Desert Creek zones of Paradox Basin fields in Utah or Colorado (see Appendix). Although the UGS received numerous inquires about the offer from other operators, none followed up with a proposal which required (1) a geologic overview of the field, (2) targeted zone(s), (3) depth, length, and directions of proposed horizontal wellbore(s), (4) drilling rationale, (5) drilling cost summary (AFE), and (6) drilling timetable. Finally, the UGS and DOE elected to terminate the project without the benefit of the field horizontal drilling demonstration.

This report summarizes the research, data, analyses, and results of the project, thus providing the tools for future successful horizontal drilling programs to occur in the small reservoirs found in the Paradox Basin and other shallow-shelf carbonate deposits.

Project Benefits and Potential Application

The overall benefit of this multi-year project are expected to be enhanced domestic petroleum production by demonstrating and transferring an advanced-oil-recovery technology throughout the small oil fields of the Paradox Basin. Specifically, the benefits expected from the project are: (1) increasing recovery and reserve base by identifying untapped compartments created by reservoir heterogeneity; (2) preventing premature abandonment of numerous small fields; (3) increasing deliverability by horizontally drilling along a reservoir's optimal fluid-flow paths; (4) identifying reservoir trends for field extension drilling and stimulating exploration in Paradox Basin fairways; (5) reducing development costs by more closely delineating minimum field size and other parameters necessary for horizontal drilling; (6) allowing for minimal surface disturbance by drilling from existing, vertical, field well pads; (7) allowing limited energy investment dollars to be used more productively; and (8) increasing royalty income to the federal, state, and local governments, the Ute Mountain Ute Indian Tribe, and fee owners. These benefits may also apply to other areas, including algal-mound and carbonate buildup reservoirs on the eastern and northwestern shelves of the Permian Basin in Texas, Silurian pinnacle and patch reefs of the Michigan and Illinois Basins, and shoaling carbonate island trends of the Williston Basin.

The results of this project were transferred to industry and other researchers through Technical Advisory and Stake Holders Boards, an industry outreach program, digital project databases, and a project Web page. Project results were also disseminated via technical a core workshop, displays and technical presentations at national and regional professional meetings, and publications. Refer to the Appendix for a complete listing of these activities.

CHAPTER II
REGIONAL UTAH LITHOFACIES EVALUATION

David E. Eby, Eby Petrography & Consulting, Inc.,
and
Thomas C. Chidsey, Jr., Craig D. Morgan, and Kevin McClure,
Utah Geological Survey

Introduction

Establishment of the basic carbonate lithofacies belts and stratigraphic patterns within shallow-shelf carbonate Ismay and Desert Creek zones of the Paradox Formation in the Blanding sub-basin was critical to the understanding of the fields that were evaluated for the potential demonstration project. Geological characterization of lithofacies on a regional scale focused on reservoir heterogeneity and lateral continuity. This task utilized representative cores and modern geophysical well logs to characterize and initially grade various intervals in the Utah portion of the region for horizontal drilling suitability.

Paradox Basin Overview

The Paradox Basin is located mainly in southeastern Utah and southwestern Colorado with small portions in northeastern Arizona and the northwestern corner of New Mexico (figure 1-1). The Paradox Basin is an elongate, northwest-southeast-trending, evaporitic basin that predominately developed during the Pennsylvanian (Desmoinesian), about 330 to 310 million years ago (Ma). The most obvious structural features in the basin are the spectacular anticlines that extend for miles in the northwesterly trending fold and fault belt. The events that caused these and many other structural features to form began in the Proterozoic, when movement initiated on high-angle basement faults and fractures 1700 to 1600 Ma (Stevenson and Baars, 1986, 1987). During Cambrian through Mississippian time, this region, as well as most of eastern Utah, was the site of typical, thin, marine deposition on the craton while thick deposits accumulated in the miogeocline to the west (Hintze, 1993). However, major changes occurred beginning in the Pennsylvanian when a pattern of basins and fault-bounded uplifts developed from Utah to Oklahoma as a consequence of the collision of South America, Africa, and southeastern North America (Kluth and Coney, 1981; Kluth, 1986), or from a smaller scale collision of a microcontinent with south-central North America (Harry and Mickus, 1998). One result of this tectonic event was the uplift of the Ancestral Rockies in the western United States. The Uncompahgre Highlands (uplift) in eastern Utah and western Colorado initially formed as the westernmost range of the Ancestral Rockies during this ancient mountain-building period.

The Uncompahgre Highlands are bounded along the southwestern flank by a large basement-involved, high-angle, reverse fault identified from geophysical seismic surveys and exploration drilling. As the highlands rose, an accompanying depression, or foreland basin, formed to the southwest — the Paradox Basin. The form of the Paradox Basin was strongly influenced by rejuvenation of pre-existing (late Precambrian), northwesterly trending structures (Baars and Stevenson, 1981). Rapid subsidence, particularly during the Pennsylvanian and then continuing into the Permian, accommodated large volumes of evaporitic and marine sediments that intertongue with non-marine arkosic material shed from the highland area to the northeast (figures 2-1 and 2-2) (Hintze, 1993). Deposition in the basin produced a thick cyclical sequence of carbonates, evaporites, and organic-rich shale (Peterson and Hite, 1969; Hite and others, 1984). The Paradox Basin is defined by the maximum extent of anhydrite beds in the Paradox Formation.

The present Paradox Basin includes or is surrounded by other uplifts that formed during the Late Cretaceous-early Tertiary Laramide orogeny such as the Monument upwarp in the west-southwest, and the Uncompahgre uplift, corresponding to earlier Uncompahgre Highlands, forming the northeast boundary (figure 1-1). Oligocene-age laccolithic intrusions form the La Sal and Abajo Mountains in the north and central parts of the basin in Utah while the Carrizo Mountains in Arizona, and the Ute, La Plata, and San Miguel Mountains in Colorado are aligned along the southeastern boundary of the basin (figure 1-1).

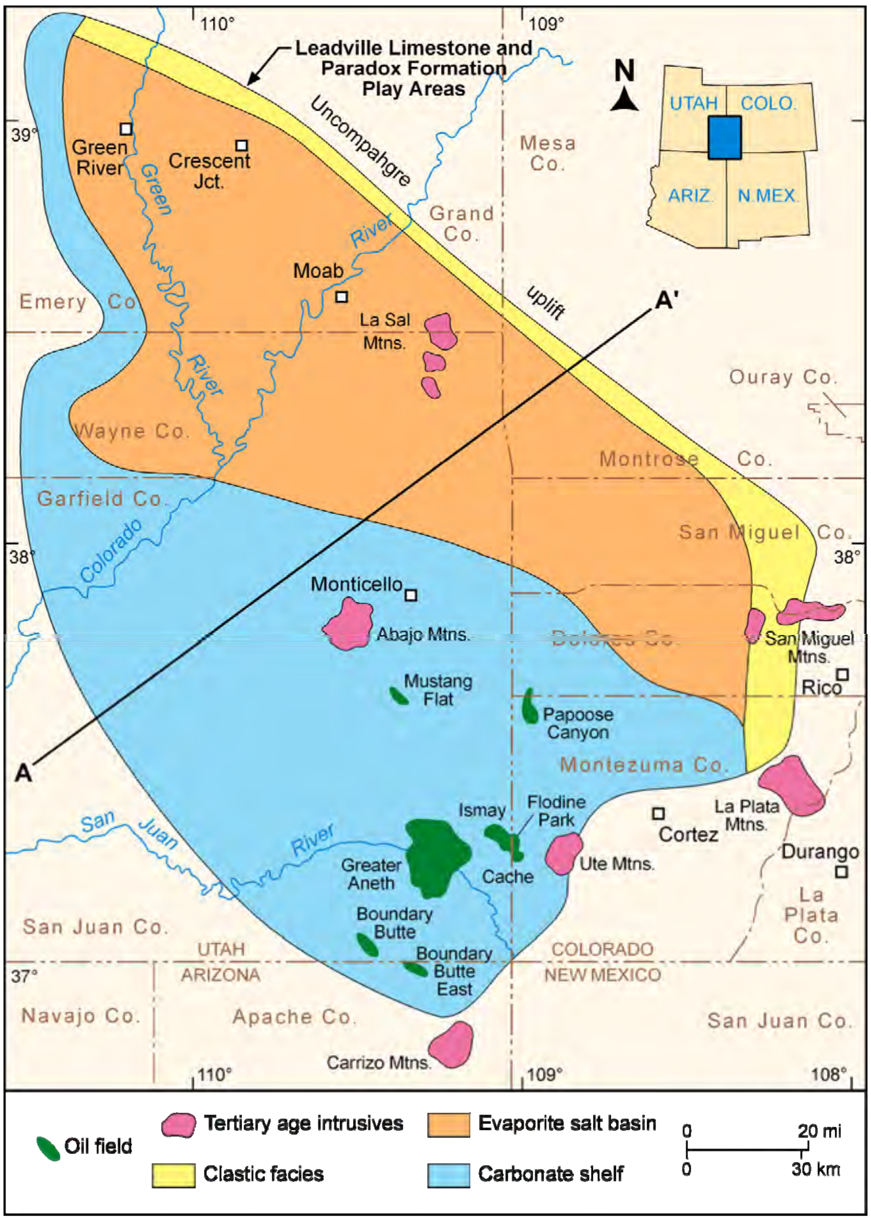

Figure 2-1. Generalized map of Paradox Formation lithofacies with clastic wedge, evaporite salt basin, and carbonate shelf (modified from Wilson, 1975). Cross section A-A' shown on figure 2-2.

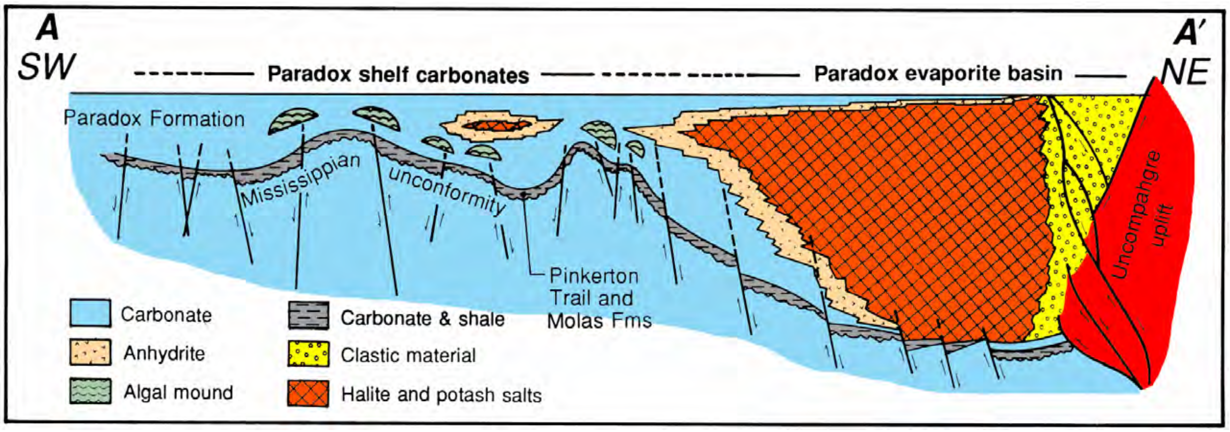

Figure 2-2. Generalized cross section across the Paradox Basin with gross lithofacies relations between Middle Pennsylvanian shelf carbonates, restricted basin evaporites, and coarse clastics proximal to the Uncompahgre uplift (modified from Baars and Stevenson, 1981). Maximum extent of anhydrite beds in the Paradox Formation that define the basin is not shown. Location of cross section shown on figure 2-1.

The Paradox Basin can generally be divided into three areas: the Paradox fold and fault belt in the north, the Blanding sub-basin in the south-southwest, and the Aneth platform in the southernmost part in Utah (figure 1-1). The Paradox fold and fault belt was created during the Tertiary and Quaternary by a combination of (1) reactivation of basement normal faults, (2) salt flowage, dissolution, and collapse, and (3) regional uplift (Doelling, 2000). The relatively undeformed Blanding sub-basin and Aneth platform developed on a shallow-marine shelf. Each area contains oil and gas fields with structural, stratigraphic, or combination traps formed on discrete, often seismically defined, closures. Most Paradox Formation oil production comes from stratigraphic traps in the Blanding sub-basin and Aneth platform that locally contain algal-mound and other carbonate lithofacies buildups. The source of the oil is several black, organic-rich shales within the Paradox Formation (Hite and others, 1984; Nuccio and Condon, 1996).

Lithofacies Mapping Database and Log-Based Correlation Scheme

A grid of regional geophysical well-log cross sections (figures 2-3 through 2-5), thickness relationships of important stratigraphic intervals (figure 1-2), and lithofacies types were combined with examination of cores throughout the Blanding sub-basin to provide a significant database for identifying potential targets for horizontal drilling within the small, heterogeneous, phylloid-algal buildups and associated lithofacies in the upper Ismay and lower Desert Creek zones. The study area covers about 750 square miles (1900 km^2) within the Blanding sub-basin of the Paradox Basin. The total number of wells drilled to the Paradox Formation within the study area is about 480 wells. We interpreted all available cores in the area (figure 2-6) – 41 wells in the upper part of the upper Ismay, 40 wells in the lower part of the upper Ismay, and 44 wells in the lower Desert Creek. Additionally, 82 geophysical well logs were interpreted from the upper Ismay and 38 from the Desert Creek. We also incorporated the work of Roylance (1984), Cannizzaro (1985), and Skinner (1996).

Isochore and structure maps, cross sections, and regional lithofacies maps (**Deliverable 1.1.1 – Regional Paradox Formation Structure and Isochore Maps, Blanding Sub-Basin,**

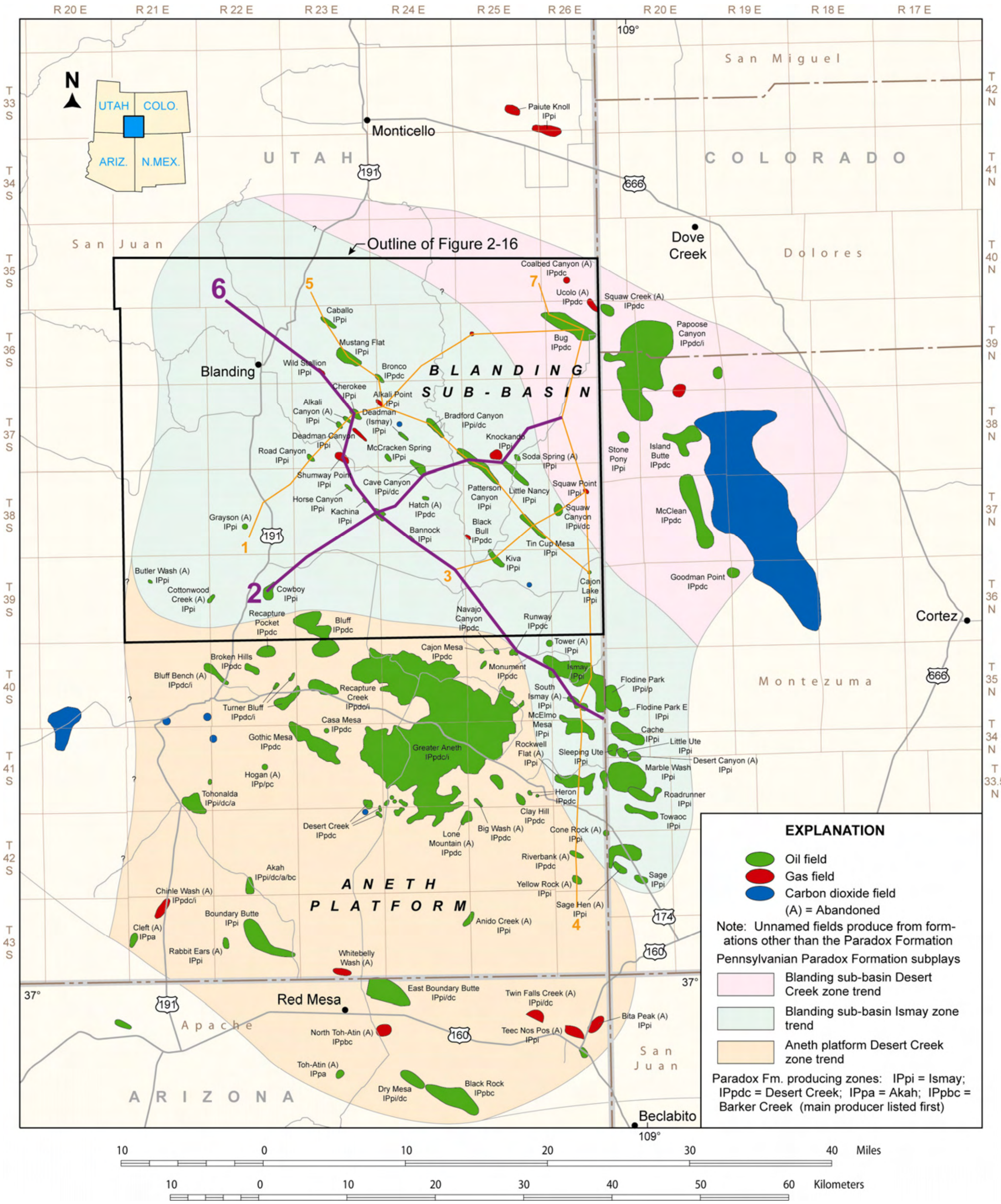

Figure 2-3. Map showing the project study area and fields within the Ismay and Desert Creek producing trends in the Blanding sub-basin, Utah and Colorado (numbered lines designate cross section locations generated in this study [cross sections 2 and 6 are shown on figures 2-4 and 2-5]).

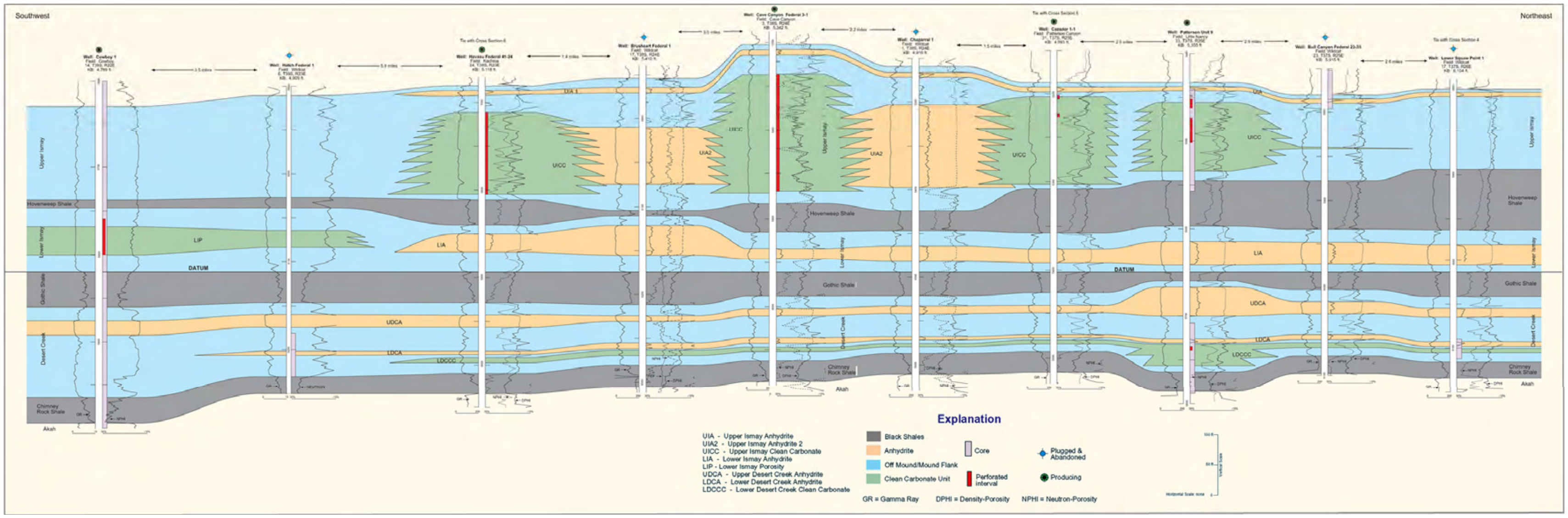

Figure 2-4. Southwest-northeast cross section number 2 through the Utah portion of the Blanding sub-basin showing regional Ismay and Desert Creek correlations.

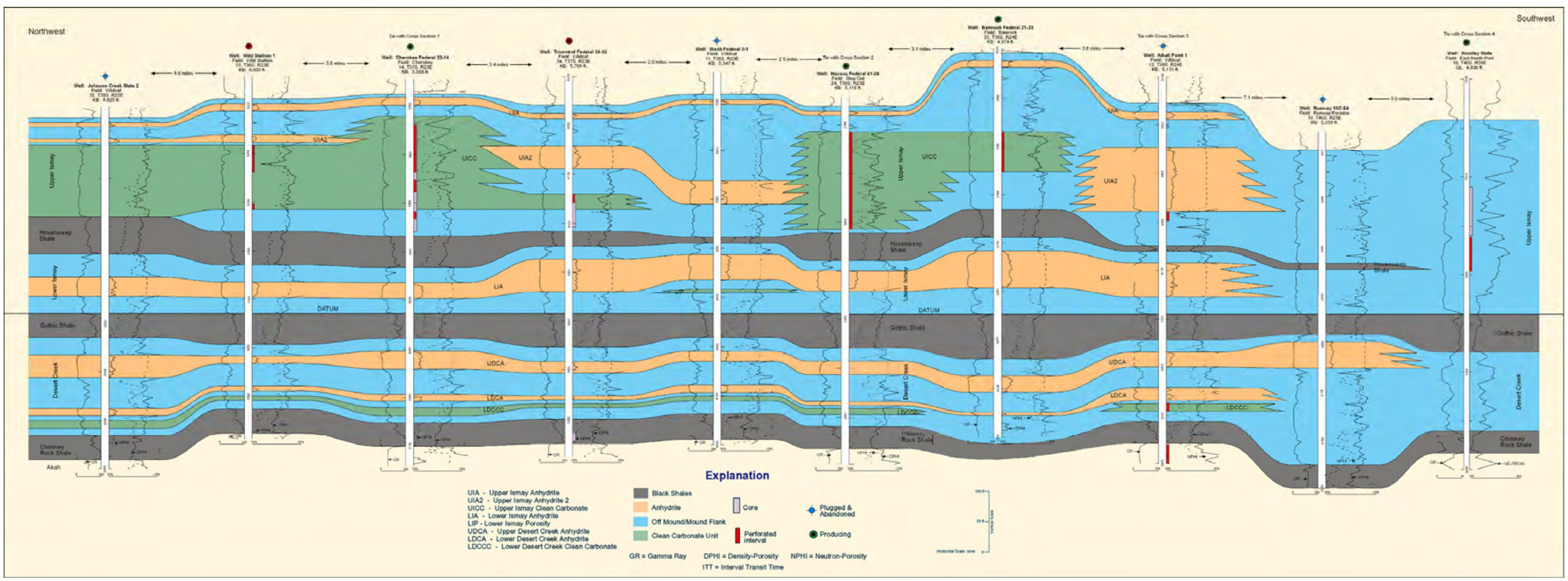

Figure 2-5. Northwest-southeast cross section number 6 through the Utah portion of the Blanding sub-basin showing regional Ismay and Desert Creek correlations.

Utah; Deliverable 1.1.2 –Regional Paradox Formation Cross Sections, Blanding Sub-Basin, Utah and Colorado; and Deliverable 1.1.3 – Regional Paradox Formation Facies Maps, Blanding Sub-Basin, San Juan County, Utah**) were constructed using a correlation scheme developed for the project. This correlation scheme tied the core-derived, typical, vertical sequence or cycle of depositional lithofacies from the Cherokee and Bug case-study fields (described later) to the corresponding gamma-ray and neutron-density curves from geophysical well logs. The correlation scheme identified the major zone contacts, seals or barriers, baffles, producing or potential reservoirs, and depositional lithofacies (figures 2-7 through 2-9, and table 2-1).

Depositionally, rock units are divided into seals or barriers (anhydrites and shales), mound (carbonate buildup [bafflestones, bindstones, grainstones, and packstones]), and off mound (mudstones and wackestones). Porosity units, and reservoir or potential reservoir layers, are identified within the mound and off-mound intervals. The mound, and some of the off-mound units, are part of the "clean carbonate" packages (figures 2-4 and 2-5) - intervals containing all of the productive reservoir lithofacies, and where carbonate mudstone and shale are generally absent. The clean carbonate packages abruptly change laterally into thick anhydrite packages, particularly in the upper Ismay zone.

The top and base of all these intervals (seals, mound, clean carbonate, as well as porosity units) were determined and coded as listed in table 2-1. The unlisted intervening units represent the baffles or non-reservoir rocks, such as non-porous packstone or wackestone (figures 2-4 and 2-4, 2-7 through 2-9). The mound/mound cap intervals usually have porosity greater than 6 percent, while the clean carbonate intervals are defined by lithology only (such as bafflestone or grainstone), although there may be occasional isolated porosity zones. The top and base of the

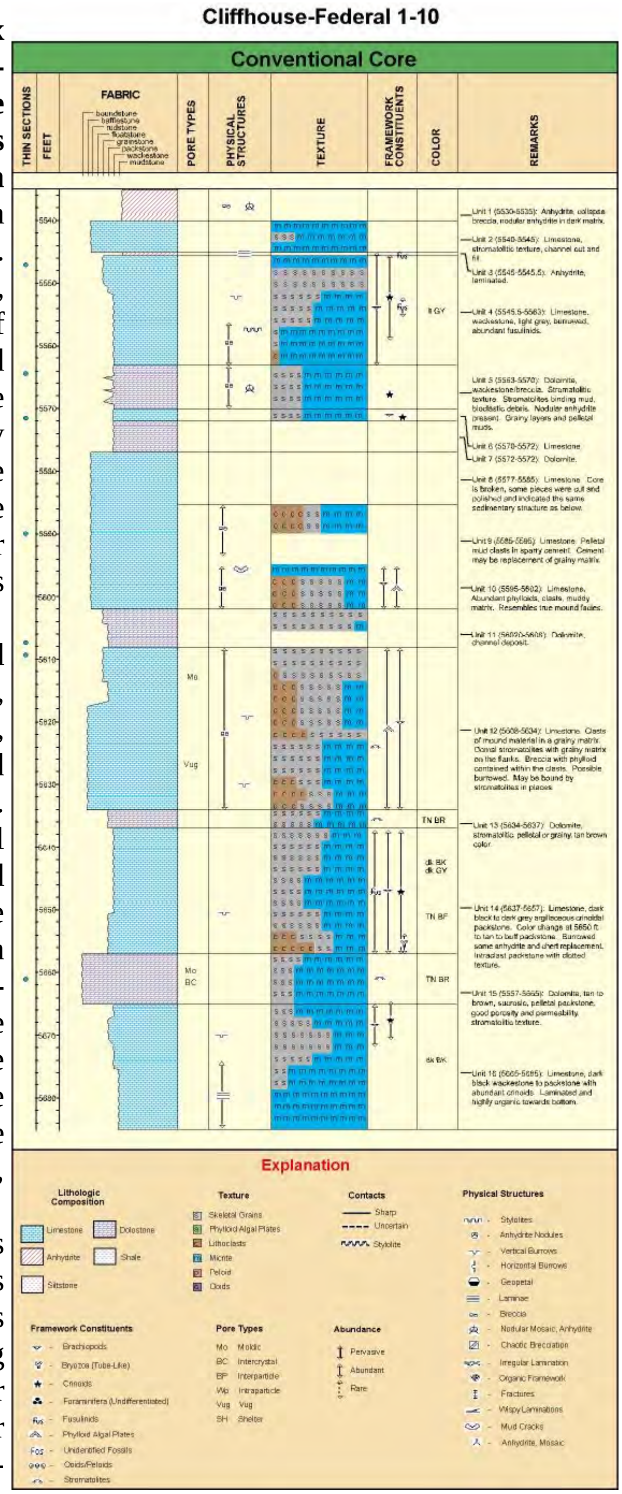

Figure 2-6. Typical core description of the Ismay zone, Cliffhouse-Federal 1-10 exploratory well, section 11, T. 38 S., R. 25 E., Salt Lake Base Line and Meridian, San Juan County, Utah.

mound/mound cap intervals are often equivalent to the clean top and base of the clean carbonate intervals. In addition, the top and base of the mound/mound cap intervals may be equivalent to the top and base of the thinner off-mound clean carbonate intervals.

Ismay Isochore Relationships

Upper Ismay "Clean Carbonate" Isochore Map

The isochore map of the upper Ismay clean-carbonate interval is shown on figure 2-10. Note that the "thicks" of upper Ismay clean carbonate (the darker green hues on this map) are often connected and nearly surround "thins" (in very pale shades). The thicks are probably the combined effect of upper Ismay platform (middle to inner shelf/tidal flat) deposition and organic (phylloid-algal and bryozoan) buildups. The thins surrounded by thicks are "intra-shelf basins" within the upper Ismay interval. These intra-shelf basins are filled with thick anhydrite deposits (see figure 2-11, "anhydrite 2" isochore map). The remaining thins that are not surrounded by, or in close proximity to, thicks are largely open-marine (deep, outer shelf) deposits.

Upper Ismay "Anhydrite 2" Isochore Map

The isochore map of the upper Ismay "anhydrite 2" is shown on figure 2-11. Note that the areas of thickest anhydrite (in darker shades of orange) roughly correlate with some of the thins on the upper Ismay clean carbonate isochore map (figure 2-10). The anhydrite 2 thicks were deposited within semi-isolated, intra-shelf basins.

Isochore "Dilemma"

The isochore relationships shown on figures 2-10 and 2-11 are too coarse or complex to accurately define prospective

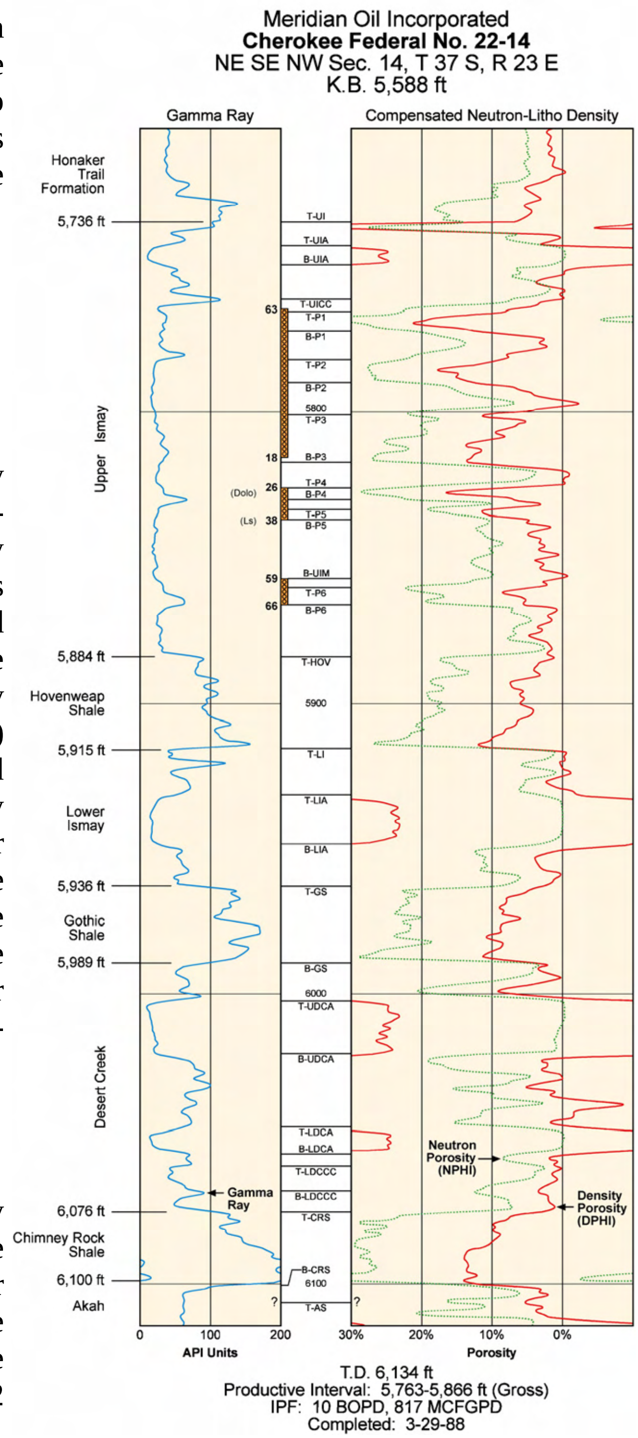

Figure 2-7. Type log for the Cherokee field (gamma-ray, compensated neutron-litho density) from the Cherokee Federal No. 22-14 well, showing the Ismay and Desert Creek correlation scheme, major units, and productive intervals (refer to table 2-1 for explanation of unit abbreviations).

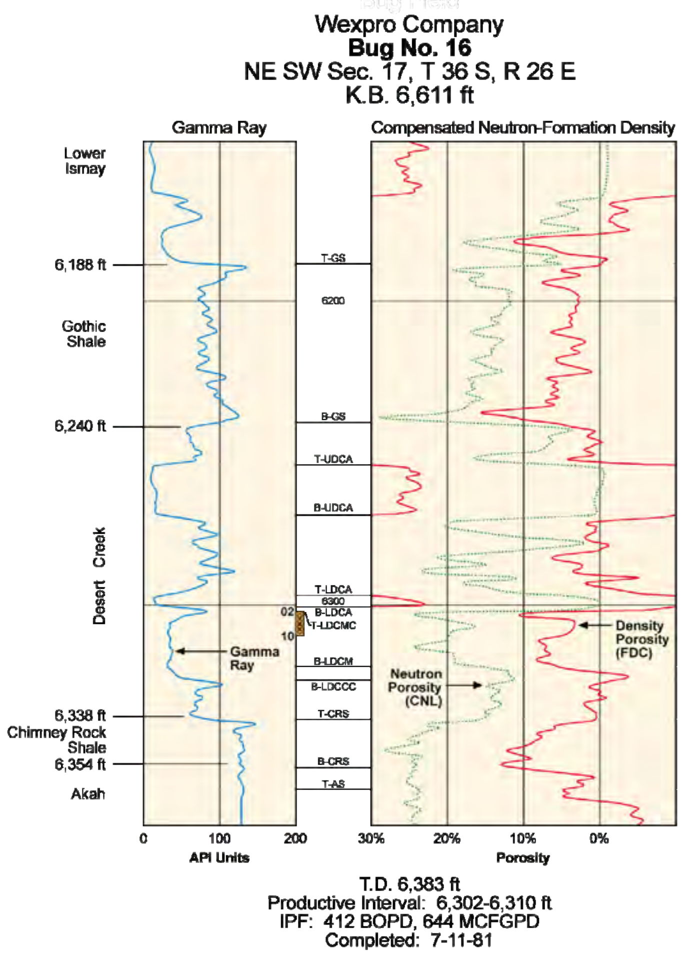

Figure 2-8. Type log for the Bug field mound (gamma-ray, compensated neutron-formation density) from the Bug No. 16 well, showing the Desert Creek correlation scheme, major units, and productive interval (refer to table 2-1 for explanation of unit abbreviations).

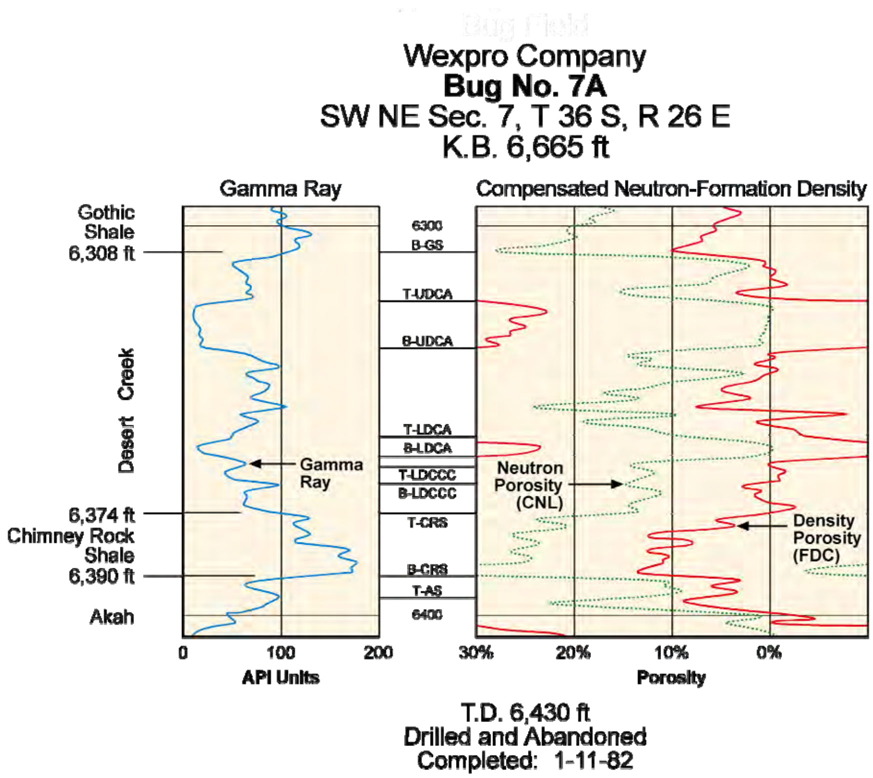

Figure 2-9. Type log for the Bug field off-mound area (gamma-ray, compensated neutron-formation density) from the Bug No. 7A well, showing the Desert Creek correlation scheme and major units (refer to table 2-1 for explanation of unit abbreviations).

Table 2-1. Correlation scheme used for Ismay and Desert Creek zones of the Paradox Formation in Cherokee and Bug fields, Blanding sub-basin, Utah.

Unit Code	**Description**
T-UI	Top - Upper Ismay Zone
T-UIA	Top - Upper Ismay Anhydrite
B-UIA	Base - Upper Ismay Anhydrite
T-UIA2	Top - Upper Ismay Anhydrite 2
B-UIA2	Base - Upper Ismay Anhydrite 2
T-UICC	Top - Upper Ismay Clean Carbonate
T-P1	Top - Porosity Unit #1
B-P1	Base - Porosity Unit #1
T-P2	Top - Porosity Unit #2
B-P2	Base - Porosity Unit #2
T-P3	Top - Porosity Unit #3
B-P3	Base - Porosity Unit #3
T-P4	Top - Porosity Unit #4
B-P4	Base - Porosity Unit #4
T-P5	Top - Porosity Unit #5
B-P5	Base - Porosity Unit #5
B-UIM	Base - Upper Ismay Mound
B-UICC	Base Upper Ismay Clean Carbonate
T-P6	Top - Porosity Unit #6
B-P6	Base - Porosity Unit #6
T-HOV	Top - Hovenweep Shale
T-LI	Top - Lower Ismay Zone
T-LIA	Top - Lower Ismay Anhydrite
B-LIA	Base - Lower Ismay Anhydrite
T-GS	Top - Gothic Shale
B-GS	Base - Gothic Shale
T-UDCA	Top - Upper Desert Creek Anhydrite
B-UDCA	Base - Upper Desert Creek Anhydrite
T-LDCA	Top - Lower Desert Creek Anhydrite
B-LDCA	Base - Lower Desert Creek Anhydrite
T-LDCMC	Top - Lower Desert Creek Mound Cap
B-LDCM	Base - Lower Desert Creek Mound

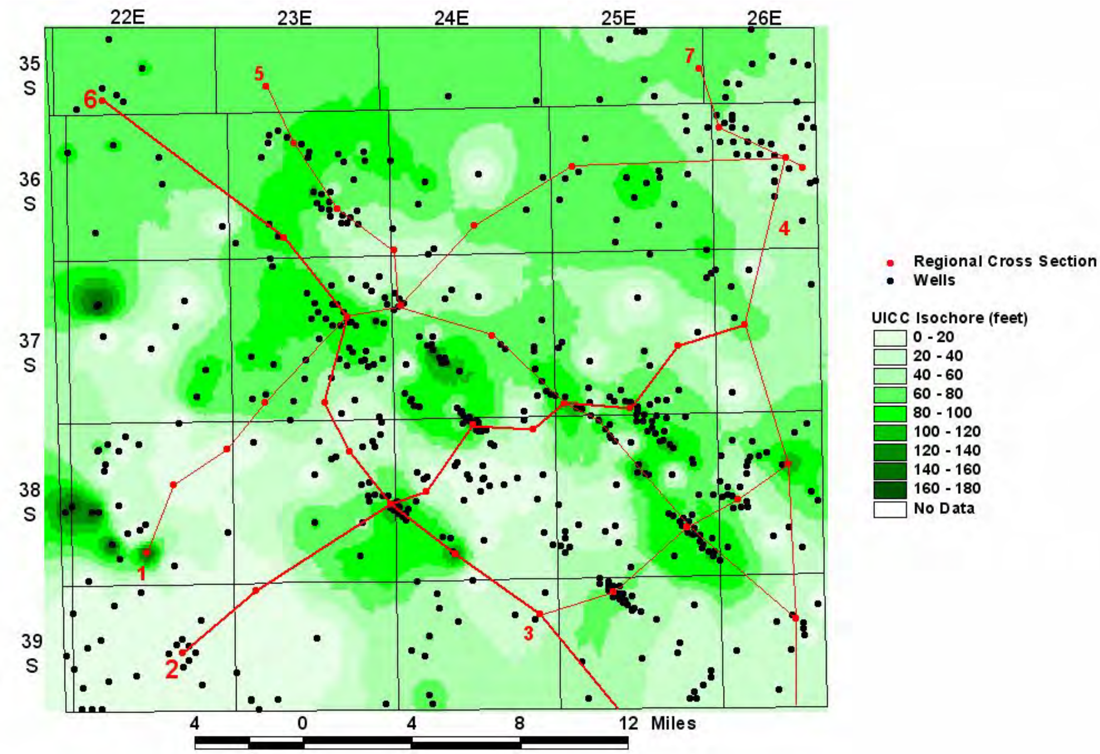

Figure 2-10. Isochore map of the upper Ismay clean carbonate (UICC) interval. The log picks and correlations of clean carbonate are shown in the regional cross sections (figures 2-4 and 2-5).

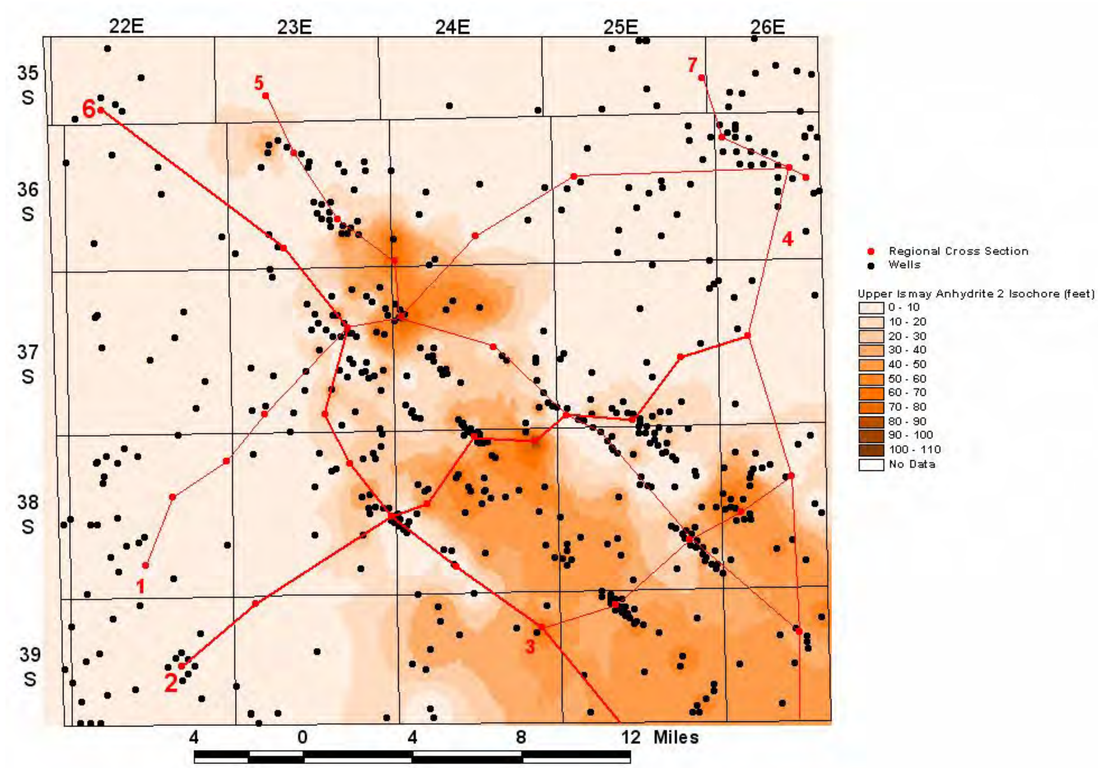

Figure 2-11. Isochore map of the upper Ismay "anhydrite 2." The log picks and correlations of anhydrite 2 are shown in the regional cross sections (figures 2-4 and 2-5).

lithofacies tracts and intra-shelf basin boundaries. Detailed examination of cores tied to geophysical well logs showed that the upper Ismay can be divided into two depositional sequences across the study area. We have termed these packages the “upper part” and “lower part” of the upper Ismay. The top of the lower part is frequently truncated by an erosional surface.

Regional Lithofacies Trends in the Upper Ismay and Lower Desert Creek Zones of the Utah Portion of the Blanding Sub-Basin

Background

In Pennsylvanian time, the Paradox Basin was rapidly subsiding along its northeast margin, but with a shallow-water carbonate shelf on the south and southwest margins of the basin that locally contained algal-mound buildups. These carbonate buildups, and the material shed from their flanks, formed petroleum traps where reservoir-quality porosity and permeability have developed.

During the Pennsylvanian, the Paradox Basin was in subtropical, dry climatic conditions along the trade-wind belt, 10° to 20° north of the paleo-equator. Prevailing winds were from present-day north (Peterson and Hite, 1969; Heckel, 1977; Parrish, 1982). Open-marine waters flowed across the shallow cratonic shelf into the basin during transgressive periods. There are four postulated normal marine access ways into the Paradox Basin. The Cabezon access way, which was located to the southeast, is generally accepted as the most likely normal marine-water conduit to maintain circulation on the shallow shelf (Fetzner, 1960; Ohlen and McIntyre, 1965; Hite, 1970). Periodic decreased circulation in the basin resulted in deposition of thick salts (halite with occasionally thinner beds of potash and magnesium salts) and anhydrite. The deeper interior of the basin to the north and northeast is composed almost entirely of salt deposits and is referred to as the evaporite salt basin (figure 2-12).

Cyclicity in Paradox Basin deposition was primarily controlled by glacio-eustatic fluctuations. The shape of the sea-level curve reflects rapid marine transgressions (rapid melting of ice caps) and slow, interrupted regression (slow ice cap buildup) (Imbrie and Imbrie, 1980; Denton and Hughes, 1983; Heckel, 1986). Irregular patterns within the transgressive-regressive cycles are thought to be a response to interference of orbital parameters (Imbrie and Imbrie, 1980). These cycles were also influenced by (1) regional tectonic activity and basin subsidence (Baars, 1966; Baars and Stevenson, 1982), (2) proximity to basin margin and evaporites (Hite, 1960; Hite and Buckner, 1981), (3) climatic variation and episodic blockage of open marine-water conduits, and (4) fluctuations in water depth and water energy (Peterson and Ohlen, 1963; Peterson, 1966; Hite and Buckner, 1981; Heckel, 1983).

Depositional Environments

Depositional environments of the Ismay and Desert Creek zones were determined based on the core descriptions. These environments are shown schematically on figure 2-13. Reservoirs within the Utah portion of the upper Ismay zone of the Paradox Formation are dominantly limestones composed of small, phylloid-algal buildups; locally variable, inner-shelf, skeletal calcarenites; and rarely, open-marine, bryozoan mounds (figure 2-13A). The Desert Creek zone is dominantly dolomite, comprising regional, nearshore, shoreline trends with highly aligned, linear lithofacies tracts (figure 2-13B).

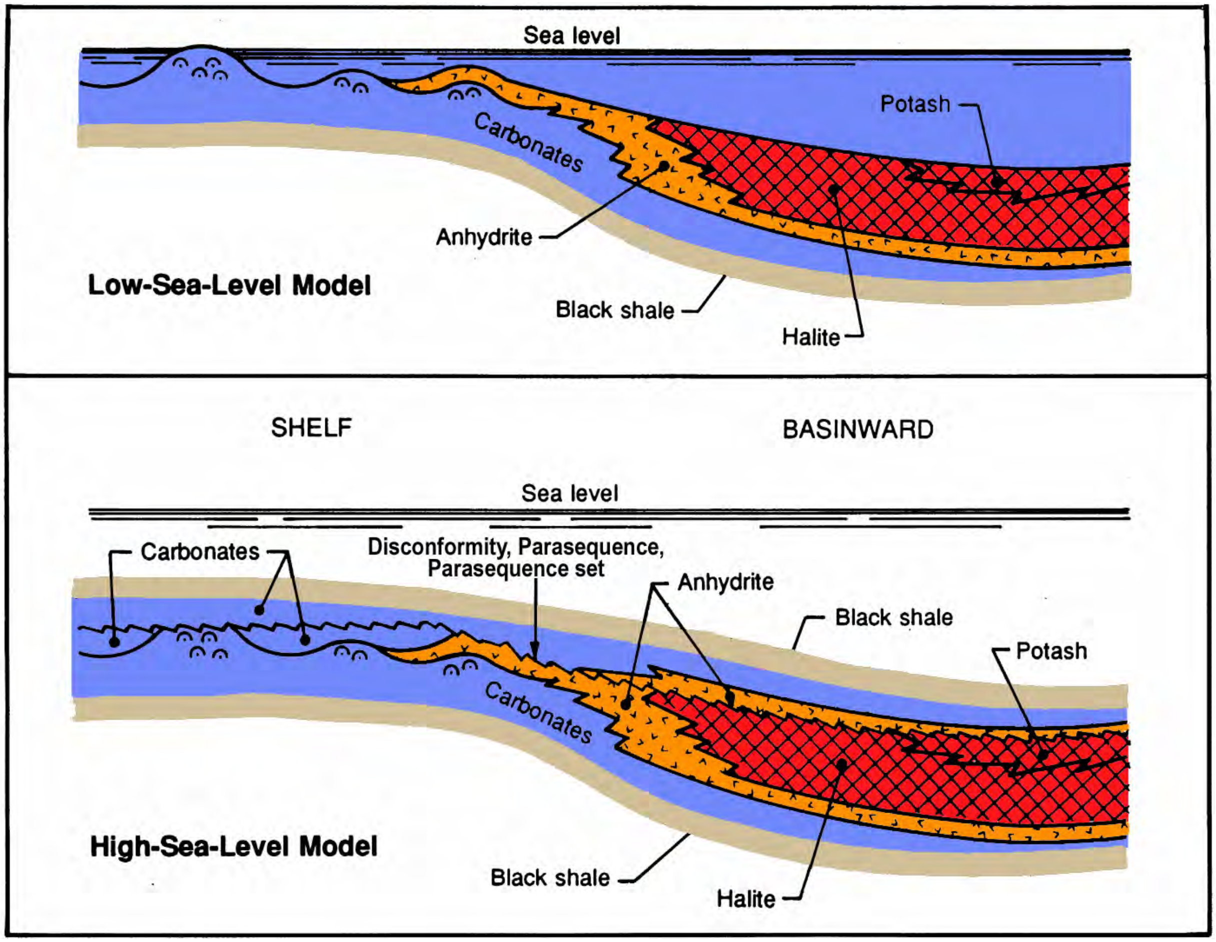

Figure 2-12. Diagram of the depositional sequence during Paradox time and the relationships of various basin and shelf lithofacies. Wavy line represents disconformity, parasequence, or parasequence set. Symbol in the shelf carbonate represents algal-mound development. Modified from Hite and Cater (1972).

The controls on the development of each depositional environment were water depth, salinity, prevailing wave energy, and paleostructural position. In the Ismay zone, the following depositional environments are recognized: open-marine shelf, organic (carbonate) buildups and calcarenites at the platform edge; middle shelf or open platform interior; quartz sand dune; and restricted inner shelf or platform interior. In the Desert Creek zone, the following depositional environments are recognized: basinal, calcarenites (carbonate islands) at the platform edge; middle shelf or open platform interior; restricted inner shelf or platform interior; platform interior salinas (evaporites); and shoreline and terrestrial.

The basinal environment represents deep water (90 to 120 feet [30-40 m]) and euxinic conditions. Deposition included (1) black to dark gray, non-calcareous, non-fossiliferous mud and silty mud, (2) spiculitic lime mud, (3) pelagic lime mud with microfossils and occasional thin-shelled bivalves such as *Halobia*, and (4) thick, deep-water siliciclastic sands. The open-marine deposition was below wave base under normal-marine salinities and low-energy conditions. Deposition consisted of argillaceous and limey mud containing crinoids, brachiopods, and byrozoans.

The middle shelf or open platform interior represents a well-circulated, low- to

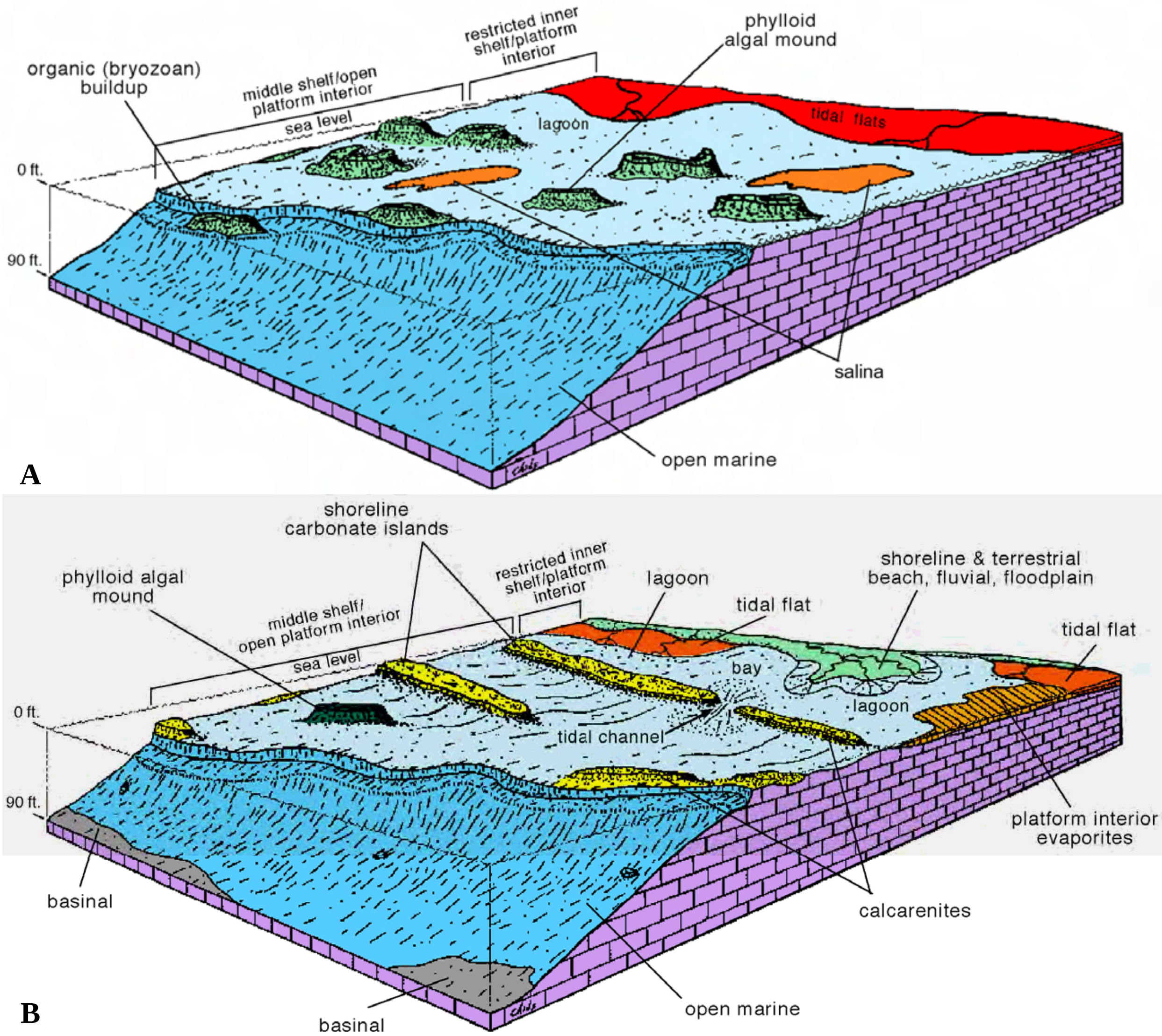

Figure 2-13. Block diagrams displaying major depositional environments, as determined from core, for the Ismay (A) and Desert Creek (B) zones, Pennsylvanian Paradox Formation, Utah and Colorado (Blanding sub-basin shown in figure 1-3).

moderate-energy, normal salinity, shallow-water (between 0 and 90 feet [0-30 m]) environment. Lithofacies from this environment form the dominant producing reservoirs in the Ismay and Desert Creek zones that trend across the Blanding sub-basin. Benthic forams, bivalve molluscs, and codiacean green algae (*Ivanovia* and *Kansasphyllum*) are common. Bryozoan mounds developed in the relatively quiet, deeper water of the middle shelf. Echinoderms are rare and open-marine cephalopods are generally absent. The principal buildup process, phylloid-algal growth, occurred during sea-level highstands. Paleotopography from Mississippian-aged normal faulting (reactivation of Precambrian faults) produced the best marine conditions for initial algal growth. Isolated dunes, composed of quartz sand, in the middle shelf of the Ismay zone represent possible subaeriel exposure and eolian conditions, although the source of the sand is uncertain.

Calcarenites are recognized in both zones and represent moderate- to high-energy, regularly agitated, marine environments where shoals and/or islands developed. Sediment deposition and modification probably occurred from 5 feet (1.5 m) above sea level to 45 feet (14 m) below sea level. These platform-edge deposits include (1) oolitic and coated grain sands, (2) crinoid, foram, algal, and fusilinid sands, (3) small, benthic foram and hard peloid sands representing stabilized peloid grain flats, and (4) shoreline carbonate islands of shell hash.

The restricted inner shelf or platform interior represents shallow water (0 to 45 feet [0-14 m]), and generally low-energy and poor circulation conditions. Fauna are limited mainly to stromatolitic algae, gastropods, certain benthic forams, and ostracods. Deposits included (1) bioclastic lagoonal to bay lime mud, (2) tidal-flat muds often with early dolomite, and (3) shoreline carbonate islands with birdseye fenestrae, stromatolites, cryptoalgal laminations, and dolomitic crusts. Platform-interior evaporites, usually anhydrite, were deposited in salinity-restricted areas.

Shoreline and terrestrial siliciclastic deposits represent beach, fluvial, and flood-plain environments. These siliciclastic deposits include argillaceous to dolomitic silt with rip-up clasts, scour surfaces, or mudcracks.

Regional Lithofacies Maps

Within these depositional environments, seven major upper Ismay and lower Desert Creek lithofacies are recognized and mapped across the Blanding sub-basin study area (figures 2-14 through 2-16). Regional subsurface mapping shows considerable spatial heterogeneity of the reservoir and non-reservoir rock types. The lower Desert Creek zone in the Blanding sub-basin contains several of the same lithofacies as the upper Ismay zone, the most notable exception being the intra-shelf evaporite basins which are discussed later. Mapping of these lithofacies delineates prospective reservoir trends containing porous and productive buildups. Upper Ismay lithofacies (both the upper and lower parts as defined above) include open marine, middle shelf, inner shelf/tidal flat, bryozoan mounds, phylloid-algal mounds, quartz sand dunes, and anhydritic salinas. Lower Desert Creek lithofacies include open marine, middle shelf, proto-mounds/collapse breccia, and phylloid-algal mounds.

Open-marine lithofacies dominate the lower Desert Creek zone in the Blanding sub-basin where there is very little hydrocarbon potential (figure 2-16). However, this lithofacies developed in different areas for both the upper part (northeastern and southern regions [figure 2-14]) and lower part (western to north-central regions [figure 2-15]) of the upper Ismay zone. Middle-shelf lithofacies cover extensive areas of the upper Ismay zone and surround important intra-shelf basins described later. Bryozoan mounds, quartz sand dunes, proto-mounds and some phylloid-algal mounds, and inner shelf/tidal flats developed on the low-energy carbonates of the middle-shelf environment (figures 2-14 through 2-16). To date, bryozoan mounds are only recognized in the lower part of the upper Ismay, at and near Mustang Flat field (figures 1-3 and 2-15). Quartz sand dune lithofacies in the upper Ismay zone are also present near Mustang Flat field and a few other isolated locations in the lower part of the upper Ismay zone (figure 2-15). This lithofacies may also be present in the lower Ismay outcrop along the Honaker Trail in the San Juan River canyon near Goosenecks State Park, southern San Juan County, Utah (Pray and Wray, 1963).

Inner shelf/tidal flat lithofacies represent relatively small areas in geographical extent, especially in the upper part of the upper Ismay zone. However, recognizing this lithofacies is

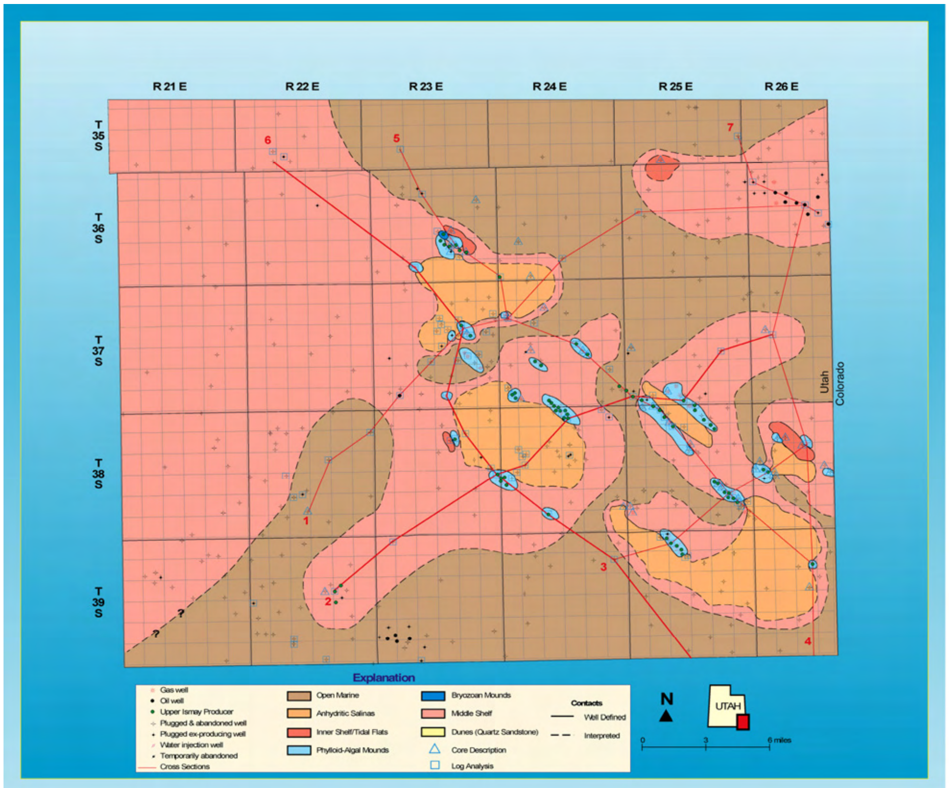

Figure 2-14. Regional lithofacies map of the upper part of the upper Ismay zone, Paradox Formation, in the Blanding sub-basin, Utah.

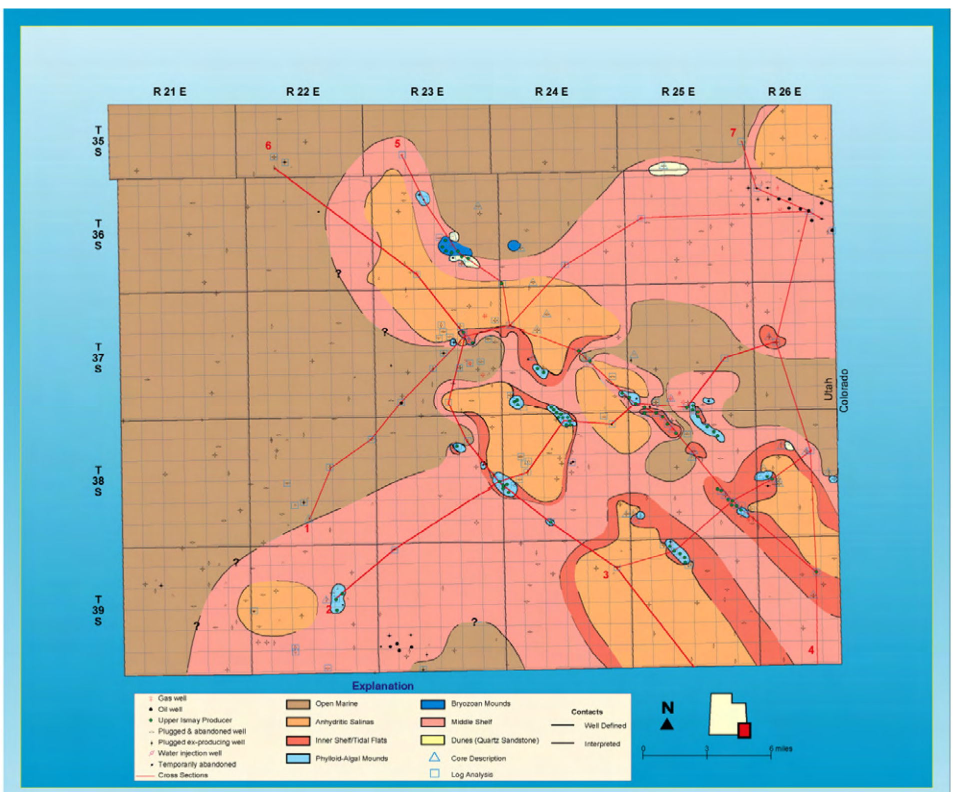

Figure 2-15. Regional lithofacies map of the lower part of the upper Ismay zone, Paradox Formation, in the Blanding sub-basin, Utah.

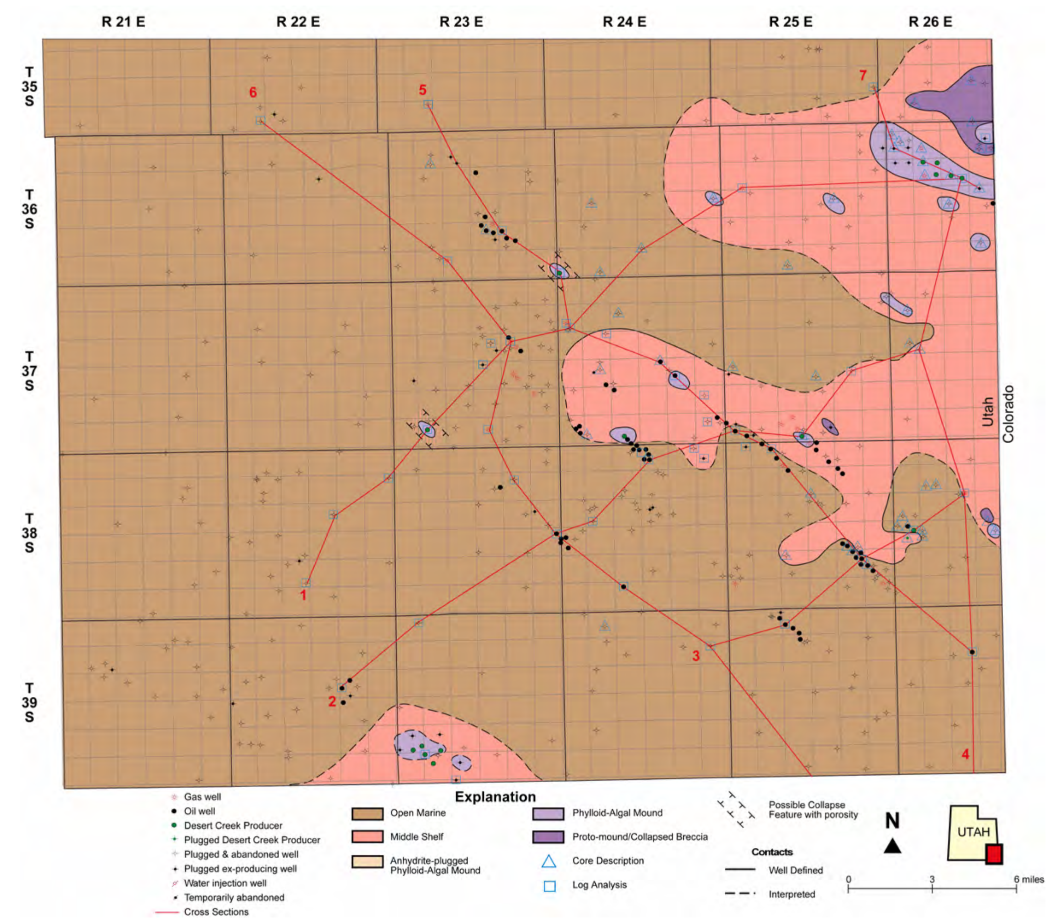

Figure 2-16. Regional lithofacies map of the lower Desert Creek zone, Paradox Formation, in the Blanding sub-basin, Utah.

important because inner shelf/tidal flats often form the substrate for phylloid-algal mound development. Proto-mounds/collapse breccia lithofacies are found in the Desert Creek zone and represent the initial stage of a mound buildup or one that never fully developed. They may appear as promising buildups on seismic, but in actuality have poor reservoir quality and little potential other than as guides to nearby fully developed mounds (figure 2-16).

In the upper Ismay zone, most phylloid-algal mounds developed adjacent to widespread intra-shelf (anhydrite-filled) basins (figures 2-14, 2-15, 2-17, and 2-18). Porous Desert Creek mound lithofacies, such as the reservoir for Bug field, appear to be linear shorelines (carbonate islands) that developed on the middle shelf (figure 2-16). Regional lithofacies mapping clearly defines anhydrite-filled, intra-shelf basins. Inner shelf/tidal flat and associated productive, phylloid-algal lithofacies trends of the Ismay are present around the anhydritic salinas of intra-shelf basins (figures 2-14, 2-15, 2-17, and 2-18). Although not present in the lower Desert Creek zone in the Blanding sub-basin, the Desert Creek reservoir lithofacies peripheral to Greater Aneth field to the south (figure 1-3) wrap around similar anhydrite-filled intra-shelf basins (Chidsey and others, 1996b; Chidsey and Eby, 2000).

The location and shape of these anhydrite-rich, intra-shelf basins play major roles in the deposition and orientation of productive phylloid-algal buildups, as well as the shoreline lithofacies that wrap around these evaporite basins. Lithofacies distant from the anhydrite-filled basins generally contain less favorable reservoir rocks, whereas most phylloid-algal buildups

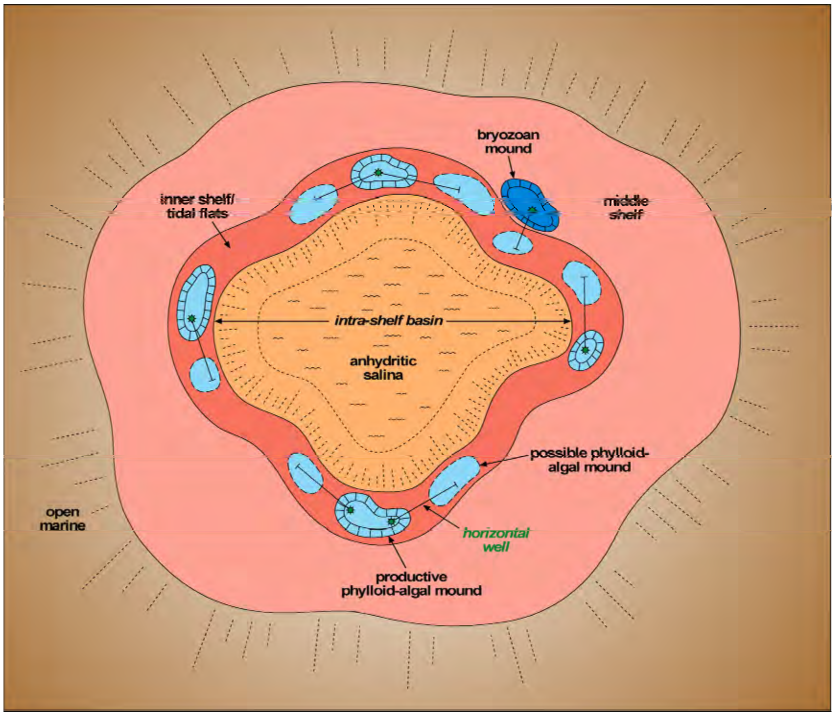

Figure 2-17. Schematic map view of an ideal upper Ismay intra-shelf basin surrounded by a ring of inner shelf/tidal flat sediments (shown in red) which encase phylloid-algal mound clusters (in light blue). The central portion of the intra-shelf basin is the location of thick anhydrite (in orange) accumulation. Outboard from the inner shelf/tidal flat and mound fairway are low-energy middle-shelf and open-marine carbonates.

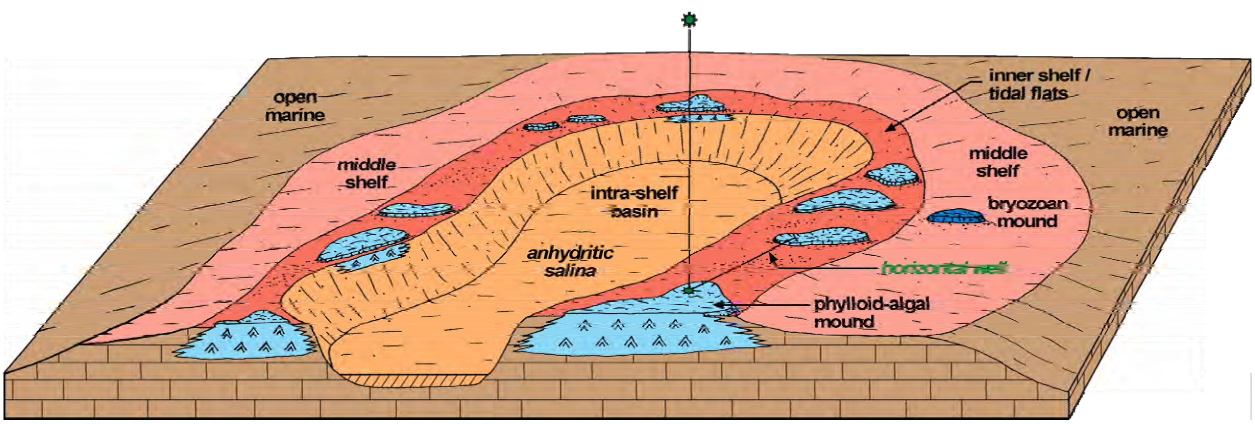

Figure 2-18. Cut-away block diagram showing the possible spatial relationships of upper Ismay lithofacies types controlled by an intra-shelf basin. Phylloid-algal mounds (in light blue) are the principal reservoir within a curvilinear band that rims the intra-shelf basin. A hypothetical vertical well into a known mound reservoir is used as a kick-off location for horizontal drilling into previously undrained mounds.

and porous inner-shelf lithofacies are very close to the intra-shelf basins. The two mapped, upper Ismay zone intervals show considerable differences in the distribution of these anhydrite basins and their surrounding lithofacies.

Lithology

Open-marine lithofacies are found in both the Ismay and Desert Creek zones of the Blanding sub-basin (figures 2-14 through 2-16, 2-19, and 21-20). Rock representing this

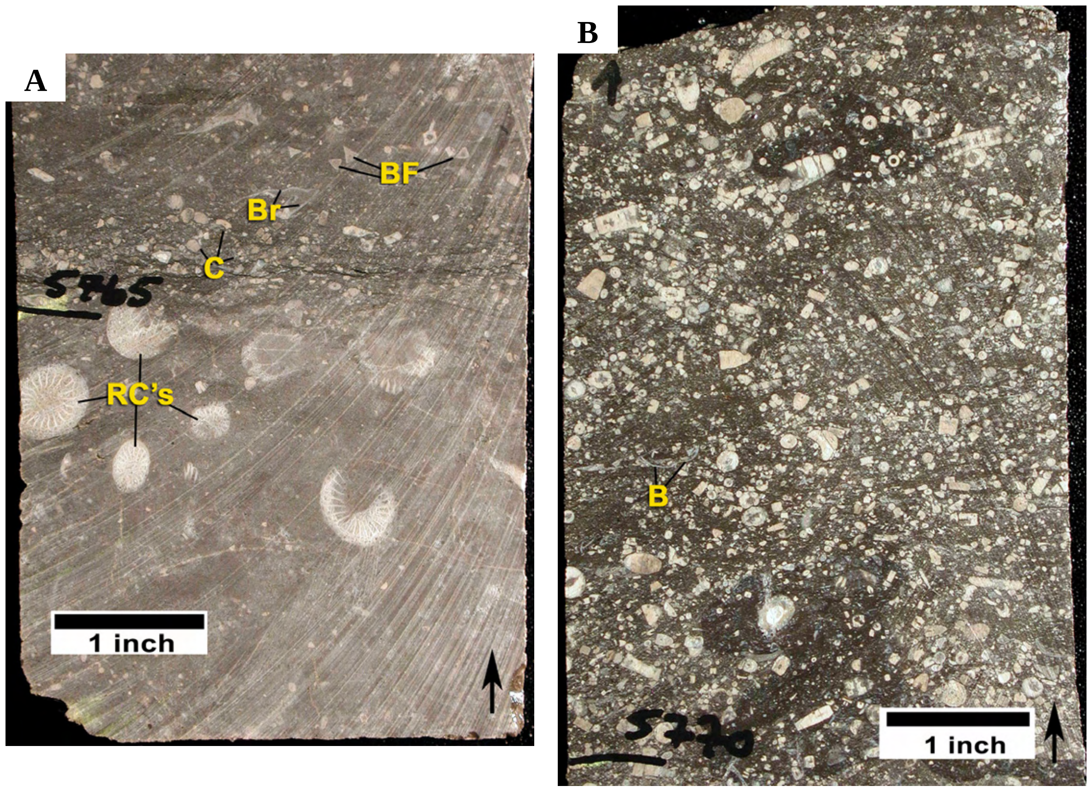

Figure 2-19. Typical, Ismay, open-marine lithofacies from the No. 1-28 Cuthair well (section 28, T. 38 S., R. 22 E., Salt Lake Base Line [SLBL]). (A) Well-preserved rugose corals (RC), crinoids (C), brachiopods (Br), and benthic forams (BF); slabbed core from 5765 feet. (B) Well-preserved, partially articulated crinoid stems and parts, as well as articulated thin-shelled bivalves (B); slabbed core from 5770 feet.

lithofacies consists of lime mudstone containing well-preserved rugose corals, crinoids, brachiopods, bryozoans, articulated thin-shelled bivalves, and benthic forams indicative of normal-marine salinities and low-energy conditions. Rock units of this lithofacies have very little effective porosity and permeability, and act as barriers and baffles to fluid flow.

Middle-shelf lithofacies are also found in both the Ismay and Desert Creek zones (figure 2-21). The most common depositional fabrics of this lithofacies are bioturbated lime to dolomitic mudstone with ubiquitous sub-horizontal feeding burrows, and fossiliferous peloidal wackstone. There are few megafossils and little visible matrix porosity. However, there is some fusulinid-rich lime wackestone to packstone also present in very tight, biogenically graded limestone.

Inner shelf/tidal flat lithofacies are found in the Ismay zone as dolomitized packstone and grainstone (figure 2-22). Clotted, lumpy, and poorly laminated microbial structures resembling small thrombolites and intraclasts are common. Megafossils and visible porosity are very rare in the inner shelf/tidal flat setting. Non-skeletal grainstone (calcarenite) composed of ooids, coated grains, and "hard peloids" occurs as high-energy deposits in some inner shelf/ tidal flat settings. Remnants of interparticle and moldic pores may be present in this lithofacies.

Bryozoan mound lithofacies are found in the Ismay zone as mesh-like networks of tubular and sheet-type (fenestrate) bryozoans (figure 2-23). These bryozoans provide the binding agent for lime mud-rich mounds. Crinoids and other open-marine fossils are common.

Large, tubular bryozoans and marine cement are also common in areas of high-energy, and possibly shallow, water. Porosity is mostly confined to preserved intraparticle spaces.

Proto-mounds/collapse breccia lithofacies in the Desert Creek zone contain dolomitized and brecciated algal plates, marine cements, and internal sediments suggesting subareal exposure (figure 2-24). They are usually near phylloid-algal mound lithofacies, but generally lack any significant porosity.

Phylloid-algal mound lithofacies are found in both the Ismay and Desert Creek zones (figures 2-14 through 2-16, and 2-25). This lithofacies contains the dominant oil-producing reservoirs in the Paradox Formation. Very large phylloid-algal plates of *Ivanovia* (the dominant genus in the Ismay zone) and skeletal grains create bafflestone or bindstone fabrics. In mound interiors, algal plates are commonly found in near-growth positions surrounded by lime mud (figure 2-25A). On the high-energy margins of algal mounds, algal plates and skeletal grains serve as substrates for substantial amounts of botryoids and other early-marine cements, and internal sediments (figure 2-25B). Desert Creek mounds are dolomitized, contain plates of the *Kansasphyllum* (figure 2-25C), and show evidence of subaerial exposure (breccia or beach rock). Pore types include primary shelter pores preserved between phylloid-algal plates and secondary moldic pores.

Figure 2-20. Typical, Desert Creek, open-marine lithofacies from the Scorpion No. 1 well (section 34, T. 36 S., R. 24 E., SLBL) containing dolomitized lime mud, and rugose corals and crinoids; slabbed core from 5892 feet.

Quartz sand dune lithofacies are found in the Ismay as very fine grained, well-sorted quartzose sandstone that display moderate- to high-angle cross-bedding (figure 2-26). The well-rounded nature of the individual quartz sand grains (visible in thin sections) is consistent with a possible eolian origin for these dunes.

Anhydrite salina lithofacies are found within locally thick accumulations in upper Ismay (upper and lower parts) intra-shelf basins (figures 2-14 and 2-15). Anhydrite growth forms include nodular-mosaic (“chicken-wire”), palmate, and banded anhydrite (figure 2-27). Large palmate crystals probably grew in a gypsum aggregate indicative of subaqueous deposition. Detrital and chemical evaporites (anhydrite) filled in the relief around palmate structures. Thin, banded couplets of pure anhydrite and dolomitic anhydrite are products of very regular chemical changes in the evaporite intra-shelf basins. These varve-like couplets are probably indicative of relatively “deep-water” evaporite precipitation.

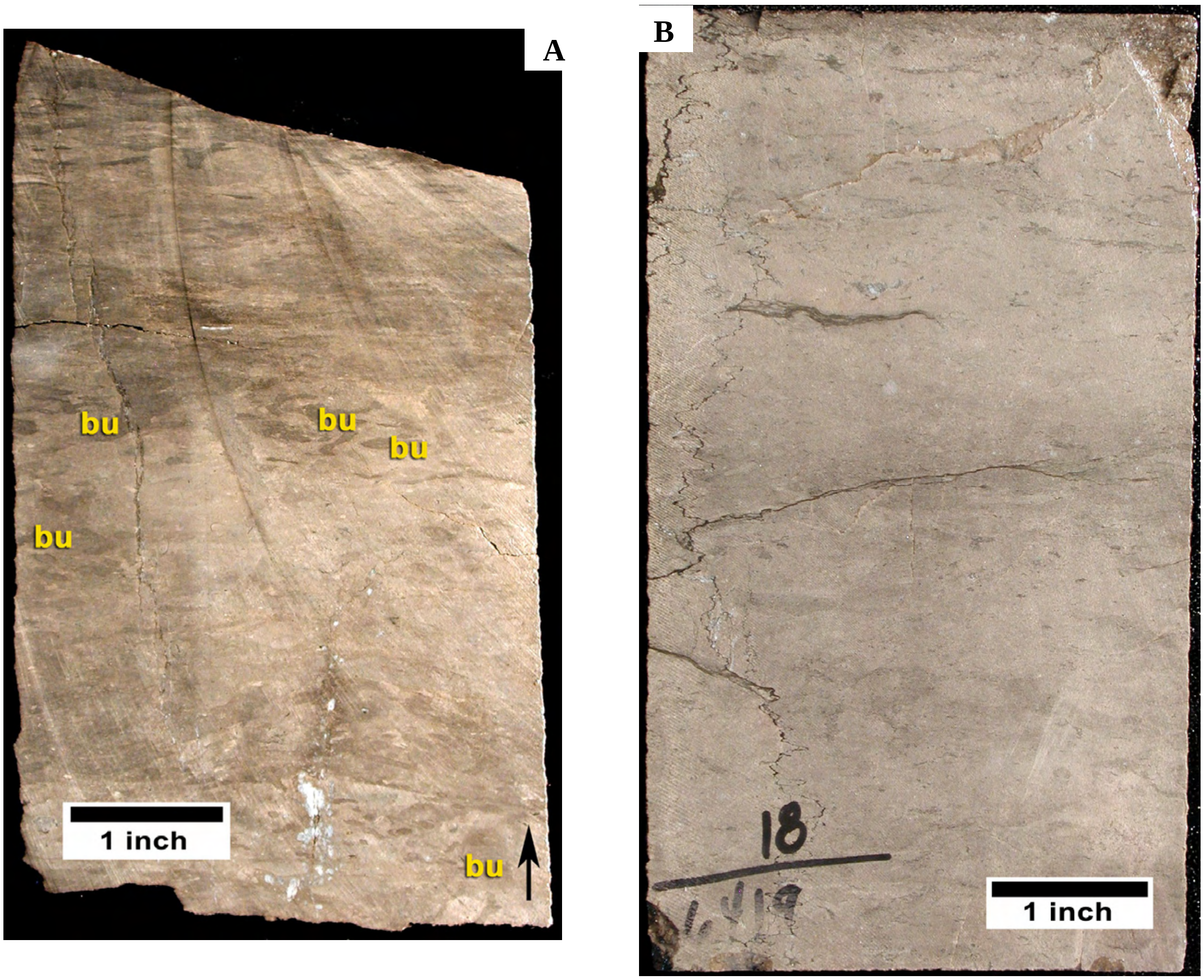

Figure 2-21. Typical middle-shelf lithofacies. (A) Ismay bioturbated lime mudstone containing compacted sub-horizontal feeding burrows (bu); Tank Canyon No. 1-9 well, section 9, T. 37 S., R. 24 E., SLBL, slabbed core from 5412.5 feet. (B) Desert Creek burrowed dolomitic mudstone; Ucolo No. 1-32 well, section 32, T. 35 S., R. 26 E., SLBL, slabbed core from 6418.7 feet.

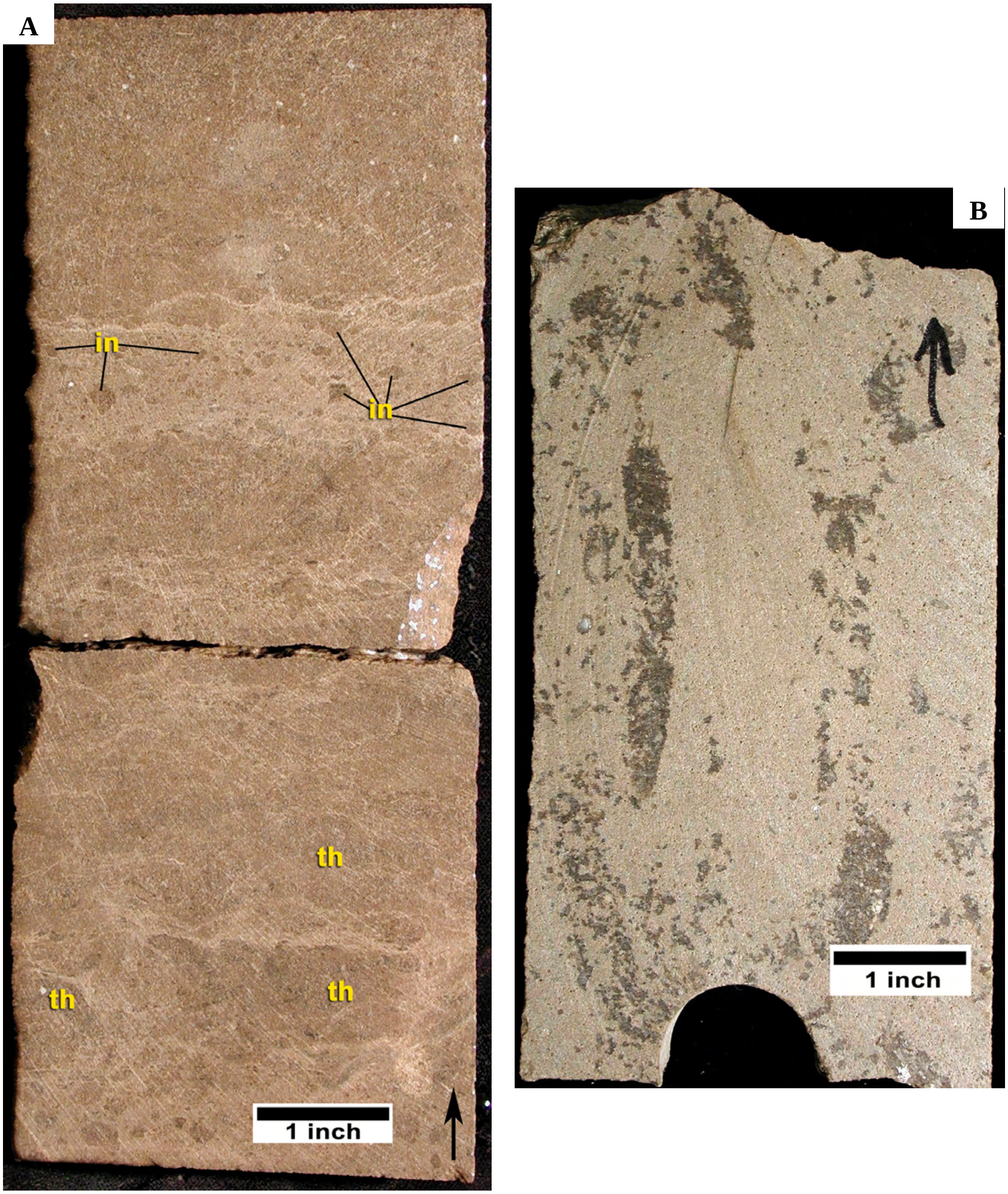

Figure 2-22. Typical, Ismay, inner shelf/tidal flat lithofacies. (A) Dolomitized lumpy microbial structures resembling small thrombolites (th) and intraclasts (in) composed of desiccated and redeposited thrombolitic fragments; Tin Cup Mesa No. 2-23 well, section 23, T. 38 S., R. 25 E., SLBL, slabbed core from 5460.5 feet. (B) Non-skeletal grainstone composed of ooids, coated grains, and peloids, with dark gray patches and columns composed of anhydrite-cemented sediments; Patterson No. 5 well, section 4, T. 38 S., R. 25 E., SLBL, slabbed core from 5443.5 feet.

Figure 2-24. Typical, Desert Creek proto-mound/collapse breccia from the Ucolo No. 1 well (section 26, T. 38 S., R. 25 E., SLBL, slabbed core from 5506 feet) showing dolomitized, broken algal plates, marine cement, and internal sediment. Note that very little porosity is preserved (white areas are anhydrite).

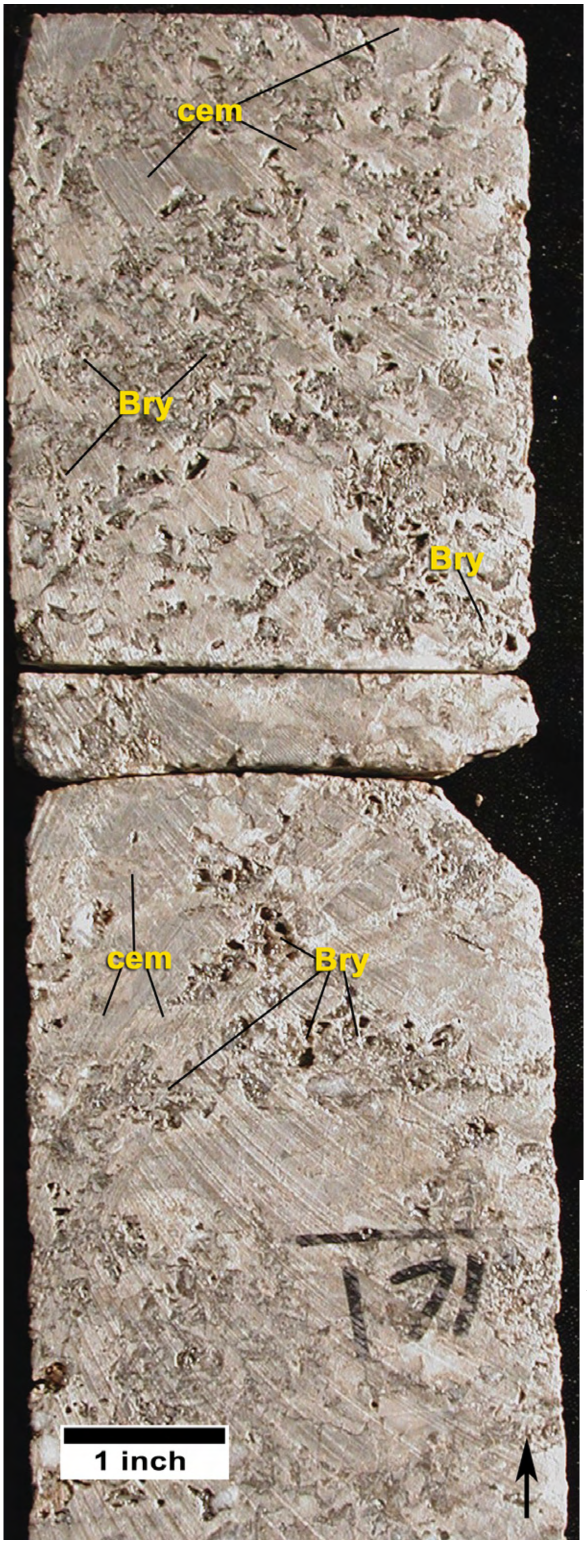

Figure 2-23. Typical, Ismay, bryozoan-mound lithofacies from the Mustang No. 3 well (section 26, T. 36 S., R. 25 E., SLBL, slabbed core from 6171 feet) containing large tubular bryozoans (Bry) and "lumps" of marine cement (cem). Occasional phylloid-algal plates are also present. This mound fabric is typical of higher energy, and possibly shallower water than the mud-dominated fabrics.

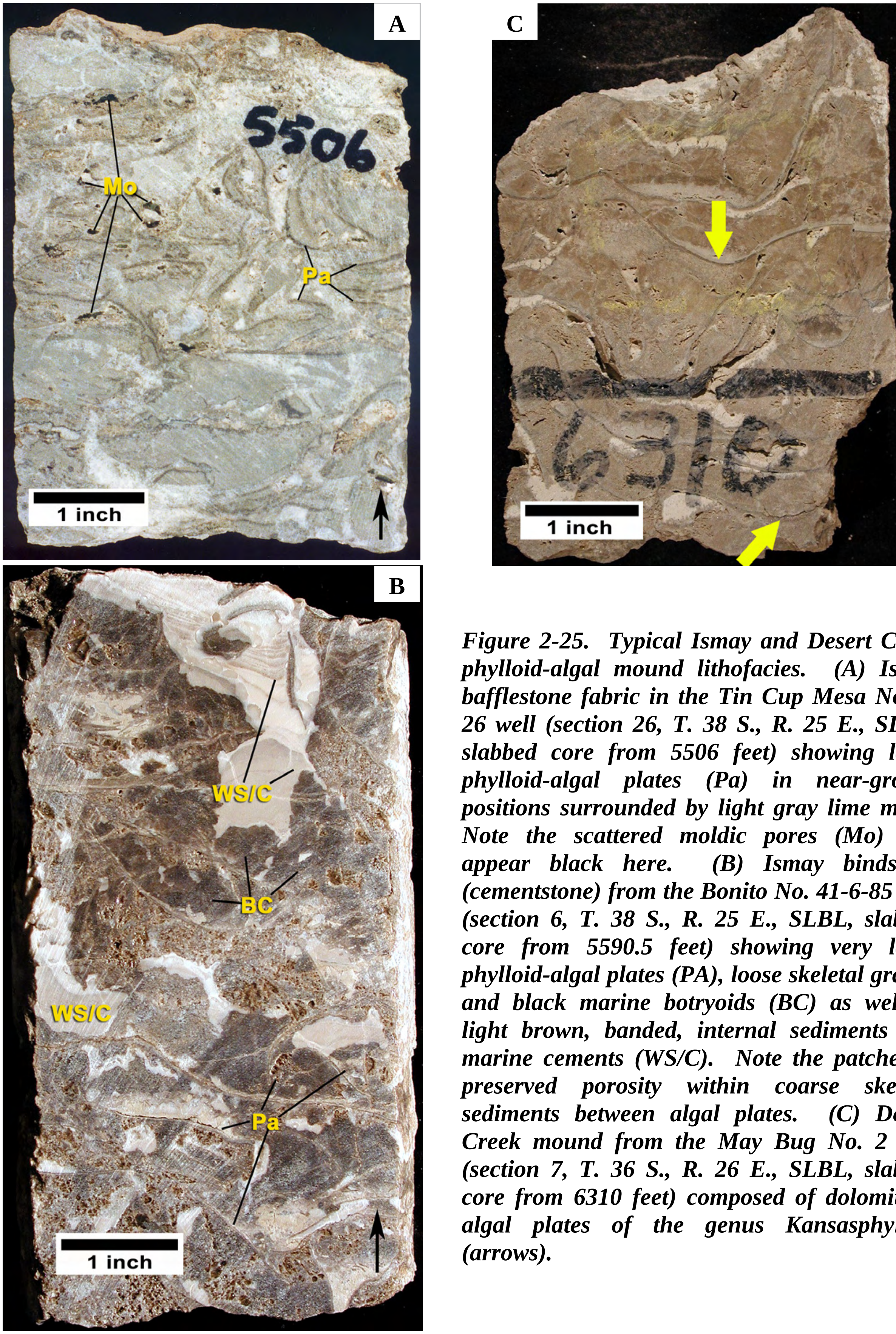

Figure 2-25. Typical Ismay and Desert Creek phylloid-algal mound lithofacies. (A) Ismay bafflestone fabric in the Tin Cup Mesa No. 3-26 well (section 26, T. 38 S., R. 25 E., SLBL, slabbed core from 5506 feet) showing large phylloid-algal plates (Pa) in near-growth positions surrounded by light gray lime muds. Note the scattered moldic pores (Mo) that appear black here. (B) Ismay bindstone (cementstone) from the Bonito No. 41-6-85 well (section 6, T. 38 S., R. 25 E., SLBL, slabbed core from 5590.5 feet) showing very large phylloid-algal plates (PA), loose skeletal grains, and black marine botryoids (BC) as well as light brown, banded, internal sediments and marine cements (WS/C). Note the patches of preserved porosity within coarse skeletal sediments between algal plates. (C) Desert Creek mound from the May Bug No. 2 well (section 7, T. 36 S., R. 26 E., SLBL, slabbed core from 6310 feet) composed of dolomitized algal plates of the genus Kansasphyllum (arrows).

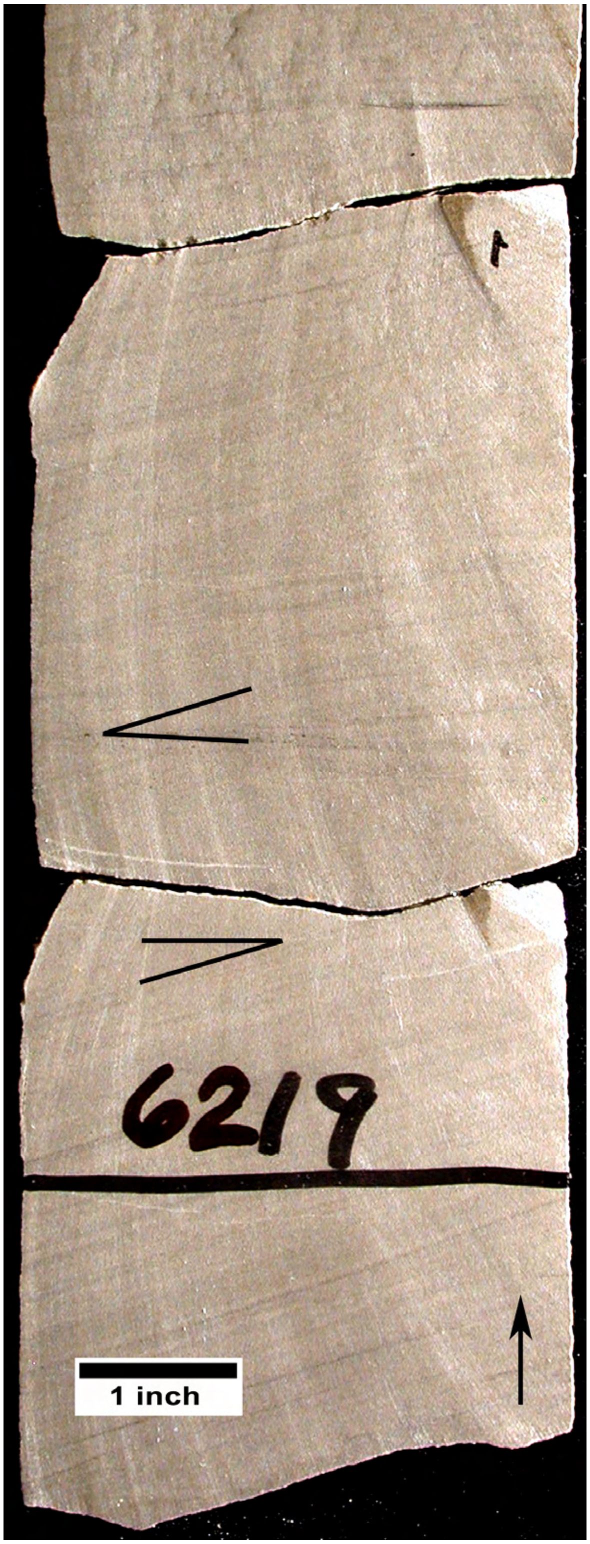

Figure 2-26. Typical upper Ismay (lower part) quartz sand dune lithofacies from the Mustang No. 22-43 well (section 26, T. 36 S., R. 43 E. SLBL, slabbed core from 6219 feet) showing high-angle cross-stratification within a 35-foot-thick sandstone encountered in wells of Mustang Flat field (figure 2-3).

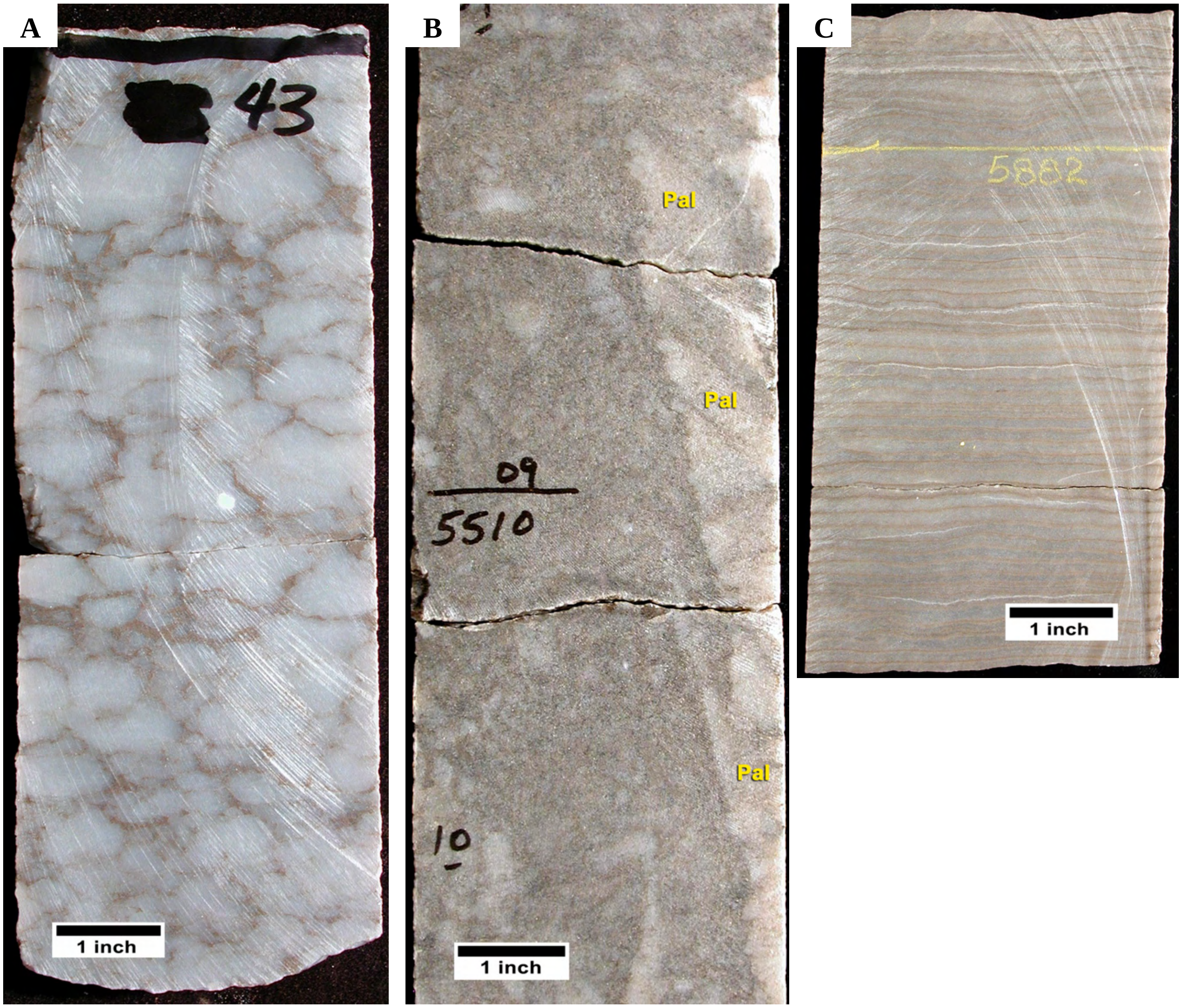

Figure 2-27. Anhydrite growth forms typically found in anhydrite salina lithofacies of upper Ismay intra-shelf basins. (A) Nodular-mosaic ("chicken-wire") anhydrite; Tank Canyon No. 1-9 well, section 9, T. 37 S., R. 24 E. SLBL, slabbed core from 5343 feet. (B) Large palmate crystals of anhydrite (Pal) along the right margin of this core segment probably grew in a gypsum aggregate that resembled an inverted candelabra while the remainder of the core segment consists of detrital and chemical anhydrite that filled in the relief around the palmate structure; Sioux Federal No. 30-1 well, section 30, T. 38 S., R. 25 E., SLBL, slabbed core from 5510 feet. (C) Thin (cm-scale), banded couplets of pure anhydrite (white to light gray) and dolomitic anhydrite (brown); Montezuma No. 41-17-74, section 17, T. 37 S., R. 24 E., SLBL, slabbed core from 5882 feet.

CHAPTER III
CASE-STUDY FIELDS

Thomas C. Chidsey, Jr., Craig D. Morgan, and Kevin McClure,
Utah Geological Survey;
Laura L. Wray, Colorado Geological Survey;
and
David E. Eby, Eby Petrography & Consulting, Inc.

Introduction

Four case-study fields were selected for local-scale reservoir characterization and evaluation during Budget Period I of the project: Bug field, San Juan County, Utah, in the Desert Creek trend; and Cherokee field, San Juan County, Utah, and Little Ute and Sleeping Ute fields, Montezuma County, Colorado, in the Ismay trend (figure 1-3). These evaluations included data collection, core photography and description, determination of a typical vertical sequence from conventional core tied to its corresponding log response, lithfacies identification, reservoir mapping, determination of diagenetic fabrics from thin sections, and plots of core plug porosity versus permeability of these fields.

The geological characterization of these fields focused on reservoir heterogeneity, quality, and lateral continuity, as well as possible compartmentalization. This utilized representative core and modern geophysical well logs to characterize and initially grade various intervals in the fields for horizontal drilling suitability. From these evaluations, untested or under-produced compartments were identified as targets for horizontal drilling. The information generated from the characterization and evaluation of the case-study fields was used for: (1) predicting changes in reservoir and non-reservoir rocks across the fields, (2) comparing field to non-field areas, (3) estimating the reservoir properties and identifying lithofacies in wells which were not cored, and (4) determining potential units suitable for horizontal drilling projects.

The models resulting from the geological and reservoir characterization of these fields can be applied to similar fields in the basin (and other basins as well) where core and other data might be limited.

Field Data Collection, Compilation, and Interpretation

Reservoir data, cores and cuttings, geophysical logs, various reservoir maps, and other information from the case-study fields were collected by the UGS and CGS. Well locations, production data, completion tests, basic core analysis, formation tops, porosity and permeability data, and other data were compiled and entered in a database developed by the UGS. This database, INTEGRAL, is a geologic-information database that links a diverse set of geologic data to records using MS Access™. The database is designed so that geological information, such as lithology, petrophysical analyses, or depositional environment, can be exported to software programs to produce strip logs, lithofacies maps, various graphs, statistical models, and other types of presentations.

All available conventional cores from the case-study fields were photographed (figures

3-1 and 3-2, and table 3-1) and described (**Deliverable 1.3.1 – Geophysical Well Log/Core Descriptions, Cherokee and Bug Fields, San Juan County, Utah, and Little Ute and Sleeping Ute Fields, Montezuma County, Colorado**). Special emphasis was placed on identifying each reservoir unit's bounding surfaces and depositional environments. The core descriptions follow the guidelines of Bebout and Loucks (1984) which include (1) basic porosity types, (2) mineral composition in percentage, (3) nature of contacts, (4) carbonate structures, (5) carbonate textures in percentage, (6) carbonate fabrics, (7) grain size (dolomite), (8) fractures, (9) color, (10) fossils, (11) cement, and (12) depositional environment. Carbonate fabrics were determined according to Dunham's (1962) and Embry and Klovan's (1971) classification schemes. Representative samples were selected from the cores for thin section description and geochemical analysis to determine diagenetic history and pore types.

The typical vertical sequence or cycle of lithofacies from the case-study fields, as determined from conventional core, was tied to its corresponding log response from geophysical well logs (figures 3-3 through 3-6, **Deliverable 1.3.1 – Geophysical Well Log/ Core Descriptions, Cherokee and Bug Fields, San Juan County, Utah, and Little Ute and Sleeping Ute Fields, Montezuma County, Colorado**), typically gamma-ray and neutron-density curves, using the log-based correlation scheme described in Chapter II. These sequences graphically include (1) carbonate fabric, pore type, physical structures, texture, framework grain, and lithofacies described from core; (2) plotted porosity and permeability analysis from core plugs; and (3) gamma-ray and neutron-density curves from geophysical well logs.

Figure 3-1. Photograph of representative slabbed core from the Desert Creek zone reservoir, Bug No. 13 well, Bug field, Utah.

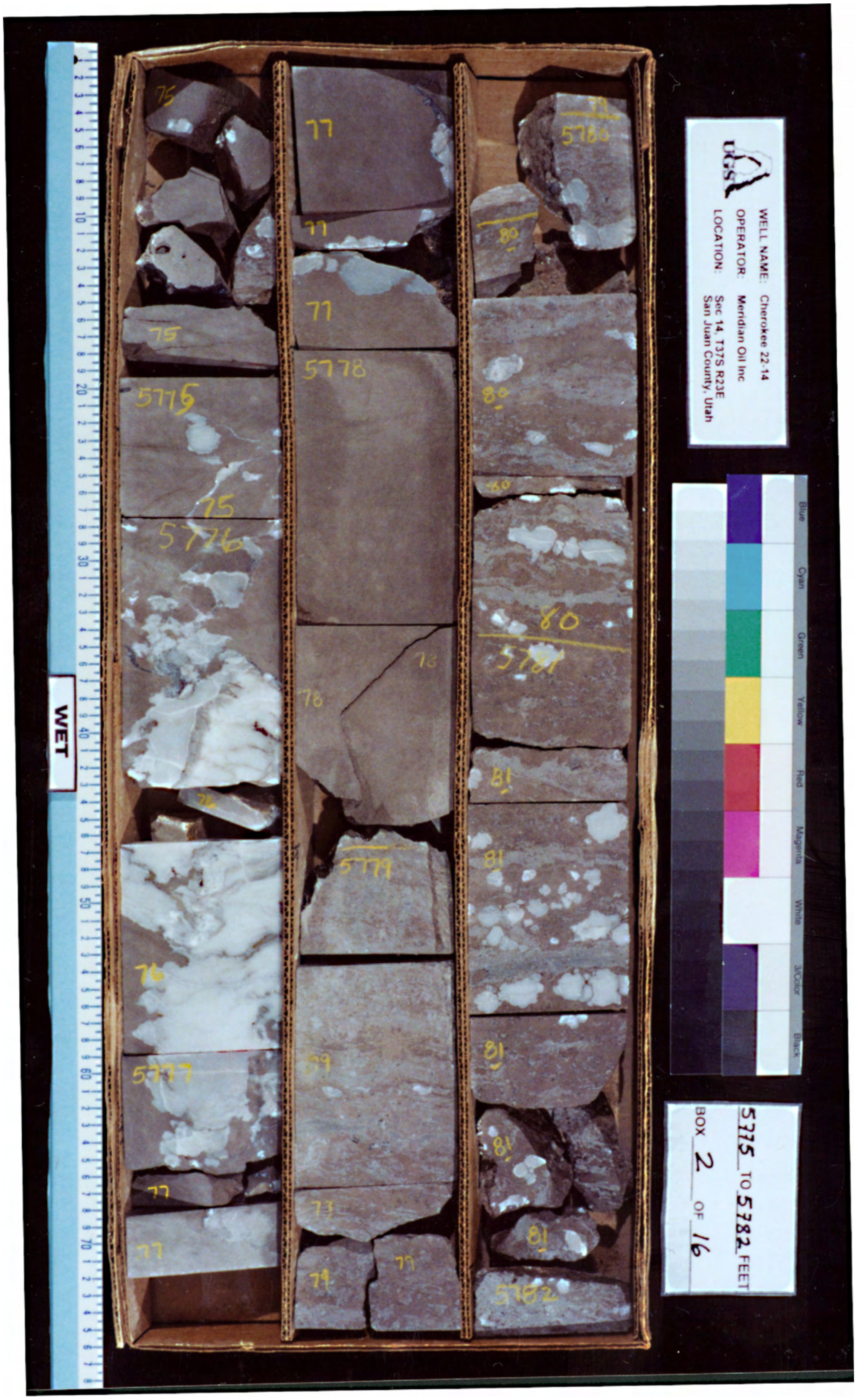

Figure 3-2. Photograph of representative slabbed core from the upper Ismay zone reservoir, Cherokee No. 22-14 well, Cherokee field, Utah.

Table 3-1. List of well conventional slabbed core examined and described from case-study fields in the Paradox Basin of Utah and Colorado.

Cherokee 22-14	14-37S-23E, UT	43-037-31367	5768-5880	Cherokee	Ismay	UGS
Cherokee 33-14	14-37S-23E, UT	43-037-31316	5770-5799	Cherokee	Ismay	UGS
May-Bug 2	7-36S-26E, UT	43-037-30543	6290-6333	Bug	Desert Creek	UGS
Bug 3	7-36S-26E, UT	43-037-30544	6316-6358	Bug	Desert Creek	UGS
Bug 4	16-36S-26E, UT	43-037-30542	6278-6322	Bug	Desert Creek	UGS
Bug 7A	7-36S-26E, UT	43-037-30730	6345-6400	Bug	Desert Creek	UGS
Bug 8	8-36S-26E, UT	43-037-30589	5737-5796.1	Bug	Desert Creek	UGS
Bug 10	22-36S-26E, UT	43-037-30591	6300-6346.5	Bug	Desert Creek	UGS
Bug 13	17-36S-26E, UT	43-037-30610	5913-5951.3	Bug	Desert Creek	UGS
Bug 16	17-36S-26E, UT	43-037-30607	6278-6333	Bug	Desert Creek	UGS
Little Ute 1	11-34N-20W, CO	05-083-06553	5836-5955.3	Little Ute	Ismay	TOS
Sleeping Ute 1	3-34N-20W, CO	05-083-06540	5533-5653	Sleeping Ute	Ismay	TOS

* UGS = Utah Geological Survey, Salt Lake City, Utah; TOS = Triple O Slabbing, Denver, Colorado

The graphical information was combined with the log-based correlation scheme to identify major Paradox Formation zone contacts, seals or barriers, baffles, and producing or potential reservoirs, and lithofacies. These major zone contacts were used to produce a variety of structure and isochore maps which were incoproated into the reservoir models. Seals or barriers include anhydite layers and thick (black) shales such as the Hovenweep shale, which separates the upper Ismay from the lower Ismay. Baffles are those rock units that restrict fluid flow in some parts of the fields, but may develop enough porosity and permeability in other parts, through diagenetic processes or lithofacies changes, to provide a conduit for fluid flow or even oil storage. The reservoirs are those units containing 6 percent or more porosity based on the average of the neutron and density porosity values.

Bug Field

Bug field (figure 1-3) is an elongate, northwest-trending carbonate buildup in the lower Desert Creek zone. Productive lithofacies of the buildup consist of a phylloid algal mound capped by shoreline carbonate island deposits. The buildup is surrounded by non-productive middle shelf fossiliferous/peloidal muds and some platform interior evaporites (see Chapter II for detailed descriptions of these lithofacies). The producing units vary from porous dolomitized bafflestone to packstone and wackestone. The trapping mechanism is an updip porosity pinchout to the northeast. The net reservoir thickness is 15 feet (4.6 m) over a 2600-acre (1052 ha) area. Porosity averages 11 percent in moldic, vuggy, and intercrystalline

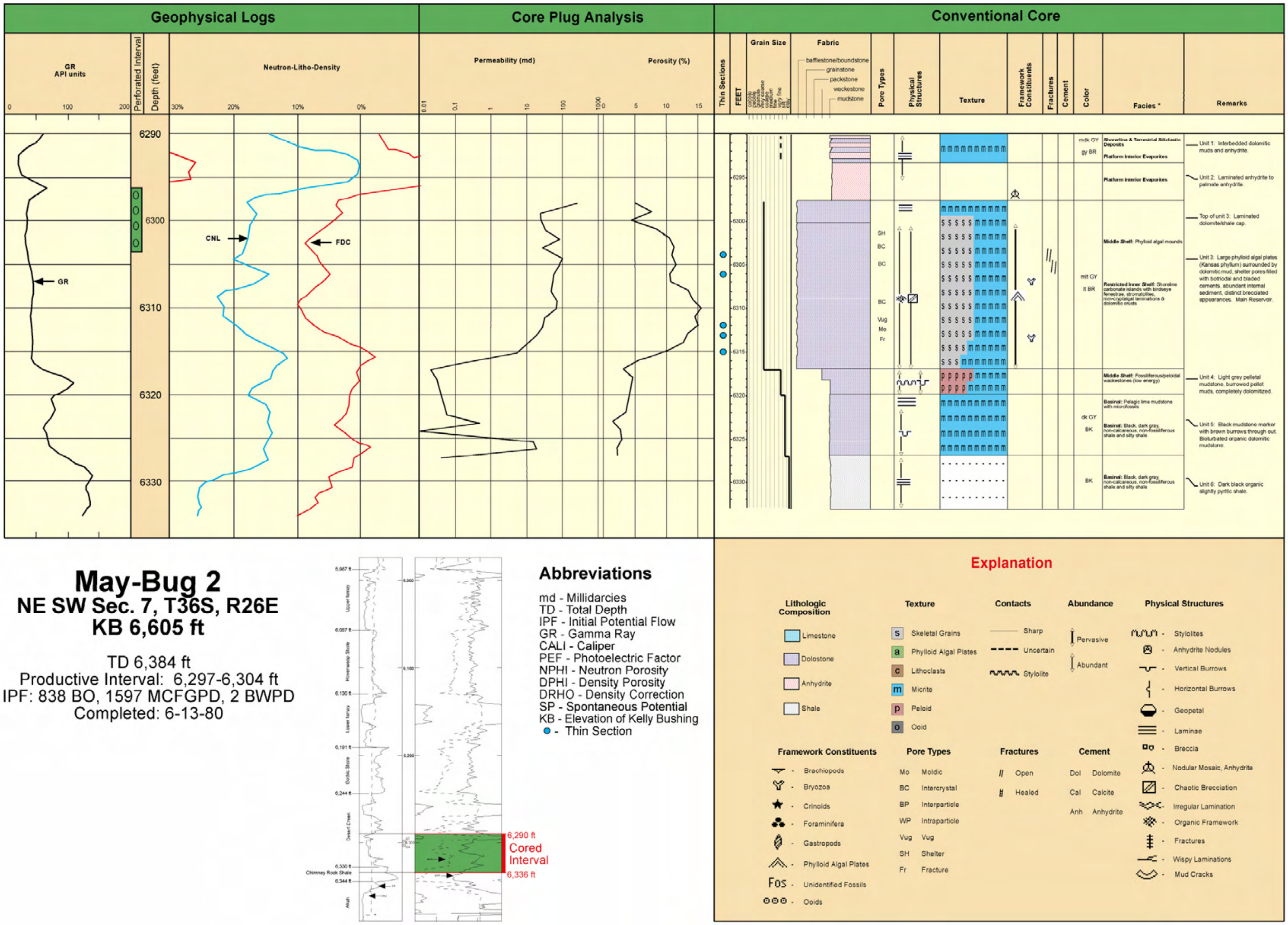

Figure 3-3. Typical vertical sequence from Bug field, including geophysical well logs, porosity/permeability plots, and core description, of the lower Desert Creek zone, May-Bug No. 2 well, San Juan County, Utah.

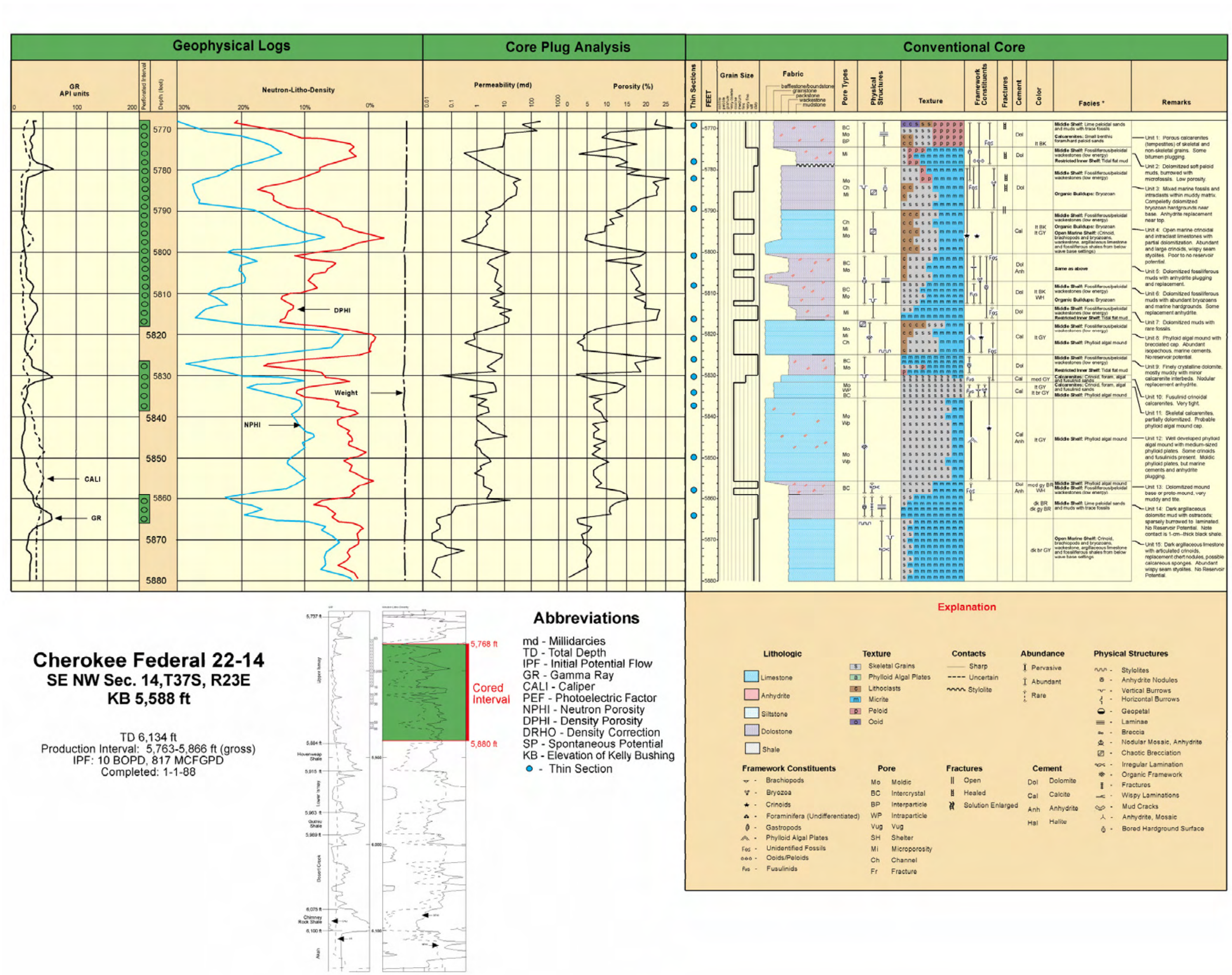

Figure 3-4. Typical vertical sequence from Cherokee field, including geophysical well logs, porosity/permeability plots, and core description, of the upper Ismay zone, Cherokee No. 22-14 well, San Juan County, Utah.

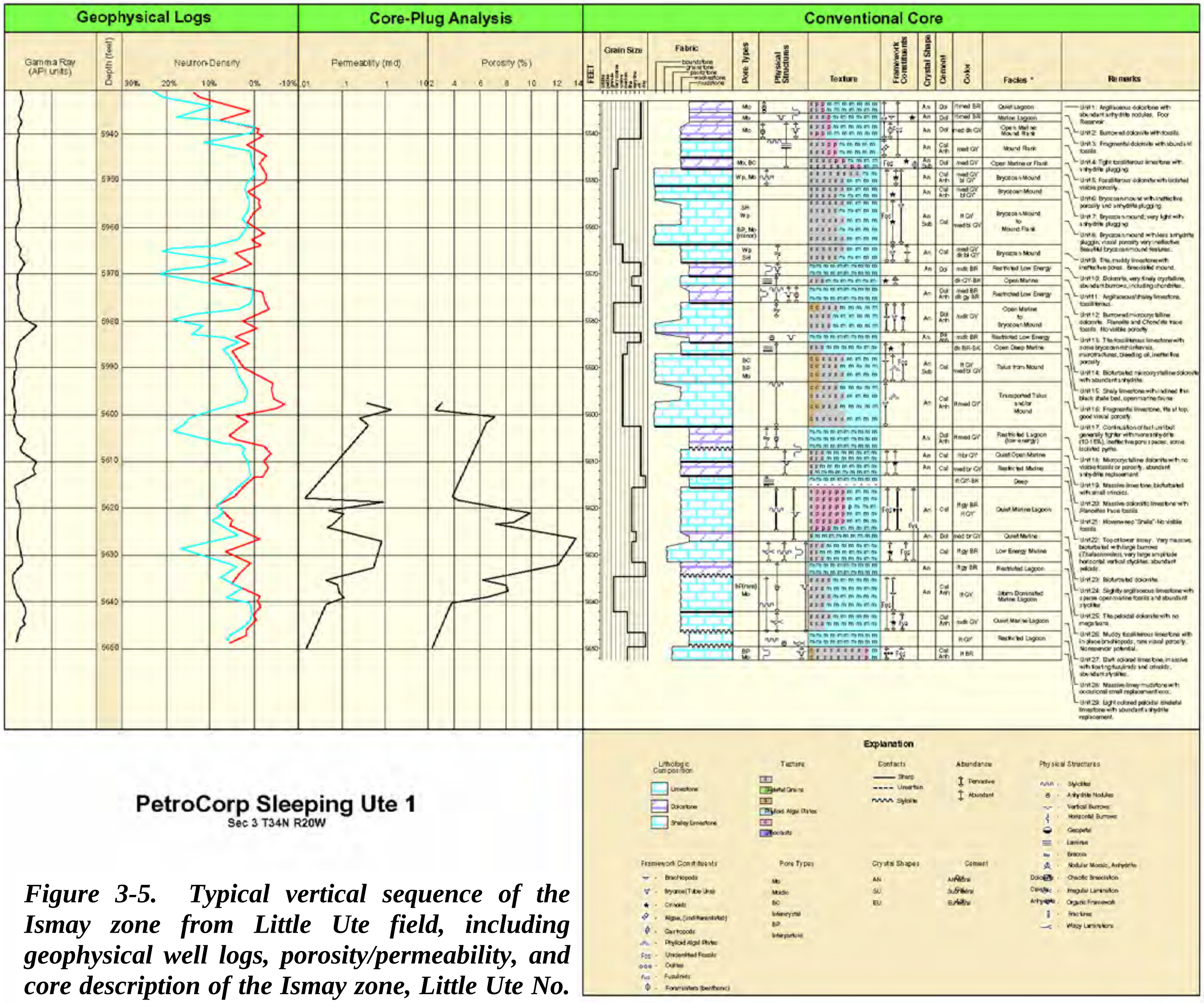

Figure 3-5. Typical vertical sequence of the Ismay zone from Little Ute field, including geophysical well logs, porosity/permeability, and core description of the Ismay zone, Little Ute No. 1 well, Montezuma County, Colorado.

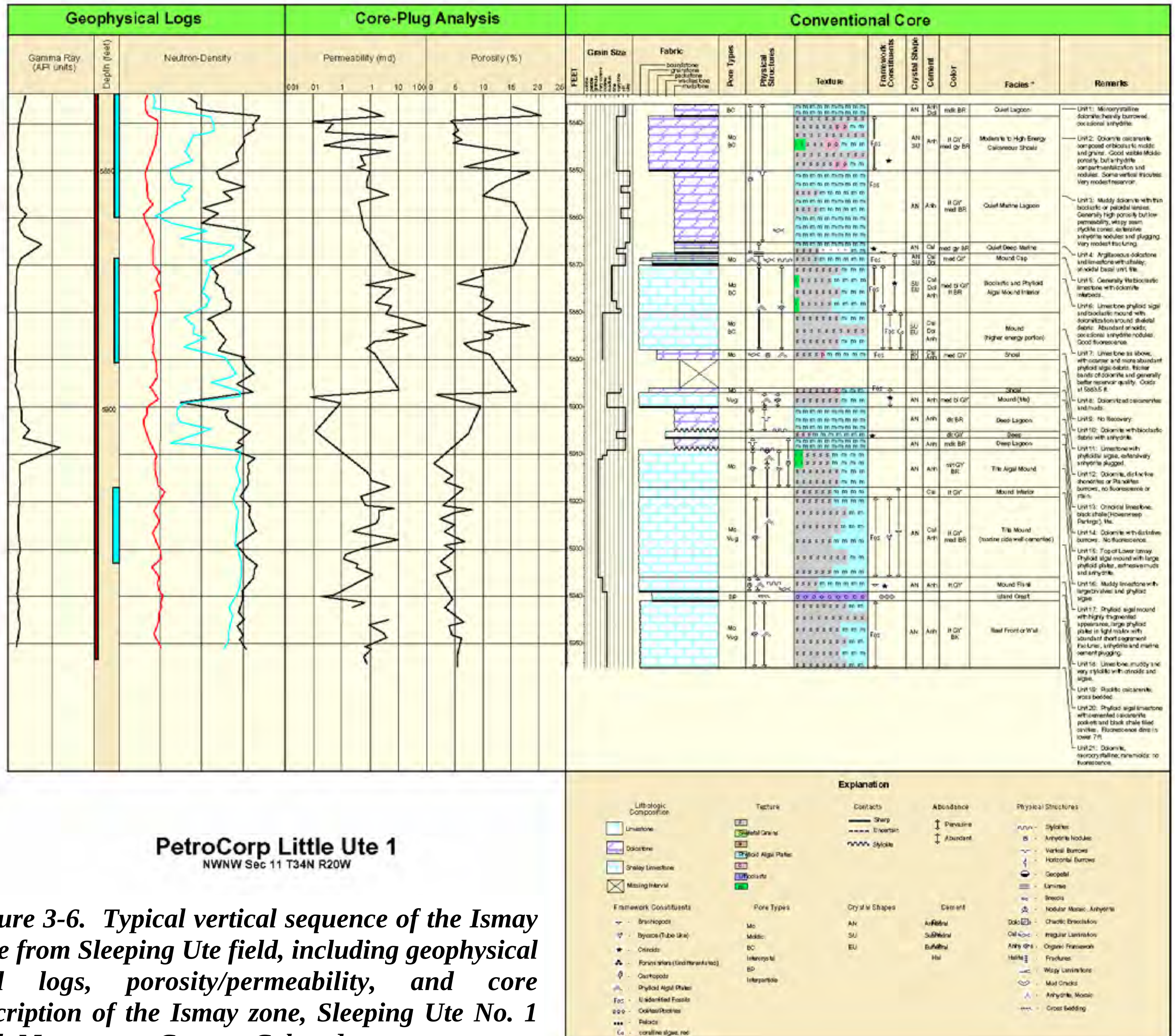

Figure 3-6. Typical vertical sequence of the Ismay zone from Sleeping Ute field, including geophysical well logs, porosity/permeability, and core description of the Ismay zone, Sleeping Ute No. 1 well, Montezuma County, Colorado.

networks. Permeability averages 25 to 30 millidarcies (mD), but ranges from less than 1 to 500 mD. Water saturation is 32 percent (Martin, 1983; Oline, 1996).

Bug field was discovered in 1980 with the completion of the Wexpro Bug No. 1 well, NE1/SE1/4 section 12, T. 36 S., R. 25 E., Salt Lake Base Line and Meridian (SLBL&M), with an initial flowing potential (IFP) of 608 bbls of oil per day (BOPD) (96.7 m^3), 1128 thousand cubic feet of gas per day (MCFGPD) (32 MCMPD), and 180 bbls of water (28.6 m^3). There are currently seven producing (or shut-in) wells, six abandoned producers, and two dry holes in the field. The well spacing is 160 acres (65 ha). The present reservoir field pressure is 3550 pounds per square inch (psi) (24,477 kPa). Cumulative production as of September 1, 2006, was 1,623,802 bbls of oil (258,185 m^3), 4.53 billion cubic feet of gas (BCFG) (0.13 BCMG), and 3,190,328 bbls of water (507,262 m^3) (Utah Division of Oil, Gas and Mining, 2007). Estimated primary recovery was 1,600,000 bbls (254,400 m^3) of oil and 4 BCFG (0.1 BCMG) (Oline, 1996). The fact that both these estimates have been surpassed suggests significant additional reserves could remain.

Cherokee Field

Cherokee field (figure 1-3) is a phylloid-algal buildup capped by anhydrite that produces from porous algal limestone and dolomite in the upper Ismay zone. The mound is capped by crinoid/fusulinid-bearing sands. The buildup is surrounded by non-productive middle shelf fossiliferous/peloidal muds (see Chapter II for detailed descriptions of these lithofacies). The net reservoir thickness is 27 feet (8.2 m), which extends over a 320-acre (130 ha) area. Porosity averages 12 percent with 8 mD of permeability in vuggy and intercrystalline pore systems. Water saturation is 38.1 percent (Crawley-Stewart and Riley, 1993).

Cherokee field was discovered in 1987 with the completion of the Meridian Oil Company Cherokee Federal 11-14 well, NE1/4NW1/4 section 14, T. 37 S., R. 23 E., SLBL&M, with an IFP of 53 BOPD (8.4 m^3), 990 MCFGPD (28 MCMPD), and 26 bbls of water (4.1 m^3). There are currently three producing (or shut-in) wells, one abandoned producer, and three dry holes in the field. The well spacing is 80 acres (32 ha). The present field reservoir pressure is estimated at 150 psi (1034 kPa). Cumulative production as of September 1, 2006, was 183,945 bbls of oil (29,247 m^3), 3.7 (BCFG) (0.1 BCMG), and 3485 bbls of water (554 m^3) (Utah Division of Oil, Gas and Mining, 2007). The original estimated primary recovery was 172,000 bbls of oil (27,348 m^3) and 3.28 BCFG (0.09 BCMG) (Crawley-Stewart and Riley, 1993). Again, since the original reserve estimates have been surpassed and the field is still producing, significant additional reserves likely remain.

Little Ute and Sleeping Ute Fields

Little Ute and Sleeping Ute fields are located in Montezuma County, Colorado (sections 3, 10, and 11, T. 34 N., R. 20 W. (figure 1-3). Six representative lithofacies were identified from core and geophysical well correlation from the Little Ute and Sleeping Ute fields: (1) phylloid-algal mounds, (2) bryozoan mounds, (3) mound talus, (4) calcarenite shoals, (5) open-marine carbonates, and (6) lagoonal/restricted shelf carbonates. The producing reservoirs consist of phylloid-algal buildups in the Ismay zone flanked by bryozoan mounds and mound talus (flank debris). In terms of cumulative production from the wells in Little Ute and Sleeping Ute fields, the phylloid-algal mound lithofacies, developed in three separated intervals in the Little Ute No. 1 well, is the best reservoir in the area. These porous mounds, capped by impermeable anhydritic dolomite, produce primarily from porous phylloid-algal limestones, some of which have been dolomitized. The net reservoir thickness is 30 feet (9.1 m), which extends over approximately 640 acres (260 ha). Porosity ranges from 4 to 20 percent with 1 to 98 mD of permeability in vuggy and intercrystalline pore systems. Water saturation is 50 percent (Ghazal, 1978).

The first well drilled in the Little Ute/Sleeping Ute study area was a dry hole, completed in 1959. The Calvert Drilling Company Desert Canyon No. 1 well was drilled in the SW1/4 of section 10, T. 34 N., R. 20 W., to a total depth of 5938 feet (1810 m) to the Gothic shale as a test of the Ismay and Desert Creek zones of the Paradox Formation. The well was plugged and abandoned on September 29, 1959, after a drill-stem test and four cores were taken in the Ismay and Desert Creek. The results of the drill-stem test, taken over the interval from 5697 to 5840 feet (1736-1780 m), were discouraging in that there was a very weak blow of air to the surface that died in 5 minutes and only 55 feet (17 m) of drilling mud was recovered. Somewhat more encouraging were the cores taken from 5675 to 5729 feet (1730-1746 m), 5739 to 5782 feet (1749-1762 m), 5782 to 5820 feet (1762-1774 m), and 5880 to 5938 feet (1792-1819 m). Over that entire interval, there were favorable reports of petroliferous odor, visible vuggy and intercrystalline porosity, and bleeding oil.

There are currently three producing wells and three dry holes in the Little Ute and Sleeping Ute study area proper. Cumulative production from these three wells, plus the Desert Canyon No. 3 well that defined the Desert Canyon field, exceeds 325,000 bbls (51,675 m^3) of oil and 0.75 BCFG (0.02 BCMG) (Colorado Oil & Gas Conservation commission, 2006).

Reservoir Mapping

Various reservoir maps (top of structure, isochore [anhydrite, shale, porosity, permeability, lithology], lithofacies, and so forth) were constructed for the case-study fields (**Deliverables 1.4.1 and 1.4.2 – Cross Sections and Field Maps: Cherokee and Bug Fields, San Juan County, Utah, and Little Ute and Sleeping Ute Fields, Montezuma County, Colorado)**. Examples are shown on figures 3-7 through 3-30. These maps incorporate unit top and thickness picks from all geophysical well logs in the areas which were determined using the log-based correlation scheme (see Chapter II). The correlation scheme identifies major Paradox Formation zone contacts, seals or barriers, baffles, producing or potential reservoirs, and depositional lithofacies. Isochore maps of the upper and lower Ismay and lower Desert Creek were generated for reservoir units containing 6 percent or more porosity based on the average of the neutron and density porosity values. The maps show well names, Ismay or Desert Creek completions, completion attempts, drill-stem tests, wells with core, and display the subsea top and interval thickness for each well. These maps were combined to show carbonate buildup trends, define limits of field potential, and indicate possible horizontal drilling targets. The structure contour, isochore, and other maps produced for Bug and Cherokee fields, such as anhydrite and shale isochore maps, were incorporated into the three-dimensional (3-D) reservoir models developed for the project and described later in this report.

Bug Field

Bug field top of structure and isochore contour maps of the lower Desert Creek zone mound were combined to show the oil/water contact and updip porosity pinchout trap (figure 3-7). A structure contour map on the top of the Chimney Rock shale (the marker bed just below the lower Desert Creek zone) of the Paradox Formation was also constructed for Bug field and combined with the lower Desert Creek zone mound isochore map (figure 3-8). The field limits defined by the isochore maps corresponds to the map of porous lithofacies (figure 3-9).

In the lower Desert Creek zone of Bug field, the top of the mound/mound cap interval is equivalent to the top of the clean carbonate interval. In addition, the top mound/mound cap interval is equivalent to the top of the thin off-mound clean carbonate interval. The reservoir porosity unit is the entire mound/mound cap interval.

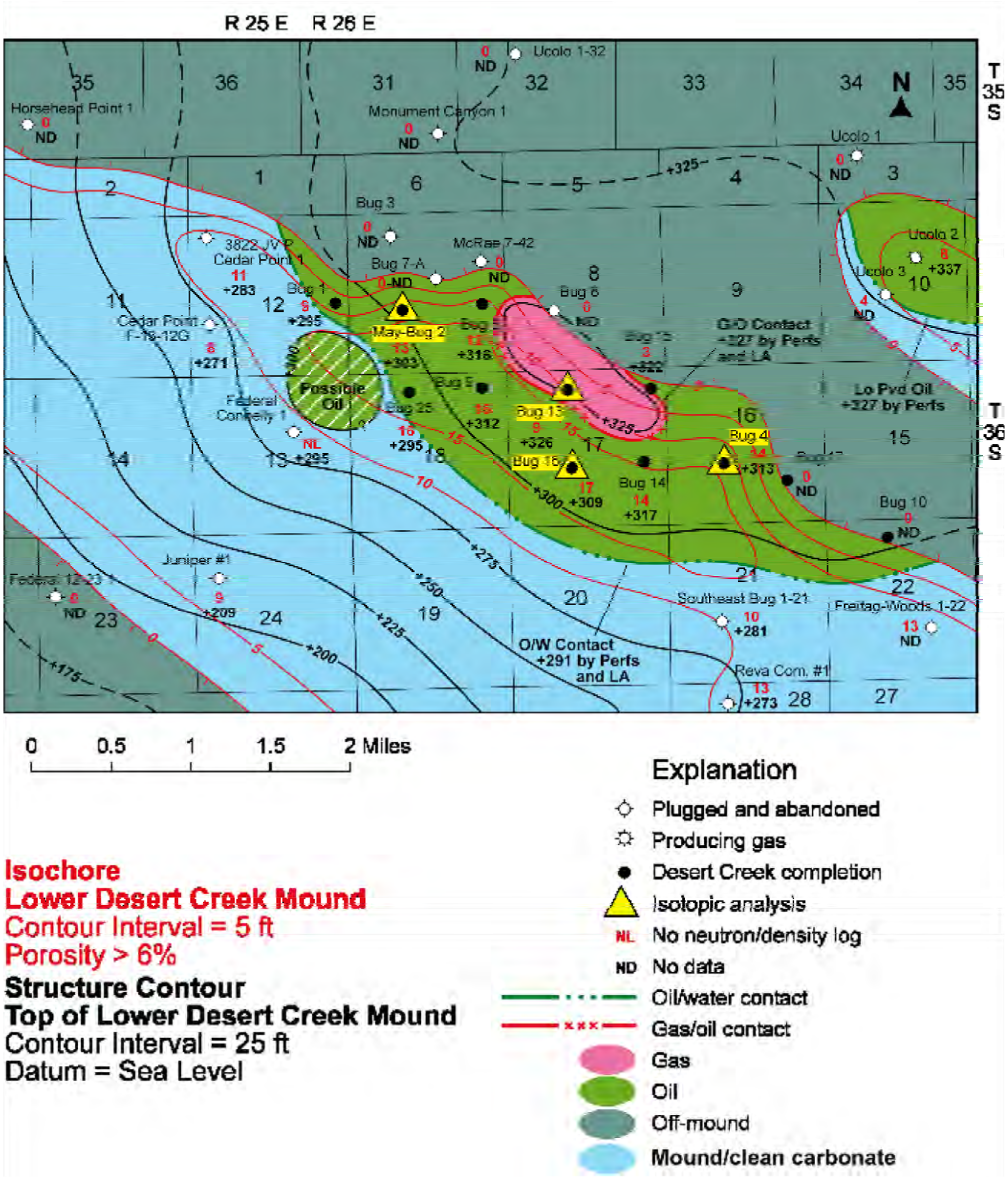

Figure 3-7. Map of combined top of structure and isochore of lower Desert Creek zone mound, Bug field, San Juan County, Utah. Well cores used for isotope sampling for this study are highlighted with a yellow triangle (discussed later in Chapter 7).

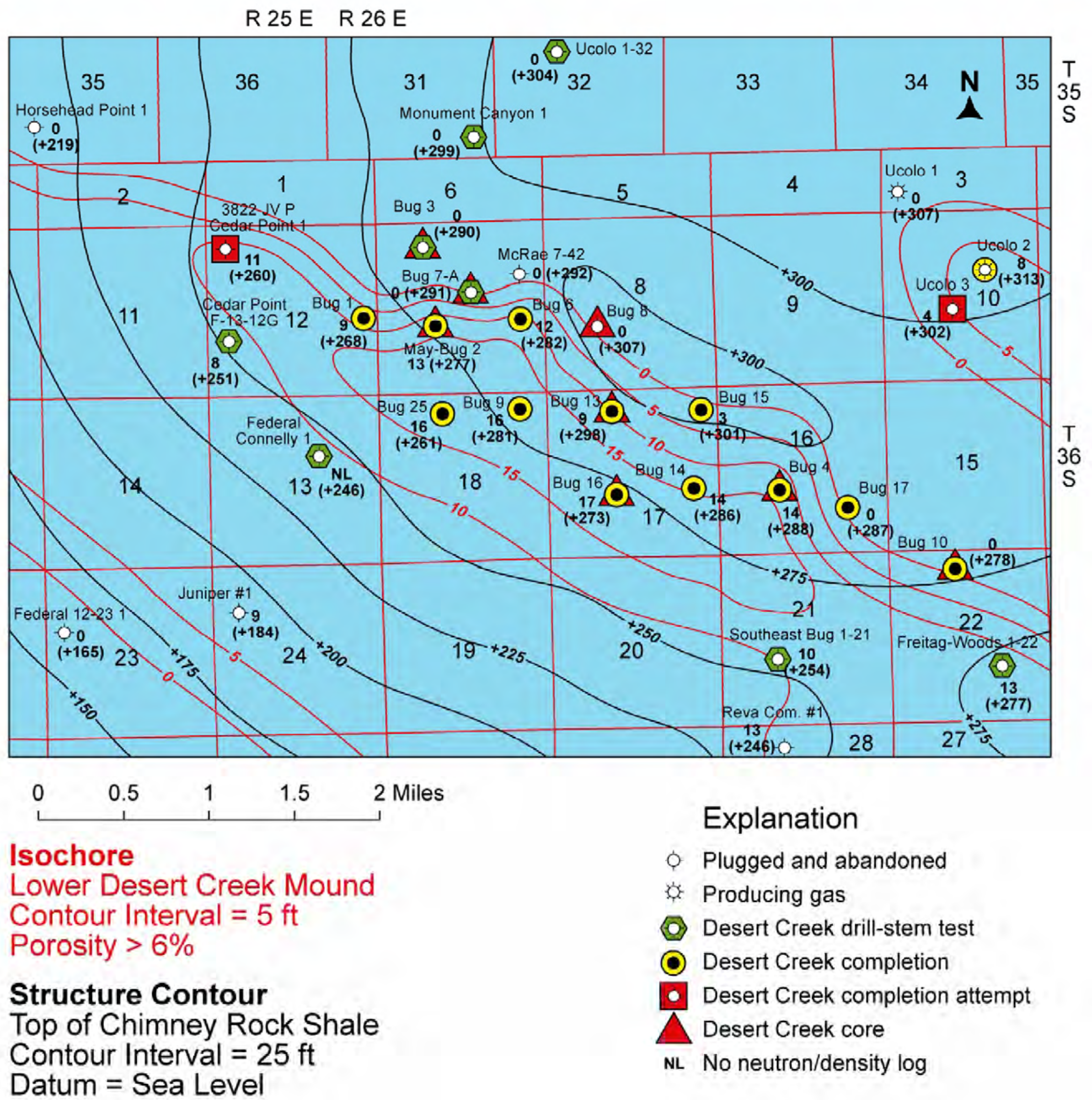

Figure 3-8. Combined Chimney Rock shale structure contour map and isochore map for the lower Desert Creek mound cap/mound core, Bug field, San Juan County, Utah.

Cherokee Field

Cherokee field structure contour maps on the top of upper Ismay clean carbonate and the upper Ismay zone were combined with isochore porosity maps of those intervals (figures 3-10 and 3-11). These maps clearly display the equant-shaped carbonate buildup on a gently southwest-plunging structural nose; the trap is especially well defined by the high proved water contact indicated on figure 3-10. They suggest untapped buildup potential to the northeast. The field limits are further defined by the lithofacies map (figure 3-12). A structure contour map on the top of the Chimney Rock shale (the marker bed just below the lower Desert Creek zone) of the Paradox Formation was also constructed for Cherokee field.

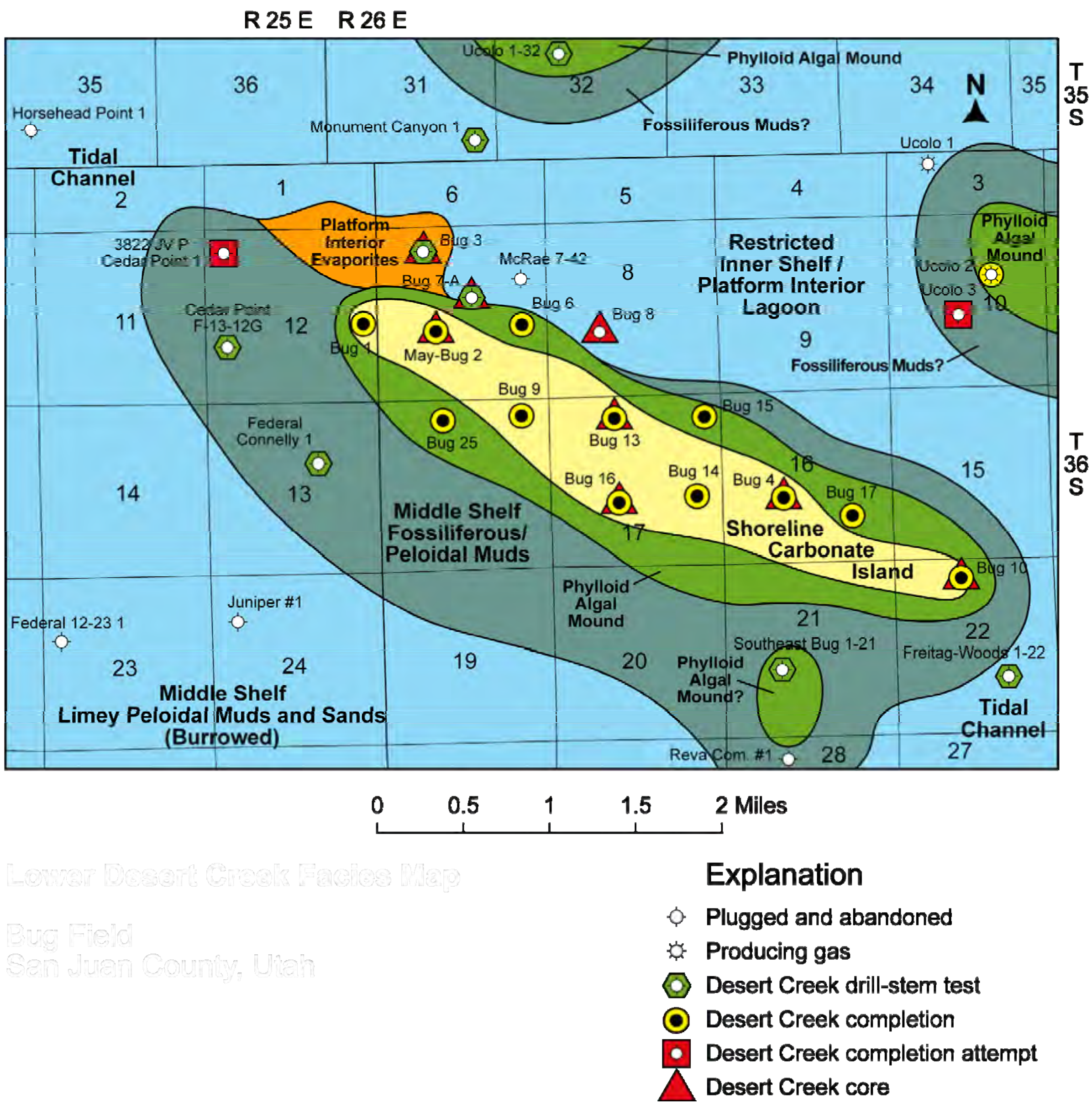

Figure 3-9. Lower Desert Creek zone lithofacies map, Bug field, San Juan County, Utah.

Isochore maps of the upper Ismay were generated for six reservoir units containing 6 percent or more porosity based on the average of the neutron and density porosity values (figures 3-13 through 3-19) identified from geophysical well logs. Five of them occur in the upper Ismay mound and the other one is in the lower part of the clean carbonate. The clean carbonate porosity unit exhibits a "false porosity" on geophysical well logs which led the operator to perforate the interval and attempt a completion. However, examination of core, thin sections, and porosity and permeability data from core plug analysis shows the unit is incapable of fluid flow due to low permeability. Therefore, porosity units 1 through 5 were mapped together to produce a gross interval isochore which represents the actual producing reservoir. Isochore maps were also constructed for the entire upper Ismay zone, upper Ismay clean carbonate, Hovenweep shale, and upper Ismay anhydrite (figures 3-20 through 3-23). The latter two units represent effective seals.

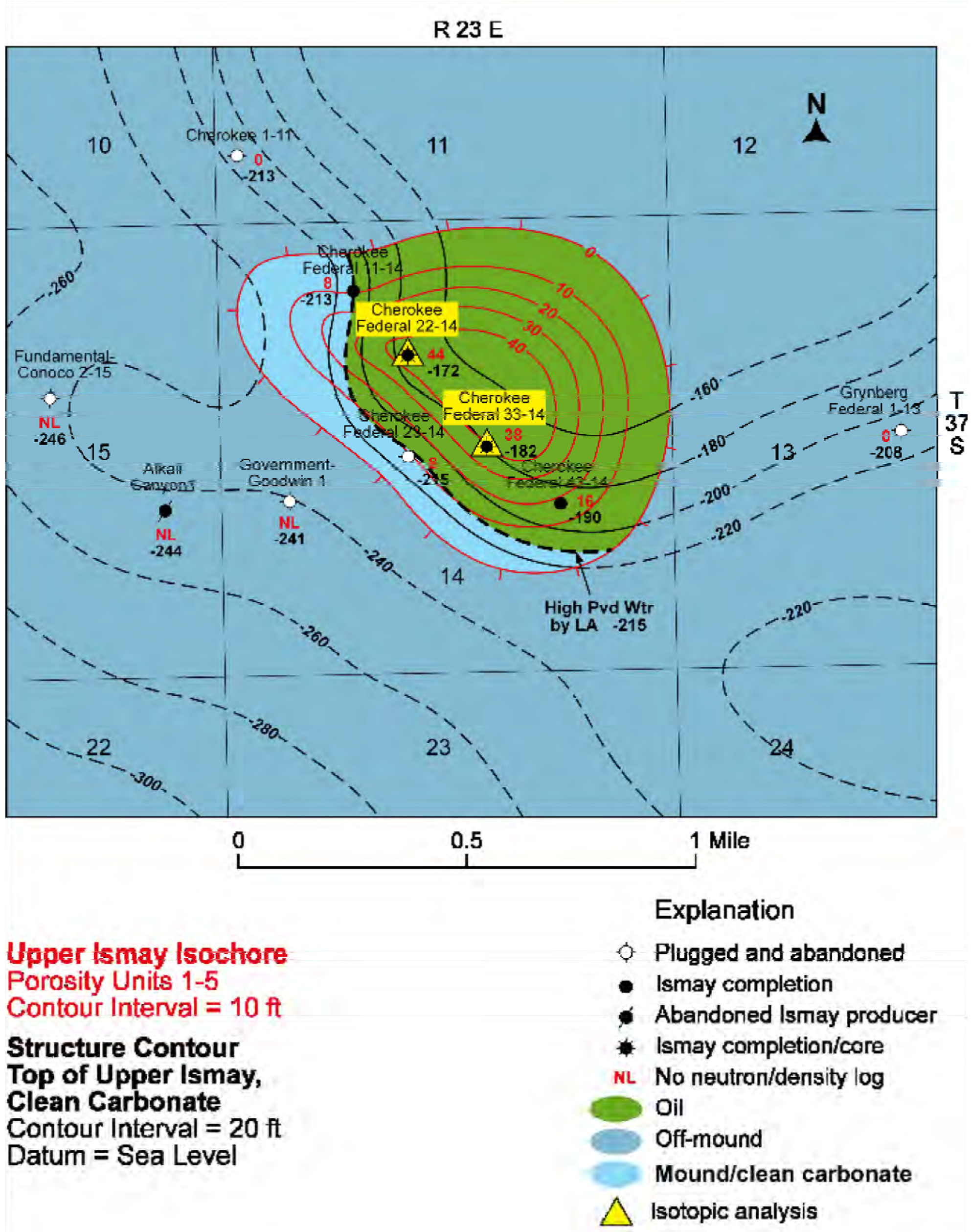

Figure 3-10. Map of combined top of "clean carbonate" structure and isochore of porosity units 1 through 5, upper Ismay zone, Cherokee field, San Juan County, Utah. Well cores used for isotope sampling for this study are highlighted with a yellow triangle (discussed later in Chapter 7).

Little Ute and Sleeping Ute Fields

Structure contour maps on the top of the upper Ismay zone (figure 3-24) and the lower Ismay zone (figure 3-25) of the Paradox Formation were constructed for Little Ute/Sleeping Ute study area. Though no cores were examined east of these fields, three additional wells, the 1 Ute C, Desert Canyon No. 2, and Desert Canyon No. 3 (see figure 3-24 for their locations), have been incorporated into all the structure contour and isopach maps described in this report.

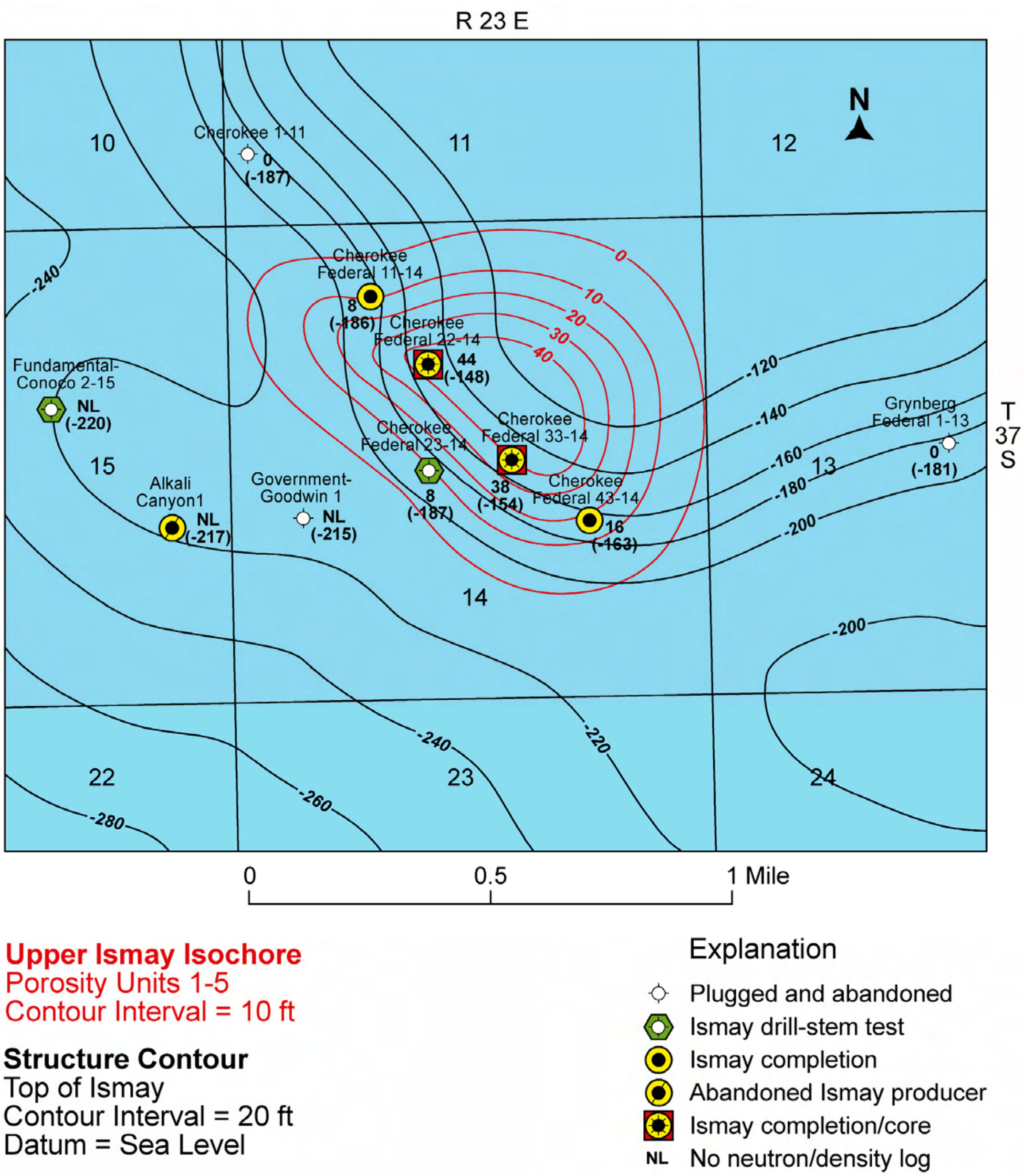

Figure 3-11. Combined upper Ismay zone structure contour map and isochore map for porosity units 1 through 5, Cherokee field, San Juan County, Utah.

The structure contour map of the upper Ismay (figure 3-24) indicates the dry, but with encouraging hydrocarbon shows, Desert Canyon No. 1 well (SW1/4 section 10, T. 34 N., R. 20 W.), to be downdip of the later-developed Little Ute and Sleeping Ute fields.

A net isopach map for the upper and lower Ismay zones was also generated (figure 3-26), showing the characteristic northwest-southeast depositional trend of the carbonate buildups in this part of the Blanding sub-basin. Interestingly, a net isopach map constructed for the underlying Gothic shale (figure 3-27) also revealed the same depositional orientation. The

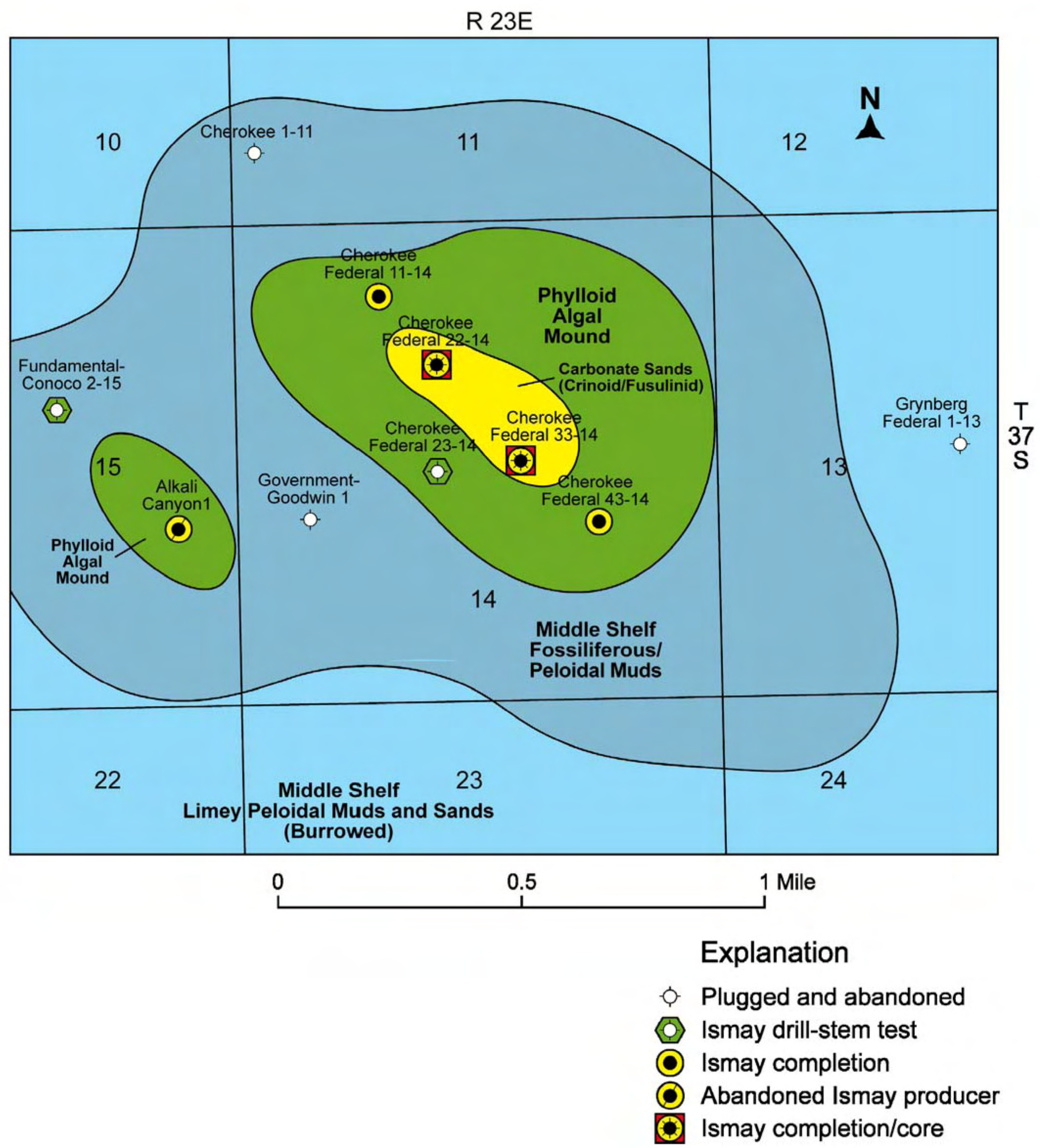

Figure 3-12. Upper Ismay zone lithofacies map, Cherokee field, San Juan County, Utah.

relationship between the thickness shown on figures 3-26 and 3-27 suggests that carbonate buildups were initiated on Gothic shale topographic highs. In comparison, the structure map on top of the Desert Creek zone below the Gothic shale (figure 3-28) displays gentle ramp dips to the southwest, giving no indication of topography that would account for the northwest-southeast-trending thick in the Gothic shale (figure 3-27). The factors responsible for these isopach trends in both the Gothic shale and the upper and lower Ismay zones (figures 13-26 and 3-27) are unknown at this time. Two additional maps, net porosity iospach of the upper Ismay zone (figure 3-29) and of the lower Ismay zone (figure 3-30), reflect the same northwest trends as mentioned above.

A larger single interval of phylloid-algal mound lithofacies is inferred to be present in

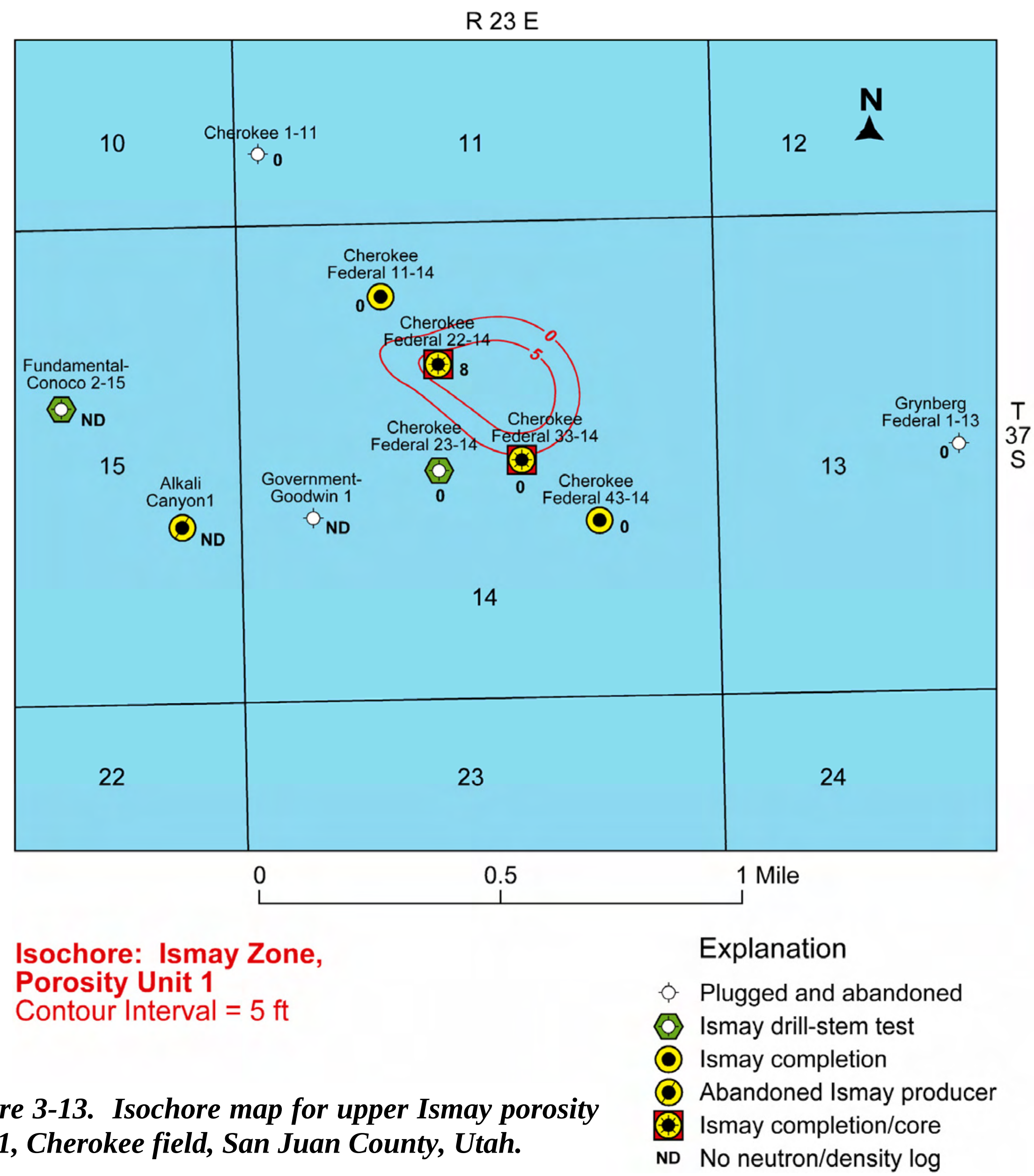

Figure 3-13. Isochore map for upper Ismay porosity unit 1, Cherokee field, San Juan County, Utah.

the Sleeping Ute No. 2 well. Though this well was cored, the core was not available for detailed analyses in this study. In comparison, the Sleeping Ute No. 1 well, the dry hole whose core was studied for this project, did not encounter the productive phylloid-algal mound lithofacies. The minor porosity zones in the bryozoan mound and mound talus lithofacies were insufficient for economic production. The Sleeping Ute No. 3 well encountered the phylloid-algal mound lithofacies, but it was not as well developed as in the adjacent wells. Low cumulative production in the Sleeping Ute No. 3 well may be caused by the lack of significant phylloid-algal mound thickness or drainage from the Sleeping Ute No. 2 well (see proximity of spacing between these two wells on figures 3-24 through 3-30). However, the actual cause is unclear at this time based on the data available to this study. Pressure and production information from the operator would give some insight into this situation.

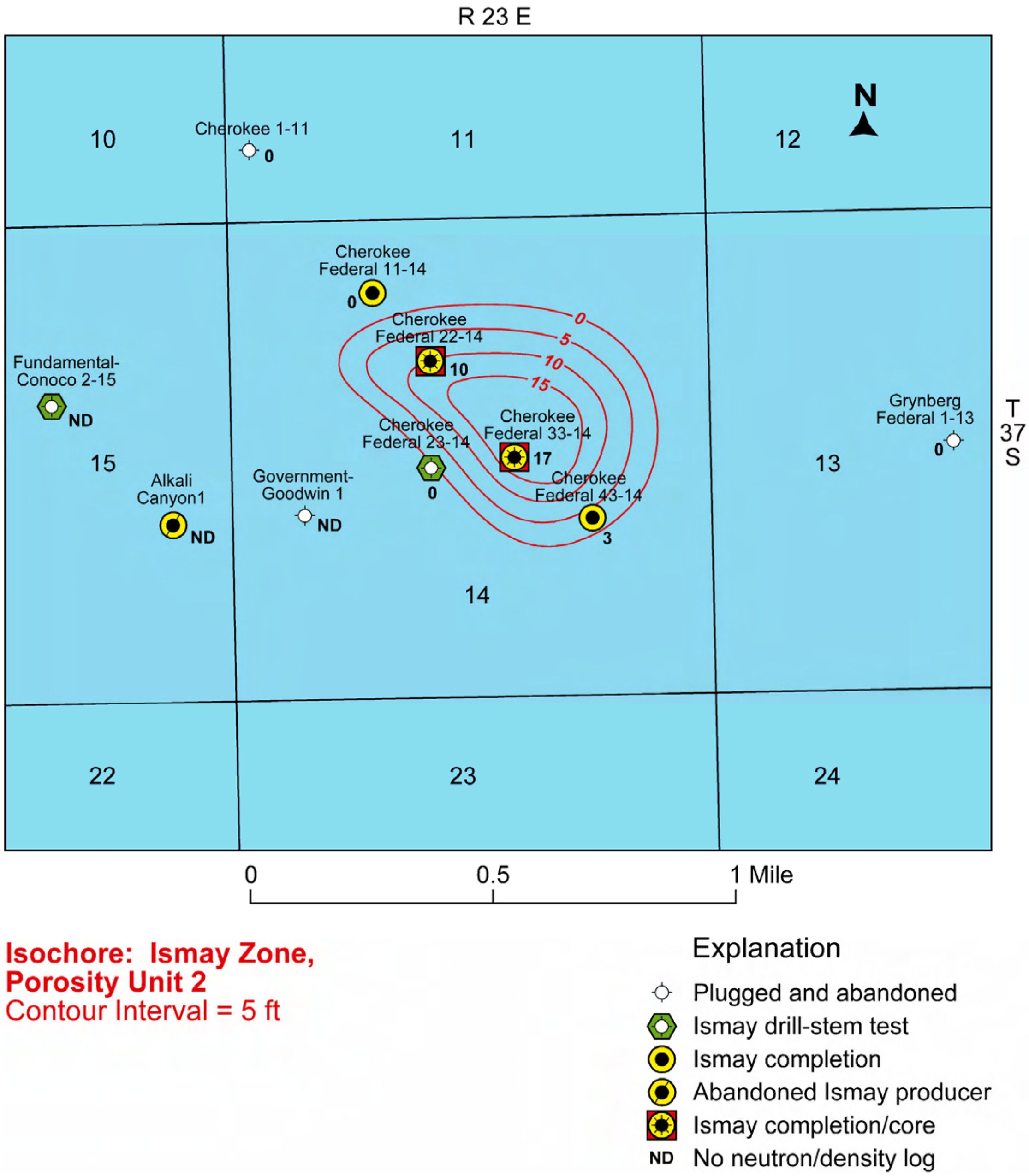

Figure 3-14. Isochore map for upper Ismay porosity unit 2, Cherokee field, San Juan County, Utah.

Reservoir Diagenetic Analysis

The diagenetic fabrics and porosity types found in the various hydrocarbon-bearing rocks of the case-study fields can be indicators of reservoir flow capacity, storage capacity, and potential for horizontal drilling. In order to determine the diagenetic histories of the various Ismay and Desert Creek reservoirs, thin sections of representative samples were selected from the conventional cores of each field for petrographic description and possible geochemical analysis (**Deliverable 1.2.1A – Thin Section Descriptions: Cherokee and Bug Fields, San Juan County, Utah, and Deliverable 1.2.1B – Thin Section Descriptions: Little Ute and**

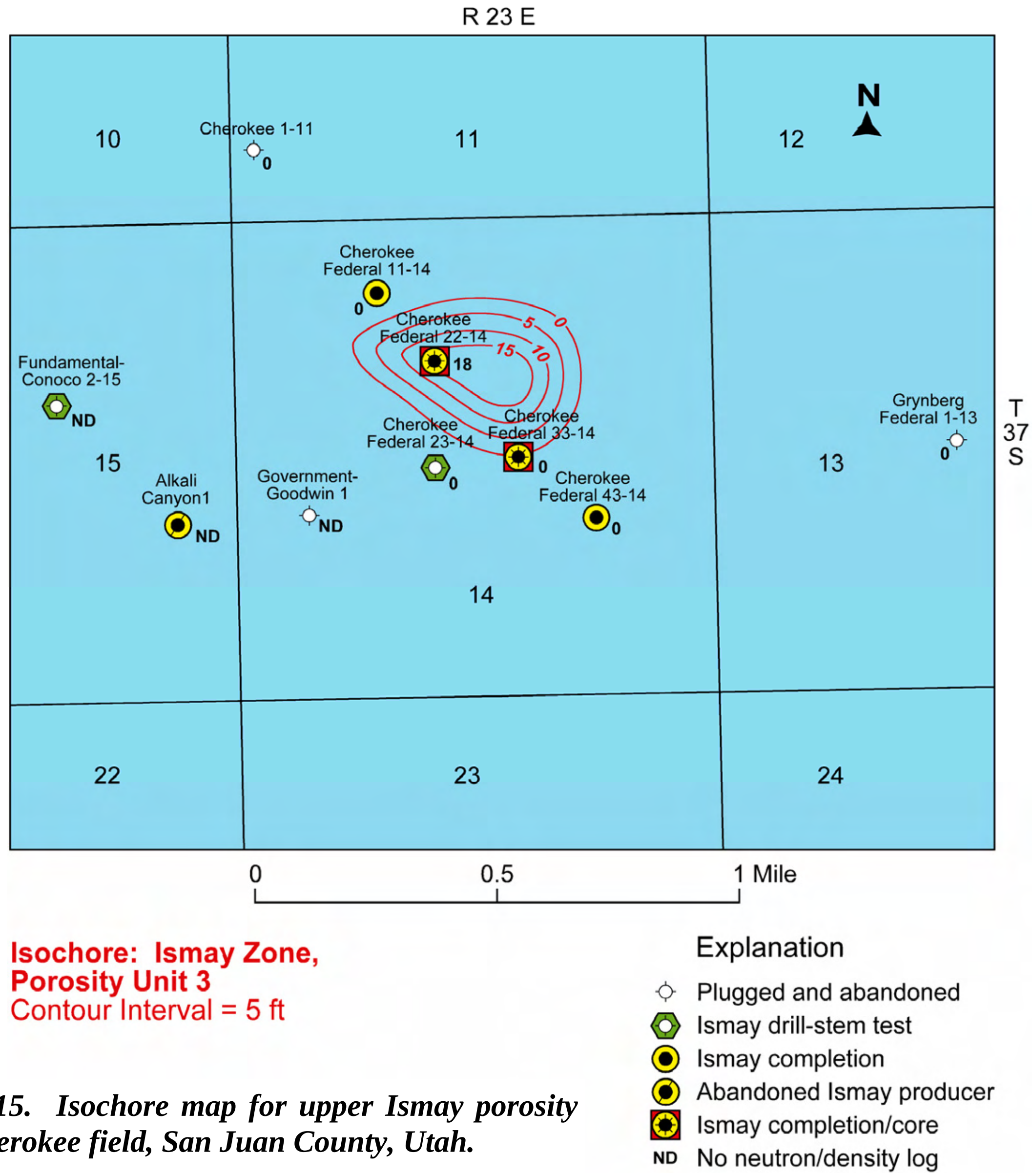

Figure 3-15. Isochore map for upper Ismay porosity unit 3, Cherokee field, San Juan County, Utah.

Sleeping Ute Fields, Montezuma County, Colorado). Carbonate fabrics were determined according to Dunham's (1962) and Embry and Klovan's (1971) classification schemes. Each thin section was photographed with additional close-up photos of (1) typical preserved primary and secondary pore types, (2) cements, (3) sedimentary structures, (4) fractures, and (5) pore plugging anhydrite and halite.

Reservoir diagenetic fabrics and porosity types of these carbonate buildups were analyzed to (1) determine the sequence of diagenetic events, (2) predict lithofacies patterns, and (3) provide data input for reservoir modeling studies. Diagenetic characterization focused on reservoir heterogeneity, quality, and compartmentalization within the case-study fields. All depositional, diagenetic, and porosity information can be combined with each field's production history in order to analyze the potential for success of each horizontal drilling candidate. Of special interest is the determination of the most effective pore systems for oil drainage versus storage.

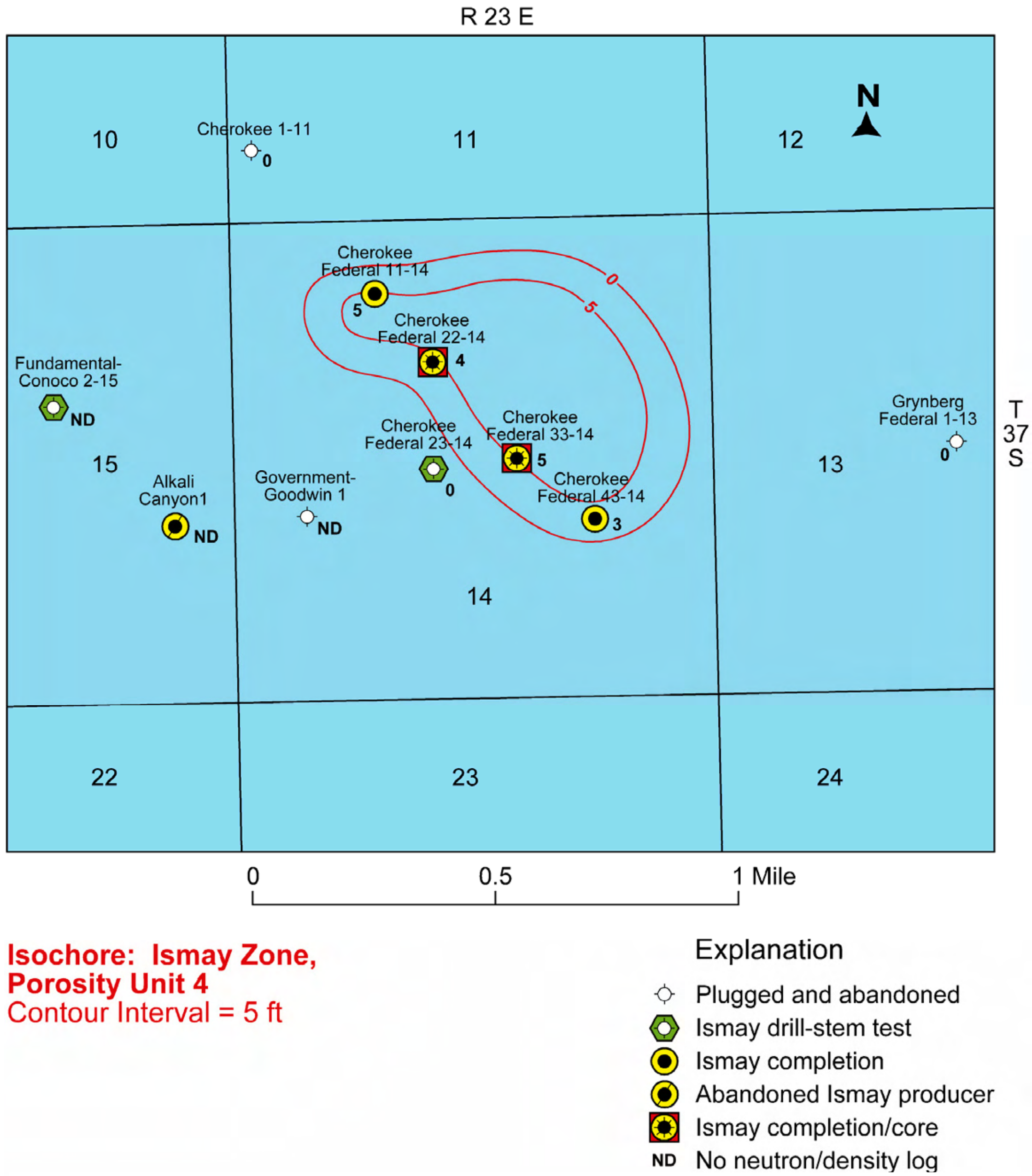

Figure 3-16. Isochore map for upper Ismay porosity unit 4, Cherokee field, San Juan County, Utah.

Bug and Cherokee fields were selected for additional petrographic, geochemical, and petrophysical techniques (described in later chapters). These techniques included (1) scanning electron microscope analysis of various dolomites to determine reservoir quality of the dolomites as a function of diagenetic history, (2) epifluorescence and cathodoluminescence petrography for the sequence of diagenesis, (3) stable carbon and oxygen isotope analysis of diagenetic components such as cementing minerals and different generations of dolomites, and (4) capillary pressure/mercury injection analysis.

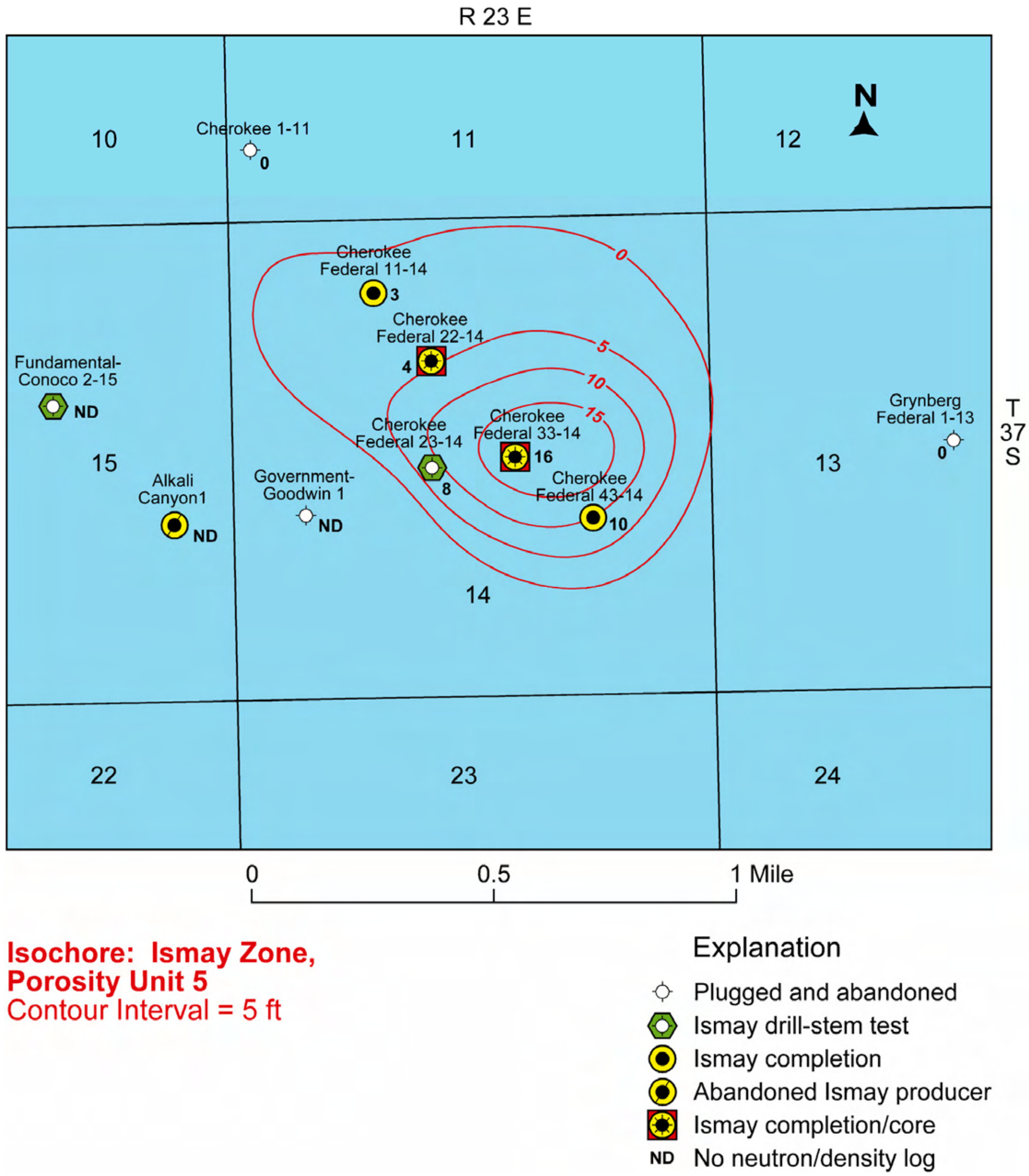

Figure 3-17. Isochore map for upper Ismay porosity unit 5, Cherokee field, San Juan County, Utah.

Bug Field

The lower Desert Creek zone in Bug field consists entirely of dolomite. The pore system observed in thin section shows a reservoir that has been predominantly affected by subaerial exposure. Solution-enlarged grain molds (sometimes originally phylloid-algal plates) and fractures are common; both of these types of pores are often lined with black bitumen. The remaining matrix consists of tight dolomite. Remnants of primary, interparticle pores are also observed between small pisolites and grain aggregates, but are often lined or plugged with late anhydrite cements or bitumen. The result is that both effective and ineffective pores are present.

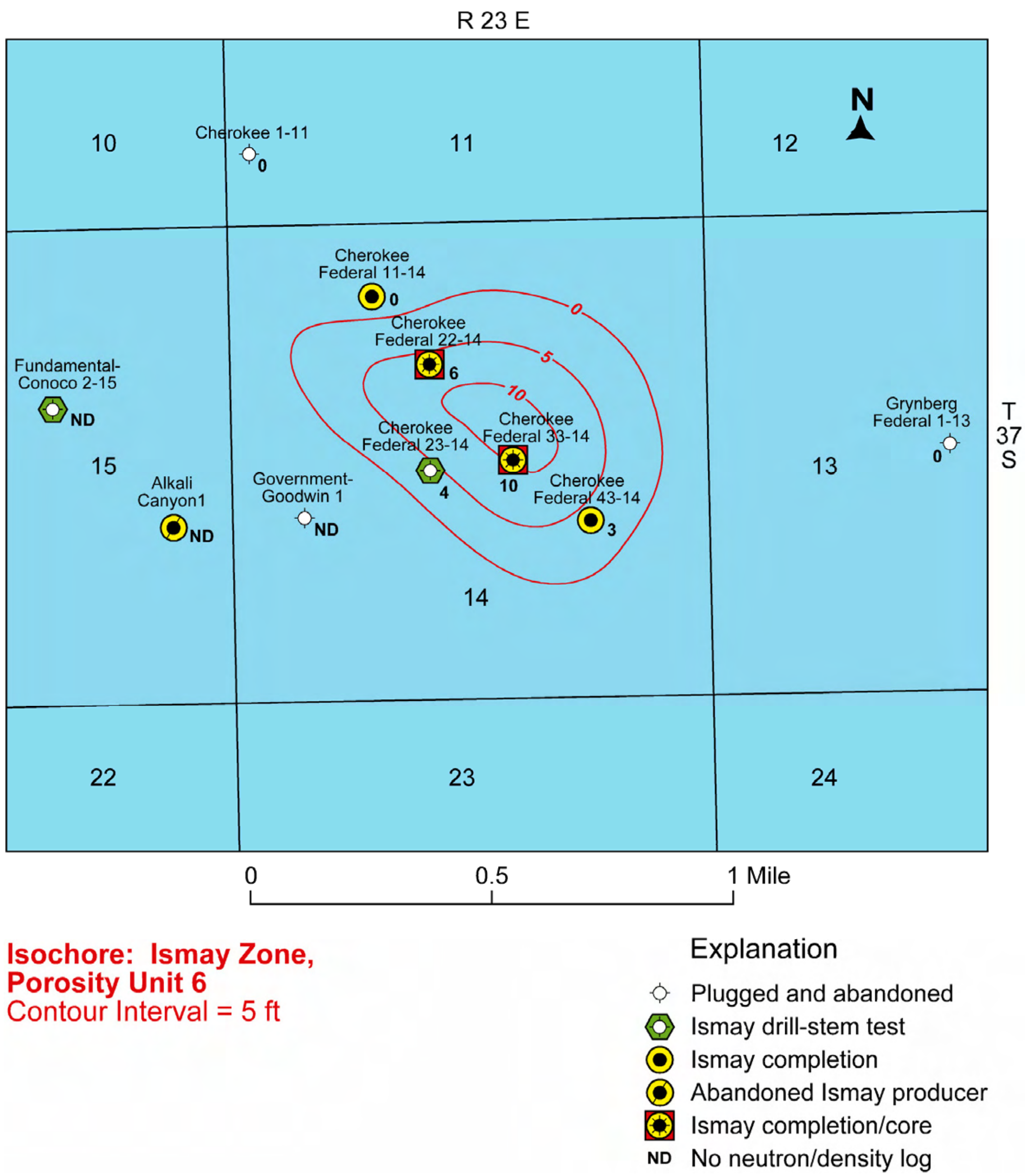

Figure 3-18. Isochore map for upper Ismay porosity unit 6, Cherokee field, San Juan County, Utah.

The most significant and unique diagenetic characteristic observed in the Bug field thin sections was extensive "micro-boxwork" porosity. Figure 3-31 is a photomicrograph showing the pattern of patchy dolomite dissolution which includes a micro-boxwork pattern of pores. Some of the pores in this view occur between elongate, rectilinear networks of dolomite "lathes." Our interpretation is that the intense micro-boxwork porosity developed early from subaerial exposure of the phylloid-algal buildup. The micro-boxwork porosity represents an important site for untapped hydrocarbons.

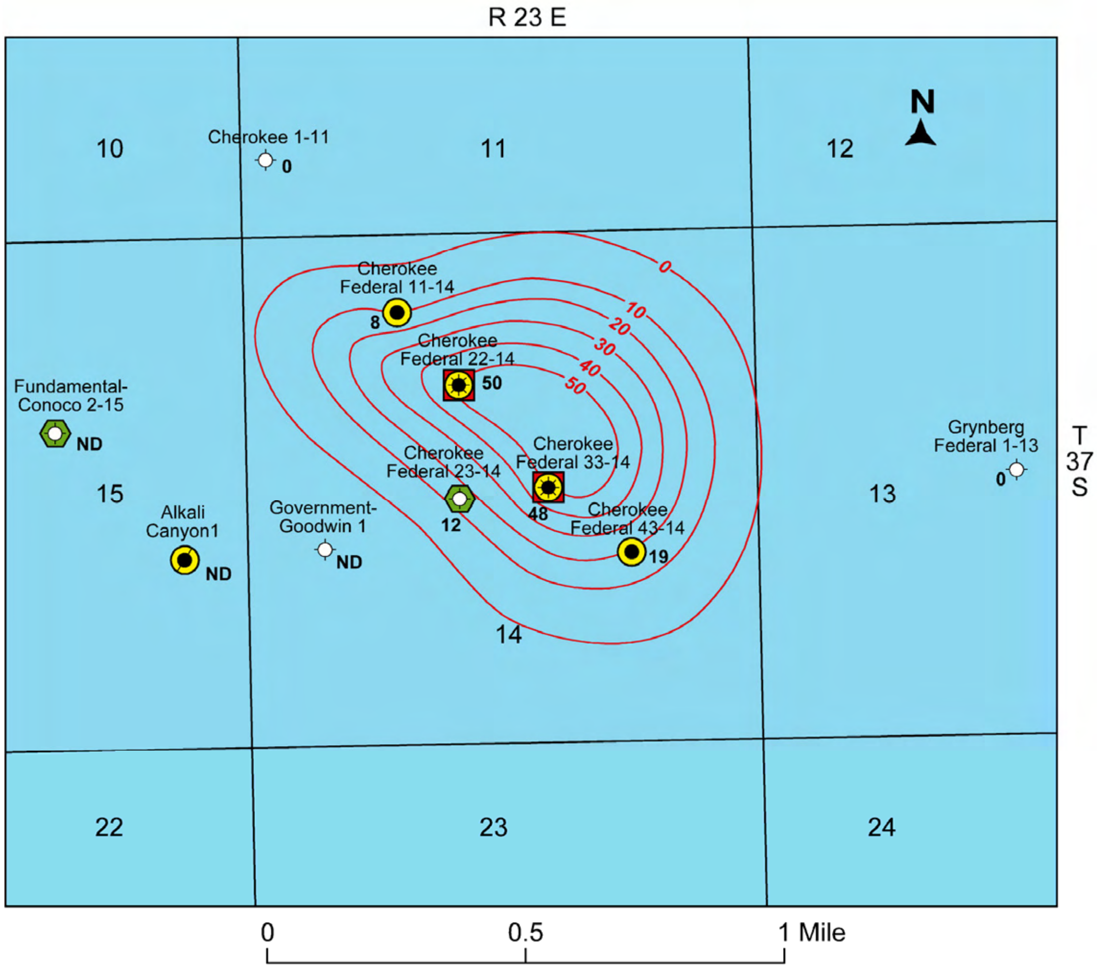

Figure 3-19. Isochore map for upper Ismay porosity units 1 through 6, Cherokee field, San Juan County, Utah.

Cherokee Field

The upper Ismay zone in Cherokee field consists of both limestone and dolomite, although there appears to be more dolomite in core than observed in thin section. Petrographic analysis shows the typical mound-lithofacies limestone consists of skeletal phylloid-algal bafflestone with anhydrite plugging early pore space. The calcarenite lithofacies consists of skeletal grainstone limestone, with primary interparticle and intraparticle porosity, and early moldic porosity. Some mixing-zone dolomite and dog-tooth spar (meteroic cement) are present. The low-energy, middle-shelf lithofacies typically consists of dolomite, packstone/ wackestone, with peloids, crinoids, and bryozoans. Early dolomitization and late solution-enlarged channels, and anhydrite and bitumen plugging are common.

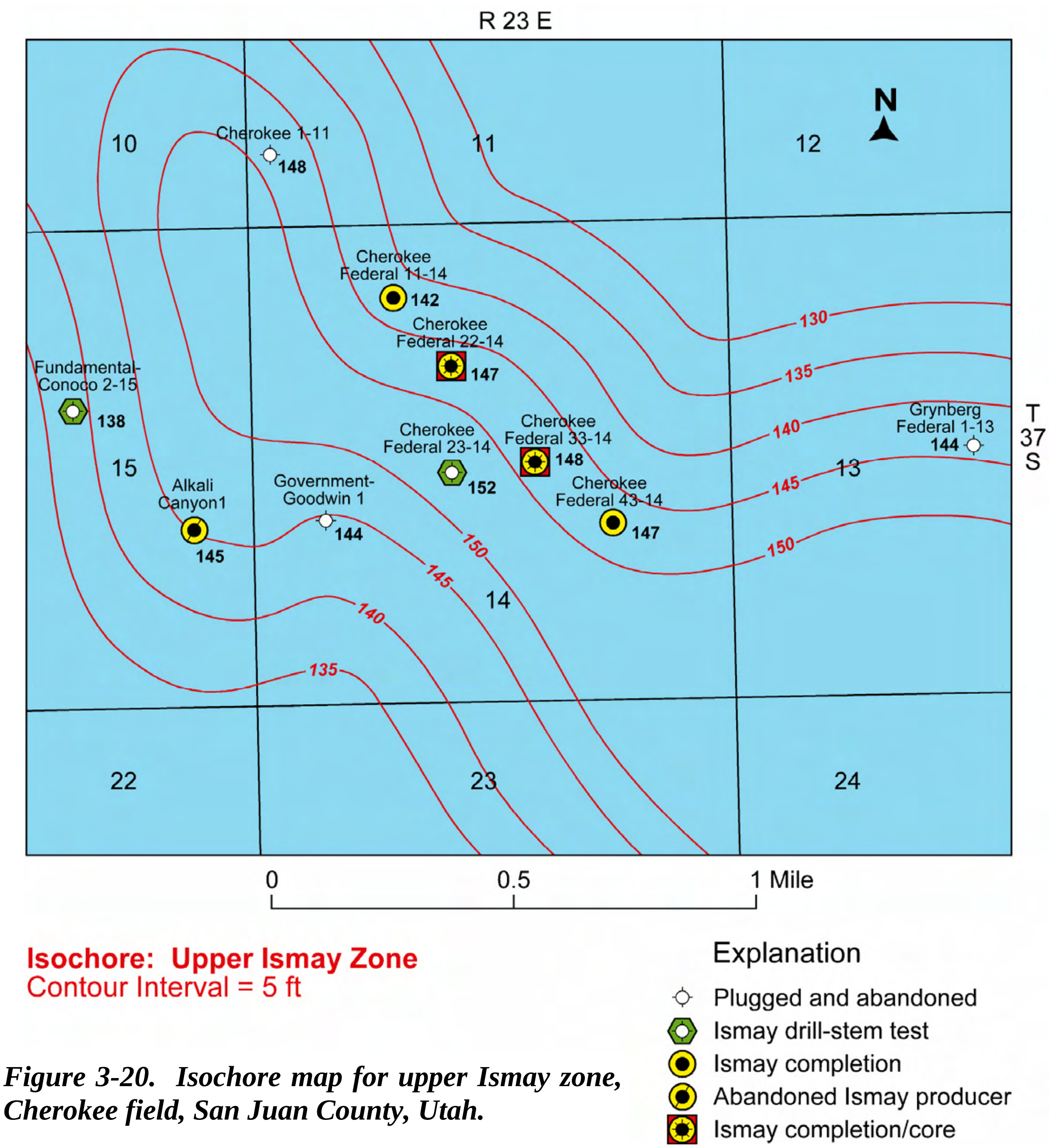

Figure 3-20. Isochore map for upper Ismay zone, Cherokee field, San Juan County, Utah.

The most significant and unique diagenetic characteristic observed in the Cherokee field thin sections was extensive microporosity. In fact, much of the "dolomite" observed on the slabbed surface of the core is alteration which features microporosity. Figure 3-32 is a photomicrograph of peloidal packstone/grainstone dominated by microporosity. The sequence of diagenetic events consisted of (1) early dolomitization by hypersaline or mixing zone brines, (2) styolitization, (3) late dissolution/micropores, (4) anhydrite replacement, and (5) bitumen plugging. We believe the intense microporosity developed late, along solution fronts by the action of aggressive hydrothermal solutions from depth (carbon dioxide escaping from Mississippian Leadville Limestone or from deep decarboxylation of organic matter). At any rate, like the microporosity in Bug field, this microporosity represents an important site for untapped hydrocarbons.

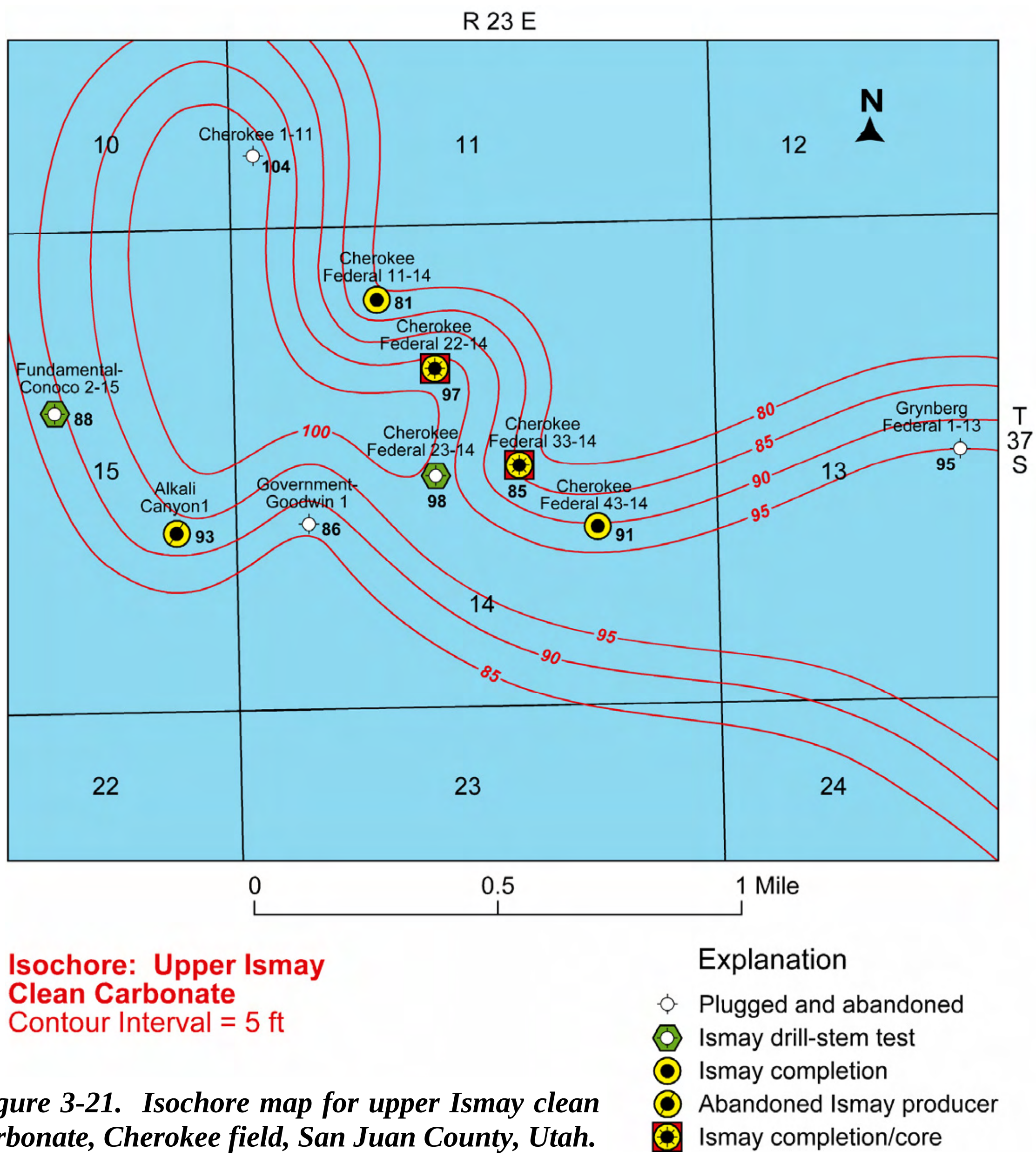

Figure 3-21. Isochore map for upper Ismay clean carbonate, Cherokee field, San Juan County, Utah.

Little Ute and Sleeping Ute Fields

Representative photomicrographs of various Little Ute/Sleeping Ute lithofacies display the nature and extent of the reservoir porosity and permeability. The phylloid-algal mound lithofacies photomicrograph (figure 3-33) shows the stunning reservoir development as seen by the blue impregnated pores. Leaching of the carbonate constituents, with porosity enhancement from dolomitization, creates an excellent reservoir. In comparison, the reservoir capability of the bryozoan mound lithofacies (figure 3-34) is limited due to the isolated pores that are restricted to minor corrosion and intraparticle spaces. The mound talus lithofacies, in general, is not a good reservoir as shown in figure 3-35. The porosity that is present is remnant interparticle and some solution porosity as shown in blue in figure 3-35. The lagoonal/ restricted marine lithofacies (figure 3-36) has excellent porosity developed in a dolomitic

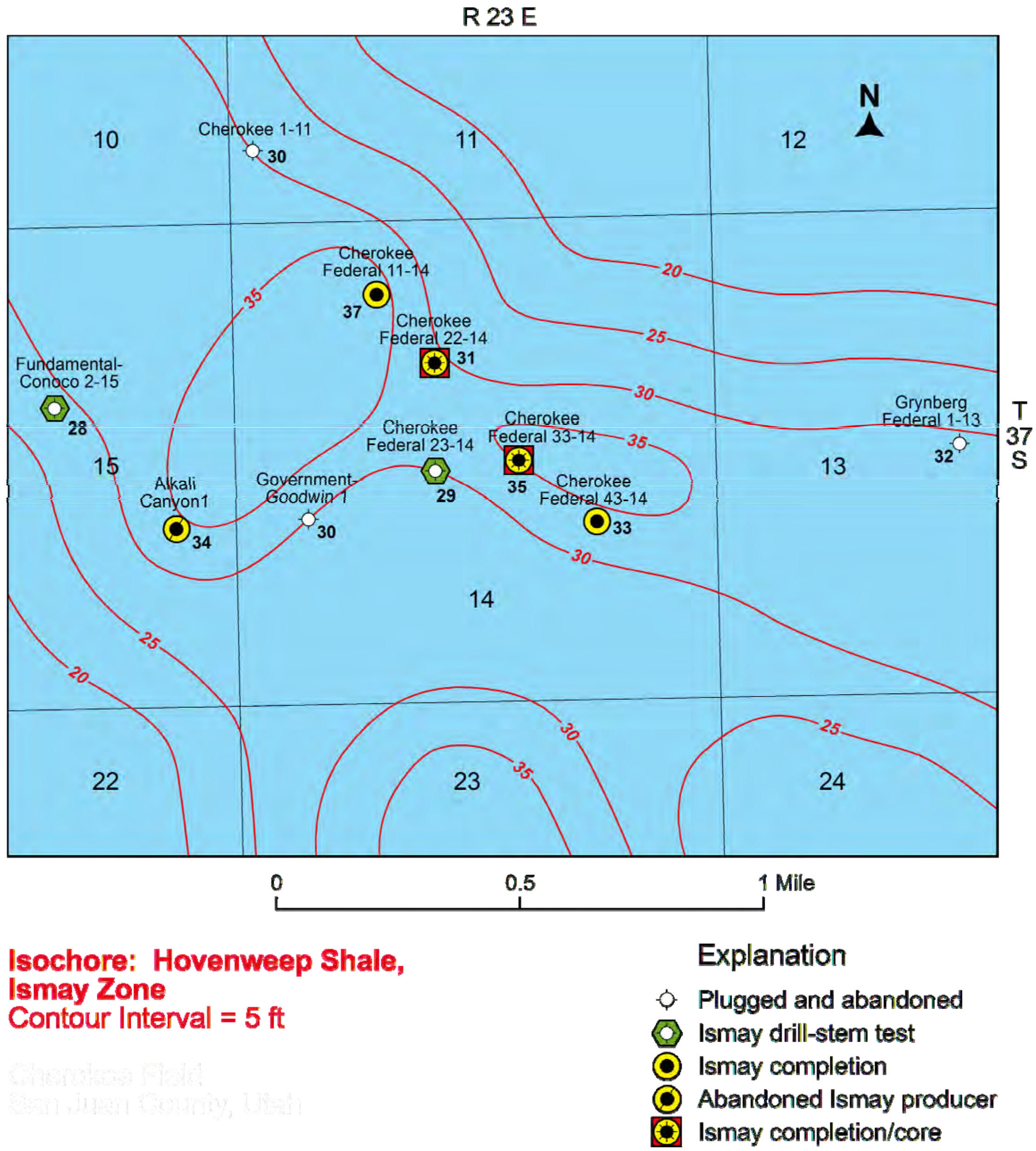

Figure 3-22. Isochore map for Hovenweep shale of the Ismay zone, Cherokee field, San Juan County, Utah.

mudstone with limited and variable permeability. The calcarenite shoal lithofacies is one that, on geophysical well logs, appears to exhibit fair to good reservoir porosity development. The problem, however, is that the intergranular and moldic porosity seen in figure 3-37 is isolated, and thus the permeability is extremely low. Finally, the open-marine lithofacies is replete with fossil fragments, some of which contain isolated moldic pores. Porosity, such as shown in figure 3-38, is actually quite good, but the lack of permeability connecting these isolated pores results in a poor reservoir rock.

The Little Ute/Sleeping Ute Ismay lithofacies contain a wide variety of pore types and associated reservoir characteristics. Interparticle porosity, shown in figure 3-39, contains pores that are remnants of the original interparticle pore system between the skeletal components in

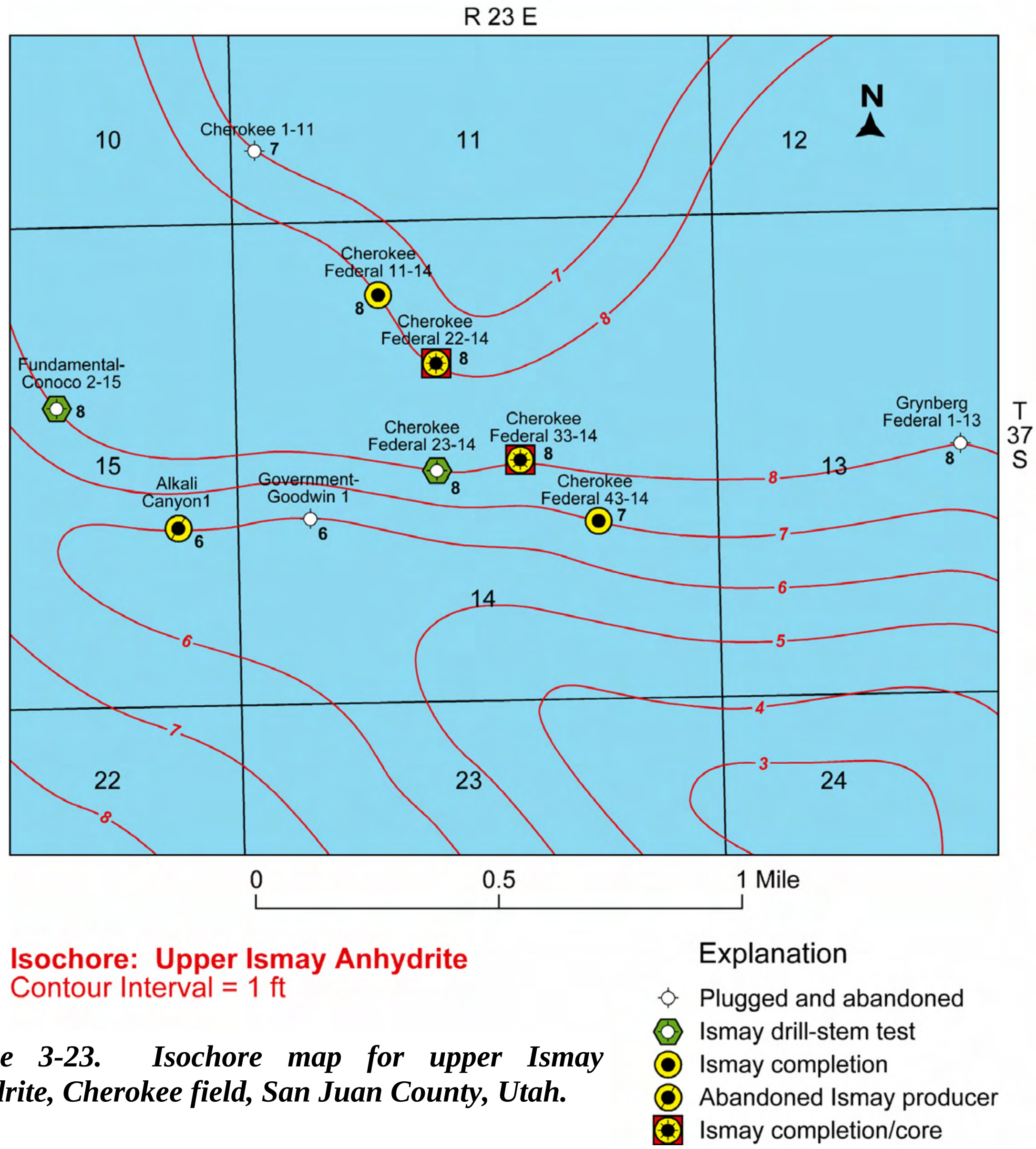

Figure 3-23. Isochore map for upper Ismay anhydrite, Cherokee field, San Juan County, Utah.

this grainstone. The paragenetic sequence of diagenesis suggests that most of the original pore space has been occluded by early marine cements, meteoric calcite spar, and minor anhydrite precipitation. The diagenetic overprint on what was originally an excellent reservoir rock renders the resultant sample poor reservoir rock due to lack of permeability between the isolated pores. Intraparticle porosity can create either good or poor reservoir rock, depending once again on the permeability network. Figure 3-40 shows good reservoir porosity, but a range in permeability that appears to be dependent upon the type of organisms in which the intraparticle porosity develops. This figure illustrates nicely that the phylloid-algal mound lithofacies comprises superior reservoir characteristics compared to the bryozoan mound lithofacies. The phylloid-algal mound lithofacies also contains examples of shelter porosity as seen in figure 3-41. Large pores develop under or between platy phylloid algal plates and/or curvilinear bivalve shells. Reservoir quality is degraded, however, when early cementation occludes these pores either partially or completely.

Early dissolution of skeletal grains and evaporite mineral crystals can also create moldic

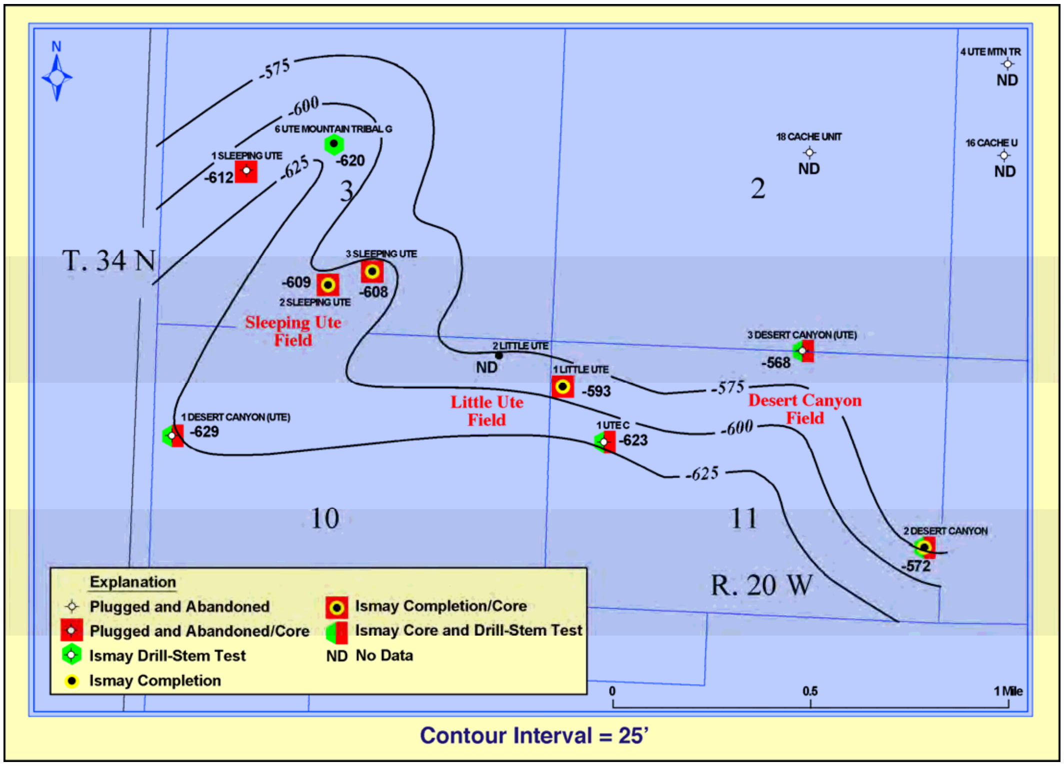

Figure 3-24. Upper Ismay zone structural contour map, Little Ute, Sleeping Ute, and Desert Canyon fields, Montezuma County, Colorado.

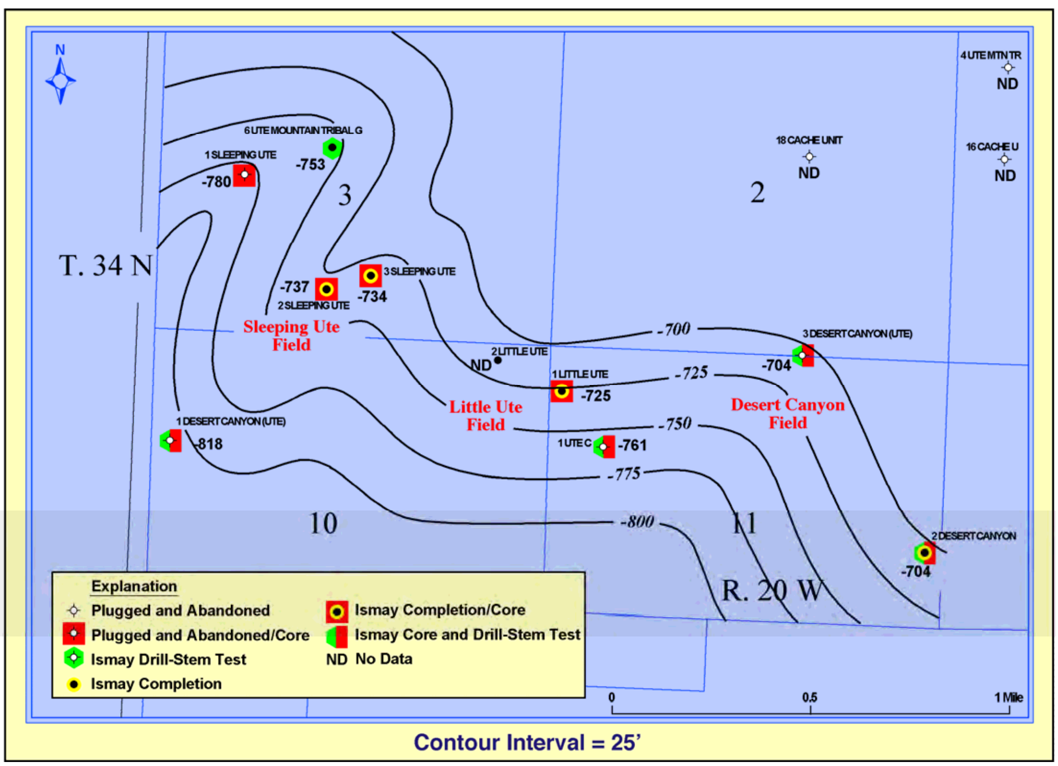

Figure 3-25. Lower Ismay zone structural contour map, Little Ute, Sleeping Ute, and Desert Canyon fields, Montezuma County, Colorado.

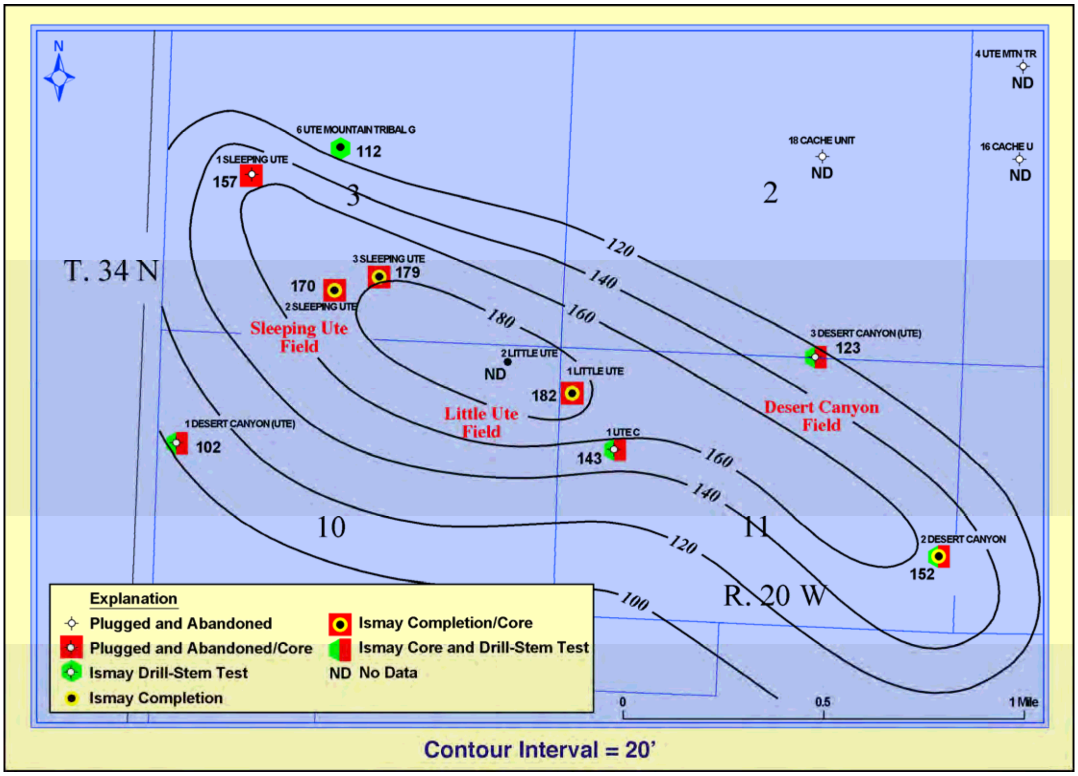

Figure 3-26. Upper and lower Ismay zone net isopach map, Little Ute, Sleeping Ute, and Desert Canyon fields, Montezuma County, Colorado.

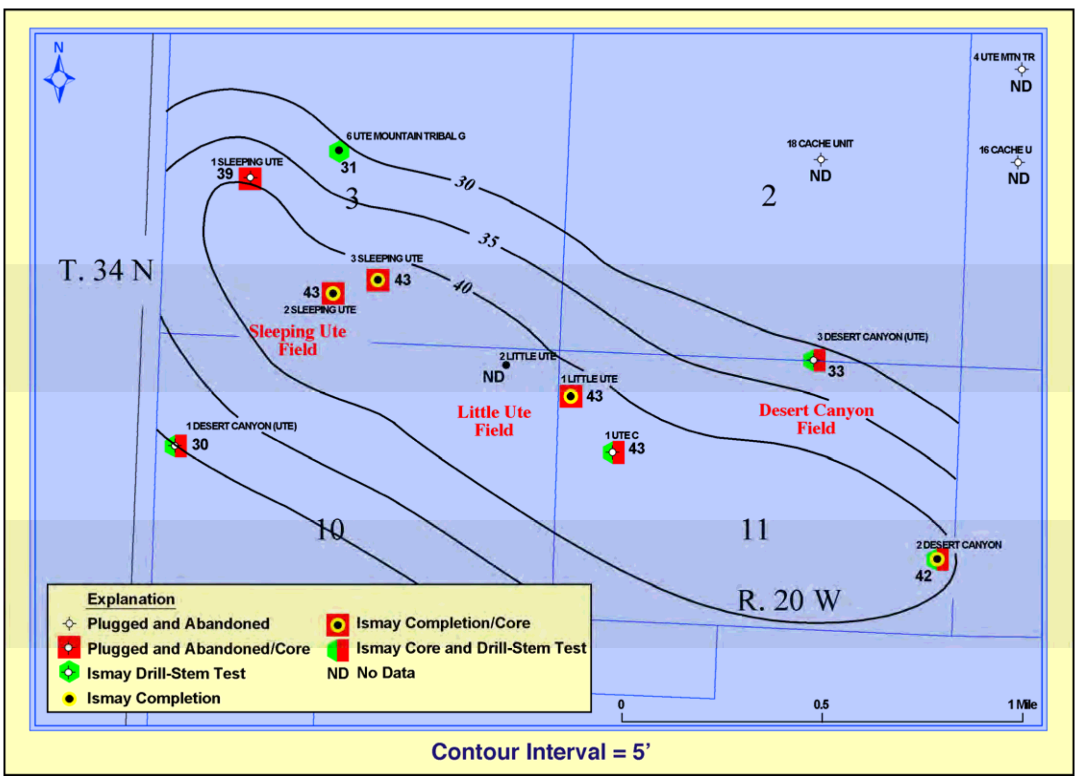

Figure 3-27. Gothic shale isopach map, Little Ute, Sleeping Ute, and Desert Canyon fields, Montezuma County, Colorado.

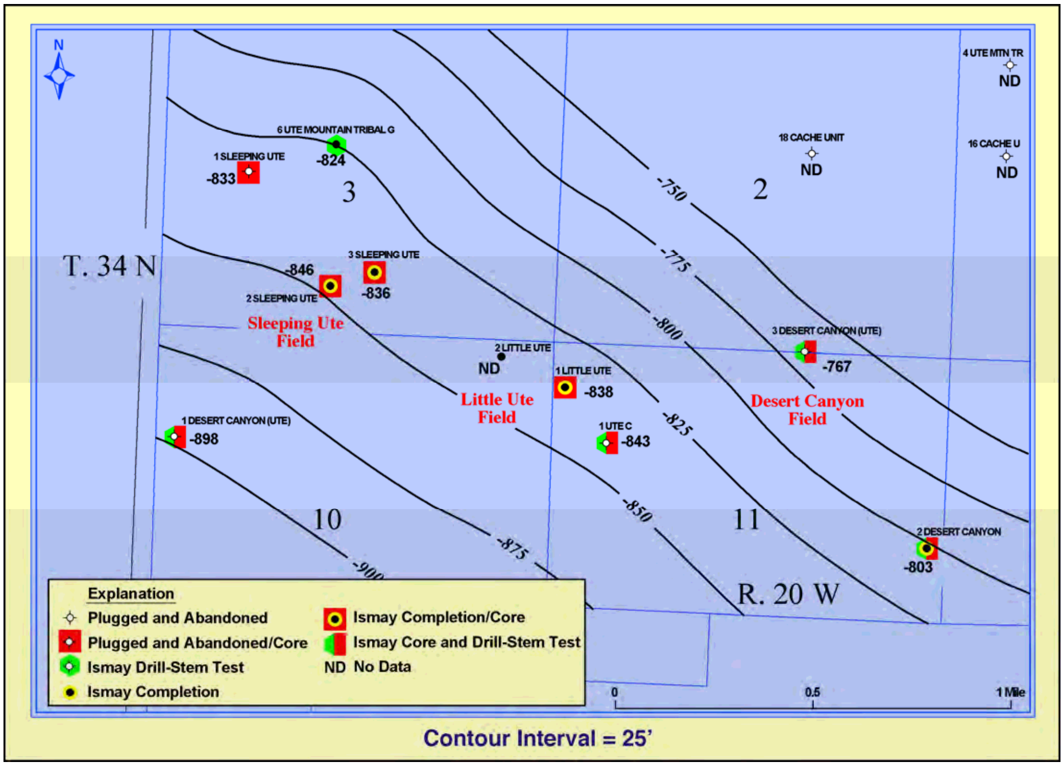

Figure 3-28. Desert Creek zone structural contour map, Little Ute, Sleeping Ute, and Desert Canyon fields, Montezuma County, Colorado.

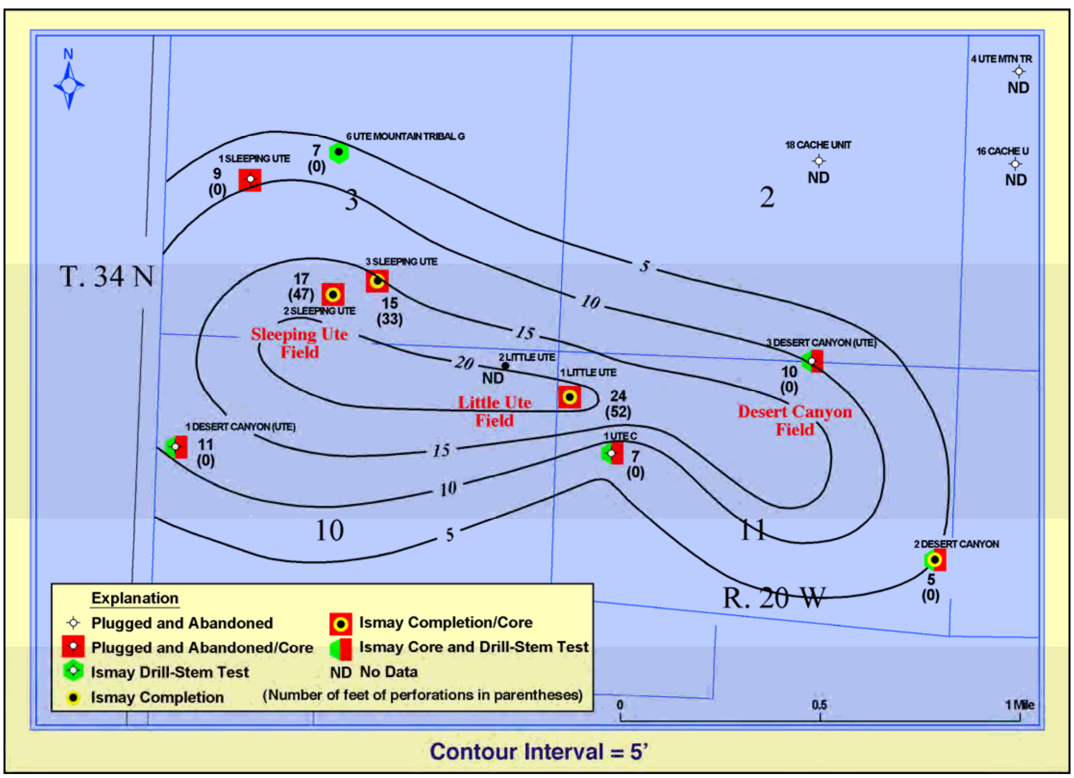

Figure 3-29. Upper Ismay zone net porosity (≥ 6 percent) isopach map, Little Ute, Sleeping Ute, and Desert Canyon fields, Montezuma County, Colorado.

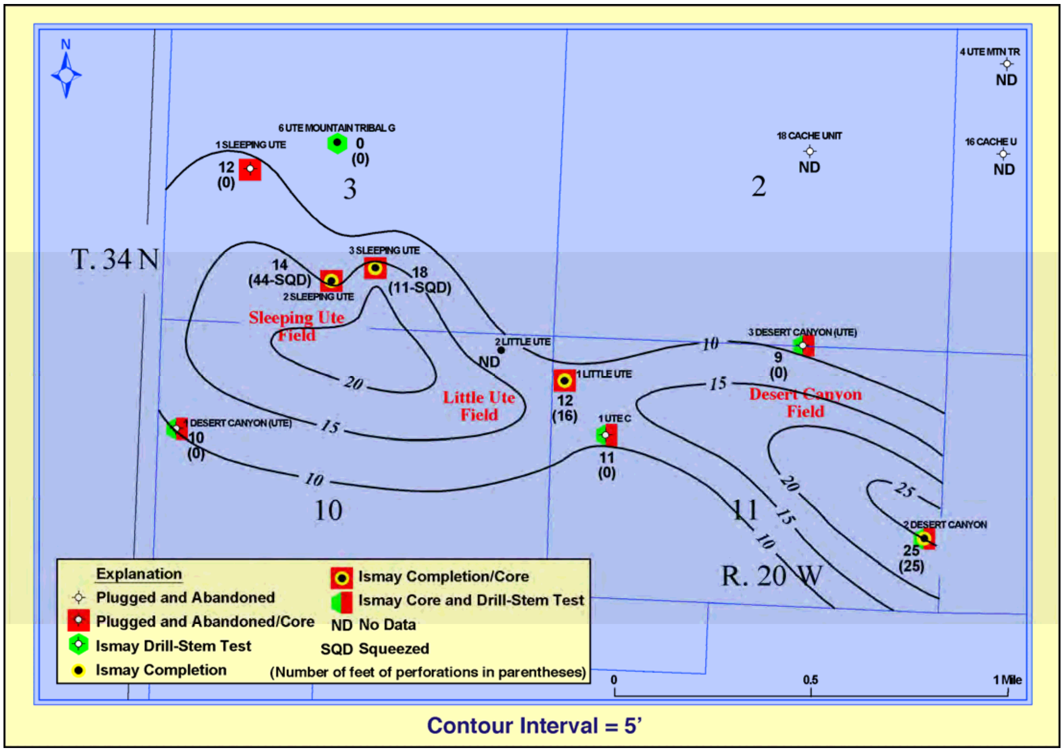

Figure 3-30. Lower Ismay zone net porosity (≥ 6 percent) isopach map, Little Ute, Sleeping Ute, and Desert Canyon fields, Montezuma County, Colorado.

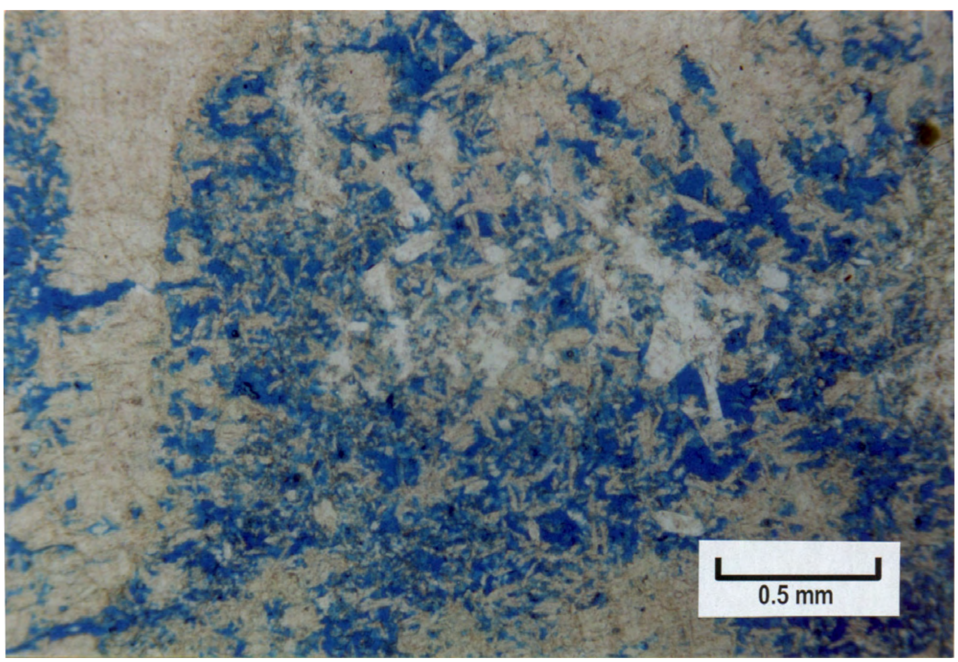

Figure 3-31. Photomicrograph (plane light with white card technique [diffused light using a piece of paper on the stage of the microscope]) showing a pattern of patchy dolomite dissolution which includes a “micro-boxwork” pattern of pores (in blue). Bug No. 10, 6327.5 feet, porosity = 10.5 percent, permeability = 7.5 mD.

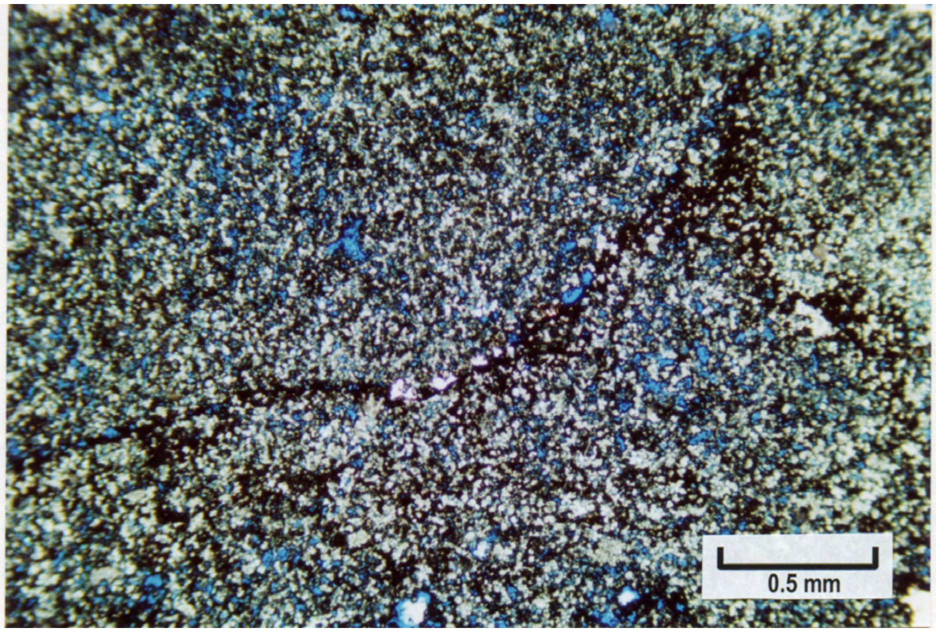

Figure 3-32. Photomicrograph (plane light) of a peloidal packstone/ grainstone dominated by microporosity. Cherokee No. 22-14, 5768.7 feet, porosity = 22.9 percent, permeability = 215 mD.

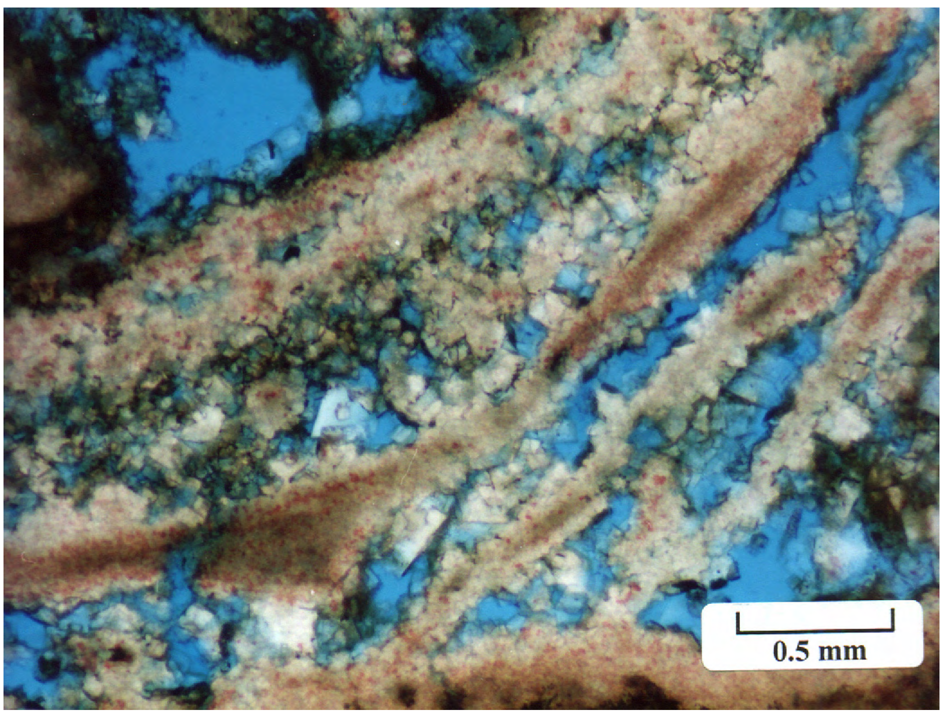

Figure 3-33. Photomicrograph (plane light with white card technique) showing a phylloid-algal mound bafflestone with a partially dolomitized and leached limestone stained with Alizarin Red-S solution. This sample exhibits much higher porosity and permeability than the undolomitized examples. Micritized remnants of phylloid algal plate rims (in red) are surrounded by partially dolomitized lime muds (white rhombs) and open pores (in blue). Little Ute No. 1 well, 5882.5 feet, porosity = 18.4 percent, permeability = 95.6 mD.

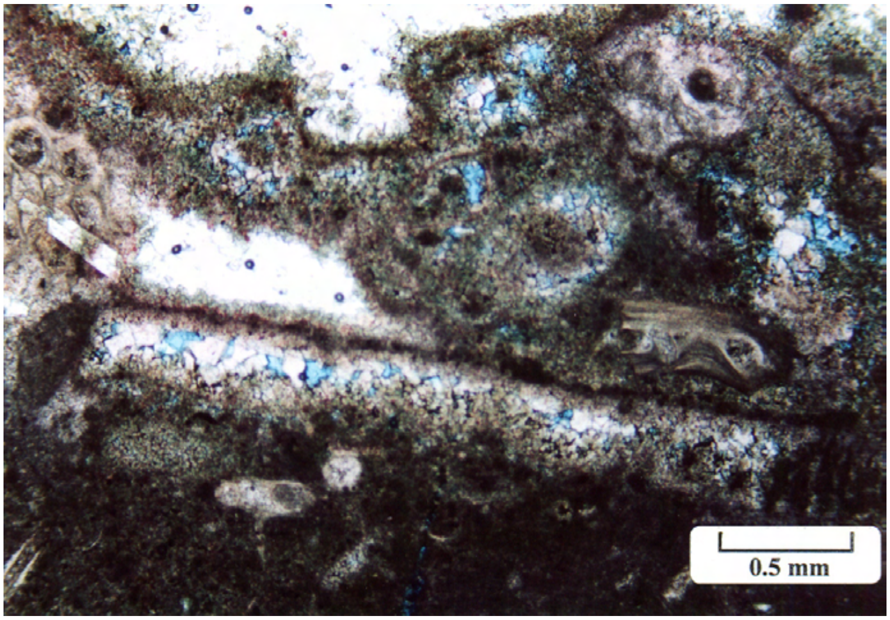

***Figure 3-34.** Photomicrograph (plane light) showing a bryozoan mound. This low-magnification micrograph shows poorly preserved remnants of bryozoan tubular clusters surrounded by vaguely peloidal lime muds. The large white masses in this view are composed of replacement anhydrite. Most of the porosity (in blue) is very isolated and restricted to minor corrosion and intraparticle spaces. Sleeping Ute No. 1 well, 5599.3 feet, porosity = 2.5 percent, permeability = 1.30 mD.*

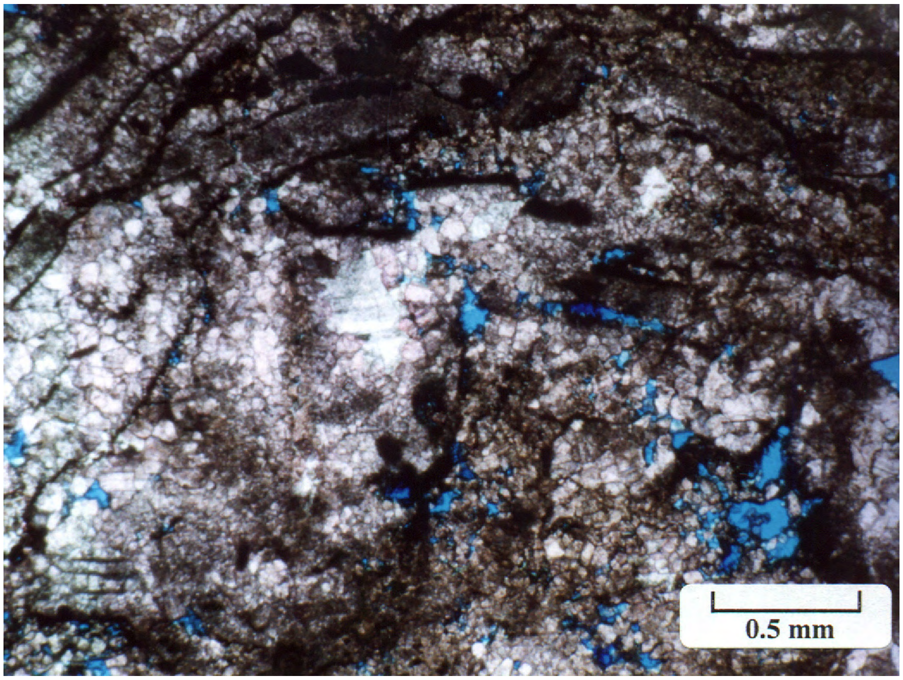

***Figure 3-35.** Photomicrograph (plane light) of mound talus showing elongate clasts of mud and fossil fragments that were probably derived from nearby bryozoan and phylloid-algal mounds. Remnant interparticle and modest solution porosity can be seen in blue. Sleeping Ute No. 1 well, 5561.4 feet, porosity = 3.9 percent, permeability = 0.491 mD.*

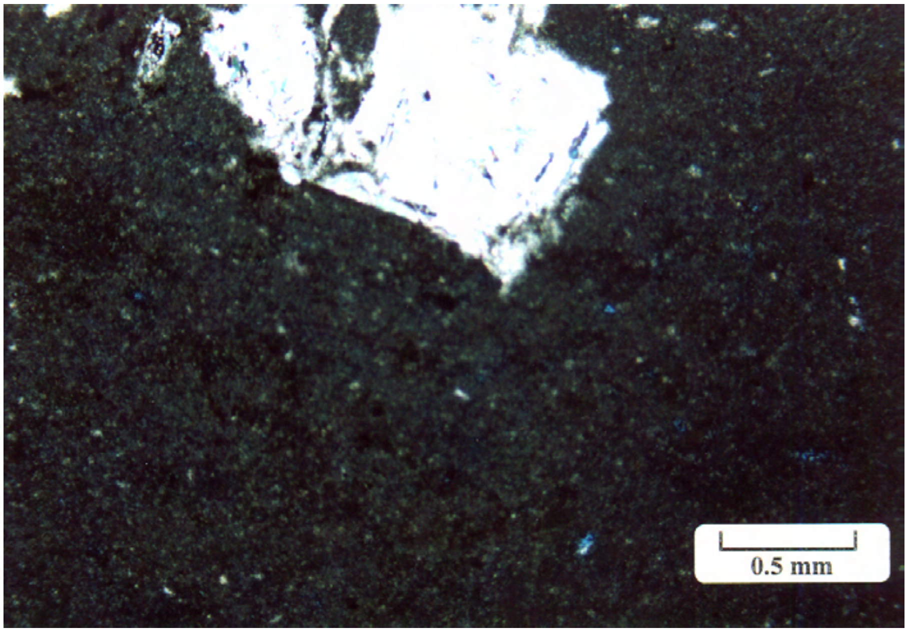

Figure 3-36. Low-magnification photomicrograph (plane light) of lagoonal/restricted marine lithofacies showing crystal casts (in white) of early evaporite minerals (now anhydrite) surrounded by a dark-colored, dolomitic mudstone with sponge spicules (the very small white specks). Note the vague peloid outlines and microporosity (in blue) within this sample. Little Ute No. 1 well, 5837.8 feet, porosity = 20.5 percent, permeability = 2.87 mD.

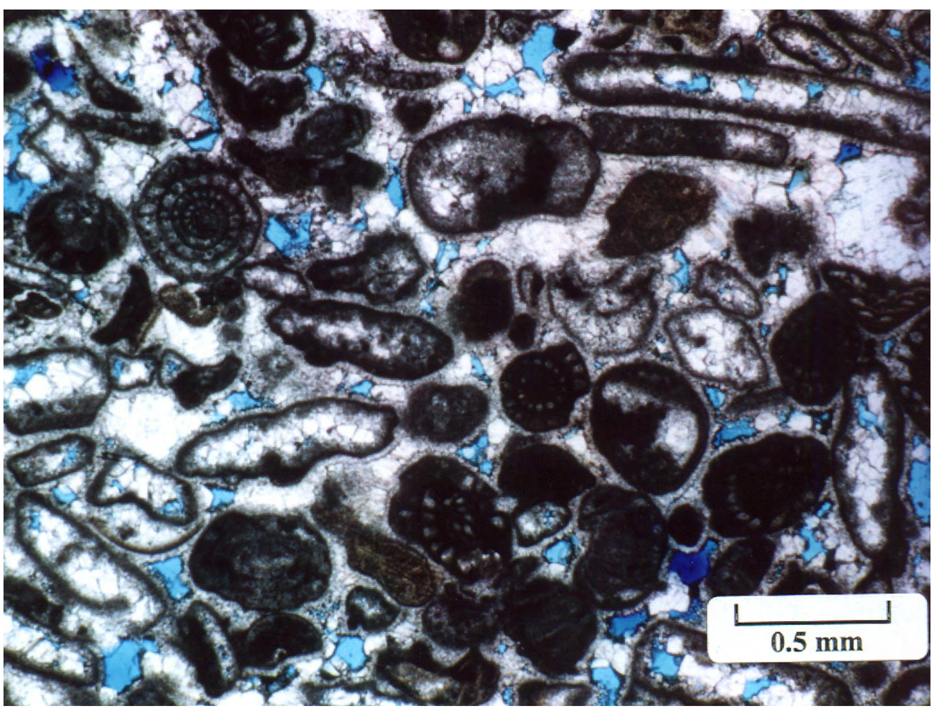

Figure 3-37. Photomicrograph (plane light) of high-energy shelf lithofacies (calcarenite shoals) showing skeletal and aggregate grains within a high-energy grainstone. Among the typical grains of this lithofacies are benthic forams (including fusulinids), phylloid-algal plates, "hard" peloids or micritized skeletal grains, and grain aggregates. Isopachous marine cements and "dogtooth" meteoric spar cements are present. Little Ute No. 1 well, 5940.5 feet, porosity = 4.6 percent, permeability = 0.018 mD.

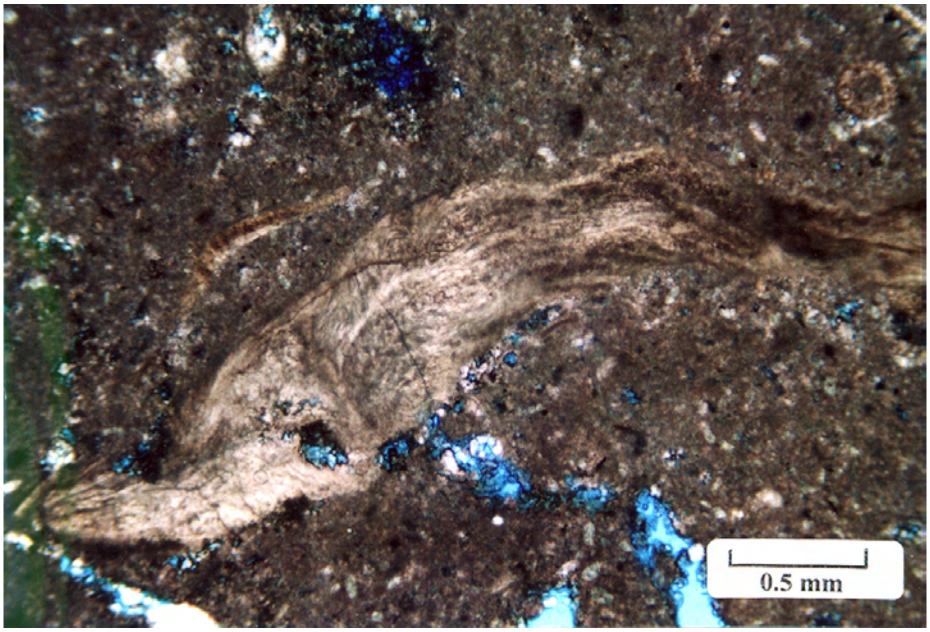

Figure 3-38. Photomicrograph (plane light) of open marine lithofacies showing fossiliferous wackestone with part of a well-preserved brachiopod shell as well as much smaller sponge spicules, echinoderm parts, and other bivalves. Note the vague peloidal fabric within the muds. Sleeping Ute No. 1 well, 5636.6 feet, porosity = 8.0 percent, permeability = 0.080 mD.

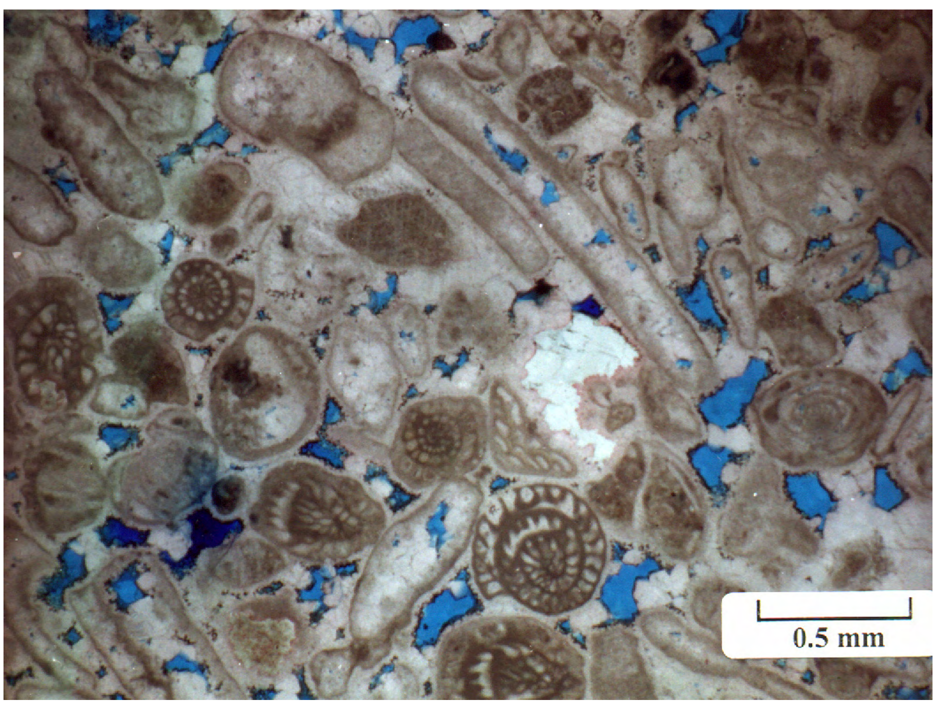

Figure 3-39. Photomicrograph (plane light with white card technique) of interparticle porosity. The scattered pores (in blue) visible in this micrograph are principally the remnants of primary interparticle space between the skeletal components of this grainstone. Early marine cements, followed by probable meteoric calcite spar and minor anhydrite (in white) have occluded most of the original interparticle porosity. Little Ute No. 1 well, 5940.5 feet, porosity = 4.6 percent, permeability = 0.018 mD.

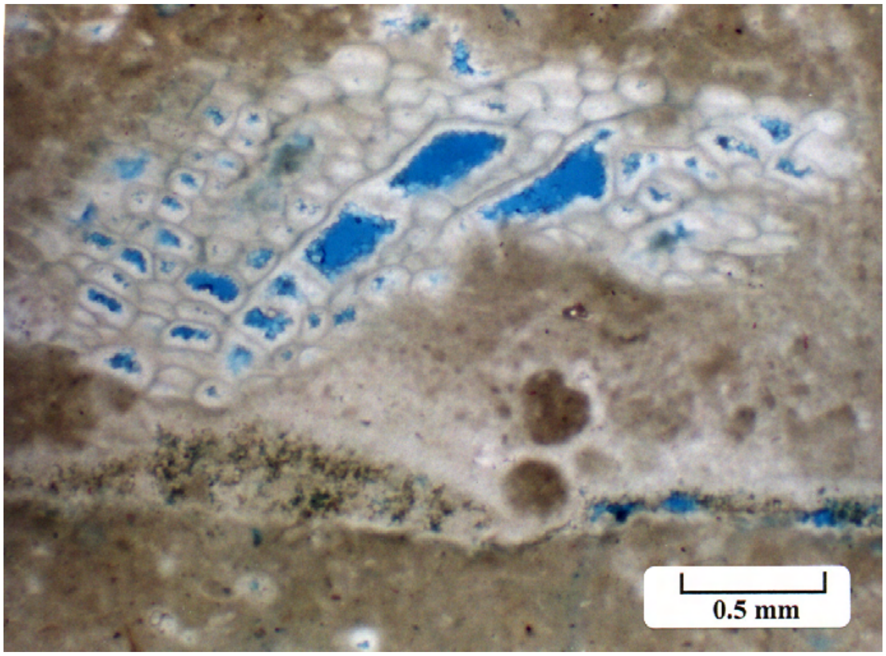

Figure 3-40. Photomicrograph (plane light with white card technique) of interparticle porosity. Open pores (in blue) are shown here within the uncemented chambers of encrusting organisms surrounded by lime muds. This sample is from within a phylloid-algal mound core. Little Ute No. 1 well, 5870.9 feet, porosity = 9.8 percent, permeability = 12.2 mD.

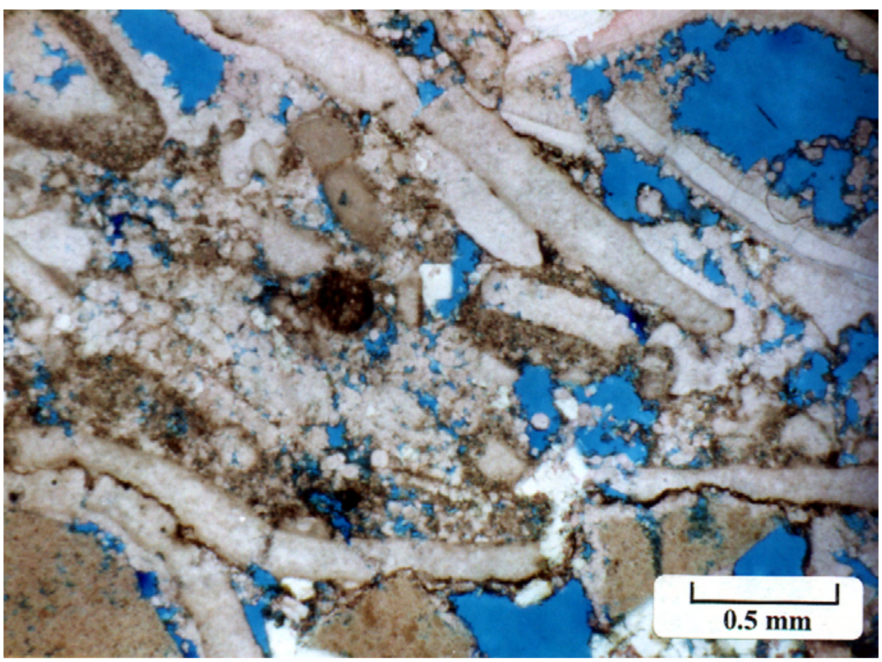

Figure 3-41. Photomicrograph (plane light with white card technique) of shelter porosity. Most of the large pores (in blue) occurring between platy phylloid-algal plates and the curvilinear bivalve shells are sheltered from internal sediment fillings. These preserved primary pores are often lined with early cements, thus limiting permeability. Some of the original grains and muds in this sample are associated with a phylloid-algal mound core. Little Ute No. 1 well, 5946.3 feet, porosity = 3.9 percent, permeability = 0.881 mD.

porosity, as seen in figure 3-42. These molds are large but isolated, creating very little permeability. Figure 3-43 shows large, open pores created by widespread dissolution of skeletal grains, carbonate clasts, and early carbonate cements. However, the permeability is ineffective in connecting this well-developed vuggy porosity. Though not abundant in the Little Ute and Sleeping Ute fields, intercrystalline porosity, developed between dolomite microcrystals, can create excellent reservoir rock as seen in figure 3-44. The introduction of evaporites that replace grains and occlude porosity prevent this sample from having much higher permeability. An excellent example of effective intercrystalline porosity is seen in figure 3-45. Not surprisingly, this example is from the phylloid-algal mound lithofacies and has excellent porosity and permeability developed between rhombic dolomite crystals, allowing large, well-connected pores. The final pore type seen in Little Ute and Sleeping Ute fields is microfractures, as displayed in figure 3-46. Reservoir quality is enhanced with extensive and abundant microfractures.

Five distinct mineralogies are seen in Little Ute and Sleeping Ute fields. Simple limestone deposited as calcite remains of phylloid-algal plates, marine fossils, and lime muds (figure 3-47), can have excellent porosity and permeability as a result of early dissolution by fresh waters. Dolomite created during the diagenesis of organic mudstone (figure 3-48) can preserve high porosities and good effective permeabilities. Several mixed mineralogies are created and preserved as well. Anhydritic limestone, in which the original calcite fossils have been partially replaced by anhydrite, does not create a good reservoir (figure 3-49). In contrast, anhydritic dolomite, as seen in figure 3-50, has abundant microporosity but very little permeability.

Porosity and Permeability Cross Plots

Porosity and permeability data from core plugs were available from five of the eight Bug wells that were cored and the two cored Cherokee wells (table 3-1), and for the two cored Little Ute/Sleeping Ute wells. Cross plots of these data are used to (1) determine the most effective pore systems for oil storage versus drainage, (2) identify reservoir heterogeneity, (3) predict potential untested compartments, (4) infer porosity and permeability trends where core-plug data are not available, and (5) match diagenetic processes, pore types, mineralogy, and other attributes to porosity and permeability distribution. Approximately 50 porosity and permeability cross plots were constructed using the available data (**Deliverable 2.1.1 – Porosity/Permeability Cross Plots: Cherokee and Bug Fields, San Juan County, Utah, and Little Ute and Sleeping Ute Fields, Montezuma County, Colorado**). Data classes within the plots included perforated limestone intervals, perforated dolomite intervals, total perforated intervals, reservoir lithofacies, carbonate fabric, pore type, and core with a 6 percent porosity cutoff.

The graph for the May-Bug No. 2 well from Bug field indicates that those samples representing intercrystalline porosity with micro-boxwork dolomite have the best reservoir potential (figure 3-51). The dominant lithofacies type (mound/breccia, calcarenites, and open marine and middle/inner shelf) was also assigned to each porosity/permeability data point that was cross plotted. No specific trend between lithofacies type and porosity/permeability was identified, although in Bug field (figure 3-52) the better reservoir qualities are found in mound/breccia lithofacies, and in Cherokee field, better reservoir qualities are generally found in calcarenite lithofacies over other lithofacies. Thus, our initial conclusion is that the reservoir quality of the rocks in Bug and Cherokee fields is most dependent on pore types and diagenesis.

In general, analysis of these plots for Cherokee field shows that those zones that have

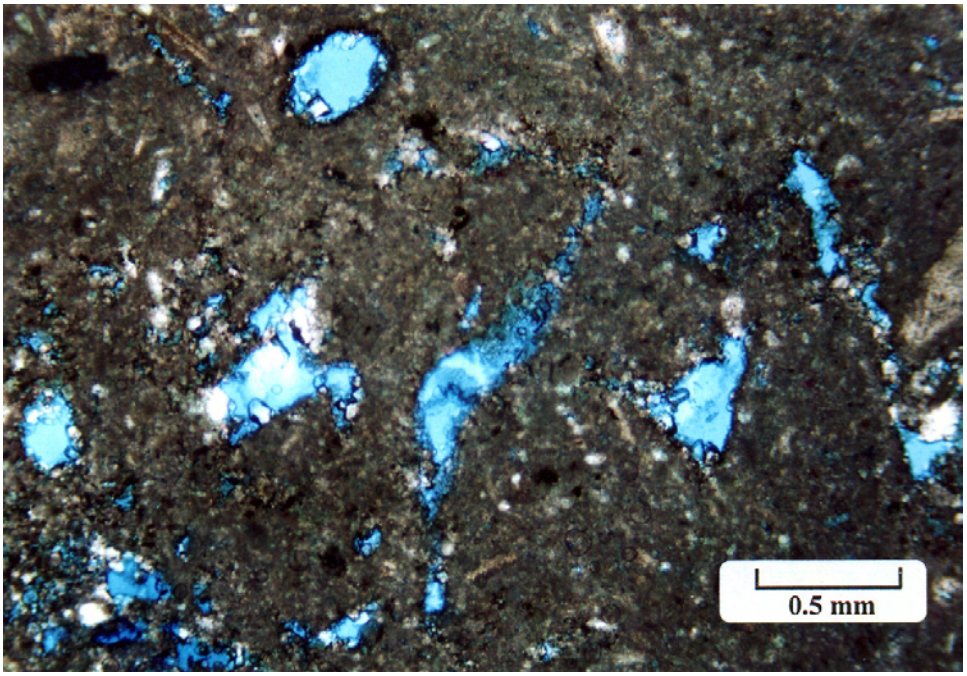

Figure 3-42. Photomicrograph (plane light) of moldic porosity. The isolated pores (in blue) are mostly from dissolved skeletal grains and early evaporite mineral crystals. These fossil and crystal molds are surrounded by dense lime muds. Sleeping Ute No. 1 well, 5636.6 feet, = 8.0 percent, permeability = 0.080 mD.

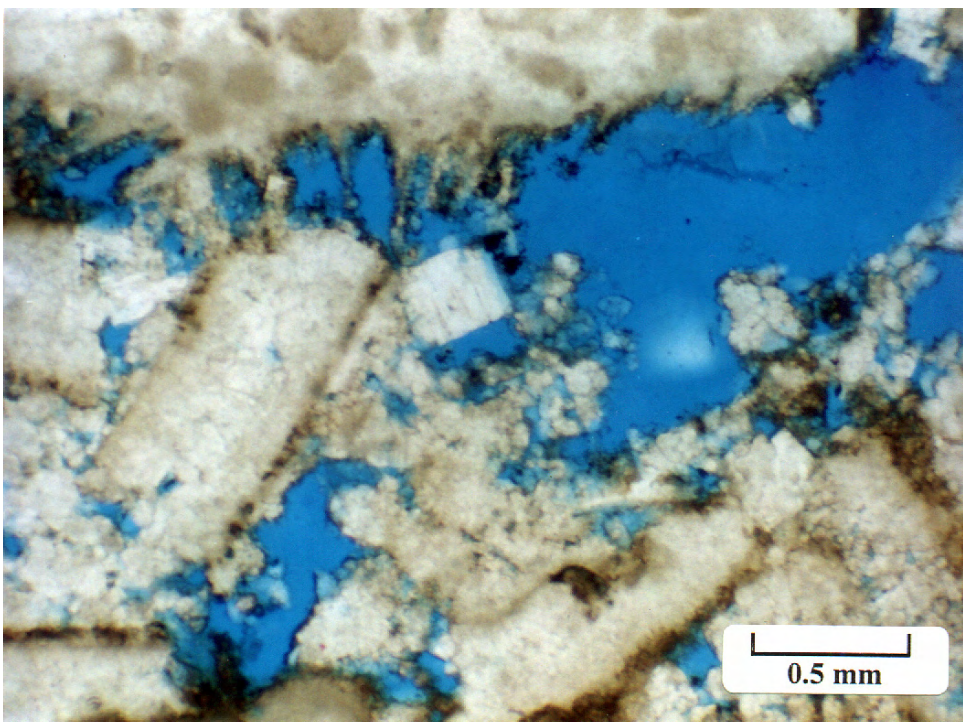

Figure 3-43. Photomicrograph (plane light with white card technique) of vuggy porosity. The oversized pores (in blue) shown here are solution-enlarged vugs. Early dissolution of skeletal grains, clasts and cements created these large, isolated pores. Little Ute No. 1 well, 5946.3 feet, porosity = 3.9 percent, permeability = 0.881 mD.

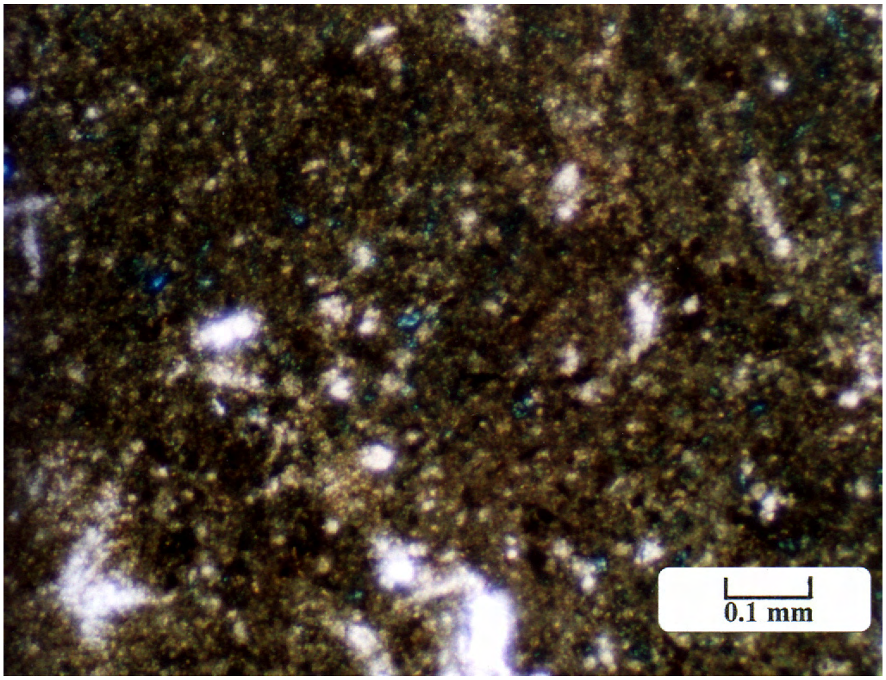

Figure 3-44. Photomicrograph (plane light) of intercrystalline porosity. The extremely small pores (in blue) of this view mostly occur between dolomite microcrystals. Crystal casts of evaporite minerals (in white) have grown displacively or replaced the dolomitic mud sediment. Little Ute No. 1 well, 5837.8 feet, porosity = 20.5 percent, permeability = 2.86 mD.

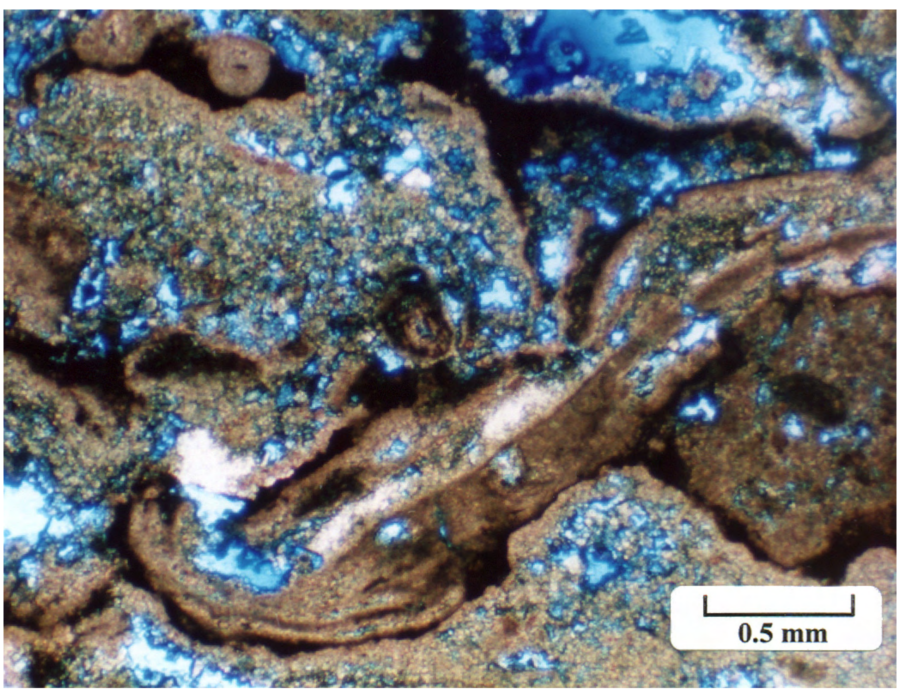

Figure 3-45. Photomicrograph (plane light) of intercrystalline porosity. The large, well-connected pores (in blue) in this view mostly occur between rhombic dolomite crystals. Some of the original grains and muds in this sample are associated with a phylloid-algal mound core. Little Ute No. 1 well, 5882.5 feet, porosity = 18.4 percent, permeability = 95.6 mD.

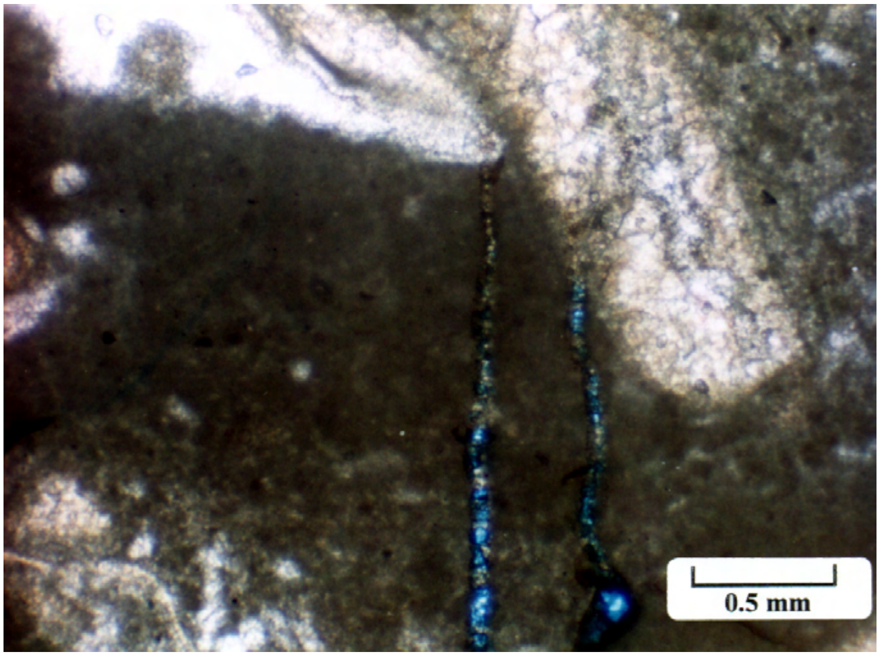

Figure 3-46. Photomicrograph (plane light) of microfractures. A pair of open microfractures (in blue) are illustrated here that cross lime muds within the sediments of a phylloid-algal mound interior. Recrystallized skeletal fragments (including phylloid-algal plates) are the white areas in this view. Little Ute No. 1 well, 5919.2 feet, porosity = 8.0 percent, permeability = 0.398 mD.

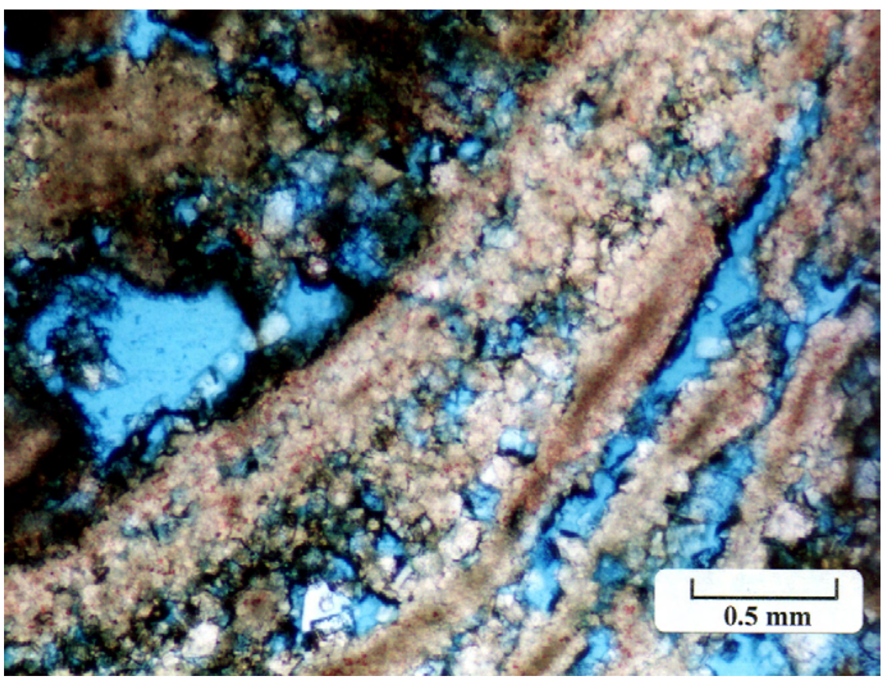

Figure 3-47. Photomicrograph (plane light with white card technique) of limestone where Alizarin Red-S staining shows the calcite composition of corroded remnants from phylloid-algal plates, marine fossils, and lime muds. Early dissolution by fresh waters has created some of the porosity (in blue). Little Ute No. 1 well, 5882.5 feet, porosity = 18.4 percent, permeability = 95.6 mD.

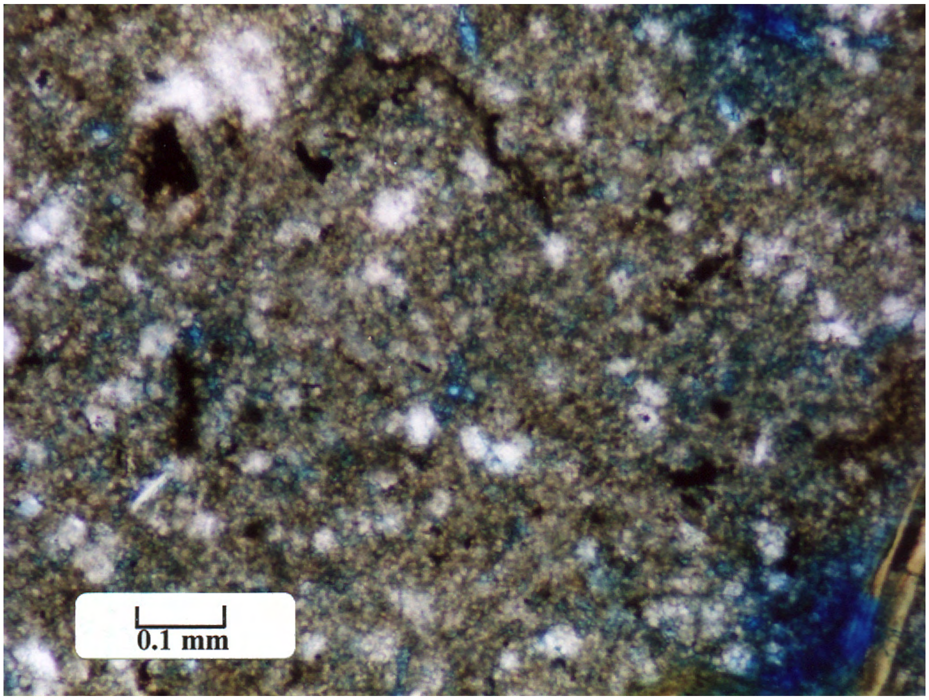

Figure 3-48. Photomicrograph (plane light with white card technique) of dolomite where sponge spicule-bearing, organic mudstone has been replaced by very finely crystalline dolomite. Note the very small intercrystalline and micro-moldic pores (in blue). Little Ute No. 1 well, 5837.8 feet, porosity = 20.5 percent, permeability = 2.87 mD.

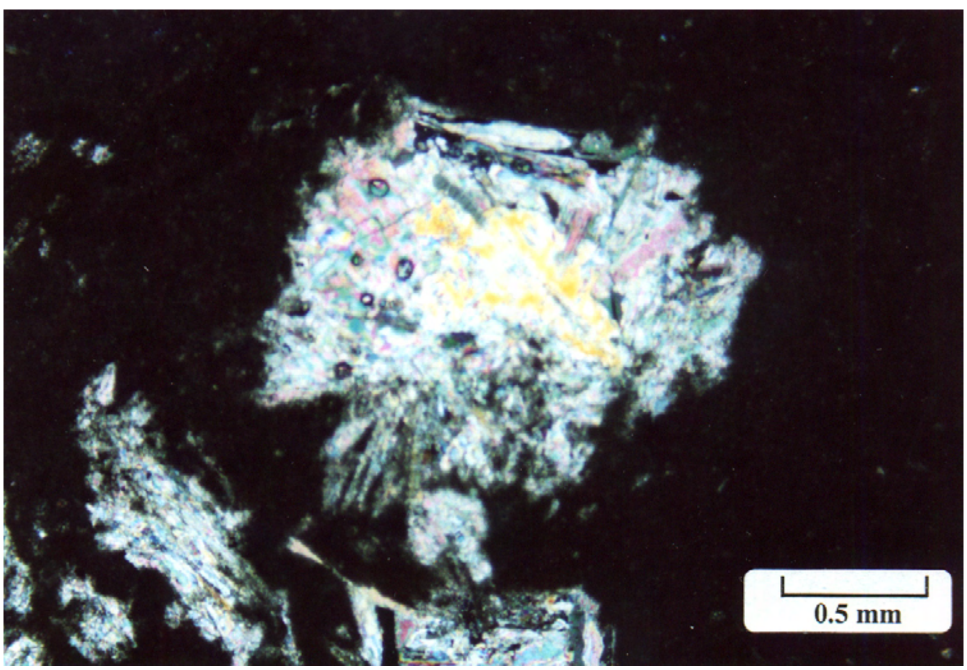

Figure 3-49. Low-magnification photomicrograph (crossed nicols) of anhydritic dolomite showing clusters of early evaporite minerals (now anhydrite) surrounded by a dark-colored, dense dolomitic mudstone. Sleeping Ute No. 1 well, 5575.4 feet, porosity = 13.2 percent, permeability = 0.283 mD.

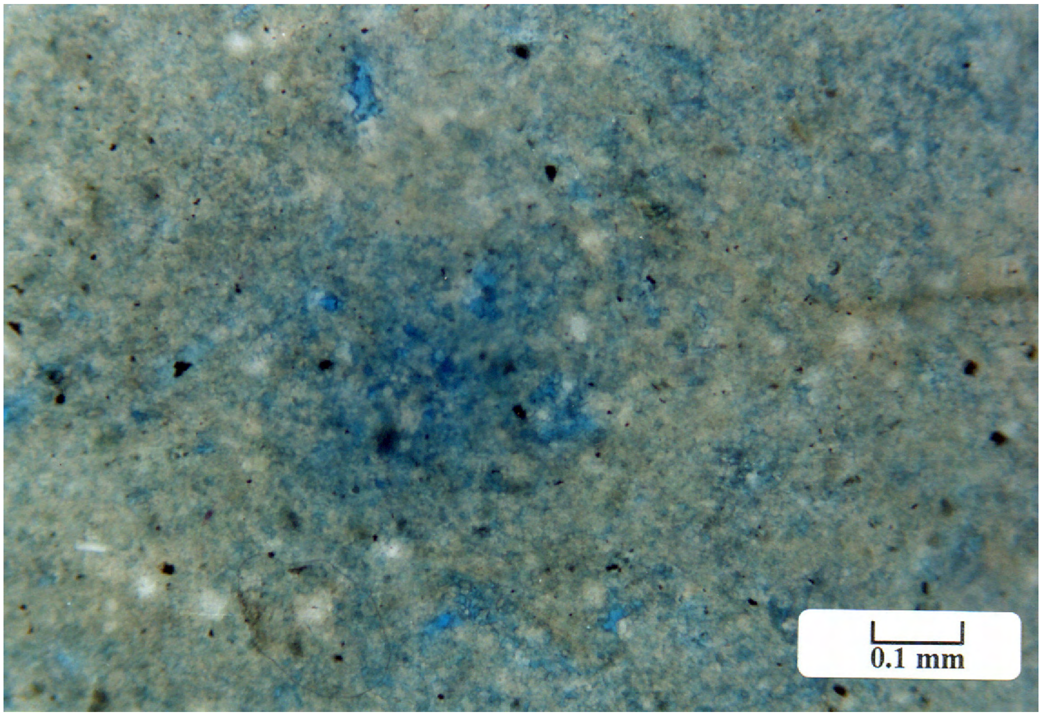

Figure 3-50. High-magnification photomicrograph (plane light with white card technique) of the same sample in figure 3-49 showing the very small crystal size of the dolomite matrix in this mixed mineralogy sample. Note the microporosity (in blue) within this sample.

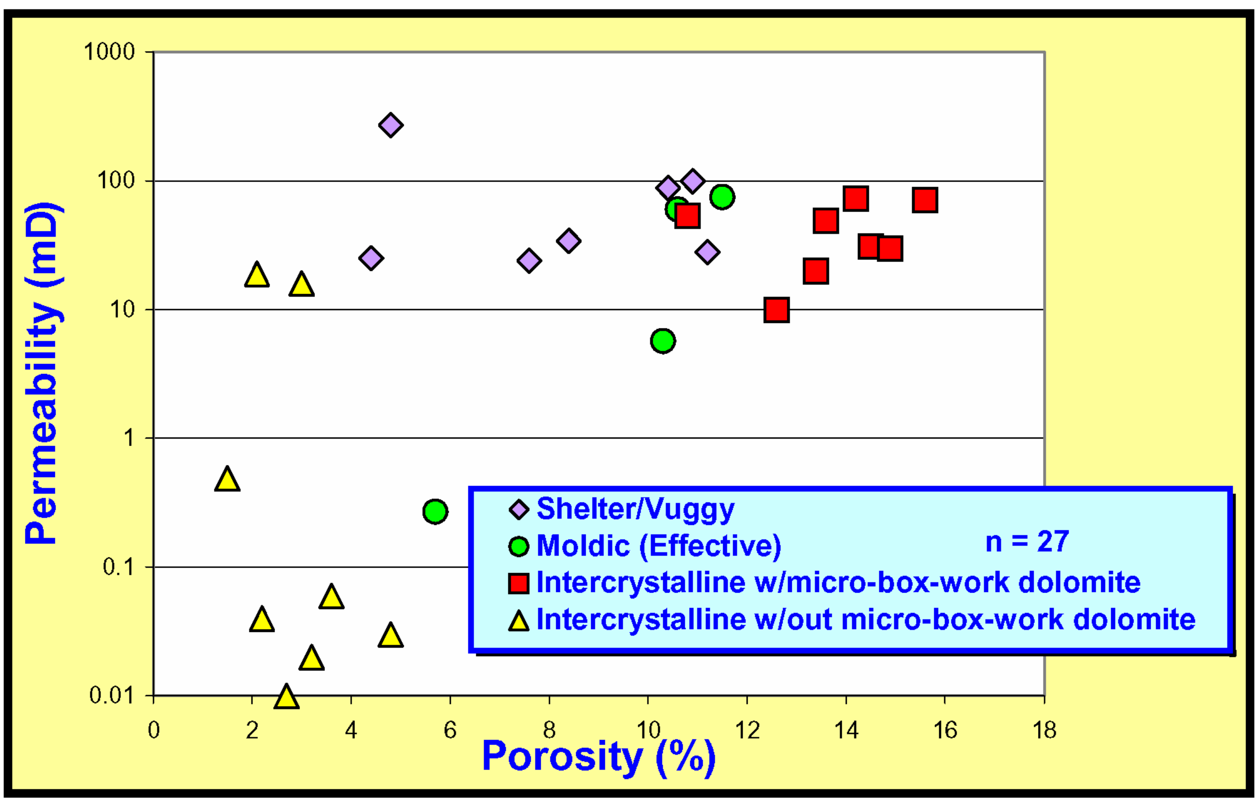

Figure 3-51. May-Bug No. 2 well permeability versus porosity cross plot by pore types and diagenesis.

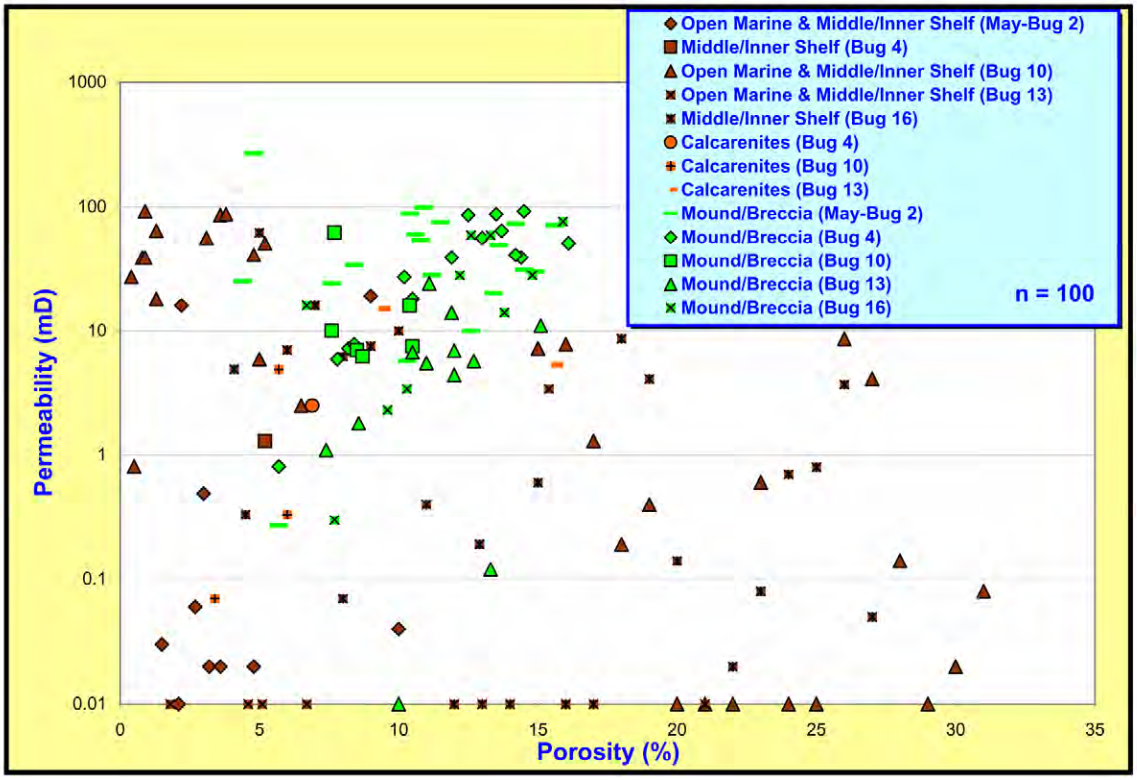

Figure 3-52. Bug field permeability versus porosity cross plot by lithofacies.

been dolomitized have better reservoir potential than those that remain limestone (figure 3-53). The dominant pore type (microporosity/channel, moldic, intercrystalline, interparticle, and shelter/vuggy) was assigned to each porosity/permeability data point that was cross plotted. The graph for the Cherokee No. 22-14 well from Cherokee field indicates that those samples representing microporosity have the best reservoir potential, while those representing intercrystalline porosity have the poorest reservoir potential (figure 3-54).

Cross plots of porosity versus permeability for the various pore types for the two cored Little Ute/Sleeping Ute wells, seen in figures 3-55 and 3-56, show that intercrystalline and moldic pore types have the highest porosity and permeability of any pore types. They also have a wide range of values with some samples being among the lowest for porosity and permeability. Note that the pore type symbols differ for this set of plots. From project work on Ismay reservoirs, a rough economic cut-off for permeability was found to be 2 mD. Cross plots of porosity versus permeability for the various lithofacies are seen in figures 3-57 and 3-58. Using the 2 mD economic cut-off, the productive Little Ute No. 1 well (figure 3-57) contains numerous phylloid-algal mound reservoir intervals. In comparison, the non-productive Sleeping Ute No. 1 well contains no phylloid-algal mound lithofacies. Only a few intervals in the Sleeping Ute No. 1 core (figure 3-58) exceed the 2 mD cut-off. Cross plots of the mineralogy are shown for the two cored wells in figures 3-59 and 3-60. Once again, the intervals that exceed 2 mD are greater in number in the productive Little Ute No. 1 well (figure 3-59) than in the non-productive Sleeping Ute No. 1 well (figure 3-60). No single mineralogy seems to dominate the reservoir intervals in the Little Ute No. 1 core. In contrast, the non-productive Sleeping Ute No. 1 core has very few intervals with permeabilities greater than 2 mD. The few samples that do fall into the higher permeability range are almost exclusively anhydritic dolomites.

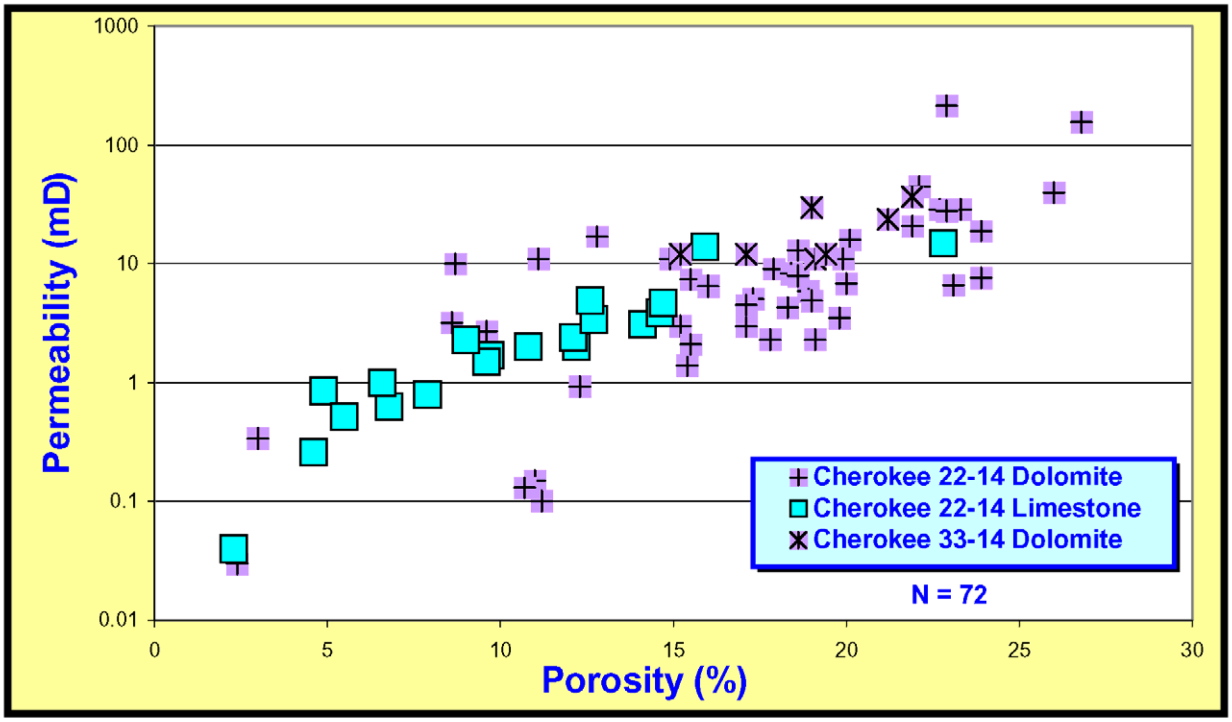

Figure 3-53. Cherokee field permeability versus porosity cross plot of perforated limestone and dolomite intervals.

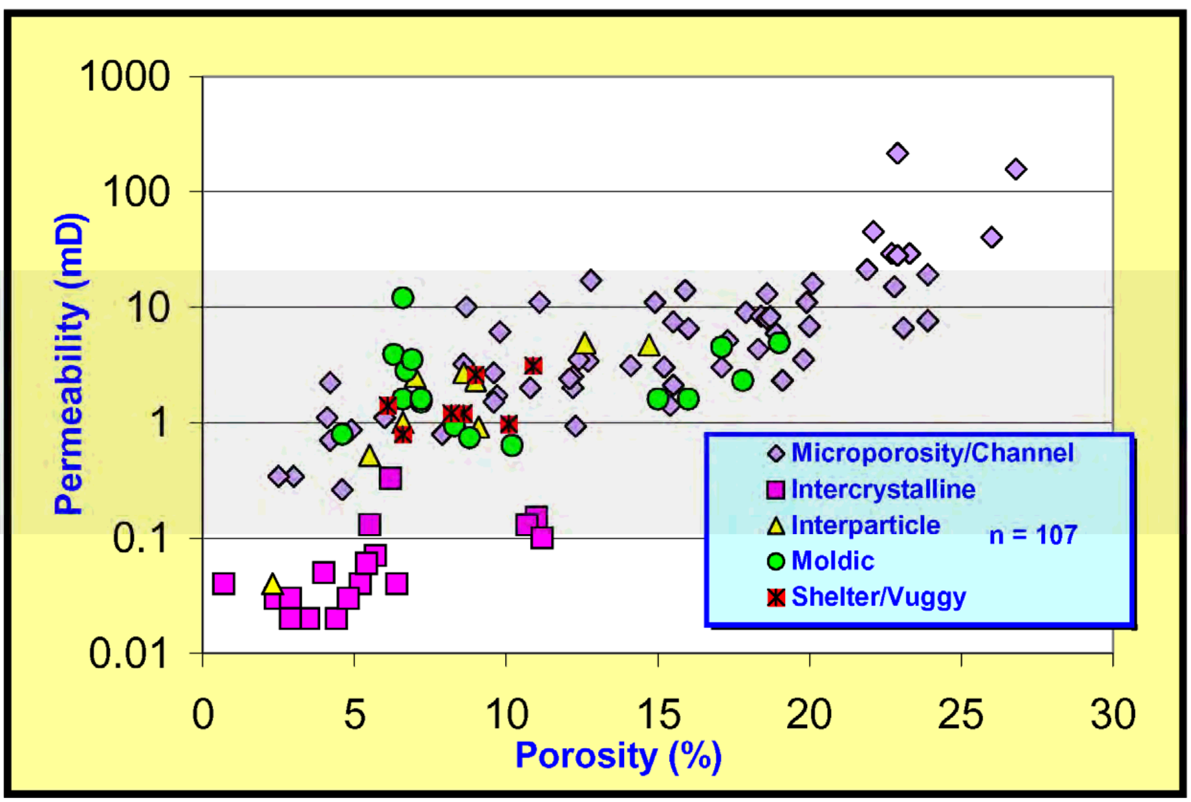

Figure 3-54. Cherokee No. 22-14 well permeability versus porosity cross plot by pore types and diagenesis.

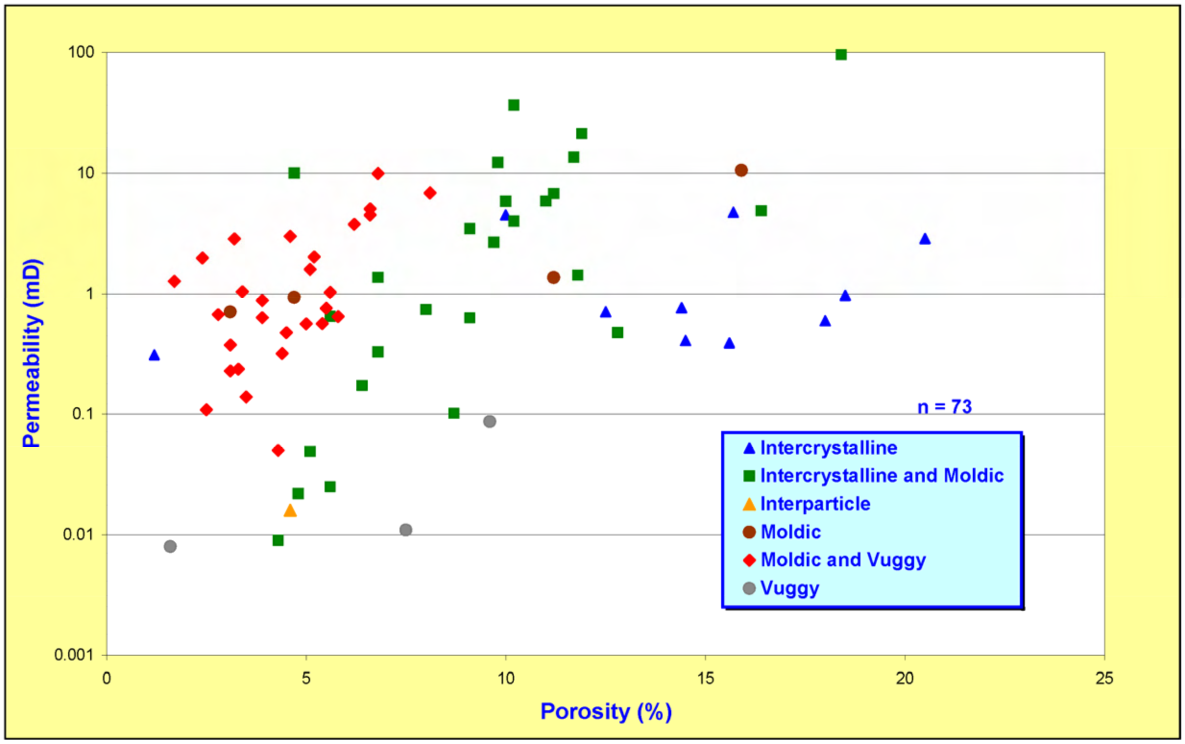

Figure 3-55. Little Ute No. 1 well permeability versus porosity cross plot by pore types.

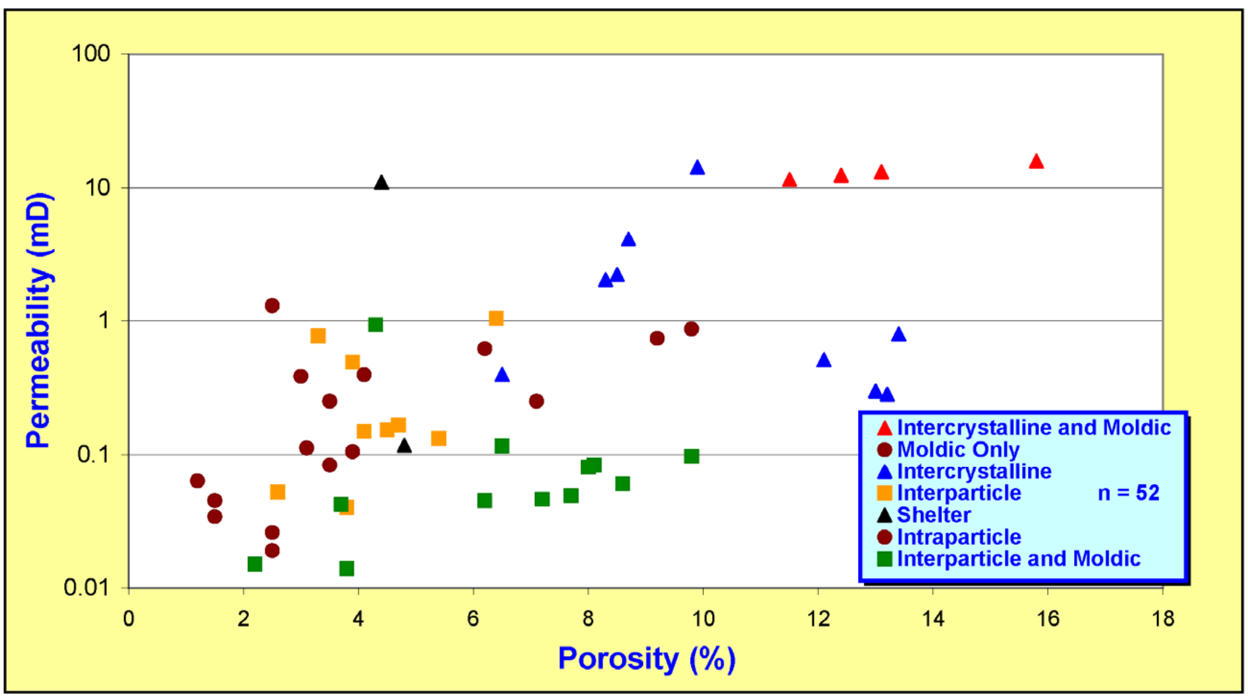

Figure 3-56. Sleeping Ute No. 1 well permeability versus porosity cross plot by pore types.

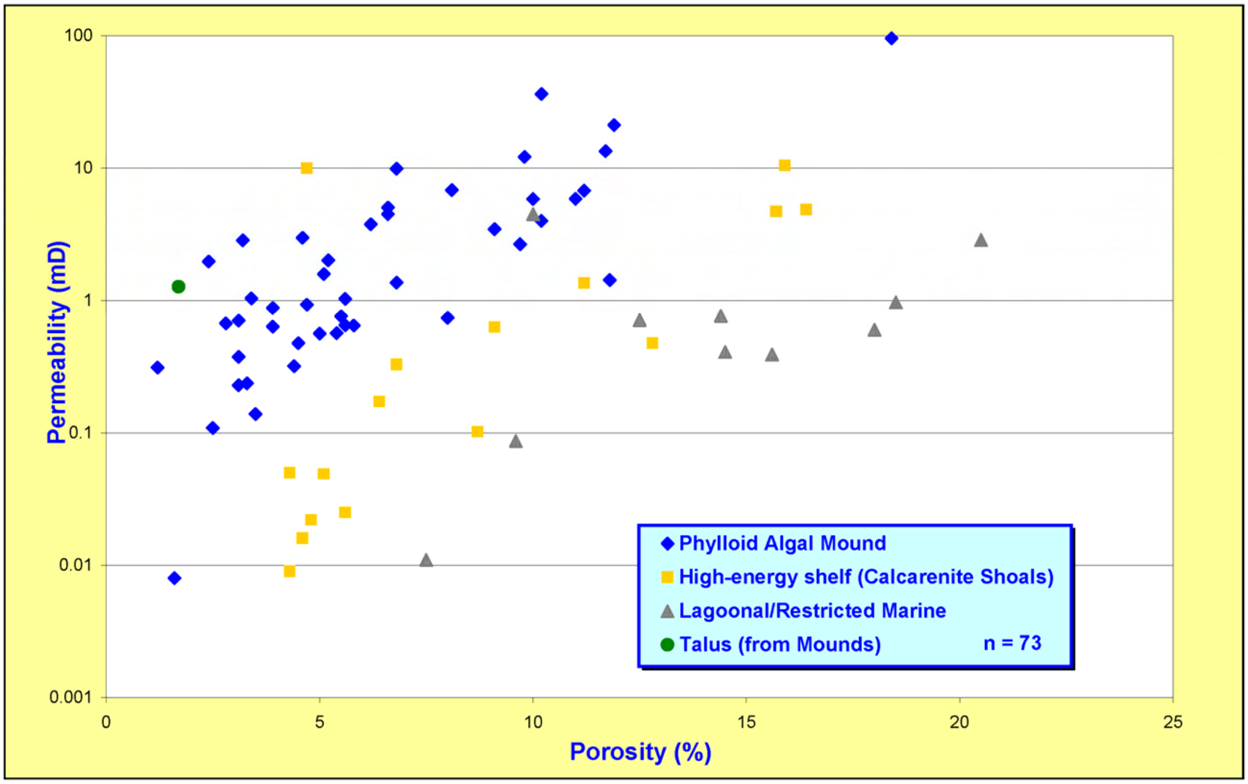

Figure 3-57. Little Ute No. 1 well permeability versus porosity cross plot by lithofacies.

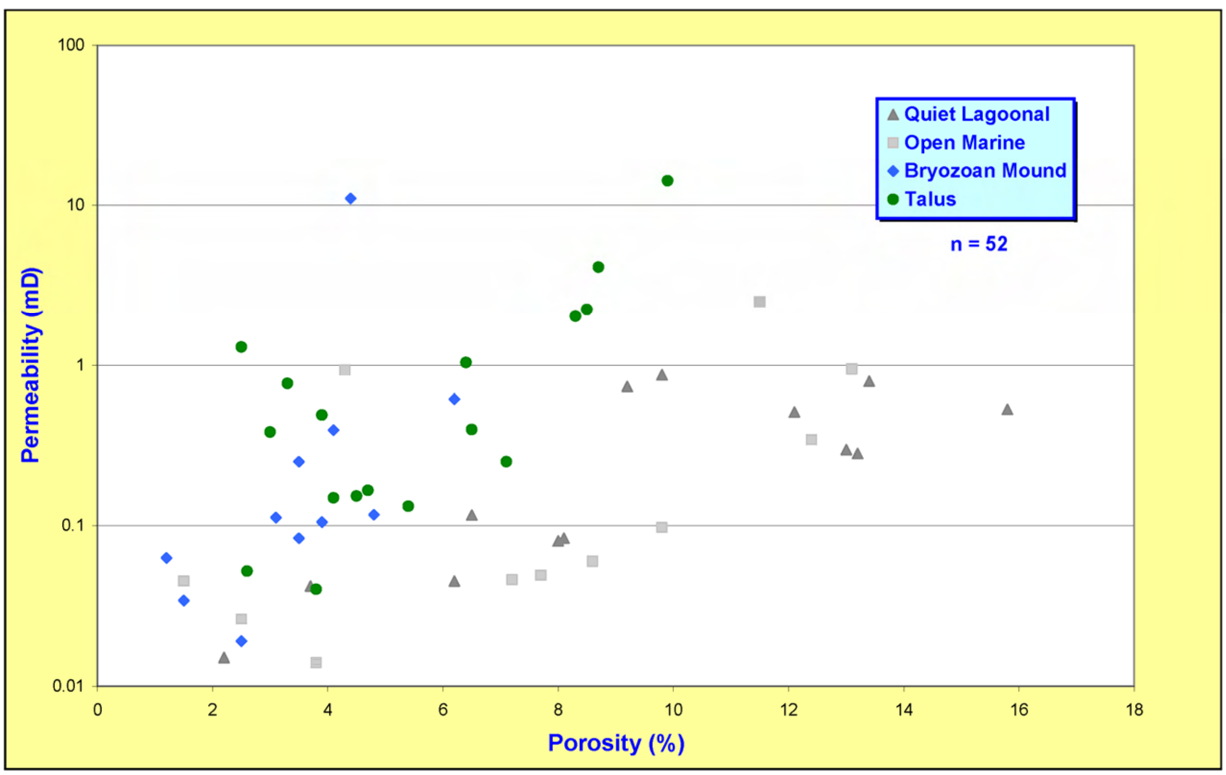

Figure 3-58. Sleeping Ute No. 1 well permeability versus porosity cross plot by lithofacies.

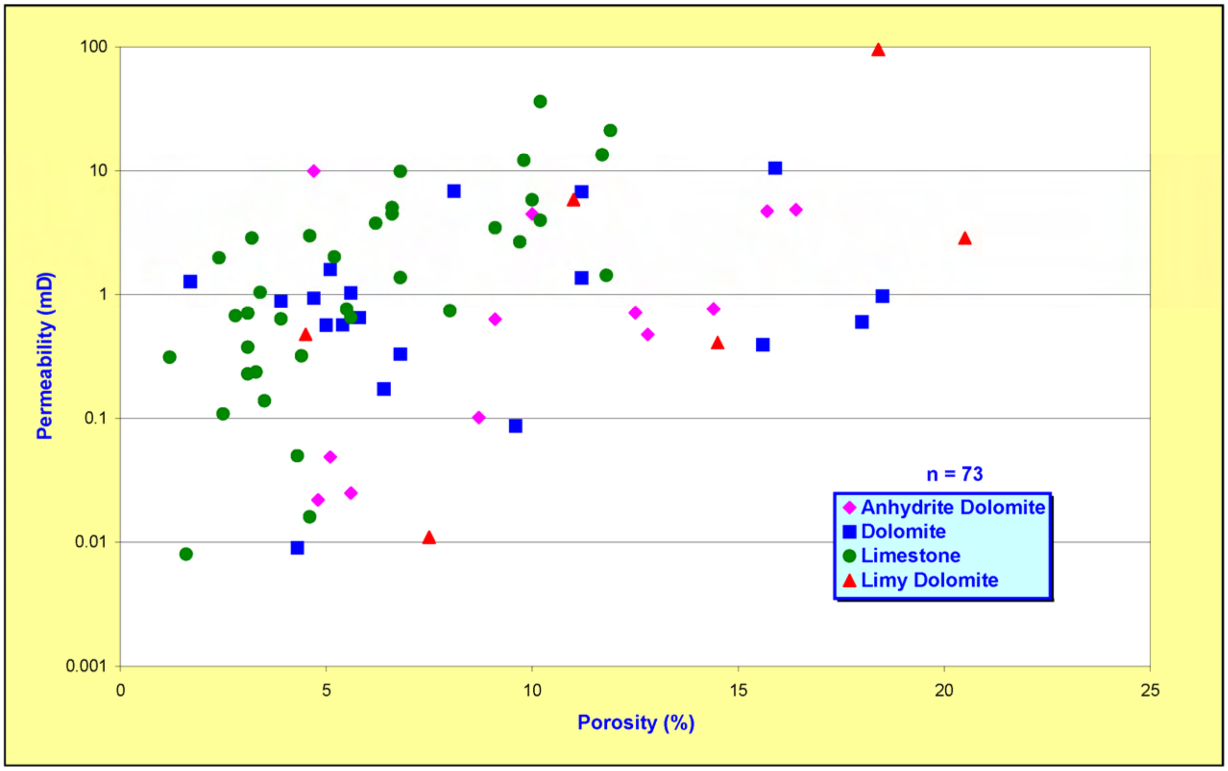

Figure 3-59. Little Ute No. 1 well permeability versus porosity cross plot by mineralogy.

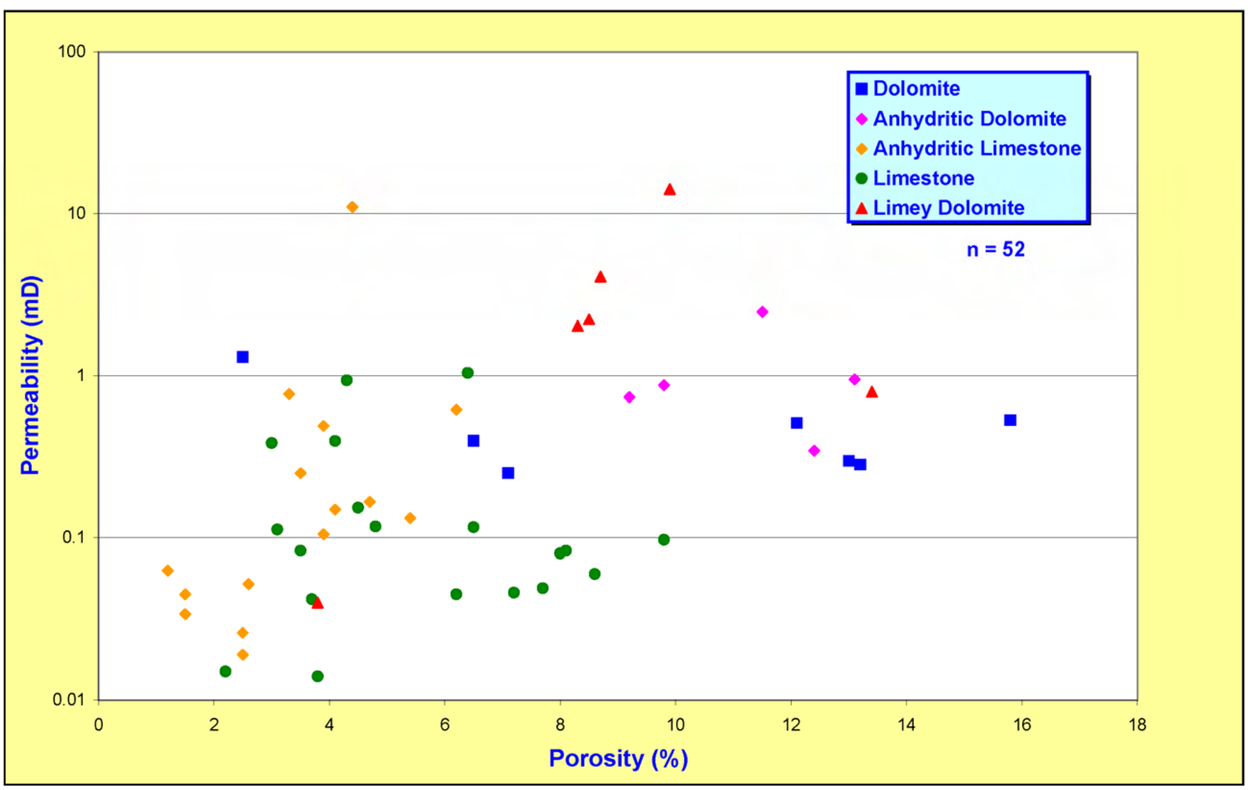

Figure 3-60. Sleeping Ute No. 1 well permeability versus porosity cross plot by mineralogy.

CHAPTER IV
SCANNING ELECTRON MICROSCOPY AND PORE CASTING: CHEROKEE AND BUG CASE-STUDY FIELDS

Thomas C. Chidsey, Jr.,
Utah Geological Survey;
Louis H. Taylor, Standard Geologic Services;
and
David E. Eby, Eby Petrography & Consulting, Inc.

Introduction

Cherokee and Bug fields (figure 1-3) were selected for scanning electron microscope (SEM) and/or pore casting analyses because they had high-quality core material available which exhibited a variety of diagenetic fabrics and porosity types as observed in thin sections. These characteristics, when found in various hydrocarbon-bearing rocks, can be indicators of reservoir flow capacity, storage capacity, and potential for horizontal drilling. Scanning electron microscope and pore casting analyses were conducted on eight thin section blanks from core samples that displayed particular characteristics of interest (table 4-1, **Deliverable 1.2.3 – Scanning Electron Microscopy and Pore Casting: Cherokee and Bug Fields, San Juan County, Utah**). The objectives of these analyses were to (1) characterize the cements present, (2) characterize the types of porosity present, and (3) identify diagenetic events.

Table 4-1. List of samples examined in this study and the characteristics of interest.

Well	Depth	SEM	Pore Casting	Characteristics of Interest
Cherokee 22-14	5768.7	X	X	Microporosity dolomite with bitumen
Cherokee 22-14	5827.7	X		Moldic porosity and micro-crystalline dolomite
Cherokee 33-14	5773.9	X		Dolomite, microporosity and moldic porosity, relatively low porosity and permeability
Cherokee 33-14	5781.2	X	X	Microporosity only dolomite, high porosity and permeability
May Bug 2	6304	X	X	Micro-boxwork dolomite/hollow dolomite fabric
May Bug 2	6312B	X		B - (second sample) botryoidal cement/dolomite
May Bug 2	6315A	X	X	A – yellow internal sediment/dolomite
Bug 4	6289.7	X	X	Microporosity/with bitumen and micro-boxwork dolomite
TOTAL	-	8	5	

Methodology

In order to determine the diagenetic histories of the various Ismay and Desert Creek reservoirs, representative examples of key lithofacies were selected from the suite of 44 samples used for thin sections, which had been taken from conventional cores of each field (table 3-1). Carbonate fabrics were determined according to Dunham's (1962) and Embry and Klovan's (1971) classification schemes. A scanning electron microscope was used to photograph (1) typical preserved primary and secondary pore types and pore throats, (2) cements, (3) sedimentary structures, (4) fractures, and (5) pore-plugging anhydrite, halite, and bitumen.

Pore casting is a special technique where the carbonate matrix of an epoxy-impregnated thin section blank is dissolved by hydrochloric acid. What remains is only the epoxy that represents the entire pore system of the sample (pores and pore throats). The pore cast is then coated with gold, and studied and photographed with the SEM (the same method used on the actual thin section blank).

The results of this SEM work are summarized in table 4-2. Porosity types and associated abbreviations included in this chapter are from Choquette and Pray (1970) (figure 4-1). Some porosity descriptions provided here vary from those determined by the thin section analysis (**Deliverable 1.2.1A – Thin Section Descriptions: Cherokee and Bug Fields, San Juan County, Utah**). The descriptions presented in this chapter are from SEM examination and measurement only.

Table 4-2. Summary of porosity, cement, and diagenetic characters of samples examined.

WELL	**Cherokee 22-14**		**Cherokee 33-14**		**May Bug 2 ****			**Bug 4**
DEPTH (ft)	5768.7'	5826.7'	5773.9'	5781.2'	6304.0'	6312.0' B	6315.0' A	6289.7'
POROSITY								
Intergranular/Microcrystalline	X	X	X	X	X	X	X	X
Dissolution (moldic)	X	X	X			X		
Dissolution (vug)	X				X	X		X
Dissolution (channel)	X	X	X					X
Fractures	X				X			X
CEMENTS								
Anhydrite	X	X	X			X		X
Calcite		X	X			X		
Quartz		X	X	X		X		
Dolomite					X			
Smectite	X	X	X					
Pyrobitumen	X	X	X	X				
DIAGENESIS								
Botryoidal Calcite Deposition					X	X	X	X
Dolomitization	X	X	X	X	X	X	X	X
Dissolution	X	X	X	X	X	X		X
Calcite Cementation		X	X					
Quartz Cementation		X	X	X		X		
Smectite Deposition	X	X	X	X				
Anhydrite Cementation	X	X	X			X		X
Pyrobitumen Emplacement	X	X	X	X				
Fracturing					X			

** Limited observation of the 6312-foot B specimen.

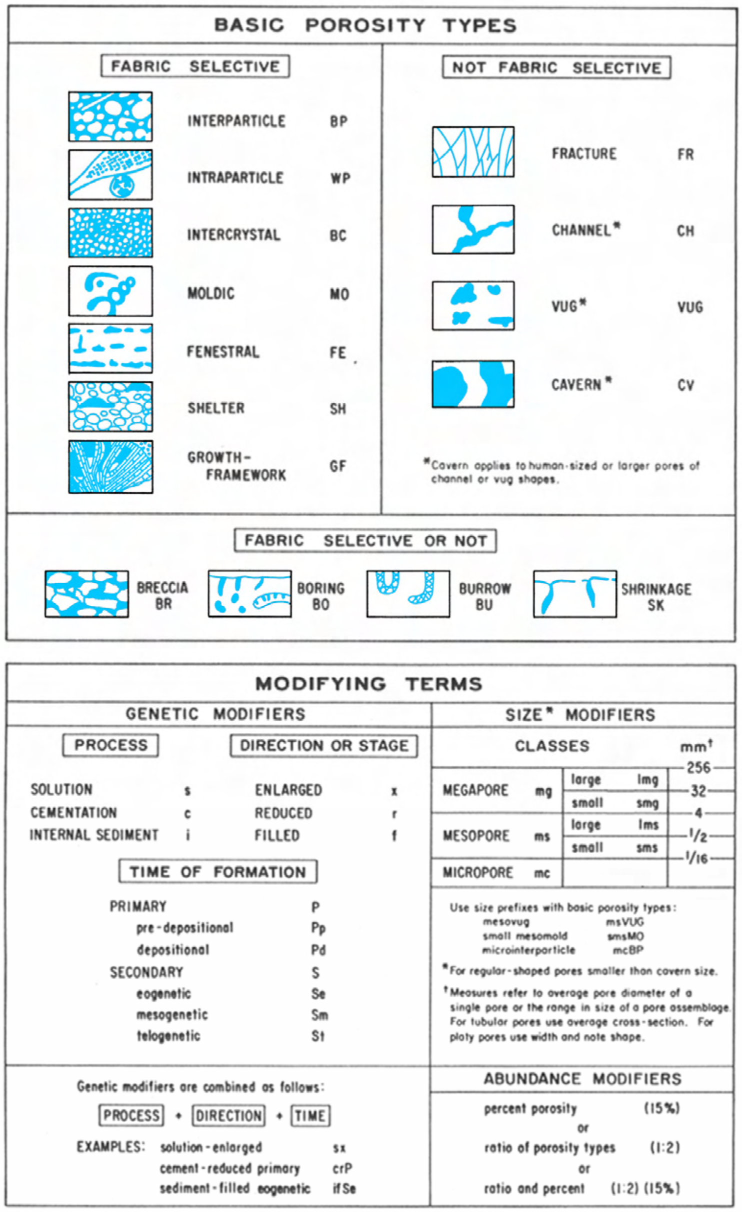

Figure 4-1. Classification of pores and pore systems in carbonate rocks (Choquette and Pray, 1970).

Porosity Types

All samples exhibit microporosity in the form of intercrystalline microporosity (figure 4-2) and micro-boxwork porosity (figure 4-3). Microporosity represents an important site for untapped hydrocarbons and possible targets for horizontal drilling. Dissolution has contributed to porosity in most samples (figure 4-2). It has created moldic, vuggy, and channel porosity. Dissolution pores are most often in the mesopore size range (see figure 4-1 for definition of pore-size classes).

Permeability is related to the size and number of pore throats, and, particularly, to the connectivity of pore throats (figures 4-4 and 4-5). In general, permeability is limited in these samples by the presence of "dead end" pore throats, as well as the presence of pore-throat-blocking cements, pyrobitumen, and tight dissolution remnants.

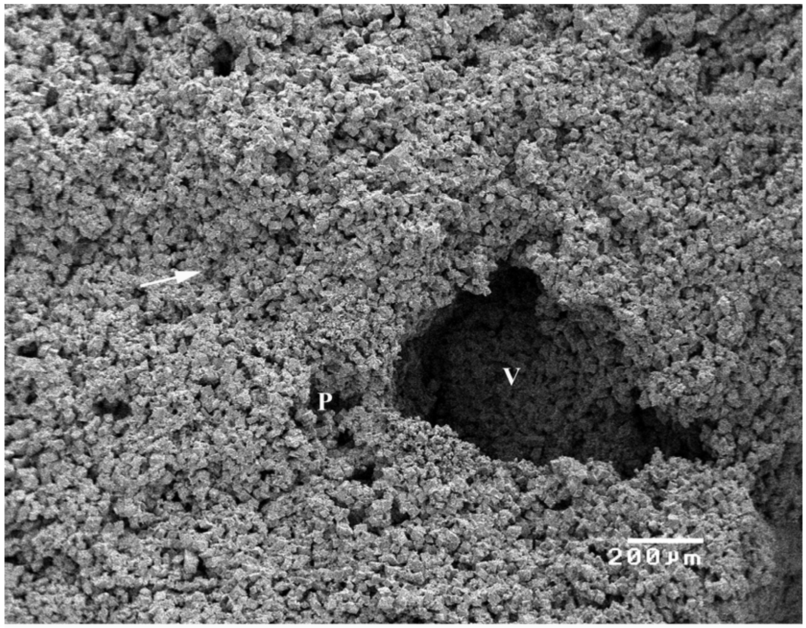

Figure 4-2. Scanning electron microscope photomicrograph of a core plug from 5768.7 feet, Cherokee No. 22-14 well. Dolomite exhibits three porosity types: intercrystalline microporosity (arrow); moldic microporosity (P); and a large mesovug (V). Oil drainage is mainly from macro- and mesopores, but not from micropores. Scale represents 200 microns (0.2 mm). Porosity = 22.9 percent; permeability = 215 mD based on core-plug analysis.

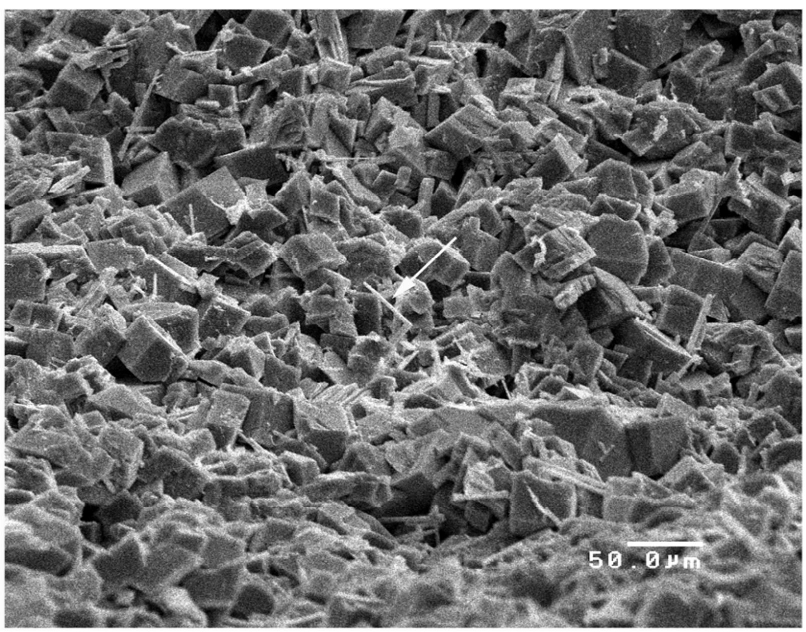

Figure 4-3. Scanning electron microscope photomicrograph of a core plug from 6315 feet, May Bug No. 2 well, showing dolomite with intercrystalline microporosity (black). Fragments (lathes) (arrow) of dolomite represent partially dissolved dolomite rhombs present within a yellow portion of the sample. The collapse and/or crushing of dolomite rhombs within the internal hollow dolomite sediment indicate early dolomitization and early meteoric dissolution resulting in micro-boxwork porosity. Scale represents 50 microns (0.05 mm). Porosity = 10.3 percent; permeability = 5.7 mD based on core-plug analysis.

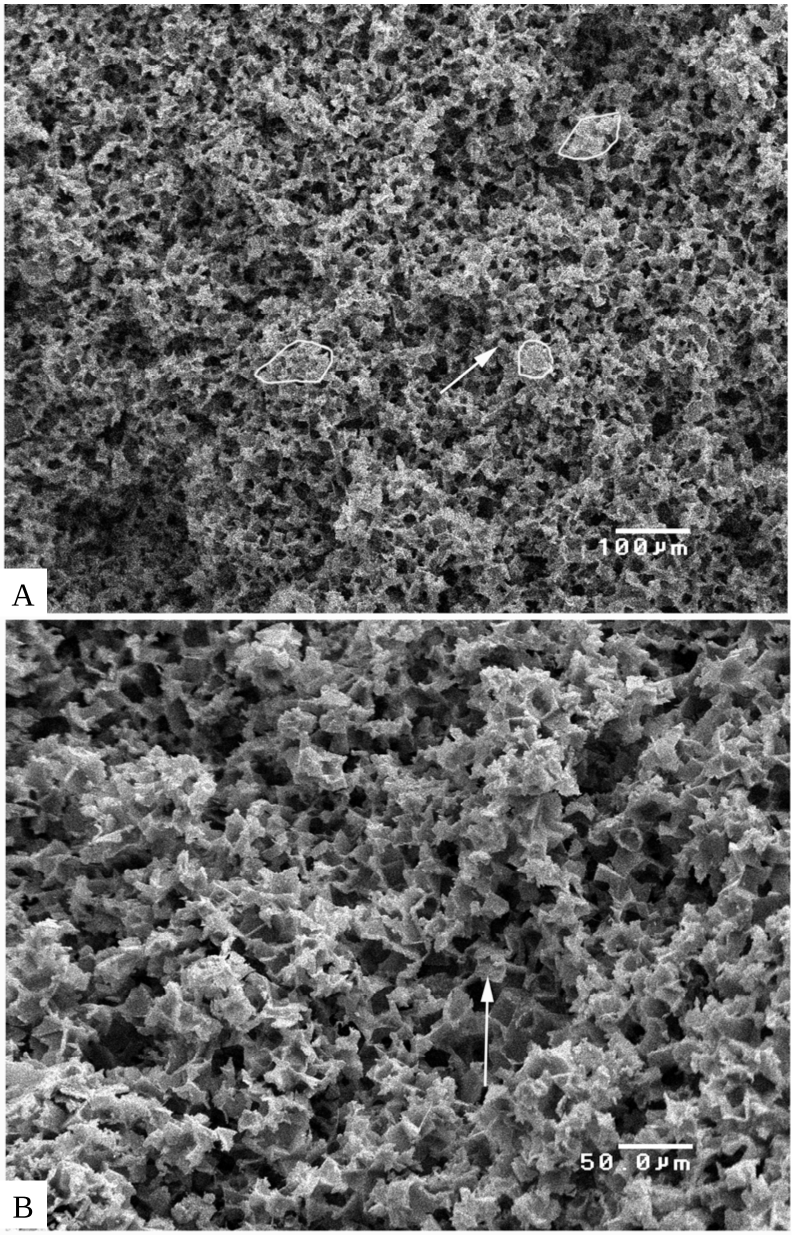

Figure 4-4. Scanning electron microscope photomicrograph of a pore cast from 5768.7 feet, Cherokee No. 22-14 well. (A) The overall intercrystalline microporosity (arrow) is relatively uniform. A few larger micropores are visible (outline). Note that the solid areas (light gray) represent porosity and the open areas (dark gray to black) represent matrix. Scale represents 100 microns (0.1 mm). (B) Enlargement of (A) showing microporosity. Impressions of dolomite rhombs are visible (arrow). Scale represents 50 microns (0.05 mm). Porosity = 22.9 percent; permeability = 215 mD based on core-plug analysis.

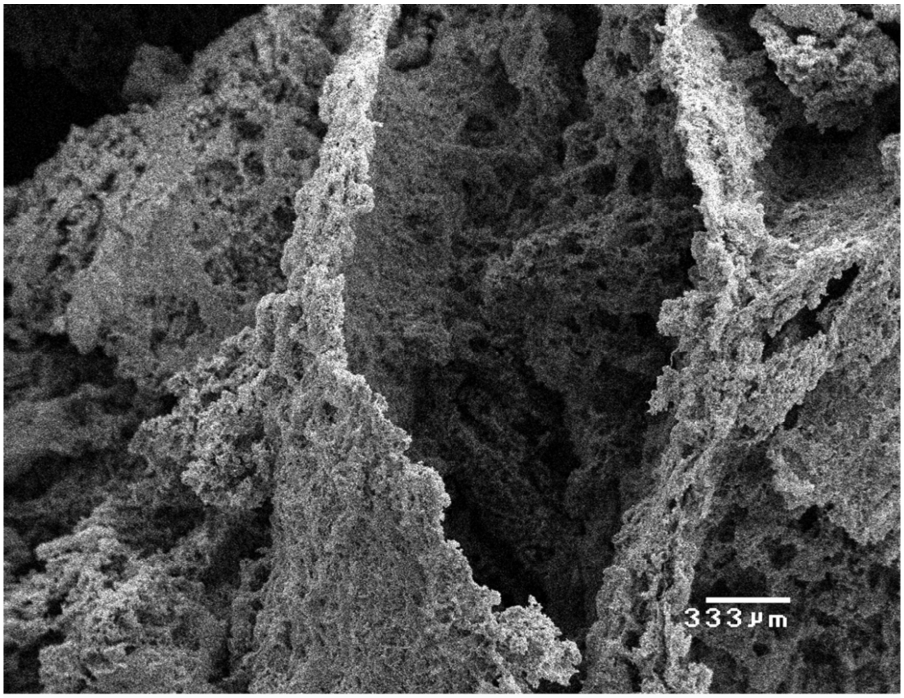

Figure 4-5. Scanning electron microscope photomicrograph of a pore cast from 6304 feet, May Bug No. 2 well. Sheet-like linear pores are associated with phylloid-algal fronds. Note that the solid areas represent porosity. Scale represents 333 microns (0.333 mm). Porosity = 10.9 percent; permeability = 99 mD based on core-plug analysis.

Fractures enhance the permeability in three samples: the sample from the depth of 5768.7 feet (1758.2 m) from the Cherokee No. 22-14 well, the sample from the depth of 6304 feet (1921 m) from the May Bug No. 2 well (figure 4-6), and the sample from the depth of 6289.7 feet (1917.0 m) from the Bug No. 4 well (figure 4-7). The permeability of these three samples is among the highest of those examined.

Lithology, Cements, and Diagenesis

All samples examined contain dolomite (figure 4-2 and 4-8). Anhydrite, calcite, smectite clays, and pyrobitumen are present in some samples. The dominant cement occluding porosity and permeability in the Cherokee wells is anhydrite (figure 4-9). Although we did not observe anhydrite in the sample from the depth of 5781.2 feet (1762.0 m) from the Cherokee No. 33-14 well during SEM analysis, thin section analyses suggest that it is present.

Porosity reduction in the Bug wells is the result of dolomitization of former calcite cements. Later anhydrite cementation also contributes to porosity and permeability reduction in these wells; anhydrite was found at the following sample depths – 6312 feet (1924 m) from the May Bug No. 2 well and 6289.7 feet (1917.0 m) from the Bug No. 4 well. Pyrobitumen commonly lines pores and plugs pore throats in many samples (figure 4-10).

Calcite (figure 4-11) and quartz (figure 4-12) cementation are very rare, but are present in the Cherokee wells and in one sample (6312 feet [1924 m]) of the May Bug No. 2 well. Smectite clay deposition (figure 4-11) is also extremely rare, and is visible in the Cherokee wells only. The minor cement constituents of calcite, quartz, and smectite contribute little to the overall lithology and are relatively insignificant to reservoir quality.

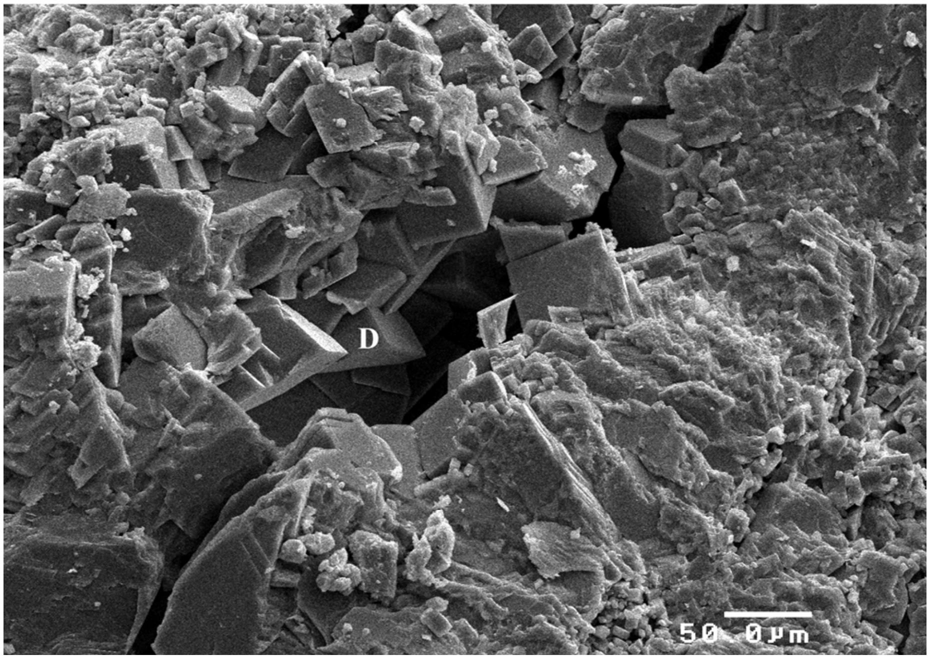

Figure 4-6. Scanning electron microscope photomicrograph of a core plug from 6304 feet, May Bug No. 2 well, showing a fracture pore and dolomite (D) within it. This demonstrates that the fracture was open during dolomite deposition. Scale represents 50 microns (0.5 mm). Porosity = 10.9 percent; permeability = 99 mD based on core-plug analysis.

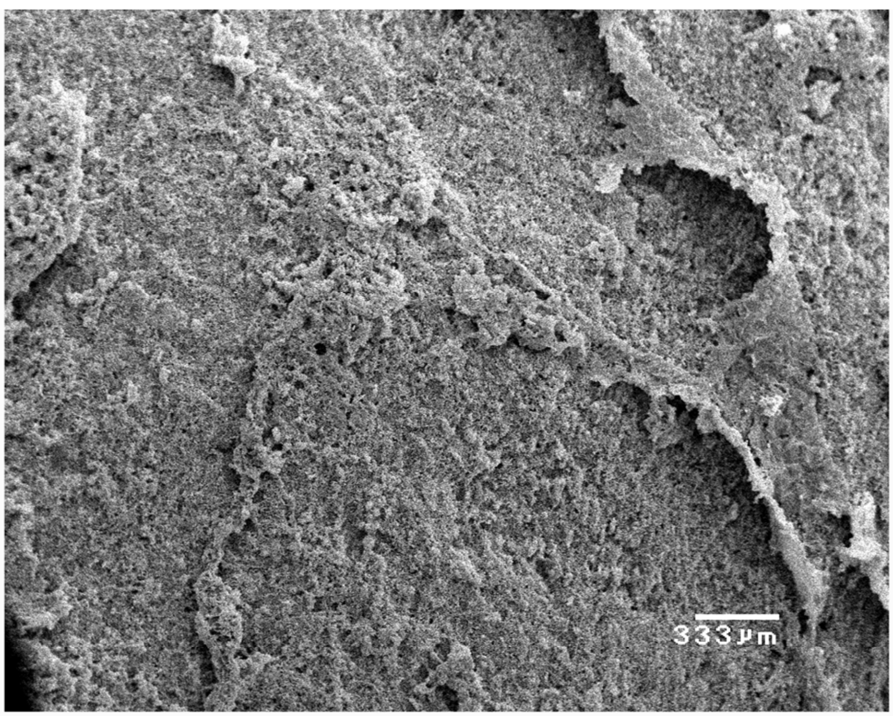

Figure 4-7. Scanning electron microscope photomicrograph of a pore cast from 6289.7 feet, Bug No. 4 well, showing pattern of intersecting fractures in a tight portion of the sample. The linear feature in the upper right may represent artificially bent fracture-filling epoxy. The circular feature is a grain. Note that the solid areas represent porosity. Scale represents 333 microns (0.333 mm). Porosity = 14.5 percent; permeability = 92 mD based on core-plug analysis.

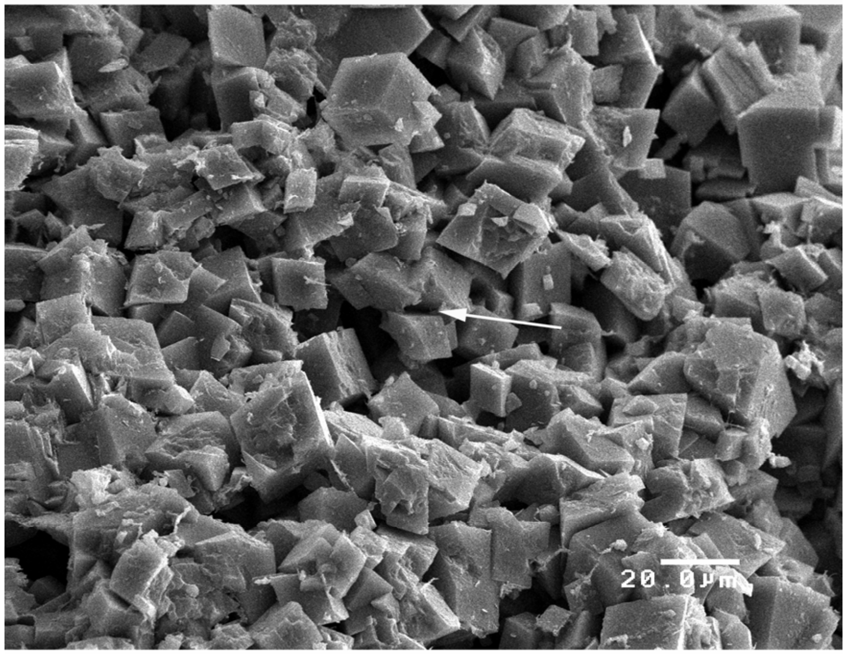

Figure 4-8. Scanning electron microscope photomicrograph of a core plug from 5781.2 feet, Cherokee No. 33-14 well, showing well-developed dolomite rhombs exhibiting abundant intercrystalline microporosity (arrow). Scale represents 20 microns (0.02 mm). Porosity = 23.6 percent; permeability = 103 mD based on core-plug analysis.

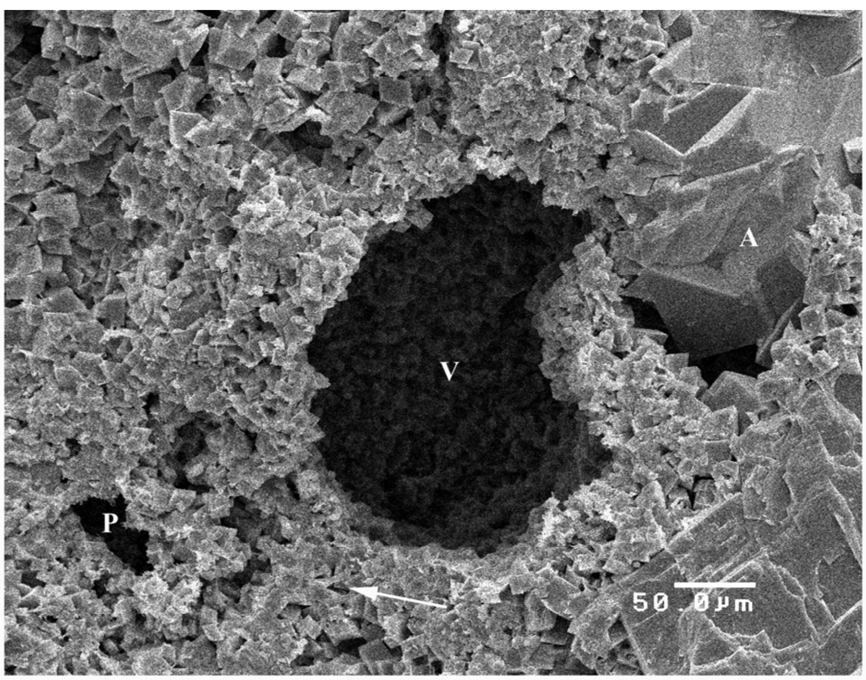

Figure 4-9. Scanning electron microscope photomicrograph of a core plug from 5827.7 feet, Cherokee No. 22-14 well, showing dolomite with a mesovug (V) and visible anhydrite (A) cement, smaller mesopores (P), and intercrystalline micropores (arrow). Scale represents 50 microns (0.05 mm). Porosity = 17.1 percent; permeability = 4.5 mD based on core-plug analysis.

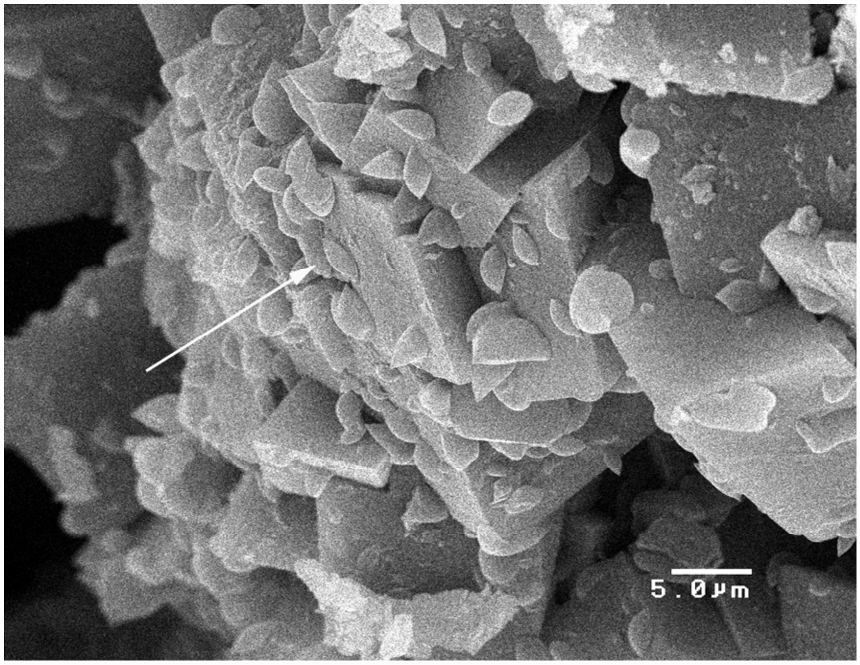

Figure 4-10. Scanning electron microscope photomicrograph of a core plug from 5768.7 feet, Cherokee No. 22-14 well, showing pyrobitumen (arrow) on dolomite, within a microfracture. Micropores are black areas. Scale represents 5 microns (0.005 mm). Porosity = 22.9 percent; permeability = 215 mD based on core-plug analysis.

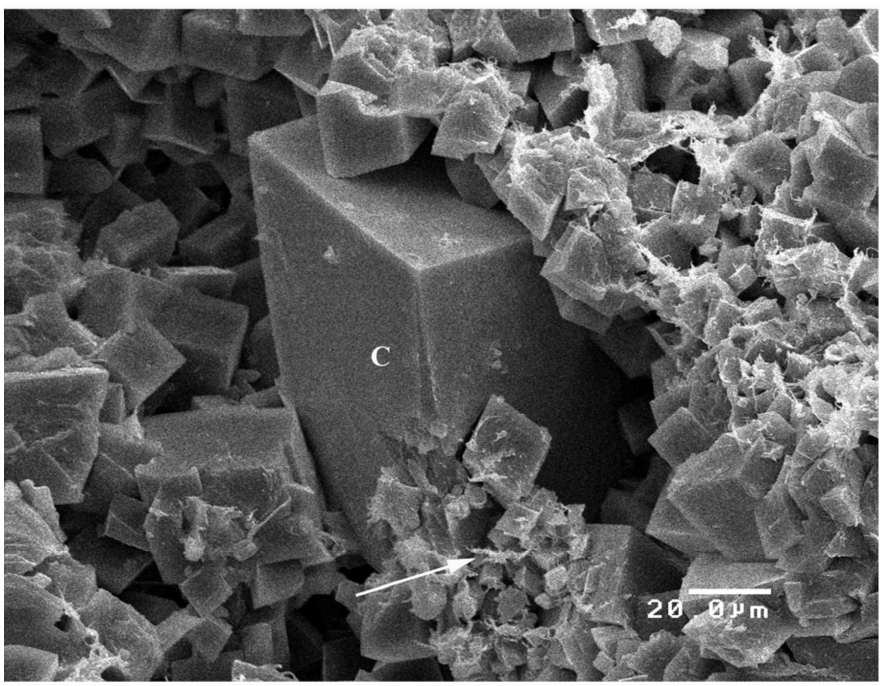

Figure 4-11. Scanning electron microscope photomicrograph of a core plug from 5827.7 feet, Cherokee No. 22-14 well, showing equant spar calcite (C), a burial cement, as well as minor smectite clay (arrow) present in a large moldic pore on the dolomite. Scale represents 20 microns (0.02 mm). Porosity = 17.1 percent; permeability = 4.5 mD based on core-plug analysis.

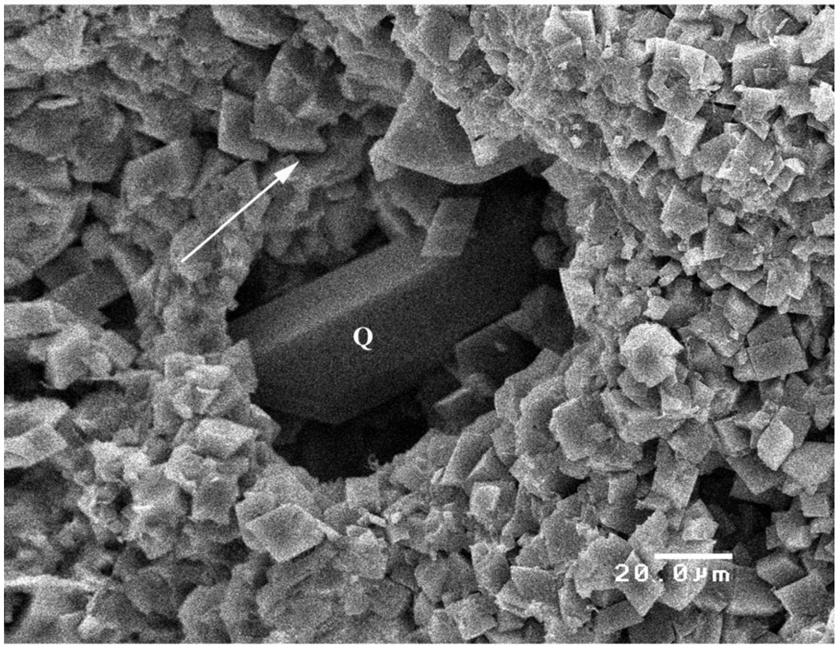

Figure 4-12. Scanning electron microscope photomicrograph of a core plug from 5773.9 feet, Cherokee No. 33-14 well, showing authigenic quartz crystal (Q) within a mesovug. Note the presence of intercrystalline microporosity (arrow). Scale represents 20 microns (0.02 mm). Porosity = 19.1 percent; permeability = 11 mD based on core-plug analysis.

Sequence of Diagenetic Events

The general diagenetic sequence for the Paradox Formation samples, based on SEM and pore casting analyses, is listed below (not all diagenetic events were identified in every sample). The various diagenetic events are included in table 4-2.

1. Calcite cementation
2. Dissolution
3. Dolomitization
4. Dissolution
5. Fracturing
6. Calcite cementation
7. Quartz cementation
8. Clay deposition
9. Anyhydite cementation
10. Pyrobitumen emplacement

Diagenesis played a major role in the development of reservoir heterogeneity in Bug and Cherokee fields as well as throughout all of the Paradox Formation fields. Based on the combined examination of samples in thin sections, core, scanning electron microscopy, and pore casts, the diagenetic processes started during Paradox Formation deposition and continued throughout its burial history. A complete listing of diagenetic events through time and their individual significance is shown on (figure 4-13). Major early (eogenetic) events were dominated by marine cement cementation, seepage reflux/hypersaline and mixing zone dolomitization, and micro-boxwork dissolution. Late (mesogenetic) events were dominated by micro-porosity dissolution and fracturing.

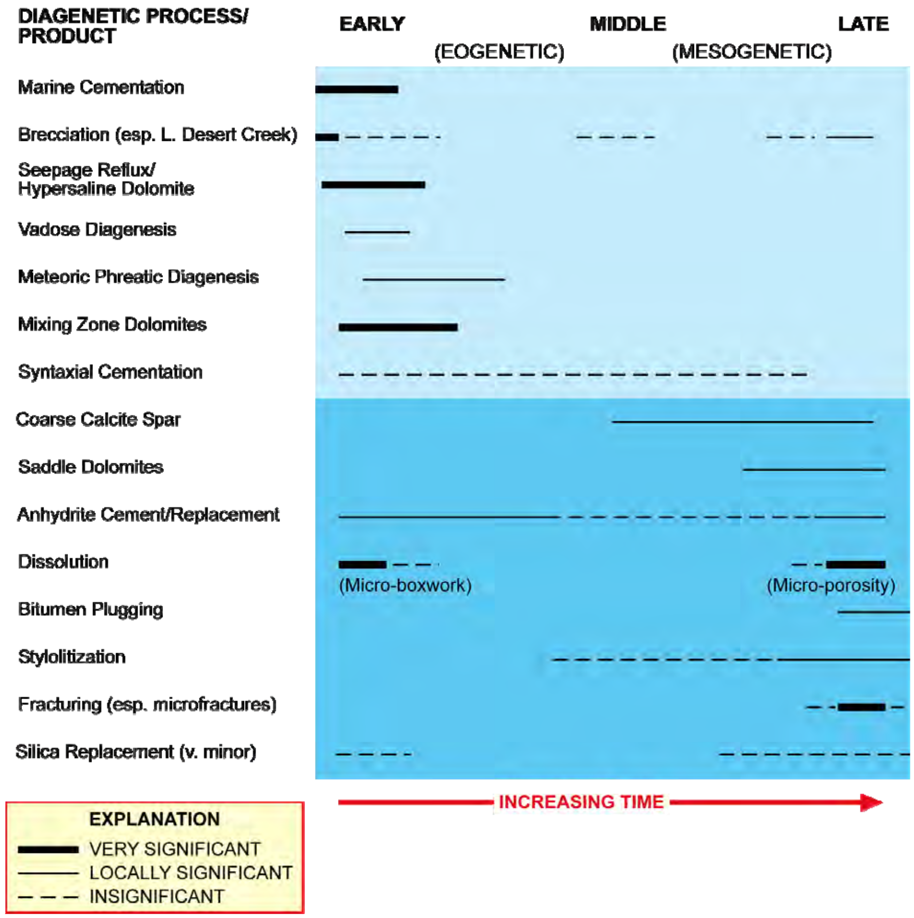

Figure 4-13. Ideal diagenetic sequence through time based on thin sections, core, scanning electron microscopy, and pore casts from the Ismay and Desert Creek zones, Cherokee and Bug fields.

CHAPTER V
EPIFLUORESCENCE ANALYSIS: CHEROKEE AND BUG CASE-STUDY FIELDS

David E. Eby, Eby Petrography & Consulting, Inc.;
and
Thomas C. Chidsey, Jr., Utah Geological Survey

Introduction

Cherokee and Bug case-study fields (figure 1-3) were chosen for blue-light epifluorescence photomicroscopy, examination, description, and interpretation of selected thin sections of samples taken from wells in the fields (**Deliverable 1.2.5 – Thin Section Epifluorescence: Cherokee and Bug Fields, San Juan County, Utah)**. Epifluorescence microscopy is a technique that has been used successfully in recent years to provide additional information on diagenesis, pores, and organic matter (including "live" hydrocarbons) within sedimentary rocks. It is a rapid, non-destructive procedure that can be done using a high-quality petrographic (polarizing) microscope equipped with reflected light capabilities. The basic principles and equipment for epifluorescence were largely developed in the 1960s and 1970s for applications in coal petrology and palynology (see reviews by van Gijzel, 1967; Teichmuller and Wolf, 1977). All applications depend upon the emission of light (by a material capable of producing fluorescence) that continues only during absorption of the excitation-generating light beam (Rost, 1992; Scholle and Ulmer-Scholle, 2003).

Epifluorescence techniques have been used within industry and research for three objectives. First, epifluorescence microscopy has been used extensively for enhancing petrographic observations, including the recognition of depositional and diagenetic fabrics within recrystallized limestone and massive dolomite (see, for instance, Dravis and Yurowicz, 1985; Cercone and Pedone, 1987; Dravis, 1991; LaFlamme, 1992). Second, the study of pore structures, microfractures, and microporosity within both carbonates and sandstones has been greatly facilitated by impregnating these voids with epoxy spiked with fluorescing dyes (Yanguas and Dravis, 1985; Gies, 1987; Cather and others, 1989a, 1989b; Soeder, 1990; and Dravis, 1991). Third, the evaluation of "oil shows" (Eby and Hager, 1986; Kirby and Tinker, 1992) and determination of the gravity or type cements and minerals has been facilitated by epifluorescence microscopy (Burruss, 1981, 1991; Burruss and others, 1986; Guihaumou and others, 1990; Lavoie and others, 2001). Only the first two objectives were pursued in this study. Also, fluid inclusions were not evaluated in this project.

Previous Work

There is no known published use of epifluorescence microscopy on the upper Ismay and lower Desert Creek subsurface rocks of the Blanding sub-basin. However, the published work cited above, applications to carbonate reservoirs listed in Eby and Hager (1986) for a study done within a Permian Basin carbonate field, and case studies documented by Dravis (1988, 1992) provided incentives to apply epifluorescence petrography to Paradox Formation reservoir rocks within the Cherokee case-study field.

Methodology

Epifluorescence petrography for this project used incident (reflected) blue light fluorescence microscopy employing the general procedures outlined by Dravis and Yurewicz (1985), including the use of the modified "white card" technique outlined by Folk (1987) and Dravis (1991). Ultraviolet (UV) fluorescence did not effectively add any textural or pore structure information that could not otherwise be seen under blue-light excitation, even though some workers utilize UV fluorescence for evaluating fluid inclusions and compositional zoning within dolomite crystals (see Scholle and Ulmer-Scholle, 2003). Fluorescence data and observations collected for this study utilized a Jena (now part of Carl Zeiss) research-grade combination polarizing-reflected light microscope equipped with a high-pressure mercury vapor lamp for epifluorescence excitation, a Zeiss IIIRS epifluorescence nosepiece, and a 35-mm camera system. Magnification ranges for examination and photo-documentation were between ~130 and 320x. The epifluorescence optical configuration used is similar to that shown in figure 5-1.

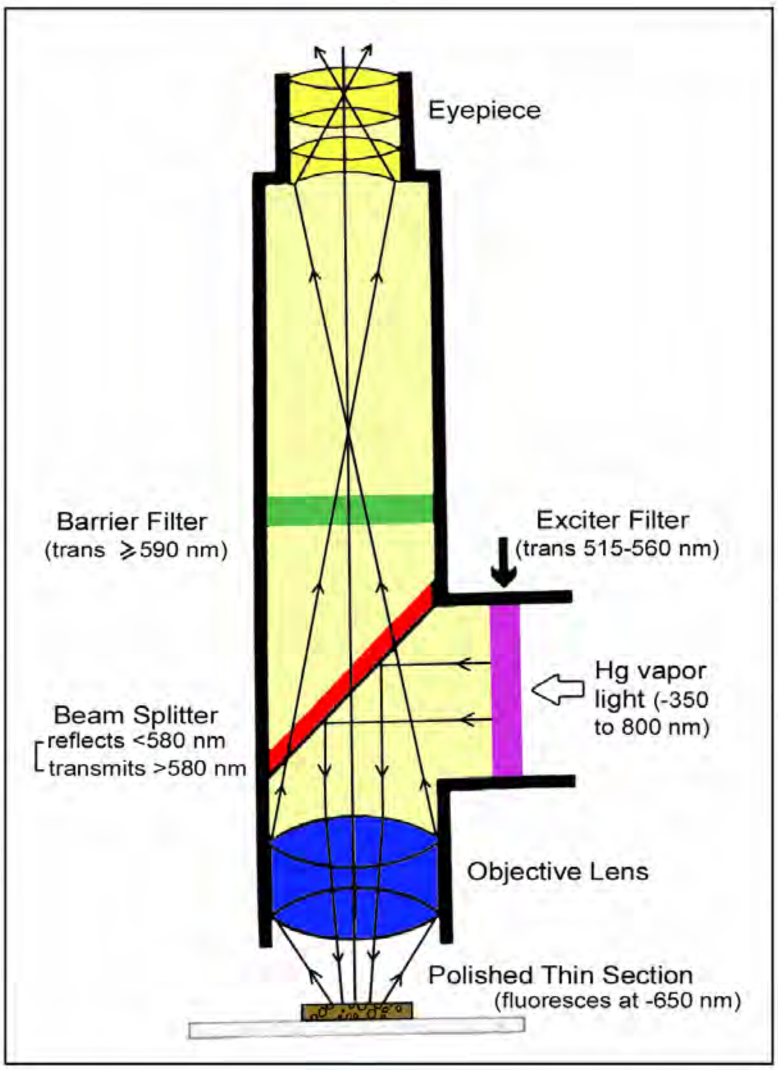

Figure 5-1. Generalized microscope optical configuration for observing fluorescence under incident light (modified from Soeder, 1990).

The light pathways and mechanics of the epifluorescence used in this study have been generally described by Soeder (1990). As described by Burruss (1991), "these excitation wavelengths are reflected to the microscope objective and sample by a dichroic beamsplitter which has a dielectric coating that reflects a specific short wavelength range. Fluorescence emission and reflected short wavelength excitation light is collected by the objective. The dichroic beamsplitter transmits the long wavelength fluorescence emission, but reflects the short wavelengths back toward the light source. The fluorescence emission passes through a barrier filter which removes any remaining short wavelength excitation light." Blue light (~420-490 nm exciter filter/520 nm barrier filter) was used to excite the cuttings and core-chip samples. We have found broad-band, blue-light epifluorescence to be the most helpful in observational work on dolomite, although some workers report applications using UV light (330-380 nm exciter filter/420 nm barrier filter) or narrow-band, blue-violet light (400-440 nm exciter filter/480 nm barrier filter). Finally, the greater depth of investigation into a sample by the reflected fluorescence technique than by transmitted polarized light or other forms of reflected light make it possible to resolve grain boundary and compositional features that are normally not appreciated in cutting or thin-section petrography.

Sample preparation is inexpensive and rapid, involving standard thin section preparation techniques. Thin sections were prepared from representative upper Ismay fabrics. These thin sections were vacuum- and pressure-impregnated with blue-dyed epoxy (see Gardner, 1980) that was spiked with a fluorescing compound. Microscopy used only uncovered polished surfaces. Examination for each thin section area of interest included photo-documentation under epifluorescence and plane-polarized light at the same magnification. Photomicrography of the compositional, textural, and pore structure attributes was done using high-speed film (ISO 800 and 1600) with some bracketing of exposures as camera metering systems do not always reliably read these high-contrast images in the yellow and green light spectrum. Since the image brightness is directly proportional to magnification, the best images are obtained at relatively high magnifications (such as greater than 100x). Low-power fluorescence is often too dim to effectively record on film. These techniques are applicable to thin sections from both core and cuttings samples.

Epifluorescence Petrography of Upper Ismay Thin Sections, Cherokee Field

Blue-light, epifluorescence (EF) microscopy was completed on six core samples for a variety of rock textures and diagenetic phases from upper Ismay zone limestone and dolomite within Cherokee field. These samples were selected to be representative of compositional, diagenetic, and pore types encountered within the two cored wells (Cherokee Federal No. 22-14 and Cherokee Federal No. 33-14). A detailed description and interpretation of the fluorescence petrography of each sample follows below along with photomicrographs (as figures 5-2 through 5-7) to show representative views under both blue-light EF and plane-polarized light. Short descriptive captions for these photomicrographs are included with each photo pair.

Cherokee Federal No. 22-14 Well

Blue-light EF microscopy of the sample from 5768.7 feet (1758 m) nicely shows pore spaces and structures that are not readily seen under transmitted, plane-polarized lighting. Black bitumen linings and interlocking, dolomite, crystalline aggregates mask clear definition

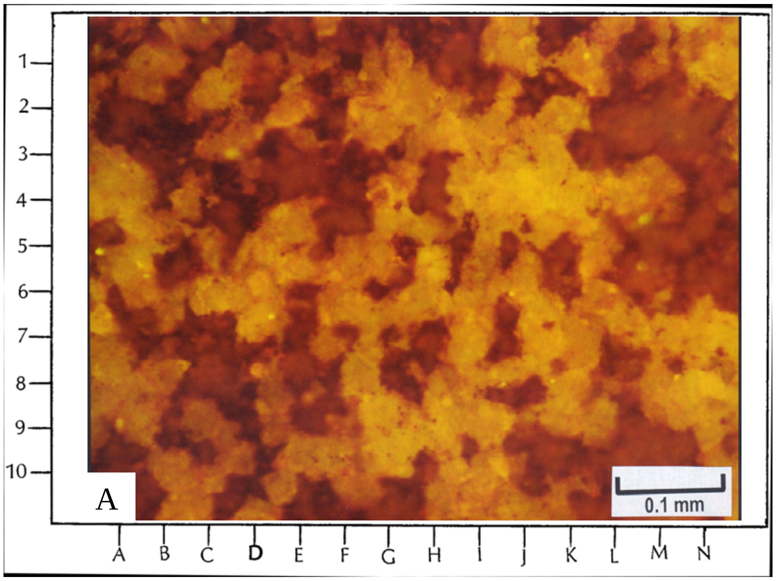

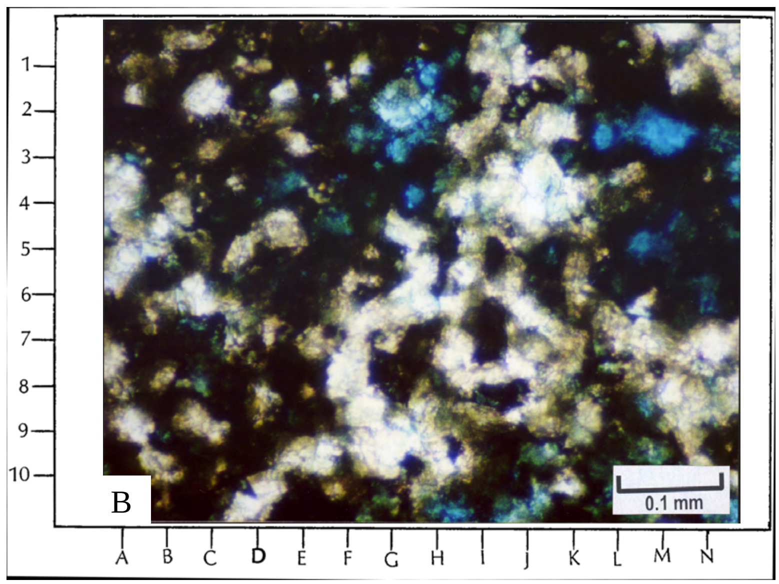

Figure 5-2. Photomicrographs from Cherokee No. 22-14 well at 5768.7 feet. A - Epifluorescence under moderate magnification of a representative area of microporosity shows outlines of small dolomite crystals (fluorescing yellow here due to oil staining). The reddish areas are pores with abundant bitumen linings and plugging (see figure 5-2B). Fluorescence petrography makes it possible to clearly see the dolomite crystals versus the pore space. In places, very small rhombic outlines of dolomite crystals can be resolved (see, for instance, E-9, G-4 and N-1). Most of the pores appear in cross section to be poorly size-sorted and of dissolution origin. Many of these pores appear to be completely surrounded by an interlocking network of dolomite crystals (see, for instance, H-3, H-6.5, and J-4). B - The same field of view as above is shown under plane light at the same magnification. Note that the black (and opaque) areas composed of bitumen mask the crystal boundaries of the dolomite as well as individual pore outlines. The white and gray areas are remnants of the dolomite matrix that are not masked by the bitumen. Only a small amount of pore space (blue-dyed areas) can be seen in this view compared to the fluorescence photomicrograph above.

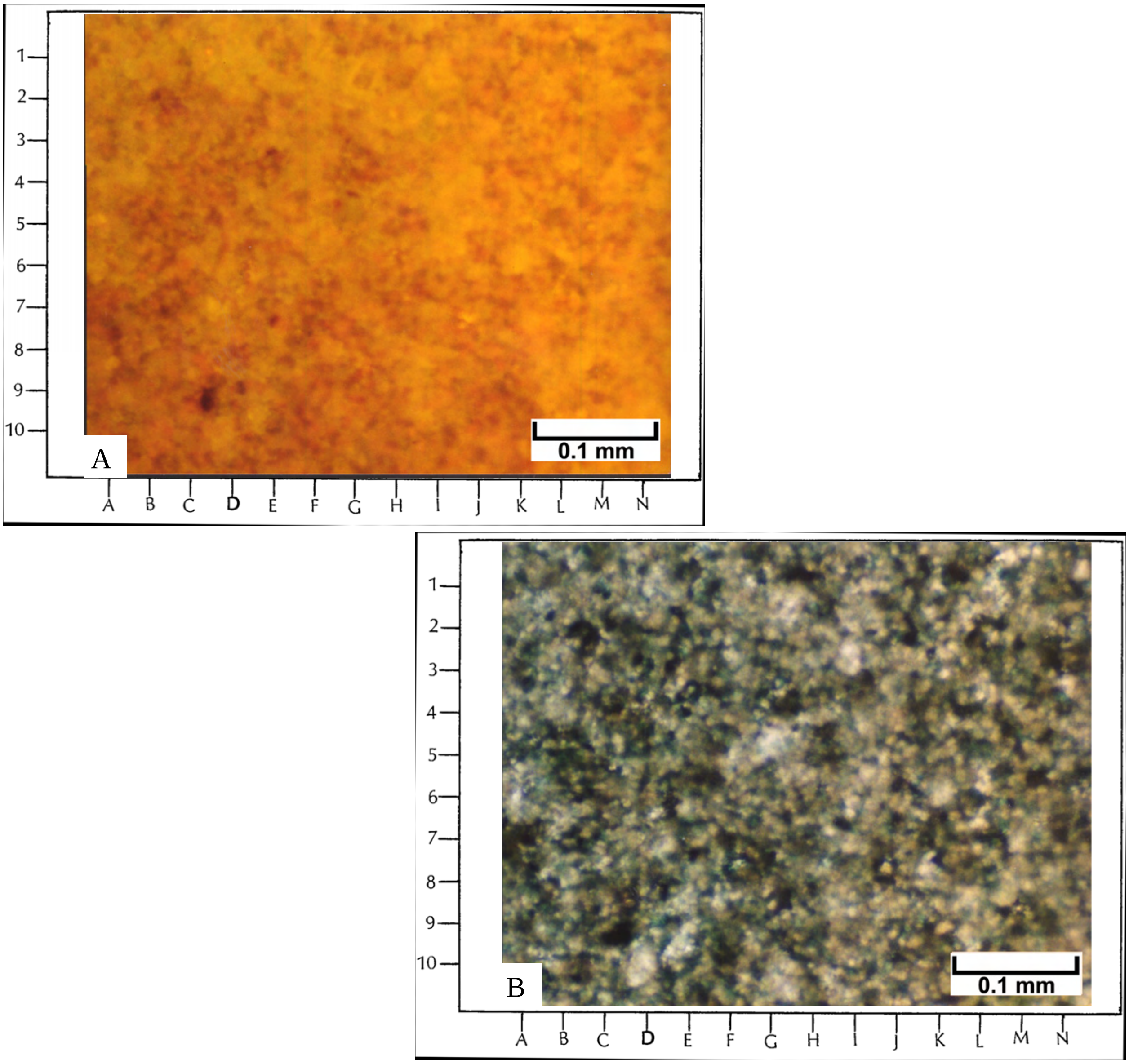

Figure 5-3. Photomicrographs from Cherokee No. 22-14 well at 5778.1 feet. A - A representative EF photomicrograph of a dense dolomitic limestone under moderate magnification distinguishes porosity from oil-stained matrix. The reddish areas represent the epoxy-impregnated pores within this sample. The yellow areas are the oil-stained, carbonate, mineral matrix. Note that the fluorescence image helps to identify occult carbonate grains such as probable fossils (for example G-2, H-2, and J-9) and small peloids (for example C-1, I-5, K-8, and so forth) that are not visible in the plane-light image. This dense limestone was deposited as a bioclastic-peloidal grainstone to packstone. B - The same field of view as above is shown under plane light at the same magnification. This portion of the sample has been artificially stained with Alizarin Red-S solution. The pink areas are calcite while the white and gray areas are mostly dolomite. The indistinct black patches are indicative of some bitumen plugging within microporous spaces. The bluish areas within this view are due to the impregnation of blue-dyed epoxy into the micropores. However, it is impossible to see any of the carbonate components, the depositional texture, or the open pores without use of EF lighting as shown above.

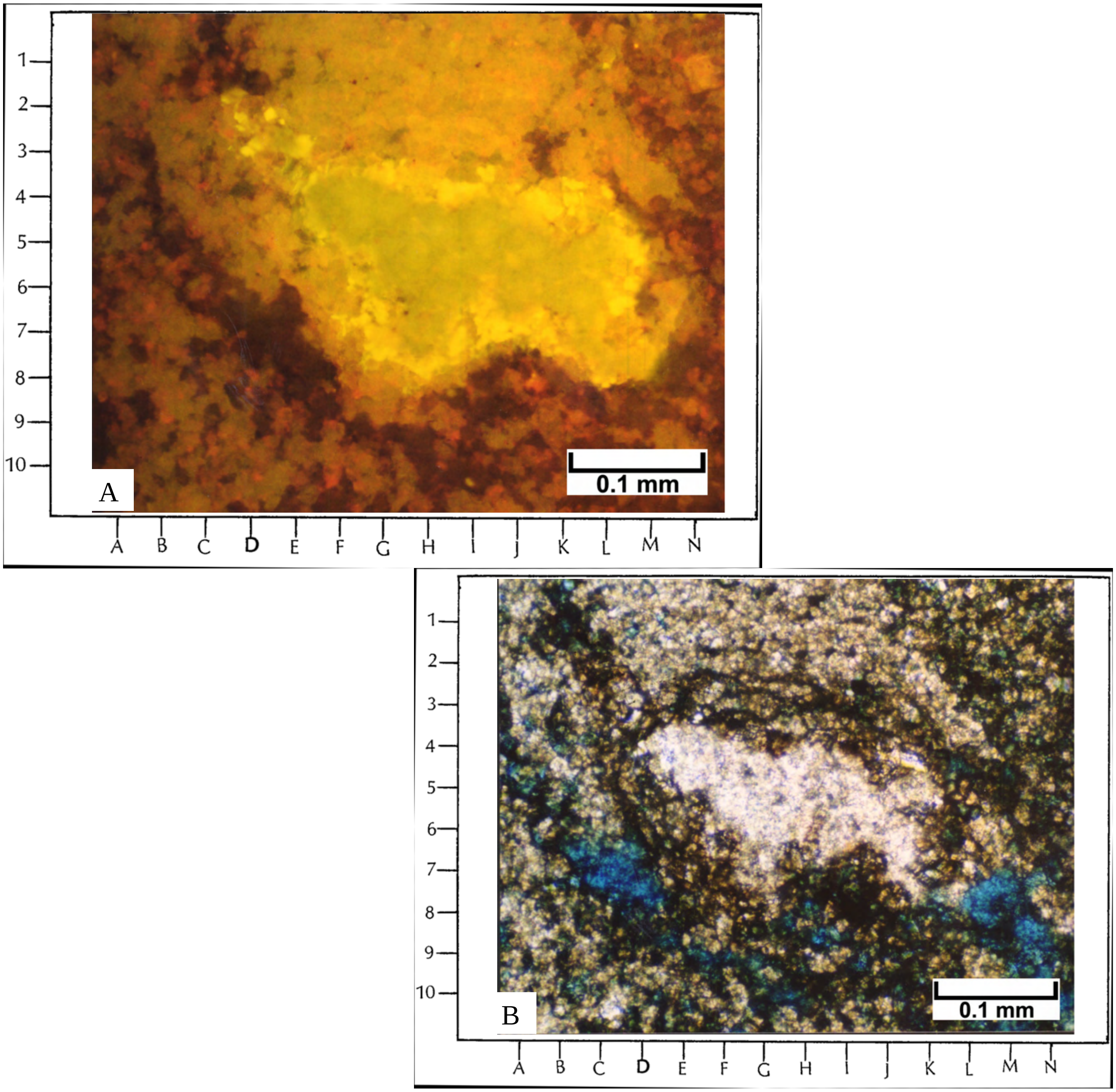

Figure 5-4. Photomicrographs from Cherokee No. 22-14 well at 5783.5 feet. A - A wide range of information can be seen in this EF image. The amoeboid, greenish-yellow feature in the center (from F-4 to M-7) is a small nodule of anhydrite surrounded by finely crystalline dolomite. The bright-yellow rim around the anhydrite is due to live oil bleeding out of the dolomite and trapped against the impervious nodule. The dull-yellow areas throughout the remainder of this image consist of dolomite containing small amounts of fluorescing oils. The solid patch of dull fluorescence across the top of this photomicrograph (from E-2 to K-2) is a tight area with interlocking dolomite crystals. The black and dark red areas show where the open pore spaces occur, including pores with some bitumen coatings. Finally, the orangish areas are mostly likely weakly fluorescing portions of bitumen. B - The same field of view as above is shown under plane light at the same magnification. Even though it is possible to identify the white nodule of anhydrite in the center of this field of view, the details of pore distribution, as well as the fluorescence of live oils and bitumen distribution, are not easy to see in this transmitted-light image.

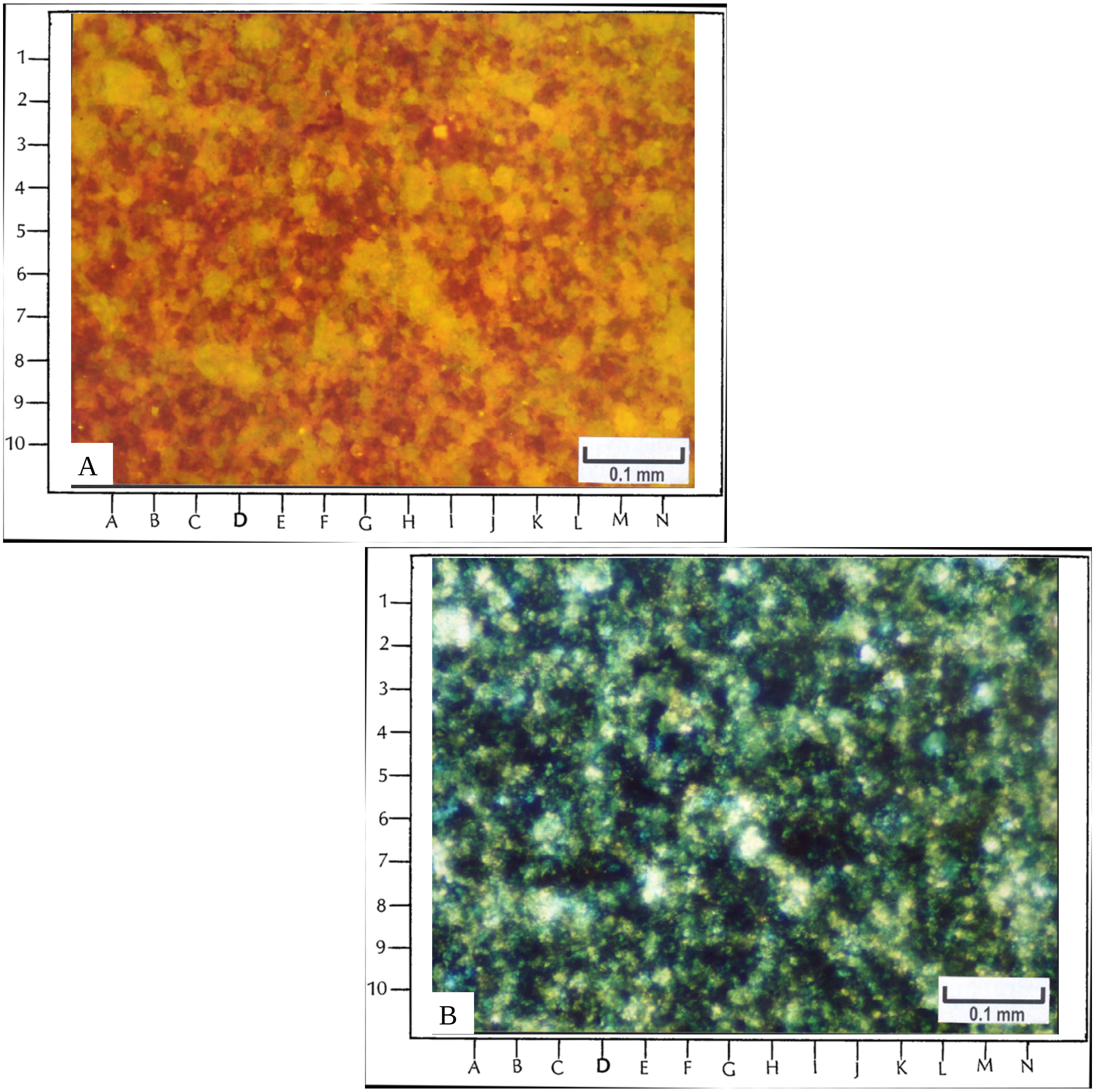

Figure 5-5. Photomicrographs from Cherokee No. 22-14 well at 5801.3 feet. A - Abundant pore space can be seen in this fluorescence image, where the epoxy-impregnated pores appear red. Despite the heterogeneity of the distribution of pores, most of this microporosity seems to be moderately well connected. The greenish-yellow and yellow colors in this image are from matrix areas composed of dolomite and limestone. The brightest yellow areas reflect staining of the matrix by live oil. Note the hints of earlier sand-sized carbonate grains (for example F-1.5, H-2, and L-5) and occasional, isolated, larger, dolomite rhombs (for example B-1.5, G-7, and K-2). B - The same field of view as above is shown under plane light at the same magnification. Note that the details of the pore sizes and shapes cannot be seen in this transmitted light photo. Abundant black bitumen throughout this microporous network makes it nearly impossible to see the amount of visible porosity. At best, the microporosity in this image shows up as an indistinct "blue haze." In addition, it is not possible to see any hints of original grains or the sizes of dolomite crystals.

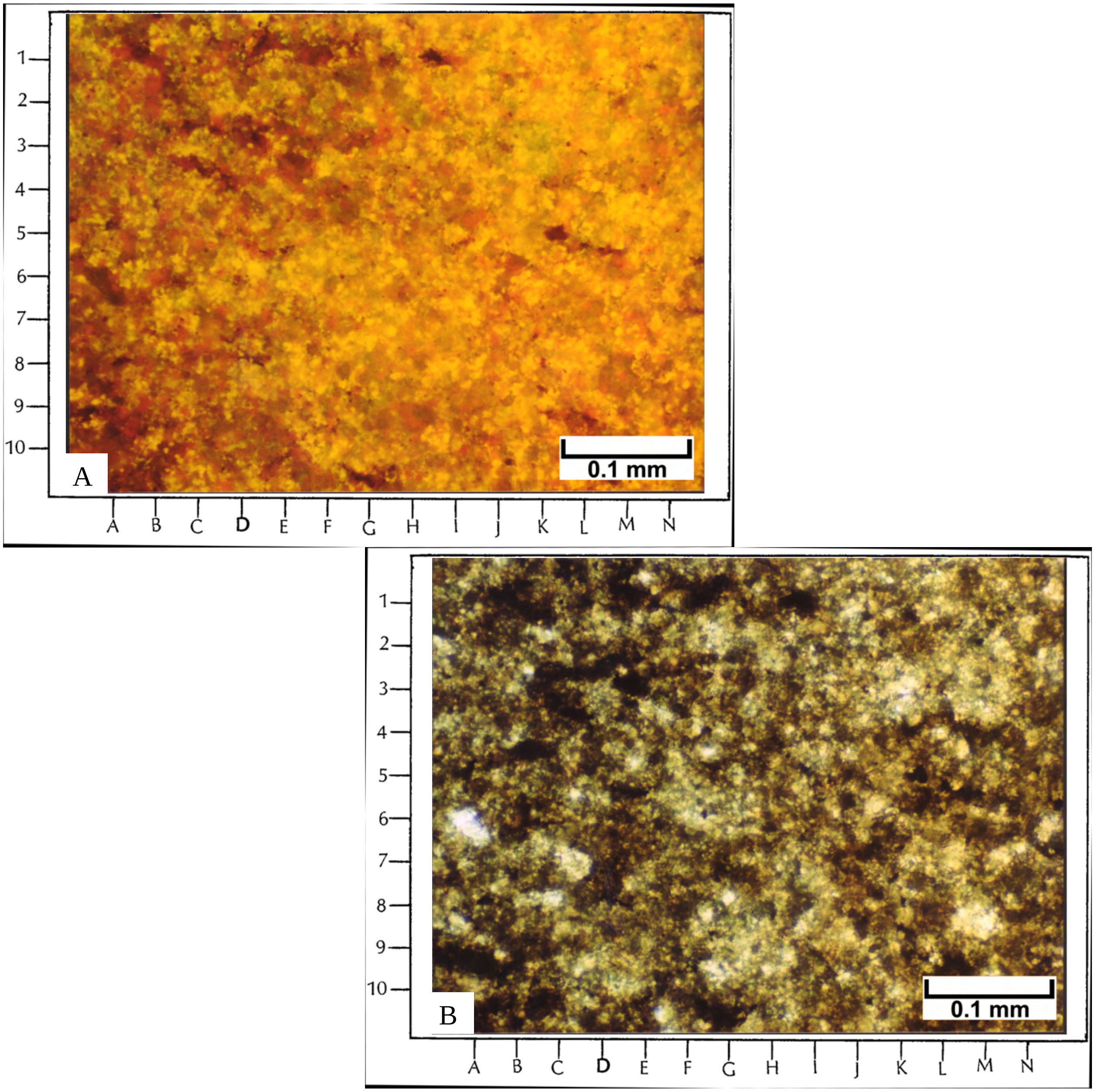

Figure 5-6. Photomicrographs from Cherokee No. 22-14 well at 5864.1 feet. A - This sample comes from a rather tight limestone than has no visible matrix porosity under transmitted lighting (see photomicrograph below). However, under EF microscopy, there is some red fluorescence from spike epoxy that has been impregnated into matrix pore spaces. Therefore, the scattered red spots in this image show the presence of some porosity. The abundant bright-yellow specks across the image are probably the result of live-oil staining throughout this relatively low-porosity sample. Note the dull-green areas which show some relict preservation of the peloids (for example E-3, F-4, and L-8) that were the principal constituent of this carbonate sediment. B - The same field of view as above is shown under plane light at the same magnification. There is no visible matrix porosity in this image (that is, no blue colors) despite the appearance in some areas of fluorescing epoxy-filled pores in the image above. In addition, the peloids that can be seen in the fluorescence view are very difficult to make out in this transmitted-light view.

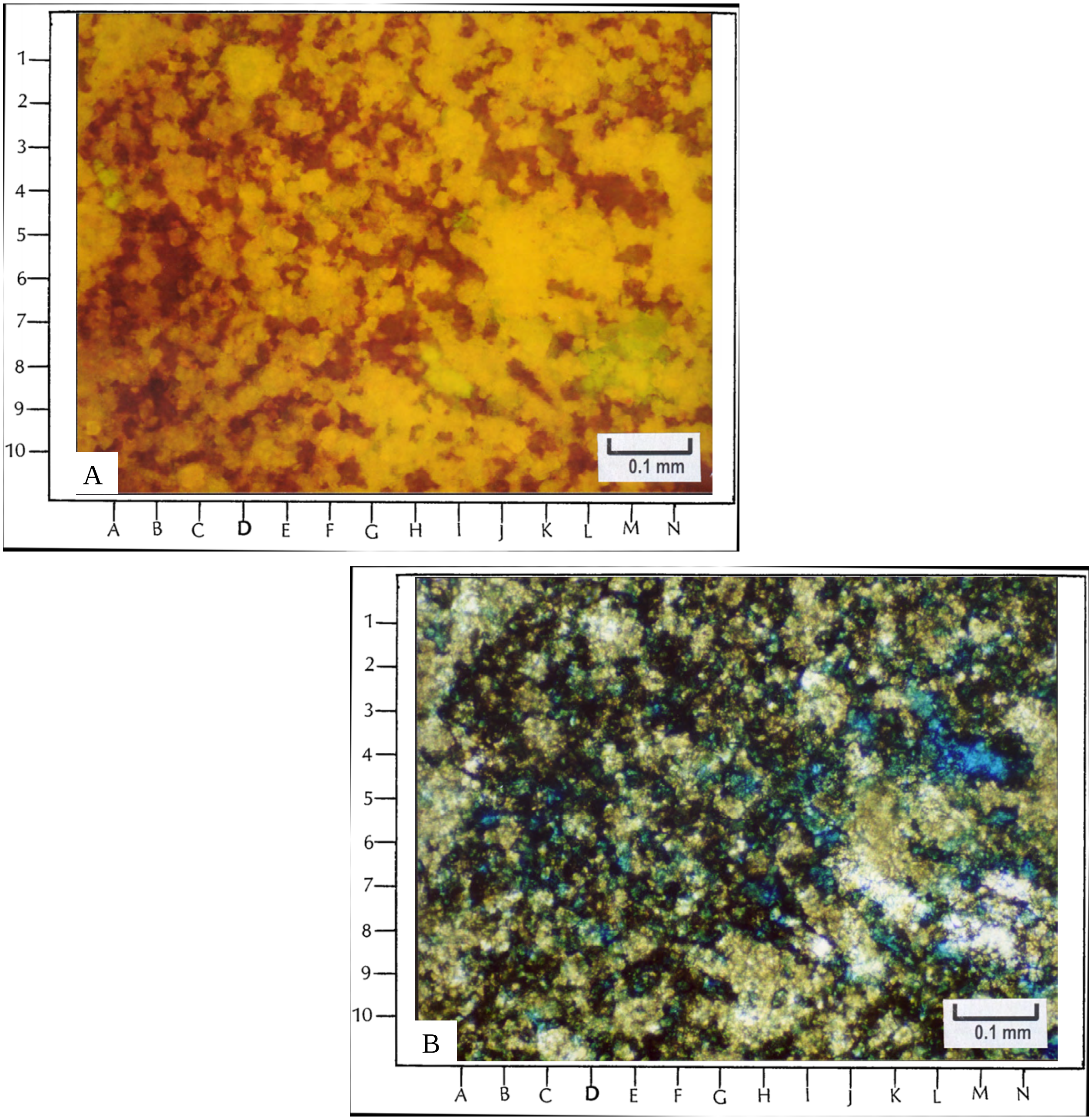

Figure 5-7. Photomicrographs from Cherokee No. 33-14 well at 5773.9 feet. A - This representative EF photomicrograph nicely shows the distribution and shapes of open pores which appear here in the shades of red. Many of these pores are somewhat elongate and are moldic in origin. Most result from the dissolution of small, phylloid-algal plates and possibly other fossil skeletons. Many of these dissolution pores appear to be well connected. The yellow areas are oil-stained carbonates which are mostly composed of limestone here. The light green areas (for example B-3.5 and M-7) are patches of anhydrite cementation. B - The same field of view as above is shown under plane light at the same magnification. Note that the areas of blue-dye colored epoxy are not abundant or as distinct as the areas in red within the fluorescence photomicrograph above. Without the aid of the fluorescence view, the amount of visible open pore space would be underestimated in the plane-light image.

of the blue-dyed epoxy that has been impregnated into the open pore spaces. However, the reddish fluorescence of the epoxy makes it possible to image pores in cross section very nicely (figure 5-2). Despite the significant amount of open porosity visible under EF, many of these voids appear to be completely surrounded by a micro-boxwork of dolomite crystals. Much of the dolomite has a dull- to bright-yellow fluorescence, due in part to the presence of live-oil films around many of the tight intercrystalline spaces. There are no identifiable remnants of the original depositional fabric of this carbonate sediment, although the appearance of probable micro-moldic and slightly larger dissolution pores (figure 5-2) suggests that there were original detrital carbonate grains present. Where anhydrite has secondarily plugged earlier intercrystalline pores (see figure 5-7), the differences in fluorescence between oil-impregated dolomite and very massive anhydrite cement are easy to see.

Blue-light EF microscopy assists with the identification of fossil fragments and peloids that populate this massive, partially dolomitized limestone. Under plane polarized lighting, the sample from 5778.1 feet (1761.1 m) appears dense and muddy. However, the fluorescence petrography reveals depositional textures that range from a fine grainstone to packstone (figure 5-3). In addition, the distribution and types of pores are difficult to identify without examination under fluorescence. Abundant open micropores with some bitumen linings are much easier to see under EF microscopy than trying to resolve the blue-dyed epoxy that has been impregnated into the sample.

Blue-light EF microscopy of the sample from 5783.5 feet (1762.7 m) displays considerable heterogeneity of porosity and its effect on permeability. The EF petrography nicely shows the location and distribution of pores in cross sections and provides good visual discrimination boundaries (figure 5-4). Areas of low porosity and permeability show up particularly well because fluorescent live oil is trapped in the tighter (low-permeability) portions of this sample. In addition, this sample displays some relatively large dolomite crystals (>100 µm across) that have replaced the finer carbonate matrix. Without EF, the size variation of dolomite crystals and some of the related intercrystalline pore space would be nearly impossible to resolve.

Blue-light EF microscopy of the sample from 5801.3 feet (1768.2 m) also displays significant heterogeneity in porosity distribution. Blue-light EF made it possible to image the quantity and quality of microporosity throughout the sample (figure 5-5). "Micro-sucrosic" dolomite appears to dominate this sample with an excellent micro-intercrystalline pore structure that could not be resolved without EF microscopy. Low-amplitude stylolites act as significant vertical permeability barriers between different layers of well-developed matrix microporosity. Replacement of the matrix rock by dolomite and the development of micro-intercrystalline porosity appears to be greatly reduced in areas immediately adjoining the stylolites.

Blue-light EF microscopy of the sample from 5864.1 feet (1787.3 m) shows a very dense limestone containing abundant, closely spaced, wispy, stylolite seams and reveals some very interesting textural and porosity information (figure 5-6). Under plane transmitted light, this sample appears to be a dense lime mudstone, whereas fluorescence examination clearly shows distinct grain-supported peloids. More importantly, EF reveals small compartments of good porosity separated from much tighter rocks by subhorizontal stylolitic seams. Hence, some of the stylolites and wispy seams with concentrations of insoluble residues act as barriers to vertical fluid flow between the porous compartments. Epifluorescence also suggests that the origin of the porosity may be related to dissolution of the peloidal limestone matrix after the formation of the stylolites.

Cherokee Federal No. 33-14 Well

Blue-light EF microscopy of the sample from 5773.9 feet (1760 m) shows slightly dolomitic limestone with high amounts of microporosity and solution-enlarged pores that are difficult to image under plane-polarized lighting. Blue-light EF images nicely show the open pores and their shapes despite the presence of variable amounts of black bitumen lining pore walls (figure 5-7). In addition, EF nicely shows remnants of fossils and non-skeletal grains (peloids and possibly ooids), as well as excellent examples of zoned, replacement, dolomite crystals.

Epifluorescence Petrography of Lower Desert Creek Thin Sections, Bug Field

Blue-light EF microscopy was completed on four samples for a variety of rock textures and diagenetic phases in core samples from oil-productive, lower Desert Creek zone dolomites within Bug field. These samples were selected to be representative of the compositional, diagenetic, pore, and fracture types encountered within the three cored wells (Bug Nos. 7, 10, and 16 [two samples]) from Bug field. A detailed description and interpretation of the fluorescence petrography of each sample follows below along with photomicrographs (as figures 5-8 through 5-11) to show representative views under both blue-light EF and plane-polarized light. Short descriptive captions for these photomicrographs are included with each photo pair.

Bug No. 7 Well

Blue-light EF microscopy of the sample from 6359.3 feet (1938 m) shows very tight dolomites with fairly uniform oil saturation throughout (figure 5-8). Much of the dolomite fluoresces a dull to bright yellow, due in part to the presence of live oil films around many of the tight inter-crystalline spaces. Non-fluorescent areas (which appear red to black in the photomicrographs) indicate extremely tight places where oil could not penetrate. In places, fluorescence petrography makes it possible to see outlines of carbonate grains as well as occasional larger dolomite rhombs. Perhaps the best application of EF in this sample is to determine open, oil-bearing fractures and "stylo-fractures" from healed fractures and tight microstylolites.

Bug No. 10 Well

Epifluorescence examination of the sample from 6327.9 feet (1929 m) aids in two very important aspects of the Bug dolomite oil reservoir. First, the definition of open, crystal-lined microfractures within dense portions of this dolomite is aided considerably with EF. Second, this sample displays well-developed micro-boxworks of dolomite crystal aggregates that serve to isolate a number of the open pores within some of the most porous parts of this sample (figure 5-9). While some pore throats are wide and open, other megascopic pores are "blind" and dead end into dolomite partitions. Only EF petrography techniques allow visual definition of this type of reservoir heterogeneity, as standard plane-light petrography does not image the micro-boxwork patterns very well.

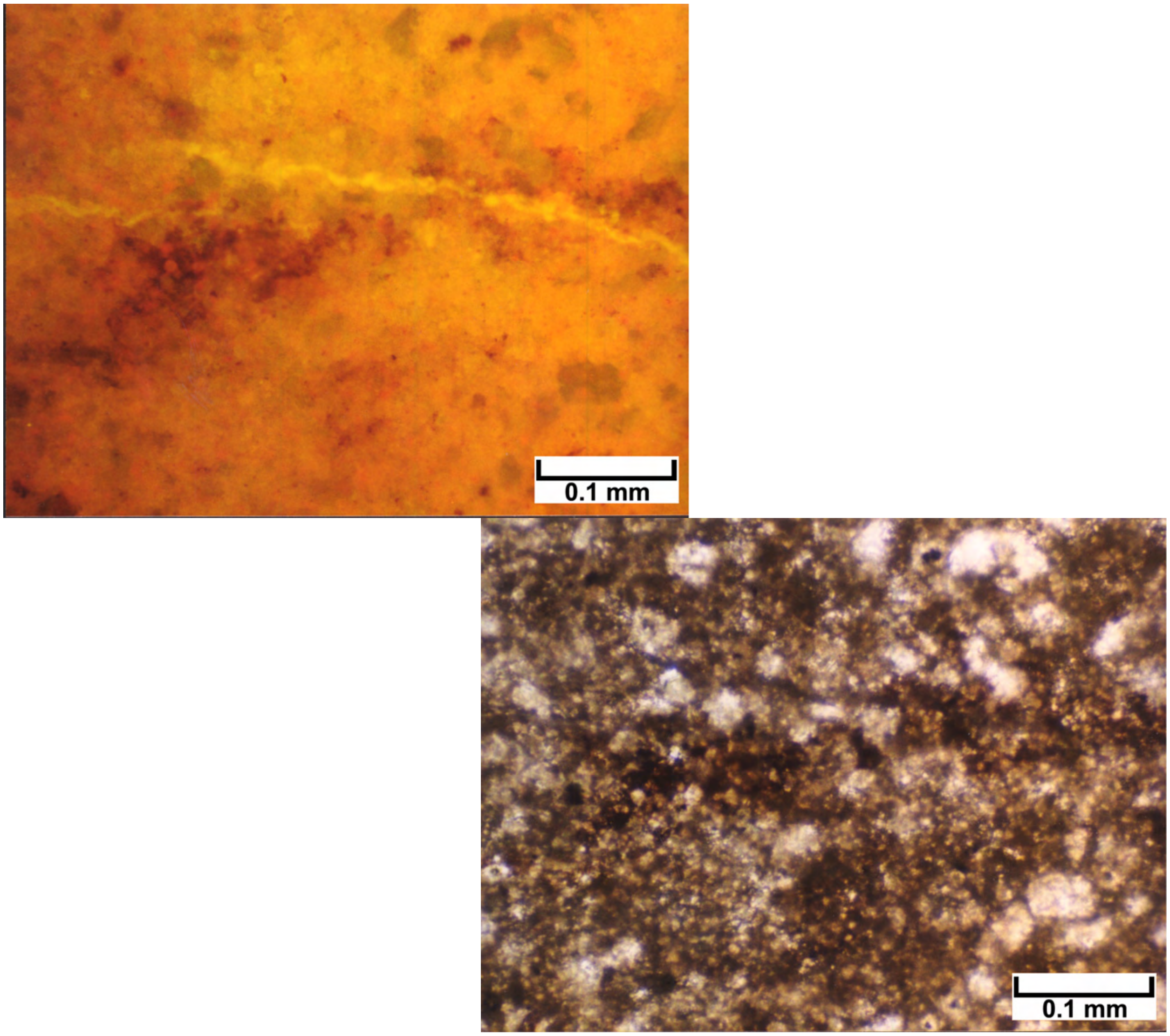

Figure 5-8. Photomicrographs from Bug No. 7 well at 6359.3 feet. A - A representative EF view of a very tight microcrystalline dolomite shows the absence of any significant megascopic matrix porosity. However, the matrix displays a yellowish orange color, indicating probable live oil saturation of this tight dolomite. Notably, there is an open microfracture, with an offset in the upper left center portion of the photomicrograph. It appears bright yellow here due to the fluorescence of "live" hydrocarbons. This microfracture crosses and post-dates a microstylolite marked by the black, jagged pattern across this view from lower left to right center. Most of the rest of the massive (mud-rich) matrix displays a mottled yellow and orange color due to oil saturation in this dolomite. Although there are no readily visible grains in the field of view, there are a few discrete dolomite crystals that appear as the dark green areas. B - The same field of view as above is shown under plane light at the same magnification. Some of the medium to dark-brown color of this dolomite may be the result of oil staining as indicated by the yellowish orange color in the EF view above. Note the poorly preserved peloids and possible fossils in this aphanitic to anhedral dolomite. Some of the larger non-planar dolomite crystals appear white in this view. The open, en echelon (offset) fractures and the wispy microstylolites seen in the top image are very indistinct across the length of this photomicrograph.

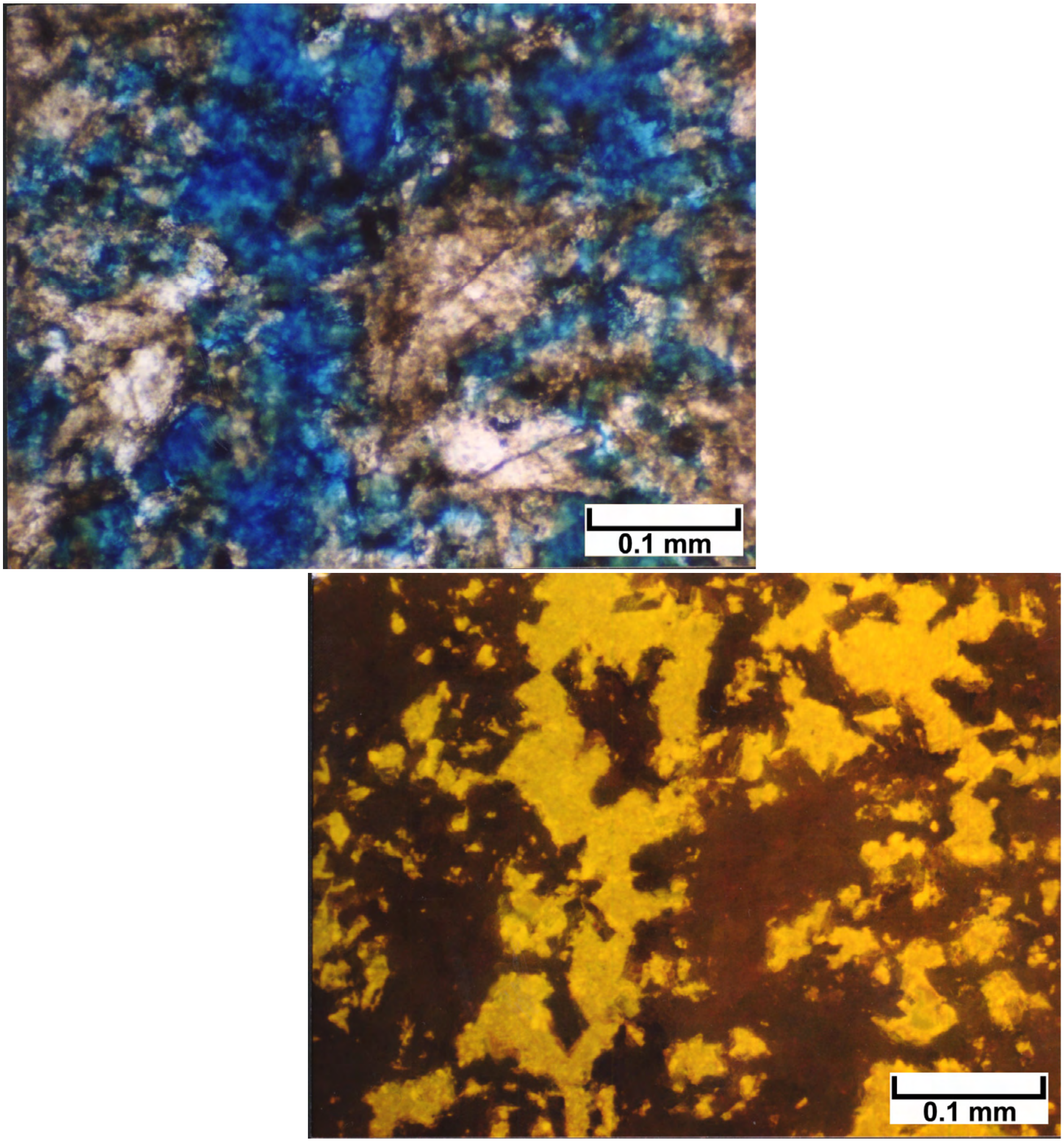

Figure 5-9. Photomicrographs from Bug No. 10 well at 6327.9 feet. A - A heterogeneous micro-boxwork of dolomite is displayed here, where the dolomite crystal aggregates appear dark gray and the open pores between the dolomite are bright yellow (due to spiked epoxy and "live oil" lining pores). Some of the pores appear to be well connected while others are isolated by interlocking dolomite crystals. Hence, some of these large pores may be "blind" or lack interconnections. Note that there is very little evidence of intercrystalline porosity within the dense dolomite areas. B - The same field of view as above under plane light at the same magnification shows fuzzy relationships between the cross section of pores (impregnated with blue epoxy) and the poorly sorted dolomite crystal matrix. No grains or structures are visible within the dolomites in this image.

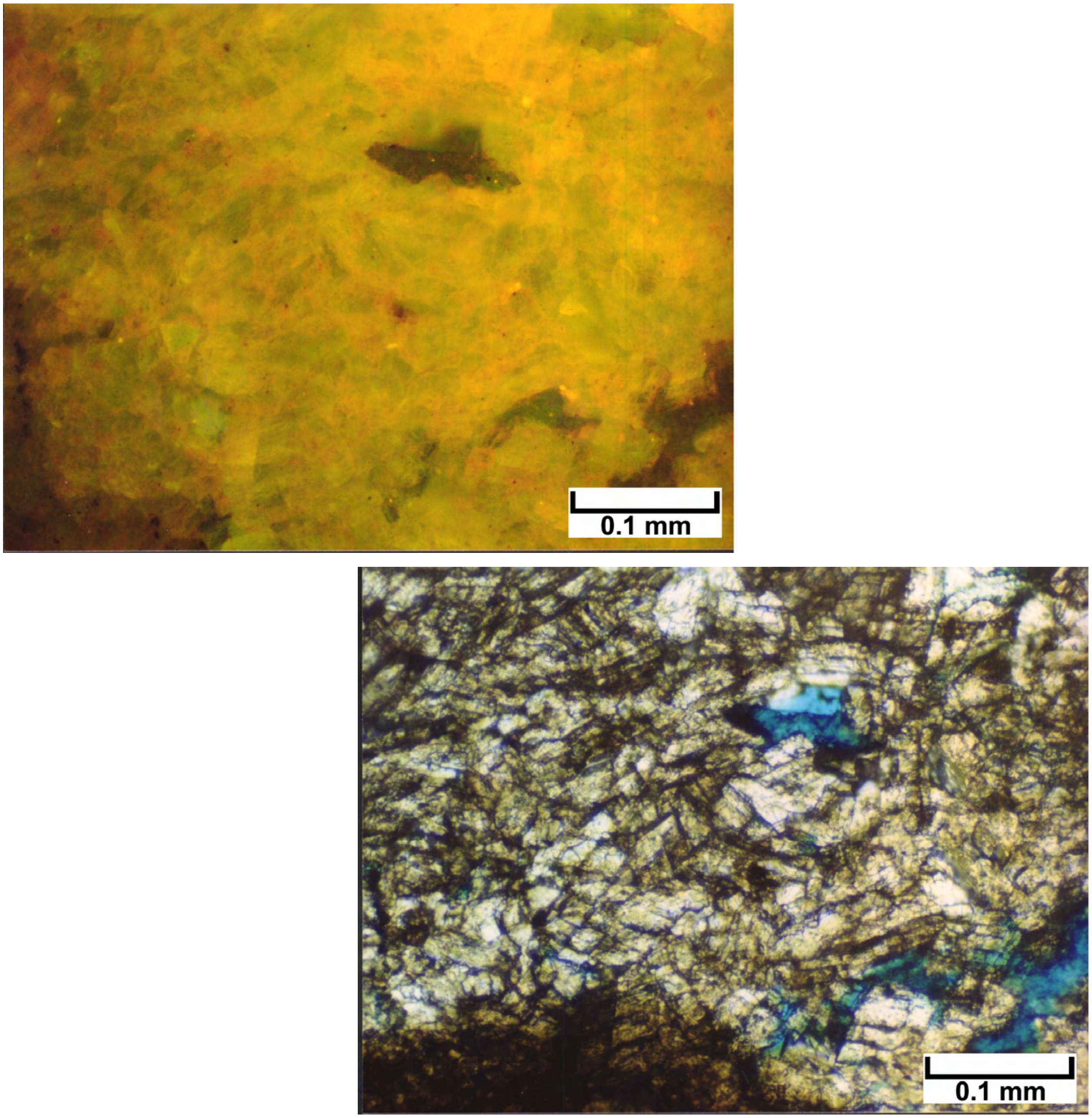

Figure 5-10. Photomicrographs from Bug No. 16 well at 6299.3 feet. A - This portion of the sample displays very tight, moderately coarse, interlocking dolomite crystals with low visible porosity. Note the intense yellow to orangish yellow fluorescence that appears to surround the dolomite subcrystals and microfractures. This yellow fluorescence is probably due to the presence of "live" and/or relict hydrocarbons within the tight intercrystalline spaces. Some of the black and reddish colors in this view may be the result of bitumen lining some of the few isolated open pores. B - The same field of view as above is shown under plane light at the same magnification. The dark gray areas within the interlocking dolomite crystals are probably due to organic matter or oil staining. This staining makes it possible to see the subcrystal boundaries and probable microfractures within them. The small amount of open-pore space in this view is shown in blue, with black bitumen linings.

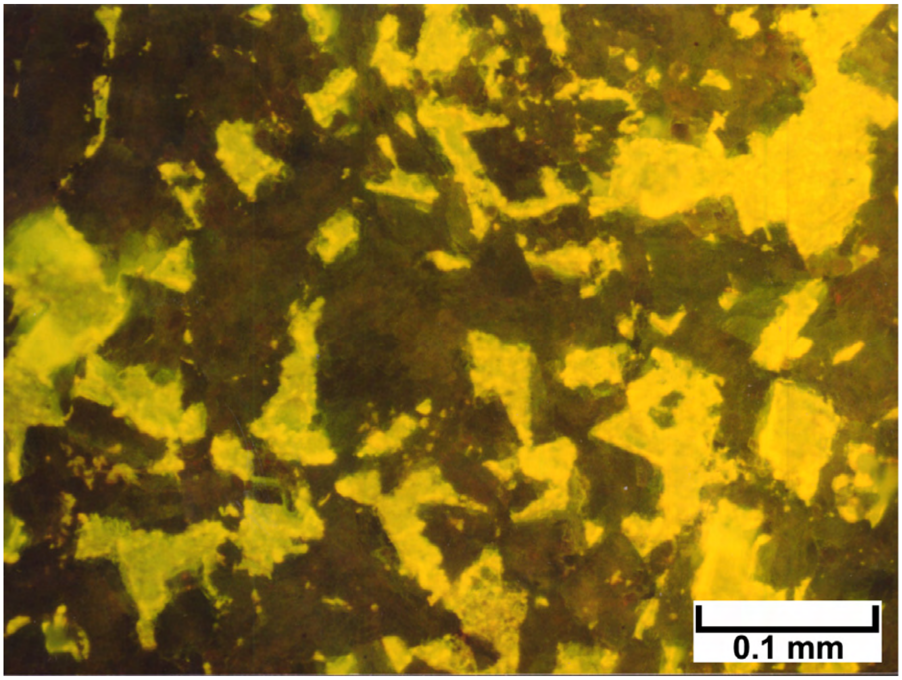

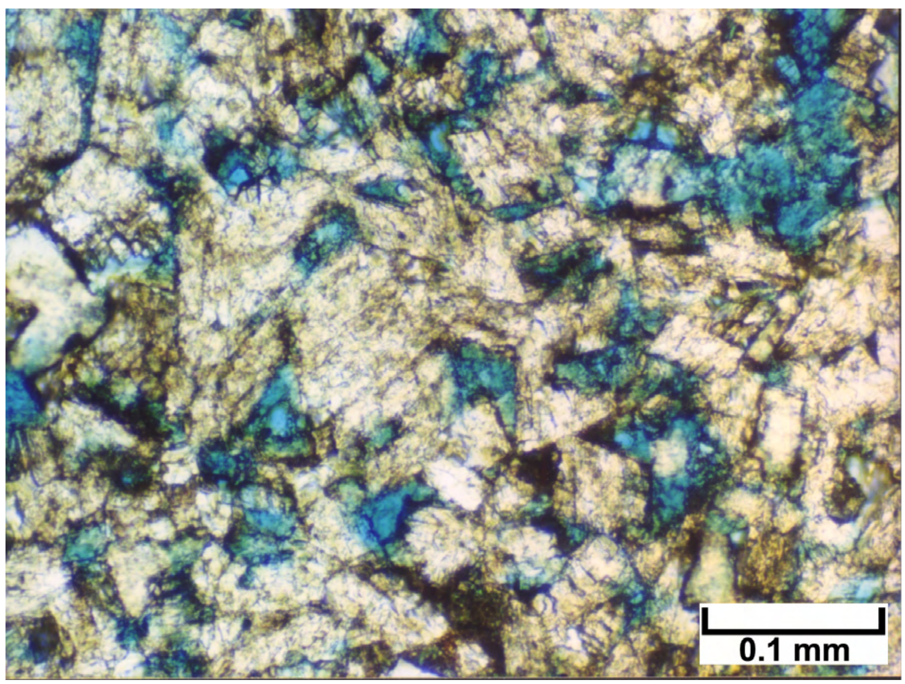

Figure 5-11. Photomicrographs from Bug No. 16 well at 6300.5 feet. A - This EF view nicely displays rhombic and highly angular pores that fluoresce bright yellow. The rhombic dolomite crystals and crystal aggregates are dull gray and gray green in color. Note the sharp contacts between the dolomite crystals and the intercrystalline pores. This image is probably representative of a cross-sectional view of a typical sucrosic dolomite from the lower Desert Creek interval at Bug field. B - The same field of view as above is shown under plane light at the same magnification. Although this view shows the sucrosic dolomite crystals well (in the white to light brown areas), the definition of pore/dolomite contacts is indistinct, in part because of bitumen linings. Pore outlines are much easier to see in the EF image.

Bug No. 16 Well

Blue-light EF microscopy of the sample from 6299.3 feet (1920 m) shows fine- to medium-sized, interlocking crystals in a sucrosic dolomite that displays some intercrystalline porosity (figure 5-10). Epifluorescence examination nicely shows that many of these types of rhombic, sucrosic, dolomite crystals display internal zonation with occasional ghosts of the original replaced carbonate grains. As in other Bug field samples, the definition of pore to matrix boundaries, especially where there are bitumen linings, can be seen much more clearly under EF.

Blue-light EF microscopy of the sample from 6300.5 feet (1920 m) shows excellent examples of rhombic dolomite crystals and crystal aggregates. Fluorescence photomicrographs show sharp contacts between the dolomite crystals and the intercrystalline pores (figure 5-11). This thin section is probably representative of a cross sectional view of a typical sucrosic dolomite from the lower Desert Creek interval at Bug field. In addition, this sample also contains complex networks of micro-boxwork structure. Many of the pores within this network appear to be isolated or "blind." Therefore, drainage of oil from this type of pore system may be inefficient. Under high magnification, EF imaging makes it easy to see highly corroded or scalloped margins of many dolomite crystals in this sample. The corroded dolomite rhomb contacts indicate that there has been some partial dissolution of dolomite rhombs.

CHAPTER VI
CATHODOLUMINESCENCE ANALYSIS: CHEROKEE AND BUG CASE-STUDY FIELDS

David E. Eby, Eby Petrography & Consulting, Inc.;
and
Thomas C. Chidsey, Jr., and Craig D. Morgan, Utah Geological Survey

Introduction

Cherokee and Bug case-study fields (figure 1-3) were selected for cathodoluminescence (CL) photomicroscopy, examination, description, and interpretation of selected thin sections of samples taken from wells in the fields (**Deliverable 1.2.6 – Thin Section Cathodoluminescence: Cherokee and Bug Fields, San Juan County, Utah**). Cathodoluminescence is the emission of light resulting from the bombardment of materials using a cathode ray (Allan and Wiggins, 1993). This technique, which can be an invaluable tool in petrographic studies of carbonate rocks, provides important information about the complex modification of rock fabrics and porosity within the lower Desert Creek and upper Ismay zones of the Blanding sub-basin (see figure 4-13 for sequence of diagenetic events). A complete discussion of the diagenetic history based upon visual core examination, thin section petrography, SEM, and pore casting was documented in **Deliverable 1.2.1A – Thin Section Descriptions: Cherokee and Bug Fields, San Juan County, Utah; Deliverable 1.2.3 – Scanning Electron Microscopy and Pore Casting: Cherokee and Bug Fields, San Juan County, Utah**; and discussed previously in Chapters III and IV.

Cathodoluminescence (CL) has been used in recent years to provide insights into the chemical differences between preserved remnants of depositional components resulting from various diagenetic events in carbonate rocks as recognized from core examination and thin section petrography. In particular, CL provides visual information on the spatial distribution of certain trace elements, especially manganese (Mn^{2+}) and iron (Fe^{2+}) in calcites and dolomites (Machel and Burton, 1991; Scholle and Ulmer-Scholle, 2003). The visible CL responses are red to orange in color, and their intensity is usually described as non-luminescent, dully luminescent, and brightly luminescent. As a general rule, incorporation of Mn^{2+} into the calcite lattice stimulates luminescence and the incorporation of Fe^{2+} quenches or reduces luminescence (Fairchild, 1983; Allan and Wiggins, 1993; Scholle and Ulmer-Scholle, 2003). Qualitative interpretation of CL usually assigns nonluminescent responses to oxidizing settings in which the reduced forms of both Mn and Fe are unavailable for incorporation into the lattices of carbonate mineral precipitates. Oxidized forms of Mn and Fe are not incorporated into calcite or dolomite crystals. Therefore, there is nothing in these crystals to excite luminescence. Bright luminescence is related to carbonate precipitates with high Mn/Fe trace element ratios, typically as a result of reducing environments during early (near-surface) to intermediate stages of burial diagenesis. Dull luminescence seems to happen where the Mn/Fe trace element ratios are present in carbonate precipitates. Thus, dull luminescence is usually thought to be the result of intermediate to late stages of burial diagenesis. It appears that elements other than Mn and Fe do not have any appreciable effect in enhancing or reducing luminescence (Budd and others, 2000).

Particularly useful references on the uses and limitations of CL interpretations in ancient carbonate studies include Sipple and Glover (1965), Frank and others (1982, 1996), Marshall (1988), Hemming and others (1989), Barker and Kopp (1991), Gregg and Karakus (1991), Machel (2000), Lavoie and others (2001), Coniglio and others (2003), and Lavoie and Morin (2004).

Previous Work

There is no known published work to date on the application of CL petrography to Pennsylvanian rocks from the Blanding sub-basin. Unpublished work includes observations of carbonate cements and dolomites in thin sections from Ismay-zone outcrop samples along the San Juan River and from five Ismay-zone cores in Ismay field by Brinton (1986).

Methodology

The analysis done in this study was completed using uncovered, polished thin sections, although rock chips and unpolished thin sections could be used. The equipment needed for CL can be installed on almost any polarizing microscope (see Marshall, 1988; Miller, 1988). A Nulcide Corporation luminocope model (figure 6-1; see also Marshall, 1988) belonging to the Colorado School of Mines Department of Geological Engineering was used for this analysis. Operating conditions were generally at 10-12kV accelerating potential, 0.5-0.7 mA of beam current and a beam focused at ~2 cm. All the work involved visual observations and some photographic documentation. Photomicrographs were taken using Fuji 1600 ASA color negative film. No attempt was made to measure intensities or spectral information on the CL responses (for example, Marshall, 1991; Filippelli and Delaney, 1992) to the Ismay and Desert Creek samples. Image analysis and regional mapping of cement zones (that is "cement stratigraphy") have been done by some workers on carbonate cements (for example, Meyers, 1974, 1978; Dorobek and others, 1987; Cander and others, 1988; Dansereau and Bourque, 2001), but these applications are beyond the scope of diagenesis documentation attempted in this project.

Cathodoluminescence Petrography of Upper Ismay and Lower Desert Creek Limestone and Dolomite Thin Sections

Cathodoluminescence examination was completed on five thin-section samples from the upper Ismay zone limestones and dolomites within Cherokee field, and five samples of lower Desert Creek zone dolomite thin sections in Bug field (table 6-1). These thin section samples were selected to be representative of mineralogical (for example, calcite, dolomite, anhydrite, and quartz), compositional, diagenetic, and pore types encountered within one core from the upper Ismay limestones of Cherokee field and within four cores from the lower Desert Creek dolomites of Bug field.

In the appendix of **Deliverable 1.2.6 – Thin Section Cathodoluminescence: Cherokee and Bug Fields, San Juan County, Utah**, there are 34 representative paired CL and transmitted plane light (Pl) photomicrographs from the five Cherokee Federal No. 22-14 well upper Ismay samples, and five of the lower Desert Creek samples throughout Bug field. In

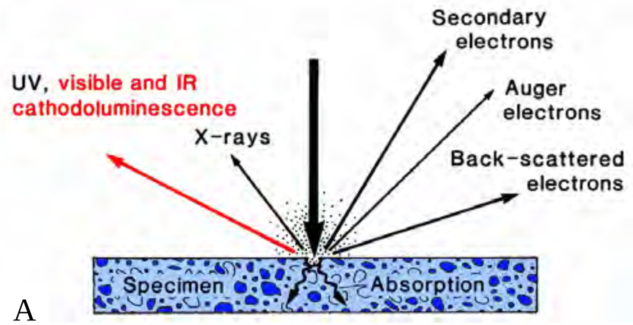

A

Figure 6-1. Generalized microscope optical configuration for observing cathodoluminescence (A - modified from Walker and Burley, 1991; B - modified from Marshall, 1991; and C - modified from Marshall, 1988).

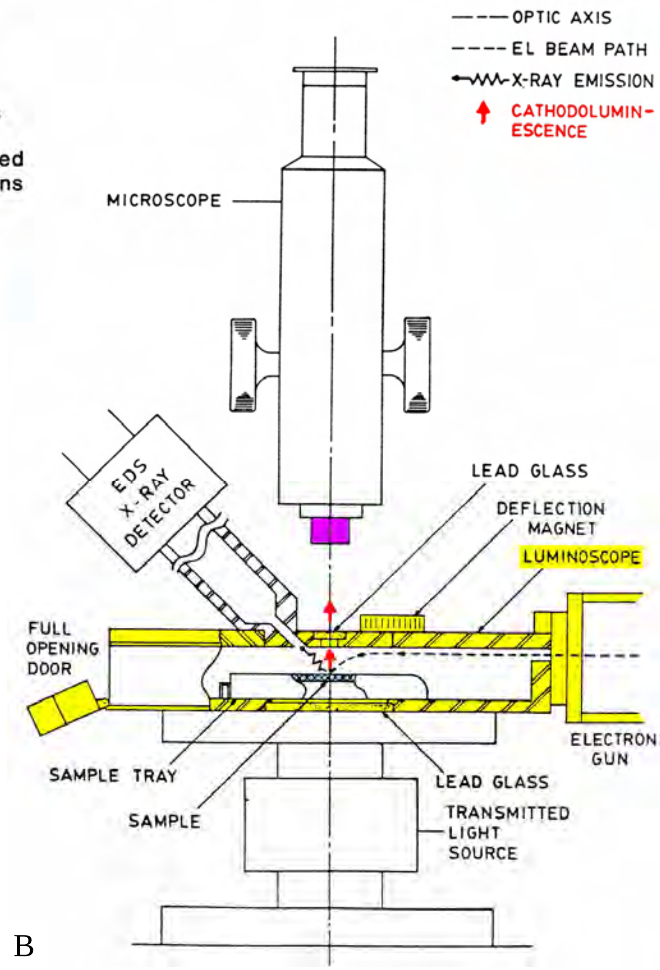

B

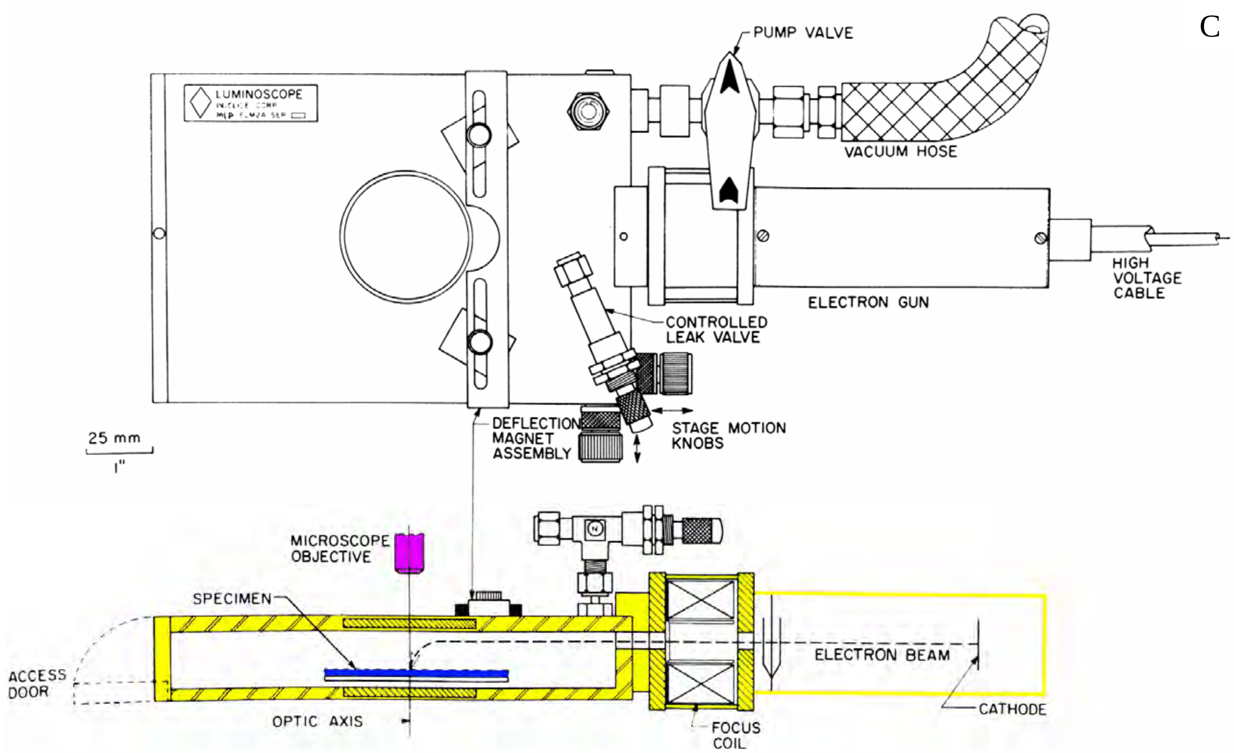

C

Table 6-1. Upper Ismay (Cherokee field) and lower Desert Creek (Bug field) samples used for cathodoluminescence microscopy.

Well	Depth	Comments
Cherokee Fed. 22-14	5773.9	Tight dolomite with no visible fabrics or differences under CL. No photomicrograph examples in this report.
Cherokee Fed. 22-14	5778.1	Micro-porous dolomite; only dim to no visible CL differences. No photomicrograph examples in this report.
Cherokee Fed. 22-14	5821.2	Radiating cement crystals & microporosity. No photomicrograph examples in this report.
Cherokee Fed. 22-14	5836.8	Micro-zoned dolomite cements & bladed to equant calcite cements. Two pairs of photomicrographs included in this report.
Cherokee Fed. 22-14	5870.3	Saddle dolomite replacement of limestone matrix & saddle dolomite cements. Two pairs of photomicrographs included in this report.
May Bug 2	6306	Dolomitized micro-fibrous botryoidal cements. One pair of photomicrographs included in this report.
May Bug 2	6312	Zone mega- and micro-dolomite crystals within brecciated fabric. One pair of photomicrographs included in this report
Bug 10	6327.9	Alternating tight and streaks within dolomites. One pair of photomicrographs included in this report.
Bug 13	5930.6	"Soil" pisolites and coated grain aggregates (grapestone?). One pair of photomicrographs included in this report.
Bug 16	6300.5	Micro-boxwork dolomite. One pair of photomicrographs included in this report.
TOTAL	10 thin sections	18 CL-PL pairs of photomicrographs included in this report.

addition, short descriptive captions are included adjacent to each photomicrograph. Thus, the report serves as a photomicrographic catalogue for cathodoluminescence in the Cherokee and Bugs fields.

Cathodoluminescence Petrography of Upper Ismay Thin Sections at Cherokee Field

Cathodoluminescence microscopy was completed on core-sample thin sections with a variety of rock textures and diagenetic phases from the upper Ismay zone limestones within the Cherokee Federal No. 22-14 well (table 6-1). However, only two of the five samples showed any significant visible response to CL.

Cathodoluminescence imaging provides good to excellent resolution of grains (both skeletal and non-skeletal) as well as different generations of calcite cements within the limestone in the thin section from 5836.8 feet (1778.9 m) in the Cherokee Federal No. 22-14 well (figures 6-2 and 6-3). Fine details of the microstructures within skeletal fragments, such as brachiopods, bryozoans, and phylloid-algal plates, are more readily visible under CL than with transmitted plane light. In addition, calcite cements that rim leached skeletal grains, as well as early generations of isopachous cements, can be easily seen. Some of the cements display a series of concentric bright and dull luminescent bands that represent multiple generations of cementation under varying water chemistries. Such concentrically banded cements are similar to those cements used in calcite cement stratigraphy within Carboniferous carbonate systems in North America by Meyers (1974, 1978, 1991) and Goldstein (1988, 1991). Finally, CL makes it easier to see the pore outlines and boundaries than under Pl light viewing. Thus, it becomes possible to qualitatively interpret how interconnected the remaining pore systems are within this sample.

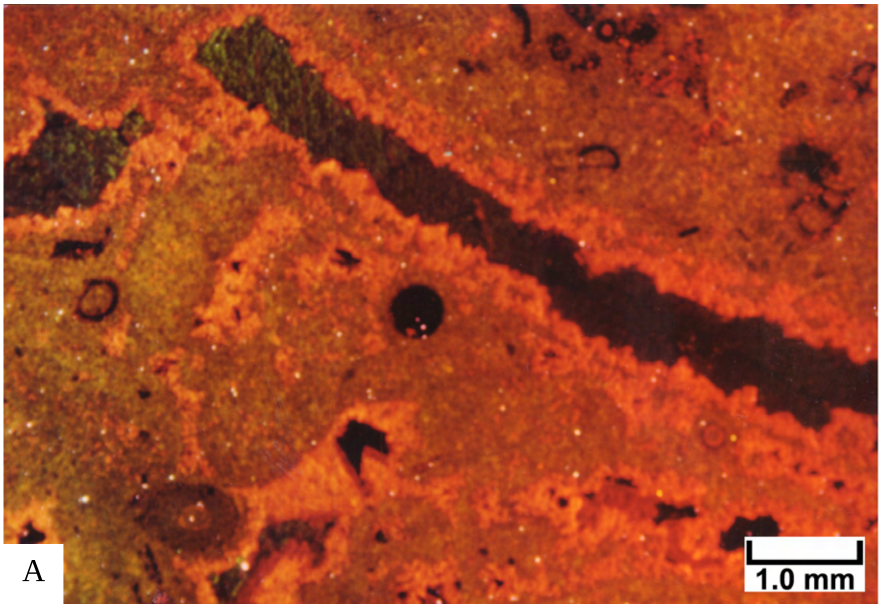

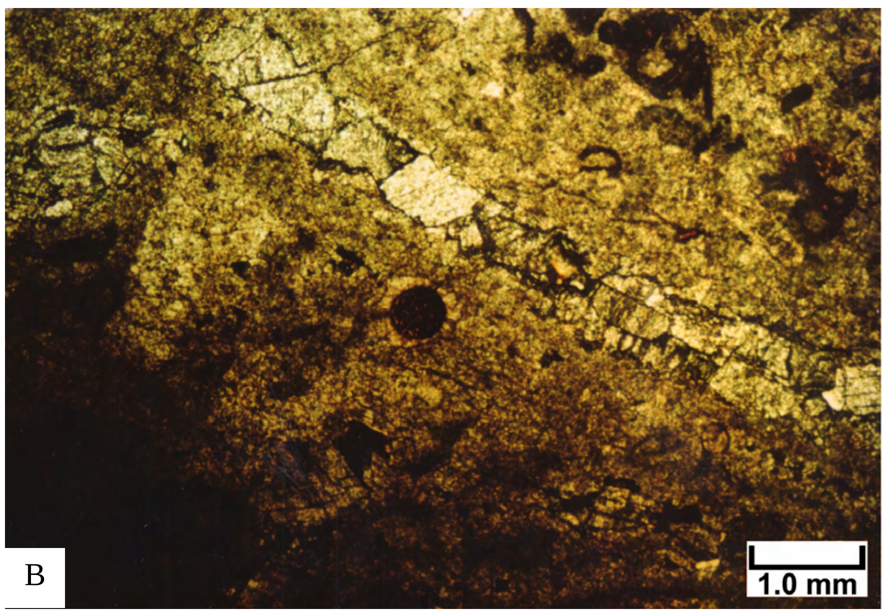

Figure 6-2. Photomicrographs from Cherokee Federal No. 22-14 well at 5836.8 feet. A - Cathodoluminescence overview of a representative skeletal/peloidal grainstone shows the details of grain preservation as well as different generations of calcite cement. Note the elongate non-luminescent area (from the upper left to right-central portions of this photomicrograph) which represents a dissolved phylloid-algal plate which is now a moldic pore. Other non-luminescent (black) portions of this view are also open pores or are filled with the same generation of calcite cement. A series of banded bright and dull cement generations represent an earlier generation of pore-filling cements. B - The same field of view is shown here under Pl at the same magnification. Note that the preservation of original grains, leached skeletal grains such as the dissolved phylloid-algal plate, and the multiple generations of cement are not visible under plane light. Without CL, many of these features would be difficult to identify.

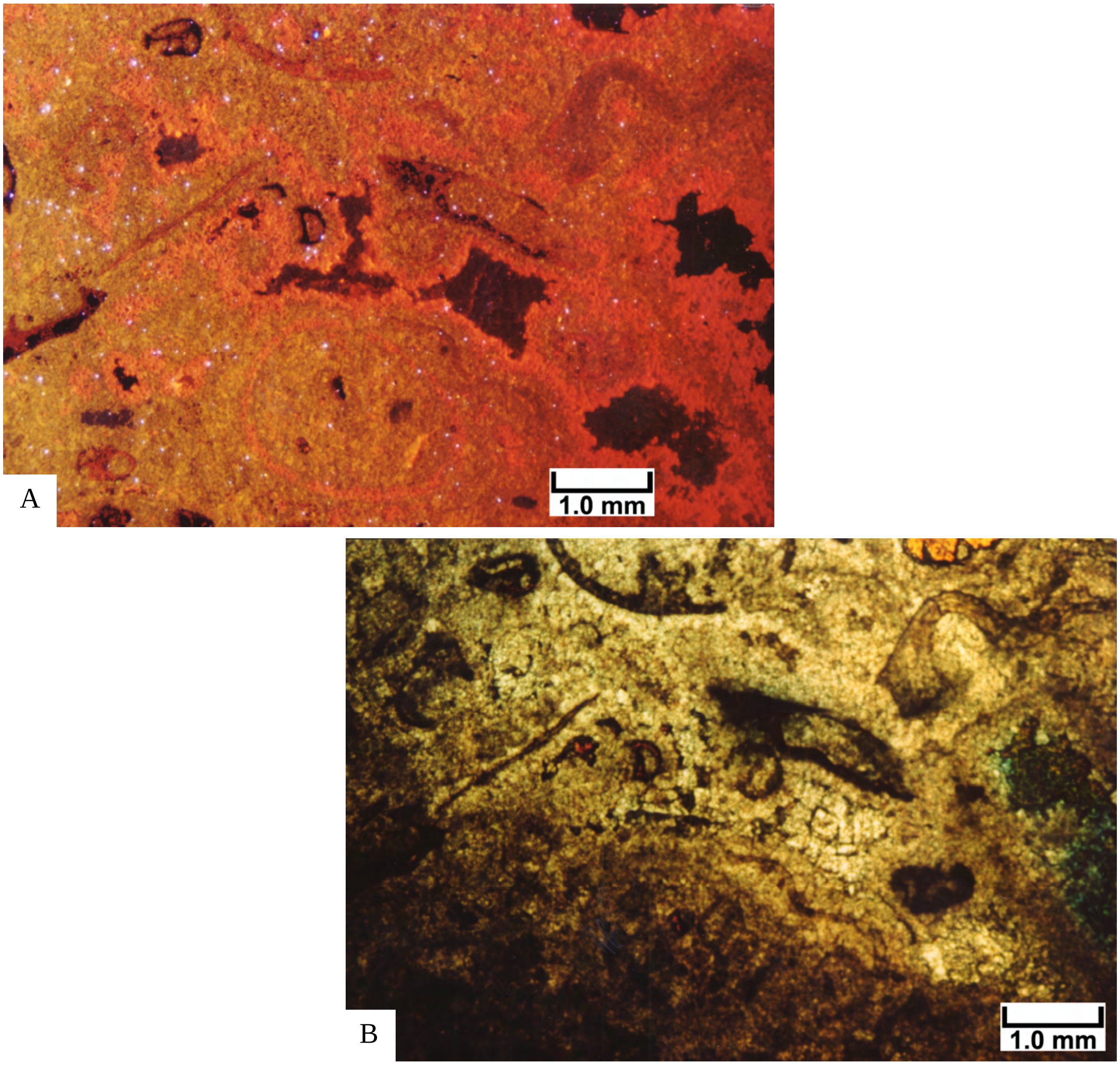

Figure 6-3. Photomicrographs from Cherokee Federal No. 22-14 well at 5836.8 feet. A - This CL view shows various skeletal grains in the dull red shapes and colors surrounded by banded generations of early pore-filling cements. Note the non-luminescent (black) patches that represent largely secondary pores that have either been filled with equant calcite spar cement, or are isolated, open moldic pores. The numerous light blue specs across this photomicrograph are mostly detrital quartz silt grains within this carbonate sediment. B - The same field of view is shown here under Pl at the same magnification. Vague outlines of skeletal grains, including broken phylloid-algal plates, brachiopod shells, and bryozoan fragments, are seen in the dark grains. This view does not provide much detail to differentiate various generations of calcite cement seen in CL view above.

Cathodoluminescence imaging was very useful in identifying the presence of saddle dolomites (Radke and Mathis, 1980) within microporous dolomites in the sample from the Cherokee Federal No. 22-14 well core at 5870.3 feet (1789.2 m). Large dolomite crystals (1.0 to 2.0 mm in diameter) with distinctly curved crystal faces occur as both replacements of finer, earlier dolomites and as pore-filling cements (figures 6-4 and 6-5). These saddle dolomites display dull, red luminescence in their core areas and slightly bright, orange-red luminescence toward their rim areas. In addition, CL makes it possible to see the growth bands in these coarse dolomite crystals due to slight luminescent differences between each growth zone.

In general, the presence of saddle dolomites within a carbonate sample is indicative of the growth of strained, slightly iron-rich, dolomite replacements and cements under elevated temperatures during burial conditions (Radke and Mathis, 1980). Additional published descriptive work on saddle dolomites using CL may be found in Lavoie and Morin (2004).

Cathodoluminescence Petrography of Lower Desert Creek Thin Sections at Bug Field

Cathodoluminescence microscopy was completed on core-sample thin sections exhibiting a variety of rock textures and diagenetic phases from the lower Desert Creek zone dolomites within the May Bug No. 2, Bug No. 10, Bug No. 13, and Bug No. 16 wells (table 6-1). Cathodoluminescence imaging was used to examine the details of early, fibrous, marine cements that occur as distinct botryoidal fans within the sample from the May Bug No. 2 well core at 6306 feet (1922 m) of lower Desert Creek reservoir dolomites (figure 6-6). Most of these fibrous cements exhibit fairly uniform orange and red luminescence. Hints or ghosts of the radiating cement fibers are visible. The blunt to squares ends of several radiating bundles of fibrous cements can be seen. These blunt ends have been used by some carbonate workers (Frank and others, 1982; Goldstein, 1988, 1991) to suggest original aragonite mineralogy of these cements, since modern aragonite botryoidal cements exhibit similar morphologies. In addition, small, internal dissolution pores crossing these early marine cements are also more readily visible using CL.

The dolomites replacing brecciated phylloid-algal mound fabrics are distinctly zoned when viewed under CL (figure 6-7) in the sample from the May Bug No. 2 well core at 6312 feet (1924 m). Replacement dolomite crystals and crystal aggregates that average 100 to 200 μm display dull to non-luminescent cores and bright red luminescent rims. In one of the photomicrographs from this sample, up to four growth zones can be seen within individual dolomite rhombs. The resulting dolomitization and crystal size growth creates small sucrosic crystals that form an effective intercrystalline pore system. These intercrystalline pores augment the vuggy and shelter pores created by the brecciated phylloid-algal mound fabric.

Cathodoluminescence imaging makes it easier to see the contacts between dolomite matrix and pores. Cathodoluminescence brings out significant detail in areas of anhydrite replacement of the dolomitized sediment. Islands of red luminescing dolomite can be easily seen within the plethora of bladed-anhydrite crystal aggregates. Within other portions of this sample, carbonate grains such as peloids and fragmented skeletal debris can be distinguished from carbonate cements in this completely dolomitized interval. The dolomitized grains exhibit deep red colors under CL while the carbonate cements are bright reddish orange. Finally, CL does an excellent job in imaging microfractures and microfracture swarms cutting through the lower Desert Creek dolomites. In this sample, an orthogonal set of microfractures cuts across the thin section. Most of these microfractures can be seen as the dark-gray to black (non-

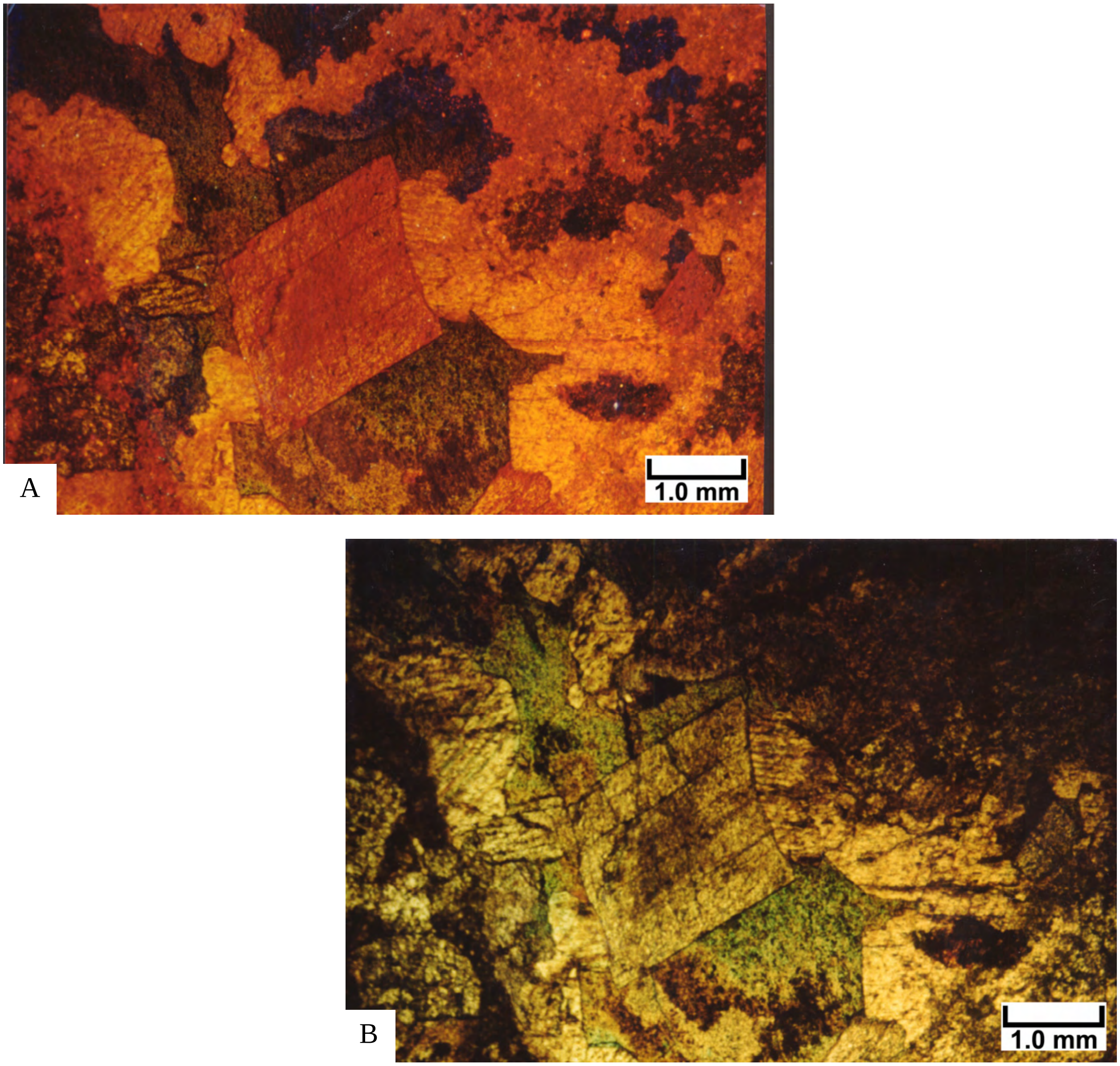

Figure 6-4. Photomicrographs from Cherokee Federal No. 22-14 well at 5870.3 feet. A - Most of the large crystals in this CL view consist of dolomite. Note in particular that the large crystal in the center displays strongly curved crystal faces. This "saddle dolomite" (see Radke and Mathis, 1980) as well as the other coarse dolomite crystals with reddish luminescence are probably late, burial or hydrothermal dolomites that precipitated under elevated temperatures. B - The same field of view is shown here under cross-polarized light at the same magnification. Note the sweeping extinction within the large crystal in the center, indicative of a strained crystal lattice. The bluish areas surrounding these replacement dolomites are remnants of intercrystalline pores.

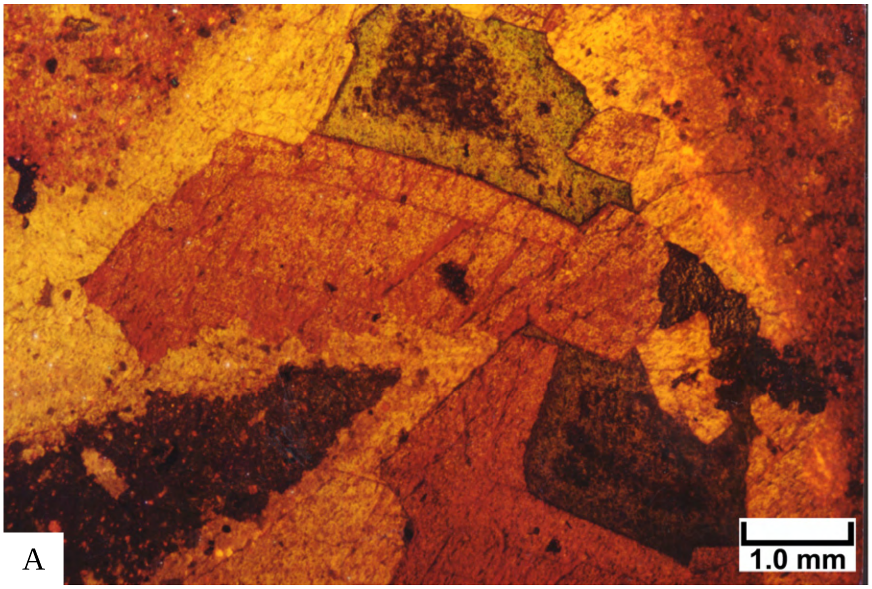

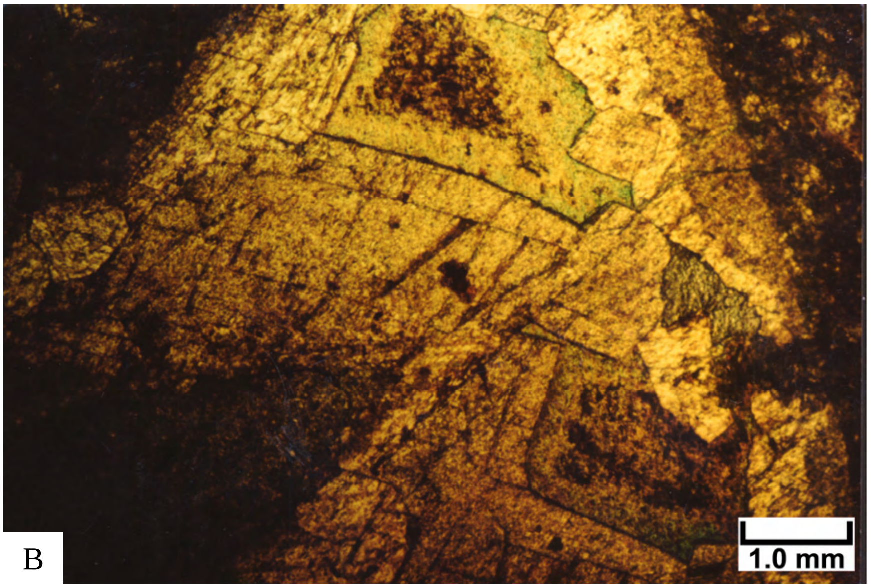

Figure 6-5. Photomicrographs from Cherokee Federal No. 22-14 well at 5870.3 feet. A - This CL view shows remnants of a muddy limestone matrix (wackestone) in the lower left and upper right corners of this photomicrograph that has been partially replaced by coarse dolomite crystals displaying curved faces. These "saddle dolomites" have a distinctive dull red and orange luminescence in which hints of the dolomite growth bands can be seen. Small inclusions of dark-colored, lime, wackestone matrix can be seen scattered throughout the coarse dolomite saddles, indicating that these saddle dolomites are replacing previous carbonates rather than being entirely cements. B - The same field of view is shown here under cross-polarized light at the same magnification. Note the intercrystalline pores (blue areas) between some of the saddle dolomites. This view makes it possible to see where dolomite has replaced lime wackestone matrix (in the medium and dark brown areas) and where dolomite is a cement growing into open pores (the clear areas).

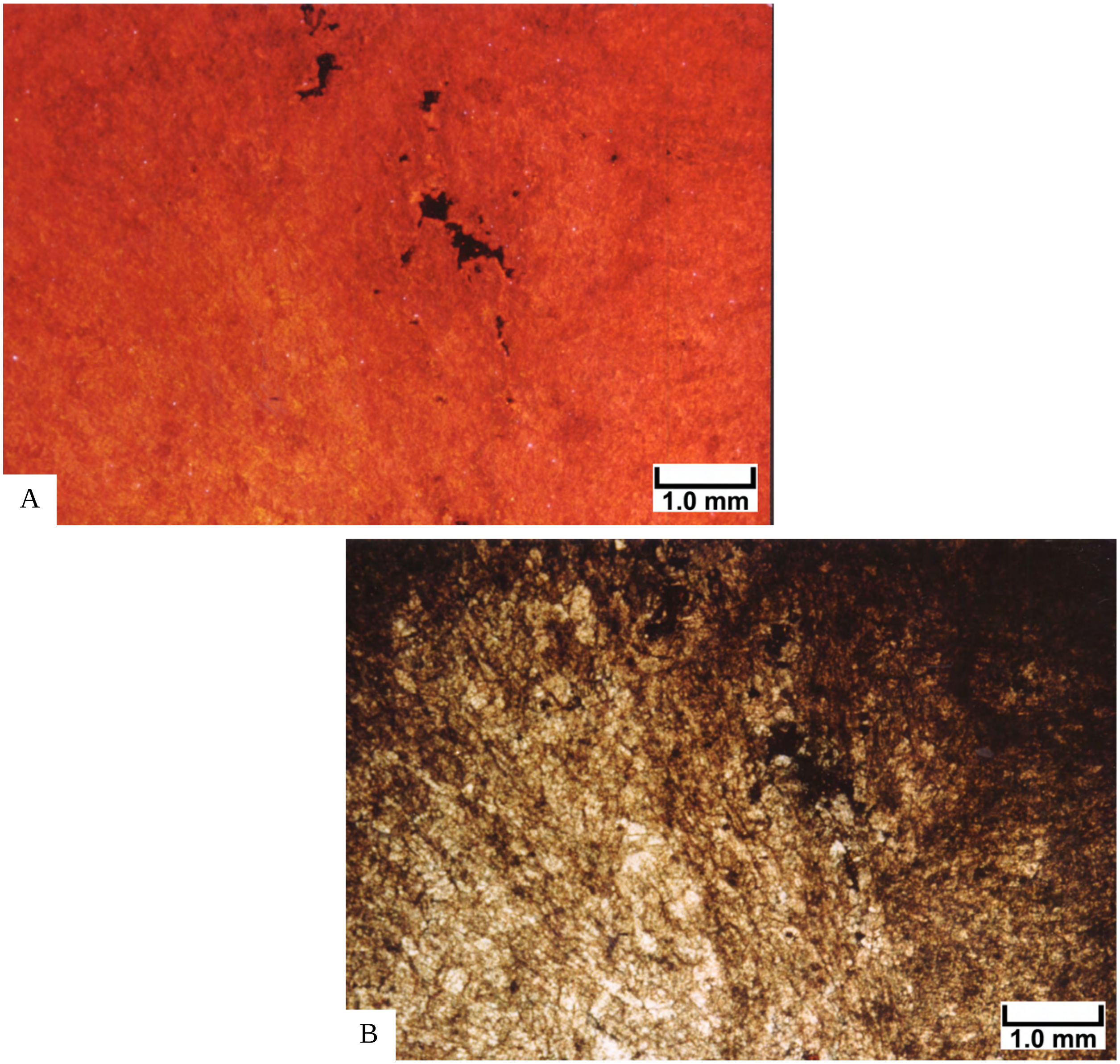

Figure 6-6. Photomicrographs from May Bug No. 2 well at 6306 feet. A - Cathodoluminescence imaging of a large botryoidal fan of dolomitized cements (originally aragonite) shows reasonably uniform orange and red luminescence. Note the blunt-shaped or square-ended crystal bundles evident in the area just to the right of center. Hints of radiating fibrous cements can be seen from bottom of the photograph to the top in this view. The black (non-luminescent) patches represent secondary pores within these early marine botryoidal cements. B - The same field of view is shown here under Pl at the same magnification. This photomicrograph shows ghosts of the radiating fibrous crystal habit of these completely dolomitized, early marine botryoidal cements. Without the CL view (see A above), it would be difficult to see either the blunt crystal fan terminations or the dissolution pores.

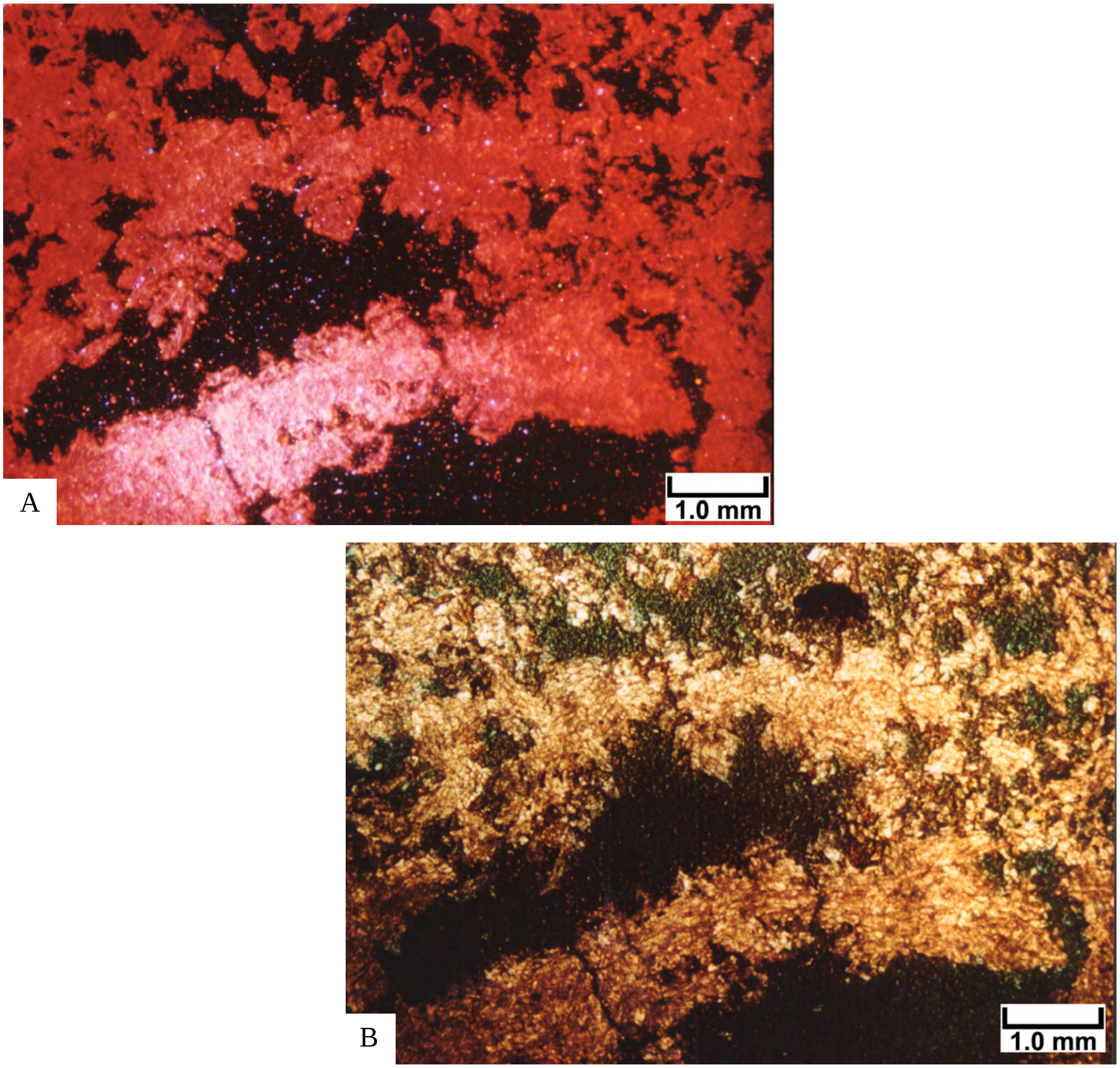

Figure 6-7. Photomicrographs from May Bug No. 2 well at 6312 feet. A - This CL view nicely shows micro-rhombic dolomites that have completely replaced a brecciated phylloid-algal mound fabric. Despite the dull red luminescence of these dolomites, growth zones and different crystal sizes can readily be seen within the replacement fabric. For instance, note the dolomite crystals (in the upper center portion of this photomicrograph) with dead (black) cores and bright luminescent (red) rims. This zonation is probably related to two distinct growth stages of this replacement dolomite. The resulting dolomitization of this mound fabric creates small sucrosic or rhombic crystals that produce an effective intercrystalline pore system. The large black patches in the lower half of this photomicrograph consist of open pores within this brecciated phylloid-algal mound fabric. B - The same field of view is shown here under Pl at the same magnification. Note that there is very little detail within this replacement dolomite that is visible under plane-transmitted light. For instance, it is impossible to see any of the zoned dolomite rhombs or the precursor fabrics before dolomite replacement without the use of CL.

luminescent) curvilinear lines. It is possible that some of these open microfractures may have originated from dissolution along microstylolites.

Cathodoluminescence imaging of the sample from the Cherokee Bug No. 10 well core at 6327.5 feet (1928.5 m) was particularly useful in identifying the shape and distribution of phylloid-algal plates, even though most of the plates have been partially dissolved, lined with early cements, and dolomitized (figure 6-8). Micro-boxwork arrays of bladed dolomite crystals are also very distinctive. In addition, CL provides a very vivid image of the distribution of both megapores and micropores within this dolomite. In particular, CL provides sharp definition of the pore boundaries with the dolomite matrix and crystal boundaries. Evidence of a brecciated fabric, as well as dissolution and corrosion of early sediments and cement, are easier to identify in this sample under CL than under plane polarized light.

A sample from the Bug No. 13 well at 5930.6 feet (1807.6 m) consists of dolomitized pisolites and coated grain aggregates (similar to “grapestone”). Cathodoluminescence imaging aids in distinguishing the smaller grains incorporated into the grapestone, or aggregate grains, versus the early marine cements (figure 6-9). Portions of this sample consist of internal sediment composed of carbonate mud and silt-sized, detrital quartz. The pelleted nature of the muddy portion of this sample is very evident under CL, despite the complete dolomitization of this interval. Interestingly, detrital quartz silt grains of probable eolian origin are easily visible within the internal sediments of this sample. In addition, CL imaging makes it much easier to see the open (versus cemented) pores and microfractures within this sample.

Cathodoluminescence imaging of the sample from the Bug No. 16 well core at 6300.5 feet (1920.3 m) was particularly useful in identifying dense, dolomitized, micro-boxwork arrays as well as bundles of fibrous marine cements (figure 6-10). Original grains and cement fabrics can be seen in the brighter red portions of the luminescing dolomites. Somewhat later cements and zonation within coarser dolomites can be seen in the orangish-red areas. Cathodoluminescence imaging also provides sharp definition of rhombic dolomite crystal terminations as well as intercrystalline pores.

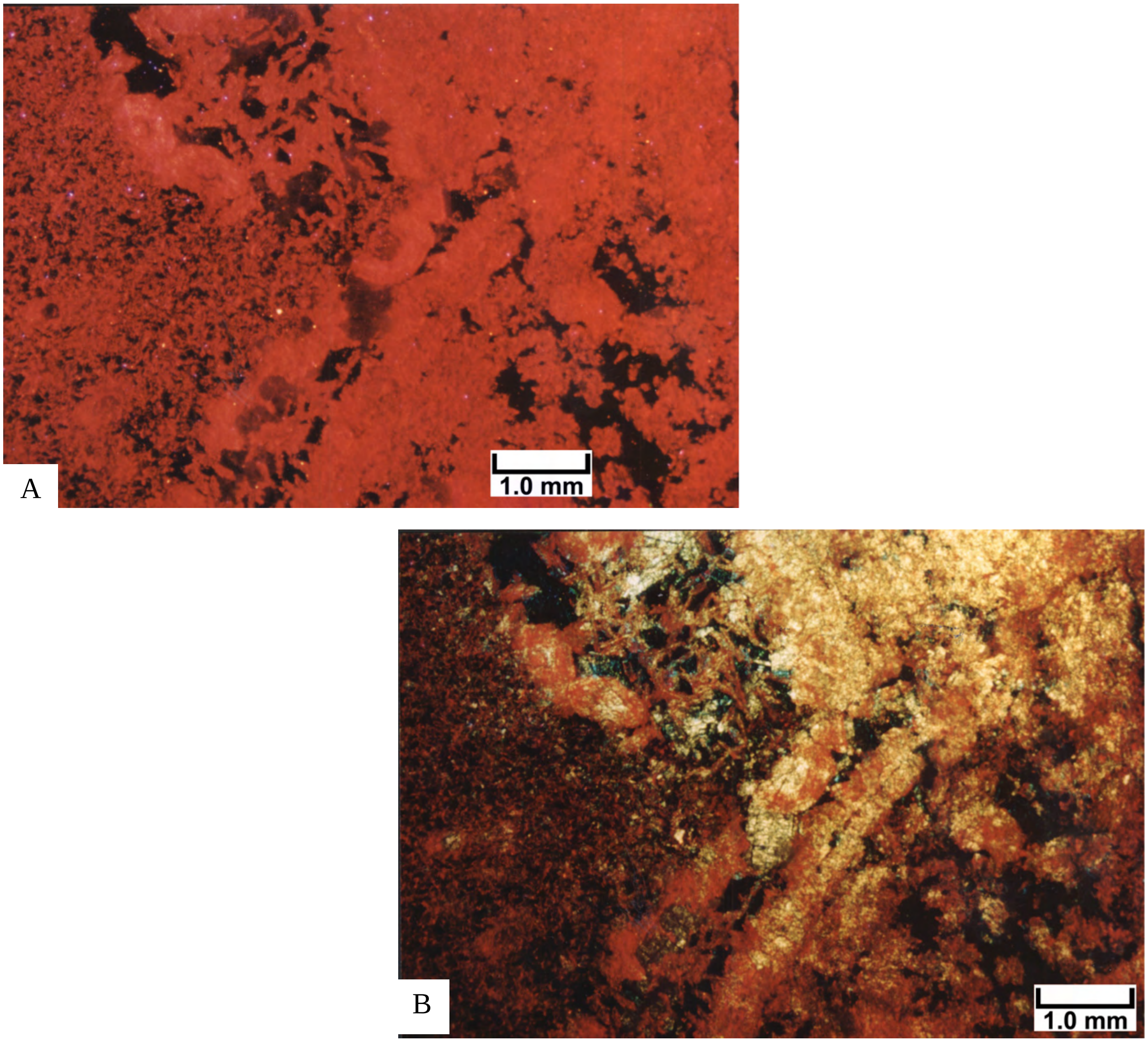

Figure 6-8. Photomicrographs from Bug No. 10 well at 6327.5 feet. A - Cathodoluminescence imaging clearly shows some of the distinctive fabric elements within a completely dolomitized, phylloid-algal/skeletal, grain-rich sediment. Note the elongate blades of poorly preserved phylloid-algal plates from bottom center to upper right in this photomicrograph. Within these blades are preserved remnants of skeletal materials in bright red, and cements in dull reddish gray. For the most part, dolomitized skeletal grains, or their remnants, appear as bright red luminescent areas with clear skeletal shapes. Some of the grains easily visible in this field of view are rounded crinoids with their distinctive circular cores and single crystal, red luminescent rims. Early cements (prior to dolomitization) are very dull red. Porous microdolomites dominate the left quarter of this photomicrograph. Note also the remnants of dolomitized bladed cements and micro-boxwork dolomite fabrics visible in the upper left center of this view. The black areas throughout this field of view are open pores. B - The same field of view is shown here under combined Pl and CL (that is, a double exposed image) at the same magnification. In this view, remnants of bright red luminescence show through the coarse and fine dolomite crystal patterns. The blue and black areas of this slide consist of open pores.

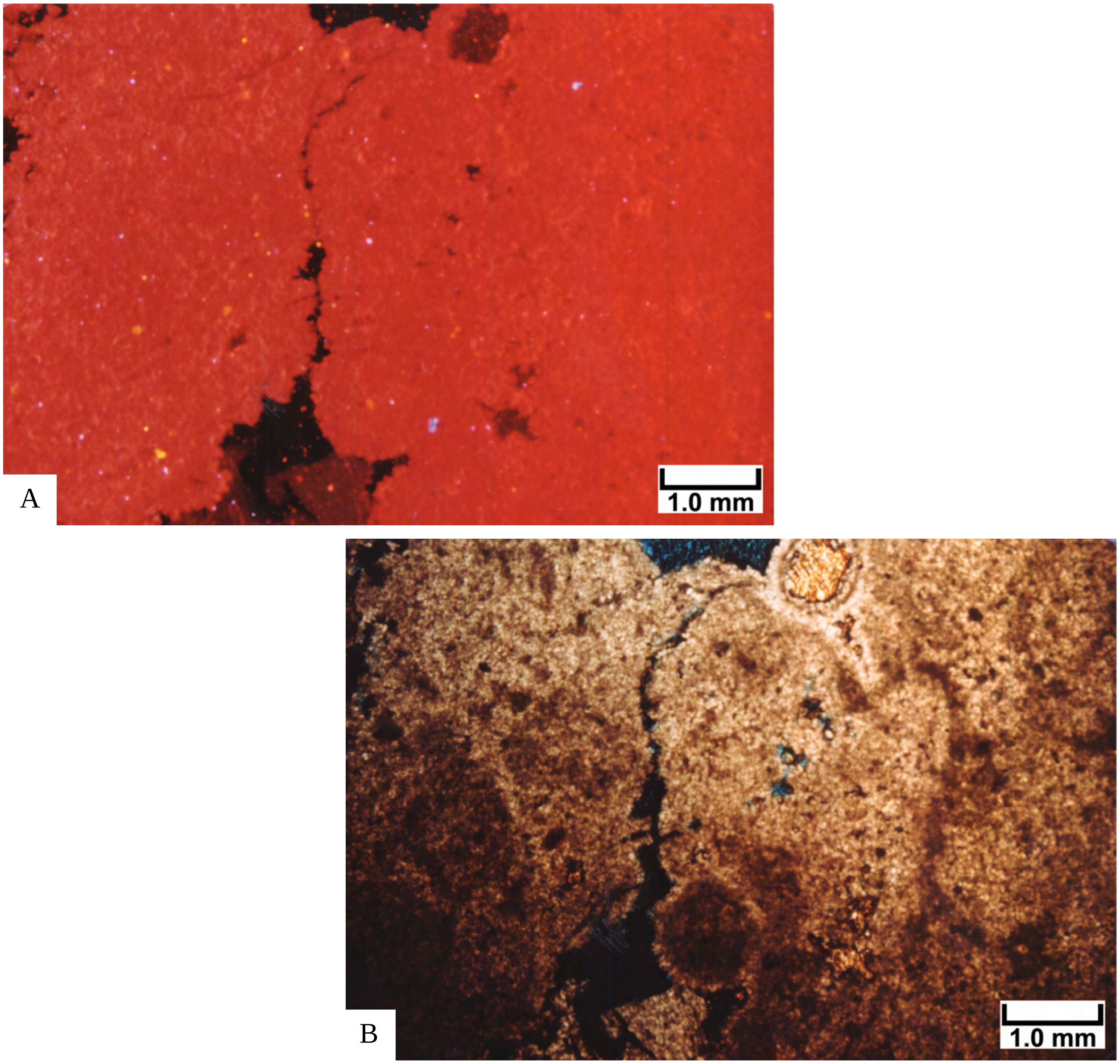

Figure 6-9. Photomicrographs from Bug No. 13 well at 5930.6 feet. A - This CL view is from a sample of pisolites and coated-grain aggregates. Note that it is possible to see the carbonate-grain outlines (in uniformly dull red) versus early carbonate cements (in orangish red). Late-stage, dolomitized, spar crystals can be seen in the dull-gray patches in the lowermost and uppermost center of this view. The black (non-luminescent) areas clearly image the open pores and microfractures. B - The same field of view is shown here under Pl at the same magnification. In this view, it is possible to see the large coated grain aggregates (pisolites and possible grapestones). However, Pl viewing does not show the individual carbonate grains that compose the larger grain aggregates as well as the CL imaging.

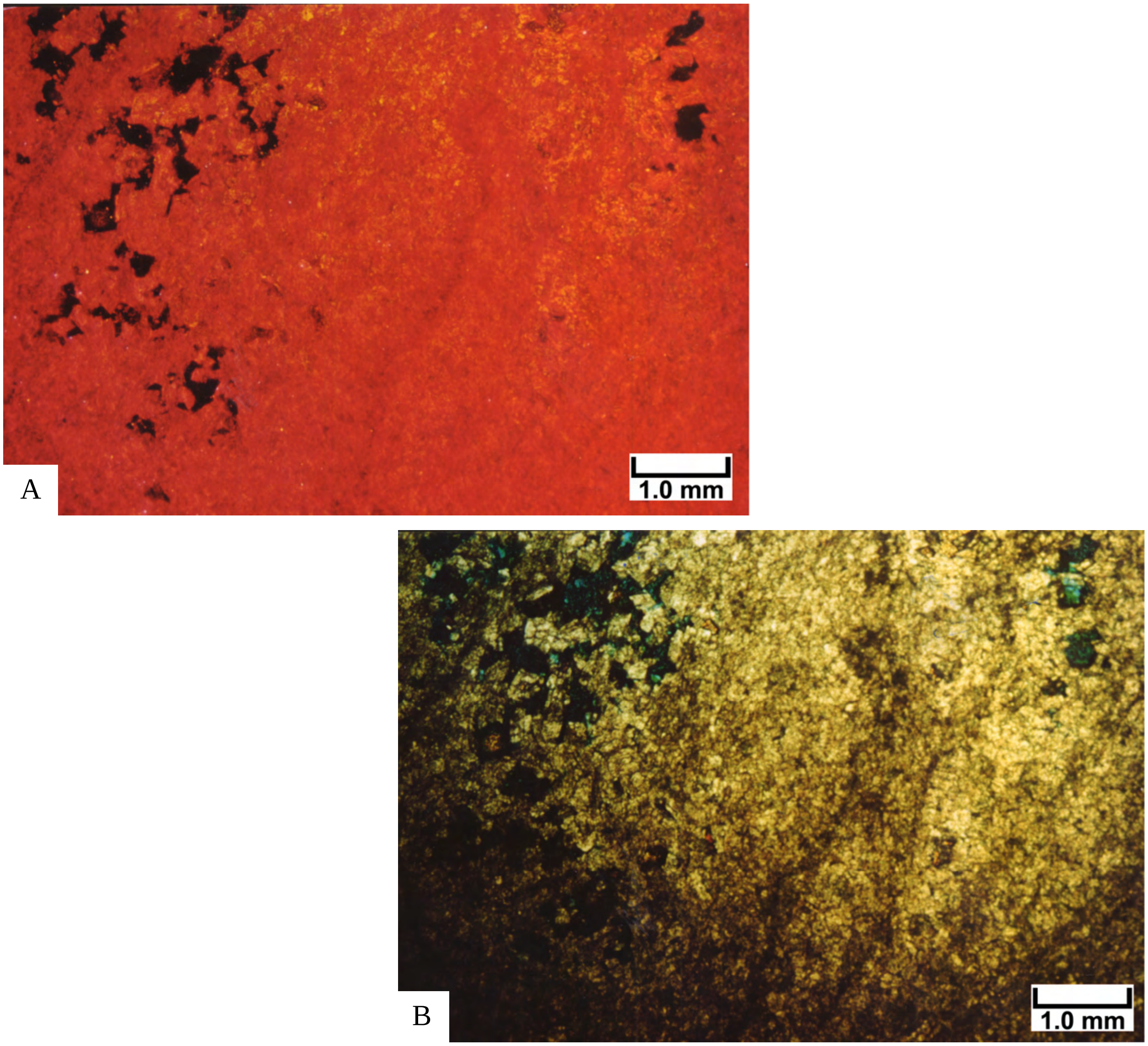

Figure 6-10. Photomicrographs from Bug No. 16 well at 6300.5 feet. A - Cathodoluminescence of an area displaying micro-boxwork dolomite and early fibrous marine cements is imaged here. Note the patterns of dull red, bright red, and orangish red throughout this dense, tight dolomite. Most of the original carbonate fabric associated with carbonate sediment and early marine cements can be seen in the dull and bright red patterns. The orangish red areas represent later dolomite cement growth bands. In some areas of this view (especially in the left third of the image), there are dolomite crystals that have developed a clear rhombic shape. The black areas clearly define open pores associated with dissolution as well as the development of intercrystalline porosity. B - The same field of view is shown here under Pl at the same magnification. Only the outlines of larger dolomite crystals are visible here. Cathodoluminescence imaging, as shown above, brings out the internal original fabric versus later dolomite growth zones much more clearly. The blue patches are open pores lined with black bitumen. The presence of bitumen makes it difficult to clearly discern the outlines of dolomite matrix versus open pores under Pl. Cathodoluminescence (above) images the pore/rock boundaries very well.

CHAPTER VII
ISOTOPE GEOCHEMISTRY: CHEROKEE, BUG, AND PATTERSON CANYON FIELDS

David E. Eby, Eby Petrography & Consulting, Inc.;
Stephen T. Nelson, Brigham Young University;
and
Thomas C. Chidsey, Jr., Kevin McClure, and Craig D. Morgan,
Utah Geological Survey

Introduction

Diagenesis played a major role in the development of reservoir heterogeneity in Bug, Cherokee, and Patterson Canyon fields and probably throughout the Paradox Formation fields (figures 3-1 and 4-13). Stable isotope geochemistry has been used in recent years to provide insights into the chemical differences between preserved remnants of depositional components from various diagenetic events in carbonate rocks as recognized from core examination and thin section petrography. Figure 7-1 shows a graph of carbon versus oxygen isotope compositions for a range of carbonate rock types from various published sources as compiled by Roylance (1990). Broad fields of carbon and oxygen isotope compositions for various carbonate rock settings are indicated, including modern marine ("subsea") cements, various marine skeletons and sediments, deep-water ("pelagic") limestones, Pleistocene carbonates, and meteoric carbonates ("speleothems and veins").

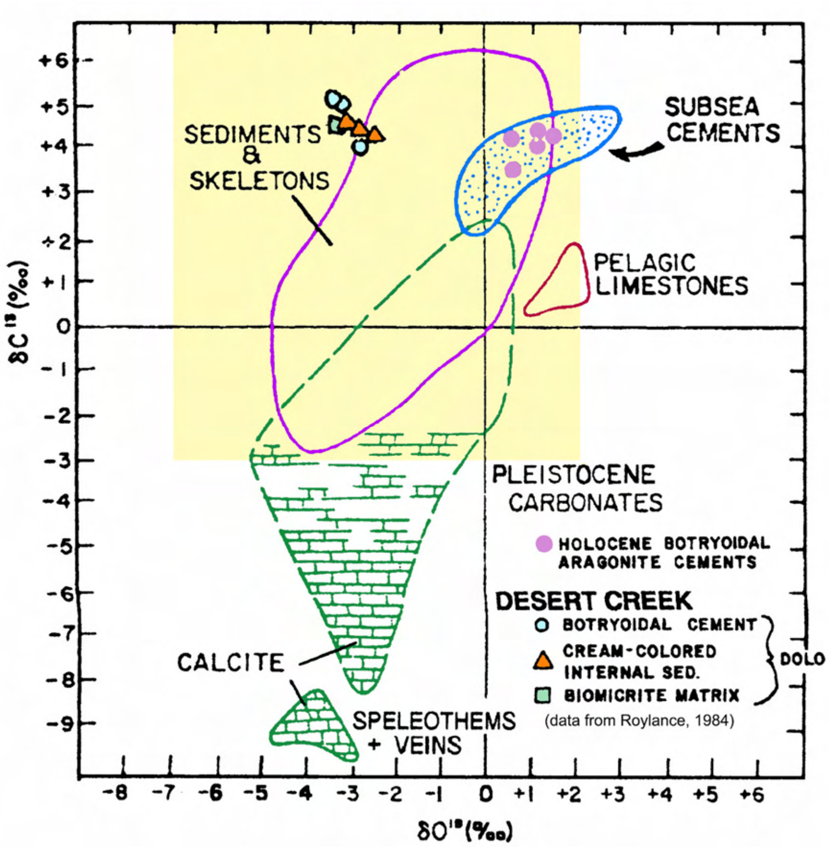

Figure 7-1. Graph of carbon versus oxygen isotope compositions. Other compositional lithofacies compiled from various published work (modified from James and Ginsburg, 1979 by Roylance, 1990). The yellow area in this cross plot is the same part of the graph shown in figures 7-2, 7-5, 7-6, 7-7, 7-9, and 7-11 of this study.

Previous Work

The only previously published isotope composition data for lower Desert Creek rocks for the project area was completed at the Marathon Petroleum Technology Lab in Littleton, Colorado for the M.S. thesis work of Roylance (1984). That data and the location of the wells sampled can be seen in tables 7-1 and 7-2, and figures 3-7 and 7-2. Brinton (1986) collected and interpreted a robust data set of carbon and oxygen isotopes (84 samples) from four cores in Ismay field, Utah and Colorado, which is outside the project area. Comments about the general isotopic ranges of various diagenetic rock components within the Ismay zone in cores from Ismay and Greater Aneth fields (outside of the Blanding sub-basin project area) have been published by Dawson (1988).

Table 7-1. Location of cores used in the isotope geochemistry study.

Zones	Well Name	Location
Lower Desert Creek	*Wexpro May-Bug 2 (this study)	NE1/4 SW1/4 Sec. 7, T36S, R26E UT
	*Wexpro Bug 4 (this study)	NE1/4 SW1/4 Sec. 16, T36S, R26E UT
	*Wexpro Bug 13 (Roylance, 1984)	NE1/4 NW1/4 Sec. 17, T36S, R26E UT
	*Wexpro Bug 16 (Roylance, 1984)	NE1/4 SW1/4 Sec. 17, T36S, R26E UT
	MOC Tin Cup Mesa 1-25	SW1/4 NW1/4 Sec. 25, T38S, R25E UT
Upper Ismay	† Cherokee 22-14 (this study)	SE1/4 NW1/4 Sec. 14, T38S, R23E UT
	† Cherokee 33-14 (this study)	NE1/4 NW1/4 Sec. 14, T38S, R23E UT
	Samedan Bonito 41-6-85 (this study)	NE 1/4 NE1/4 Sec. 6, T38S, R25E UT

*Well locations are shown in figure 3-7
†Well locations are shown in figure 3-10

Table 7-2. Previous stable carbon and oxygen isotope data from lower Desert Creek zone, Bug and Tin Cup Mesa fields (analyses from Roylance, 1984).

Sample Groups:	del 13C	del 18O
BUG FIELD - Lower Desert Creek Cores Dolomitized Whole Rock Matrix (biomicrite in algal bafflestone)		
Bug 13: 5940.7'C	+4.7	-3.3
Dolomitized Internal Sediment (within phylloid-algal bafflestone)		
Bug 13: 5939.3'A	+4.4	-2.9
Bug 13: 5940.7'A	+4.3	-2.5
Bug 16: 6313.4'A	+4.8	-3.3
Dolomitized Botryoidal Cements		
Bug 13: 5939.3'B	+5.0	-3.3
Bug 13: 5940.7'B	+4.0	-2.9
Bug 16: 6313.4'B	+5.2	-3.4
TIN CUP MESA FIELD - Lower Desert Creek Cores Limestone Whole Rock Matrix (calcite fraction [micrite and crinoid, bryozoan and brachiopod fragments] of dolomitized bioclastic wackestone)		
Tin Cup Mesa #1-25: 5667' calcite	+0.9	-3.3
Dolomite Fraction of Whole Rock Matrix (dolomitized micrite matrix of bioclastic wackestone)		
Tin Cup Mesa #1-25: 5667' dolomite	+0.9	-1.6

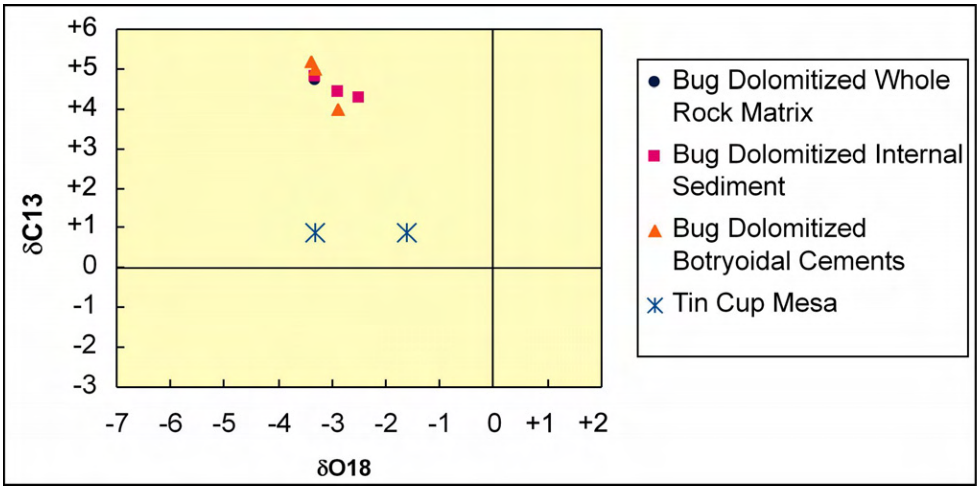

Figure 7-2. Graph of carbon versus oxygen compositions for Bug and Tin Cup Mesa fields determined by Roylance, 1984.

Methodology

Isotopic composition analyses for carbon and oxygen were completed for a variety of whole rock and diagenetic phases for core samples from the lower Desert Creek zone from Bug field and the upper Ismay zone from Cherokee field (tables 7-1, 7-3, and 7-4). In addition, a series of samples from whole rock, dolomite, and various cement generations were selected from an upper Ismay buildup in a recently drilled well at Patterson Canyon field (the Samedan Bonito No. 41-6-85, completed in July 2002) containing well-cemented oolitic beds and phylloid-algal mound fabrics (table 7-5). Figure 7-3 shows the location of the fields or well names sampled for isotope geochemistry. Individual samples were collected as powdered rock using a Dremel drill equipped with precision bits. All analyses were completed at the Brigham Young University (BYU) Department of Geology Stable Isotope Laboratory, Provo, Utah. The internal standard used in the BYU lab is the UCLA Carrara marble. The accepted values for this internal standard were matched consistently during the analysis of the Paradox core samples selected for this study. All isotopic compositions are reported relative to PeeDee Belemnite (PDB) (see Land, 1980, figure 6 for definition relative to SMOW).

Carbon and Oxygen Isotopes from Lower Desert Creek Dolomites

Isotopic composition analyses for carbon and oxygen were completed for a variety of whole rock and diagenetic phases for core samples from the lower Desert Creek dolomite interval from Bug field (table 7-1, figure 3-7). Values obtained in this project were compared to stable carbon and oxygen isotopic measurements reported by Roylance (1984, 1990), and included in this report in figure 7-2 and table 7-2. A total of eight powdered samples were drilled from core samples from two Bug field wells and analyzed (table 7-3). The samples were selected to analyze dolomitized phylloid-algal mound fabrics and breccias, cream-colored dolomitized internal sediments, and dolomitized void-filling cements (mostly botryoids and blunt-ended fibrous fans). Annotated close-up core photos (figure 7-4) show the approximate locations of the drilled and powdered samples from the May Bug No. 2 and Bug No. 4 wells. A plot of carbon versus oxygen compositions for all Bug field samples obtained in this study is shown on figure 7-5 (see also table 7-3). Comparison of the new data with previously reported Bug field isotope compositions (Roylance, 1984, 1990) is shown in figure 7-6.

Table 7-3. New stable carbon and oxygen isotope data from lower Desert Creek zone Bug field dolomites.

Sample Groups:	del 13C	del 18O
BUG FIELD - Lower Desert Creek Cores		
Whole Rock Dolomite		
May Bug 2: 6304'A (phylloid-algal mound & marine sediment)	+4.49	-4.72
May Bug 2: 6315' B (phylloid-algal mound fabric)	+4.03	-4.42
Dolomitized Internal Sediment (cream-colored)		
May Bug 2: 6304'B	+4.30	-4.50
May Bug 2: 6315'A	+4.16	-4.15
May Bug 4: 6297.4'B	+4.52	-4.67
Dolomitized Micro-Boxwork Fabric (probably botryoidal cements)		
May Bug 2: 6304'C	+4.40	-4.56
May Bug 4: 6289.7'	+4.77	-4.58
May Bug 4: 6297.4'A	+4.76	-4.46

Table 7-4. New stable carbon and oxygen isotope data from upper Ismay zone Cherokee field.

Sample Groups:	del 13C	del 18O
CHEROKEE FIELD - Upper Ismay Cores		
Whole Rock		
Cherokee 22-14: 5827.7' (mostly dolomite, w/ moldic porosity)	+5.41	-2.90
Cherokee 22-14: 5836.8' (limestone; phylloid-algal mound fabric)	+5.02	-4.55
Cherokee 33-14: 5781.2'A (mostly dolomite)	+4.67	-6.08
Micro-Porous Dolomite Zones (often w/ pyrobitumen)		
Cherokee 22-14: 5768.7'	+3.57	-2.92
Cherokee 33-14: 5781.2'B	+4.85	-4.54

Table 7-5. New stable carbon and oxygen isotope data from upper Ismay buildup zone Samedan Bonito No. 41-6-85 core.

Sample Groups:	del 13C	del 18O
Whole Rock (dolomitized oolite)		
Bonito 41-6-85: 5544'A	+4.53	-5.10
Dolomitized Cements (in oolite)		
Bonito 41-6-85: 5544'B	+4.51	-5.15
Calcite Cements (within phylloid-algal buildup)		
Bonito 41-6-85: 5592'A (black cement)	+6.30	-5.10
Bonito 41-6-85: 5592'B (gray cement)	+5.67	-5.68
Bonito 41-6-85: 5592'C (brown cement ? w/sediment?)	+5.56	-5.87
Bonito 41-6-85: 5592'D (white cap cement; no sediment)	+5.73	-5.05
Bonito 41-6-85: 5592'E (coarse blocky cement)	+5.69	-6.41

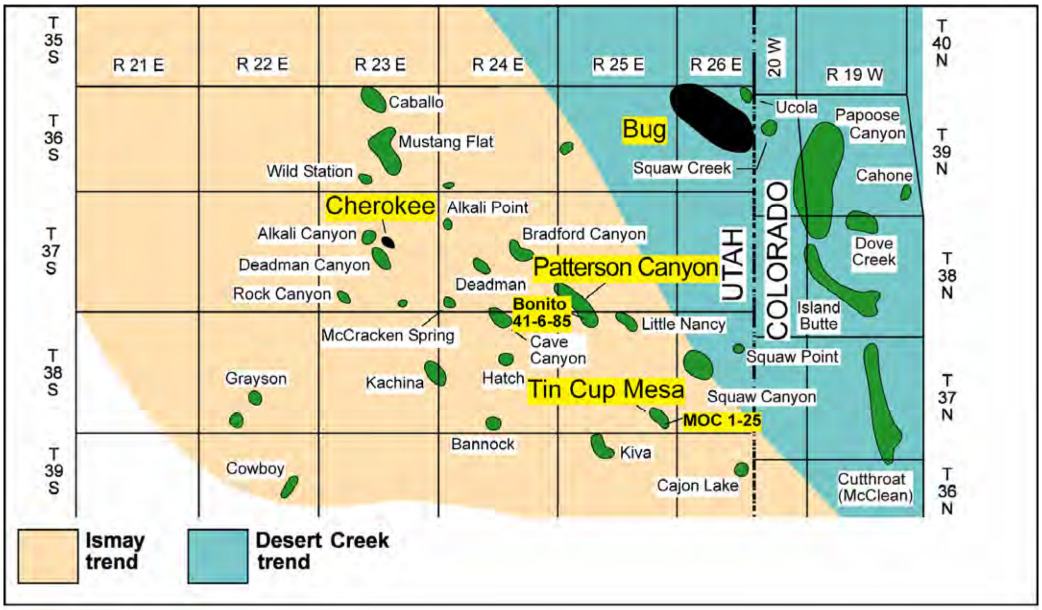

Figure 7-3. Map showing project study area and fields (case-study fields in black) within the Ismay and Desert Creek producing trends, Utah and Colorado. Fields sampled for isotope analyses are highlighted in yellow.

Carbon isotopic compositions for the eight Bug field dolomite samples (figure 7-4) all cluster very close around a mean value of +4.43‰ PDB (range of +4.03 to +4.77‰). Interestingly, the range for del ^{13}C values is slightly higher for the Bug 4 well (+4.03 to +4.77‰) than for the May Bug No. 2 well (+4.52 to +4.77‰), although their means (+4.28 versus 4.68‰) may not be significantly different. The carbon isotope values for Bug field dolomites are remarkably similar for all the rock components analyzed, including “whole rock” samples from the phylloid-algal mound fabrics and associated marine sediments, internal sediments within shelter pores, and early cements lining original pores. The mean value of del ^{13}C for all Bug field samples in this study is also very close to the mean of +4.6‰ (range of +4.0 to +5.2‰) for seven samples from two other Bug field cores (Bug No. 13 and Bug No. 16) analyzed by Marathon’s lab (see table 3, p. 125 in Roylance, 1984; see figure 7-2). Despite dolomitization, all of the lower Desert Creek samples from Bug field analyzed in this project, as well as analyzed by Marathon, show carbon isotope compositions that are very close in value to modern marine carbonates (“sediments and skeletons” on figure 7-1) and Holocene botryoidal marine aragonite cements (James and Ginsburg, 1979; “subsea cements” on figure 7-1). Furthermore, carbon isotopic compositions for former aragonite marine cements from the Late Permian Capitan Reef complex in southeastern New Mexico are calculated to be about +5.3‰ by Given and Lohmann (1985). Hence, it appears that the carbon isotope geochemistry of all of the lower Desert Creek dolomites at Bug field have retained a strong influence from Pennsylvanian marine water composition. Meteoric waters, which typically would tend to lower the carbon isotope values significantly (Hudson, 1975), do not appear to have had any effect on the composition of these lower Desert Creek dolomites.

Oxygen isotopic compositions for the eight Bug field dolomite samples (figure 7-5 and table 7-3) also cluster in a very narrow range around a mean value of -4.51‰ PDB (range of -4.15 to -4.72‰). There is no significant difference in oxygen values between the two Bug

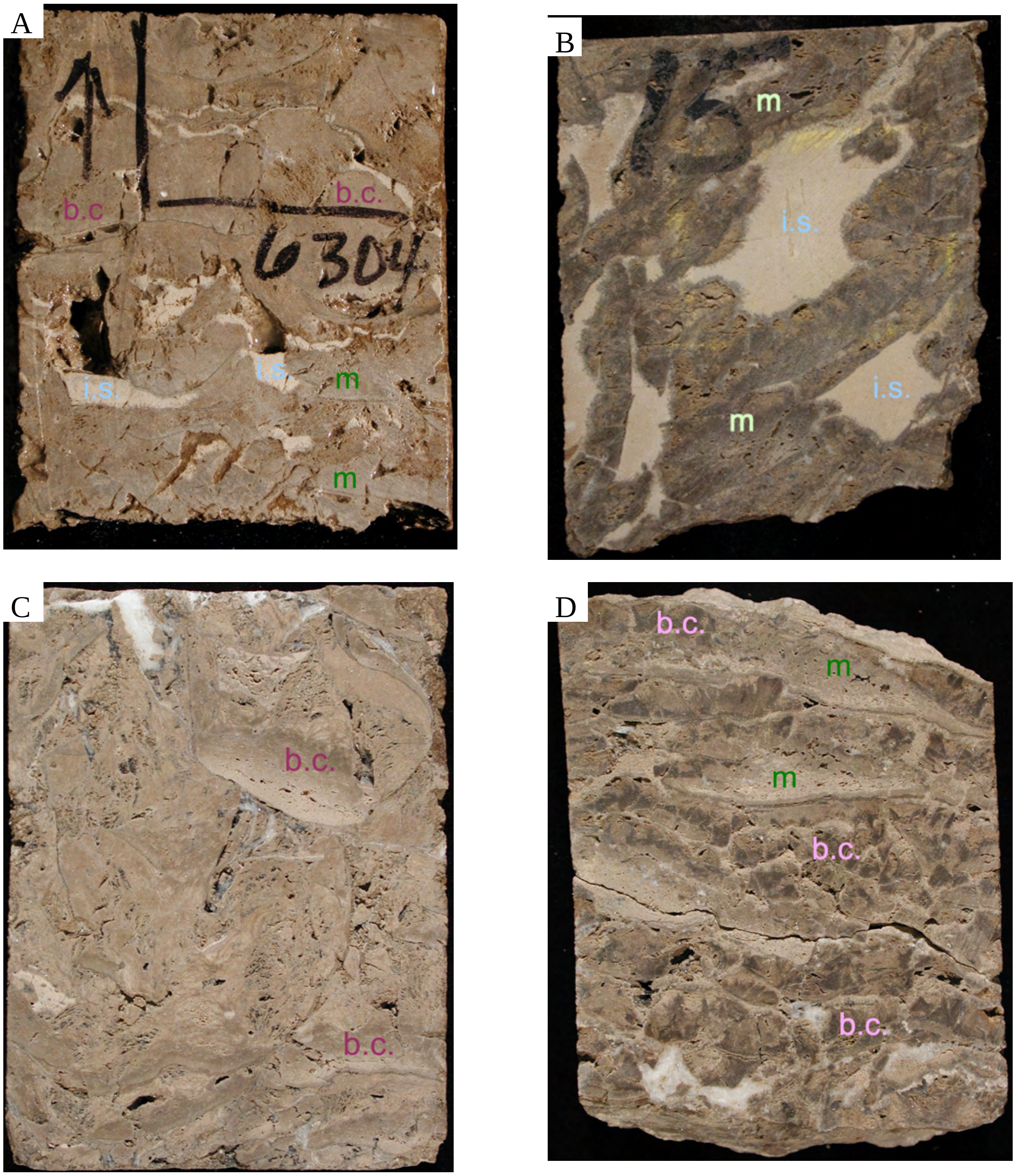

Figure 7-4. Core photos of typical Bug field components sampled for stable carbon and oxygen isotope analysis. (A) May Bug No. 2: 6304 feet - the "whole rock" dolomitized phylloid-algal mound fabric (m; sample 6304 feet A) in medium gray, the dolomitized cream-colored internal sediment (i.s.; sample 6304 feet B), and dark gray dolomitized botryoidal cements (b.c.; sample 6304 feet C) as well as associated micro-boxwork fabric were sampled for isotopic analysis. (B) May Bug No. 2: 6315 feet - both the "whole rock" dolomitized phylloid-algal mound fabric (m; sample 6315 feet B) in dark gray and the dolomitized cream-colored internal sediment (i.s.; sample 6315 feet A) were sampled for isotopic analysis. (C) Bug No. 4: 6289.7 feet - dolomitized, dark gray botryoidal cements (b.c.; sample 6289.7 feet) displaying micro-boxwork fabric were sampled for isotopic analysis. (D) Bug No. 4: 6297.5 feet - "whole rock" dolomitized phylloid-algal mound fabric (m; sample 6297.5 feet B) and dark gray dolomitized botryoidal cements (b.c.; sample 6297.5 feet A) as well as associated micro-boxwork fabric were sampled for isotopic analysis.

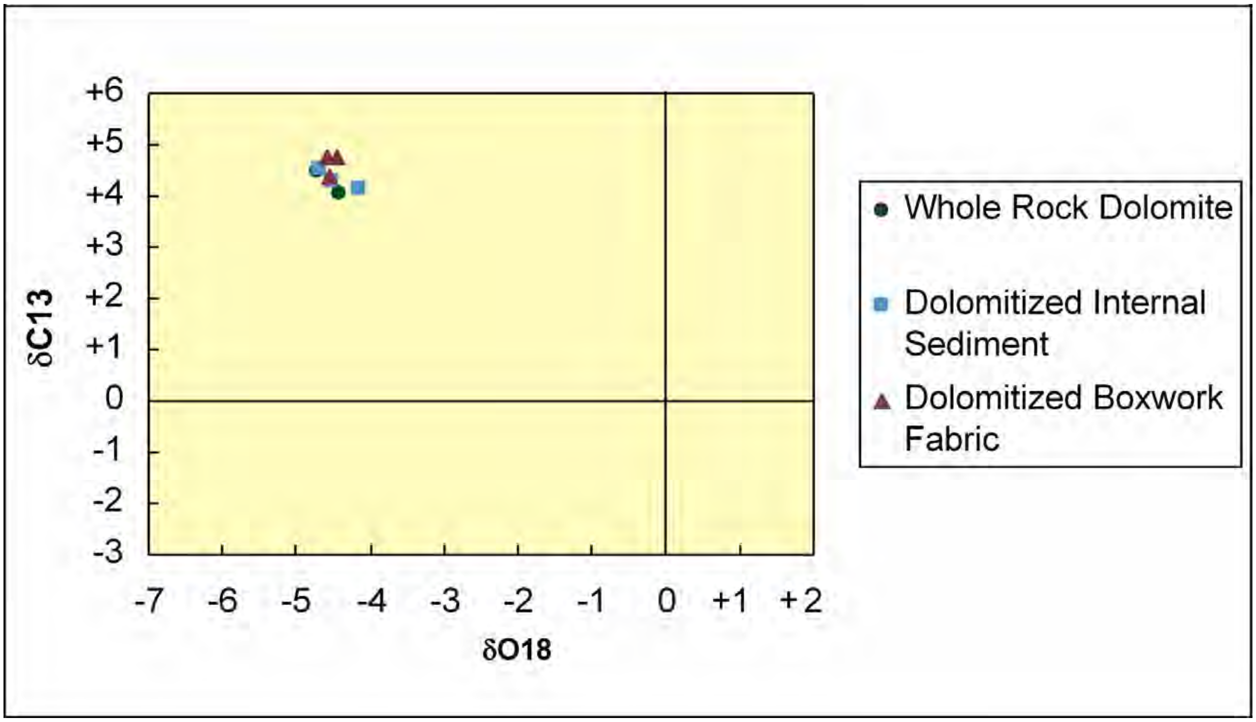

Figure 7-5. Graph of carbon versus oxygen compositions for Bug field dolomites completed for this study.

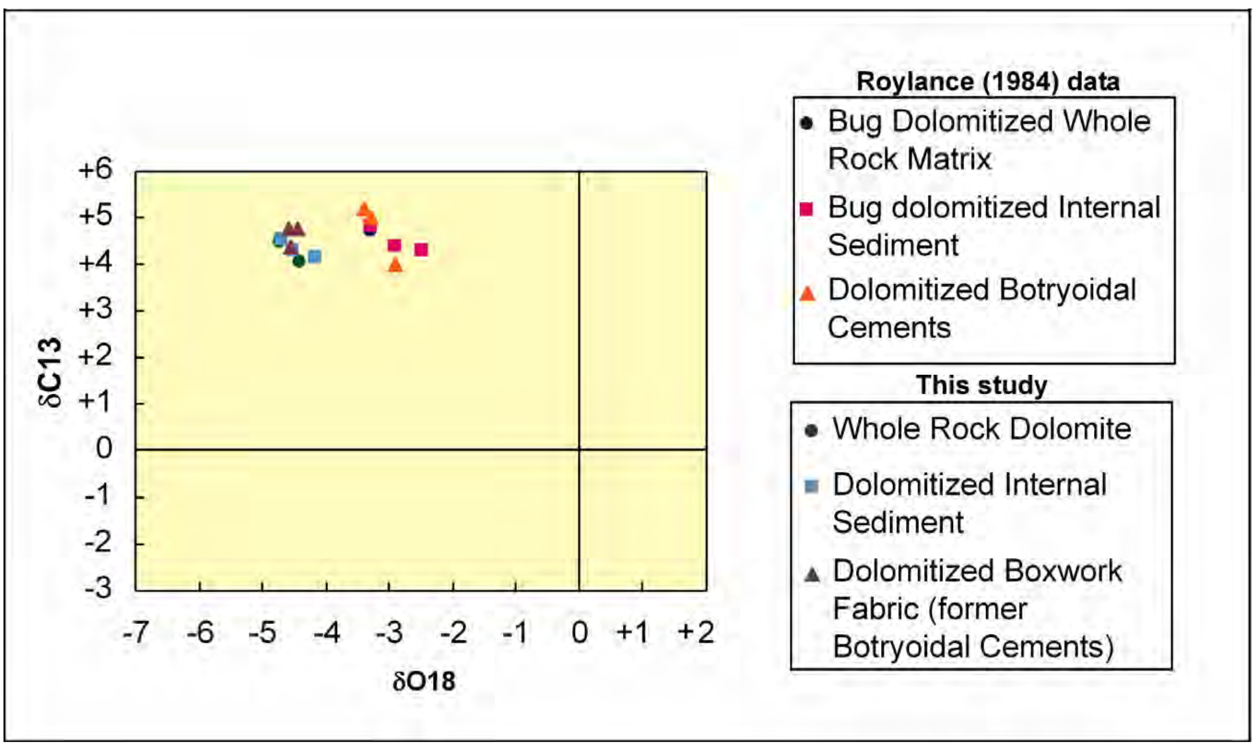

Figure 7-6. Graph comparing carbon versus oxygen compositions for Bug field dolomites by Roylance (1984) versus those completed for this study.

wells studied. However, the oxygen compositions in the dolomites sampled here for May Bug No. 2 and Bug No. 4 are significantly different from the values reported by Roylance (1984, 1990) for seven samples processed from the same stratigraphic interval in the Bug No. 13 and Bug No. 16 wells (figures 7-5 and 7-6, table 7-2). The mean oxygen isotope composition for the latter wells is -3.1‰ PDB (range of -2.5 to -3.4‰). Thus, the oxygen values in the May Bug No. 2 and Bug No. 4 cores are more negative by nearly 1.5‰. The oxygen isotope composition data from Bug No. 13 and Bug No. 16 cores, which are situated near the center of the Bug field buildup (figure 3-7), are rather close to the values for modern marine carbonates ("sediments and skeletons" on figure 7-1) and to values inferred for unaltered Pennsylvanian marine cements (Lohmann, 1983).

Oxygen isotopic compositions for former aragonite and magnesium calcite marine cements from the Late Permian Reef complex in southeastern New Mexico are calculated to be between -2.8 and -2.5‰ by Given and Lohmann (1985, 1986). The lighter oxygen values obtained from samples in the May Bug No. 2 and Bug No. 4 cores, which are located along the margins or flanks of Bug field (figure 3-7), may be indicative of exposure to higher temperatures, to fluids depleted in ^{18}O relative to sea water, or to hypersaline waters (Land, 1980, 1982) during burial diagenesis. It is also interesting to note that the two wells with the lightest oxygen isotope compositions in the lower Desert Creek dolomites (May Bug No. 2 and Bug No. 4) have produced significantly greater amounts of hydrocarbons. Production through May 2003 is 340,562 bbls of oil (54,149 m^3) and 0.76 BCFG (0.02 BCMG) for May Bug No. 2 (abandoned in 1993), and 237,285 bbls of oil (37,728 m^3) and 0.48 BCFG (0.01 BCMG) for Bug 4, while Bug No. 13 and Bug No. 16 have produced only 86,801 bbls of oil (13,801 m^3) and 0.4 BCFG (0.01 BCMG), and 24,840 bbls of oil (3950 m^3) and 0.88 BCFG (0.02 BCMG), respectively (Utah Division of Oil, Gas and Mining, 2007). The gross productive lower Desert Creek reservoir zone within each of these wells is less than 20 feet (6 m) thick. Clearly, there are economically significant changes in the reservoir quality and the diagenetic history between these well pairs.

Two samples of regional, non-reservoir, open-marine lower Desert Creek zone from Tin Cup Mesa field were analyzed by Marathon's lab for carbon and oxygen isotope composition (MOC No. 1-25 well; figure 7-3, table 7-2). The isotopic values for these samples (a limestone and a dolomite) are significantly different from the Bug field reservoir dolomites (figure 7-2 and 7-7). The biggest difference is the much lighter (by greater than 3‰) carbon isotope compositions in the Tin Cup Mesa lower Desert Creek samples than at Bug field. For oxygen isotope composition, the limestone (calcite fraction) is significantly heavier (at -1.6‰ PDB) than either the dolomite sample in the Tin Cup Mesa sample (at –3.3‰ PDB) or the mean values in the two different Bug field dolomite data sets (-3.1‰ for the two poor wells and –4.51‰ for the two excellent wells).

Carbon and Oxygen Isotopes from the Upper Ismay of Cherokee Field

Isotopic composition analyses for carbon and oxygen were completed for a variety of whole rock and diagenetic phases for core samples from the upper Ismay zone in Cherokee field (figures 7-3 and 3-10; table 7-1). A total of five powdered samples were drilled from core samples of the two cored, upper Ismay wells at Cherokee field and were analyzed (table 7-3). The samples were selected to analyze typical dolomitized calcarenite (bioclastic grainstone), limestone phylloid-algal fabric, dolomitized cryptalgal (stromatolitic) laminites, and

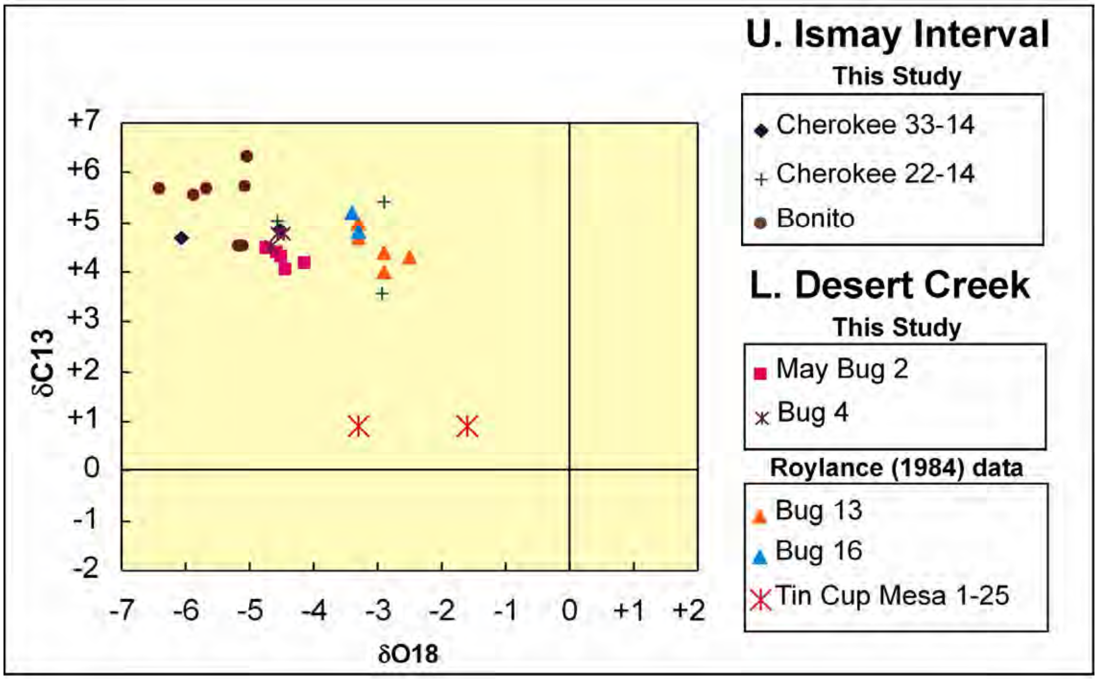

Figure 7-7. Summary graph of carbon versus oxygen compositions for all components sampled for this study and previously published data by Roylance (1984).

microcrystalline, microporous dolomite. Annotated close-up core photos (figure 7-8) show the approximate locations of the drilled and powered samples from the Cherokee Federal No. 22-14 and Cherokee Federal No. 33-14 wells. A plot of carbon versus oxygen compositions for all Cherokee field samples obtained in this study is shown on figure 7-9 (see also table 7-4).

Carbon isotopic compositions for the five upper Ismay dolomite samples from Cherokee field (figure 7-9) have a mean value of +4.70‰ PDB (range of +3.57 to +5.11‰). Although the mean carbon isotopic composition appears to be higher in the upper Ismay carbonate samples from Cherokee field than in the lower Desert Creek dolomites at Bug field, the values are not distinguishable at the 95 percent confidence level (t-test). In addition, the limestone (calcite) sample from representative phylloid-algal mound fabrics displays a del ^{13}C value within the same range as the dolomite samples (table 7-4). Brinton (l986, p. 217-218) reported a possible mean marine del ^{13}C value of +3.9‰ PDB during the time of Ismay deposition from analysis of unaltered brachiopods from Ismay field core. Carbon isotopic compositions for former aragonite marine cements from the Late Permian Capitan Reef complex in southeastern New Mexico are about +5.3‰ (Given and Lohmann, 1985). This may suggest that the fluids responsible for upper Ismay carbonates within Cherokee field have slightly heavier carbon isotope compositions than marine brachiopods at Ismay field, or slightly lighter than late Paleozoic seawater. But as with the Bug field dolomite samples, the Cherokee field carbonates fall within the same range of carbon isotope compositions as modern marine sediments, skeletons, and marine cements (see figure 7-1).

The del ^{13}C values of the Cherokee field upper Ismay components overlap or are slightly heavier than any of the diagenetic components reported by Dawson (1988) in Ismay field for meteoric-phreatic cements (del ^{13}C = +2.5 to +4.8‰), and are uniformly heavier than either deep burial ferroan calcite cements (del ^{13}C = +1.8 to +3.2‰) or saddle dolomites (mean del

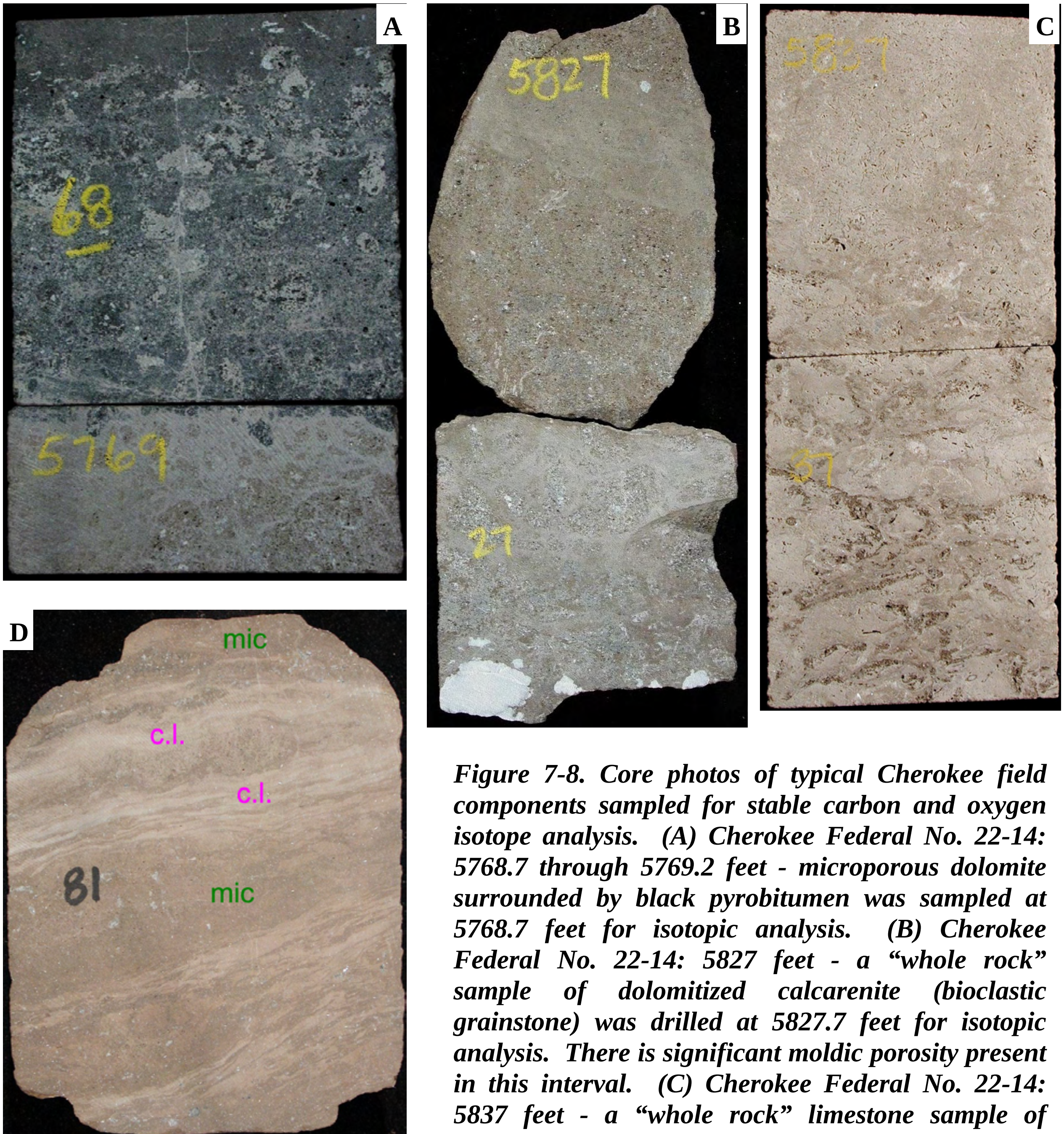

Figure 7-8. Core photos of typical Cherokee field components sampled for stable carbon and oxygen isotope analysis. (A) Cherokee Federal No. 22-14: 5768.7 through 5769.2 feet - microporous dolomite surrounded by black pyrobitumen was sampled at 5768.7 feet for isotopic analysis. (B) Cherokee Federal No. 22-14: 5827 feet - a "whole rock" sample of dolomitized calcarenite (bioclastic grainstone) was drilled at 5827.7 feet for isotopic analysis. There is significant moldic porosity present in this interval. (C) Cherokee Federal No. 22-14: 5837 feet - a "whole rock" limestone sample of phylloid-algal mound fabric was drilled at 5826.8 feet for isotopic analysis. (D) Cherokee No. 33-14: 5781 feet - both the "whole rock" dolomitized cryptalgal laminite (c.l.; sample 5781.2 feet A) and microporous dolomite (mic; sample 5781.2 feet B) were sampled for isotopic analysis.

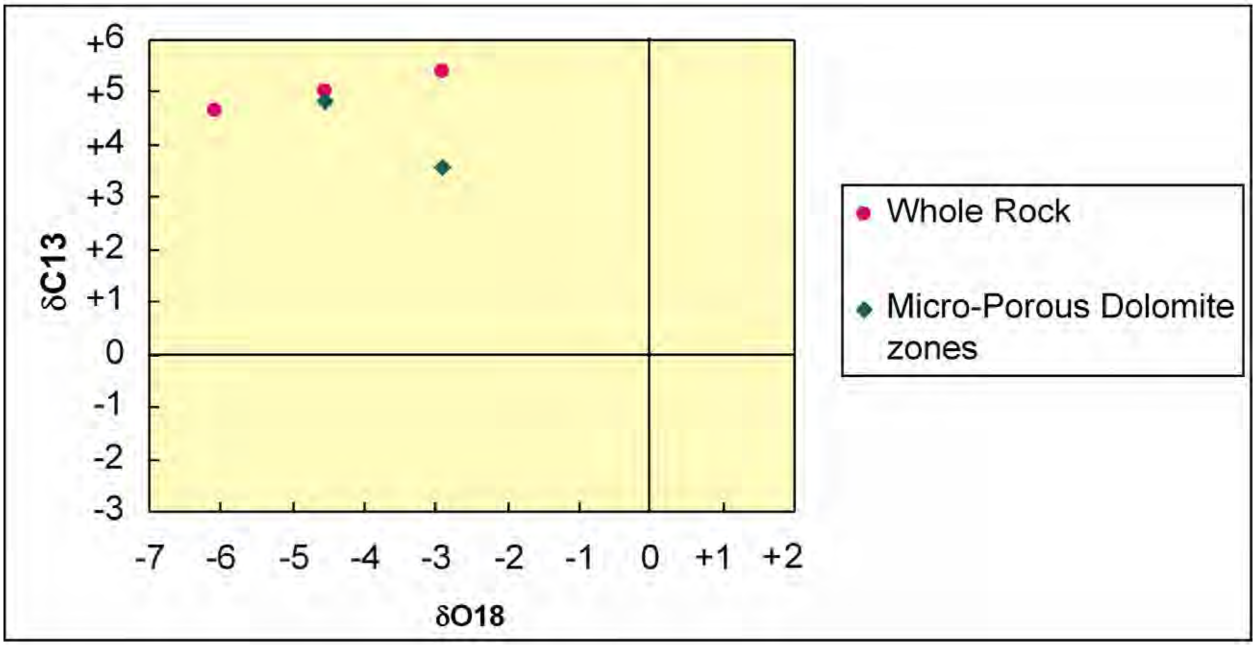

Figure 7-9. Graph of carbon versus oxygen compositions for Cherokee field components completed for this study.

^{13}C = +3.4‰). The range of del ^{13}C values at Cherokee field has a better overlap with values reported from marine botyroidal-fibrous (marine) cements and "neomorphosed matrix sediments" in Ismay field cores (Brinton, 1986) that range between +4.2 to +5.0‰. In addition, Brinton (1986, figure 62) shows that various forms of microcrystalline dolomite in Ismay field have isotopic values that cluster between +3.0 and +6.0‰ for del ^{13}C. As with the lower Desert Creek dolomites in Bug field, it does not appear that meteoric waters, which typically would precipitate carbonates with more depleted carbon isotope values, have had major effects on the composition of the Ismay carbonate components in Cherokee field. Rather, it is likely that most of the carbonates present within Ismay carbonates (as well as throughout the lower Desert Creek) have retained a marine-influenced isotope geochemistry throughout marine cementation as well as through post-burial recycling of marine carbonate components during dolomitization, stylolitization, dissolution, and late cementation. Such an explanation is in agreement with the model for the positive carbon isotope values of many ancient carbonates proposed by Hudson (1975).

Oxygen isotopic compositions for the Cherokee field limestone and dolomite samples (figure 7-9 and table 7-4) form a wide range of values around a mean value of -4.20‰ PDB (range of –2.90 to –6.08‰). As with the carbon isotope data, there is no significant difference between the oxygen isotope compositions from lower Desert Creek dolomite samples in Bug field and the upper Ismay limestones and dolomites from Cherokee field. There is no apparent pattern in the Cherokee field del ^{18}O values other than the deeper samples contain the more depleted (more negative) values. However, the range of values is probably too wide to suggest a depth-related temperature increase for the lowered del ^{18}O values. A similar range of del ^{18}O values was reported by Dawson (1988) from a variety of cement generations from Ismay field cores. Only very late ferroan calcites and baroque dolomites in Dawson's (1988) data displayed more negative oxygen isotope compositions than the Cherokee field limestones and dolomites.

Brinton (l986, p. 217-218) reported a possible mean marine del ^{18}O value of –4.7‰, during the time of Ismay deposition, from analysis of unaltered brachiopods from Ismay field core. This proposed Ismay marine value is very close to two of the Cherokee field values (see table 7-4), and to the mean value of all the samples. However, two of the samples (at –2.90 and –2.92‰) are significantly heavier than Brinton's (1986) marine del ^{18}O value calculated from unaltered marine fossils. They are closer to Given and Lohmann's (1985, 1986) marine diagenesis as determined from former aragonite and magnesium calcite marine cements in the Capitan Reef. These heavier del ^{18}O samples (both dolomites) contain oxygen values similar to two cement-filled crinoids and many of the microcrystalline dolomites analyzed by Brinton (1986). One of the dolomitized samples in Cherokee field, from cryptalgal laminites, has a much lighter oxygen composition (-6.08‰). Only certain saddle dolomite cements, late equant calcite spars, and neomorphosed calcites commonly had such light compositions in Brinton's (1986) work on Ismay field cores. The depleted del ^{18}O value of this one dolomite sample (Cherokee Federal No. 33-14: 5781.2 feet A [1762 m]) suggests neomorphism, cementation, and/or dolomitization from warm or isotopically light subsurface waters.

Carbon and Oxygen Isotopes from an Upper Ismay Buildup, Patterson Canyon Field

Carbon and oxygen isotopic analysis was completed on various whole rock and diagenetic cement generations from the upper Ismay oolite/phylloid-algal buildup along the southwest margin of Patterson Canyon field (figure 7-3, table 7-1). The Samedan Bonito No. 41-6-85 well cored approximately 25 feet (8 m) of very well-cemented, phylloid-algal mound limestone (a "reef wall" at the margin of the Patterson Canyon phylloid-algal reservoir) and 31 feet (10 m) of overlying tight oolitic and pelloidal calcarenites. Two samples were drilled from core near the top of the oolitic grainstone section, and five samples were drilled from the cements near the base of the well-cemented mound section. Annotated close-up core photos (figure 7-10) show the approximate locations of the drilled and powdered samples from the oolite and "reef cementstone" interval selected in the Bonito No. 41-6-85 well. This particular core was analyzed, despite its location outside of either of the two project fields (Bug and Cherokee) because of the spectacular development of cements that display visual characteristics suggesting different generations of development, most of which appear to have been early, or prior to significant burial. A plot of carbon versus oxygen compositions for all Samedan Bonito No. 41-6-85 limestone samples obtained in this study is shown on figure 7-11 (see also table 7-5).

Carbon isotopic compositions for the seven upper Ismay limestone samples in the core from the cemented buildup in Patterson Canyon field have a mean value of +5.43‰ PDB (range of +4.51 to +6.30‰). These values are distinguishable at the 95 percent confidence level (t-test) from the Cherokee field carbonate samples and at the 90 percent level from the Bug field dolomites, but like the Bug and Cherokee values of del ^{13}C, they are much heavier than the mean value of +0.56‰ (standard deviation of 1.55) for a large sampling ($n = 272$) of Phanerozoic marine limestones (Hudson, 1975). However, the samples can really be divided into two populations with regard to carbon isotopic composition. The five calcite samples from the deeper cemented phylloid-algal buildup have a mean value of +5.79 ‰ PDB (range of +5.56 to +6.30‰) while the oolite and cement samples from the capping grainstone have a mean value of +4.52‰ PDB (range of +4.51 to +4.53‰). Since both of these carbon isotope

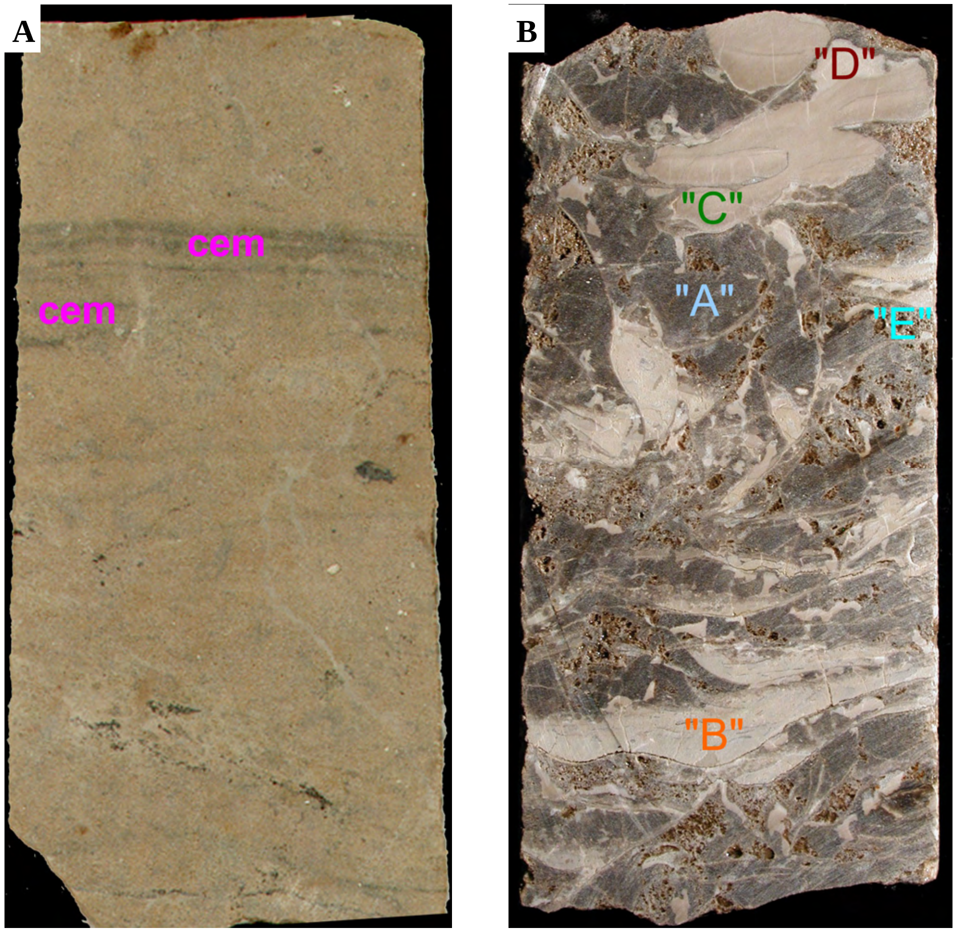

Figure 7-10. Core photos of whole rock and cement components sampled for stable carbon and oxygen isotope analysis in the upper Ismay buildup of the Samedan Bonito No. 41-6-85 well. (A) Bonito No. 41-6-85: 5544 feet - both the "whole rock" limestone (an oolitic grainstone; sample 5544 feet A) and calcite cement bands (cem; sample 5544 feet B) along bedding were sampled for isotopic analysis. (B) Bonito No. 41-6-85: 5592 feet – five calcite cement generations were sampled for isotopic analysis. Sample 5592 feet A – black cements that appear to have originally been botryoidal cement fans. Sample 5592 feet B – gray marine cements. Sample 5592 feet C – brown cements containing sediments at the bottoms of pores, often display geopetal relationships. Sample 5592 feet D – white cements that fill the tops of geopetal cores. Sample 5592 feet E – coarse, blocky calcite spar cements.

populations are significantly heavier than Brinton's (1986) value for unaltered brachiopods from Ismay field, it is likely that an isotopically heavier fluid, possibly from concentrated (higher salinity) or closed-system sea water, is recorded in both populations.

Interestingly, Given and Lohmann's (l985) calculated value (+5.3‰ PDB) from Late Paleozoic marine cements from the Permian Basin reef front falls between the two Bonito No. 41-6-85 well populations. It does not appear that meteoric waters, which typically would precipitate calcites with more depleted carbon isotope values, were involved in the diagenesis of the tight Patterson Canyon well buildup. But why the significant difference in del ^{13}C values between the well-cemented oolite samples and the cements present in the underlying reef? Clearly the waters were somehow different in composition between the phylloid-algal mound

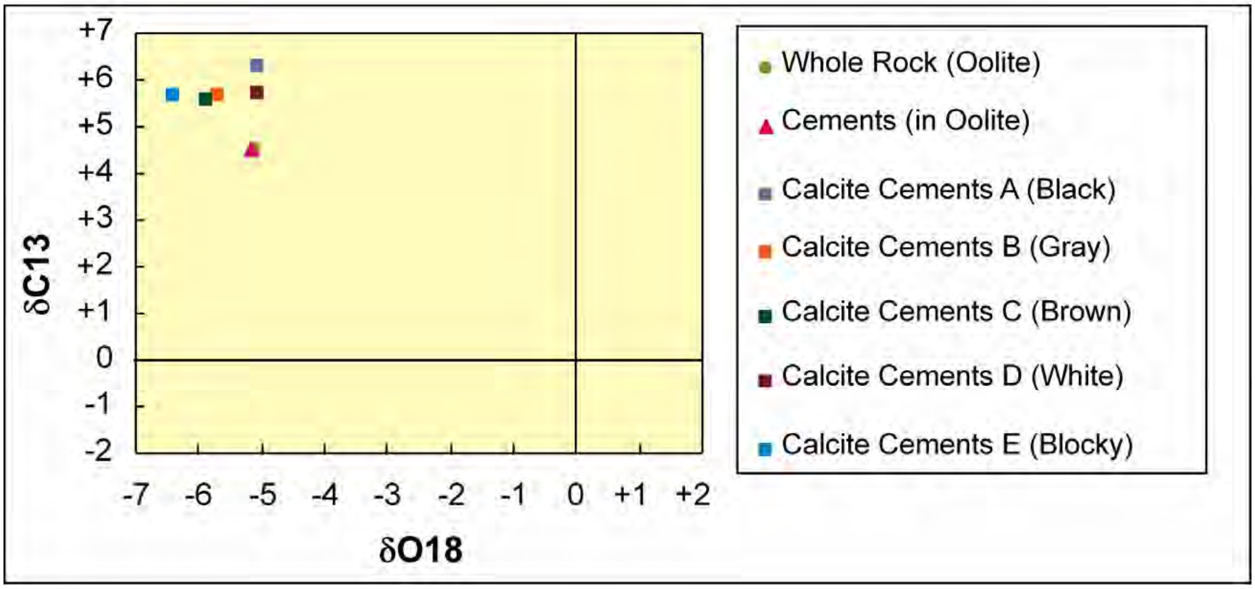

Figure 7-11. Graph of carbon versus oxygen compositions for whole rock and cement components in an upper Ismay buildup, Samedan Bonito No. 41-6-85 well, completed for this study.

cements and the lithified oolites. One possible scenario is that the waters responsible for the several generations ("A" through "E") of mound cement were confined to a "closed hydrologic system" that allowed a fluid with heavier carbon to evolve. The oolite and cement bands therein may have been in a more open system allowing water exchange such that waters with a composition slightly lighter than Brinton's proposed Ismay marine value (derived from unaltered brachiopods) were involved in the lithification and diagenesis of the capping oolite.

Oxygen isotopic compositions for the seven upper Ismay limestone samples of the cemented buildup in Patterson Canyon field form a moderate range of values around a mean value of –5.48‰ PDB (range of –5.05 to –6.41‰). As with the carbon isotope data, there is a significant difference (at the 95 percent confidence level) between the Bonito No. 41-6-85 oxygen isotope compositions and those from both the lower Desert Creek dolomites and the upper Ismay at Cherokee field. There is no significant difference in the del ^{18}O values between the deeper mound, early cement samples (mean value of -5.62‰ PDB) and the overlying lithified oolite (mean of -5.58‰ PDB). All seven of the Bonito No. 41-6-85 limestone samples, regardless of component or cement type, are lighter on average by about 1.0‰ PDB than the Bug and Cherokee field samples. These Patterson Canyon samples' del ^{18}O values from diagenetic components are also lighter than either Brinton's marine del ^{18}O value calculated from unaltered marine fossils or Given and Lohmann's (1985, 1986) values of –2.8 to -2.5‰ for former aragonite and magnesium calcite marine cements from the Late Permian Reef complex in southeastern New Mexico. The reasons for these significant differences are not immediately clear. It is possible that the oxygen isotope signatures indicate waters with depleted ^{18}O characteristics evolved in the mound cavities and ooid grainstone pores, without any influence by hypersaline waters. Alternatively, the limestones in this sample set may have all been modified via neomorphism by isotopically light subsurface waters.

CHAPTER VIII
CAPILLARY PRESSURE/MERCURY INJECTION ANALYSIS: CHEROKEE AND BUG CASE-STUDY FIELDS

David E. Eby, Eby Petrography & Consulting, Inc.;
and
Thomas C. Chidsey, Jr.,
Utah Geological Survey

Introduction

The Cherokee and Bug case-study fields (figure 1-3) were chosen for capillary pressure/ mercury injection analysis due to the quality and amount of core available from those fields. Capillary pressure/mercury injection analysis evaluates reservoir fluid saturation, and relates pore aperture size and distribution to porosity and permeability (Pittman, 1992). These data were used to assess reservoir potential and quality by: (1) determining the most effective pore systems for oil storage versus drainage, (2) identifying reservoir heterogeneity, (3) predicting potential untested compartments, (4) inferring porosity and permeability trends, and (5) matching diagenetic processes, pore types, mineralogy, and other attributes to porosity and permeability distribution. High-pressure, mercury-injection porosimetry (MIP) measurements were conducted on five core samples (table 8-1, **Deliverable 1.2.2 – Capillary Pressure/ Mercury Injection Analysis: Cherokee and Bug Fields, San Juan County, Utah**). The core samples include: (1) a dolomitic peloidal packstone to grainstone with anhydrite replacement and bitumen plugging from the Cherokee No. 22-14 well (5768.7 feet [1758.2 m]), (2) a micritic dolomitic mudstone to wackestone with a large amount of bitumen from the Cherokee No. 33-14 well (5781.2 feet [1762.0 m]), (3) a dolomitic phylloid-algal bafflestone with both early marine cement and leaching from the May Bug No. 2 well (6304 feet [1921 m]), (4) a dolomitic phylloid-algal bafflestone with internal sediment and leaching, also from the May Bug No. 2 well (6315 feet [1925 m]), and (5) a dolomitic phylloid-algal bafflestone with both early marine cement and leaching from the Bug No. 4 well (6289.1 feet [1916.8 m]).

Methodology

Capillary pressure/mercury injection analysis was conducted by TerraTek, Inc., Salt Lake City, Utah (now part of Schlumberger). Core plugs were obtained from the two Cherokee wells and three of the eight Bug wells that were cored. Core plugs were no more than 2 inches (5 cm) in length. Prior to MIP testing, the samples were dried in a low-temperature convection oven, and then ambient helium porosity and grain density measurements were conducted on each sample (table 8-1). These porosity values, along with the volume of mercury injected into each sample, were used to calculate cumulative saturation. The samples were also visually examined for open fractures that can contribute to anomalous results at low injection pressures. None of the samples tested contained open fractures or coring-induced cracks.

Table 8-1. Well core-plug samples selected for capillary pressure/mercury injection analysis.

Sample Depth (feet)	Well Name	Porosity (%)	Grain Density (g/cm^3)
5768.7	Cherokee 22-14	24.38	2.875
5781.2	Cherokee 33-14	20.89	2.934
6304.0	May Bug 2	11.06	2.865
6315.0	May Bug 2	22.24	2.834
6289.1	Bug 4	12.45	2.857

Results and Interpretation

All samples tested exhibited 100 percent mercury saturation at pressures less than 10,000 psi (68,950 kPa) injection pressure. The selected reservoir rock samples vary in porosity from 11 to 24 percent, and have grain densities of 2.8 to 2.9 g/cm^3. Pore-throat-radius histograms and saturation profiles are presented in figures 8-1 through 8-7.

Cherokee Field

The pore-throat-radius histograms for both the Cherokee No. 22-14 and Cherokee No. 33-14 well samples (5768.7 feet [1758.2 m] and 5781.2 feet [1762.0 m], respectively) (figures 8-1 and 8-2), show that half of the pore size distribution falls under 2.0 microns, or in the microporosity realm. For the Cherokee No. 22-14 well sample, the distribution of pore-throat radii appears to be trimodal. Mode 1 ranges from 7.0 to 3.6 microns (the modal class [the most abundant radii in the mode] is 4.0 microns), and accounts for 3.8 to 8 percent of the pore space, with 30 percent of the pores saturated on the cumulative injection curve. Mode 2 ranges from 2.4 to 1.04 microns (the modal class is 1.6 microns), and accounts for 10 to 15 percent of the pore space, also with 30 percent of the pores saturated on the cumulative injection curve. Mode 3 ranges from 0.7 to 0.13 microns (the modal class is 0.7 microns), and accounts for the remaining pore space, but with 20 percent of the pores saturated on the cumulative injection curve. Modes 1 and 2 account for 60 percent of the injection and need 16 percent porosity to be effective for oil and gas production. Mode 3 needs 19.5 percent porosity to be effective for oil (1.0 micron radii) and gas (0.5 micron radii) production. The measured porosity is 24.4 percent.

For the Cherokee No. 33-14 well sample, the distribution of pore-throat radii appears to be unimodal. The primary mode ranges from 3.0 to 1.04 microns (modal class is 2.0 microns), accounts 6 to 15 percent of the pore space, but only 40 percent saturation of the cumulative curve at 2.0 microns. Thus of the two wells, the Cherokee No. 33-14 is a poorer producer than the Cherokee No. 22-14. This primary mode needs 15.5 percent porosity to be effective for oil and 19.5 percent porosity for gas production. The measured porosity is 20.1 percent.

The saturation profile for the Cherokee No. 22-14 well sample shows mode 1 covers 2 to 30 percent of the mercury saturation (percent of the pore volume) and requires injection pressure of 2 to 20 psi (14-138 kPa) (figure 8-3). Mode 2 covers 30 to 70 percent of the mercury saturation and requires injection pressure of 20 to 40 psi (138-276 kPa), and is the most important in terms of contribution to production. The first 50 percent of the mercury saturation requires 28 psi (193 kPa) and is thus a good pore system; the second 45 percent requires 400 psi (2758 kPa). Most pores are filled under 1000 psi (6895 kPa).

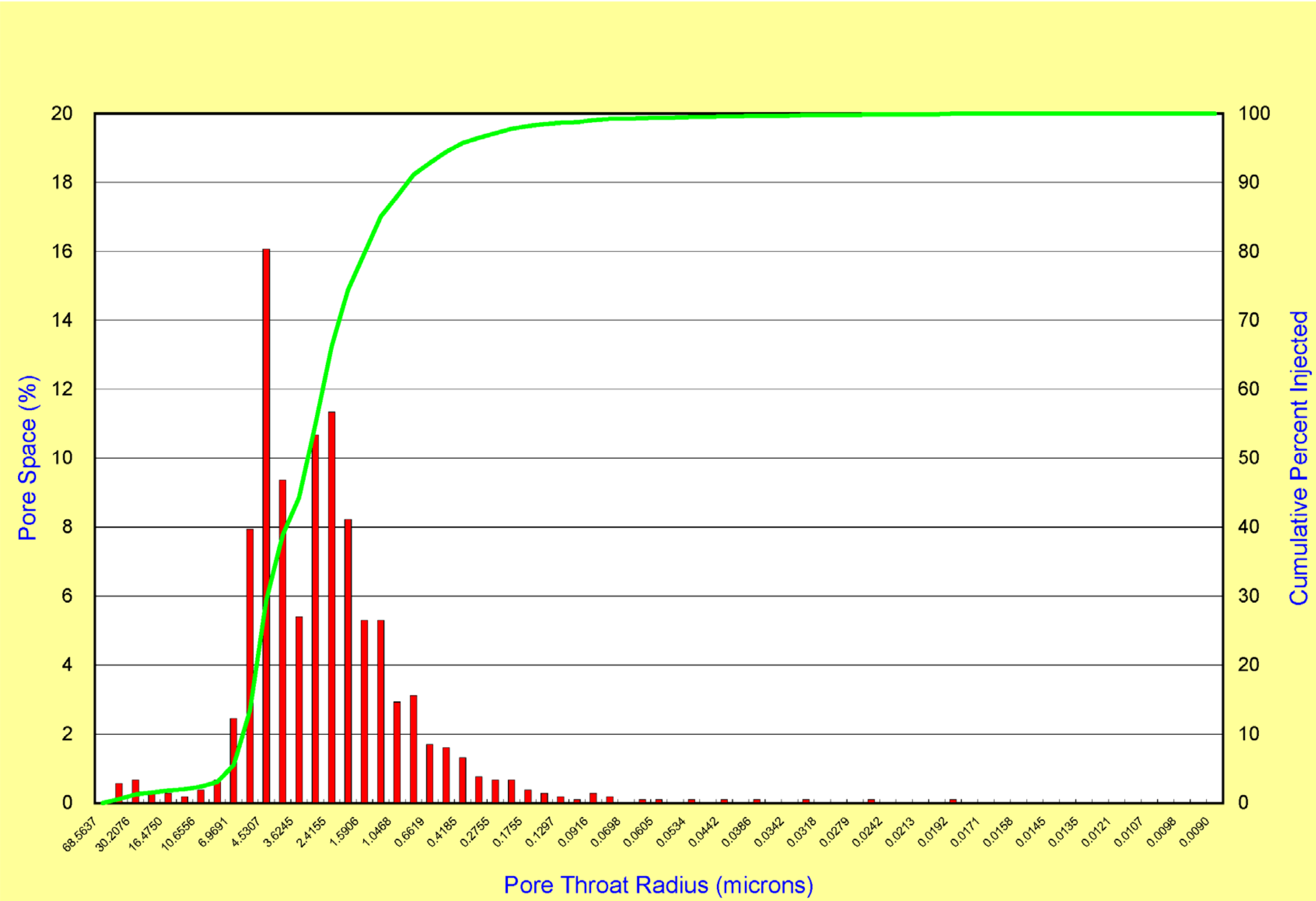

Figure 8-1. Pore throat radius histogram – sample depth, 5768.7 feet – Cherokee No. 22-14 well.

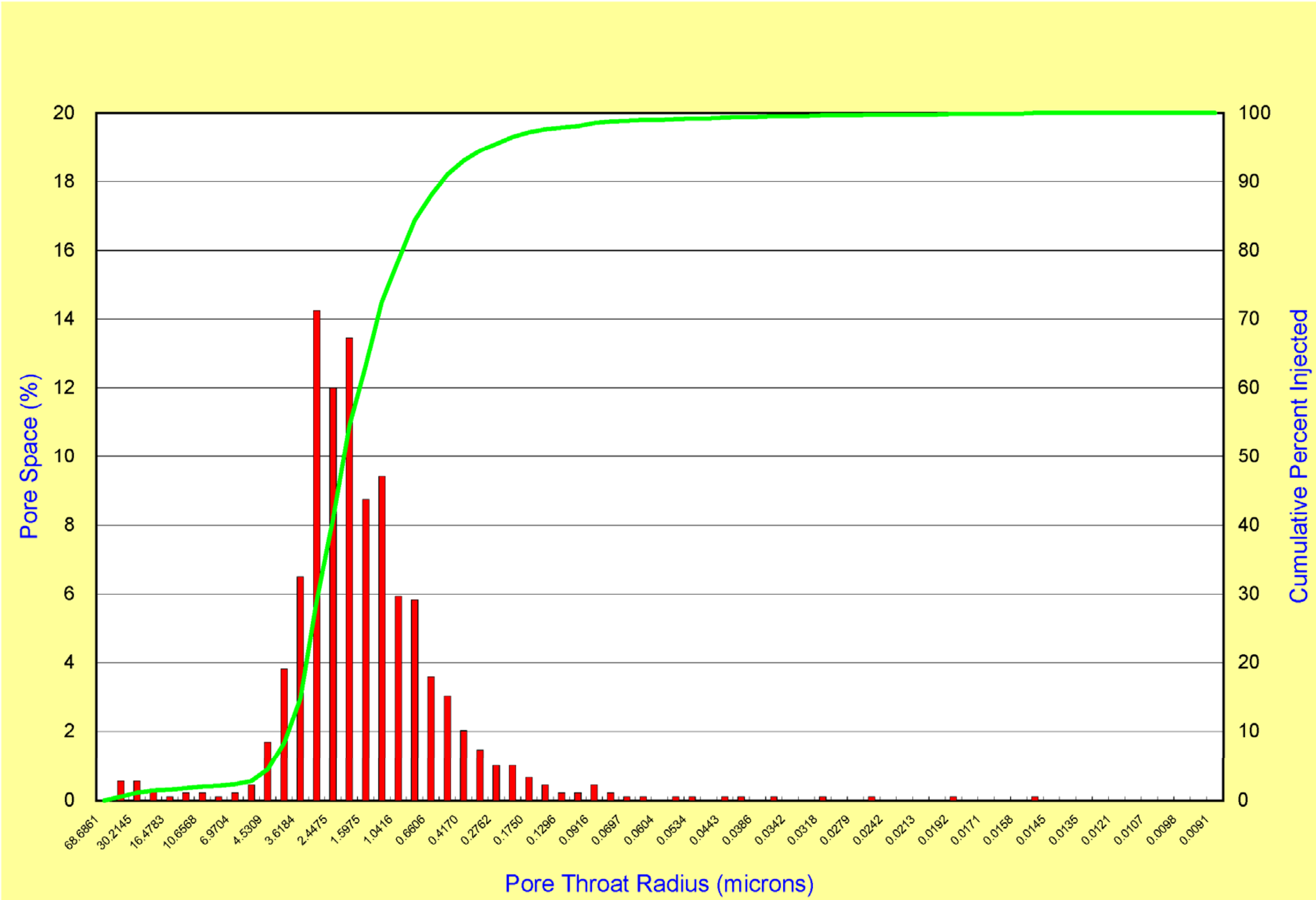

Figure 8-2. Pore throat radius histogram – sample depth, 5781.2 feet – Cherokee No. 33-14 well.

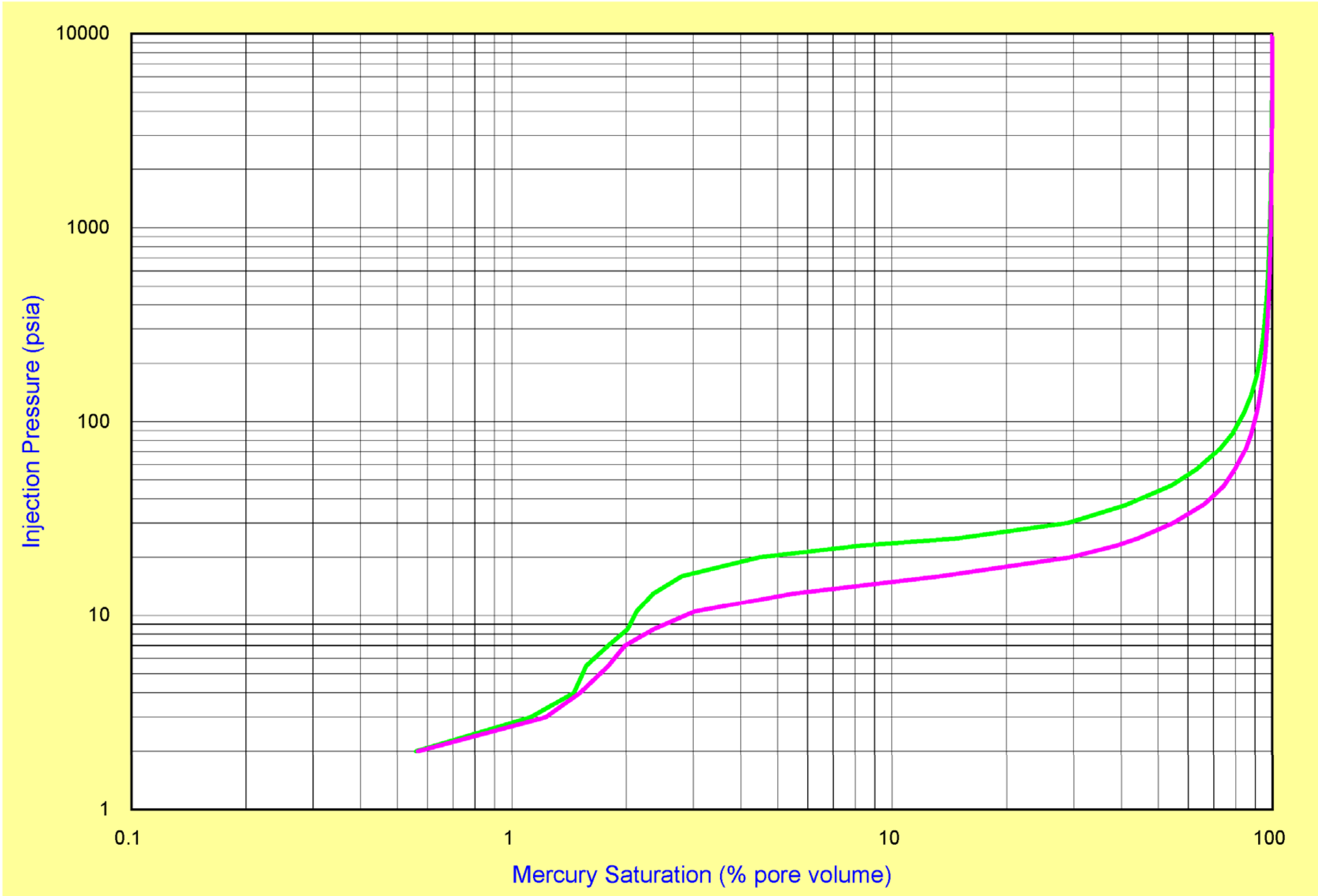

Figure 8-3. Saturation profiles, Cherokee No. 22-14 and Cherokee No. 33-14 wells.

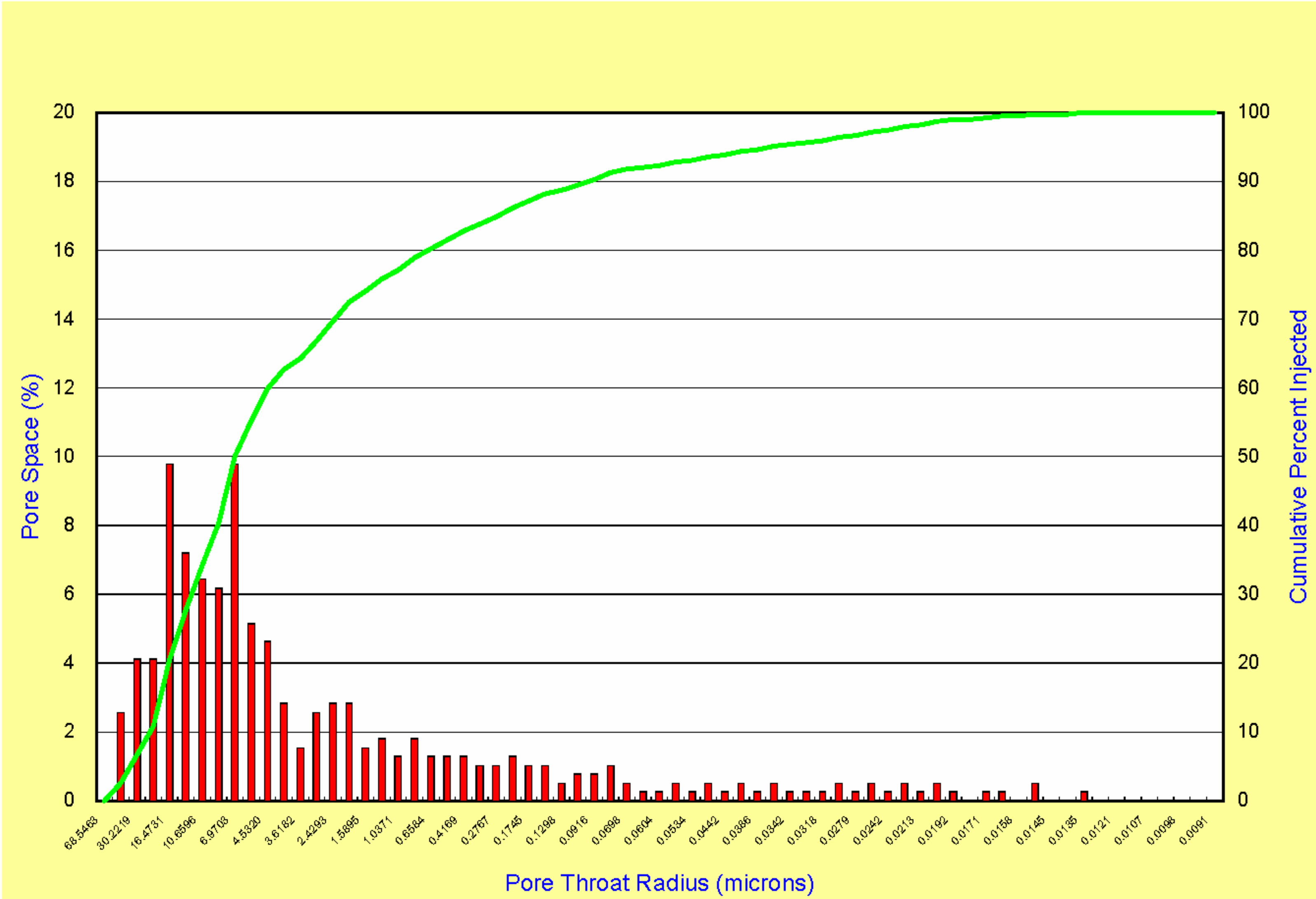

Figure 8-4. Pore throat radius histogram – sample depth, 6304 feet – May Bug No. 2 well.

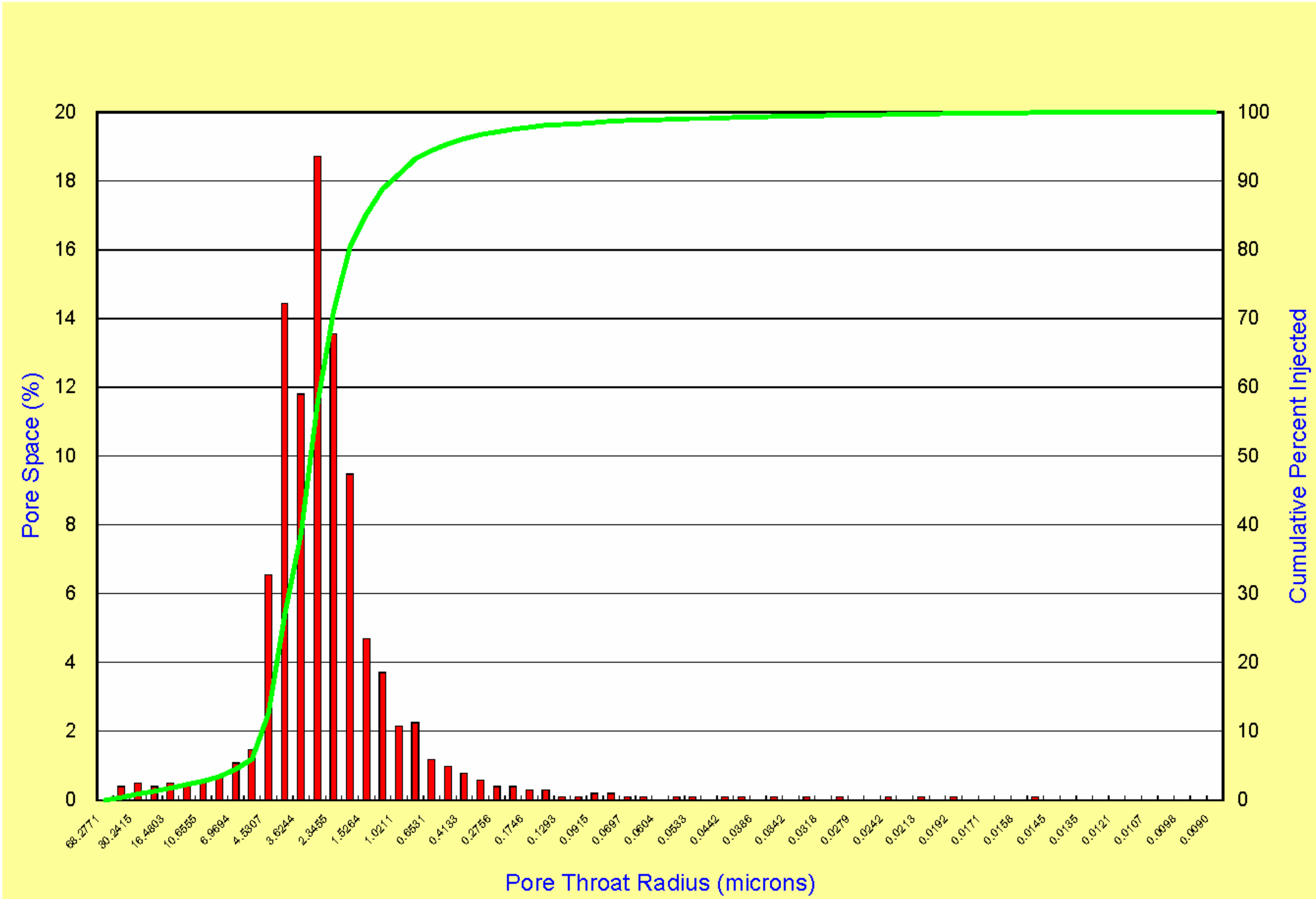

Figure 8-5. Pore throat radius histogram – sample depth, 6315 feet – May Bug No. 2 well.

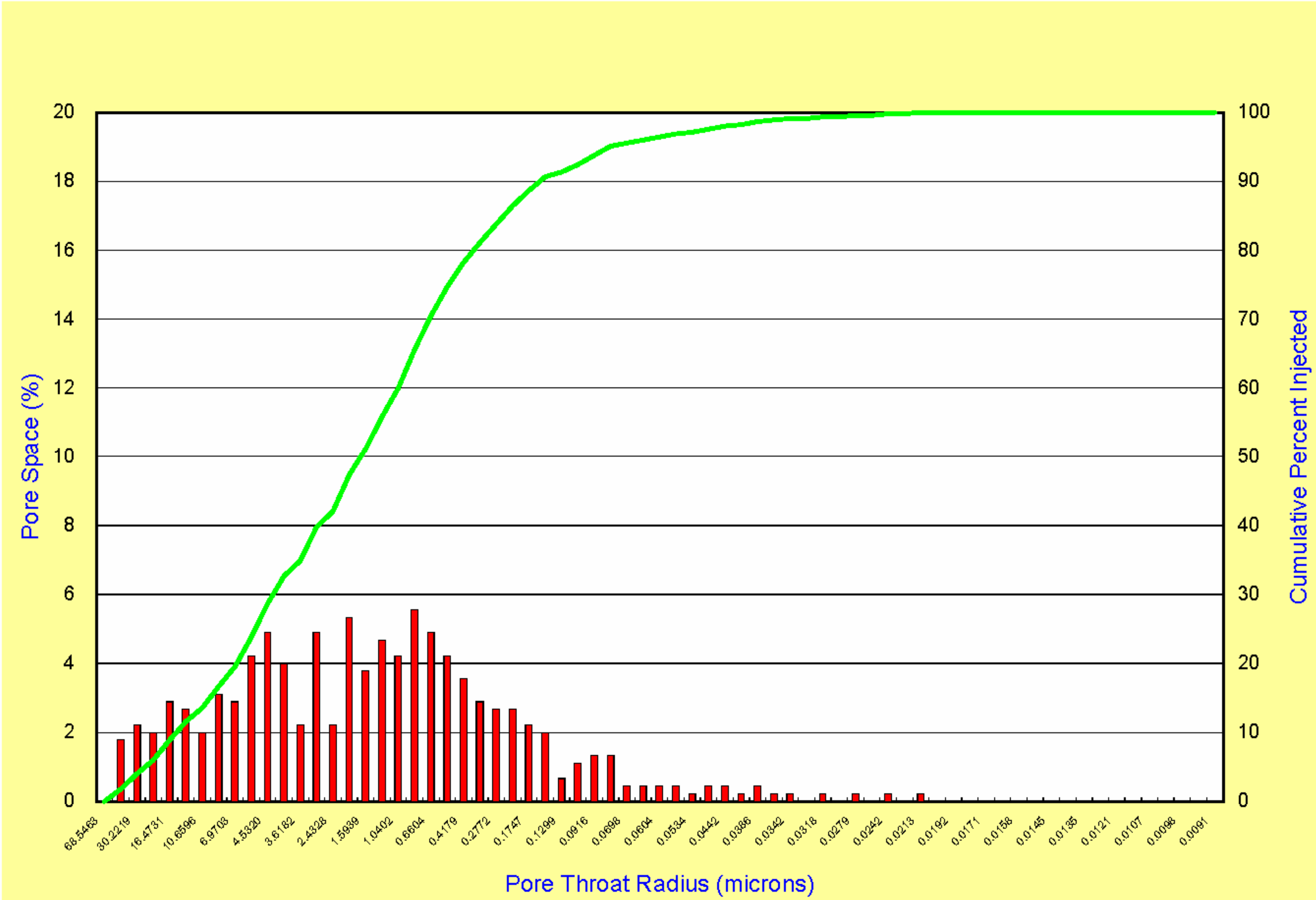

Figure 8-6. Pore throat radius histogram – sample depth, 6289.1 feet – Bug No. 4 well.

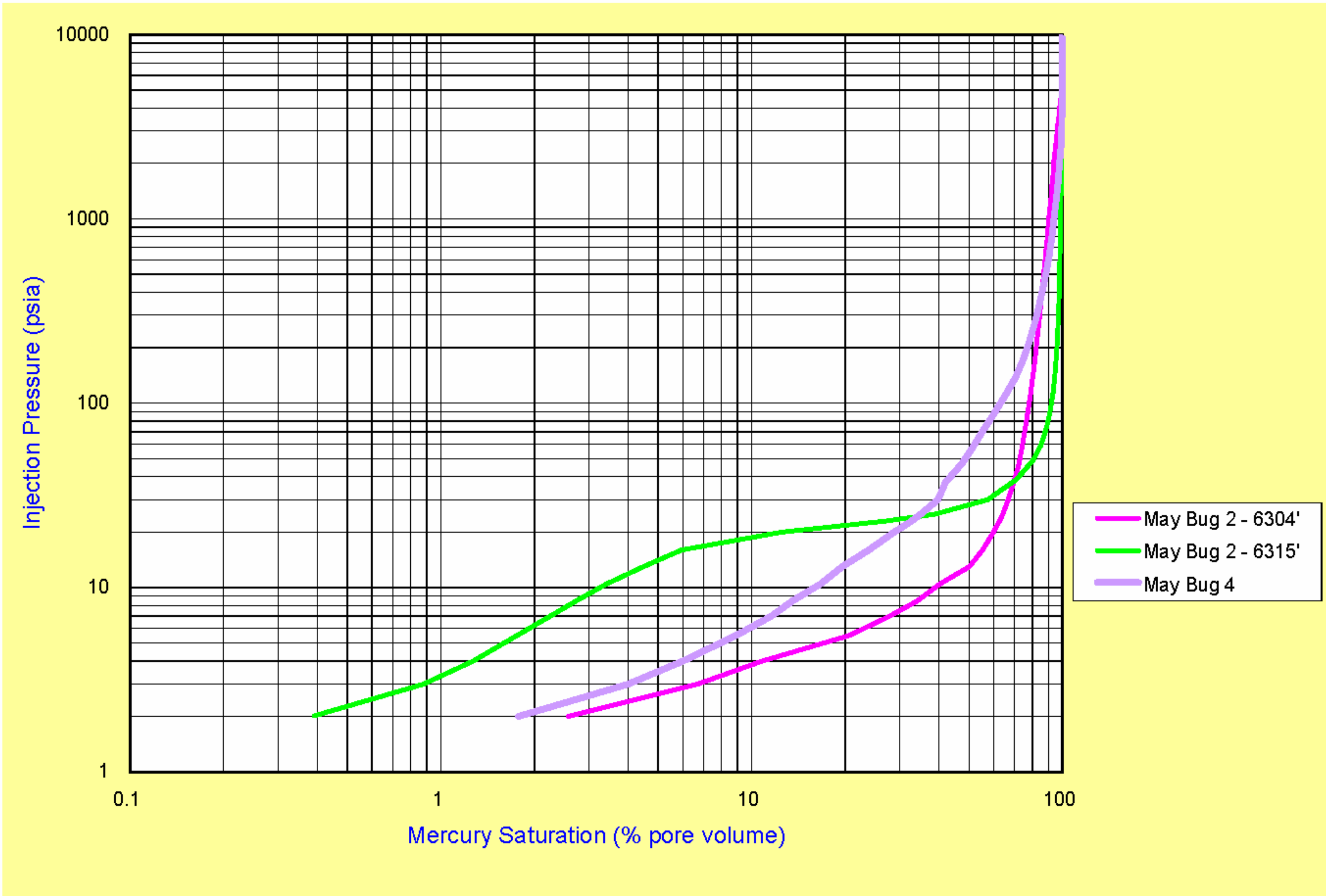

Figure 8-7. Saturation profiles, May Bug No. 2 and Bug No. 4 wells.

The saturation profile for the Cherokee No. 33-14 well sample shows the primary mode covers 2.5 to 70 percent of the mercury saturation and requires injection pressure of 15 to 70 psi (103-483 kPa) (figure 8-3). The first 50 percent of the mercury saturation requires 45 psi (310 kPa); the second 45 percent requires 600 psi (4137 kPa).

Both samples show that a relatively high injection pressure is required to occupy more than the last 70 percent of the pores (figure 8-3). The Cherokee No. 33-14 well sample has a steeper saturation profile than the Cherokee No. 22-14 well sample indicating a greater amount of microporosity, and corresponding to the lower IFP (336 BOPD [53 m^3/D] and 349 MCFGPD [10 MCMGPD] for the Cherokee No. 33-14 well compared to 688 BOPD [109 m^3/D] and 78,728 MCFGPD [2230 MCMGPD] for the Cherokee No. 22-14 well). However, the well has a high potential for untapped reserves.

Bug Field

Three capillary pressure/mercury injection tests were run on samples from Bug field: two from the May Bug No. 2 well (6304 feet [1921 m] and 6315 feet [1925 m]), and one from the Bug No. 4 well. The sample from 6304 feet (1921 m) from the May Bug No. 2 well, the distribution of pore-throat radii is trimodal (figure 8-4). Mode 1 ranges from 10 to 20 microns (the modal class is 10.65 microns), and accounts for 2 to 4 percent of the pore space, with 20 percent of the pores saturated on the cumulative injection curve. Mode 2 ranges from 6.9 to 4.5 microns (the modal class is 5.0 microns), and accounts for 10 to 12 percent of the pore space, with 10 percent of the pores saturated on the cumulative injection curve. The minor mode 3 ranges from 3.0 to 1.5 microns (the modal class is 2.0 microns), and accounts for 13 to 15 percent of the pore space, also with 10 percent of the pores saturated on the cumulative injection curve. Modes 1 and 2 account for 30 percent of the injection and need 16 percent porosity to be effective for oil and 17.5 percent porosity for gas production. The measured porosity is 11.1 percent.

For the sample from 6315 feet (1925 m) from the May Bug No. 2 well, the distribution of pore-throat radii appears to be unimodal (figure 8-5). The primary mode ranges from 4.5 to 1.5 microns (modal class is 2.3 microns), and accounts 2 to 17 percent of the pore space, with 75 percent saturation of the cumulative curve. This primary mode needs 18 percent porosity to be effective for oil and 19.5 percent porosity for gas production. The measured porosity is 22.2 percent.

The distribution of pore-throat radii in the Bug No. 4 well is trimodal (figure 8-6). Mode 1 ranges from 5.5 to 3.6 microns (the modal class is about 4.0 microns), and accounts for 4.2 to 6.3 percent of the pore space, with 10 percent of the pores saturated on the cumulative injection curve. Mode 2 ranges from 2.4 to 1.0 microns (the modal class is 1.6 microns), and accounts for 8.3 to 10.3 percent of the pore space, also with 10 percent of the pores saturated on the cumulative injection curve. Mode 3 ranges from 1.0 to 0.4 microns (the modal class is 0.66 microns), and accounts for 12.3 to 14.3 of the remaining pore space, again with 10 percent of the pores saturated on the cumulative injection curve. Modes 1 and 2 account for 20 percent of the injection and need 11 percent porosity to be effective for oil production. Mode 3 needs 18 percent porosity to be effective for gas production. The measured porosity is 12.3 percent.

The saturation profile for the sample from 6304 feet (1921 m) from the May Bug No. 2 well shows mode 1 covers 1 to 60 percent of the mercury saturation and requires injection pressure of 1 to 20 psi (7-138 kPa) (figure 8-7). Mode 2 covers 60 to 75 percent of the mercury saturation and requires injection pressure of 20 to 50 psi (138-345 kPa). The first 50 percent of the mercury saturation requires 15 psi (103 kPa); the second 45 percent requires 400 psi (2758 kPa).

The saturation profile for the sample from 6315 feet (1925 m) from the May Bug No. 2 well shows the primary mode covers 6 to 60 percent of the mercury saturation and requires injection pressure of 15 to 30 psi (103-207 kPa) (figure 8-7). The first 50 percent of the mercury saturation requires 28 psi (193 kPa); the second 45 percent requires 400 psi (2758 kPa).

The saturation profile for the Bug No. 4 well sample shows mode 1 covers 4 to 28 percent of the mercury saturation and requires injection pressure of 3 to 20 psi (21-138 kPa) (figure 8-7). Mode 2 covers 45 to 70 percent of the mercury saturation and requires injection pressure of 40 to 150 psi (276-1034 kPa). Mode 3 covers 88 to 92 percent of the mercury saturation and requires injection pressure of 500 to 1500 psi (3448-10,343 kPa). The first 50 percent of the mercury saturation requires 55 psi (379 kPa); the second 45 percent requires 2000+ psi (13,782+ kPa).

As in Cherokee field, relatively high injection pressures are required to occupy more than the last 70 percent of the pores (figure 8-7). The steeper saturation profiles indicate a significant amount of micro-boxwork porosity, and thus, an excellent target for horizontal drilling.

CHAPTER IX
PRODUCTION ANALYSIS: CHEROKEE AND BUG CASE-STUDY FIELDS

Thomas C. Chidsey, Jr.,
Utah Geological Survey

Introduction

The two Utah case-study fields were selected for reservoir-modeling studies: Cherokee in the Ismay trend and Bug in the Desert Creek trend (figure 1-3). Before modeling studies could be conducted, analyses of well-test and oil production data were required (**Deliverable 2.1.2 – Production Analysis: Cherokee and Bug Fields, San Juan County, Utah**). These data were compiled through two principal tasks: (1) review of existing well-completion data, and (2) determination of production history from monthly production reports available through the Utah Division of Oil, Gas and Mining. This information was merged with geological characterization data and incorporated into the interpretation of reservoir models. Production "sweet spots" and potential horizontal drilling candidates, both wells and fields, were identified. Using the results, various horizontal drilling methods and the ultimate recovery can be estimated for Cherokee and Bug fields.

Well-Test Data Evaluation

Well-test data can provide key insight into the nature of reservoir heterogeneities, and also provide "large-scale" quantitative data on actual reservoir properties and lithofacies from case-study reservoirs. Although a number of well tests have been conducted in all of the target reservoirs, only the IFP well tests were determined to provide quantitative reservoir property information. Initial potential flow well tests were graphed and plotted for each well (figures 9-1 through 9-4). The graphs include both oil (in BOPD) and gas (in MCFGPD) production.

In Cherokee field, the highest IFP was recorded from the Cherokee Federal No. 22-14 well (figures 9-1 and 9-2), located on the crest of the structural nose where the thickest part of the upper Ismay zone mound lithofacies developed (figures 3-10 and 3-12). The lowest recorded IFP was recorded from the Cherokee Federal No. 11-14 well (figures 9-2 and 9-3), located on the structural low and on the thin flank of the mound buildup (figures 3-10 and 3-12). Both wells had relatively high gas-to-oil ratios (GOR) in comparison to the other two producing field wells (figure 9-1) in the southeastern part of the field (figure 9-2).

In Bug field, the highest IFPs were recorded from the Bug No. 1, May Bug No. 2, Bug No. 9, and Bug No. 4 wells (figures 9-3 and 9-4), located structurally downdip from the updip porosity pinch out that forms the trap, and in the main part of the lower Desert Creek zone carbonate buildup (figures 3-7 and 3-9); Bug No. 9 was tested from the thickest section of the mound. These wells penetrated both the phylloid-algal mound and the shoreline carbonate island lithofacies of the carbonate buildup. The lowest recorded IFPs were from wells closest to the updip porosity pinch out, or just downdip from the oil/water contact (figures 9-3, 9-4, and 3-7). These wells penetrated only the phylloid-algal mound lithofacies (figure 3-9).

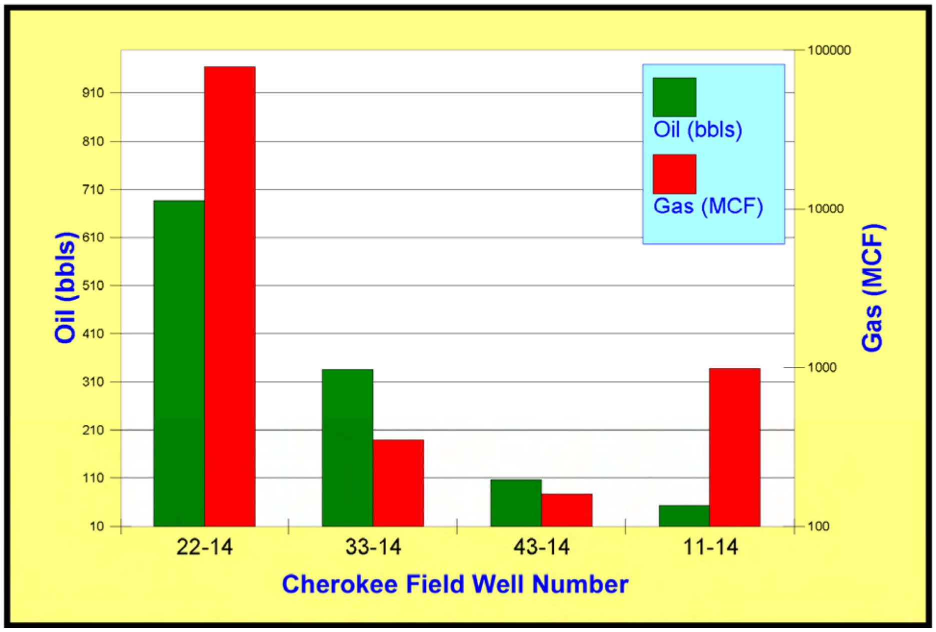

Figure 9-1. Initial flowing potential of oil and gas from upper Ismay producing wells in Cherokee field (data source: Utah Division of Oil, Gas and Mining).

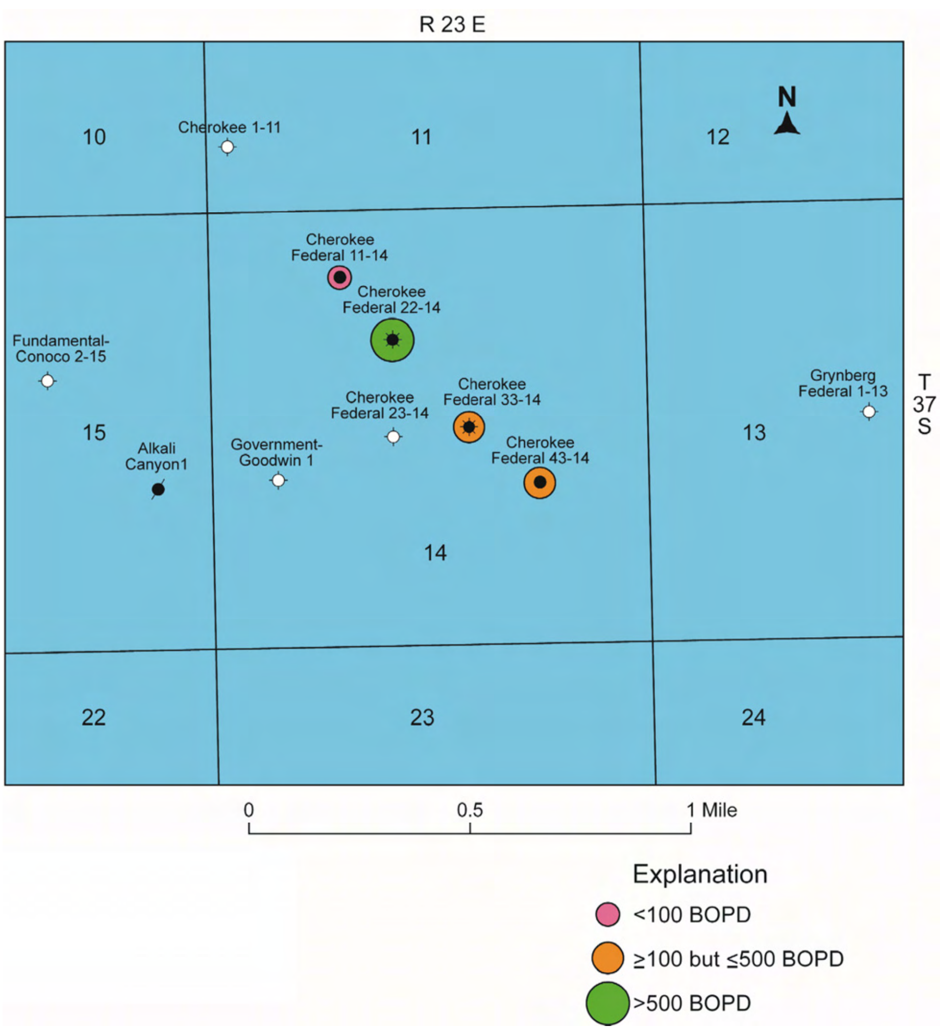

Figure 9-2. Bubble map of initial flowing potential of oil (in BOPD) from upper Ismay producing wells in Cherokee field (data source: Utah Division of Oil, Gas and Mining).

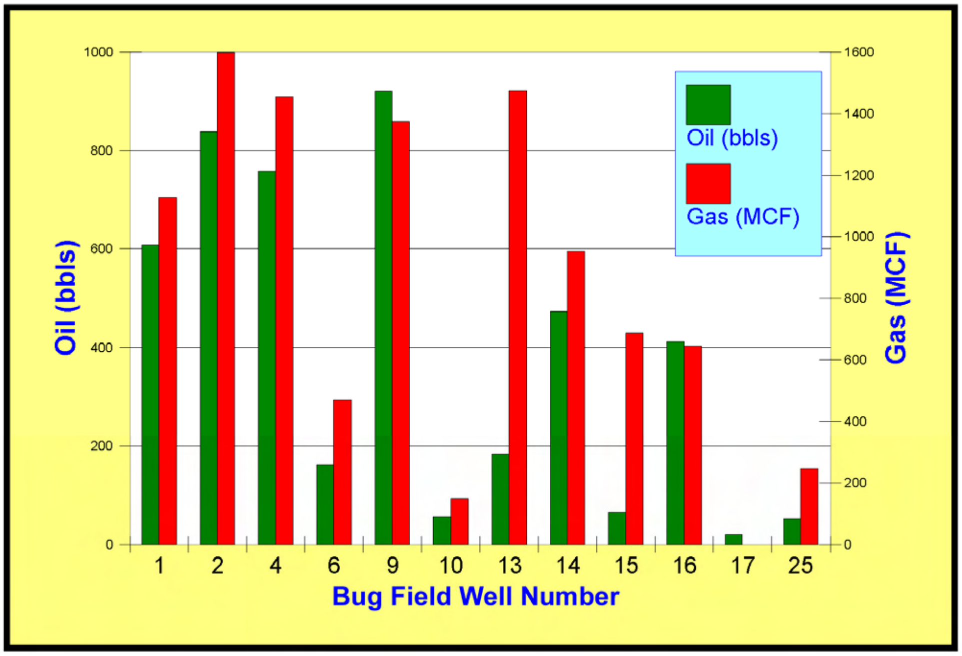

Figure 9-3. Initial flowing potential of oil and gas from lower Desert Creek producing wells in Bug field (data source: Utah Division of Oil, Gas and Mining).

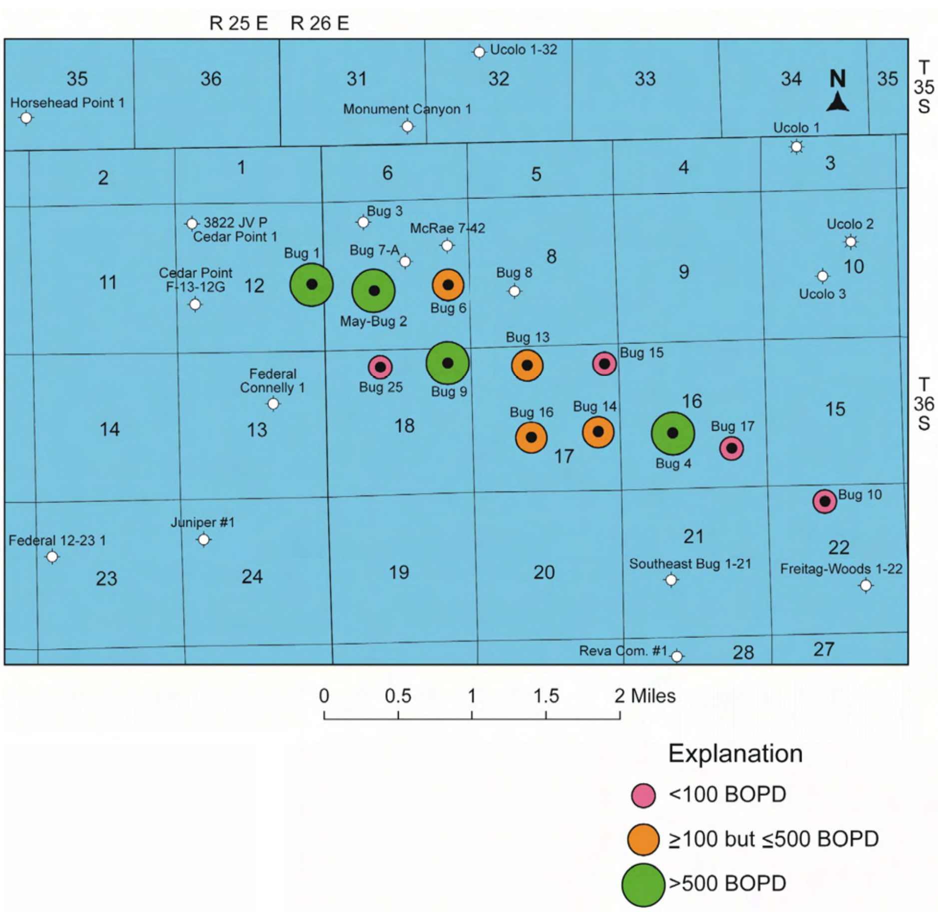

Figure 9-4. Bubble map of initial flowing potential of oil (in BOPD) from lower Desert Creek producing wells in Bug field (data source: Utah Division of Oil, Gas and Mining).

Cumulative Production

Oil and gas production from Cherokee field has shown a steady decline since peaking in the late 1980s (figure 9-5). Cumulative production was graphed and plotted for each well (figures 9-6 and 9-7). The graphs include both oil and gas production. In Cherokee field, the largest volume of oil has been produced from the Cherokee Federal No. 33-14 well, while the highest volume of gas has been produced from the Cherokee Federal No. 22-14 well (figure 9-6). Both wells are located where the crest of the structural nose coincides with the thickest part of the mound lithofacies (figures 3-10 and 3-12). The Cherokee Federal No. 22-14 well is slightly higher structurally than the Cherokee Federal No. 33-14 well, possibly accounting for the significantly greater volume of gas production. These wells penetrated both the phylloid-algal mound and the crinoid/fusulinid-bearing carbonate sand lithofacies of the carbonate buildup (figure 3-12). The Cherokee Federal No. 33-14 well may have encountered a significantly thicker section of microporosity and microfractures than other wells resulting in greater oil production. Microporosity is present in cores from both the Cherokee Federal No. 33-14 and Cherokee Federal No. 22-14 wells (figure 3-32). This unique pore type represents the greatest hydrocarbon storage capacity and potential horizontal drilling target in the field. The lowest volumes of hydrocarbon production are from wells on the flanks of both the structure and the mound. These wells are likely close to the oil/water contact (its exact elevation is unknown) and have penetrated only the phylloid-algal mound buildup.

In Bug field, oil and gas production peaked in 1982, and has shown a steady decline in oil and gas since 1985 and 1989, respectively (figure 9-8). The largest volumes of oil have been produced from the May Bug No. 2 and Bug No. 14 wells (figures 9-9 and 9-10). These wells, plus the Bug No. 4 and Bug No. 9 wells, have each produced over 200,000 barrels (31,800 m^3) of oil. They are all located structurally downdip from the updip porosity pinch out, and in the main part of the lower Desert Creek zone carbonate buildup (figures 3-7 and 3-9). These wells penetrated both the phylloid-algal mound and the shoreline carbonate island lithofacies. However, there are other wells that penetrated this same lithofacies combination, such as Bug No.16 well, but have produced lower volumes of oil. These wells may have encountered fewer microfractures and less micro-boxwork porosity (figure 3-31), a prime diagenetic pore type in this dolomitized reservoir, which is thought to account for the greatest hydrocarbon storage and flow capacity in the field. The lowest volumes of hydrocarbon production are from wells closest to the updip porosity pinch out (Bug No. 15 and No. Bug 17) or farther downdip near the oil/water contact (Bug No. 25) (figures 3-7, 9-9, and 9-10). These wells penetrated only the phylloid-algal mound lithofacies (figure 3-9). The Bug No. 13 and Bug No. 15 wells are the structurally highest wells in the field and are located near a presumed gas cap, thus their production history shows high GORs.

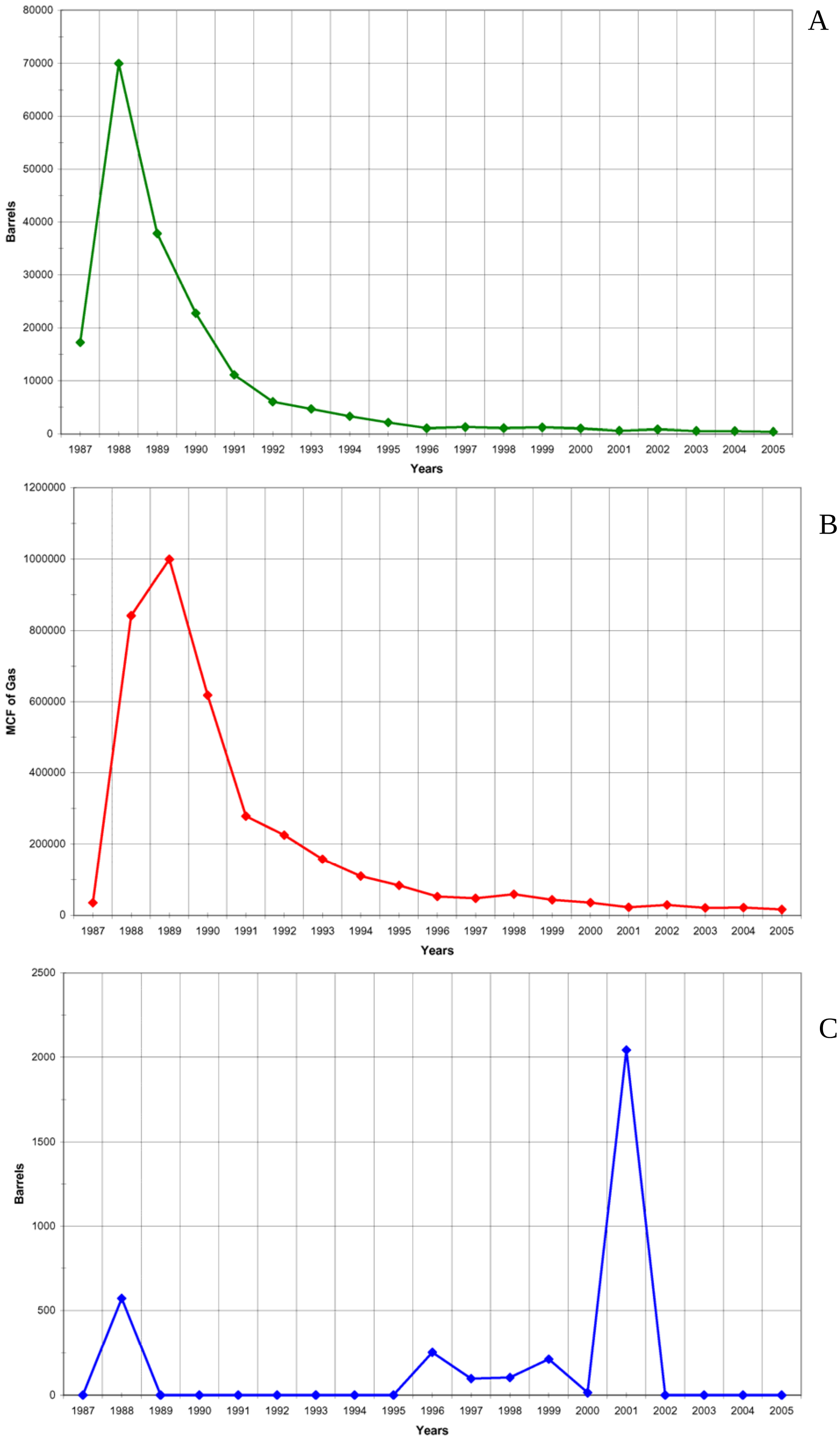

Figure 9-5. Historical oil (A), gas (B), and water (C) production for Cherokee field through 2005 (Utah Division of Oil, Gas and Mining, 2006).

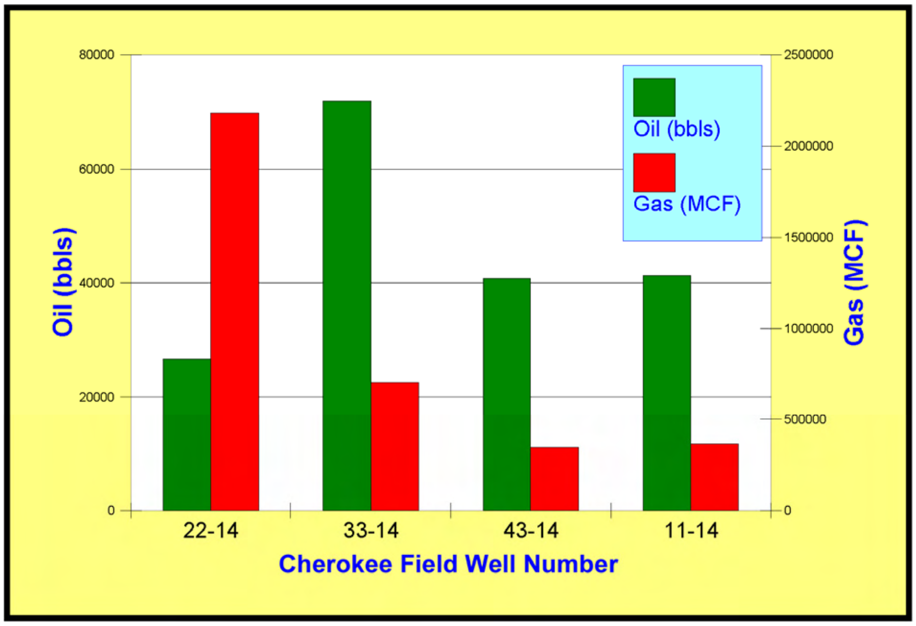

Figure 9-6. Cumulative production of oil and gas (as of January 1, 2006) from upper Ismay producing wells in Cherokee field (Utah Division of Oil, Gas and Mining, 2006).

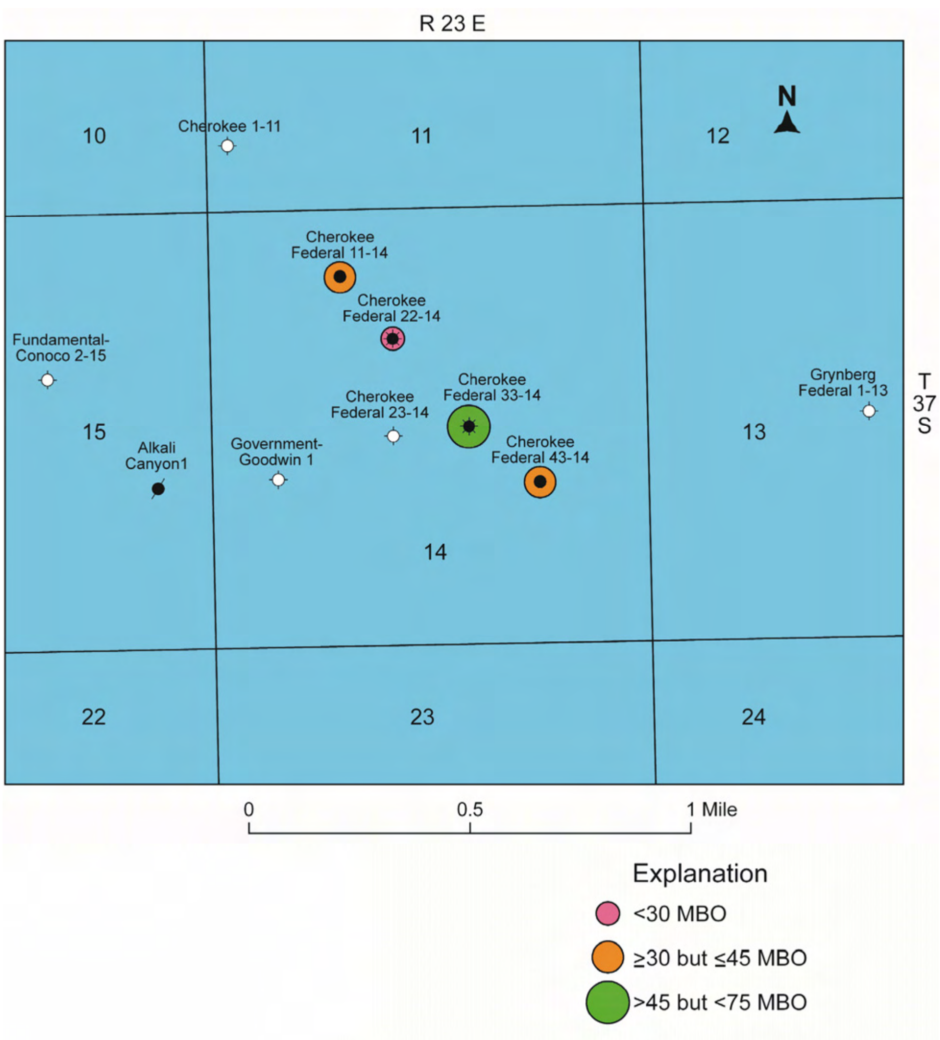

Figure 9-7. Bubble map of cumulative production of oil as of January 1, 2006 (in thousands of barrels, MBO) from upper Ismay producing wells in Cherokee field through 2005 (Utah Division of Oil, Gas and Mining, 2006).

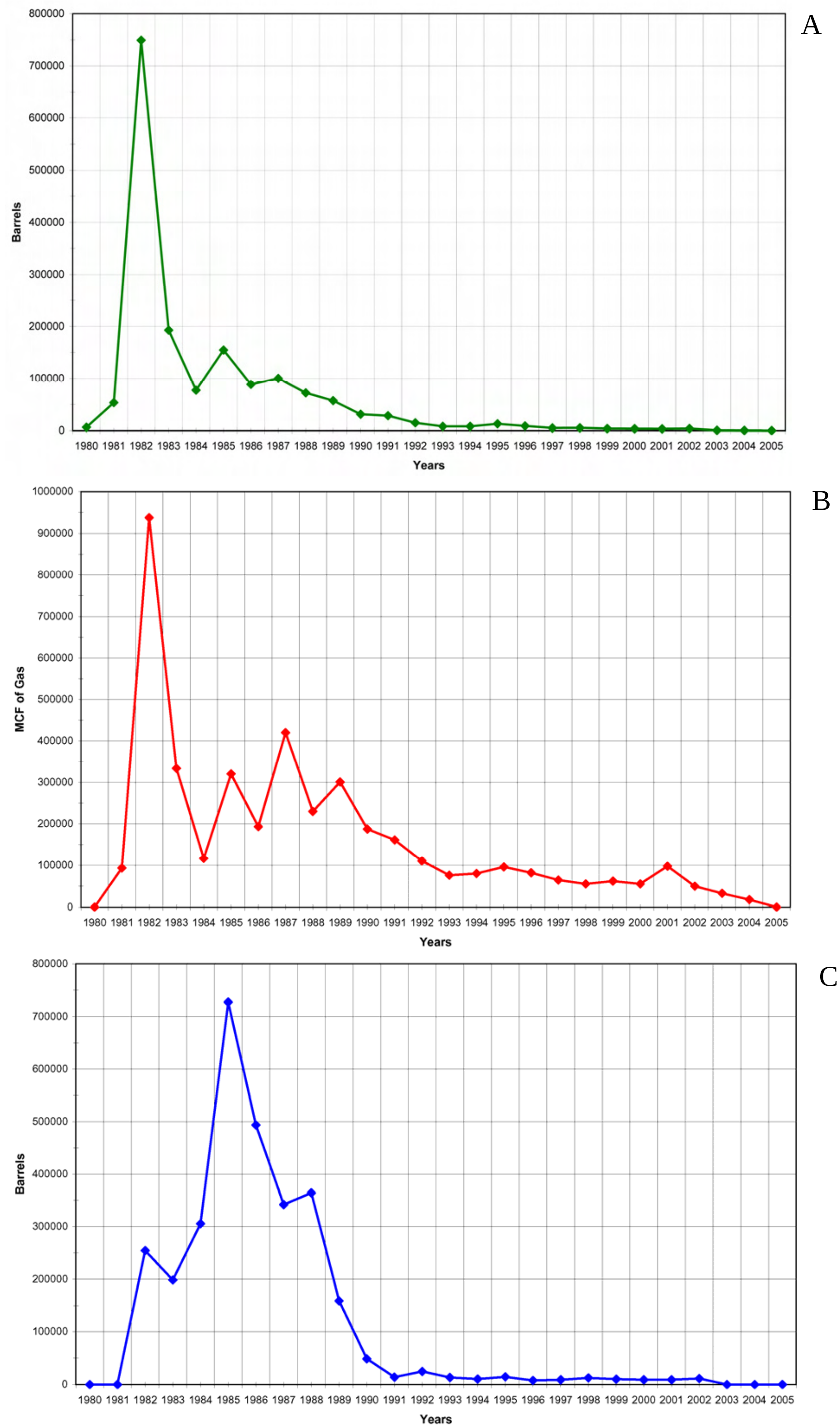

Figure 9-8. Historical oil (A), gas (B), and water (C) production for Bug field through 2005 (Utah Division of Oil, Gas and Mining, 2006).

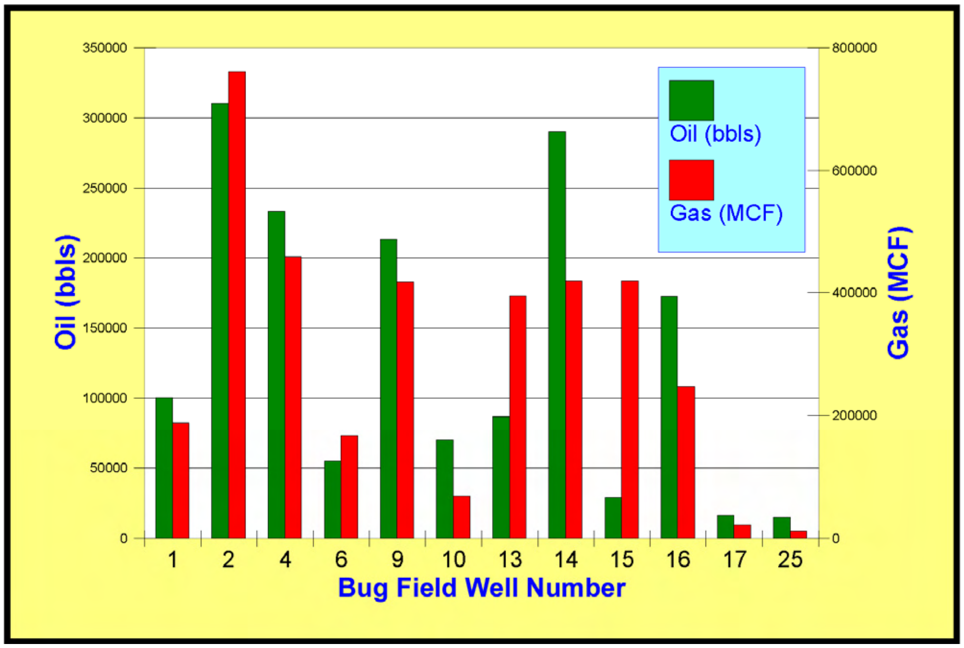

Figure 9-9. Cumulative production of oil and gas (as of January 1, 2006) from lower Desert Creek producing wells in Bug field (Utah Division of Oil, Gas and Mining, 2006).

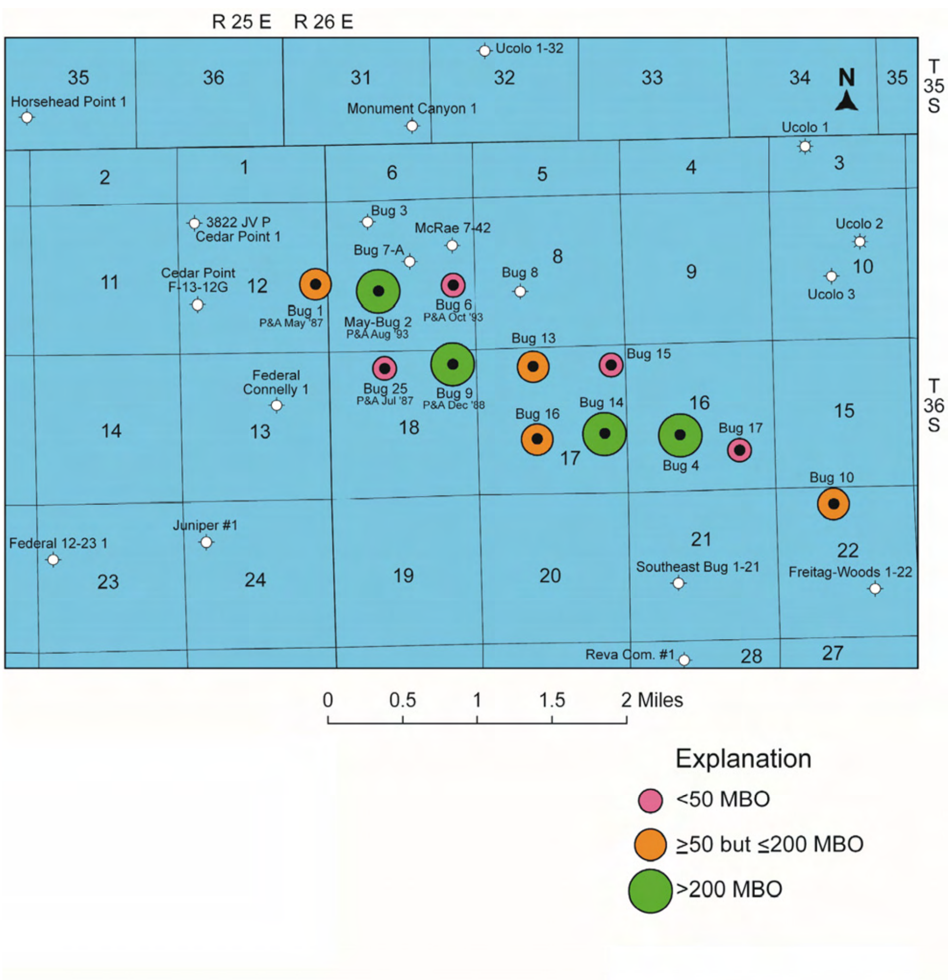

Figure 9-10. Bubble map of cumulative production (as of January 1, 2006) of oil (in thousands of barrels (MBO) from lower Desert Creek producing wells in Bug field (Utah Division of Oil, Gas and Mining, 2006).

CHAPTER X
THREE-DIMENSIONAL MODELING AND RESERVE CALCULATIONS: CHEROKEE AND BUG CASE-STUDY FIELDS

Thomas C. Chidsey, Jr., and Sharon Wakefield,
Utah Geological Survey;
and
David E. Eby, Eby Petrography & Consulting, Inc.

Introduction

Three-dimensional geologic models were created and reserves calculated for Cherokee and Bug fields (figure 1-3) (**Deliverable 2.2.1 – Three-Dimensional Geologic Models and Reserve Calculations: Cherokee and Bug Fields, San Juan County, Utah**). These models were used to identify and rank reservoir units containing significant amounts of remaining undrained oil best suited for horizontal drilling. The results were used to develop strategies for conducting horizontal drilling programs in Cherokee and Bug fields (described in Chapter 11) and elsewhere in the Paradox Basin.

Methodology

The 3-D models were created using Environmental Systems Research Institute, Inc. (ESRI) ArcView® 3D Analyst software. Structure, isochore, and other reservoir property contour maps (see Chapter 3 and **Deliverable 1.41 and 1.4.2 – Cross Sections and Field Maps: Cherokee and Bug Fields, San Juan County, Utah**) were digitized using AutoCad®, then brought into ArcView®. These AutoCad® files were first converted to shape files and then to grids. Next, Triangulated Irregular Network (TIN) files were created. A TIN is a set of contiguous, non-overlapping triangles used to represent a surface. Attribute and geometry information were stored for the points, lines, and faces that comprise each triangle. This information was used for display, query, and analysis purposes. A height value was recorded for each triangle node. Heights between nodes were also interpolated, thus allowing for the definition of a continuous surface. TINs can accommodate irregularly distributed, as well as selective data sets. This made it possible to represent a complex and irregular surface with a small data set (ESRI, 1998).

The TIN was imported into a 3D Analyst scene (called a viewer) and a projection was set selected from a specific projection or coordinate system from one of the following categories: Projections of the World, Projections of a Hemisphere, Projections of the United States, State Plane – 1927, State Plane – 1983, Universal Transverse Mercator (UTM), or National Grids. Once the map projections or coordinate system categories are selected, ArcView® displays the parameters that it uses in the projection, such as the Ellipsoid, Central Meridian, Reference Latitude and Standard Parallels. If no projection is set, TIN themes are displayed using the local coordinates found in the data set. Also brought into the scene was a feature theme for the well locations based on their UTM coordinates. Feature themes and TIN themes had to be in the same coordinate system to display them together without a projection. To set a projection, feature themes had to be in decimal degrees and TIN themes had to be in the projection set for them (ESRI, 1998).

The scene's 3-D properties were set to control certain aspects of scene display such as sun azimuth (the compass direction of the sun), sun altitude (the height of the sun), and a vertical exaggeration factor. The vertical exaggeration factor is a multiplier used to increase or decrease the vertical dimension of data displayed in the scene's 3-D viewer (ESRI, 1998).

After the viewer scene was projected, each theme property was set. Setting the theme properties allowed us to define height, extrusion, shading, navigation simplification, and transparency properties individually. Each TIN theme had its own legend display in the view's Table of Contents. A TIN theme's legend specified what triangle points, lines, or faces were drawn and what colors were used to draw them. This controlled how the TIN theme was displayed in the view (ESRI, 1998).

The scene was shifted, rotated, panned, or zoomed to any angle without disturbing the way each theme was lined up. After all the angles were set for best viewing position, they were exported as a joint photographic expert group (.jpg) or bitmap (.bmp) image file. This image file was used to create a layout. A layout is a map used to display views and is used to prepare graphics for output from ArcView® (ESRI, 1998). Layouts were printed and exported to a number of formats. The annotations (labels, descriptions, titles, and so forth) were added at this time.

Modeling Interpretation

Cherokee Field

The relative locations of Cherokee field wells used to produce reservoir structure and isochore maps are shown on figure 10-1. The 3-D diagrams with structural contours on top of the upper and lower Ismay zone (figure 10-2), the upper Ismay clean carbonate (figure 10-3), and the Gothic shale (figure 10-4A) show the same general southwest-dipping structural nose upon which the carbonate buildup developed. This structure ends abruptly, suggesting the possible presence of a northwest-southeast-trending normal fault. Intense, late-stage microporosity development along hydrothermal solution fronts in the reservoir rock likely migrated from nearby, unknown fracture and fault zones (see **Deliverable 1.2.1A – Thin Section Descriptions: Cherokee and Bug Fields, San Juan County, Utah**).

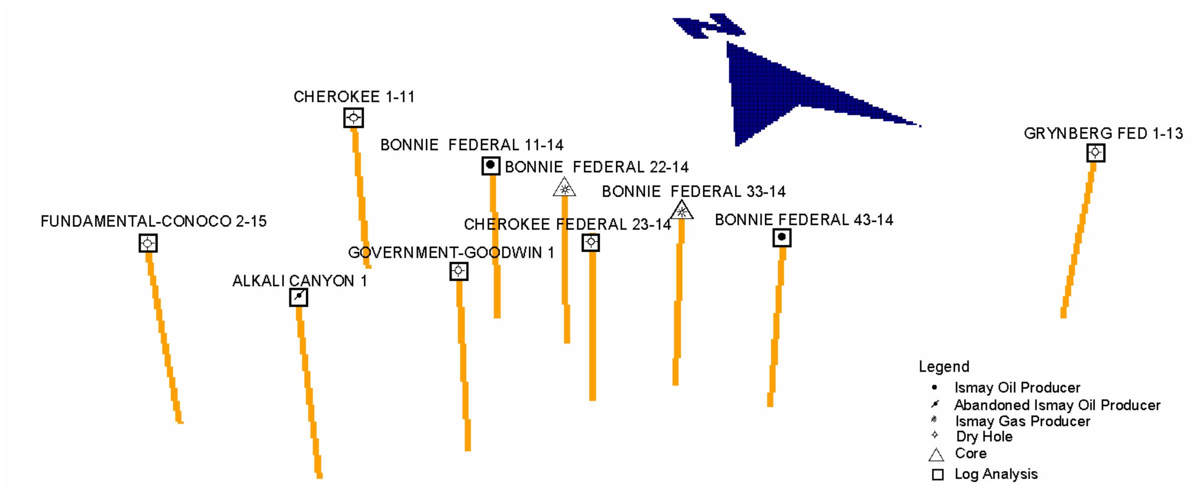

Figure 10-1. Relative locations and names of wells in the Cherokee field area, San Juan County, Utah.

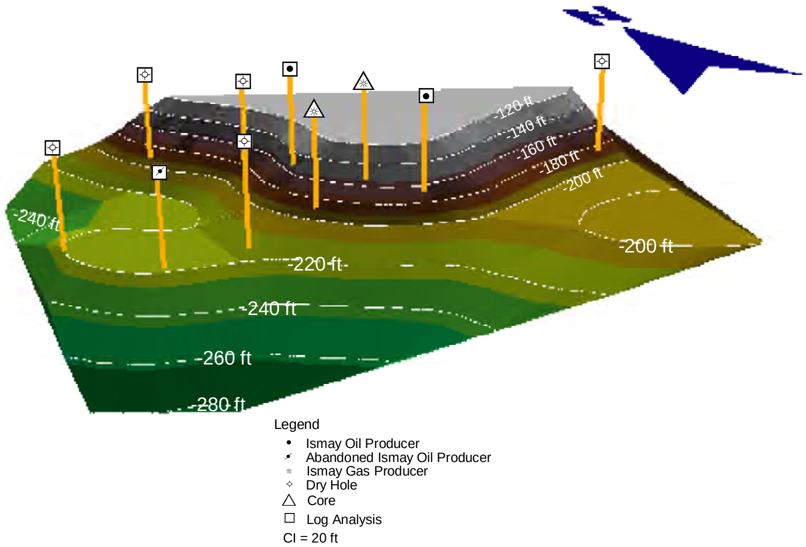

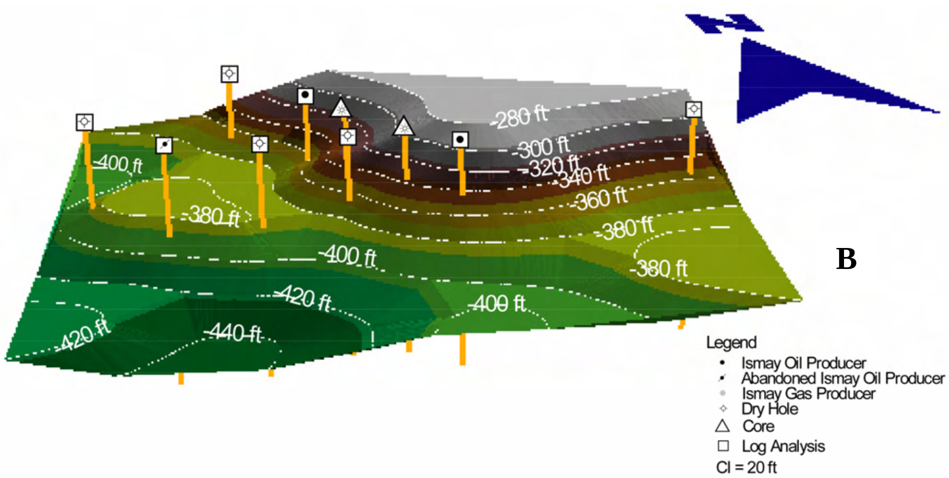

Figure 10-2. Three-dimensional models, Cherokee field. (A) Structure contours on top of upper Ismay zone. (B) Structure contours on top of lower Ismay zone.

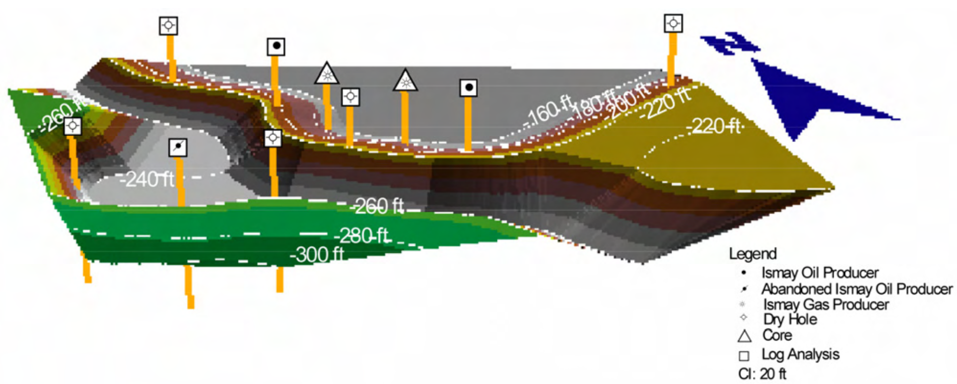

Figure 10-3. Three-dimensional model with structure contours on top of upper Ismay zone clean carbonate, Cherokee field.

The 3-D models of the thickness of the Gothic (figure 10-4B) and Hovenweap (figure 10-5) shales show a general west-northwest to east-southeast linear trend. Cherokee wells align along a subtle Gothic thick area (figure 10-4B), whereas the upper Ismay carbonate buildup may have developed on a better-defined thick in the shallower Hovenweap (figure 10-5).

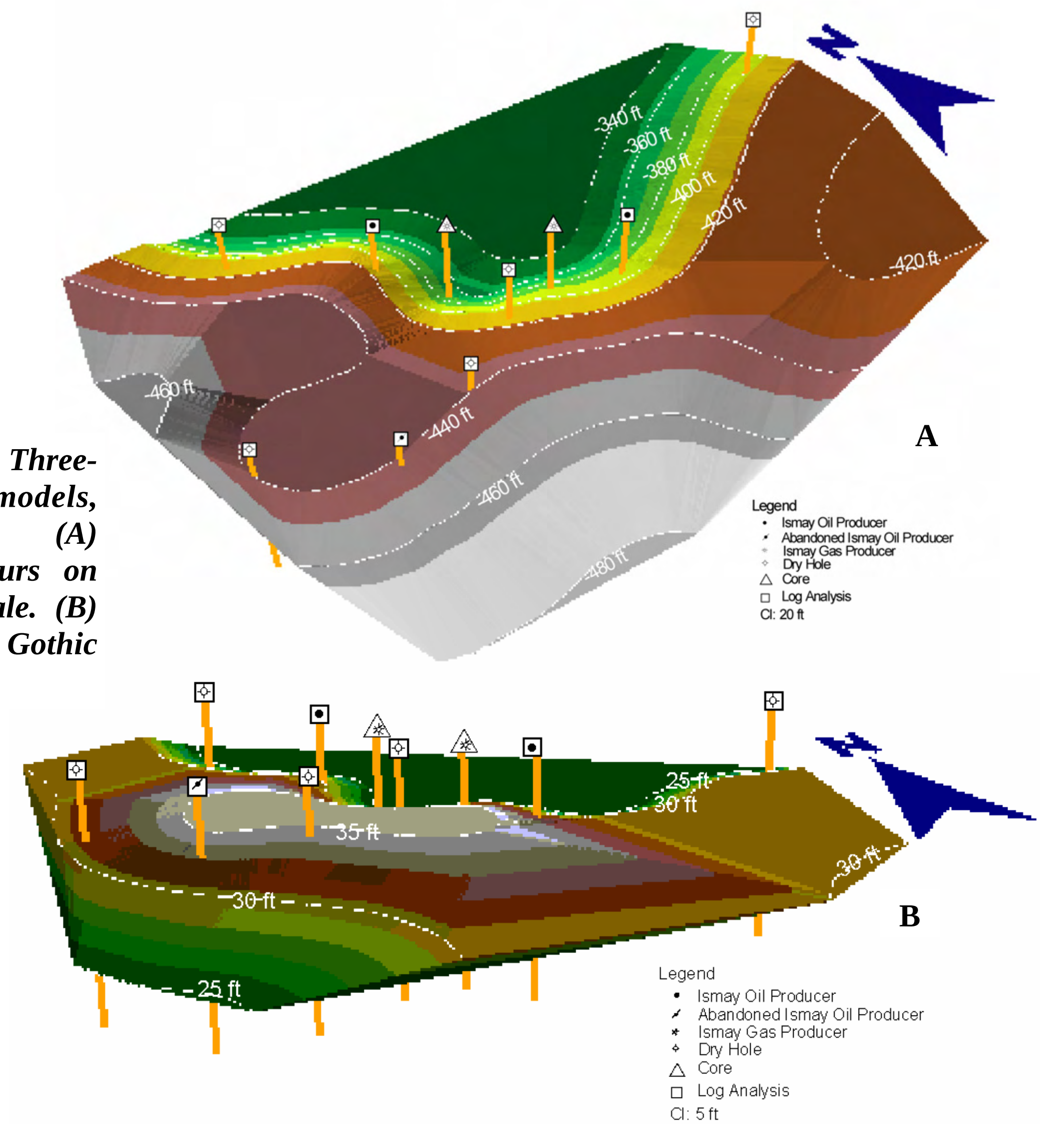

Figure 10-4. Three-dimensional models, Cherokee field. (A) Structure contours on top of Gothic shale. (B) Isochore of Gothic shale.

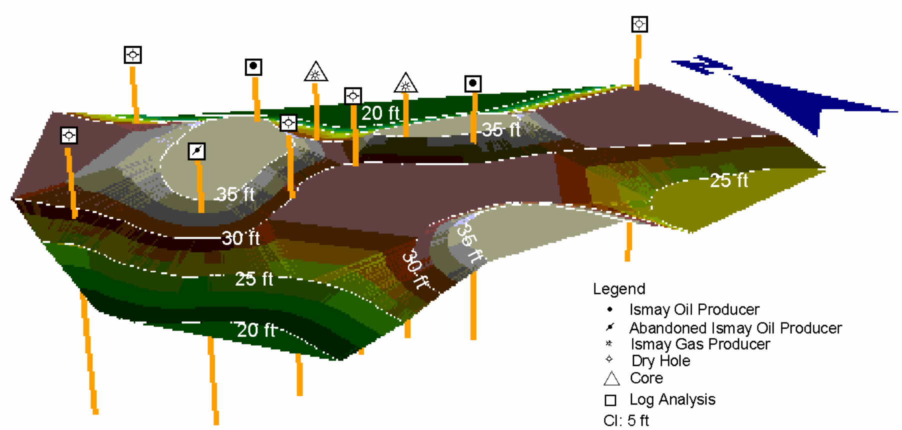

Figure 10-5. Three-dimensional model of the isochore of the Hovenweap shale, Ismay zone, Cherokee field.

There are two anhydrite units (1 and 2) in the upper Ismay zone (figure 10-6). They display a similar west-northwest to east-southeast linear trend as the Hovenweap and Gothic shales. Cherokee wells are located in the thickest part of the relatively thin upper Ismay anhydrite 1 (figure 10-6A). The upper Ismay anhydrite 2 varies in thickness from 80 feet (24 m) to 0 across the map area. This unit is 0 to 15 feet (0-5 m) thick in Cherokee wells, which lie along the edge of thick anhydrite, as seen in both isochore and inverted isochore diagrams (figures 10-6B and 10-6C). This situation is similar to the regional upper Ismay lithofacies pattern where intrashelf basins are the locations of thick anhydrite accumulations. Phylloid-algal buildups developed on inner shelf and tidal flats within curvilinear bands that rim the intrashelf basins (see Chapter II).

Three-dimensional models of the thickness of the entire Ismay zone (figure 10-7A), upper Ismay (figure 10-7B), lower Ismay (figure 10-7C), and upper Ismay clean carbonate (figure 10-8) also display the same general west-northwest to east-southeast trend punctuated by elongate to slightly equant thick areas. Cherokee field is located near thick areas shown on Ismay and upper Ismay 3-D diagrams. Surprisingly, the field is located adjacent to the thickest part of the upper Ismay clean carbonate (100 feet [30 m]), although the range from that thick area to the thinnest section in Cherokee wells is only 19 feet (6 m).

Five reservoir porosity units (figures 10-9 through 10-12), all having porosity greater than 6 percent, are present in the upper Ismay mound, separated by low-porosity/permeability barriers (mudstone and wackestone). These porosity units represent the phylloid-algal buildups composed primarily of bafflestone and grainstone that produce oil and gas in the field. Typical of the upper Ismay trend in the Blanding sub-basin, these units appear in 3-D diagrams as small, equant-shaped pods. The overall carbonate reservoir for Cherokee field is shown in a combined 3-D diagram on figure 10-11B, and the individual porosity units are shown vertically stacked in figure 10-12. Porosity unit 5 (figure 10-11A) is the largest and most likely the major production contributor, as well as holding the bulk of the remaining reserves. The 3-D thickness diagrams suggest all five porosity units have an untested northeastern area.

As expected, 3-D diagrams of the upper Ismay zone depicting net feet of porosity greater than 10 and 12 percent by log analysis (figure 10-13) show the same equant-shaped buildups as displayed by porosity units 1 through 5. The 12 percent porosity diagram shows a thickness pattern which is similar to, but smaller than the thickness pattern of porosity units 1 through 5 combined (figure 10-11B).

The upper Ismay zone's net-feet of limestone (figure 10-14A) and dolomite (figure 10-14B) were determined by log analysis. The extent of the 3-D diagrams for these two parameters is limited by the lack of neutron/density logs for older wells in the area. Characteristic of the Ismay zone in the Blanding sub-basin, limestone is the dominant lithology. However, there is an unusual amount of dolomite present. The 3-D thickness diagrams show a large buildup of limestone adjacent to (figure 10-14A), and dolomite within (figure 10-14B), Cherokee field. In both cases, a carbonate buildup continues northeast of the field wells.

Bug Field

The relative locations of Bug field wells used to produce reservoir structure and isochore maps are shown on figure 10-15. The 3-D diagram with structural contours on top of the Gothic shale (figure 10-16A) shows a general regional dip to the southwest and a subtle, elongate, northwest-southeast-trending anticline. The 3-D model of the thickness of the Gothic shale (figure 10-16B) shows a similar northwest-southeast trend. Bug producing wells align along, or adjacent to, a subtle Gothic thickness increase.

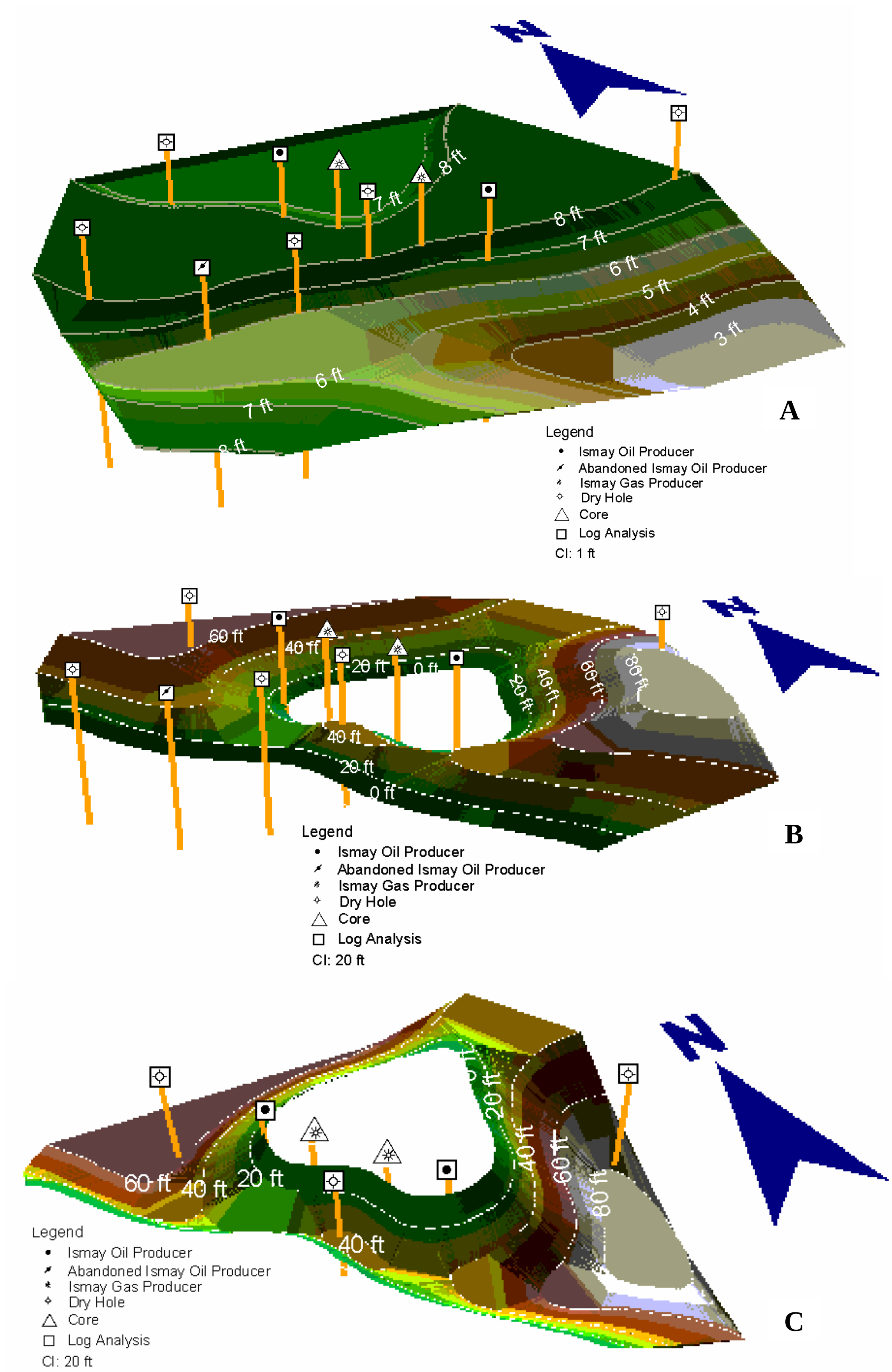

Figure 10-6. Three-dimensional models, Cherokee field. (A) Upper Ismay zone anhydrite 1 isochore. (B) Upper Ismay zone anhydrite 2 isochore. (C) Upper Ismay zone anhydrite 2 inverted isochore.

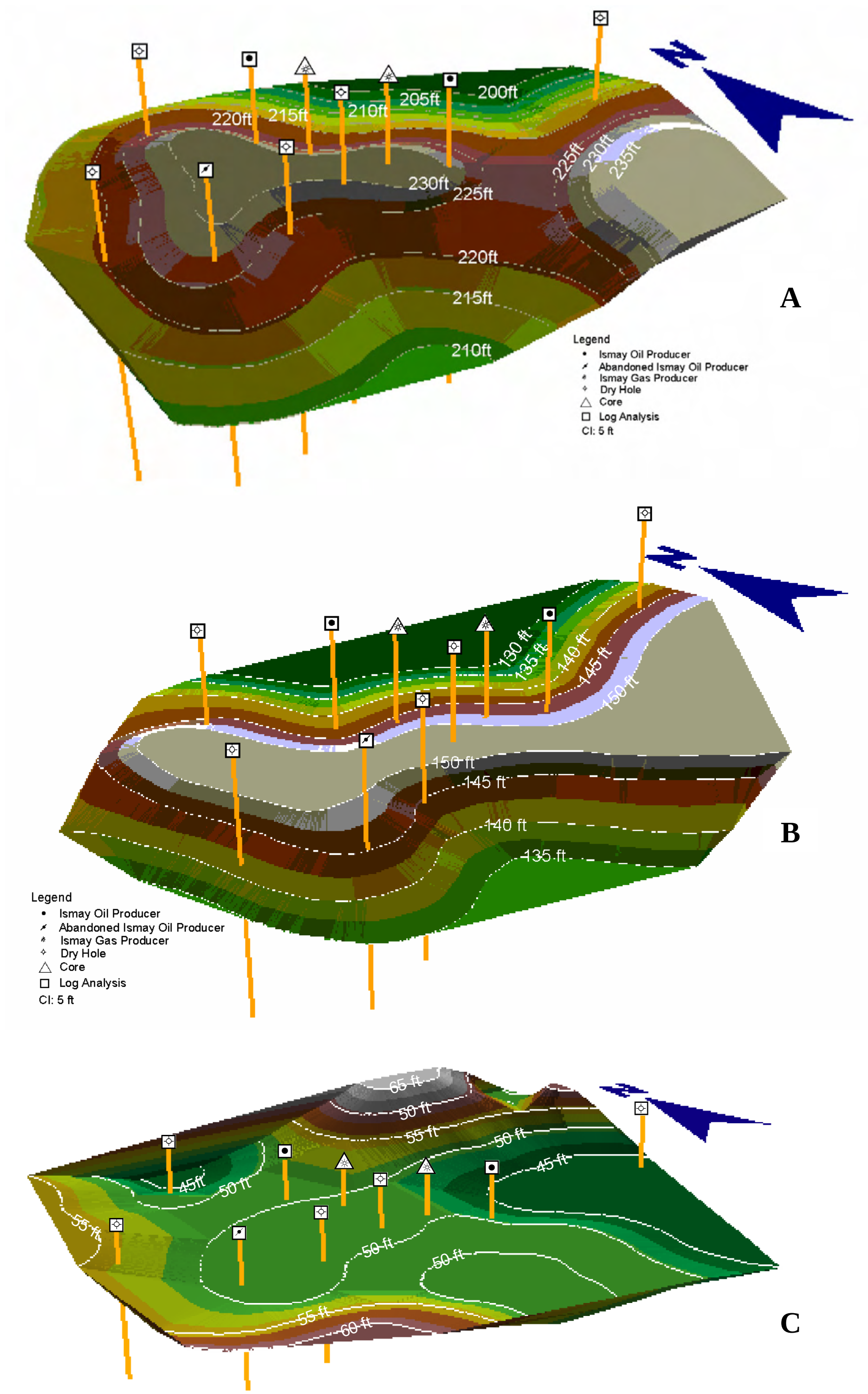

Figure 10-7. Three-dimensional models, Cherokee field. (A) Ismay zone isochore. (B) Upper Ismay zone isochore. (C) Lower Ismay zone isochore.

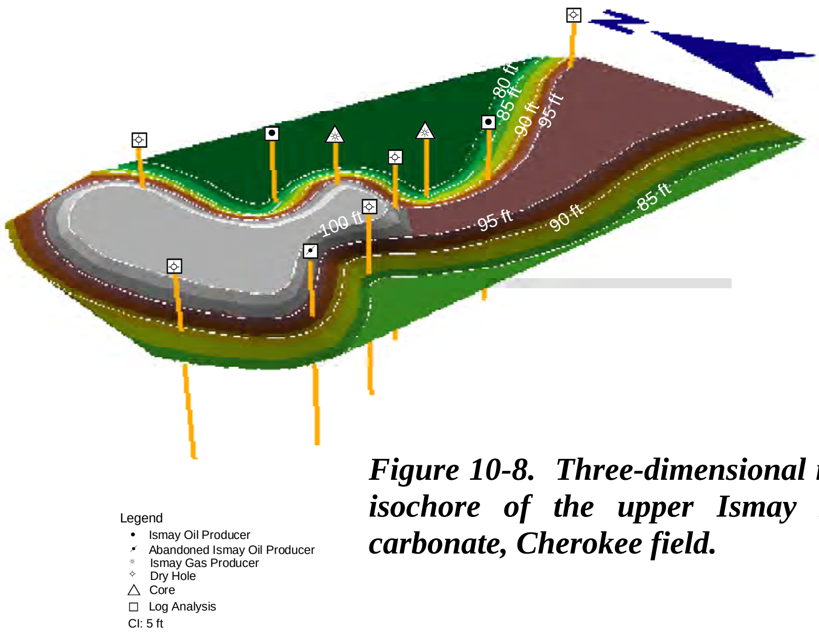

Figure 10-8. Three-dimensional model of the isochore of the upper Ismay zone, clean carbonate, Cherokee field.

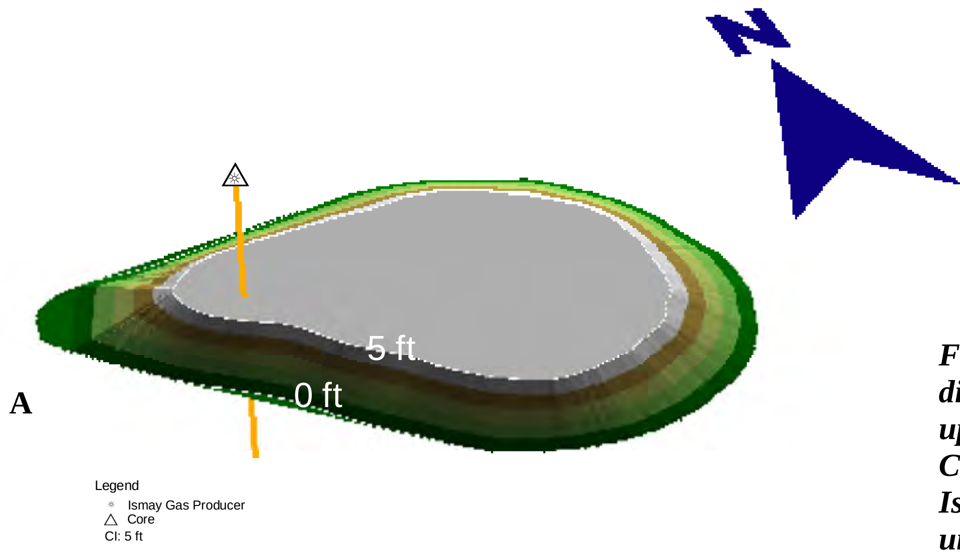

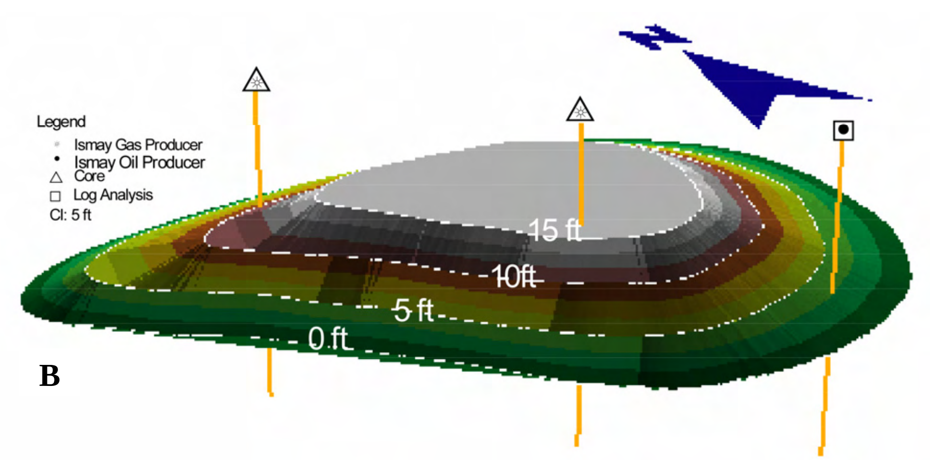

Figure 10-9. Three-dimensional models, upper Ismay zone, Cherokee field. (A) Isochore of porosity unit 1. (B) Isochore of porosity unit 2.

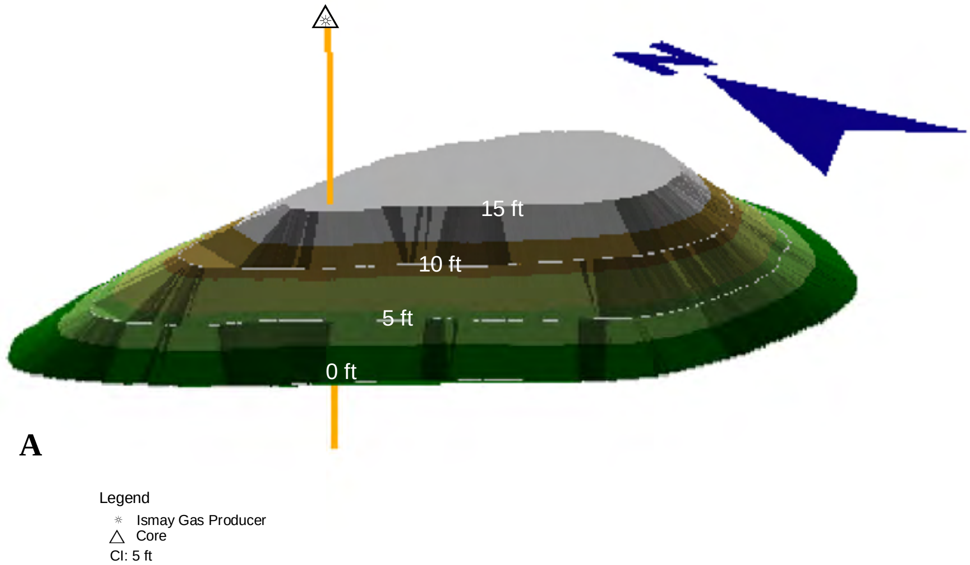

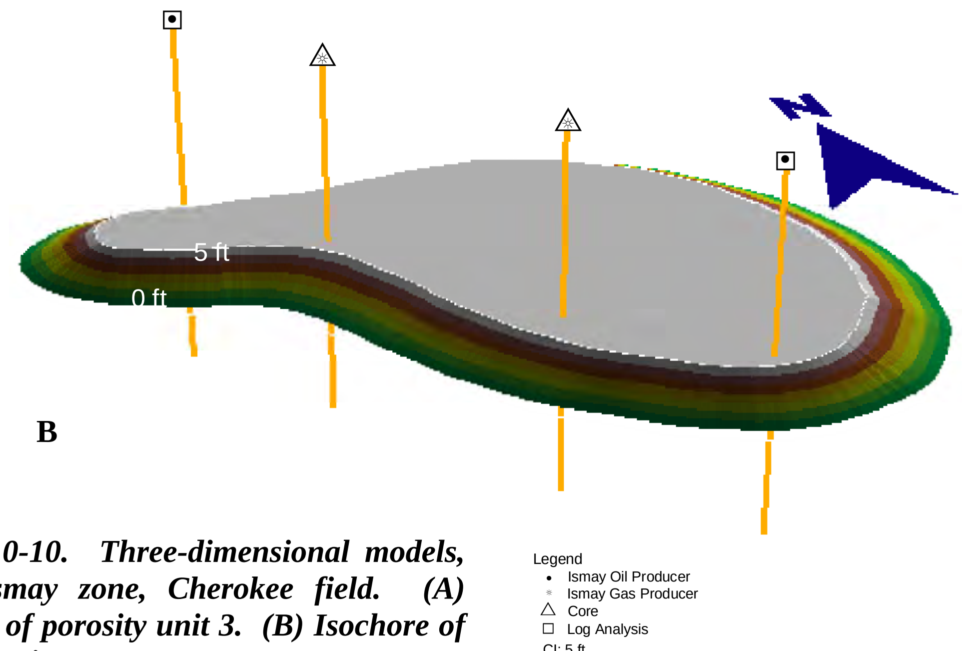

Figure 10-10. Three-dimensional models, upper Ismay zone, Cherokee field. (A) Isochore of porosity unit 3. (B) Isochore of porosity unit 4.

The 3-D diagrams with structural contours on top of the Desert Creek zone (figure 10-17A), lower Desert Creek mound (figure 10-17B), lower Desert Creek clean carbonate (figure 10-17C), and Chimney Rock shale (figure 10-17D) also each show a southwest regional dip. The top of the Desert Creek zone, which is just slightly deeper than the Gothic shale, displays the same subtle, elongate, northwest-southeast-trending anticline. The anticline broadens in the lower Desert Creek mound and clean carbonate, likely representing the buildup itself. At the Chimney Rock shale top, the anticline may depict the topographic high upon which the Bug carbonate buildup developed.

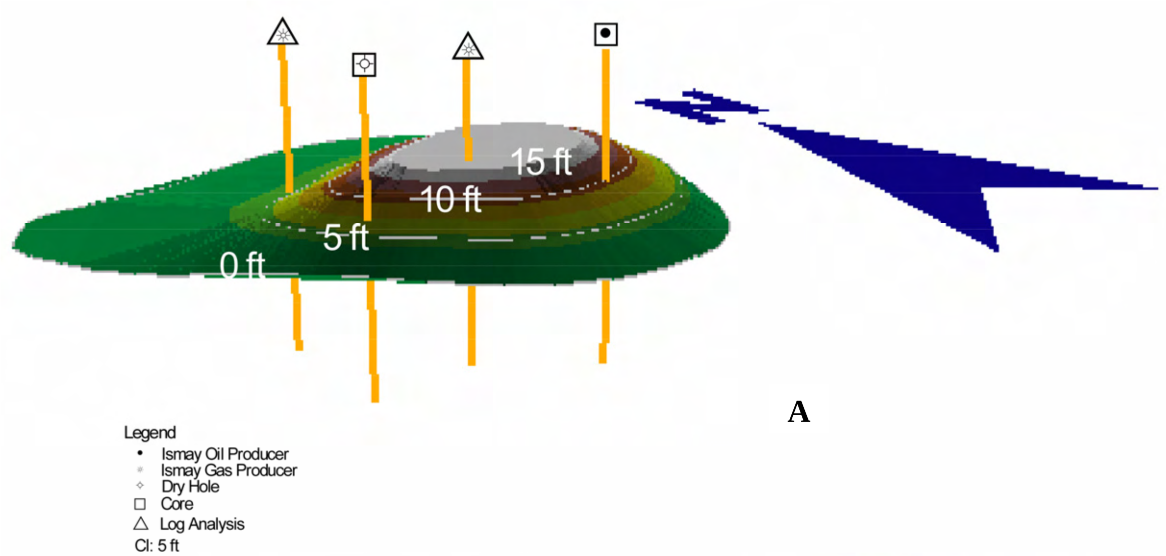

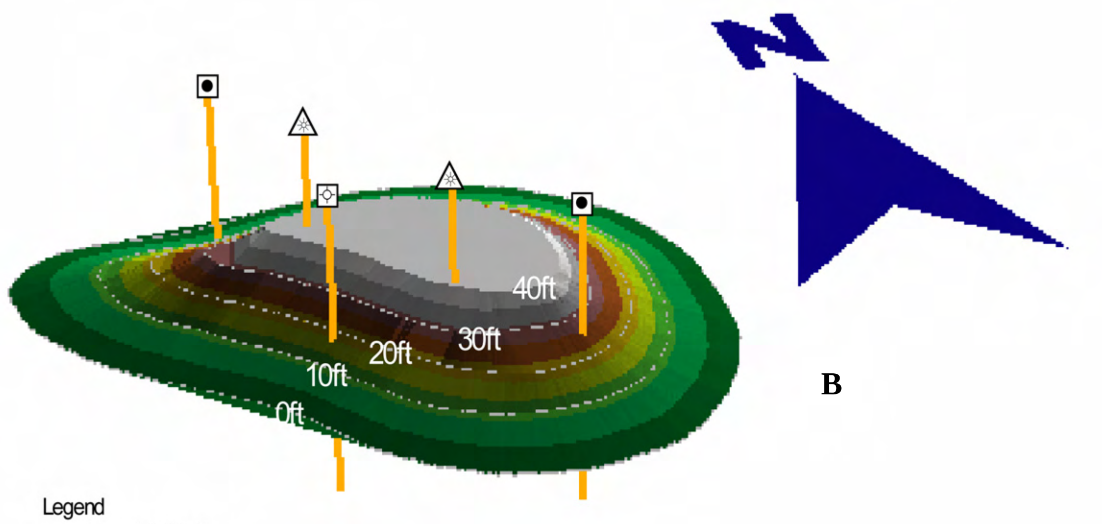

Figure 10-11. Three-dimensional models, upper Ismay zone, Cherokee field. (A) Isochore of porosity unit 5. (B) Isochore of porosity units 1 through 5 combined thickness.

Likewise, a 3-D model of the entire thickness of the Desert Creek zone (figure 10-18) also displays the same general northwest to southeast trend as does the structural diagram, with elongate thin and thick areas. Bug field is located adjacent to one of the thin areas (70 feet [21 m]), but is not situated entirely on a thick area. However, the Bug No. 6 well does contain the thickest section of Desert Creek in the mapped area at 138 feet (42 m).

There is one anhydrite unit in the lower Desert Creek zone (figure 10-19). It displays the general northwest-southeast linear trend corresponding to the trend of the Gothic shale and entire Desert Creek. The unit is a thin, widespread anhydrite of relatively uniform thickness that averages about 5 feet (1.5 m) over most of the area. Bug producing wells are located in a thicker part (up to 9 feet [3 m]) as seen in both isochore and inverted isochore diagrams (figures 10-19A and 10-19B), and the Southeast Bug 1-21 well contains an exceptionally thick section of anhydrite at 18 feet (6 m). Unlike the Ismay zone, there are no intrashelf basins that we have identified in the Desert Creek (see Chapter II).

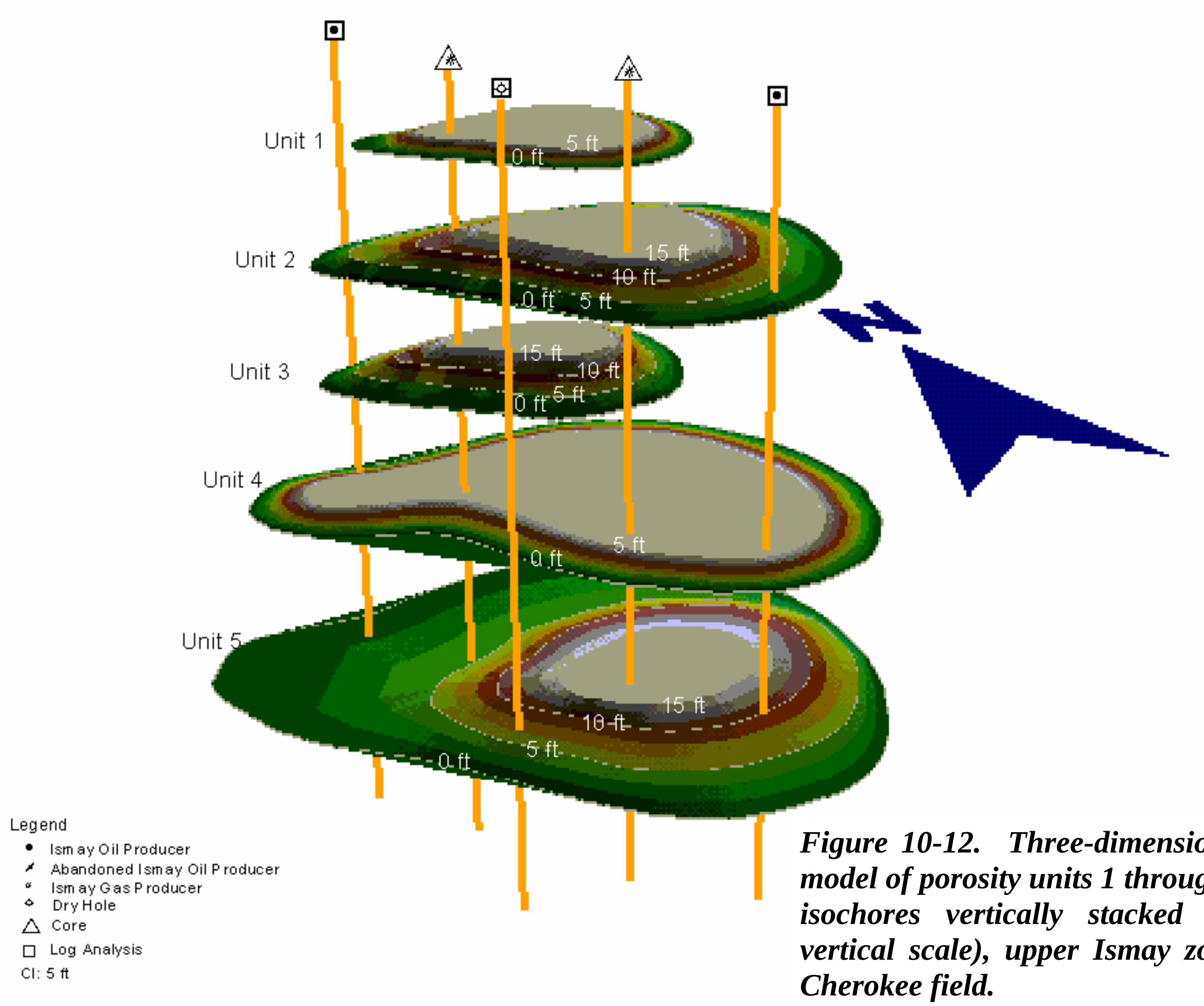

Figure 10-12. Three-dimensional model of porosity units 1 through 5 isochores vertically stacked (no vertical scale), upper Ismay zone, Cherokee field.

The 3-D models of the thickness of the lower Desert Creek clean carbonate (figure 10-20) and mound core (figure 10-21) display an elongate, northwest-southeast-trending carbonate buildup depicting the typical, nearshore, shoreline-linear lithofacies tracts of the Desert Creek zone in the northern Blanding sub-basin. Both diagrams appear similar as they represent nearly the same interval of the lower Desert Creek – the producing reservoir. The slightly thicker clean carbonate displays a small saddle between two subsidiary buildups, whereas the mound core is represented by one uniformly thick buildup.

The 3-D model of the thickness of the Chimney Rock shale (figure 10-22) shows a slight east-west trend. The Chimney Rock varies in thickness only slightly over the area, from 14 to 18 feet (5-6 m). Some Bug producing wells align along a subtle Chimney Rock thickness increase, but in general no particular pattern can be discerned.

The 3-D diagrams of the lower Desert Creek clean carbonate with the net feet of log-derived porosity greater than 10 and 12 percent (determined by geophysical log analysis; figures 10-23A and 10-23B) show an elongate reservoir buildup with two subsidiary thick areas separated by a slightly thinner saddle that may represent an intermound trough. The northern thick area trends generally east-west while the southern one trends northwest-southeast. At 12 percent porosity, as expected, the buildup is thinner and smaller in overall areal extent, but still

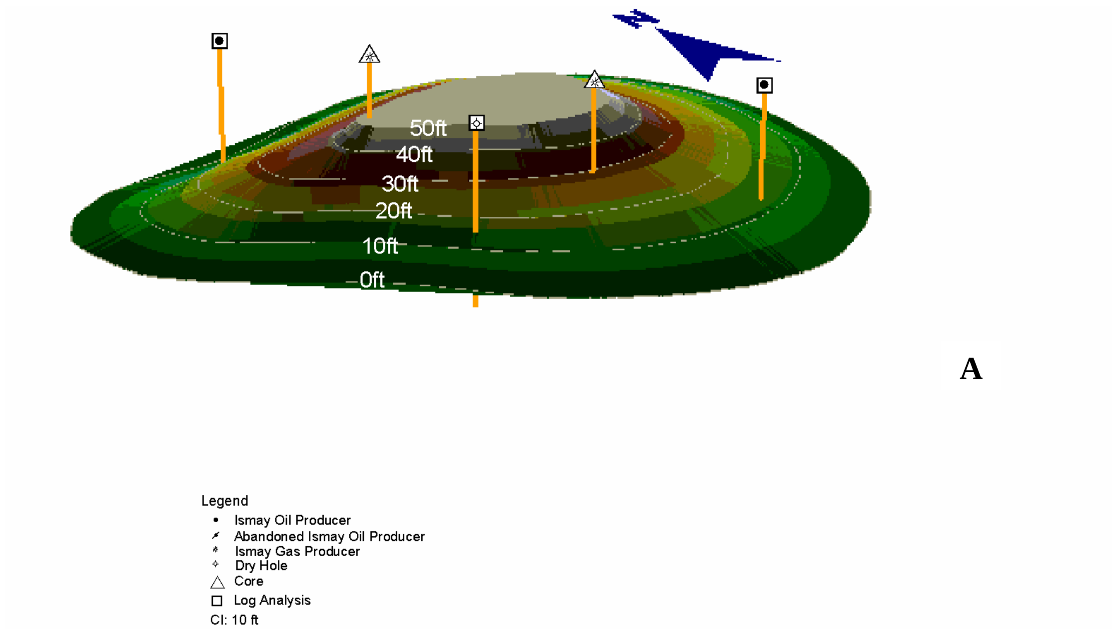

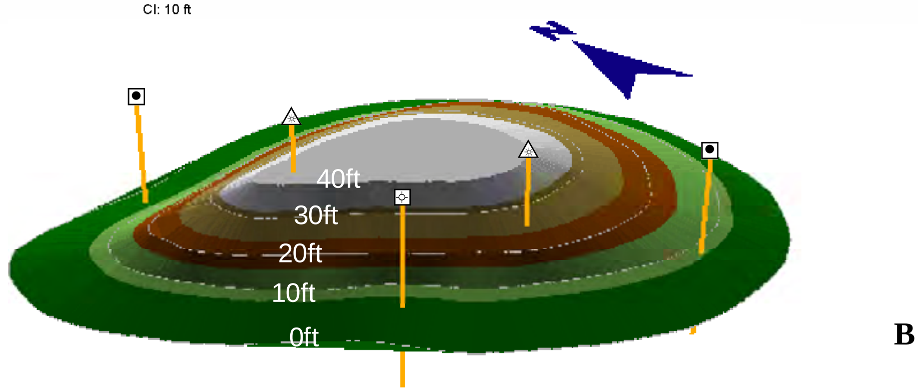

Figure 10-13. Three-dimensional models, upper Ismay zone net feet of porosity, as determined by geophysical log analysis, for greater than 10 percent porosity (A), and greater than 12 percent porosity (B), Cherokee field.

mimics the general characteristics of the buildup at 10 percent porosity. In both diagrams the porosity pinches out along the northeast flank of the buildup, which when combined with a coincident anticline in the top of the lower Desert Creek zone clean carbonate (figure 10-17) provides a combination stratigraphic/structural trap. The 3-D diagrams of the lower Desert Creek clean carbonate with the net feet of core-derived porosity greater than 10 and 12 percent (determined by core analysis; figures 10-24A and 10-24B) also show an elongate reservoir buildup, but one that is narrower and thinner than its counterpart based on geophysical log analysis. No subsidiary buildups or saddles are present; the top of the buildup is flat. The buildup trends west-northwest to east-southeast. In both diagrams (figures 10-24A and 10-24B) the entire carbonate buildup is bounded by a porosity pinchout and represents a stratigraphic trap.

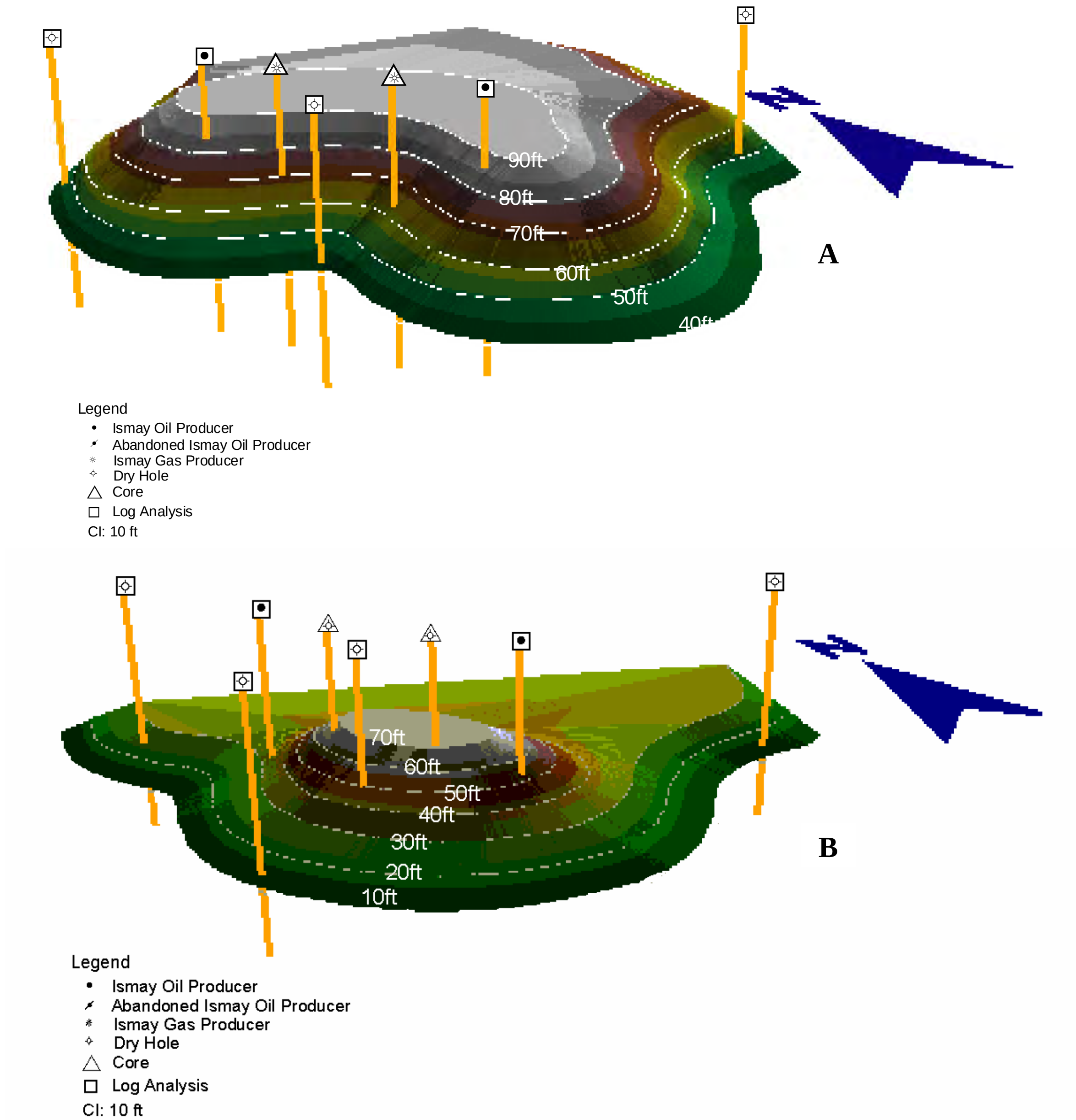

Figure 10-14. Three-dimensional models, upper Ismay zone net feet of limestone (A) and dolomite (B) as determined by geophysical log analysis, Cherokee field.

The 3-D models of the lower Desert Creek clean carbonate with the net feet of core-derived permeability greater than 2 mD (figure 10-25A), greater than 10 mD (figure 10-25B), and greater than 50 mD (figure 10-25C), portray a buildup very similar to that constructed for net feet of porosity greater than 10 and 12 percent by core analysis (figures 10-24A and 10-24B). In both diagrams the entire carbonate buildup is defined by a permeability pinchout and trends west-northwest to east-southeast. At permeability greater than 2 mD (figure 10-25A), there is a subsidiary buildup in the northwestern part of the reservoir. At permeability greater than 10 and 50 mD (figures 10-25B and 10-25C), the thinner buildups depict two subsidiary thick areas separated by an even thinner saddle.

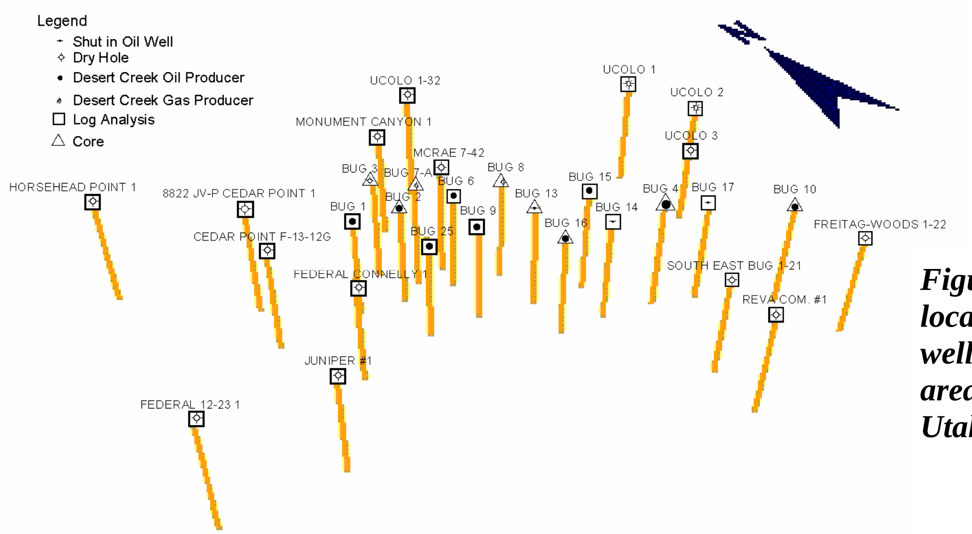

Figure 10-15. Relative locations and names of wells in the Bug field area, San Juan County, Utah.

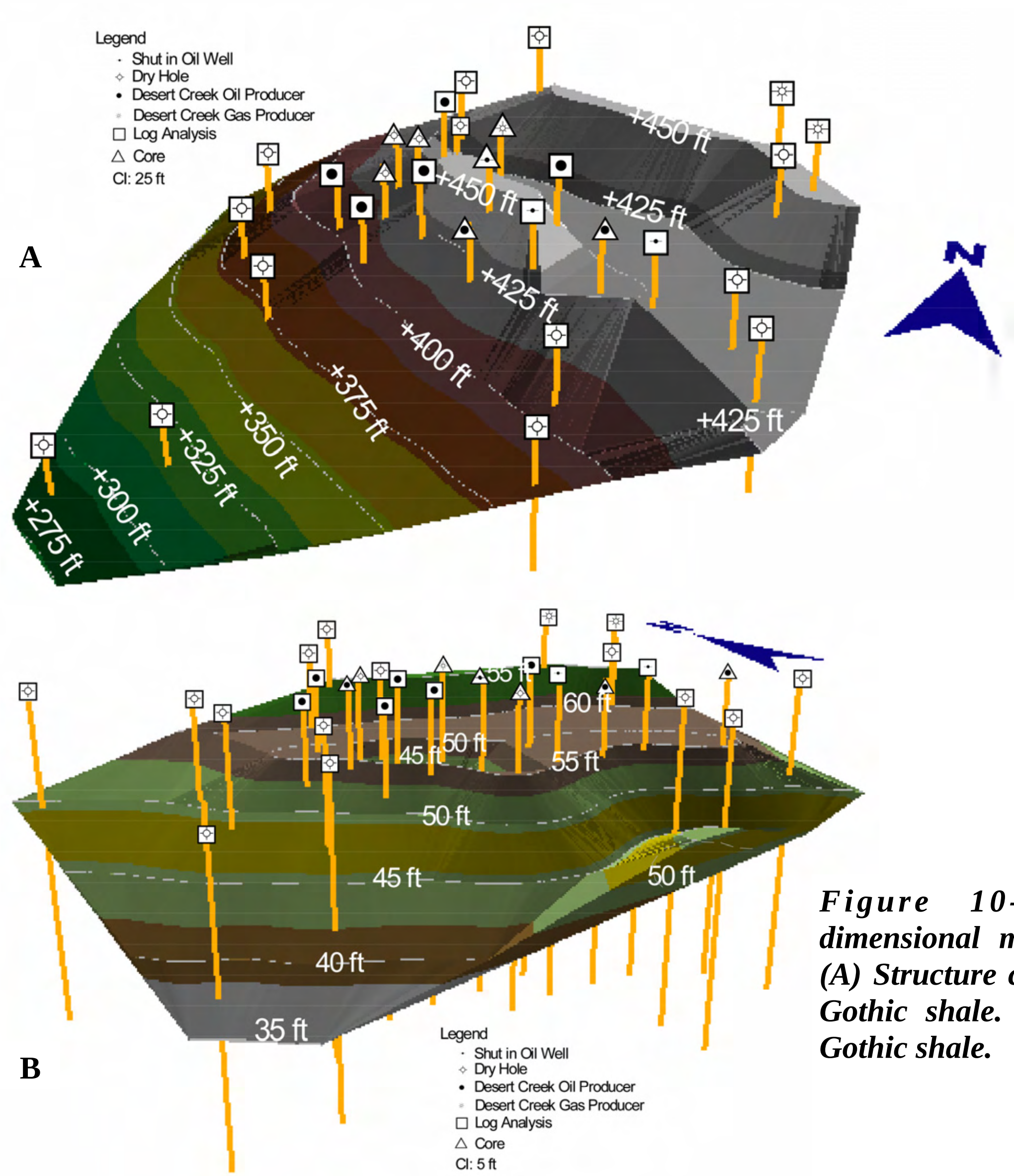

Figure 10-16. Three-dimensional models, Bug field. (A) Structure contours on top of Gothic shale. (B) Isochore of Gothic shale.

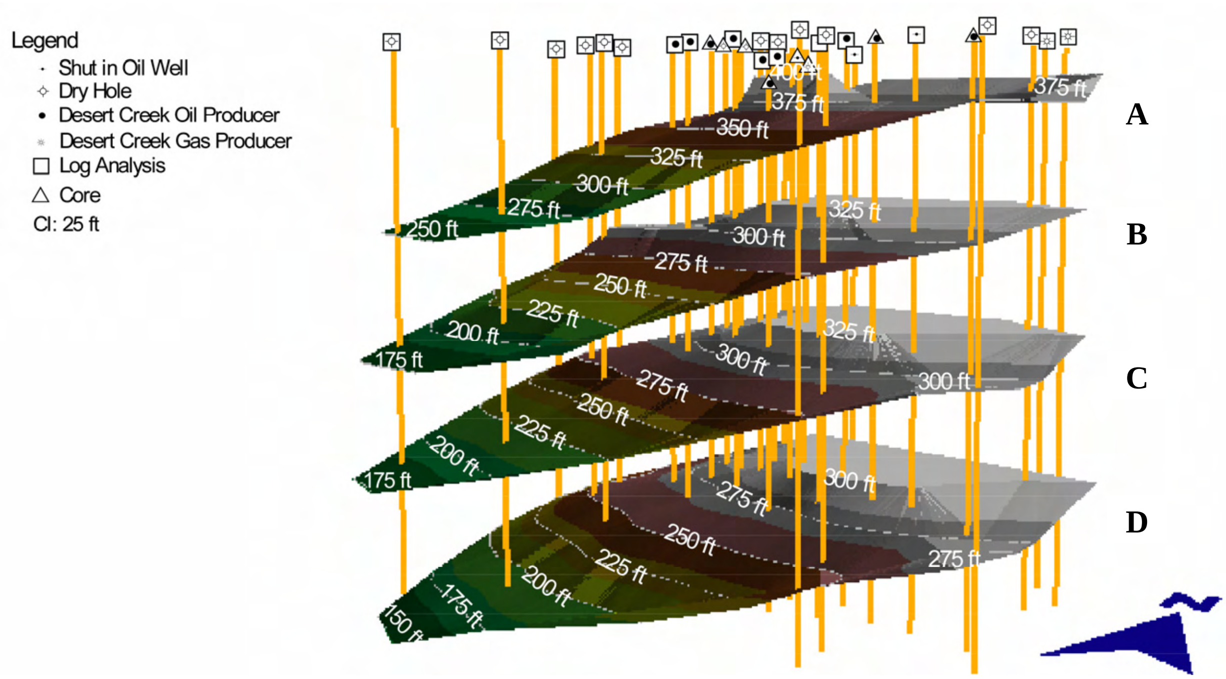

Figure 10-17. Three-dimensional models vertically stacked (no scale) with structural contours on tops of the Desert Creek zone (A), lower Desert Creek mound (B), lower Desert Creek clean carbonate (C), and Chimney Rock shale (D), Bug field.

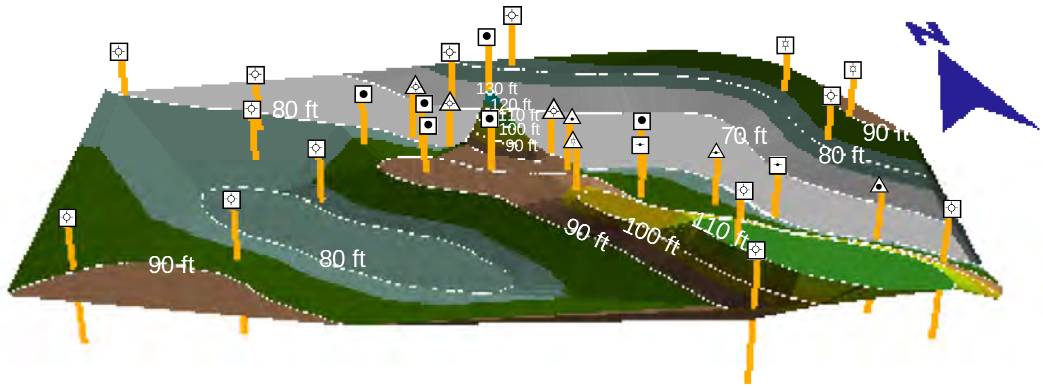

Legend
- Shut in Oil Well
- Dry Hole
- Desert Creek Oil Producer
- Desert Creek Gas Producer
- Log Analysis
- Core

CI: 10 ft

Figure 10-18. Three-dimensional model of the isochore of the Desert Creek zone, Bug field.

Lower Desert Creek clean carbonate with net feet of dolomite (figure 10-26) was determined by core analysis. The extent of the 3-D diagram is limited due to the lack of available cores in the area. Characteristic of the Desert Creek zone in the Blanding sub-basin, dolomite is the dominant lithology. The 3-D thickness diagram shows a large, northwest-southeast-trending buildup of dolomite within Bug field (figure 10-26). Not surprisingly, the buildup is divided into two subsidiary 30-foot- (10 m) thick areas separated by a saddle 20 feet (7 m) thick.

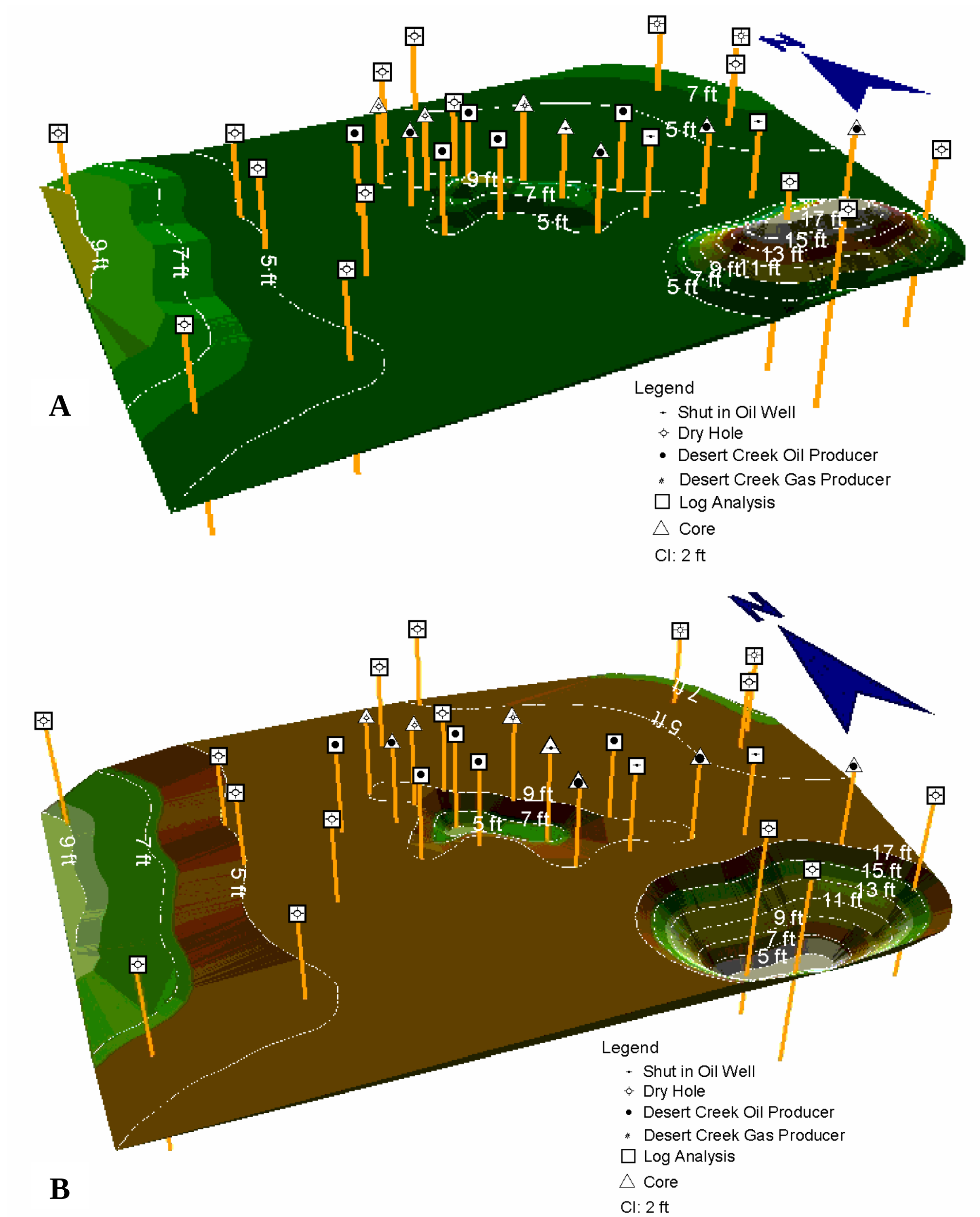

Figure 10-19. Three-dimensional models, Bug field. Lower Desert Creek zone anhydrite isochore (A) and inverted isochore (B).

Reserve Calculations

ArcView® was also used to calculate reservoir surface areas and volumes. Surface areas were measured along the slope of a surface, taking height into consideration. The surface area (feet squared) reported was that on the surface that falls above or below the specified height and was converted to acres. The volume operation calculates the cubic space between a TIN surface and the horizontal plane located at the specified height. Volumes (cubic feet) were determined either above or below the plane. In the case-study fields, reservoir volumes were determined above planes representing the oil/water or high proved water contacts. Volumes were first converted to acre-feet and then oil and gas recovery factors (in bbls and MCF per acre-foot, respectively) were applied to calculate reserves (tables 10-1 and 10-2).

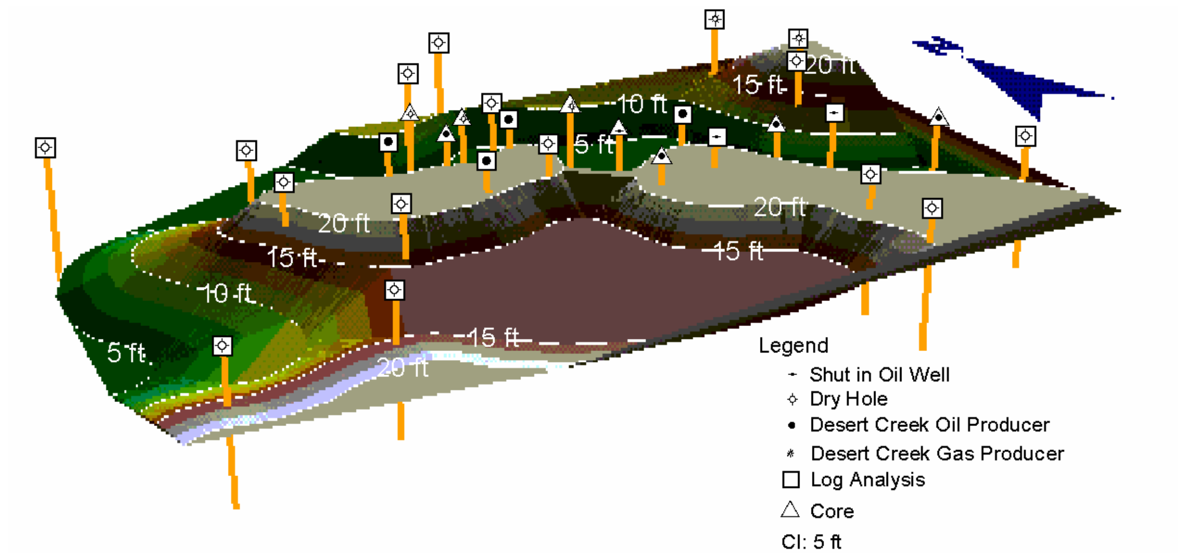

Figure 10-20. Three-dimensional model of the isochore of the lower Desert Creek zone clean carbonate, Bug field.

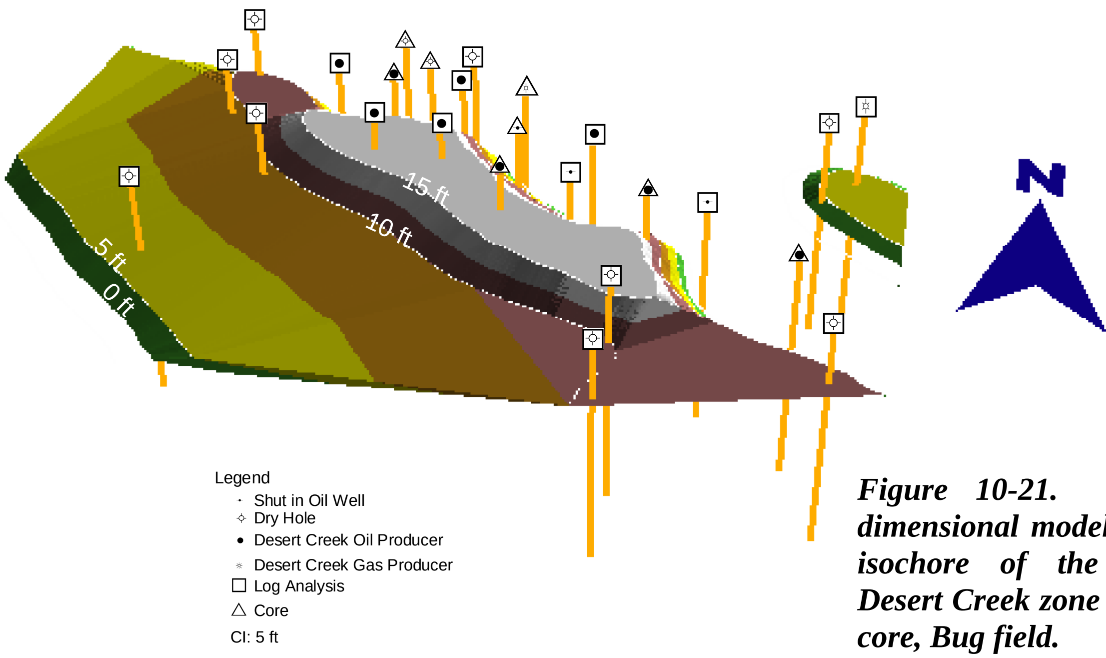

Figure 10-21. Three-dimensional model of the isochore of the lower Desert Creek zone mound core, Bug field.

Cherokee Field

Reservoir volumes (in acre-feet) (table 10-1) were calculated for porosity units 1 through 5 (figures 10-9 through 10-11) as derived from core and log analysis, and where the net feet of porosity was greater than 10 and 12 percent as derived from log analysis (figure 10-13). Recovery factors of 20 bbls of oil (3 m^3) and 380 thousand cubic feet of gas (MCFG) (11 MCMG) acre-foot, respectively, were derived from a Cherokee field study by Crawley-Stewart and Riley (1993). We applied these recovery factors to the various upper Ismay volumes to determine the primary oil and gas recovery volumes (table 10-1). Cumulative production as of September 1, 2006, was 183,945 bbls of oil (29,247 m^3), 3.7 (BCFG) (0.1 BCMG), and 3485

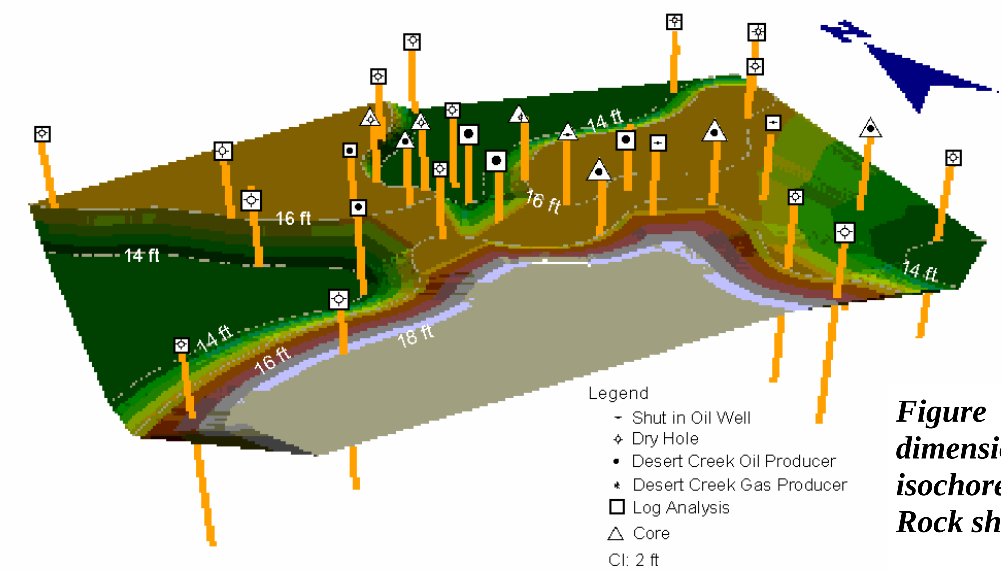

Figure 10-22. Three-dimensional model of the isochore of the Chimney Rock shale, Bug field.

bbls of water (554 m^3) (Utah Division of Oil, Gas and Mining, 2007). No single porosity unit can account for the volume of hydrocarbons produced. Therefore, all five or some combination of two or more porosity units are contributing, with porosity unit 5 having the largest volume followed by porosity unit 4, 2, 3, and 1 in decreasing order of size (table 10-1). The total volume of porosity units 1 through 5 combined (figure 10-11B) is 17,522 acre-feet, and this volume was calculated to contain over 350,000 bbls of oil (55,000 m^3) and 6.6 BCFG (0.19 BCMG) primary recovery. Based on these calculations, the remaining recoverable oil and gas reserves are nearly 168,000 bbls of oil (26,700 m^3) and 3 BCFG (0.08 BCMG). Using a price of $30/bbl and $4/MCFG, the unrisked value of the remaining recoverable reserves is over $5 million and $11 million for oil and gas, respectively.

Extending the porosity cutoff down to porosity greater than 10 percent increases the combined volumes of porosity units 1 through 5 to 19,374 acre-feet, suggesting the presence of additional undrained zones (microporosity). This increase in reservoir volume amounts to an additional 37,000 bbls of oil (5900 m^3) and 0.7 BCFG (0.02 BCMG) that may be present in the upper Ismay zone in Cherokee field. However, our primary recovery volume for the net feet of porosity greater than 12 percent was less than the combined primary oil recovery volume of porosity units 1 through 5 as calculated earlier (table 10-1).

Bug Field

Reservoir volumes were calculated for the lower Desert Creek zone clean carbonate at Bug field (table 10-2). These include volumes for net feet of porosity greater than 10 percent both by geophysical log analysis (figure 30A) and by core analysis (figure 10-24A), and volumes for net feet of permeability greater than 2 mD and 10 mD from core analysis (figures 10-25A and 10-25B, respectively). Recovery factors of 41 bbls of oil (7 m^3) and 103 MCFG (3 MCMG) per acre-foot, respectively, were derived from Oline (1996). We applied these recovery factors to the various lower Desert Creek clean carbonate volumes to determine the primary oil and gas recovery volumes (table 10-2). Cumulative production as of September 1, 2006, was 1,623,802 bbls of oil (258,185 m^3) and 4.53 BCFG (0.13 BCMG) (Utah Division of Oil, Gas and Mining, 2007).

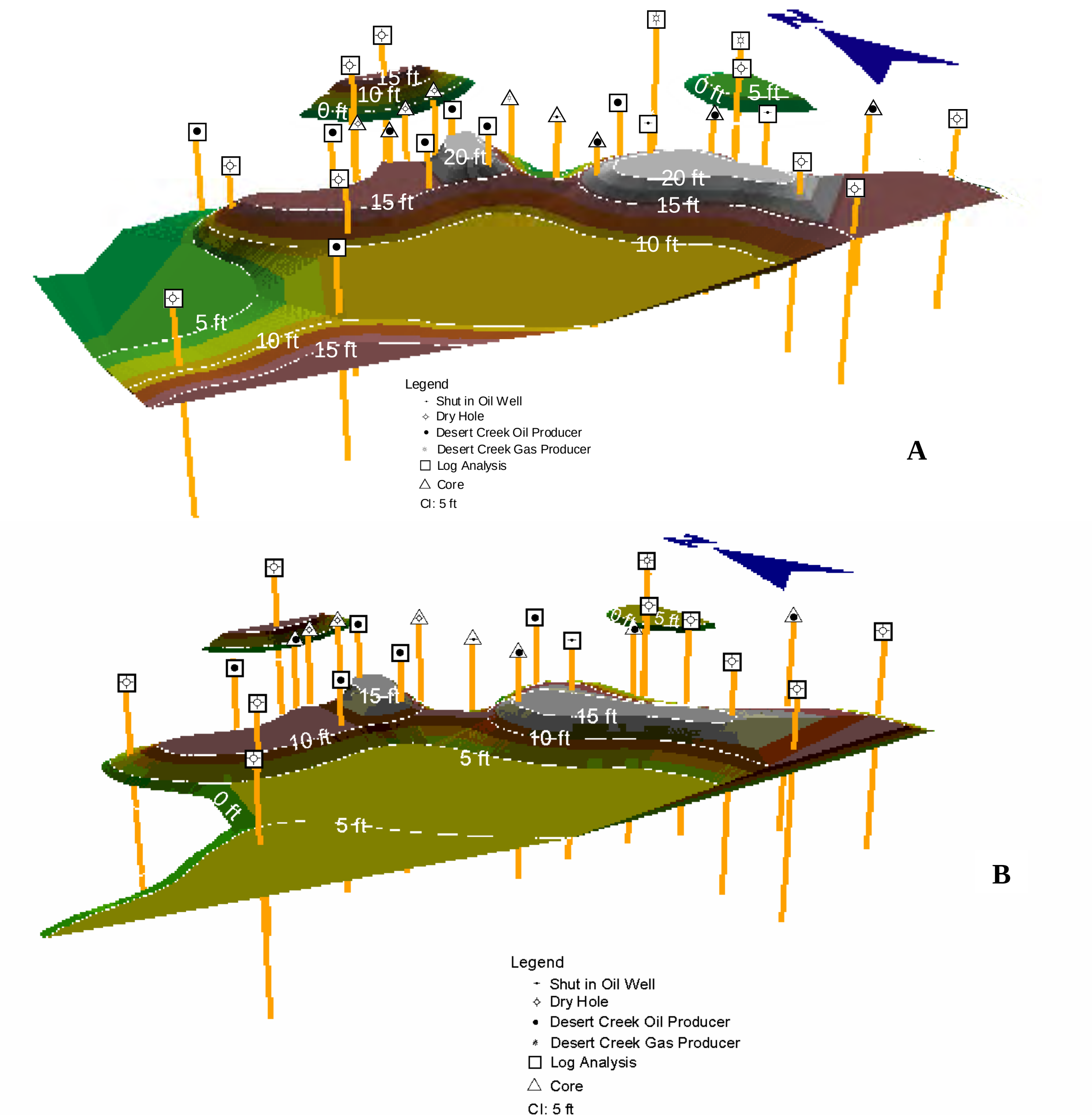

Figure 10-23. Three-dimensional models, lower Desert Creek zone clean carbonate net feet of porosity, as determined by geophysical log analysis, for greater than 10 percent porosity (A), and greater than 12 percent porosity (B), Bug field.

The volume calculated for net feet porosity greater than 10 percent by log analysis (99,057 acre-feet) is over twice that by core analysis (42,621 acre-feet). This may be a function of more data provided by well logs than by core, or that porosity determined from geophysical well logs is considerably optimistic showing ineffective (non-connected pores or "heart-break") porosity. This suggests the presence of additional undrained zones (micro-boxwork porosity). The bottom line is that from log analysis, the lower Desert Creek clean carbonate may contain recoverable oil and gas reserves of nearly 2,440,000 bbls of oil (388,000 m^3) and 5.7 BCFG (0.16 BCMG). Again, using prices of \$30/bbl and \$4/MCFG, the unrisked value of

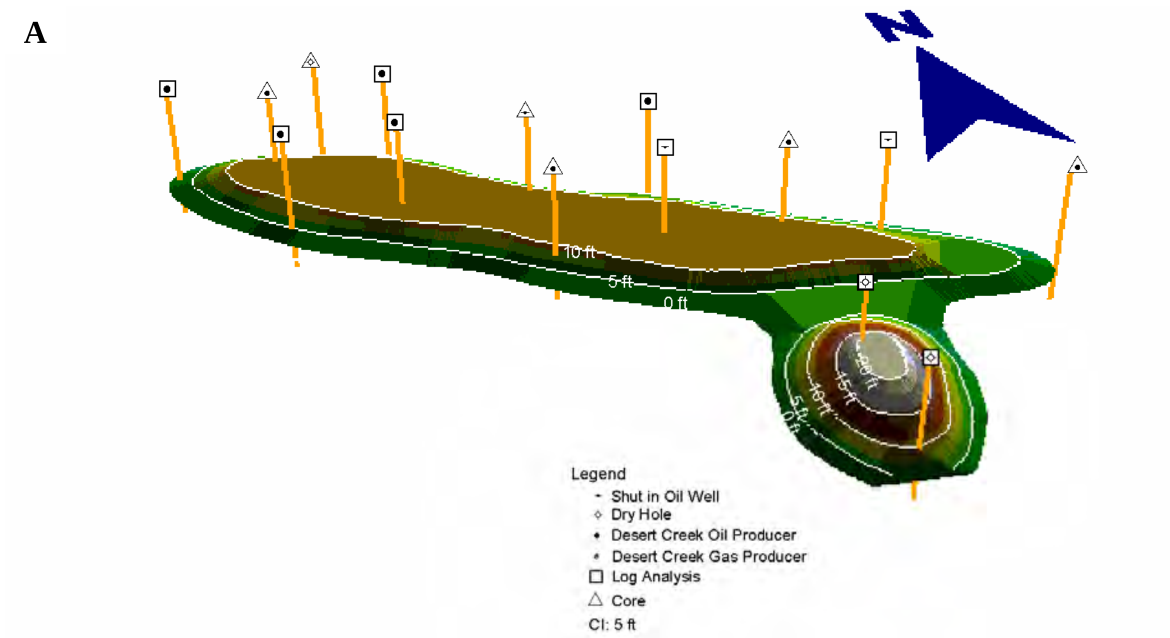

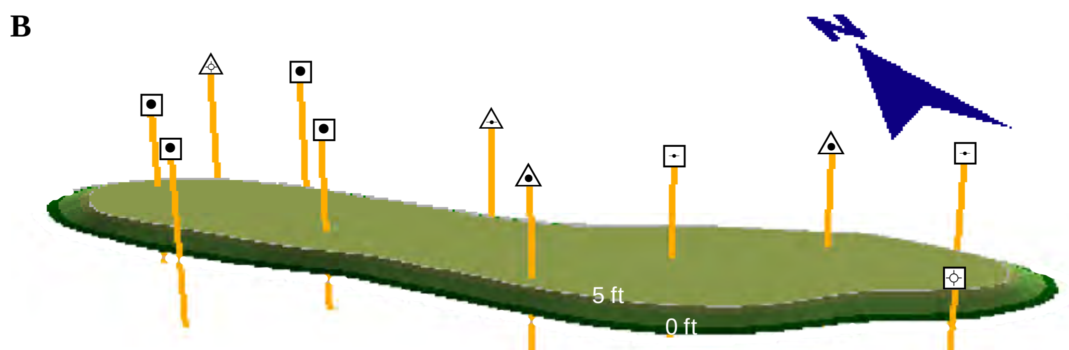

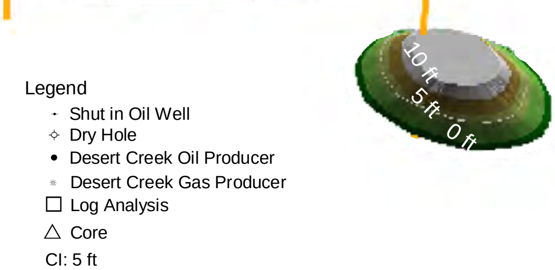

Figure 10-24. Three-dimensional models, lower Desert Creek zone clean carbonate net feet of porosity, as determined by core analysis, for greater than 10 percent porosity (A), and greater than 12 percent porosity (B), Bug field.

the remaining reserves is over $73 million and $22 million for oil and gas, respectively. However, for the porosity volume calculated from core analysis, only about 125,000 bbls of oil (19,900 m^3) remain having an unrisked value of $3.75 million. Theoretically, there are no remaining gas reserves using the calculated volume.

The volumes calculated for net feet of permeability also show significant differences (table 10-2). As expected, the net feet greater than 2 mD yielded an optimistically high volume (64,027 acre-feet) with remaining recoverable reserves of 1,000,000 bbls of oil (160,000 m^3) and 2.1 BCFG (0.06 BCMG), at an unrisked value of $30 million and $8.4 million, respectively. At 10 mD, the clean carbonate volume was a third lower (41,746 acre-feet) than at 2 mD, with about 89,000 bbls of oil (14,000 m^3) remaining at an unrisked value of $2.7 million. Again, theoretically, there are no remaining gas reserves using the calculated volume.

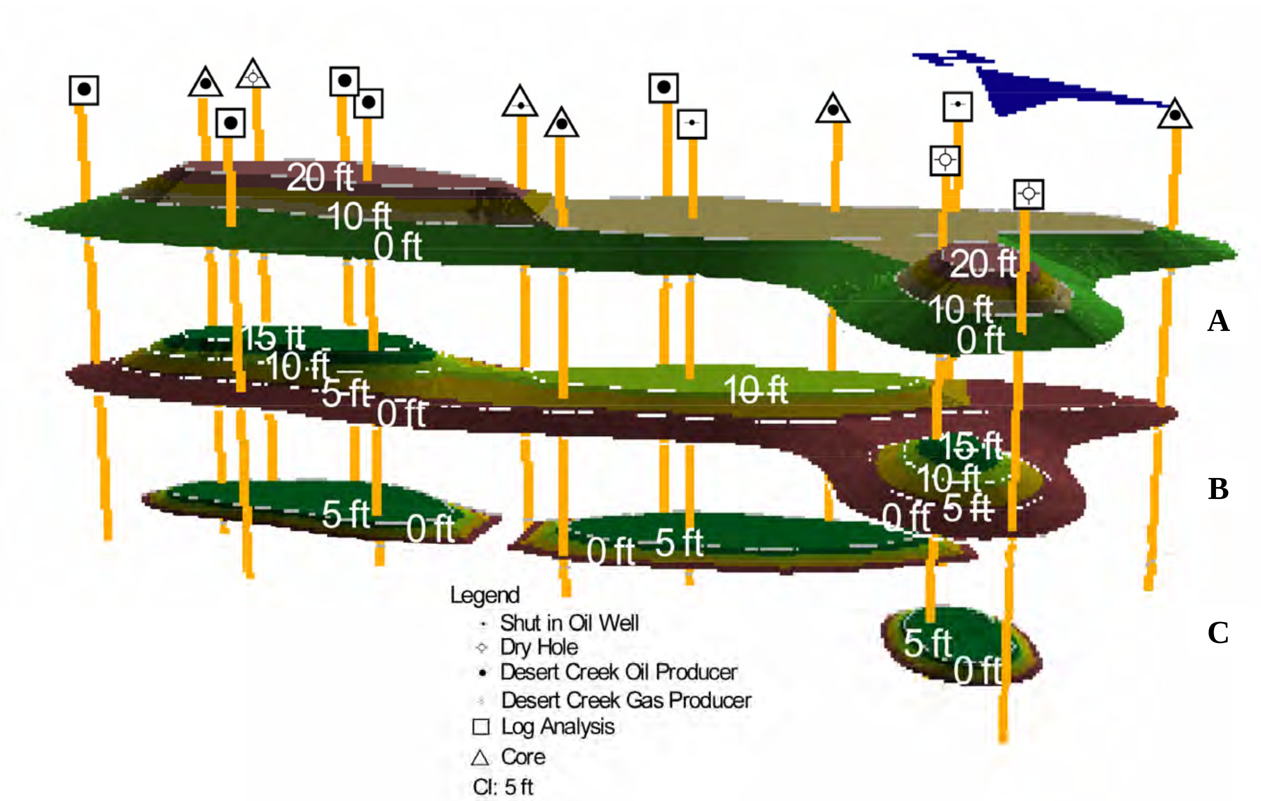

Figure 10-25. Three-dimensional models, lower Desert Creek zone clean carbonate net feet of permeability, as determined by core analysis, for greater than 2 mD (A), greater than 10 mD (B), and greater than 50 mD (C), Bug field.

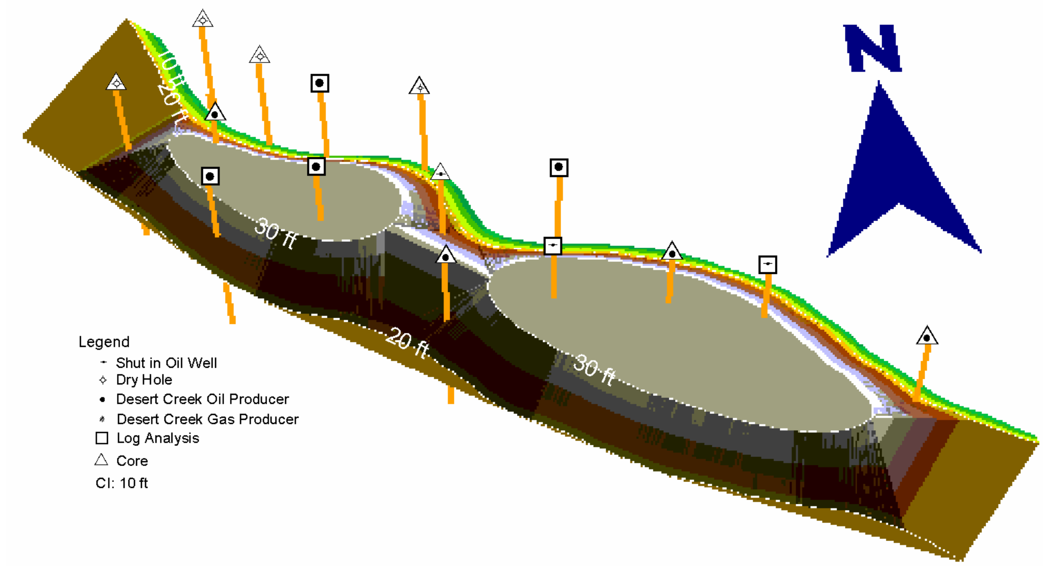

Figure 10-26. Three-dimensional model, lower Desert Creek zone clean carbonate net feet of dolomite as determined by core analysis, Bug field.

Table 10-1. Reservoir calculations, upper Ismay zone, Cherokee field.

NAME	VOLUME (AC FT)	OIL RECOVERY FACTOR (BBLS/AC FT)*	PRIMARY OIL VOLUME RECOVERY (BBLS)	GAS RECOVERY FACTOR (MCF/AC FT)*	PRIMARY GAS VOLUME RECOVERY (MCF)	CUMULATIVE FIELD OIL PRODUCTION (BBLS) AS OF 9/01/06*	REMAINING RECOVERABLE OIL (BBLS)	UNRISKED OIL VALUE BASED ON $30 PER BBL	CUMULATIVE FIELD GAS PRODUCTION (MCF) AS OF 9/01/06**	REMAINING RECOVERABLE GAS (MCF)	UNRISKED GAS VALUE BASED ON $4 PER MCF
Porosity Unit 1***	699	20	13,975	380	265,528	ND	--	--	ND	--	--
Porosity Unit 2***	4060	20	81,207	380	1,542,941	ND	--	--	ND	--	--
Porosity Unit 3***	2117	20	42,348	380	804,607	ND	--	--	ND	--	--
Porosity Unit 4***	4123	20	82,464	380	1,566,825	ND	--	--	ND	--	--
Porosity Unit 5***	6523	20	130,454	380	2,478,620	ND	--	--	ND	--	--
Total of Porosity Units 1-5***	17,522	20	350,448	380	6,658,521	183,945	166,503	$4,995,090	3,718,410	2,940,111	$11,760,444
Net Feet of Porosity (>10% by LA)	19,374	20	387,474	380	7,362,015	183,945	203,529	$6,105,870	3,718,410	3,643,605	$14,574,420
Net Feet of Porosity (>12% by LA)	14,650	20	293,001	380	5,567,017	183,945	109,506	$3,271,680	3,718,410	1,848,607	$7,394,428

*Crawley-Stewart and Riley, 1993.
**Utah Division of Oil, Gas and Mining, 2007.
***>6% porosity by log analysis (LA)
ND = no data

Table 10-2. Reservoir calculations, lower Desert Creek zone, Bug field.

NAME	VOLUME (AC FT)	OIL RECOVERY FACTOR (BBLS/AC FT)*	PRIMARY OIL VOLUME RECOVERY (BBLS)	GAS RECOVERY FACTOR (MCF/AC FT)*	PRIMARY GAS VOLUME RECOVERY (MCF)	CUMULATIVE FIELD OIL PRODUCTION (BBLS) AS OF 9/01/06**	REMAINING RECOVERABLE OIL (BBLS)	UNRISKED OIL VALUE BASED ON $30 PER BBL	CUMULATIVE FIELD GAS PRODUCTION (MCF) AS OF 9/01/06**	REMAINING RECOVERABLE GAS (MCF)	UNRISKED GAS VALUE BASED ON $4 PER MCF
Clean Carbonate Net Feet of Porosity (>10% by LA)	99,057	41	4,061,352	103	10,202,909	1,623,802	2,437,550	$73,126,500	4,529,309	5,673,600	$22,694,400
Clean Carbonate – Porosity Thickness (>10% by core analysis)	42,621	41	1,747,465	103	4,389,974	1,623,802	123,663	$3,709,890	4,529,309	0	0
Clean Carbonate Net Feet of Permeability (kh>2 mD)	64,027	41	2,625,105	103	6,594,775	1,623,802	1,001,303	$30,039,090	4,529,309	2,065,466	$8,261,864
Clean Carbonate Net Feet of Permeability (kh>10 mD)	41,746	41	1,711,568	103	4,299,794	1,623,802	87,766	$2,632,980	4,529,309	0	0

* Oline, 1996.
**Utah Division of Oil, Gas and Mining, 2007.
LA = log analysis

CHAPTER XI
HORIZONTAL DRILLING OPPORTUNITIES

Thomas C. Chidsey, Jr.,
Utah Geological Survey;
and
David E. Eby, Eby Petrography & Consulting, Inc.

Historical Aspects

With the exception of the giant Greater Aneth field (figure 1-3), the value of horizontal drilling has not been demonstrated in any of the over 100 smaller shallow-shelf carbonate reservoirs in the Paradox Basin. The reservoirs are heterogeneous due to lithofacies changes and extensive diagenesis within the Ismay and Desert Creek zones, leaving untapped compartments. To date, only two horizontal wells have been drilled in small Ismay (Knockando) and Desert Creek (Mule) fields (figure 2-1). The results from these wells were disappointing in terms of encountering the objective reservoir lithofacies and production (Chidsey, 2002).

During the 1990s, horizontal drilling was proven to be viable alternative to conventional vertical drilling. Many drilling and logging problems associated with horizontal drilling have been overcome. Successful horizontal drilling programs have been applied to widespread areas in the U.S. and elsewhere including the Austin Chalk play along the Gulf Coast of Texas, the Bakken Shale play in the Williston basin, the Cane Creek shale play in the northern Paradox basin of Utah, the Niobrara Chalk play in the D-J basin, and the Lower Cretaceous Mannville Group in the Alberta basin (Fritz and others, 1992; Morgan, 1992; Stark, 1992). These plays targeted reservoirs dominated by fractures.

Carbonate reservoirs that have successfully been drilled with horizontal wells include pinnacle reefs in the Alberta basin, the Madison Group in the Williston basin, Permian Basin reefs, and Devonian and Silurian pinnacle reefs in the Michigan basin. The purpose of horizontal drilling for these carbonate reservoirs was to: solve water-, solvent-, and/or gas-coning problems; control water production; improve light oil production; and encounter off-reef lithofacies or karsted reef surfaces. These drilling programs were not designed to encounter untapped reservoir compartments. The results of these drilling projects are summarized by Jones (1992), LeFever (1992), and Wood and others (1996). The horizontal wells in these plays have generally higher success rates, higher initial flowing potentials (20 to 50 percent), lower drilling costs, and require fewer wells to drain a reservoir than vertical wells.

Horizontal Drilling Techniques

Types of Horizontal Wells

Horizontal wells may be classified as long reach (over 5000 feet [1500 m] in length) and short reach or horizontal laterals (200 to 700 feet (60-200 m] in length) (figure 11-1); both were considered for the demonstration project in Cherokee field. Long-reach and short-reach horizontal wells have advantages and disadvantages for. Short-reach horizontal drilling

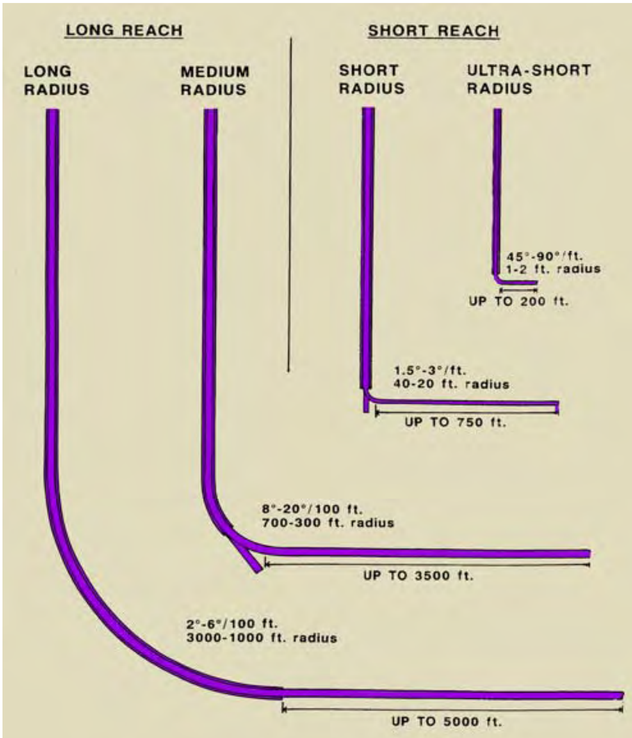

Figure 11-1. Diagrammatic cross section showing types of horizontal wells (after Fritz and others, 1992).

provides a more precise vertical placement of horizontal drains than long-reach drilling, is best for small leases, and sometimes less expensive if drilled from an existing well. Short reach wells have less risk than long-reach wells because the kickoff point is usually below fluid contacts and there is good isolation between fluid zones. The disadvantages of short-reach wells are the need for customized drilling equipment usually a short horizontal drain hole with only openhole completion. Short-reach horizontal wells are usually not logged or cored.

The advantages of long-reach horizontal wells include the fact that they use conventional drilling equipment, accomodate normal-size measurement-while-drilling (MWD) tools, can use downhole motor and steerable systems, cover over 5000 feet (1500 m) of horizontal length, and allow conventional logging, coring, and casing and completion. The disadvantages of long-reach wells are that they are less accurate on depth and cost more than short-reach wells.

Multilateral wellbores exiting a single wellbore (figure 1-4) have gained wide acceptance (Chambers, 1998). These laterals may be horizontal or deviated to reach different bottom-hole locations. The laterals are drilled from the main wellbore. Branches are drilled from a horizontal lateral into the horizontal plane. Splays (fish hooks or herringbone) are drilled from a horizontal lateral in the vertical plane. A dual lateral is a multilateral well with two laterals. Laterals may be opposed to each other or stacked. Multilaterals are drilled for cost saving reasons or reservoir production reasons associated with improved drainage or injection. They provide a means for increasing contact with the pay zones and, in the case of our project, would target untapped reservoir compartments.

The short-reach or horizontal lateral drilling program at Greater Aneth field has included wells with two opposed sets of three stacked parallel laterals with lengths of 860 to 960 feet (260-290 m); similar to that shown schematically on figure 1-4. The purpose of this program was to encounter subzones that were basically untouched by waterflooding, and to slant through vertical barriers to overcome permeability problems and increase production (Amateis, 1995). Net pay and original oil in place were the two main criteria used to choose the location of horizontal laterals. Production and injection laterals are drilled into the porosity zones to sweep oil that vertical wells could not reach. All laterals have been drilled as injector-producer pairs to maintain reservoir pressure and maximize sweep efficiency. Production tests average 700 BOPD (110 m^3/d) with rates as high as 1127 BOPD (179 m^3/d) and 461 BWPD (73 m^3/d). While the rates were encouraging, high early declines indicated the need for injection support. Amateis (1995) estimated this program would help to recover 33 percent of the 421 million barrels (66.9 milliom m^3) of oil in place.

Drilling Techniques

There have been many advances in horizontal drilling technology and cost control over the last 15 years. The use of modern angle build motors and MWD logging equipment allow accurate entry into potential reservoirs. Cost control using new methods and equipment can reduce the cost of drilling horizontally to less than 1.5 times that of drilling a vertical well.

Wells are prepared in two ways. They are either whipstocked (preferred) or sectioned, depending upon casing condition. Open-hole logs are not usually run. Mud-log interpretation and rate of penetration (ROP) are the only source of reservoir quality in the lateral. Rate of penetration is a real-time indicator used to steer the well. In good porosity lithofacies, ROP averages between 0.5 to 3 minutes/foot. In poor porosity lithofacies, ROP slows down to 9 minutes/foot (Amateis and Hall, 1997).

Cross sections serve more as a guide than an absolute target since porosity and permeability are not very predictable. Adjustments are made as the laterals are drilled using the cuttings and penetrations rates. Thermal decay time (TDT) logs along the laterals help to visualize the variability of the porosity units. The relative water saturations along the wellbore change rapidly laterally. Salinity of the water cannot be estimated so saturations are qualitative rather than quantitative, but are clear indicators of the compartmentalization of the reservoir by surfaces not easily incorporated in 3-D models (Amateis and Hall, 1997).

Wellsite Recommendations

1. Carefully collect and examine drill samples (cuttings) during horizontal drilling operations.

2. Use a good binocular (research-grade) microscope capable of high magnification. It should be equipped with a daylight-corrected fiber optics lighting system to determine porosity types, mineralogy, and lithofacies being drilled. These properties should be documented and accurately logged to accompany mudlogging data.

3. Utilize UV and blue-light fluorescence microscopy to assist with the evaluation of oil shows while drilling the horizontal leg(s).

4. Wellsite assessment of rock/fluid properties using the microscopic techniques listed above should be used in helping to determine when to cease drilling each horizontal leg/ lateral.

5. Immediately after drilling, make selective thin sections from the cuttings in order to confirm the rock and fluid properties of the section that was drilled horizontally. With thin sections, the cuttings should be thoroughly evaluated using epifluorescence, cathodoluminescence, and polarized light microscopy.

Completion Operations

Vertical wells are completed with matrix-acid stimulations, which have historically proven the best method. To obtain matrix stimulation on a multilateral well, acid must be evenly placed in each lateral. Acid must be pumped at matrix pressures and rates. Each lateral must be isolated from the other laterals. At Greater Aneth field for example (figure 1-3), matrix stimulation of a multilateral well has not been easy and has only been achieved on a few wells (Amateis and Hall, 1997).

Several different completion methods have been tried on the open-hole multilaterals at Greater Aneth field. Methods ranged from no acid stimulation, to acid washing, to bullhead acidizing, to perforated subs. After producing unacidized wells for a few months at Greater Aneth field, the same wells were acidized. The average acid stimulation paid out in four months (see Amateis and Hall, 1997, p. 134-135 for procedural notes on doing the acid-washing and bullhead acid treatments). Distribution of acid during the acid-washing treatments in the field was excellent, but injection rates and bottom-hole treating pressures were low. Bullhead acid treatments provide higher rates and bottom-hole treating pressures but poor acid distribution. A comparison of acid treatments based on early oil production per lateral at Greater Aneth shows that acid-washing and bullhead treatments have similar results.

Horizontal Drilling Targets in the Paradox Basin from the Regional Lithofacies Perspective

The Utah portion of the Blanding sub-basin shows the development of "clean carbonate" packages that contain a variety of the productive reservoir lithofacies (see Chapter II). These clean carbonates abruptly change laterally into thick anhydrite packages. Isochore maps of the upper Ismay clean carbonates and the locally thick anhydrites are consistent with a broad carbonate shelf containing several small intra-shelf basins. The intra-shelf basin centers filled with anhydrite following carbonate sedimentation on the remainder of the carbonate shelf.

Lithofacies and reservoir controls imposed by the anhydritic intra-shelf basins should be considered when selecting the optimal location and orientation of any horizontal drilling for undrained reserves, as well as identifying new exploration trends. Projections of the inner shelf/tidal flat and mound trends around the intra-shelf basins identify potential exploration targets, which could be developed using horizontal drilling techniques (figures 2-17 and 2-18). Drilling horizontally from known phylloid-algal reservoirs along the inner shelf/tidal flat trend could encounter previously undrilled porous buildups.

Intra-shelf basins are not present in the lower Desert Creek zone of the Blanding sub-basin. However, drilling horizontally from productive mound lithofacies along linear shoreline trends could also encounter previously undrilled porous Desert Creek intervals and buildups.

Reservoir Zones Targeted For Horizontal Drilling

Cherokee and Bug Fields

Carbonate buildups and extent of field potential shown on structure contour maps on the top of the upper Ismay zone and the Chimney Rock shale, and isochore maps of the upper Ismay and lower Desert Creek for Cherokee and Bug fields, respectively, also reveal possible horizontal drilling targets. In Cherokee field, the 3-D thickness models indicate the five porosity units in the Ismay zone of the northeastern field area are likely not fully drained (figure 10-12) and could be tested with a horizontal lateral from existing wellbores. In addition, horizontal laterals could test the potential of each individual limestone and dolomite unit identified in core. These two lithologies have distinct diagenetic characteristics and pore types which are often separated from each other by various baffles and barriers.

In Bug field, the 3-D model of the thickness of the lower Desert Creek clean carbonate (figure 10-20) displays an elongate, northwest-southeast-trending carbonate buildup depicting the typical, nearshore, shoreline-linear lithofacies tracts of the Desert Creek zone in the northern Blanding sub-basin. The clean carbonate model shows a small saddle, which may represent an intermound trough between two subsidiary buildups. Intermound troughs may be filled with low-permeability wackestone and mudstone, thus acting as barrier or baffle to fluid flow. The relatively small size and abundance of intermound troughs over short distances, as observed in outcrop along the San Juan River for example, suggests caution should be used when correlating these lithofacies between development wells (Chidsey and others, 1996a). Lithofacies that appear correlative and connected from one well to another may actually be separated by low-permeability lithofacies and carbonate rock fabrics which inhibit flow and decrease production potential. Horizontal wells, or laterals, increase the chance of successful drainage where these troughs are present.

The reservoir quality of Cherokee and Bug fields has been affected by multiple generations of dissolution, anhydrite plugging, and various types of cementation which act as barriers or baffles to fluid flow. Intense, late-stage microporosity development along hydrothermal solution fronts is the most significant diagenetic characteristic of the Ismay zone at Cherokee field (figure 3-32). Extensive, early-stage micro-boxwork porosity due to dissolution related to subaerial exposure of the carbonate buildup is the most significant diagenetic characteristic of the Desert Creek zone at Bug field (figure 3-31). Based on cross plots of permeability and porosity data, the reservoir quality of the rocks in Cherokee and Bugs fields is most dependent on pore types and diagenesis. The microporosity in Cherokee field and the micro-boxwork porosity in Bug field represent important targets for undrained reserves by using horizontal drilling techniques.

Little Ute and Sleeping Ute Fields

Structure contour maps on the top of the upper Ismay zone and the Desert Creek zone, as well as isopach maps of the upper and lower Ismay zones for Little Ute and Sleeping Ute fields, respectively, also showed possible horizontal drilling targets. A 3-D model with structure contours on the top of the lower Ismay zone (figure 11-2) was constructed for the Little Ute/Sleeping Ute/Desert Canyon area. This 3-D model shows general regional dip to the southwest. A prominent southwest-trending structural nose is displayed in the Sleeping Ute field area upon which the carbonate buildup likely developed. A 3-D model of the net porosity thickness (porosity greater than 6 percent by log analysis) of the lower Ismay zone (figure 11-3) shows the characteristic elongate, northwest-southeast, depositional trend of the lower Ismay carbonate buildups in this part of the Blanding sub-basin. This trend indicates a near-shoreline, linear lithofacies tract. Figure 11-3 indicates the buildup has two subsidiary thick areas separated by a slightly thinner saddle that may represent an intermound trough.

The reservoir quality of the rocks in Little Ute and Sleeping Ute fields is most dependent on lithofacies types, pore types, and diagenesis. For example, the phylloid-algal mound lithofacies (figure 3-33) shows excellent reservoir porosity development. Leaching of skeletal grains created extensive but isolated moldic porosity, and thus often resulted in low permeability. Even widespread diagenetic dissolution that produces excellent porosity does not ensure that these reservoirs can be economically produced using vertical wells.

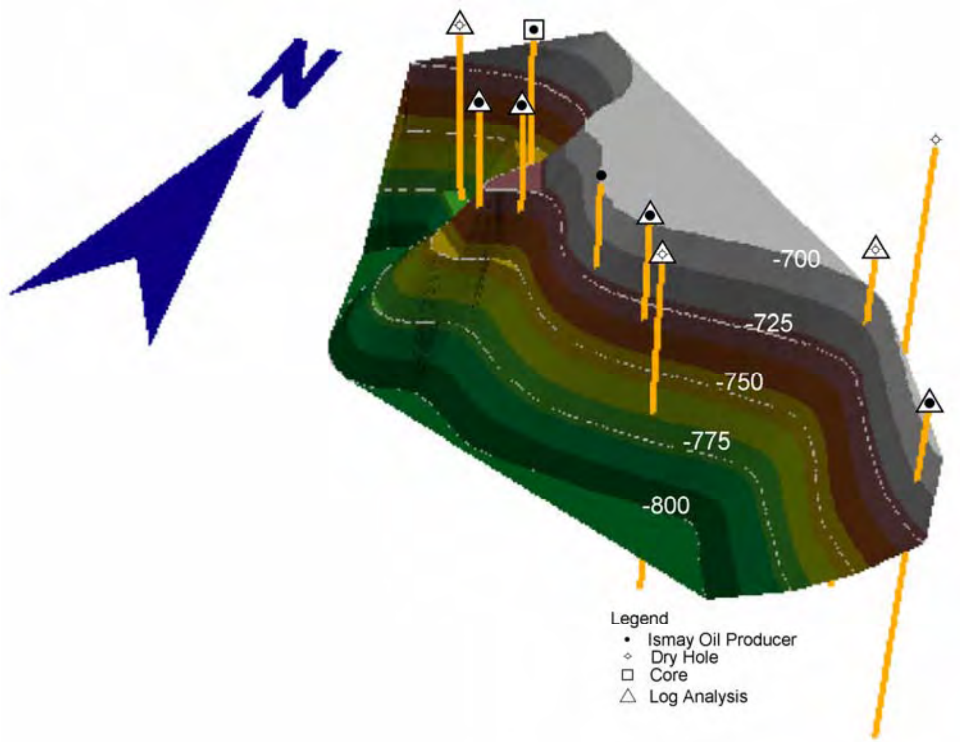

Figure 11-2. Three-dimensional model with structure contours on top of the lower Ismay zone, Little Ute, Sleeping Ute, and Desert Canyon fields, Montezuma County, Colorado.

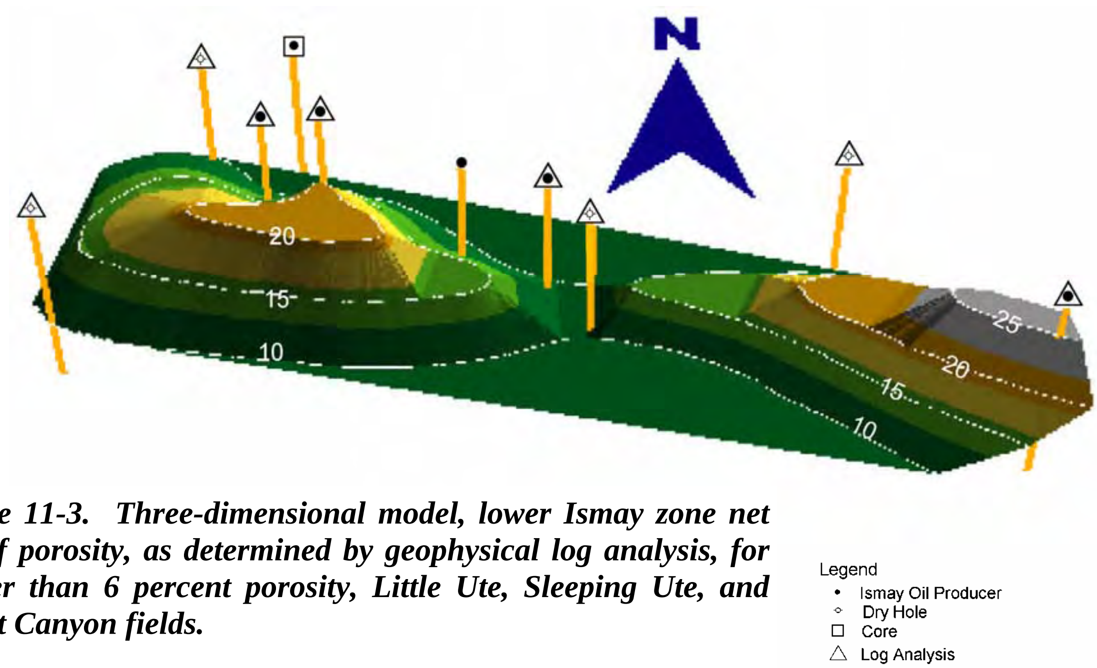

Figure 11-3. Three-dimensional model, lower Ismay zone net feet of porosity, as determined by geophysical log analysis, for greater than 6 percent porosity, Little Ute, Sleeping Ute, and Desert Canyon fields.

Paradox Basin Horizontal Drilling Strategies

Three strategies for horizontal drilling were developed for Cherokee, Bug, and similar fields in the Paradox Basin (figure 11-4). All strategies involve drilling stacked, parallel horizontal laterals or high-angle drill holes. Depositional lithofacies are targeted in both the Ismay and Desert Creek zones of Cherokee and Bug fields where, for example, multiple buildups (algal mounds and calcarenites) can be penetrated with two opposed sets of stacked, parallel horizontal laterals (figure 11-4A). The hydrothermally induced microporosity in the Ismay zone of Cherokee field does not appear to be lithofacies dependent and therefore could be drained with radially stacked, horizontal laterals and splays (figure 11-4B). Finally, much of the elongate, brecciated, beach-mound, depositional lithofacies and micro-boxwork porosity in the Desert Creek zone of Bug field could be penetrated by opposed sets of stacked, parallel horizontal laterals (figure 11-4C).

Two strategies for horizontal drilling were developed for Little Ute and Sleeping Ute fields also involving drilling stacked, parallel horizontal laterals (figure 11-5). Depositional lithofacies are targeted in the Ismay zone of Little Ute and Sleeping Ute fields where, like

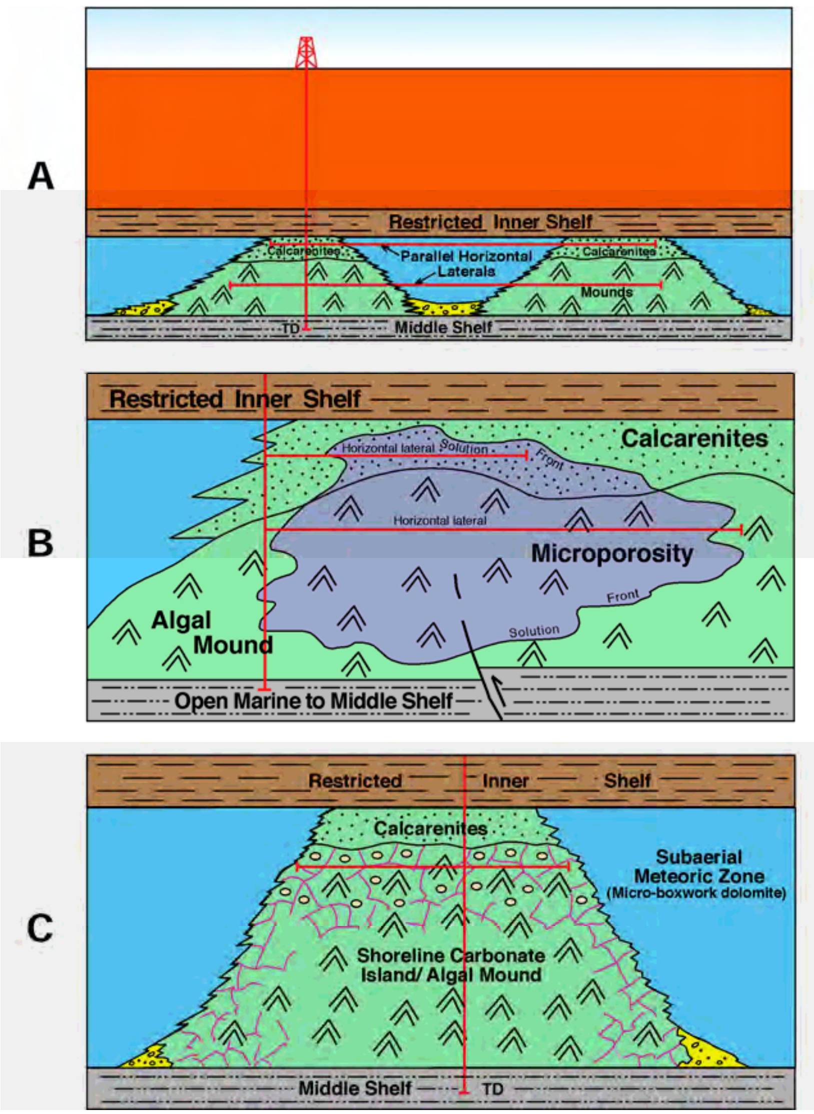

***Figure 11-4.** Schematic diagram of strategies for horizontal drilling in Cherokee and Bug fields, Utah: (A) depositional lithofacies in the Ismay and Desert Creek zones of Cherokee and Bug fields, (B) microporosity in the Ismay zone of Cherokee field, and (C) depositional lithofacies and diagenetic fabrics (micro-boxwork porosity) in the Desert Creek zone of Bug field.*

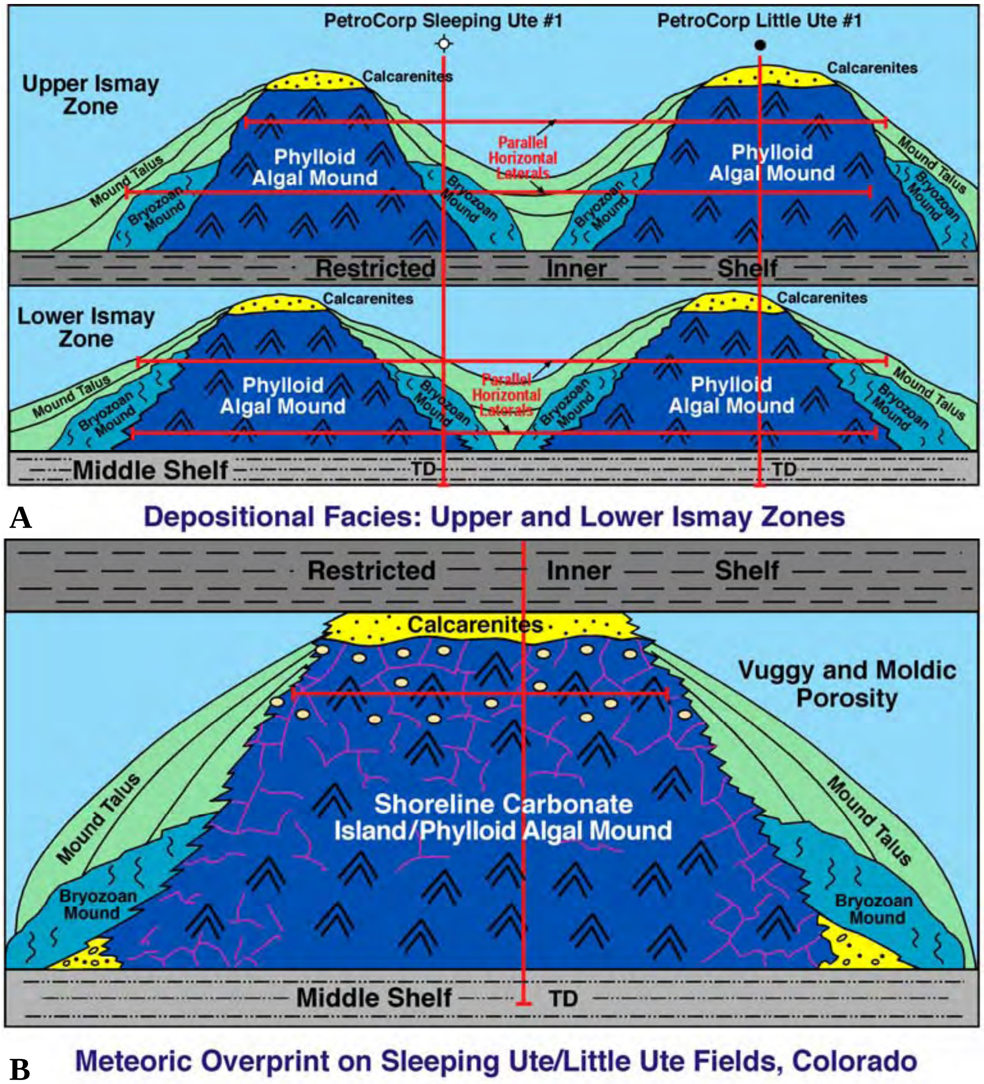

Figure 11-5. Schematic diagram of strategies for horizontal drilling in the upper and lower Ismay zones of Sleeping Ute and Little Ute fields, Colorado: (A) depositional lithofacies, and (B) meteoric overprint within the shoreline carbonate island and upper phylloid-algal mound lithofacies.

Cherokee and Bug fields, multiple buildups (algal and bryozoan mounds, calcarenites, and mound talus) can be penetrated with two opposed sets of stacked, parallel, horizontal laterals (figure 11-5A). Similarly, a second strategy involves penetrating multiple zones of diagenetically enhanced (dissolution [meteoric overprint]) reservoir intervals in these mound buildups (figure 11-5B).

Horizontal Drilling Recommendations for Cherokee and Bug Fields

Cherokee Field

The UGS made five alternative horizontal drilling recommendations to the operator of Cherokee field based on the conclusion that multiple potential Ismay intervals have not been drained due to reservoir heterogeneity, particularly to the northeast of the main field area. All alternatives would use existing vertical development wells, rather than drilling new wells, to minimize costs and surface disturbances in the environmentally sensitive areas of southeastern Utah. We provided reservoir maps that included both horizontal lengths and directions.

Alternative 1 proposed drilling stacked short and medium radius multi-laterals for porosity units 1 through 5 from the Cherokee Federal No. 22-14 well (figures 11-6 through 11-11). Horizontal lengths would range from 1320 to 2900 feet (400-880 m) generally in southeast to east-southeast directions. Alternative 2 proposed drilling a single or dual, high-angle drain hole(s) (slant hole[s]) to cross porosity units 1 through 5 from the Cherokee Federal No. 22-14

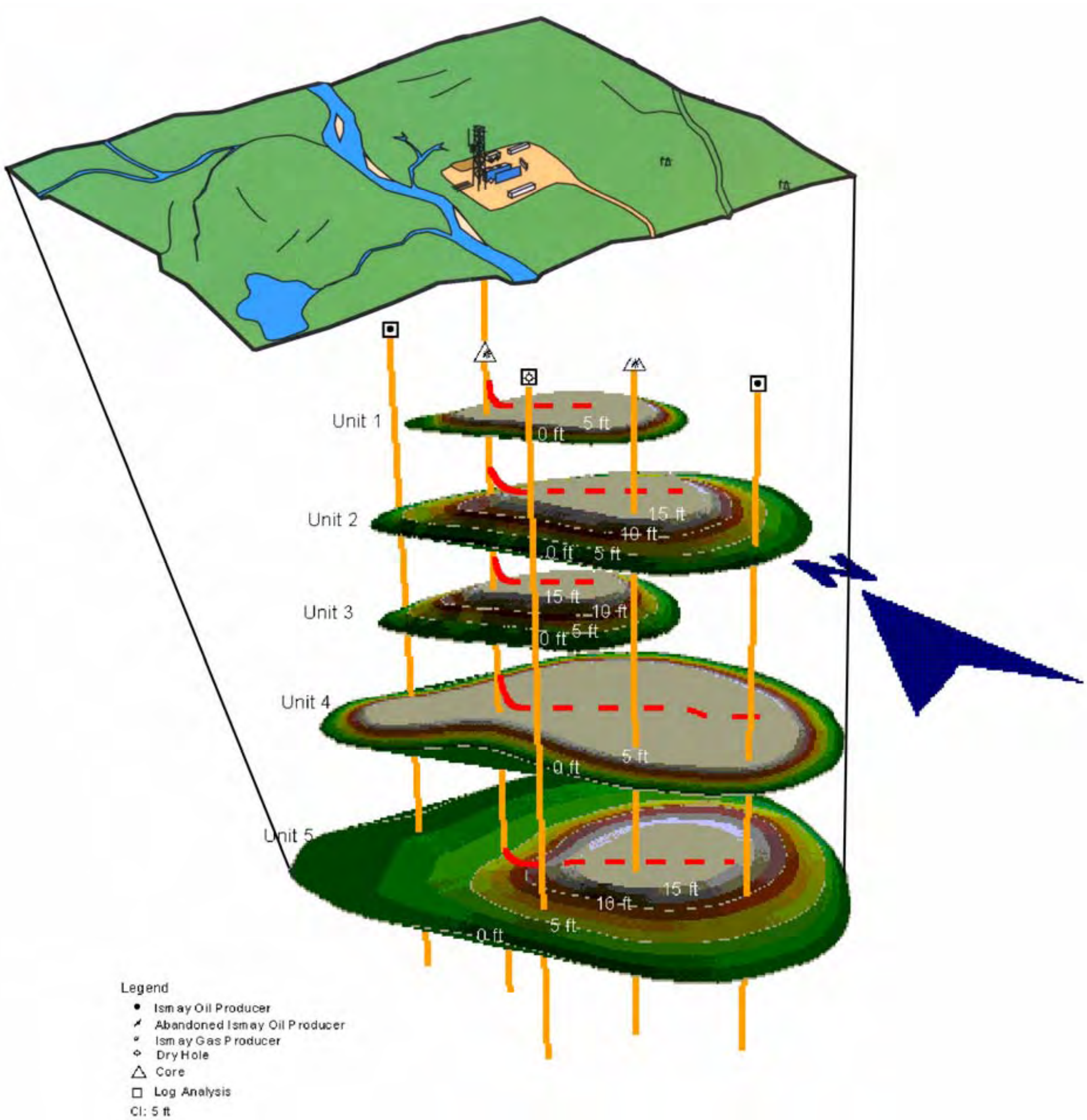

Figure 11-6. Alternative 1 - schematic of proposed short and medium radius multi-laterals for porosity units 1 through 5, Cherokee field, shown on 3-D model of porosity units 1 through 5 isochores vertically stacked (no vertical scale).

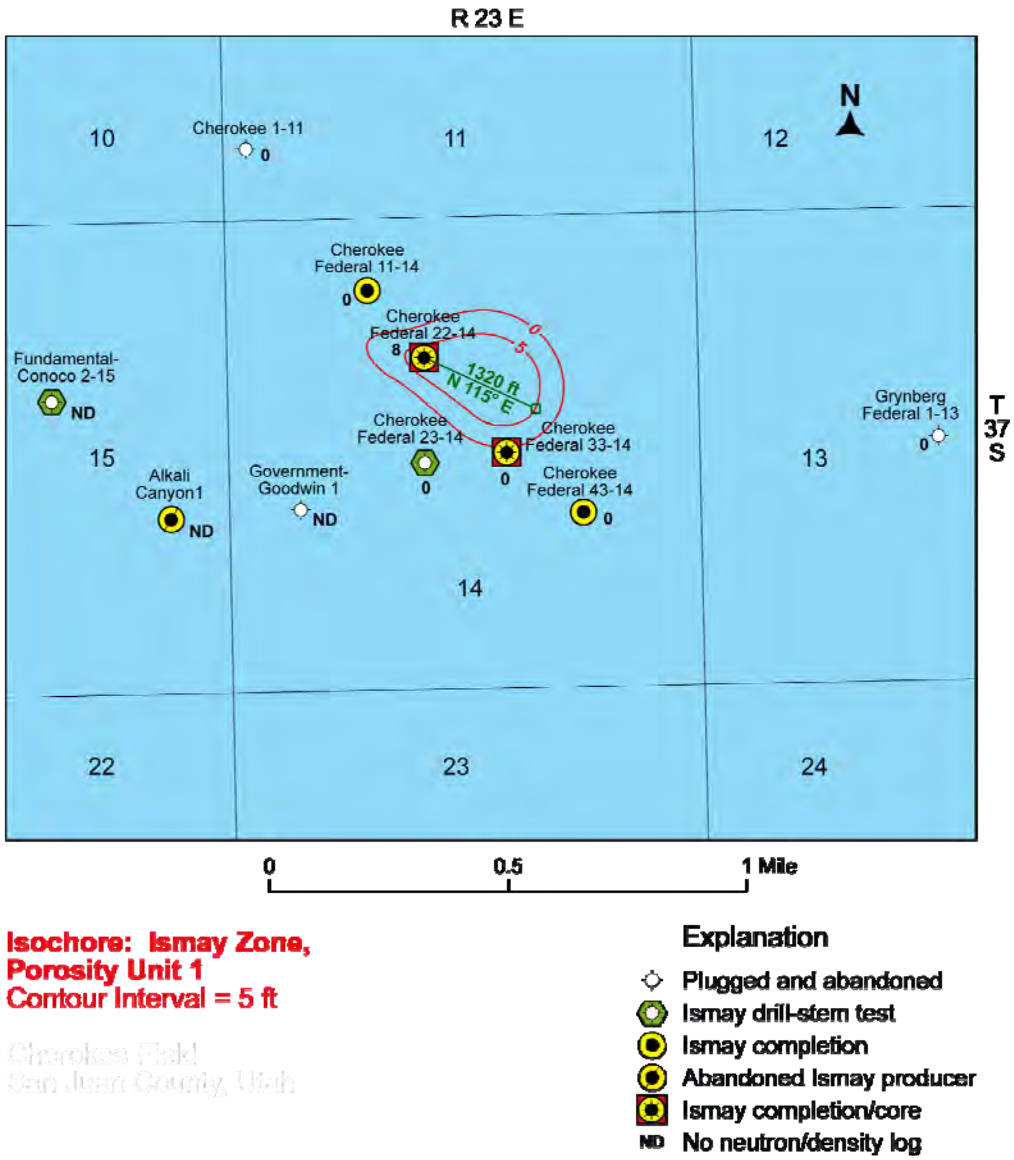

Figure 11-7. Recommended horizontal length and direction targeting porosity unit 1, Cherokee field, shown on isochore of porosity unit 1.

well (figure 11-12 through 11-14). Two directions were proposed – 3000 feet (900 m) to the southeast and 2460 feet (750 m) to the northeast. Alternative 3 proposed a medium radius horizontal drain hole for a single mound unit only from the Cherokee Federal No. 22-14 well (figure 11-15). Alternative 4 proposed drilling a combination of medium and short radius laterals (up to three) targeting just limestones (figure 11-16). Alternative 5 proposed drilling a combination of medium and short radius laterals (up to four) targeting just dolomites (figure 11-17).

Bug Field

The UGS proposed drilling opposing, dual, long-radius horizontal laterals from the Bug

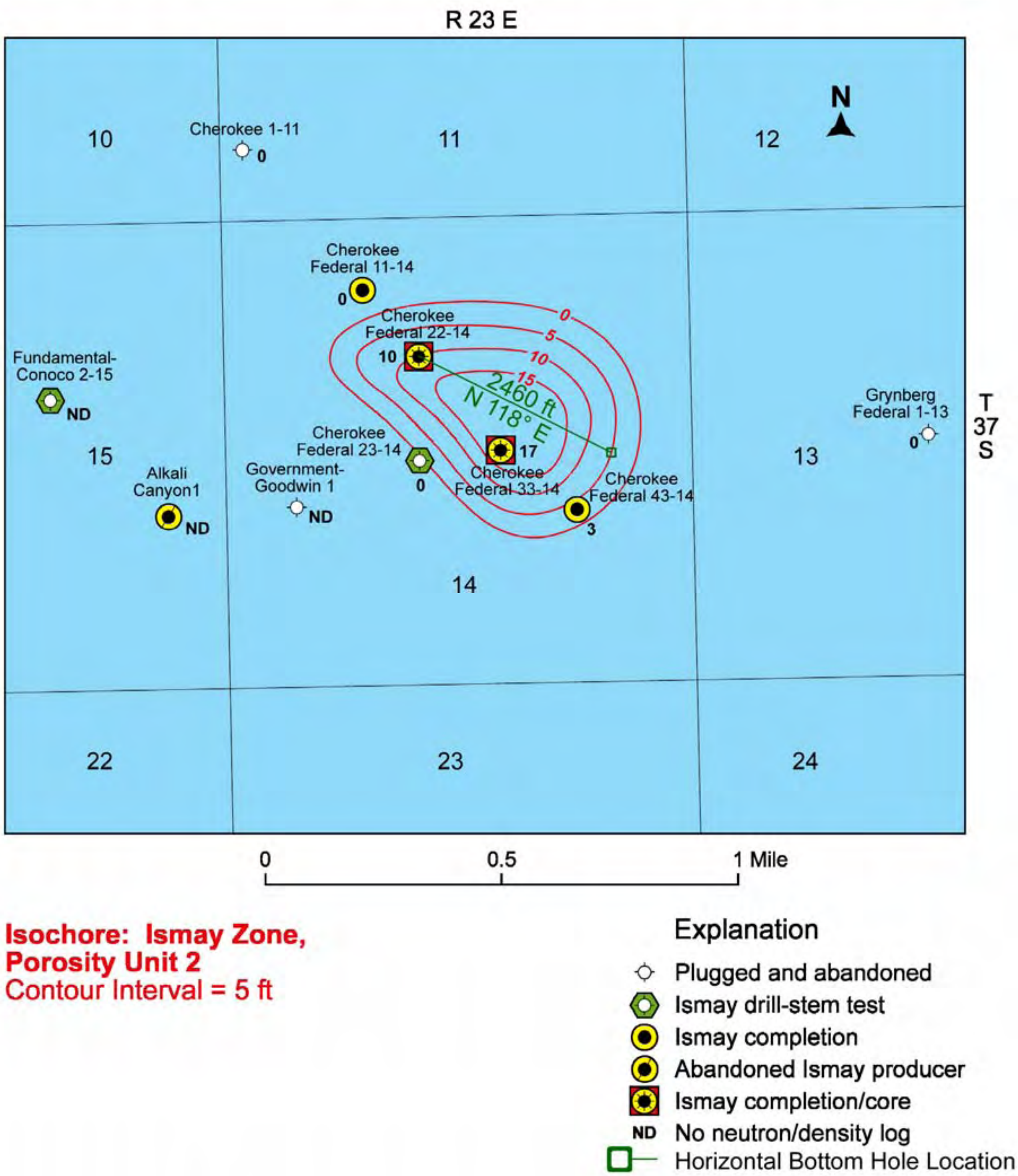

Figure 11-8. Recommended horizontal length and direction targeting porosity unit 2, Cherokee field, shown on isochore of porosity unit 2.

No. 13 well located essentially in the center of the field (figures 11-18 through 11-24). Horizontal lengths would run along the length of the field 7400 feet (2300 m) in a west-northwest direction and 11,000 feet (3400 m) generally in an east-southeast direction. These laterals would target the thickest and highest porosity and permeability in lower Desert Creek clean carbonate (figures 11-18 through 11-20). These laterals would also follow either the nearshore, shoreline trend (shoreline carbonate island) or phylloid-algal mound lithofacies (figure 11-21).

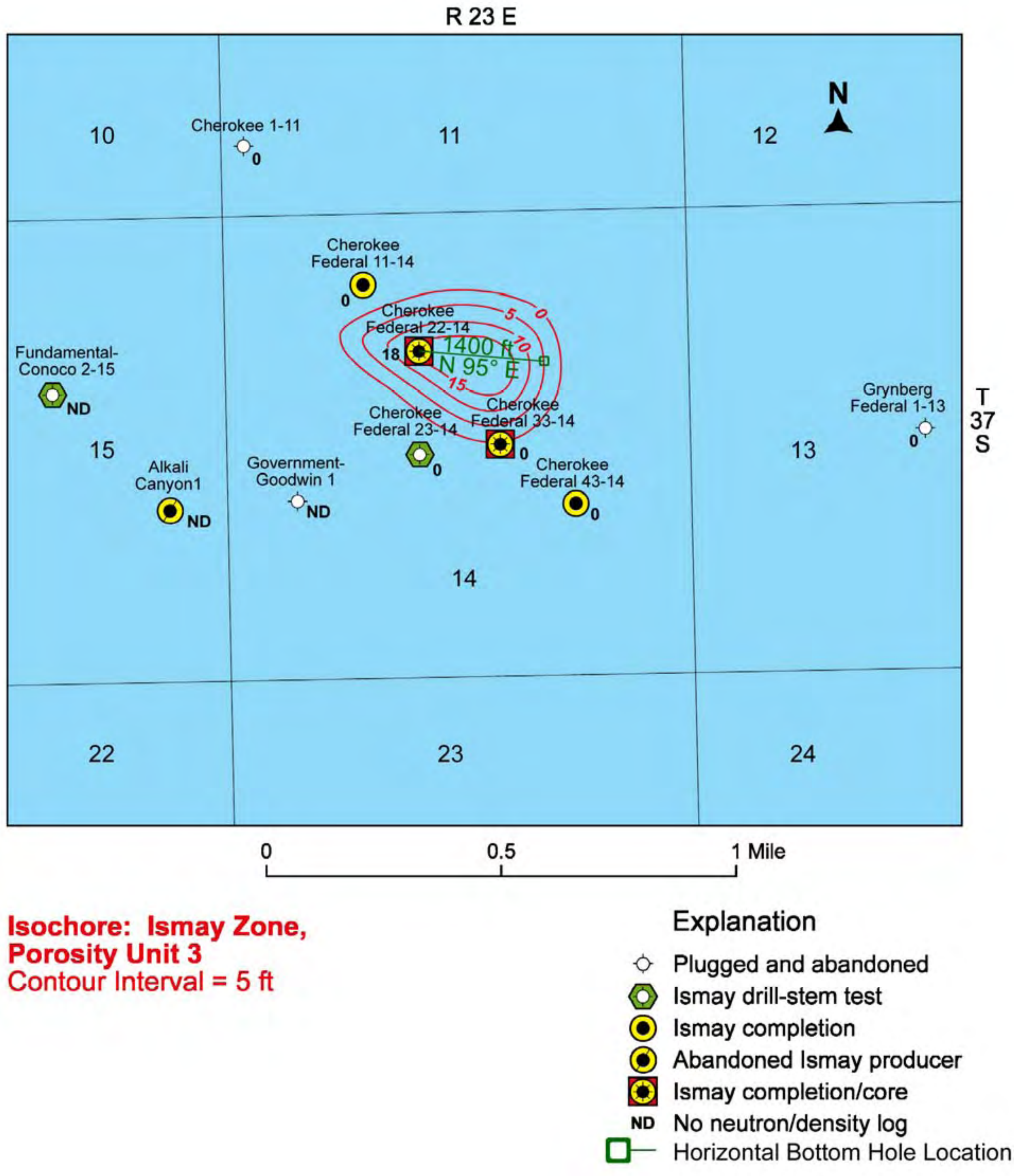

Figure 11-9. Recommended horizontal length and direction targeting porosity unit 3, Cherokee field, shown on isochore of porosity unit 3.

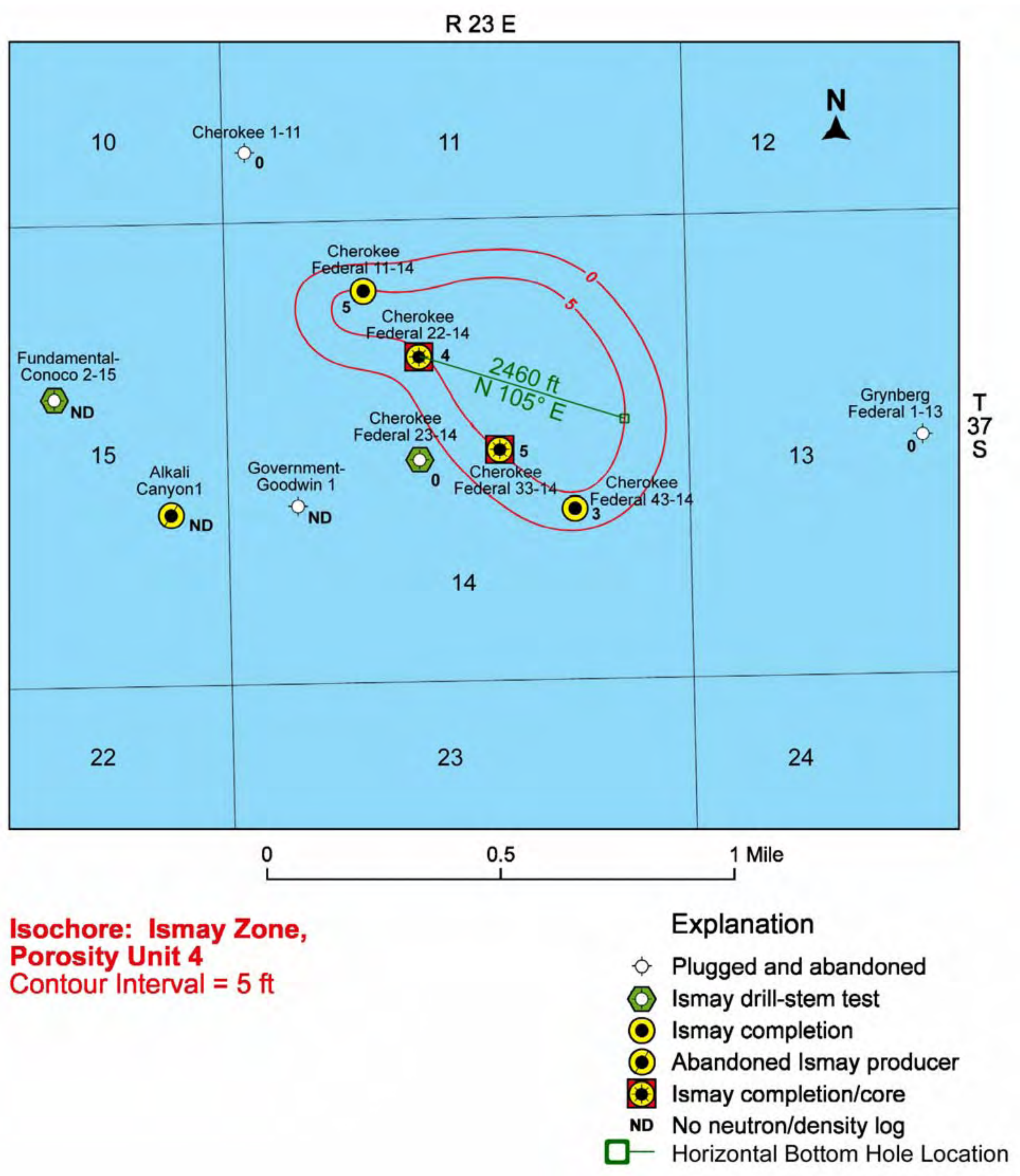

Figure 11-10. Recommended horizontal length and direction targeting porosity unit 4, Cherokee field, shown on isochore of porosity unit 4.

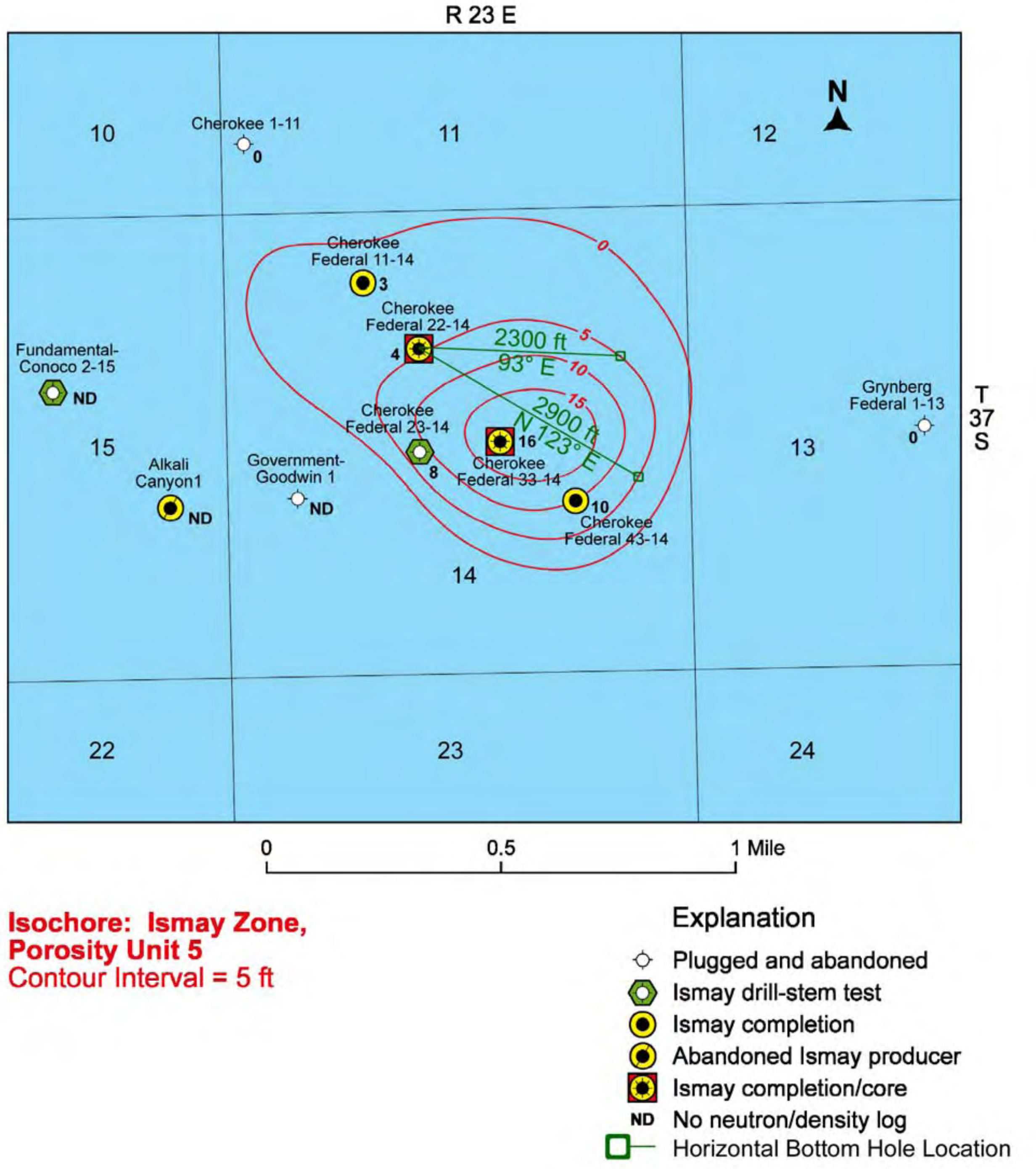

Figure 11-11. Recommended horizontal length and direction targeting porosity unit 5, Cherokee field, shown on isochore of porosity unit 5.

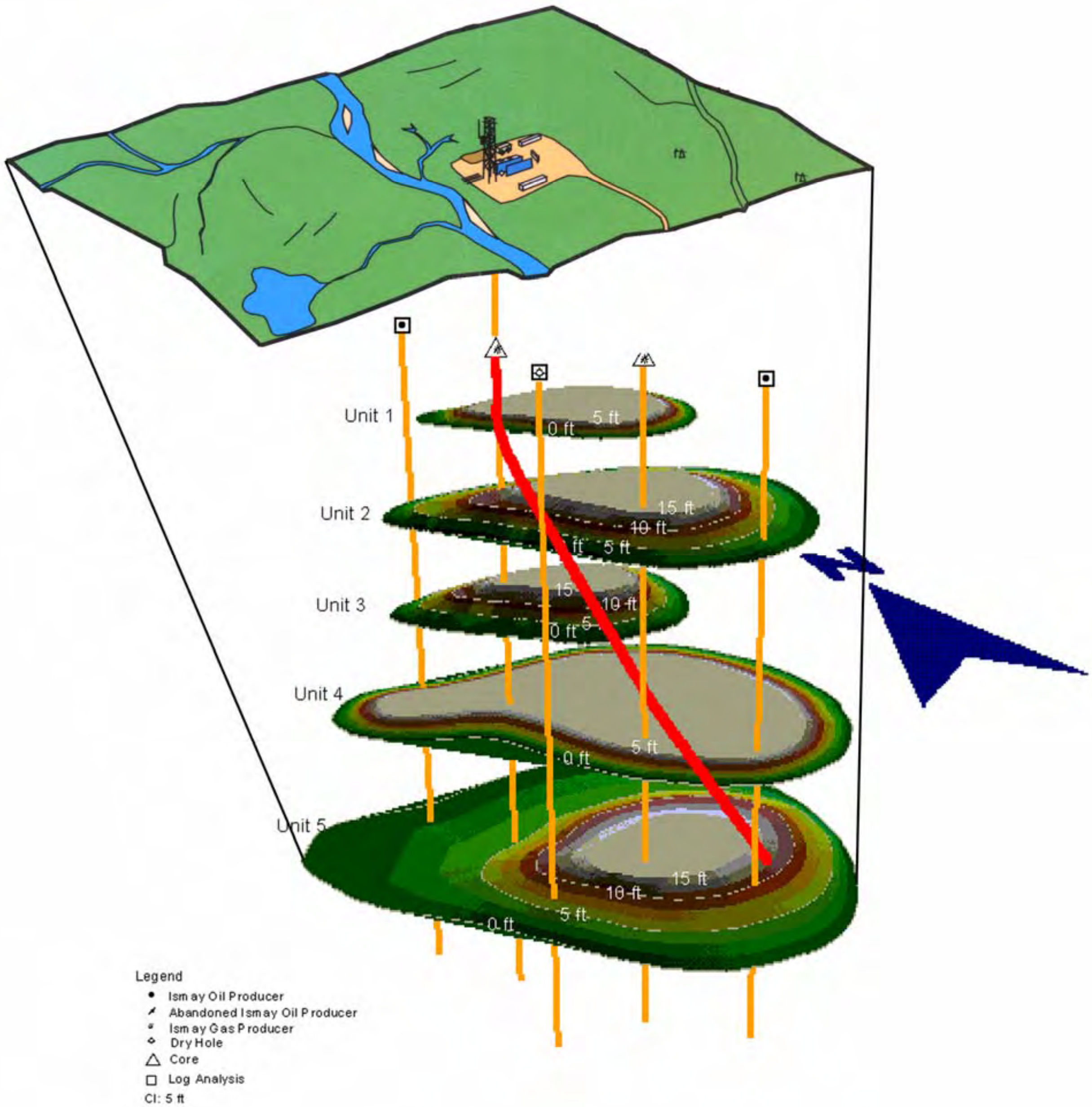

Figure 11-12. Alternative 2 - schematic of a proposed high-angle drain hole for porosity units 1 through 5, Cherokee field, shown on 3-D model of porosity units 1 through 5 isochores vertically stacked (no vertical scale).

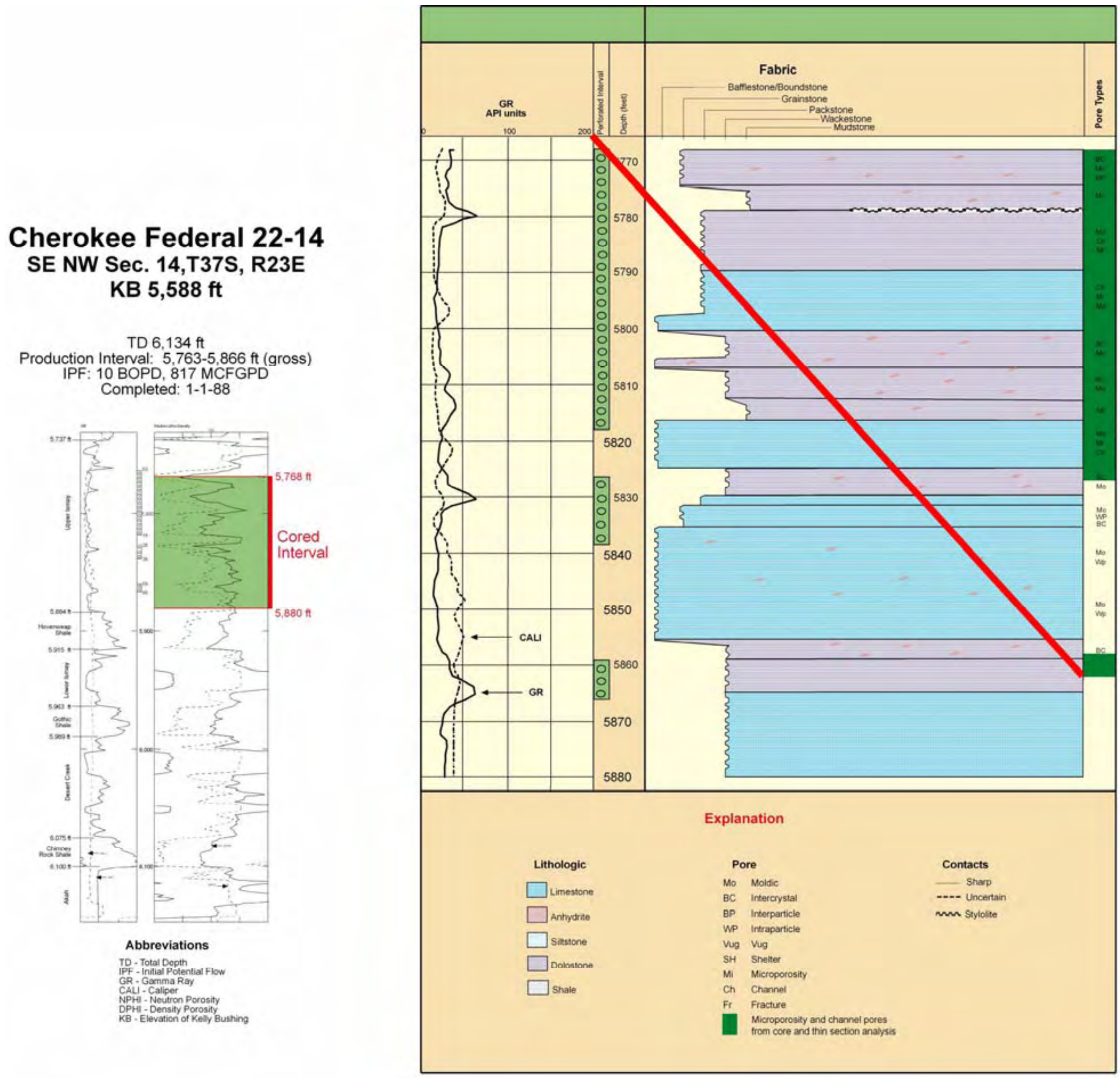

Figure 11-13. Proposed high-angle drain hole (slant hole) to cross porosity units 1 through 5, shown on core description, displaying carbonate fabrics and pore types, for the Cherokee Federal No. 22-14 well.

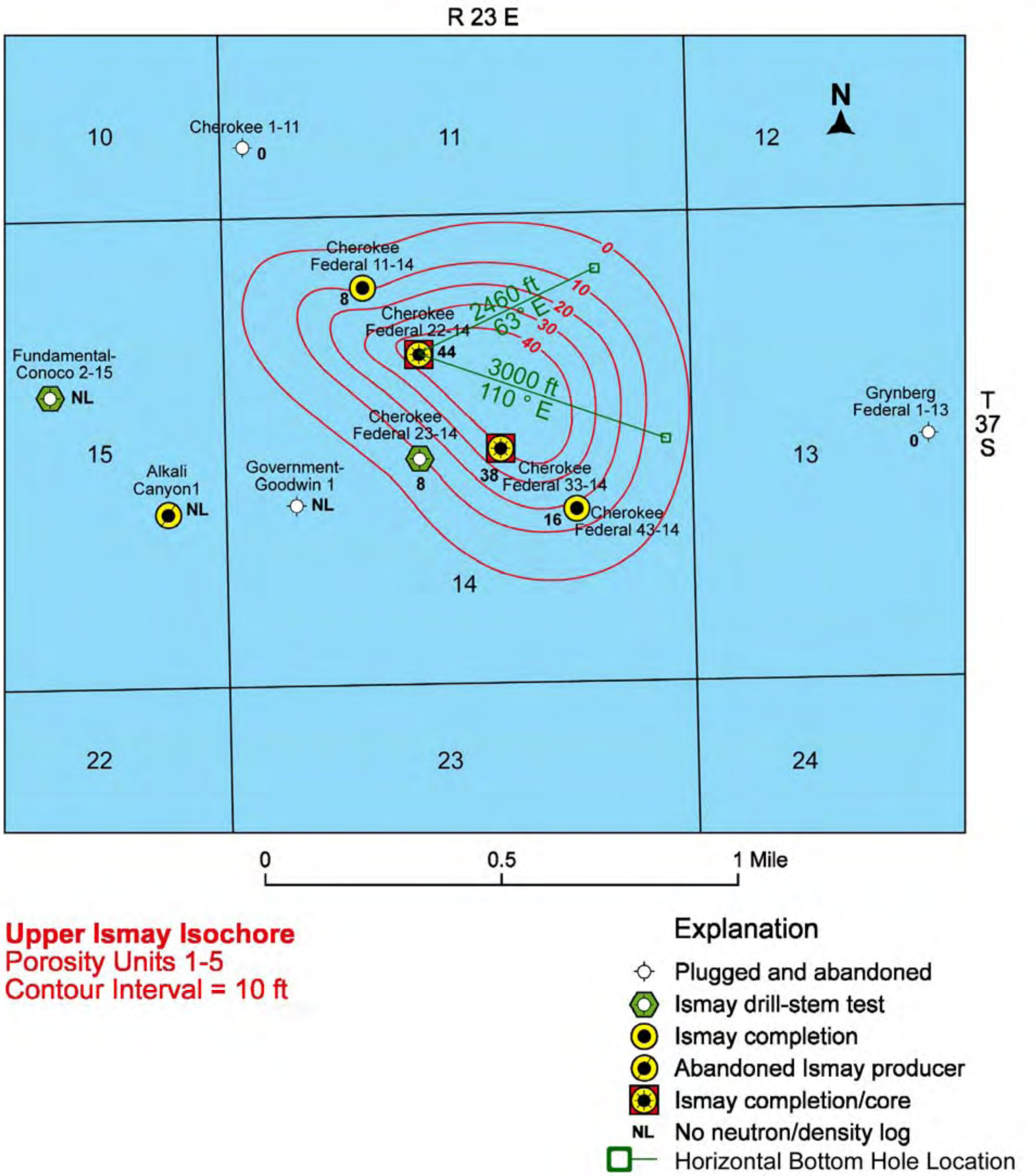

Figure 11-14. Recommended horizontal lengths and directions of high-angle drain holes targeting porosity units 1 through 5, Cherokee field, shown on the combined isochore of porosity units 1 through 5.

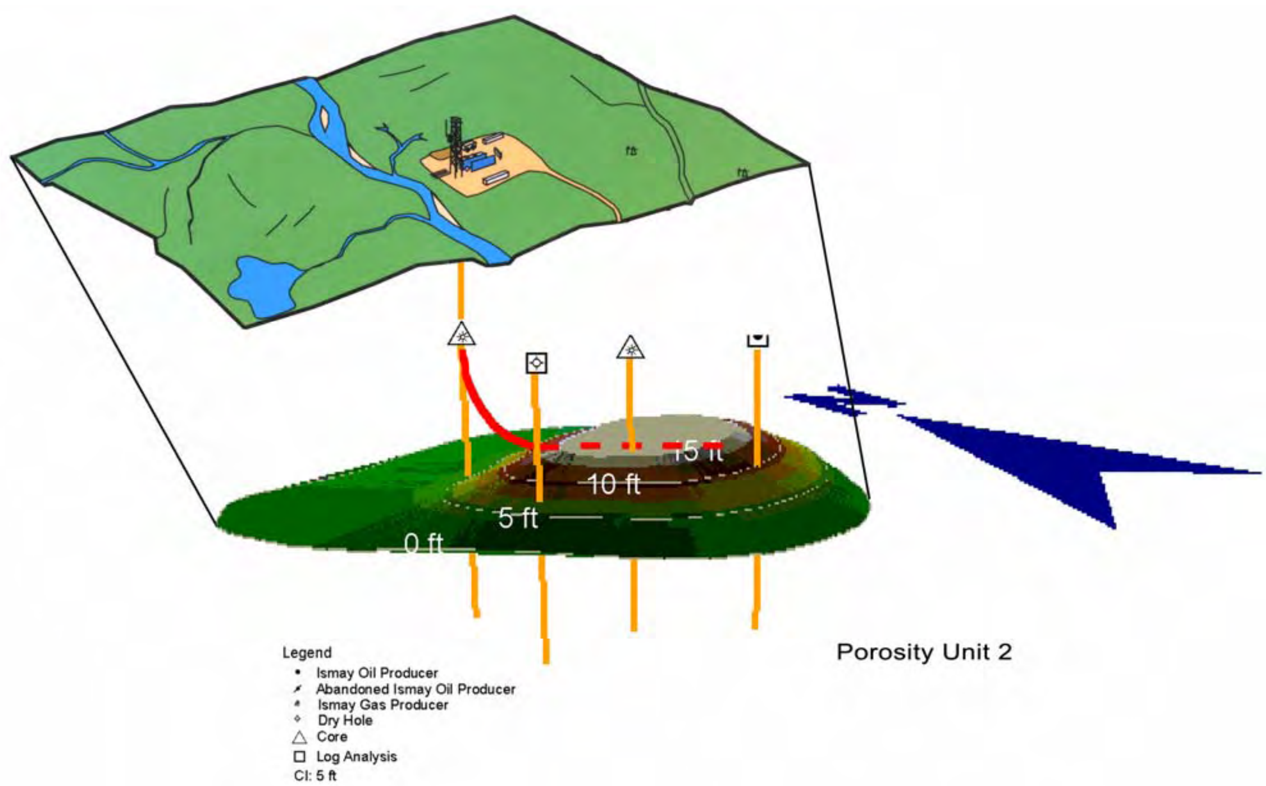

Figure 11-15. Alternative 3 - schematic of a proposed medium radius horizontal drain hole for a mound only, shown on 3-D model of porosity unit 2.

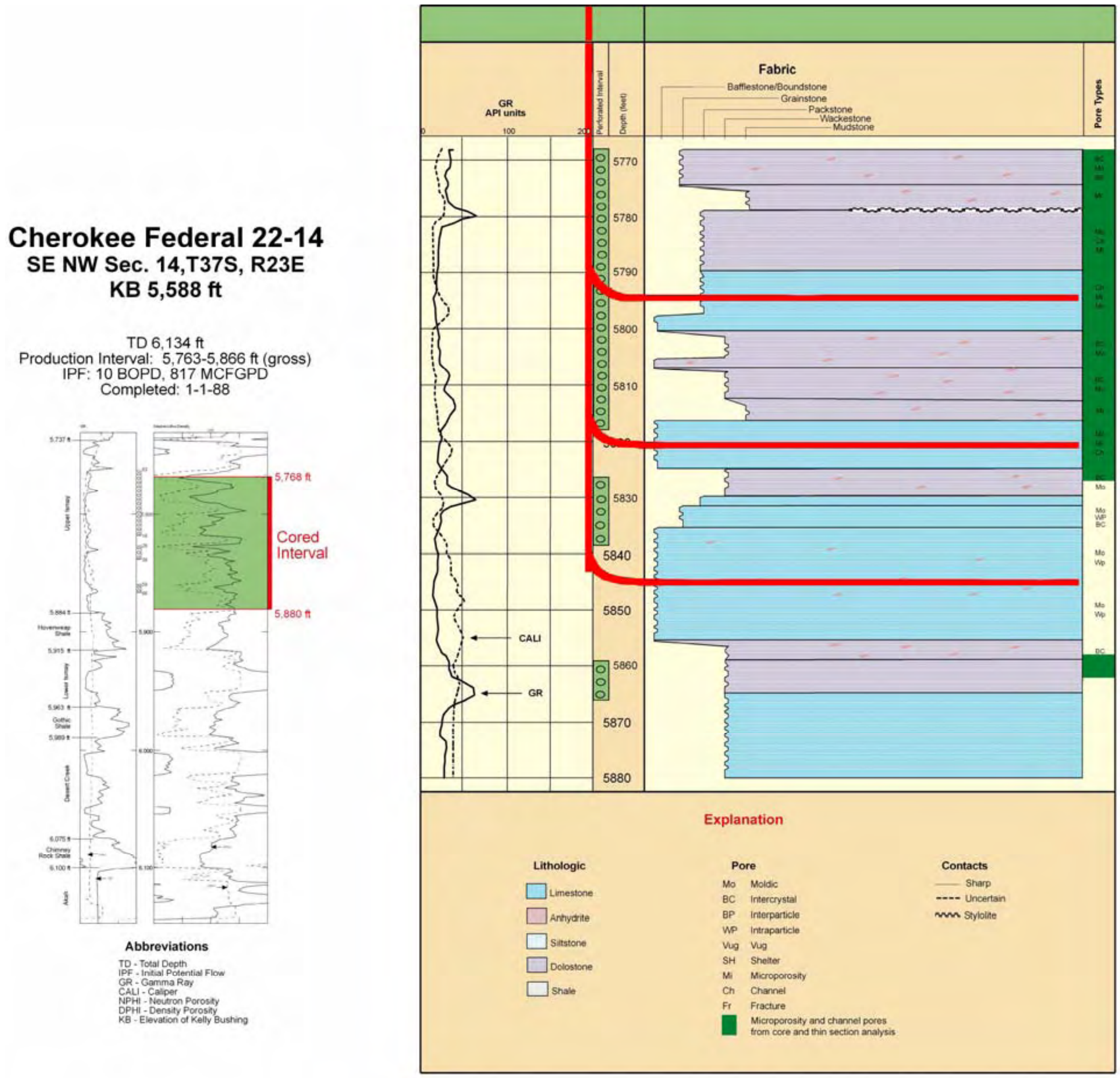

Figure 11-16. Alternative 4 - combination of medium and short radius laterals (up to three laterals) targeting limestones, shown on core description, displaying carbonate fabrics and pore types, for the Cherokee Federal No. 22-14 well.

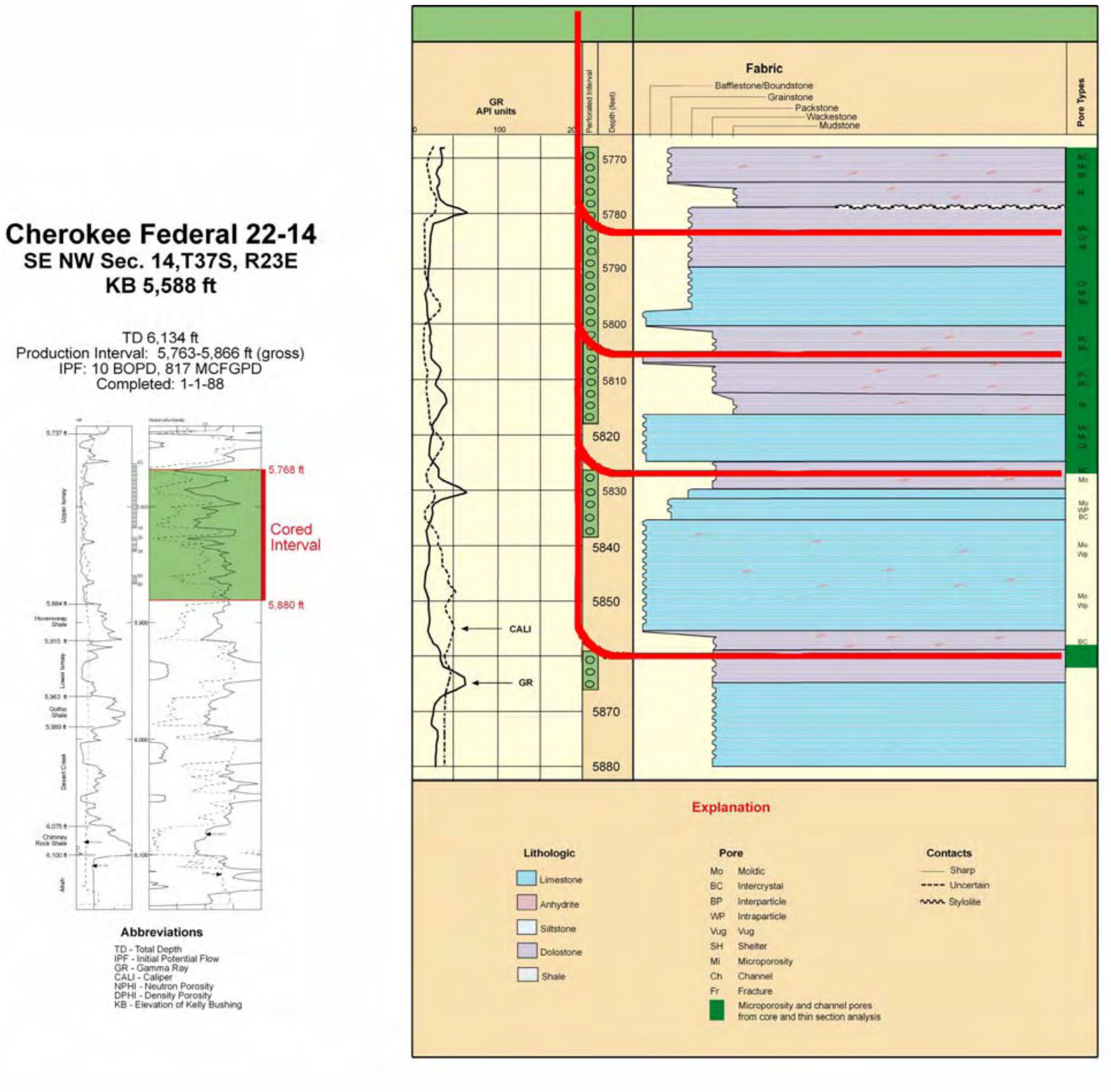

Figure 11-17. Alternative 5 - combination of medium and short radius laterals (up to four laterals) targeting dolomites, shown on core description, displaying carbonate fabrics and pore types, for the Cherokee Federal No. 22-14 well.

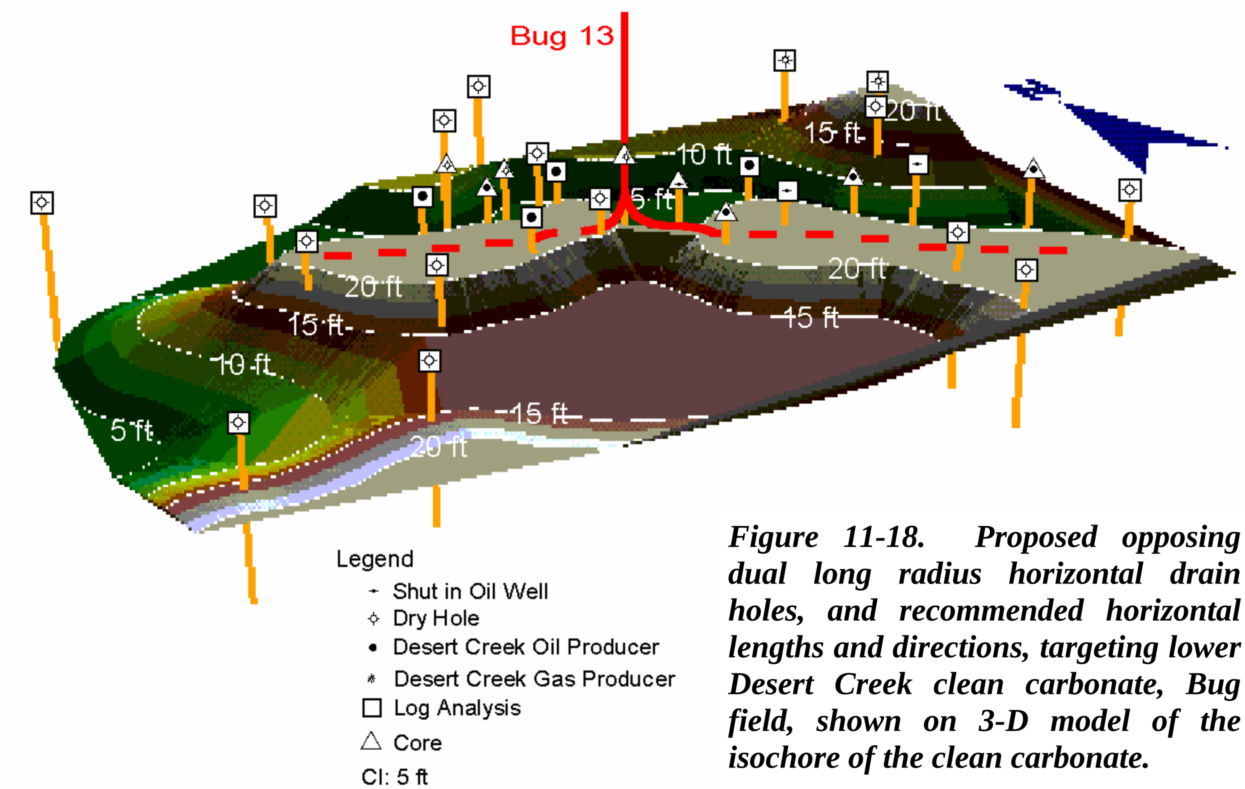

Figure 11-18. Proposed opposing dual long radius horizontal drain holes, and recommended horizontal lengths and directions, targeting lower Desert Creek clean carbonate, Bug field, shown on 3-D model of the isochore of the clean carbonate.

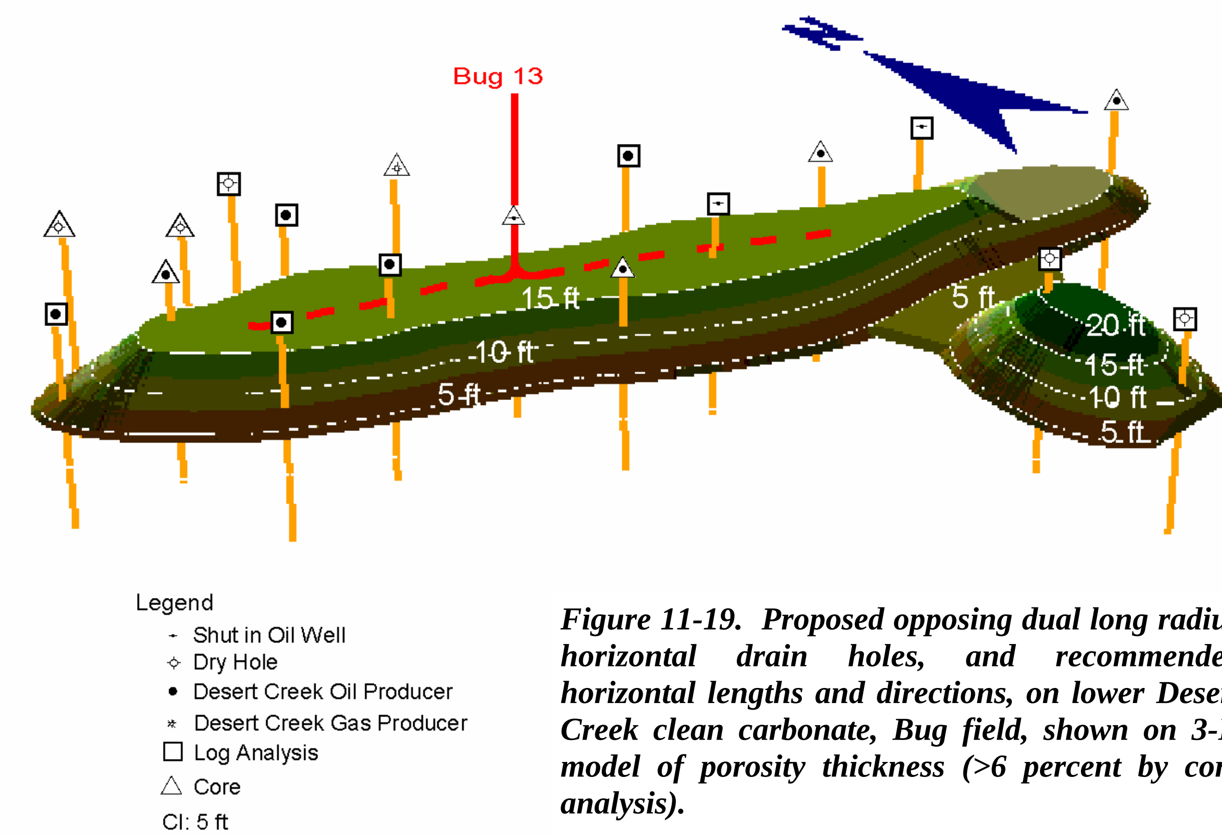

Figure 11-19. Proposed opposing dual long radius horizontal drain holes, and recommended horizontal lengths and directions, on lower Desert Creek clean carbonate, Bug field, shown on 3-D model of porosity thickness (>6 percent by core analysis).

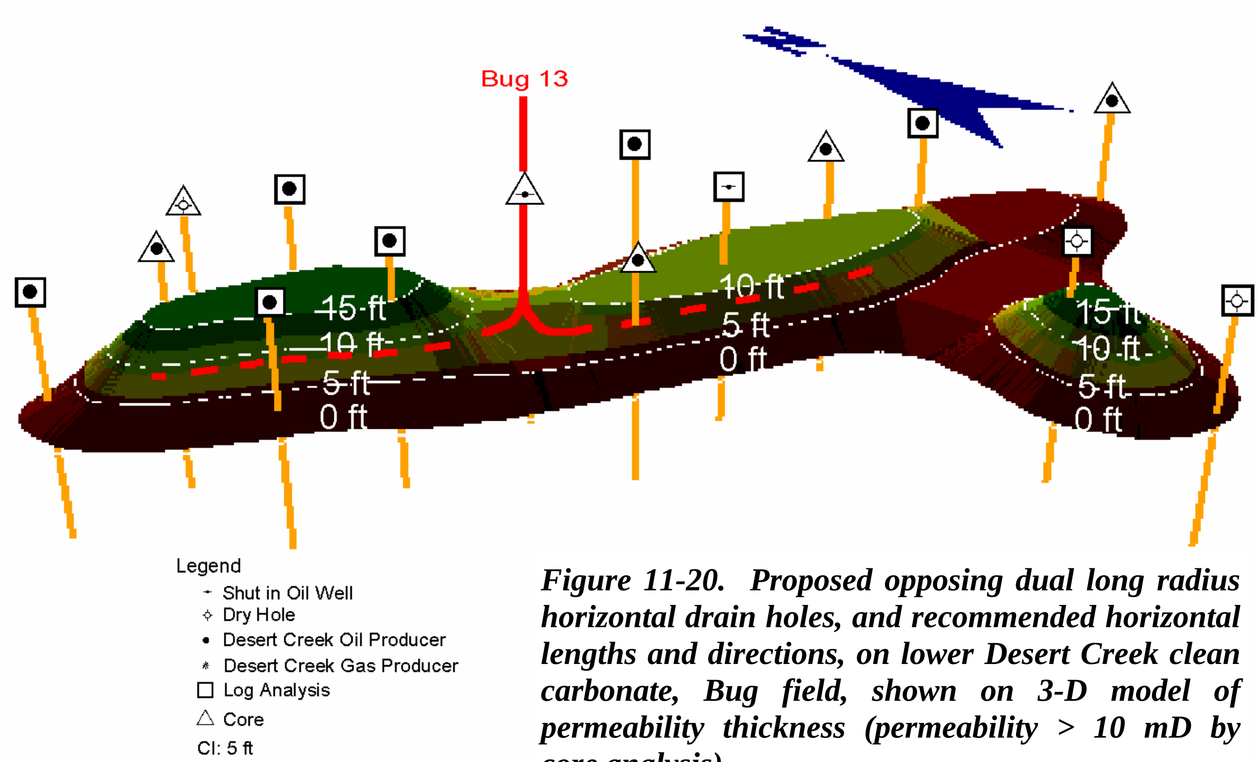

Figure 11-20. Proposed opposing dual long radius horizontal drain holes, and recommended horizontal lengths and directions, on lower Desert Creek clean carbonate, Bug field, shown on 3-D model of permeability thickness (permeability > 10 mD by core analysis).

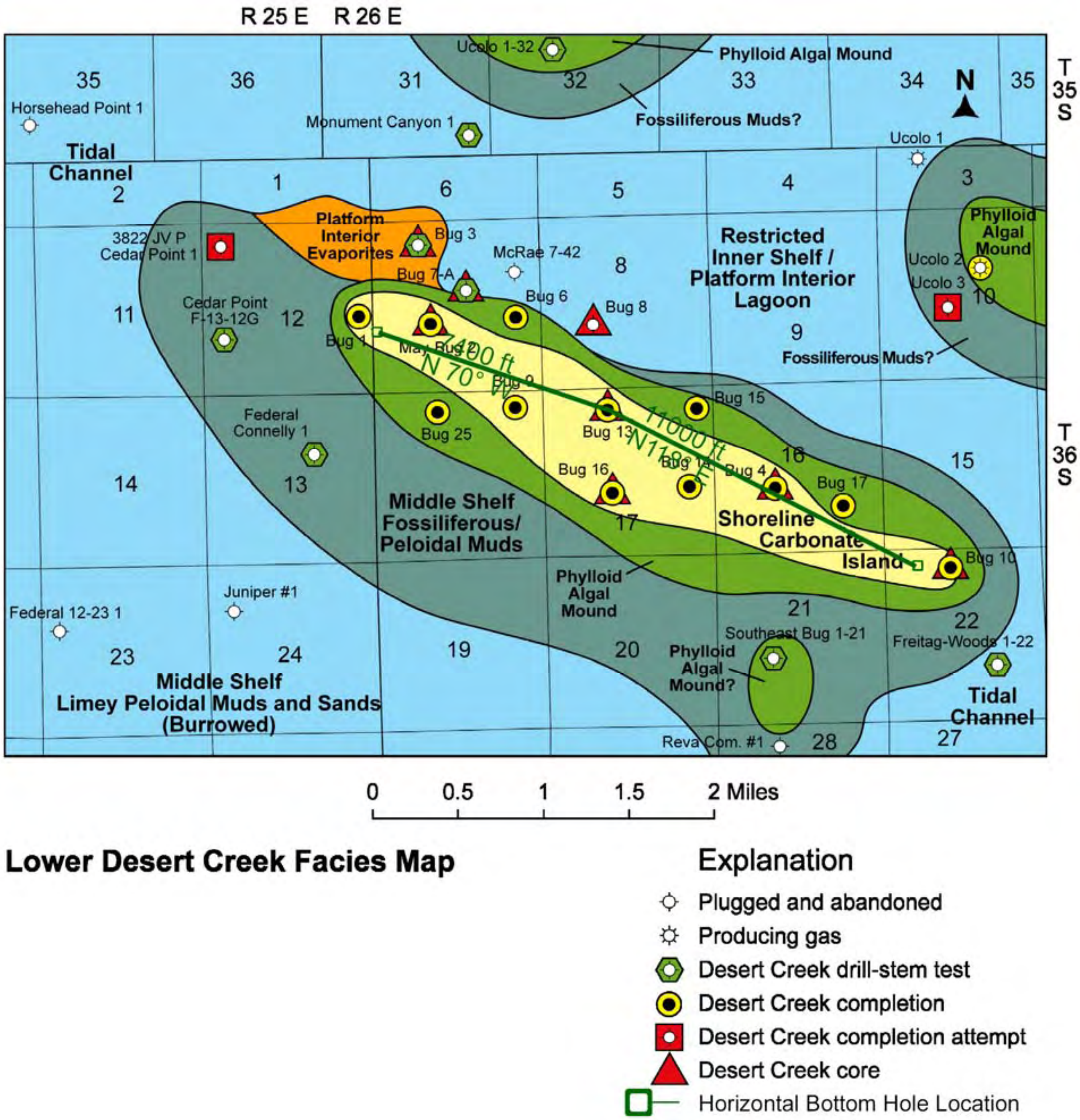

Figure 11-21. Proposed opposing dual long radius horizontal drain holes, and recommended horizontal lengths and directions, Bug field, shown on lower Desert Creek lithofacies map.

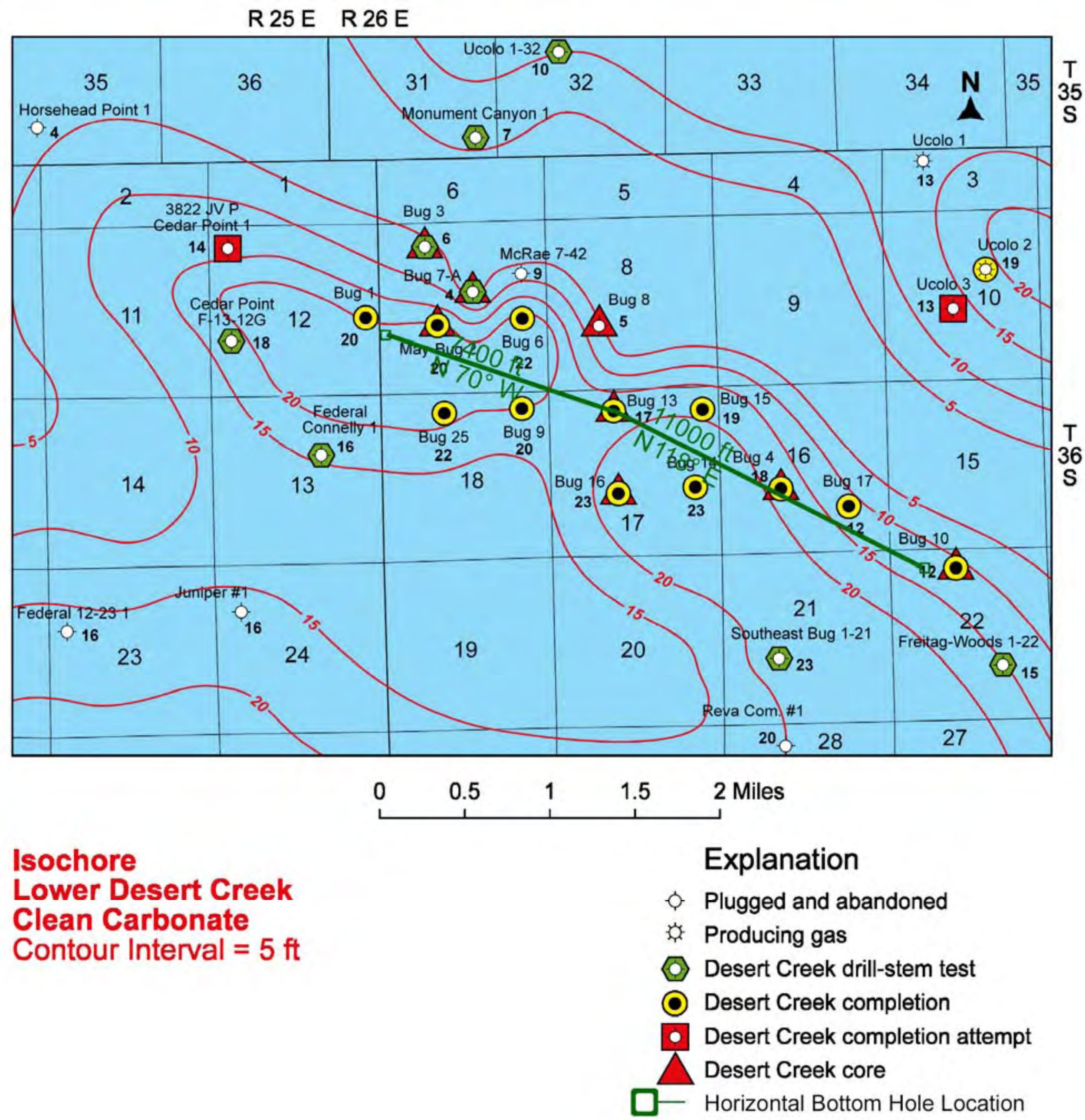

Figure 11-22. Proposed opposing dual long radius horizontal drain holes, and recommended horizontal lengths and directions, Bug field, shown on isochore of lower Desert Creek clean carbonate.

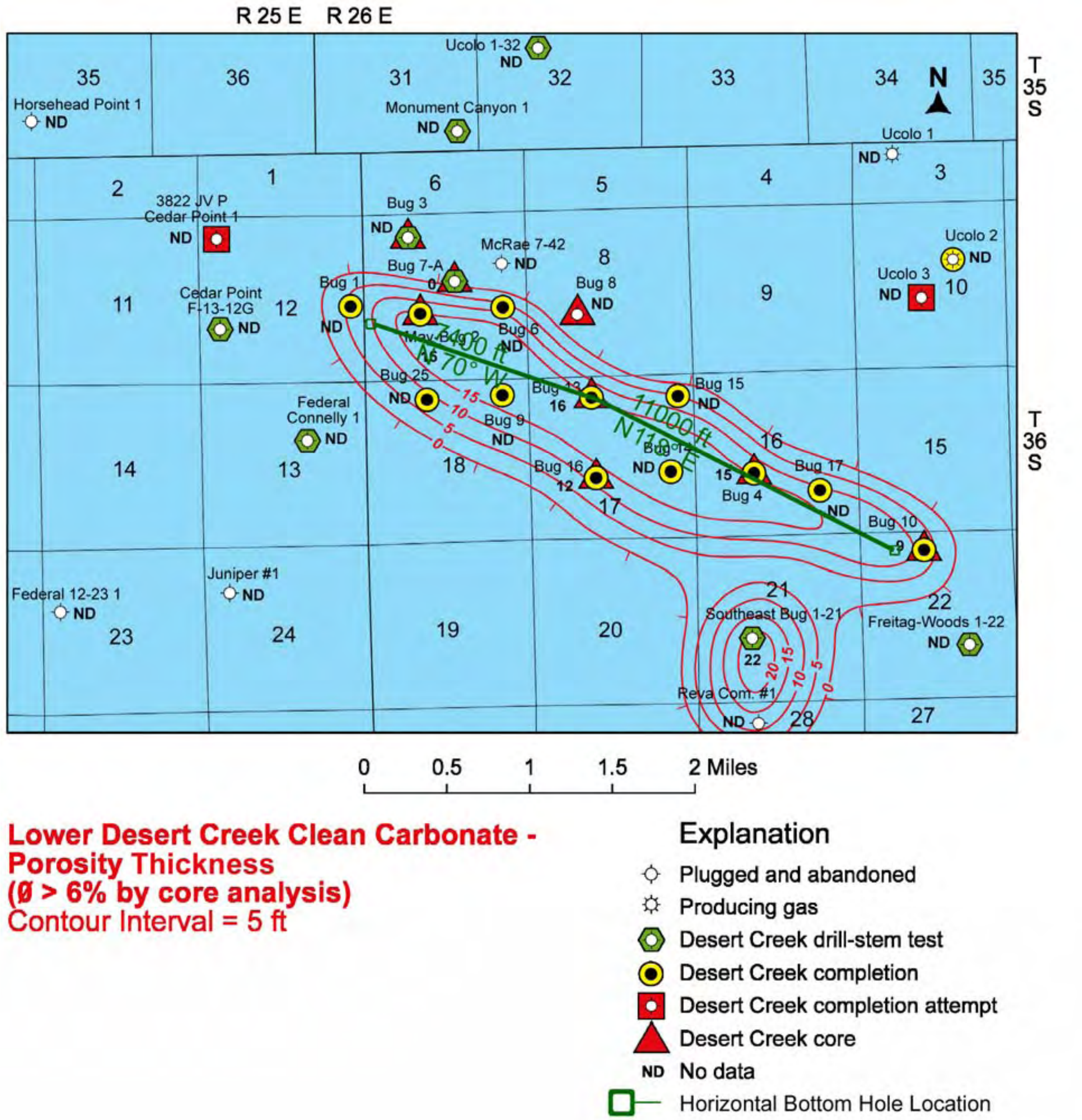

Figure 11-23. Proposed opposing dual long radius horizontal drain holes, and recommended horizontal lengths and directions, Bug field, shown on lower Desert Creek clean carbonate porosity thickness map.

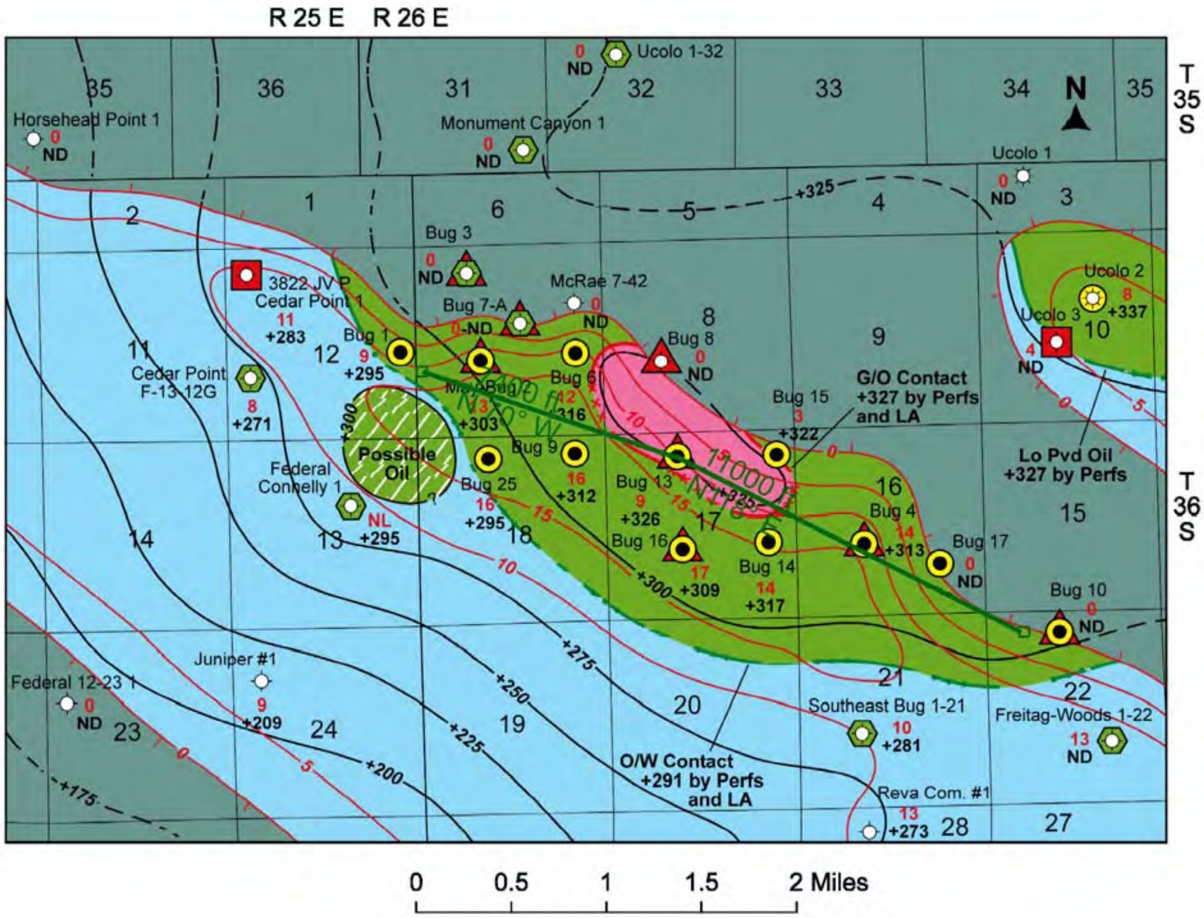

Isochore
Lower Desert Creek Mound
Contour Interval = 5 ft
Porosity > 6%

Structure Contour
Top of Lower Desert Creek Mound
Contour Interval = 25 ft
Datum = Sea Level

Explanation

- Plugged and abandoned
- Producing gas
- Desert Creek drill-stem test
- Desert Creek completion
- Desert Creek completion attempt
- Desert Creek core
- NL No neutron/density log
- ND No data
- Oil/water contact
- Gas/oil contact
- Horizontal Bottom Hole Location
- Gas
- Oil
- Off-mound
- Mound/clean carbonate

Figure 11-24. Proposed opposing dual long radius horizontal drain holes, and recommended horizontal lengths and directions, Bug field, shown on map of combined top of structure and isochore of lower Desert Creek zone mound, Bug field.

CHAPTER XII
SUMMARY AND CONCLUSIONS

Thomas C. Chidsey, Jr.,
Utah Geological Survey

The Paradox Basin of Utah, Colorado, Arizona, and New Mexico contains nearly 100 small oil fields producing from carbonate buildups within the Pennsylvanian (Desmoinesian) Paradox Formation. These fields typically have one to 10 wells with primary production ranging from 700,000 to 2,000,000 barrels (111,300-318,000 m^3) of oil per field and a 15 to 20 percent recovery rate of original oil in place. At least 200 million barrels (31.8 million m^3) of oil will not be recovered from these small fields because of inefficient recovery practices and undrained heterogeneous reservoirs.

The two main producing zones of the Paradox Formation are informally named the Ismay and the Desert Creek. The Ismay zone is dominantly limestone, comprising small, equant buildups of phylloid-algal material; locally variable, inner-shelf, skeletal calcarenites; rare, open-marine, bryozoan mounds; and anhydrite caps. The Ismay produces oil from fields in the southern Blanding sub-basin. The Desert Creek zone is dominantly dolomite, comprising regional, nearshore, shoreline trends with highly aligned, linear lithofacies tracts. The Desert Creek produces oil in fields in the central Blanding sub-basin. Both the Ismay and Desert Creek buildups generally trend northwest-southeast. Various lithofacies changes and extensive diagenesis have created complex reservoir heterogeneity within these two diverse zones.

Four case-study fields were selected for local-scale reservoir characterization and evaluation during Budget Period I of the project: Bug field, San Juan County, Utah in the Desert Creek trend, and Cherokee, San Juan County, Utah, and Little Ute and Sleeping Ute fields, Montezuma County, Colorado, in the Ismay trend. Geological characterization on a local scale focused on reservoir heterogeneity, quality, and lateral continuity, as well as possible reservoir compartmentalization, within these fields. This study utilized representative cores, geophysical logs, and thin sections to characterize and grade each field's potential for drilling horizontal laterals from existing development wells.

The project's primary objective was to enhance domestic petroleum production by demonstration and transfer of horizontal drilling technology in the Paradox Basin. If this project demonstrated technical and economic feasibility, then the technique could be applied to approximately 100 additional small fields in the Paradox Basin alone, and result in increased recovery of 25 to 50 million barrels (4-8 million m^3) of oil. Based on our evaluations, we choose the best candidate fields for pilot demonstration projects to drill horizontally from existing vertical wells, monitor well performance, and report associated validation activities. The two case-study fields were Cherokee field, operated by our industry partner Seeley Oil Company, and Bug field, operated by Wexpro Company. Our work indicated that horizontal wells drilled from existing vertical wells in each field would likely encounter unproduced oil reserves, and could be done economically. Both operators elected not to participate in the demonstration project (Budget Period II) citing limited drilling budgets and commitments elsewhere as the primary reasons for their decisions.

The UGS conducted an aggressive promotion program to offer other operators the opportunity to participate in the project demonstration to drill a lateral(s) from an existing vertical well(s) or new horizontal well(s) in the Ismay and Desert Creek zones of Paradox Basin fields in Utah or Colorado. Although the UGS received numerous inquires about the offer from other operators, none followed up with a proposal. Finally, the UGS and DOE elected to terminate the project without the benefit of the field horizontal drilling demonstration. However, the results of the various project studies can be applied to similar fields elsewhere in the Paradox Basin and the Rocky Mountain region, the Michigan and Illinois Basins, and the Midcontinent region.

Regional Lithofacies Evaluation

1. The depositional environments of the Ismay and Desert Creek zones, based on the core descriptions, show that the controlling factors were water depth, salinity, prevailing wave energy, and, in the case of phylloid-algal growth, paleostructural position. Lithofacies from the middle shelf, principally the phylloid-algal mounds, form the dominant producing reservoirs in the Ismay and Desert Creek zones.

2. Examination of upper Ismay cores identified seven depositional lithofacies: open marine, middle shelf, inner shelf/tidal flat, bryozoan mounds, phylloid-algal mounds, quartz sand dunes, and anhydritic salinas. Lower Desert Creek lithofacies include open marine, middle shelf, proto-mounds/collapse breccia, and phylloid-algal mounds.

3. A grid of regional log cross sections within the Utah portion of the Blanding sub-basin shows the development of “clean carbonate” packages which contain all of the productive reservoir lithofacies. These clean carbonates abruptly change laterally into thick anhydrite packages. Isochore maps of the upper Ismay clean carbonates and the locally thick anhydrites are consistent with a broad carbonate shelf containing several small intra-shelf basins. The intra-shelf basin centers filled with anhydrite following carbonate sedimentation on the remainder of the carbonate shelf.

4. Mapping the upper Ismay zone lithofacies into two intervals (upper and lower parts) delineated very prospective reservoir trends that contain porous, productive buildups. The mapped lithofacies trends clearly define anhydrite-filled intra-shelf basins. Intra-shelf basins are not present in the lower Desert Creek zone of the Blanding sub-basin.

Case-Study Fields

1. The log-based correlation scheme developed for the project ties the typical, vertical, core-derived sequence or cycle of depositional lithofacies from Cherokee and Bug case-study fields to their corresponding gamma-ray and neutron-density curves from geophysical well logs. The correlation scheme identifies major zone contacts, seals or barriers, baffles, producing or potential reservoirs, and depositional lithofacies. Seals or barriers include anhydrite layers and shales. Baffles are those rock units that restrict fluid flow in some parts of the field, but may develop enough porosity and permeability in other parts through diagenetic processes or lithofacies changes to provide a conduit for fluid flow or even oil storage. In Cherokee field for example, six porosity units were identified in the upper Ismay zone. In Bug field, the porosity unit is the entire Desert Creek mound. However, geophysical logs often exhibit a "false porosity" for some units, which led to wasteful

completion attempts. The cores reveal these zones to actually represent barriers or baffles to fluid flow. Log-defined units with real porosity represent potential targets for horizontal drilling.

2. The typical vertical sequence or lithofacies from the case-study fields, as determined from conventional core and tied to its corresponding log response, helped identify reservoir and non-reservoir rock (such as false porosity zones on geophysical well logs) and determine potential units suitable for horizontal drilling projects.

3. Structure contour maps on the top of the Ismay Desert Creek zones, and seals such as the Chimney Rock shale, and isochore maps of various units of the Ismay and lower Desert Creek for case-study fields show carbonate buildup trends, lithofacies distribution, defined limits of field potential, and also indicated possible horizontal drilling targets.

4. The diagenetic fabrics and porosity types found in the various hydrocarbon-bearing rocks of the case-study fields are indicators of reservoir flow capacity, storage capacity, and potential for horizontal drilling. The reservoir quality of these fields has been affected by multiple generations of dissolution, anhydrite plugging, and various types of cementation, which act as barriers or baffles to fluid flow. The most significant and unique diagenetic characteristic observed in thin sections from Cherokee field was intense, late-stage microporosity development along hydrothermal solution fronts. This late-stage diagenetic overprint is not present in the Little Ute and Sleeping Ute fields of Colorado. The thin sections from Bug field show extensive, early-stage micro-boxwork porosity due to dissolution related to subaerial exposure of the carbonate buildup.

5. Based on cross plots of permeability and porosity data, the reservoir quality of the rocks in the case-study fields is most dependent on pore types and diagenesis; in the Colorado fields quality depends on lithofacies as well.

Scanning Electron Microscopy and Pore Casting

1. Scanning electron microscope and/or pore casting analyses helped disclose the diagenetic fabrics and porosity types found in the various hydrocarbon-bearing rocks of Cherokee and Bug fields.

2. All samples exhibit microporosity in the form of intercrystalline (primarily in Cherokee field) or micro-boxwork porosity (primarily in Bug field). Dissolution has contributed to porosity in most samples. It has created moldic, vuggy, and channel porosity. All samples contain dolomite. Anhydrite, calcite, smectite clays, and pyrobitumen are present in some samples. The dominant cement occluding porosity and permeability in the Cherokee wells is anhydrite.

3. The general diagenetic sequence for these samples, based on SEM and pore casting analyses, is: (1) deposition of calcite cement, (2) dissolution, (3) dolomitization, (4) dissolution, (5) fracturing, (6) calcite cementation, (7) quartz cementation, (8) clay deposition, (9) anhydrite cementation, and (10) pyrobitumen emplacement.

Epifluorescence Analysis

1. Epifluorescence petrography makes it possible to clearly identify grain types and shapes, within both limestone and dolomite reservoir intervals in upper Ismay zone thin sections from cores examined in this study. In particular, identification of peloids, skeletal grain types, and coated grains is easy in rocks where these grains have been poorly preserved, partially leached, or completely dolomitized.

2. Depositional textures that are frequently occult or poorly preserved can often be clearly distinguished using blue-light EF microscopy. In many of the microporous limestones and finely crystalline dolomites of the upper Ismay reservoir at Cherokee field, the differences between muddy and calcarenitic fabrics can only be clearly appreciated with fluorescence lighting.

3. Epifluorescence petrography clearly and rapidly images pore spaces that cannot otherwise be seen in standard viewing under transmitted polarized lighting. In addition, the cross-sectional size and shape of pores are easy to determine.

4. Much of the upper Ismay zone porosity is very heterogeneous and poorly connected as viewed under EF. In particular, microporosity within some of the upper Ismay reservoir section in Cherokee field can be resolved much more clearly than with transmitted polarized lighting. The EF examination helps in seeing the dissolution origin of most types of the microporosity. Transmitted polarized lighting does not image microporosity in carbonate samples very well, even though blue-dyed epoxy can be impregnated into even very small pores. This porosity does not show up very well because the pores are much smaller than the thickness of the thin section, hence carbonate crystallites on either side of micropores are seen rather than the pores. In addition, opaque bitumen linings prevent light from passing through some of the pores to the observer. Without the aid of the EF view, the amount of visible open pore space would be underestimated in the plane-light image.

5. Where dolomitization has occurred, EF petrography often shows the crystal size, shape, and zonation far better than transmitted plane or polarized lighting. This information is often very useful when considering the origin and timing of dolomitization as well as evaluating the quality of the pore system within the dolomite.

6. Permeability differences within these dolomite and limestone samples are also easy to image because of the differential oil saturations between the tighter areas and the more permeable lithologies. Low-permeability carbonates from this study area show bright yellow fluorescence due to trapped live oil that is retained within tighter parts of the reservoir system. More permeable rocks show red fluorescence due to the epoxy fluorescence where oil has almost completely drained from the better quality portions of the reservoir.

7. Fluorescence of dense, “muddy” limestone and dolomite containing abundant, closely spaced, wispy stylolite seams often reveals some very interesting textural and porosity

information. Under plane transmitted light, these types of samples appear to be a dense lime mudstone whereas EF examination clearly shows distinct grain-supported peloids. More importantly, EF frequently reveals small compartments of good porosity separated from much tighter rocks by subhorizontal stylolitic seams. Hence, some of the stylolites and wispy seams with concentrations of insoluble residues act as barriers to vertical fluid flow between the porous compartments. Epifluorescence also suggests that the origin of the porosity may be related to dissolution of the peloidal limestone matrix after the formation of the stylolites.

Cathodoluminescence Analysis

1. Examination of upper Ismay limestones and lower Desert Creek dolomites under CL makes it possible to more clearly identify grain types and shapes, early cements (such as botryoidal, fibrous marine, bladed calcite cements), and brecciated phylloid-algal mound fabrics. In addition, identification of pelleted fabrics in muds, as well as various types of skeletal grains, is improved by CL examination in rocks where these grains have been poorly preserved, partially leached, or completely dolomitized. In many ways, CL imaging of samples nicely complements the types of information derived from EF of carbonate thin sections.

2. Cathodoluminescence imaging clearly and rapidly images pore spaces that cannot be easily seen in standard viewing under transmitted, plane-polarized lighting. In addition, the cross sectional size, shape, and boundaries of pores are easy to determine. This information is often very useful when considering the origin and timing of dolomitization as well as evaluating the quality of the pore system within the dolomite.

3. Imaging of microfractures as well as dissolution along microstylolites, is greatly facilitated under CL. Many open microfractures cannot be easily seen in a normal 3-µm–thick petrographic thin section, especially within dense, lower Desert Creek dolomites. Routine CL examination of the same thin section often reveals the presence of individual microfractures or microfracture swarms.

4. Examination of saddle dolomites, when present within the clean carbonate intervals of the upper Ismay or lower Desert Creek interval, can provide more information about these late, elevated temperate (often hydrothermal) mineral phases. For instance, saddle dolomites from the Cherokee Federal No. 22-14 well showed nice growth banding. They also exhibited the difference between replacement and cement types of saddle dolomites under CL.

Isotope Geochemistry

1. Diagenesis is the main control on the quality of Ismay and Desert Creek reservoirs. Much of the porosity development occurred in a mesogenetic (burial) setting, mostly post-dating stylolitization. Maximum porosity is developed as dissolution adjacent to stylolites, especially in phylloid-algal mounds. It is likely that most of the carbonates present within the Ismay zone (as well as throughout the lower Desert Creek) have retained a marine-

influenced isotope geochemistry through marine cementation as well as post-burial recycling of marine carbonate components during dolomitization, stylolitization, dissolution, and late cementation. Such an explanation agrees with the model for the positive carbon isotope values of many ancient carbonates.

2. Carbon isotopic compositions for Bug field dolomite samples have a mean value of +4.43‰ PDB. Despite dolomitization, all of the lower Desert Creek samples from Bug field show carbon isotope compositions that are very close in value to modern marine carbonates and Holocene botryoidal marine aragonite cements.

3. The carbon isotope geochemistry of all of the lower Desert Creek dolomites at Bug field has retained a strong influence from Pennsylvanian marine water composition. Meteoric waters do not appear to have had any effect on the composition of these lower Desert Creek dolomites.

4. Oxygen isotopic compositions for the Bug field dolomite samples have a mean value of -4.51‰ PDB. The lighter oxygen values obtained from wells located along the margins or flanks of Bug field may be indicative of exposure to higher temperatures, to fluids depleted in ^{18}O relative to sea water, or to hypersaline waters during burial diagenesis.

5. The wells in Bug field with the lightest oxygen isotope compositions in the lower Desert Creek dolomites have produced significantly greater amounts of hydrocarbons.

6. Carbon isotopic compositions for the upper Ismay dolomite samples at Cherokee field have a mean value of +4.70‰ PDB. As with the Bug field dolomite samples, the Cherokee field carbonates fall within the same range of carbon isotope compositions as modern marine sediments, skeletons, and marine cements. It does not appear that meteoric waters, which typically would precipitate carbonates with more depleted carbon isotope values, have had major effects on the composition of the Ismay carbonate components.

7. Oxygen isotopic compositions for the Cherokee field limestone and dolomite samples form a wide range of values around a mean value of -4.20‰ PDB. There is no significant difference between the oxygen isotope compositions from lower Desert Creek dolomite samples in Bug field and the upper Ismay limestones and dolomites from Cherokee field.

8. One of the dolomitized samples in Cherokee field, from cryptalgal laminites, has a much lighter oxygen composition. The depleted del ^{18}O value of this one dolomite sample suggests neomorphism, cementation, and/or dolomitization from warm or isotopically light subsurface waters.

9. Carbon isotopic compositions for upper Ismay limestone samples in the cemented buildup of Patterson Canyon field have a mean value of +5.43‰ PDB. However, the samples can be divided into two populations with regard to carbon isotopic composition: isotopically heavier mound cemented and isotopically lighter oolite and cement bands.

10. Mound cements were confined to a “closed hydrologic system” that allowed a fluid with

heavier carbon to evolve. The oolite and cement bands therein may have been in a more open system allowing water exchange such that waters with a composition slightly lighter were involved in the lithification and diagenesis of the capping oolite.

11. Oxygen isotopic compositions for upper Ismay limestone samples of the cemented buildup in Patterson Canyon field have a mean value of –5.48‰ PDB, lighter than Bug and Cherokee samples.

12. The oxygen isotope signatures indicate waters with depleted ^{18}O characteristics evolved in the mound cavities and ooid grainstone pores, without any influence by hypersaline waters. Alternatively, the limestones in this sample set may have all been modified via neomorphism by isotopically light subsurface waters.

Capillary Pressure /Mercury Injection Analysis

1. Capillary pressure/mercury injection analyses were used to assess reservoir potential and quality in Cherokee and Bug fields by: (1) determining the most effective pore systems for oil storage versus drainage, (2) identifying reservoir heterogeneity, (3) predicting potential untested compartments, (4) inferring porosity and permeability trends, and (5) matching diagenetic processes, pore types, mineralogy, and other attributes to porosity and permeability distribution.

2. The pore-throat-radius histogram for both the Cherokee No. 22-14 and Cherokee No. 33-14 wells, shows that half of the pore size distribution falls under 2.0 microns or in the microporosity realm. The saturation profiles for both wells show that a relatively high injection pressure is required to occupy more than the last 70 percent of the pores. The Cherokee No. 33-14 well has a steeper saturation profile than the Cherokee No. 22-14 indicating a greater amount of microporosity and thus, a high potential for untapped reserves.

3. The pore-throat-radius histograms for Bug field show that some zones likely have significant microporosity (micro-boxwork porosity), while other zones are dominated by moldic porosity. Steeper saturation profiles for Bug field indicate a significant amount of micro-boxwork porosity and excellent targets for horizontal drilling.

Production Analysis

1. Production "sweet spots" and potential horizontal drilling candidates were identified for Cherokee and Bug fields. In Cherokee field, the highest IFPs as well as the largest volumes of oil and gas produced are from wells located on the crest of the structural nose where the upper Ismay zone buildup developed and in the thickest part of the mound facies. These wells penetrated both the phylloid-algal mound and the crinoid/fusulinid-bearing, carbonate sand facies of the carbonate buildup where there may be a thick section of microporosity. This unique pore type represents the greatest hydrocarbon storage capacity and potential horizontal drilling target in the field.

2. In Bug field, the highest IFPs and largest volumes of oil were recorded from wells located structurally downdip from the updip porosity pinch out that forms the trap, and in the main part of the lower Desert Creek zone carbonate buildup. These wells penetrated both the phylloid-algal mound and the shoreline carbonate island facies where significant micro-boxwork porosity has likely developed - the diagenetic pore type with the greatest hydrocarbon storage and flow capacity in this dolomitized reservoir.

Three-Dimensional Modeling and Reserve Calculations

1. The 3-D models were created using ESRI ArcView® 3D Analyst. Structure, isochore, and other reservoir property contour maps were digitized using AutoCad®, then brought into ArcView®.

2. Cherokee field 3-D diagrams with structural contours on top of the upper and lower Ismay zone, upper Ismay clean carbonate, and Gothic shale show the same general southwest-dipping structural nose upon which the carbonate buildup developed. The abrupt termination of the structure suggests the possible presence of a northwest-southeast-trending normal fault where late-stage microporosity may have developed.

3. Two anhydrite units in the upper Ismay zone display a similar west-northwest to east-southeast linear trend as the Hovenweap and Gothic shales at Cherokee field. Cherokee wells that contain phylloid-algal buildups lie along the edge of thick anhydrite and follow the regional upper Ismay lithofacies pattern where intrashelf basins are the locations of thick anhydrite accumulations. Phylloid-algal buildups developed on inner shelf and tidal flats within curvilinear bands that rim the intrashelf basins.

4. The 3-D models of the thickness of the entire Ismay zone, upper Ismay, lower Ismay, and upper Ismay clean carbonate at Cherokee field, display a general west-northwest to east-southeast trend punctuated by elongate to slightly equant thick areas. Five reservoir porosity units with porosity greater than 6 percent are present in the upper Ismay mound separated by low-porosity/permeability barriers. These high-porosity units represent the phylloid-algal buildups and, typical of the upper Ismay trend in the Blanding sub-basin, are viewed in 3-D as small equant-shaped pods. Porosity unit 5 is the largest and most likely the major production contributor, as well as holding the bulk of the remaining reserves. The 3-D thickness diagrams suggest all five porosity units have an untested northeastern area.

5. The 3-D thickness of net feet of limestone and dolomite show a large buildup of both limestone adjacent to and dolomite within Cherokee field. Characteristic of the Ismay zone in the Blanding sub-basin, limestone is the dominant lithology. However, there is an unusual amount of dolomite present. In both cases, a carbonate buildup continues northeast of the present field wells.

6. Bug field 3-D diagrams with structural contours on top of the Desert Creek zone, lower Desert Creek mound, lower Desert Creek clean carbonate, and Chimney Rock shale each show southwest regional dip and a subtle, elongate, northwest-southeast-trending anticline.

7. A 3-D model of the entire thickness of the Desert Creek zone at Bug field like wise displays the same general northwest-southeast trend, as do the structural diagrams, with elongate thin and thick areas. The 3-D models of the thickness of the lower Desert Creek clean carbonate and mound core display an elongate, northwest-southeast-trending carbonate buildup depicting the typical, nearshore, shoreline-linear facies tracts of the Desert Creek zone in the northern Blanding sub-basin.

8. The 3-D diagrams of the lower Desert Creek clean carbonate with log-derived net feet of porosity greater than 10 and 12 percent show an elongate reservoir buildup with two subsidiary thick areas separated by a slightly thinner saddle that may represent an intermound trough. In both diagrams, the porosity pinches out along the northeast flank of the buildup, which, when combined with the coincident anticlinal structure on the top of the lower Desert Creek zone clean carbonate, provides a combination stratigraphic/structural trap.

9. Reservoir volumes (in acre-feet) were calculated for the Cherokee and Bug fields. Recovery factors of 20 bbls of oil (3 m^3) and 380 MCFG (11 MCFG) per acre-foot, respectively, were used for Cherokee field to determine the upper Ismay primary oil and gas recovery. The total volume of porosity units 1 through 5 is 17,522 acre-feet, and may contain over 350,000 bbls and 6.6 BCFG primary recovery. Based on these calculations, the remaining recoverable oil and gas reserves are nearly 168,000 bbls (26,700 m^3) and 3 BCFG (0.08 BCMG), suggesting the presence of additional undrained zones (microporosity). Using a price of $30/bbl and $4/MCFG, the unrisked value of the remaining recoverable reserves is over $5 million and $11 million for oil and gas, respectively.

10. Recovery factors of 41 bbls of oil (7 m^3) and 103 MCFG (3 MCFG) per acre-foot, respectively, were used for Bug field to determine the lower Desert Creek clean carbonate primary oil and gas recovery. The volume calculated for net feet of reservoir with porosity greater than 10 percent by log analysis is 99,057 acre-feet. This suggests the presence of additional undrained zones (micro-boxwork porosity). The lower Desert Creek clean carbonate may contain recoverable oil and gas reserves of nearly 2,440,000 bbls of oil (388,000 m^3) and 5.7 BCFG (0.16 MCMG). Again, using $30/bbl and $4/MCFG, the unrisked value of the remaining reserves is over $73 million and $22 million for oil and gas, respectively.

Horizontal Drilling Opportunities

1. With the exception of the giant Greater Aneth field, the value of horizontal drilling has not been demonstrated in any of the small shallow-shelf carbonate reservoirs in the Paradox Basin. These reservoirs are heterogeneous due to lithofacies changes and extensive diagenesis within the Ismay and Desert Creek zones leaving untapped compartments.

2. Production and injection laterals could be drilled into the porosity zones to sweep oil that vertical wells could not reach. At the well site, care collection and examination of drill samples (cuttings) during horizontal drilling operations can determine porosity types,

mineralogy, and lithofacies being drilled. These properties should be documented and accurately logged to accompany mudlogging data. Ultraviolet- and blue-light fluorescence microscopy can assist with the evaluation of oil shows while drilling the horizontal leg(s).

3. While initial production rates may be encouraging from laterals, high early declines will likely indicate the need for injection support. Half of horizontal laterals may be converted to injection to maintain reservoir pressure and maximize sweep efficiency. To obtain matrix stimulation on a multilateral well, acid must be evenly placed in each lateral. Acid must be pumped at matrix pressures and rates. Each lateral must be isolated from the other laterals.

4. Lithofacies and reservoir controls imposed by the anhydritic intra-shelf basins should be considered when selecting the optimal location and orientation of any horizontal drilling for undrained reserves, as well as identifying new exploration trends. In the Ismay zone, projections of the inner shelf/tidal flat and mound trends around the intra-shelf basins identify potential exploration targets, which could be developed using horizontal drilling techniques. Drilling horizontally from known phylloid-algal reservoirs along the inner shelf/tidal flat trend could encounter previously undrilled porous buildups. In the Desert Creek zone, drilling horizontally from productive mound lithofacies along linear shoreline trends could also encounter previously undrilled porous intervals and buildups.

5. Strategies for horizontal drilling were developed for case-study and similar fields in the Paradox Basin. All strategies involve drilling stacked, parallel horizontal laterals. Depositional lithofacies are targeted in both the Ismay and Desert Creek zones where, for example, multiple buildups can be penetrated with two opposed sets of stacked, parallel horizontal laterals. Much of the elongate, brecciated beach-mound depositional lithofacies in the Desert Creek zone of Bug field could be penetrated by opposed sets of stacked, parallel horizontal laterals. Similarly, a second strategy involves penetrating multiple zones of diagenetically enhanced reservoir intervals in these mound buildups. The microporosity in Cherokee, the micro-boxwork porosity in Bug, and the meteoric overprint at Little Ute/ Sleeping Ute fields represent important sites for untapped hydrocarbons and possible targets for horizontal drilling. The hydrothermally induced microporosity in the Ismay zone of Cherokee field does not appear to be lithofacies dependent and therefore could be drained with radially stacked, horizontal laterals and splays.

6. The UGS presented five alternative horizontal drilling recommendations to the operator of Cherokee field based on the conclusion that multiple potential Ismay intervals have not been drained due to reservoir heterogeneity, particularly to the northeast of the main field area. All alternatives would use existing vertical development wells, rather than drilling new wells, to minimize costs and surface disturbances in the environmentally sensitive areas of southeastern Utah.

7. The UGS proposed drilling opposing, dual, long-radius horizontal laterals from the center of the Bug field. These laterals would target the thickest and highest porosity and permeability in lower Desert Creek clean carbonate and would run along the length of the field, following either nearshore, shoreline trend (shoreline carbonate island) or phylloid-algal mound lithofacies.

REFERENCES

Allan, J.R., and Wiggins, W.D., 1993, Dolomite reservoirs - geochemical techniques for evaluating origin and distribution: American Association of Petroleum Geologists, Continuing Education Course Note Series 36, 129 p. (Ch-6).

Amateis, L.J., 1995, Application of sequence stratigraphic modeling to integrated reservoir management at Aneth Unit, Greater Aneth field, Utah: Society of Petroleum Engineers, SPE 030534, p. 35-49 (Ch-11).

Amateis, L.J., and Hall, S., 1997, Drilling multilaterals in a complex carbonate reservoir, Aneth field, Utah, *in* Coalson, E.B., Osmond, J.C., and Williams, E.T., editors, Innovative petroleum technology in the Rocky Mountain area: Rocky Mountain Association of Geologists Guidebook, p. 125-135 (Ch-11).

Baars, D.L., 1966, Pre-Pennsylvanian paleotectonics-key to basin evaluation and petroleum occurrences in Paradox Basin, Utah and Colorado: American Association of Petroleum Geologists Bulletin, v. 50, no. 10, p. 2082-2111 (Ch-2).

Baars, D.L., and Stevenson, G.M., 1981, Tectonic evolution of the Paradox Basin, Utah and Colorado, *in* Wiegand, D.L., editor, Geology of the Paradox Basin: Rocky Mountain Association of Geologists Guidebook, p. 23-31 (Ch-2).

---1982, Subtle stratigraphic traps in Paleozoic rocks of Paradox Basin, *in* Halbouty, M.T., editor, The deliberate search for the subtle trap: American Association of Petroleum Geologists Memoir 32, p. 131-158 (Ch-2).

Barker, C.E., and Kopp, O.C., editors, 1991, Luminescence microscopy - quantitative and qualitative aspects: Society for Sedimentary Geology (SEPM) Short Course 25 Notes, p. 1-7 (Ch-6).

Bebout, D.G., and Loucks, R.G., 1984, Handbook for logging carbonate rocks: Bureau of Economic Geology, University of Texas at Austin, Handbook 5, 43 p. (Ch-3).

Brinton, L., 1986, Deposition and diagenesis of Middle Pennsylvanian (Desmoinesian) phylloid algal banks, Paradox Formation, Ismay zone, Ismay field and San Juan Canyon, Paradox Basin, Utah and Colorado: Golden, Colorado School of Mines, M.S. thesis, 315 p. (Ch-6, Ch-7).

Budd, D.A., Hammes, U., and Ward, W.B., 2000, Cathodoluminescence in calcite cements - new insights on Pb and Zn sensitizing, Mn activation, and Fe quenching at low trace-element concentrations: Journal of Sedimentary Petrology, v. 70, p. 217-226 (Ch-6).

Burruss, R.C., 1981, Hydrocarbon fluid inclusions in studies of sedimentary diagenesis, *in* Hollister, L.S., and Crawford, M.L., editors, Fluid inclusions - applications in petrology:

Mineralogical Association of Canada Short Course Notes, v. 6, p. 138-156 (Ch-5).

---1991, Practical aspects of fluorescent microscopy of petroleum fluid inclusions, *in* Barker, C.E., and Kopp, O.C., editors, Luminescence microscopy - quantitative and qualitative aspects: Society for Sedimentary Geology (SEPM) Short Course 25 Notes, p. 1-7 (Ch-5).

Burruss, R.C., Cercone, K.R., and Harris, P.M., 1986, Timing of hydrocarbon migration - evidenced from fluid inclusions in calcite cements, tectonics and burial history, *in* Schneidermann, N., and Harris, P.M., editors, Carbonate cements: Society for Sedimentary Geology (SEPM) Special Publication 36, p. 277-289 (Ch-5).

Cander, H.S., Kauffman, J., Daniels, L.D., and Meyers, W.J., 1988, Regional dolomitization in the Burlington-Keokuk Formation (Mississippian), Illinois and Missouri - constraints from cathodoluminescent zonal stratigraphy, *in* Shukla, V., and Baker, P.A., editors, Sedimentology and geochemistry of dolostones: Society for Sedimentary Geology (SEPM) Special Publication No. 43, p. 129-144 (Ch-6).

Cannizzaro, C.R., 1985, Depositional analysis of the upper Ismay and lower Desert Creek intervals (Pennsylvanian) of the southern Paradox Basin: Troy, Rensselaer Polytechnic Institute, 85 p. (Ch-2).

Cather, M.E., Morrow, N.R., Brower, K.R., and Buckley, J.S., 1989a, Uses of epi-fluorescent microscopy in evaluation of Mesaverde tight gas sands [abs.]: American Association of Petroleum Geologists Bulletin, v. 73, p. 1150-1151 (Ch-5).

Cather, M.E., Morrow, N.R., and Klich, I., 1989b, Applications of fluorescent dye staining techniques to reservoir studies of tight gas sands, Measverde Group, southwestern Colorado [abs.]: American Association of Petroleum Geologists Bulletin, v. 73, p. 342 (Ch-5).

Cercone, K.R., and Pedone, V.A., 1987, Fluorescence (photoluminescence) of carbonate rocks - instrumental and analytical sources of observational error: Journal of Sedimentary Petrology, v. 57, p. 780-782 (Ch-5).

Chambers, M.R. 1998, Multilateral technology gains broader acceptance: O&G Journal, v. 96, no. 47, p. 47-52 (Ch-1, Ch-11).

Chidsey, T.C., Jr., compiler and editor, 2002, Increased oil production and reserves utilizing secondary/tertiary recovery techniques on small reservoirs in the Paradox Basin, Utah – final report: U.S. Department of Energy (NETL/NPTO) Oil Recovery, Field Demonstrations, Program Class II, compact disc, p. 5-2-5-6 (Ch-11).

Chidsey, T.C., Jr., Brinton, Lisë, Eby, D.E., and Hartmann, Kris, 1996a, Carbonate mound reservoirs in the Paradox Formation - an outcrop analogue along the San Juan River, southeastern Utah, *in* Huffman, A.C., Jr., Lund, W.R., and Godwin, L.H., editors, Geology and resources of the Paradox Basin: Utah Geological Association Publication 25, p. 139-156 (Ch-11).

Chidsey, T.C., Jr., and Eby, D.E., 2000, Facies of the Paradox Formation, southeastern Utah, and modern analogs - tools for exploration and development [abs.]: American Association of Petroleum Geologists, Annual Convention Program with Abstracts, v. 9, p. A26 (Ch-2).

Chidsey, T.C., Jr., Eby, D.E., and Lorenz, D.M., 1996b, Geological and reservoir characterization of small shallow-shelf fields, southern Paradox Basin, Utah, *in* Huffman, A.C., Jr., Lund, W.R., and Godwin, L.H., editors, Geology and resources of the Paradox Basin: Utah Geological Association Publication 25, p. 39-56 (Ch-2).

Chidsey, T.C., Jr., Wakefield, S., Hill, B.G., and Hebertson, M., 2004, Oil and gas fields of Utah: Utah Geological Survey Map 203DM, scale 1:700,000 (Ch-1).

Choquette, P.W., and Pray, L.C., 1970, Geologic nomenclature and classification of porosity in sedimentary carbonates: American Association of Petroleum Geologists Bulletin, v. 54, no. 2, p. 207-250 (Ch-4).

Colorado Oil & Gas Conservation Commission, 2006, Colorado oil and gas information system (COGIS) - production data inquiry: Online, <oil-gas.state.co.us/cogis/ProductionSearch2.asp>, accessed May 25, 2006 (Ch-1, Ch-3).

Coniglio, M., Zheng, Q., and Carter, T.R., 2003, Dolomitization and recrystallization of Middle Silurian reefs and platformal carbonates of the Guelph Formation, Michigan Basin, southwestern Ontario: Bulletin of Canadian Petroleum Geology, v. 51, p. 177-199 (Ch-6).

Crawley-Stewart, C.L., and Riley, K.F., 1993, Cherokee, *in* Hill, B.G., and Bereskin, S.R., editors, Oil and gas fields of Utah: Utah Geological Association Publication 22, non-paginated (Ch-3, Ch-10).

Dansereau, P., and Bourque, P.A., 2001, The Neigette breccia - remnant of the West Point reef tract in the Matapedia Valley area, and witness to Late Silurian synsedimentary faulting, Gaspe Belt, Northern Appalachians, Quebec: Bulletin of Canadian Petroleum Geology, v. 49, p. 327-345 (Ch-6).

Dawson, W.C., 1988, Ismay reservoirs, Paradox Basin - diagenesis and porosity development, *in* Goolsby, S.M., and Longman, M.W., editors, Occurrence and petrophysical properties of carbonate reservoirs in the Rocky Mountain region: Rocky Mountain Association of Geologists, p. 163-174, 442-443 (Ch-7).

Denton, G.H., and Hughes, T.J., 1983, Milankovitch theory of ice ages - hypothesis of ice-sheet linkage between regional insolation and global climate: Quaternary Research, v. 20, p. 125-144 (Ch-2).

Doelling, H.H., 2000, Geology of Arches National Park, Grand County, Utah, *in* Sprinkel, D.A., Chidsey, T.C., Jr., and Anderson, P.B., editors, Geology of Utah's parks and monuments: Utah Geological Association Publication 28, p. 11-36 (Ch-2).

Dorobek, S.L., Read, J.F., Niemann, J.M., Pong, T.C., and Haralick, R.M., 1987, Image analysis of cathodoluminescence-zoned calcite cements: Journal of Sedimentary Petrology, v. 57, p. 766-770 (Ch-6).

Dravis, J.J., 1988, Deep-burial microporosity in Upper Jurassic Haynesville oolitic grainstones, East Texas: Sedimentary Geology, v. 63, p. 325-341 (Ch-5).

---1991, Carbonate petrography – update on new techniques and applications: Journal of Sedimentary Petrology, v. 61, p. 626-628 (Ch-5).

---1992, Burial dissolution in limestones and dolomites – criteria for recognition and discussion of controls: a case study approach (Pt. 1: Upper Jurassic Haynesville limestones, East Texas; Pt. 2: Devonian Upper Elk Point dolomites, western Canada): American Association of Petroleum Geologists Bulletin/Canadian Society of Petroleum Geologists Short Course Notes, Subsurface dissolution porosity in carbonates (Ch-5).

Dravis, J. J., and Yurewicz, D.A., 1985, Enhanced carbonate petrography using fluorescence microscopy: Journal of Sedimentary Petrology, v. 55, p. 795-804 (Ch-5).

Dunham, R.J., 1962, Classification of carbonate rocks according to depositional texture, *in* Ham, W.E., editor, Classification of carbonate rocks: American Association of Petroleum Geologists Memoir 1, p. 108-121 (Ch-3, Ch-4).

Eby, D.E., and Hager, R.C., 1986, Fluorescence petrology of San Andres dolomites – H.O. Mahoney lease, Wasson field, Yoakum County, Texas: Permian Basin Section, Society for Sedimentary Geology (SEPM) Publication 86-26, p. 37-38 (Ch-5).

Embry, A.R., and Klovan, J.E., 1971, A Late Devonian reef tract on northeastern Banks Island, Northwest Territories: Canadian Petroleum Geologists Bulletin, v. 19, p. 730-781 (Ch-3, Ch-4).

Environmental Systems Research Institute, Inc. (ESRI), 1998, ArcView® GIS 3.2, 3D Analyst Version 1.0 (Ch-10).

Fairchild, I.J., 1983, Chemical studies of cathodoluminescence of natural dolomites and calcites: Sedimentology, v. 30, p. 572-583 (Ch-6).

Fetzner, R.W., 1960, Pennsylvanian paleotectonics of the Colorado Plateau: American Association of Petroleum Geologists Bulletin, v. 44, no. 8, p. 1371-1413 (Ch-2).

Filippelli, G.M., and DeLaney, M.L., 1992, Quantifying cathodoluminescent intensity with an on-line camera and exposure meter: Journal of Sedimentary Petrology, v. 62, p. 724-725 (Ch-6).

Folk, R.L., 1987, Detection of organic matter in thin sections of carbonate rocks using a white card: Sedimentary Geology, v. 54, p. 193-200 (Ch-5).

Frank, J.R., Carpenter, A.B., and Oglesby, T.W., 1982, Cathodoluminescence and composition of calcite cement in Taum Sauk Limestone (Upper Cambrian), southeast Missouri: Journal of Sedimentary Petrology, v. 52, p. 631-638 (Ch-6).

Frank, T.D., Lohmann, K.C., and Meyers, W.J., 1996, Chemostratigraphic significance of cathodoluminescence zoning in syntaxial cement - Mississippian Lake Valley Formation, New Mexico: Sedimentary Geology, v. 105, p. 29-50 (Ch-6).

Fritz, R.D., Horn, M.K., and Joshi, S.D., 1992, Geological aspects of horizontal drilling: American Association of Petroleum Geologists Continuing Education Course Notes Series No. 33, 563 p. (Ch-11).

Gardner, K.L., 1980, Impregnation technique using colored epoxy to define porosity in petrographic thin sections: Canadian Journal of Earth Sciences, v. 17, p. 1104-1107 (Ch-5).

Ghazal, R.L., 1978, Desert Canyon, *in* Fassett, J.E., editor, Oil and gas fields of the Four Corners area: Four Corners Geological Society, v. 1, p. 116-117 (Ch-3).

Gies, R.M., 1987, An improved method for viewing micropore systems in rocks with the polarizing microscope: Society of Petroleum Engineers Formation Evaluation, v. 2, p. 209-214 (Ch-5).

Given, R.K., and Lohmann, K.C., 1985, Derivation of the original isotopic composition of Permian marine cements: Journal of Sedimentary Petrology, v. 55, p. 430-439 (Ch-7).

---1986, Isotopic evidence for the early meteoric diagenesis of the reef facies, Permian reef complex of West Texas and New Mexico: Journal of Sedimentary Petrology, v. 56, p. 183-193 (Ch-7).

Goldstein, R.H., 1988, Cement stratigraphy of Pennsylvanian Holder Formation, Sacramento Mountains, New Mexico: American Association of Petroleum Geologists Bulletin, v. 72, p. 425-438 (Ch-6).

---1991, Practical aspects of cement stratigraphy with illustrations from Pennsylvanian limestone and sandstone, New Mexico and Kansas, *in* Barker, C.E., and Kopp, O.C., editors, Luminescence microscopy - quantitative and qualitative aspects: Society for Sedimentary Geology (SEPM) Short Course 25 Notes, p. 123-131 (Ch-6).

Gregg, J.M., and Karakus, M., 1991, A technique for successive cathodoluminescence and reflected light microscopy: Journal of Sedimentary Petrology, v. 61, p. 613-635 (Ch-6).

Guihaumou, N., Szydlowskii, N., and Padier, B., 1990, Characterization of hydrocarbon fluid inclusions by infra-red and fluorescence microspectrometry: Mineralogical Magazine, v. 54, p. 311-324 (Ch-5).

Harr, C.L., 1996, Paradox oil and gas potential of the Ute Mountain Ute Indian Reservation, *in* Huffman, A.C., Jr., Lund, W.R., and Godwin, L.H., editors, Geology of the Paradox Basin: Utah Geological Association Publication 25, p. 13-28 (Ch-1).

Harry, D.L., and Mickus, K.L., 1998, Gravity constraints on lithospheric flexure and the structure of the late Paleozoic Ouachita orogen in Arkansas and Oklahoma, south-central North America: Tectonics, v. 17, no. 2, p. 187-202 (Ch-2).

Heckel, P.H., 1977, Origin of phosphatic black shale facies in Pennsylvanian cyclothems of mid-continent North America: American Association of Petroleum Geologists Bulletin, v. 61, no. 7, p. 1045-1068 (Ch-2).

---1983, Diagenetic model for carbonate rocks in midcontinent Pennsylvanian eustatic cyclothems: Journal of Sedimentary Petrology, v. 53, p. 733-759 (Ch-2).

---1986, Sea-level curve for Pennsylvanian eustatic marine transgressive-regressive depositional cycles along midcontinent outcrop belt, North America: Geology, v. 14, p. 330-334 (Ch-2).

Hemming, N.G., Meyers, W.J., and Grams, J.C., 1989, Cathodoluminescence in diagenetic calcites - the roles of Fe and Mn as deduced from electron probe and spectrophotometric measurements: Journal of Sedimentary Petrology, v. 59, p. 404-411 (Ch-6).

Hintze, L.F., 1993, Geologic history of Utah: Brigham Young University Geology Studies Special Publication 7, 202 p. (Ch-2).

Hite, R.J., 1960, Stratigraphy of the saline facies of the Paradox Member of the Hermosa Formation of southeastern Utah and southwestern Colorado, *in* Smith, K.G., editor, Geology of the Paradox Basin fold and fault belt: Four Corners Geological Society, Third Field Conference Guidebook, p. 86-89 (Ch-2).

---1970, Shelf carbonate sedimentation controlled by salinity in the Paradox Basin, southeast Utah, *in* Ran, J.L., and Dellwig, L.F., editors, Third symposium on salt: Northern Ohio Geological Society, v. 1, p. 48-66 (Ch-2).

Hite, R.J., Anders, D.E., and Ging, T.G., 1984, Organic-rich source rocks of Pennsylvanian age in the Paradox Basin of Utah and Colorado, *in* Woodward, Jane, Meissner, F.F., and Clayton, J.L., editors, Hydrocarbon source rocks of the greater Rocky Mountain region: Rocky Mountain Association of Geologists Guidebook, p. 255-274 (Ch-2).

Hite, R.J., and Buckner, D.H., 1981, Stratigraphic correlation, facies concepts and cyclicity in Pennsylvanian rocks of the Paradox Basin, *in* Wiegand, D.L., editor, Geology of the Paradox Basin: Rocky Mountain Association of Geologists 1981 Field Conference, p. 147-159 (Ch-2).

Hite, R.J., and Cater, F.W., 1972, Pennsylvanian rocks and salt anticlines, Paradox Basin, Utah and Colorado, *in* Mallory, W.W., editor, Geologic atlas of the Rocky Mountain region: Rocky Mountain Association of Geologists Guidebook, p. 133-138 (Ch-2).

Hudson, J.D., 1975, Carbon isotopes and limestone cements: Geology, v. 3, p. 19-22 (Ch-7).

Imbrie, John, and Imbrie, J.Z., 1980, Modeling the climatic response to orbital variations: Science, v. 207, p. 943-953 (Ch-2).

James, N.P., and Ginsburg, R.N., 1979, The seaward margin of Belize barrier and atoll reefs: International Association of Sedimentologists Special Publication 3, 191 p. (Ch-7).

Jones, G.S., 1992, A geologist's perspective on horizontal drilling in a pinnacle reef, Rainbow Basin, Alberta, *in* Schmoker, J.W., Coalson, E.B., and Brown, C.A., editors, Geological studies relevant to horizontal drilling--examples from western North America: Rocky Mountain Association of Geologists Guidebook, p. 171-175 (Ch-11).

Kirby, K.C., and Tinker, S.W., 1992, The Keg River/Winnipegosis petroleum system in northeast Alberta [abs.]: American Association of Petroleum Geologists Annual Convention, Official Program with Abstracts, v. 1, p. A66 (Ch-5).

Kluth, C.F., 1986, Plate tectonics of the Ancestral Rocky Mountains: American Association of Petroleum Geologists Memoir 41, p. 353-369 (Ch-2).

Kluth, C.F., and Coney, P.J., 1981, Plate tectonics of the Ancestral Rocky Mountains: Geology, v. 9, p. 10-15 (Ch-2).

LaFlamme, A.K., 1992, Replacement dolomitization in the Upper Devonian Leduc and Swan Hills Formations, Caroline area, Alberta, Canada [abs.]: American Association of Petroleum Geologists Annual Convention, Official Program with Abstracts, v. 1, p. A70 (Ch-5).

Land, L.S., 1980, The isotopic and trace elements geochemistry of dolomite - the state of the art, *in* Zenger, D.H., Dunham, J.B., and Ethington, R.L., editors, Concepts and models of dolomitization: Society for Sedimentary Geology (SEPM) Special Publication 28, p. 87-110 (Ch-7).

---1982, Dolomitization: American Association of Petroleum Geologists Short Course Note Series No. 24, 20 p. (Ch-7).

LaVoie, D., Chi G., and Fowler, M.G., 2001, The Lower Devonian Upper Gaspe Limestones in eastern Gaspe - carbonate diagenesis and reservoir potential: Bulletin of Canadian Petroleum Geology, v. 49, p. 346-365 (Ch-5, Ch-6).

LaVoie, D., and Morin, C., 2004, Hydrothermal dolomitization in the Lower Silurian Sayabee Formation in northern Gaspe – Matapedia (Quebec) - constraint on timing of porosity and regional significance for hydrothermal reservoirs: Bulletin of Canadian Petroleum Geology, v. 52, p. 256-269 (Ch-6).

LeFever, J.A., 1992, Horizontal drilling in the Williston Basin, United States and Canada, *in* Schmoker, J.W., Coalson, E.B., and Brown, C.A., editors, Geological studies relevant to horizontal drilling--examples from western North America: Rocky Mountain Association of Geologists Guidebook, p. 177-197 (Ch-11).

Lohmann, K.C., 1983, Diagenetic history of carbonate reservoirs – integration of petrographic and geochemical techniques, *in* Wilson, J.L., Wilkinson, B.H., Lohmann, K.C., and Hurley, N.F., editors, New ideas and methods of exploration for carbonate reservoirs: Dallas Geological Society, unpaginated (Ch-7).

Machel, H.G., 2000, Application of cathodoluminescence to carbonate diagenesis, *in* Pagel, M., Barbin, V., Blanc P., and Ohnenstetter, D., editors, Cathodoluminescence in geosciences: New York, Springer, p. 271-301 (Ch-6).

Machel, H.G., and Burton, E.A., 1991, Factors governing cathodoluminescence in calcite and dolomites and their implications for studies of carbonate diagenesis, *in* Barker, C.E., and Kopp, O.C., editors, Luminescence microscopy - quantitative and qualitative aspects: Society for Sedimentary Geology (SEPM) Short Course 25 Notes, p. 37-57 (Ch-6).

Marshall, D.J., 1988, Cathodoluminescence of geological materials: Winchester, Massachusetts, Allen & Unwin, 128 p. (Ch-6).

---1991, Combined cathodoluminescence and energy dispersive spectroscopy, *in* Barker, C.E., and Kopp, O.C., editors, Luminescence microscopy - quantitative and qualitative aspects: Society for Sedimentary Geology (SEPM) Short Course 25 Notes, p. 27-36 (Ch-6).

Martin, G.W., 1983, Bug, *in* Fassett, J.E., editor, Oil and gas fields of the Four Corners area, volume III: Four Corners Geological Society, p. 1073-1077 (Ch-3).

Meyers, W.J., 1974, Carbonate cement stratigraphy of the Lake Valley Formation (Mississippian), Sacramento Mountains, New Mexico: Journal of Sedimentary Petrology, v. 44, p. 837-861 (Ch-6).

---1978, Carbonate cements: their regional distribution and interpretation in Mississippian limestones of southwestern New Mexico: Sedimentology, v. 25, p. 371-400 (Ch-6).

---1991, Cement stratigraphy - an overview, *in* Barker, C.E., and Kopp, O.C., editors, Luminescence microscopy - quantitative and qualitative aspects: Society for Sedimentary Geology (SEPM) Short Course 25 Notes, p. 133-148 (Ch-6).

Miller, J., 1988, Cathodoluminescence microscopy, *in* Tucker, M., editor, Techniques in sedimentology: Oxford, Blackwell Publications, p. 174-190 (Ch-6).

Morgan, C.D., 1992, Horizontal drilling potential of the Cane Creek Shale, Paradox Formation, Utah, *in* Schmoker, J.W., Coalson, E.B., and Brown, C.A., editors, Geological studies relevant to horizontal drilling--examples from western North America: Rocky Mountain Association of Geologists Guidebook, p. 257-265 (Ch-11).

Nuccio, V.F., and Condon, S.M., 1996, Burial and thermal history of the Paradox Basin, Utah and Colorado, and petroleum potential of the Middle Pennsylvanian Paradox Formation, *in* Huffman, A.C., Jr., Lund, W.R., and Godwin, L.H., editors, Geology of the Paradox Basin: Utah Geological Association Publication 25, p. 57-76 (Ch-2).

Ohlen, H.R., and McIntyre, L.B., 1965, Stratigraphy and tectonic features of Paradox Basin, Four Corners area: American Association of Petroleum Geologists Bulletin, v. 49, no. 11, p. 2020-2040 (Ch-2).

Oline, W.F., 1996, Bug, *in* Hill, B.G., and Bereskin, S.R., editors, Oil and gas fields of Utah: Utah Geological Association Publication 22 Addendum, non-paginated (Ch-3, Ch-10).

Parrish, J.T., 1982, Upwelling and petroleum source beds, with reference to the Paleozoic: American Association of Petroleum Geologists Bulletin, v. 66, no. 6, p. 750-774 (Ch-2).

Peterson, J.A., 1966, Stratigraphic vs. structural controls on carbonate-mound accumulation, Aneth area, Paradox Basin: American Association of Petroleum Geologists Bulletin, v. 50, no. 10, p. 2068-2081 (Ch-2).

Peterson, J.A., and Hite, R.J., 1969, Pennsylvanian evaporite-carbonate cycles and their relation to petroleum occurrence, southern Rocky Mountains: American Association of Petroleum Geologists Bulletin, v. 53, p. 884-908 (Ch-2).

Peterson, J.A., and Ohlen, H.R., 1963, Pennsylvanian shelf carbonates, Paradox Basin, *in* Bass, R.O., editor, Shelf carbonates of the Paradox Basin: Four Corners, Geological Society Symposium, 4th Field Conference, p. 65-79 (Ch-2).

Pittman, E.D., 1992, Relationship of porosity and permeability to various parameters derived from mercury injection-capillary pressure curves for sandstone: American Association of Petroleum Geologists Bulletin, v. 76, no. 2, p. 191-198 (Ch-8).

Pray, L.C., and Wray, J.L., 1963, Porous algal facies (Pennsylvanian) Honaker Trail, San Juan Canyon, Utah, *in* Bass, R.O., editor, Shelf carbonates of the Paradox Basin: Four

Corners Geological Society Guidebook, p. 204-234 (Ch-2).

Radke, B.M., and Mathis, R.L., 1980, On the formation and occurrence of saddle dolomite: Journal of Sedimentary Petrology, v. 50, p. 1149-1168 (Ch-6).

Rost, F.W.D., 1992, Fluorescence microscopy, v. 1: New York, Cambridge University Press, 253 p. (Ch-5).

Roylance, M.H., 1984, Depositional and diagenetic control of petroleum entrapment in the Desert Creek interval, Paradox Formation, southeastern Utah and southwestern Colorado: Lawrence, University of Kansas, M.S. thesis, 191 p. (Ch-2, Ch-7).

---1990, Depositional and diagenetic history of a Pennsylvanian algal-mound complex - Bug and Papoose Canyon fields, Utah and Colorado: American Association of Petroleum Geologists Bulletin, v. 74, p. 1087-1099 (Ch-7).

Scholle, P.A., and Ulmer-Scholle, D.S., 2003, A color guide to the petrography of carbonate rocks: American Association of Petroleum Geologists Bulletin Memoir 77, p. 427-440 (Ch-5, Ch-6).

Sipple, R.F., and Glover, E.D., 1965, Structures in carbonate rocks made visible by luminescence petrography: Science, v. 150, p. 1283-1287 (Ch-6).

Skinner, M.R., 1996, Carbonate microfacies and conodont biostratigraphy of the subsurface upper Ismay interval (Desmoinesian, Paradox Formation), Mustang Flat oil field, Utah: Provo, Brigham Young University, M.S. thesis, 110 p. (Ch-2).

Soeder, D.J., 1990, Applications of fluorescent microscopy to study of pores in tight rocks: American Association of Petroleum Geologists Bulletin, v. 74, p. 30-40 (Ch-5).

Stark, P.H., 1992, Perspectives on horizontal drilling in western North America, *in* Schmoker, J.W., Coalson, E.B., and Brown, C.A., editors, Geological studies relevant to horizontal drilling--examples from western North America: Rocky Mountain Association of Geologists Guidebook, p. 3-14 (Ch-11).

Stevenson, G.M., and Baars, D.L., 1986, The Paradox—a pull-apart basin of Pennsylvanian age, *in* Peterson, J.A., editor, Paleotectonics and sedimentation in the Rocky Mountain region: American Association of Petroleum Geologists Memoir 41, p. 513-539 (Ch-2).

---1987, The Paradox—a pull-apart basin of Pennsylvanian age, *in* Campbell, J.A., editor, Geology of Cataract Canyon and vicinity: Four Corners Geological Society, 10th Field Conference, p. 31-55 (Ch-2).

Teichmuller, M., and Wolf, M., 1977, Application of fluorescence microscopy in coal petrology and oil exploration: Journal of Microscopy, v. 109, p. 49-73 (Ch-5).

Utah Division of Oil, Gas and Mining, 2006, Oil and gas production report, December 2005: Online, <http://www.ogm.utah.gov/oilgas/PUBLICATIONS/Reports/PROD_book_list.htm>, accessed February 16, 2007 (Ch-9).

---2007, Oil and gas production report, August 2006: Online, <http://www.ogm.utah.gov/oilgas/PUBLICATIONS/Reports/PROD_book_list.htm>, accessed January 17, 2007 (Ch-1, Ch-3, Ch-7, Ch-10).

van Gijzel, P., 1967, Palynology and fluorescence microscopy: Reviews of Paleobotany and Palynology, v. 1, p. 49-79 (Ch-5).

Walker, G., and Burley, S., 1991, Luminescence petrography and spectroscopic studies of diagenetic minerals, *in* Barker, C.E., and Kopp, O.C., editors, Luminescence microscopy - quantitative and qualitative aspects: Society for Sedimentary Geology (SEPM) Short Course 25 Notes, p. 83-96 (Ch-6).

Wilson, J.L., 1975, Carbonate facies in geologic history: New York, Springer-Verlag, 471 p. (Ch-2).

Wood, J.R., Allan, J.R., Huntoon, J.E., Pennington, W.D., Harrison, W.B., Taylor, E., and Tester, C.J., 1996, Horizontal well taps bypassed Dundee oil in Crystal field, Michigan: Oil & Gas Journal, October, p. 60-63 (Ch-11).

Wray, L.L., Apeland, A.D., Hemborg, T., and Brchan, C., 2002, Oil and gas fields map of Colorado: Colorado Geological Survey Map Series 33, scale 1:500,000 (Ch-1).

Yanguas, J.E., and Dravis, J.J., 1985, Blue fluorescent dye technique for recognition of microporosity in sedimentary rocks: Journal of Sedimentary Petrology, v. 55, p. 600-602 (Ch-5).

APPENDIX
TECHNOLOGY TRANSFER

Project Presentations

"Class II Oil Revisit Project - Heterogeneous Shallow-Shelf Carbonate Buildups in the Blanding Sub-Basin of the Paradox Basin, Utah and Colorado: Targets for Increased Oil Production and Reserves Using Horizontal Drilling Techniques" by Laura Wray, U.S. Department of Energy, Contractors Review Meeting, Denver, Colorado, June 28, 2000.

"Heterogeneous Shallow-Shelf Carbonate Buildups in the Blanding Sub-Basin of the Paradox Basin, Utah and Colorado: Targets for Increased Oil Production and Reserves Using Horizontal Drilling Techniques" by David E. Eby, 10th Annual National Indian Energy & Minerals Conference sponsored by the Bureau of Indian Affairs, Colorado School of Mines, Golden, Colorado, June 21, 2000.

"Heterogeneous Carbonate Buildups in the Blanding Sub-Basin of the Paradox Basin, Utah and Colorado: Targets for Increased Oil Production Using Horizontal Drilling Techniques" by David E. Eby and Thomas C. Chidsey, Jr., American Association of Petroleum Geologists Annual Convention, Denver, Colorado, June 4-5, 2001.

"Heterogeneous Carbonate Buildups in the Colorado Portion of the Blanding Sub-Basin of the Paradox Basin, Colorado and Utah: Possible Targets for Increased Oil Production Using Horizontal Drilling Techniques" by Laura L. Wray, Neal DeShazo, and David E. Eby, American Association of Petroleum Geologists Annual Convention, Houston, Texas, March 12, 2002.

"Reservoir Diagenesis and Porosity Development in the Upper Ismay Zone, Pennsylvanian Paradox Formation, Cherokee Field, Utah" by Thomas C. Chidsey, Jr., and David E. Eby, American Association of Petroleum Geologists Rocky Mountain Section Meeting, Laramie, Wyoming, September 9, 2002.

"Heterogeneous Shallow-Shelf Carbonate Buildups in the Paradox Basin, Utah and Colorado: Targets for Increased Oil Production and Reserves Using Horizontal Drilling Techniques" by Thomas C. Chidsey, Jr., at a Class II Review conference sponsored by the National Energy Technology Laboratory at the Center for Energy and Economic Diversification (CEED) in Odessa, Texas, December 12, 2002.

"Regional Facies Trends in the Upper Ismay Zone of the Blanding Sub-basin of the Paradox Basin, Utah – Aids for Identifying Possible Targets for Horizontal Drilling" by David E. Eby, Thomas C. Chidsey, Jr., Craig D. Morgan, and Kevin McClure, at the AAPG annual convention, Salt Lake City, Utah, May 13, 2003.

"Heterogeneous Shallow-Shelf Carbonate Buildups in the Blanding Sub-Basin of the Paradox Basin, Utah and Colorado: Targets for Increased Oil Production & Reserves Using Horizontal Drilling Techniques" by Thomas C. Chidsey, Jr., American Association of Petroleum Geologists Student Chapter Meeting, University of Utah, Salt Lake City, Utah, January 23, 2004.

"Regional Facies Trends in the Upper Ismay Zone of the Blanding Sub-basin of the Paradox Basin, Utah" by David E. Eby, at the Society for Sedimentary Geology (SEPM), Rocky Mountain Section Luncheon Meeting, Denver, Colorado, March 30, 2004.

"Heterogeneous Shallow-Shelf Carbonate Buildups in the Blanding Sub-Basin of the Paradox Basin, Utah and Colorado: Targets for Increased Oil Production & Reserves Using Horizontal Drilling Techniques" by Thomas C. Chidsey, Jr., Moab, Utah, May 4, 2004.

Project Publications

Abstracts

Eby, D.E., and Chidsey, T.C., Jr., 2001, Heterogeneous shallow-shelf carbonate buildups in the Blanding sub-basin of the Paradox Basin, Utah and Colorado: targets for increased oil production using horizontal drilling techniques [abs.]: American Association of Petroleum Geologists Annual Convention, Official Program with Abstracts, v. 10, p. A55.

Chidsey, T.C., Jr., and Eby, D.E., 2002, Reservoir diagenesis and porosity development in the upper Ismay zone, Pennsylvanian Paradox Formation, Cherokee field, Utah [abs.]: American Association of Petroleum Geologists Rocky Mountain Section Meeting, Official Program Book p. 20-21.

Wray, L.L., DeShazo, Neal, and Eby, D.E., 2002, Heterogeneous carbonate buildups in the Colorado portion of the Blanding sub-basin of the Paradox Basin, Colorado and Utah – possible targets for increased oil production using horizontal drilling techniques [abs.]: American Association of Petroleum Geologists Annual Convention, Official Program with Abstracts, v. 11, p. A192-193.

Eby, D.E., Chidsey, T.C., Jr., Morgan, C.D., and McClure, Kevin, 2003, Regional facies trends in the upper Ismay zone of the Blanding sub-basin of the Paradox Basin, Utah – aids for identifying possible targets for horizontal drilling [abs.]: American Association of Petroleum Geologists Annual Convention, Official Program with Abstracts, v. 12, p. A48.

Eby, D.E., 2004, Regional facies trends in the upper Ismay zone of the Blanding sub-basin of the Paradox Basin, Utah [abs.]: Society for Sedimentary Geology (SEPM), Rocky Mountain Section Newsletter, v. 29, no. 6, p. 1 and 3.

Non-Technical Papers

Chidsey, T.C., Jr., 2001, Carbonate buildups in the Paradox Basin, targeted for horizontal drilling: U.S. Department of Energy, The Class Act, v. 8, no. 1, p. 3-6.

Chidsey, T.C., Jr., 2003, An up close and personal view of Cherokee oil field, San Juan County,

Utah: Utah Geological Survey, Survey Notes, v. 35, no. 2, p. 1-3.

Semi-Annual Technical Progress Reports

Chidsey, T.C., Jr., Eby, D.E., and Wray, L.L., 2001, Heterogeneous shallow-shelf carbonate buildups in the Paradox Basin, Utah and Colorado: targets for increased oil production and reserves using horizontal drilling techniques – semi-annual technical progress report for the period April 6 to September 5, 2000: U.S. Department of Energy, DOE/BC15128-1, 22 p.

Chidsey, T.C., Jr., Eby, D.E., and Wray, L.L., 2001, Heterogeneous shallow-shelf carbonate buildups in the Paradox Basin, Utah and Colorado: targets for increased oil production and reserves using horizontal drilling techniques – semi-annual technical progress report for the period September 6, 2000 to April 5, 2001: U.S. Department of Energy, DOE/BC15128-2, 24 p.

Chidsey, T.C., Jr., Eby, D.E., and Wray, L.L., 2001, Heterogeneous shallow-shelf carbonate buildups in the Paradox Basin, Utah and Colorado: targets for increased oil production and reserves using horizontal drilling techniques – semi-annual technical progress report for the period April 6 to October 5, 2001: U.S. Department of Energy, DOE/BC15128-3, 32 p.

Wray, L.L., Eby, D.E., and Chidsey, T.C., Jr., 2002, Heterogeneous shallow-shelf carbonate buildups in the Paradox Basin, Utah and Colorado: targets for increased oil production and reserves using horizontal drilling techniques – semi-annual technical progress report for the period October 6, 2001 to April 5, 2002: U.S. Department of Energy, DOE/BC15128-4, 32 p.

Chidsey, T.C., Jr., 2002, Heterogeneous shallow-shelf carbonate buildups in the Paradox Basin, Utah and Colorado: targets for increased oil production and reserves using horizontal drilling techniques – semi-annual technical progress report for the period April 6, 2002 to October 5, 2002: U.S. Department of Energy, DOE/BC15128-5, 35 p.

Eby, D.E., Chidsey, T.C., Jr., McClure, Kevin, and Morgan, C.D., 2003, Heterogeneous shallow shelf carbonate buildups in the Paradox Basin, Utah and Colorado: targets for increased oil production and reserves using horizontal drilling techniques – semi-annual technical progress report for the period October 6, 2002 to April 5, 2003: U.S. Department of Energy, DOE/BC15128-6, 29 p.

Chidsey, T.C., Jr., McClure, Kevin, Morgan, C.D., Eby, D.E., and Nelson, S.T., 2003, Heterogeneous shallow-shelf carbonate buildups in the Paradox Basin, Utah and Colorado: targets for increased oil production and reserves using horizontal drilling techniques – semi-annual technical progress report for the period April 6, 2003 to October 5, 2003: U.S. Department of Energy, DOE/BC15128-7, 40 p.

Chidsey, T.C., Jr., Wakefield, Sharon, and Eby, D.E., 2004, Heterogeneous shallow-shelf carbonate buildups in the Paradox Basin, Utah and Colorado: targets for increased oil production and reserves using horizontal drilling techniques – semi-annual technical progress report for the period October 6, 2003 to April 5, 2004: U.S. Department of Energy, DOE/BC15128-8, 46 p.

Chidsey, T.C., Jr., and Eby, D.E., 2004, Heterogeneous shallow-shelf carbonate buildups in the Paradox Basin, Utah and Colorado: targets for increased oil production and reserves using horizontal drilling techniques – semi-annual technical progress report for the period April 6, 2004 to October 5, 2004: U.S. Department of Energy, DOE/BC15128-9, 22 p.

Chidsey, T.C., Jr., Morgan, C.D., and Eby, D.E., 2005, Heterogeneous shallow-shelf carbonate buildups in the Paradox Basin, Utah and Colorado: targets for increased oil production and reserves using horizontal drilling techniques – semi-annual technical progress report for the period October 6, 2004 to April 5, 2005: U.S. Department of Energy, DOE/BC15128-9, 31 p.

Project Deliverables

Deliverable 1.1.1 – Regional Paradox Formation Structure and Isochore Maps, Blanding Sub-Basin, Utah

Deliverable 1.1.2 – Regional Paradox Formation Cross Sections, Blanding Sub-Basin, Utah and Colorado

Deliverable 1.1.3 – Regional Paradox Formation Facies Maps, Blanding Sub-Basin, San Juan County, Utah

Deliverable 1.2.1A – Thin Section Descriptions: Cherokee and Bug Fields, San Juan County, Utah

Deliverable 1.2.1B – Thin Section Descriptions: Little Ute and Sleeping Ute Fields, Montezuma County, Colorado

Deliverable 1.2.2 – Capillary Pressure/Mercury Injection Analysis: Cherokee and Bug Fields, San Juan County, Utah

Deliverable 1.2.3 – Scanning Electron Microscopy and Pore Casting: Cherokee and Bug Fields, San Juan County, Utah

Deliverable 1.2.4 – Isotopic Analysis: Cherokee and Bug Fields, San Juan County, Utah

Deliverable 1.2.5 – Thin Section Epifluorescence: Cherokee and Bug Fields, San Juan County, Utah

Deliverable 1.2.6 – Thin Section Cathodoluminescence: Cherokee and Bug Fields, San Juan

County, Utah

Deliverable 1.3.1 – Geophysical Well Log/Core Descriptions, Cherokee and Bug Fields, San Juan County, Utah, and Little Ute and Sleeping Ute Fields, Montezuma County, Colorado

Deliverables 1.4.1 and 1.4.2 – Cross Sections and Field Maps: Cherokee and Bug Fields, San Juan County, Utah, and Little Ute and Sleeping Ute Fields, Montezuma County, Colorado

Deliverable 2.1.1 – Porosity/Permeability Cross-Plots: Cherokee and Bug Fields, San Juan County, Utah, and Little Ute and Sleeping Ute Fields, Montezuma County, Colorado

Deliverable 2.1.2 – Production Analysis: Cherokee and Bug Fields, San Juan County, Utah

Deliverable 2.2.1 – Three-Dimensional Geologic Models and Reserve Calculations: Cherokee and Bug Fields, San Juan County, Utah

Deliverable 3.1.1 – Demonstration Location: Cherokee and Bug Fields, San Juan County, Utah and Little Ute and Sleeping Ute Fields, Montezuma County, Colorado

Project Displays at American Association of Petroleum Geologists Annual Meetings

Project materials, plans, objectives, and results were displayed at the UGS booth during the following meetings of the American Association of Petroleum Geologists (AAPG):

AAPG Annual Convention, April 16-19, 2000, New Orleans, Louisiana
AAPG Annual Convention, June 3-6, 2001, Denver, Colorado
AAPG Annual Convention, March 10-13, 2002, Houston, Texas
AAPG Rocky Mountain Section Meeting, September 8-10, 2002, Laramie, Wyoming
AAPG Annual Convention, May 11-14, 2003, Salt Lake City, Utah
AAPG Annual Convention, April 18-24, 2004, Dallas, Texas
AAPG Rocky Mountain Section Meeting/Rocky Mountain Natural Gas Strategy Conference and Investment Forum (hosted by the Colorado Oil & Gas Association), August 9-11, 2004, in Denver, Colorado
AAPG Annual Convention, June 19-22, 2005, Calgary, Canada
APG Rocky Mountain Section Meeting, September 23-24, 2005, Jackson, Wyoming
AAPG Annual Convention, April 9-12, 2006, Houston, Texas
AAPG Rocky Mountain Section Meeting, June 10-13, 2006, Billings, Montana

Short Course

The UGS prepresented a short course, "Pennsylvanian Heterogeneous Shallow-Shelf Buildups of the Paradox Basin: A Core Workshop," instructed by David E. Eby, Thomas C. Chidsey, Jr., and Laura L. Wray, at the UGS Core Research Center, May 10, 2003, as part of the AAPG Annual Convention in Salt Lake City, Utah. The short course was co-sponsored by the DOE. Core from representative Ismay and Desert Creek fields was examined. All core displayed was placed into regional paleogeographic settings. The core workshop was organized into topical modules with participants performing a series of exercises using core, geophysical well logs, and photomicrographs from thin sections. These modules included: describing reservoir versus non-reservoir facies, determining diagenesis and porosity from core, recognizing barriers and baffles to fluid flow, correlating core to geophysical well logs, and identifying potential completion zones and candidates for horizontal drilling. There were 25 participants from oil companies around the world.

Utah Geological Survey Web Site

The UGS maintains a Web site, http://geology.utah.gov. The UGS site includes a page under the heading *Oil, Gas, Coal, & CO_2*, which describes the UGS/DOE cooperative studies past and present (Paradox Basin, Ferron Sandstone, Bluebell field, Green River Formation, PUMP II), and has a link to the DOE Web site. Each UGS/DOE cooperative study also has its own separate page on the UGS Web site. The Paradox Basin project page http://geology.utah.gov/emp/Paradox2/index.htm contains (1) a project location map, (2) a description of the project, (3) a list of project participants and their postal addresses and phone numbers, (4) a reference list of all publications that are a direct result of the project, (5) semi-annual technical progress reports, and (6) project technical poster displays.

Technical Advisory Board

Seeley Oil Co., Salt Lake City, Utah
Legacy Energy Corp., Denver, Colorado
Pioneer Oil & Gas, South Jordan, Utah
Hallwood Petroleum Inc., Denver, Colorado
Dolar Oil Properties, Sandy, Utah
Cochrane Resources Inc., Roosevelt, Utah
Wexpro Co., Salt Lake City, Utah
Samedan Oil Corp., Houston, Texas
Questar Exploration, Denver, Colorado
Tom Brown Inc., Denver, Colorado
PetroCorp Inc., Denver, Colorado
Stone Energy LLC., Denver, Colorado
Sinclair Oil Corp., Salt Lake City, Utah

Stake Holders Board

Utah School and Institutional Trust Lands Administration, Salt Lake City, Utah
Utah Division of Oil, Gas and Mining, Salt Lake City, Utah
Colorado Oil and Gas Conservation Commission, Denver, Colorado
U.S. Bureau of Land Management, Salt Lake City, Utah
U.S. Bureau of Indian Affairs, Denver, Colorado
Ute Mountain Ute Indian Tribe, Towaoc, Colorado

Utah Geological Survey Press Release

NEWS RELEASE

January 12, 2005
Contact: Tom Chidsey
(801) 537-3364

UTAH GEOLOGICAL SURVEY OFFERS DOE FUNDING FOR HORIZONTAL DRILLING IN THE PARADOX BASIN

The Utah Geological Survey (UGS), with funding from the U.S. Department of Energy (DOE), is offering operators of fields that produce from the Ismay and Desert Creek zones of the Pennsylvanian Paradox Formation in the Blanding sub-basin, Paradox Basin, Utah and Colorado, the opportunity to receive 35 percent, up to a maximum of $200,000, of the costs to drill a horizontal lateral(s) from an existing vertical development well(s) or a new horizontal development well(s). All results from this government-funded horizontal well, including production tests, drilling and completion reports, daily production, geophysical well and mud logs, core and cuttings, etc., will be in the public domain. The general public, as well as UGS and DOE officials, will be permitted to visit the well site during drilling, testing, and production phases of operation.

Interested parties are invited to submit proposals to the UGS by March 1, 2005, that include the following information: (1) a geologic overview of the field, (2) targeted zone(s), (3) depth, length, and direction(s) of proposed horizontal wellbore(s), (4) drilling rationale, (5) drilling cost summary (AFE), and (6) drilling timetable.

For further information concerning horizontal drilling proposals, please contact Roger Bon (Ph.: 801/537-3363; email: rogerbon@utah.gov) or Tom Chidsey (Ph.: 801/537-3364; email: tomchidsey@utah.gov).

The drilling of a horizontal well is part of a UGS/DOE-funded project titled *Heterogeneous Shallow-Shelf Carbonate Buildups in the Blanding Sub-Basin of the Paradox Basin, Utah and Colorado: Targets for Increased Oil Production and Reserves Using Horizontal Drilling Techniques*. The UGS maintains a Web site, http://geology.utah.gov which includes a page under the heading *Oil, Gas, Coal, & CO_2*, describing the UGS/DOE cooperative studies past and present. Each UGS/DOE cooperative study also has its own separate page on the UGS Web site. The Paradox Basin project page http://geology.utah.gov/emp/Paradox2/index.htm contains (1) a project location map, (2) a description of the project, (3) semi-annual technical progress reports, and (4) project technical poster displays.

The Utah Geological Survey is an applied scientific agency that creates, interprets, and provides information about Utah's geologic environment, resources, and hazards to promote safe, beneficial, and wise use of land.